THE STATUS OF CANADIAN ENERGY'S CO-PROCESSING TECHNOLOGIES

F.G. BOEHM AND R.D. CARON

CANADIAN ENERGY DEVELOPMENTS INC.
4222 - 97 STREET
EDMONTON, ALBERTA T6E 5Z9, CANADA

Potential commercial production of synthetic liquid fuels was for many years thought to demand liquefaction of coal or upgrading of bitumen/heavy oils. By the late 1970s, however, another concept - i.e., the simultaneous co-processing of coal and heavy oil - began to receive some serious attention; and by now co-processing technology has reached a stage of development where it may appear to be the preferred upgrading procedure. This view, and the corollary that the feedstocks used for co-processing will play an increasingly important role in Canada's energy future, is supported by what is now seen as the most probable energy scenario. This scenario being:

(a) Energy consumption, globally and in Canada, will rise by between 1 and 3 percent per year;

(b) Crude oil prices will only very slightly increase up to 1995, but rise much more rapidly thereafter;

(c) The steady depletion of Canadian light crude resources since the early 1970s will, over the next decade, be reflected in rapidly diminishing indigenous supplies of such oil; and

(d) Stiffer competition in heavy oil markets, primarily from Mexico, Saudi Arabia and Venezuela, will make it important that Canada develop its own resources rather than import increasingly large volumes of crude oil.

We can also assume that the cost of heavy oil will be slightly less than conventional crude and will rise in proportion to the crude price, as well, the cost of suitable coal will not exceed $10-13 run-of-mine/tonne and will probably only increase with inflation.

Canadian Energy Developments Inc. (CE) is therefore concentrating its efforts on developing co-processing technologies which can be shown to possess significant advantages from low feedstock costs and which, even in current market conditions, could offer acceptable rates of return. In particular, the company is working toward development of a 25,000 bbl/d (4,000 m^3/d) heavy oil upgrader that would use co-processing technology.

THE CE TECHNOLOGIES

While several agencies (such as CANMET in Canada, and EPRI, HRI, etc. in the US) are exploring a broad spectrum of coal/heavy oil co-processing as means for production of synthetic liquid hydrocarbons - Canadian Energy, in cooperation with the Alberta Office of Coal Research and Technology[1], has focussed its attention on two specific process configurations.

---

[1] A Division of the Alberta Energy, Government of Alberta

1. THE CCLC PROCESS

The CCLC Process consists of two stages which involves (i) a preparatory step and coal "solubilization" (or "solvolysis"), and (ii) hydrogenation of the solubilized product mix.

Depending on its API gravity, the heavy oil used in the process is fractionated by atmospheric or vacuum distillation, and the bottom stream is blended with coal to form a slurry. For the subsequent processing, coal loadings up to 45 wt %, with ash contents up to 10 wt % are used, and the first-stage coal solubilization is followed by hydrogenation at 440-460°C/14-18 MPa which consumes 2-3 wt % hydrogen.

Test runs with a feedstock comprised of 58 wt % Cold Lake vacuum bottoms[2], 40 wt % subbituminous C coal[3] and 2 wt % "throw-away" catalyst in a continuous 2 kg/h bench scale unit have quite consistently furnished (C_5 to -525°C) oils that accounted for over 72 wt % of the d.a.f. feedstock.

Products available for secondary upgrading typically consisted of naphtha (25%), LGO (35%), M/HGO (14%) and a residual (+525°C) oil (8%).

The CCLC Process offers a continuous operation, high conversion, and a product slate that would require very little secondary upgrading for profitable disposition.

2. THE PYROSOL PROCESS

The second processing procedure under development by Canadian Energy is the PYROSOL Process which was initially conceived by West Germany's Gesellschaft für Kohleverflüssigung mbH (GfK) as an alternative to its more conventional high-severity coal liquefaction technology. PYROSOL seeks to generate as high or higher oil yields, but employs milder process conditions (and expends correspondingly less hydrogen) by combining a mild hydrogenation step with subsequent hydrocoking.

CE considered this approach to be another logical starting point for development of a Canadian co-processing technology, and accordingly entered into a co-operation and licence agreement with GfK.

In its present configuration and operating mode, the PYROSOL Process uses coal loadings up to 55 wt % (with up to 10 wt % ash), conducts first-stage hydrogenation at 380-420°C/8/12 MPa (with 0.8-1.5 wt % hydrogen consumption), and carries out second-stage hydrocoking at 480-520°C/8-10 MPa.

Although not yet optimized, test runs with the same feedstock as used in the CCLC Process have yielded 68 wt % oil (on d.a.f. feedstock); and product slates for secondary upgrading have been found to consist mainly of naphtha (8%), LGO (25%), M/HGO (27%) and coker oil (8%).

---

[2] These represent very heavy residua from oil sand bitumen processing

[3] From Manalta's Vesta Mine in Central Alberta

Advantages offered by the PYROSOL process will accrue from relatively low capital costs and easy operability, low hydrogen consumption, and an ability to process wastes in the form of coke before taking the products to secondary upgrading.

THE CURRENT STATUS

Canadian Energy is now working with a fully integrated, flexible 15 kg/h pilot plant which can operate in both process modes. Results from this unit are sufficiently encouraging to allow us to expect completion of the development program by 1990 and then proceed to a selection of the most suitable of the two processes for testing in a full-size demonstration plant. Commercialization may thus be possible in the early 1990s.

THE ECONOMICS OF CO-PROCESSING

Large-scale application of any co-processing technology obviously depends on demonstrating

(a) that a full-scale plant can achieve a sufficient return on investment to justify the necessary capital outlay, and

(b) that the technology is competitive with other processing options and can deliver a product that can compete against alternative fuels in the market place.

Canadian Energy has therefore initiated two feasibility studies in order to define the conditions in which a technically proven co-processing technology would have potential for commercial exploitation. One is examining the economics of stand-alone 25,000 bbl/d (4,000 m^3/d) heavy oil upgrader using co-processing technology and is still in progress. But the other, which is focused on the suitability of co-processing as means for converting heavy residua to acceptable refinery feedstocks, has been completed.

In that study co-processing was assumed to be integrated with refinery operations, and five cases were explored.

The first three cases (A, B and C) envisaged a plant input of 10,000 bbl/d (1,600 m^3/d) Cold Lake vacuum residua plus 1,371 tonnes/d subbituminous coal.

Case A then assumed maximum integration into the infrastructure of a refinery - i.e., the refinery is able to process the raw liquid products from co-processing without prior hydro-treating in the co-processing facility.

Case B envisaged intermediate integration - i.e., the refinery would only be capable of processing a moderately hydro-treated product from co-processing, and the co-processing facility would therefore include capacity for upgrading high-sulphur naphtha as well as for fluid catalytic cracking of heavy gas oils.

Case C considered minimum integration - with the refinery only capable of accepting a "synthetic crude" from the co-processing plant.

Case D, also based on minimum integration, envisaged a larger co-processing facility (16,000 bbl or 2,500 m^3/d Cold Lake residua and 2,193 tonnes/d of run-of-mine subbituminous coal) in order to assess the impact of plant size on capital and operating costs.

And Case E examined upgrading of two situations (E-1 and E-2) in which <u>only heavy oils</u> were processed by conventional hydrocracking in ebullated bed and subsequent delayed coking, and compared these with C and D.

E-1 envisaged processing 10,000 bbl/d of the Cold Lake vacuum residua, while E-2 was taken to operate with 16,000 bbl/d of Cold Lake residua.

In Case C and D, the plants produced 13,000 and 21,000 bbl/d (2,070 and 3,340 m^3/d), respectively, of (C_5 to -525°C) oil, and also furnished small amounts of C_3/C_4, sulphur and ammonia.

Capital costs for the upgrader units, expressed in 1987 $Can and including all off-site facilities and utilization systems as well as project contingencies were $310, $385, $416, $539, $410 and $504 million for Cases A, B, C, D, E-1 and E-2 respectively.

The key data for the base case, all expressed in 1992 $ Can., were then chosen as follows:

Plant start-up:	1992
Coal, f.o.b. Plant:	$16.00/tonne (*)
Natural gas:	$0.085/$m^3$ (*)
Cold Lake vacuum residua:	$20.65/bbl ($129.87/m^3)
Value of liquid products:	Case A - $31.55/bbl ($197.17/m^3)
	Case B - $33.35/bbl ($209.75/m^3)
	Case C, D and E - $35.35/bbl ($222.33/m^3)
Inflation rate to 1992:	$4% per annum
Oil price forecasts:	Coles, Nikiforuk, Pennell
Equity:	100%

(*) inflated to 1992

From these data, the case studies arrived to the following after-tax DCF rates of return:

Case A:	12.4%
Case B:	11.4%
Case C:	11.8%
Case D:	14.4%

For E-1 and E-2 the corresponding figures were 4.0% and 6.4% respectively.

These findings allow several important inferences. Thus:

(a) A co-processing plant can offer an acceptable rate of return if heavy oil residua can be purchased at less then 80% of the price of crude oil, and such a plant is clearly more attractive than conventional heavy oil upgrading (cf. A, B, C and D vs. E-1 and E-2).

(b) Minimal benefits would be gained from refinery integration if the output of the upgrader is to be a synthetic crude, and a stand-alone upgrader, which would benefit by producing some light oils from the residua, would therefore also prove economically attractive.

(c) If the product price differentials used in the study are correct, the return on investment is not substantially affected by the extent of hydrotreating required to be conducted in the upgrader.

But perhaps the most interesting result of the study are the clear advantages which accrue to a co-processing facility from its lower feedstock costs. On a volume basis, and expressed in Canadian $$, feedstock and production costs per barrel of C_5 to $-525^{\circ}C$ oils would run to $18.28 in co-processing and $24.18 in conventional heavy oil upgrading (equivalent to $114.97 and $152.08 per m^3 respectively). And if the price of heavy residua were to increase by $5.00/bbl, the cost advantage to a co-processing facility would rise by $2.00/bbl ($12.58 m^3).

SUMMARY

Co-processing - i.e., simultaneous upgrading of coal and heavy oil residua - is expected to play an increasingly important role in Canada's future energy supply. Two co-processing technologies, both being developed by Canadian Energy Developments Inc., are reviewed, and six Case Studies indicating the economic potential of the process are presented. It is shown that co-processing has a significant economic advantage over conventional heavy oil upgrading, and that this advantage will increase as the cost of heavy oil increases.

Novel Dispersed-Phase Catalytic Approach to Coprocessing

by

A.V. Cugini, J.A. Ruether, D.L. Cillo, D. Krastman, and D.N. Smith
Pittsburgh Energy Technology Center
P.O. Box 10940
Pittsburgh, Pennsylvania 15236

and

Vincent Balsone
Gilbert Commonwealth, Inc.
P.O. Box 618
Library, Pennsylvania 15129

ABSTRACT

The Pittsburgh Energy Technology Center (PETC) is currently testing a new process concept for catalytically coprocessing a mixture of coal and petroleum-derived residual oils. The catalyst used in this process is molybdenum added directly to the reactor as an aqueous solution. Recent results are presented for product yield structure obtained in a 1-liter semibatch reactor. A discussion is also given for some recent findings obtained from coprocessing studies in a 1-liter continuous reactor system.

An important economic advantage in using this process can be gained if recovery of the dispersed catalyst from the product residue is demonstrated. A discussion is provided of an approach to catalyst recovery that does not require complicated processing steps and uses relatively inexpensive reagents. Results are presented from preliminary testing of the recovery process that indicate it is feasible to efficiently recover the catalytically active material for reuse in the process.

INTRODUCTION

The rapid consumption of conventional light petroleum reserves and the increasing need to refine lower quality petroleum feedstocks have recently prompted serious consideration of technology for coprocessing coal with petroleum residual oils or heavy bitumens. Coprocessing is attractive as a possible route for introducing the processing of coal in an evolutionary manner into existing refinery infrastructures without immediately incurring the large capital investment associated with other coal liquefaction alternatives.

Previous coprocessing experiments conducted at PETC in a noncatalytic operation (Lett and Cugini, 1986) have led to several conclusions. First, coal is capable of enhancing demetallation of the petroleum solvent stream. The demetallation mechanism appears to be an adsorption process whereby the metals are adsorbed onto the surface of the coal remaining undissolved at the reaction conditions. Second, distillate yields in coprocessing are larger than would be predicted from linear addition of the distillate yields based on independent processing of the coal and petroleum-derived solvent. Two factors appear to be responsible for this result. First, the petroleum-derived solvent can act as a hydrogen donor solvent (although a poor one) for the coal; and second, coal enhances the conversion of the oil through the catalytic effects of the inorganics in the coal, primarily pyrite. While these are positive results obtained in the noncatalytic coprocessing approach, the liquid product yields are too low and would not appear to justify a noncatalytic approach to coprocessing.

In our preliminary catalyst-screening studies, we evaluated a single-stage approach to catalytic coprocessing. While two-stage coprocessing has merits, mainly dealing with coal's inherent ability to remove metals from the petroleum and thereby reduce second-stage catalyst aging, the use of a supported catalyst at any point increases the difficulty of ultimately recovering the expensive metals used in formulating the catalyst. A dispersed-phase catalyst would facilitate recovery of the active metals. Also, the most active materials for single-stage upgrading have been finely dispersed catalysts, either supported or unsupported. Therefore, we chose a dispersed-phase catalyst for use in single-stage coprocessing. The form chosen was a water-soluble salt, specifically ammonium molybdate. This material is readily available, and the molybdenum in a catalyst recovery process is readily recovered as ammonium molybdate.

EXPERIMENTAL RESULTS AND DISCUSSION

Batch Operation

Catalyst (additive) screening tests were initially conducted in 42-mL microautoclave reactors. The objective of these tests was to identify potential active catalysts for coprocessing. The catalysts (additives) tested include aqueous ammonium heptamolybdate, hydrogen sulfide, hydrogen sulfide/water, and pyrite. These catalysts were tested at typical coprocessing reaction conditions; i.e. 435°C, 1200 psig cold H_2 charge, a residence time of 1 hour, and a 70 wt% concentration of Maya ATB with 30 wt% Illinois #6 coal. Analyses of the major thermophysical properties of Maya ATB and Illinois No. 6 coal are presented in Tables 1 and 2.

The products from the batch tests were removed from the reactors and separated into soluble and insoluble fractions. The product yield distributions for the catalyst-screening tests are shown in Figure 1. The molybdenum catalyst was the most active catalyst tested. The use of 0.1% Mo (based on total feed slurry) as aqueous ammonium molybdate resulted in the highest heptane-soluble-oil yield and lowest pitch (THF-insolubles) yield. The use of pyrite or H_2S resulted in an increase in conversion, with the pyrite being the more active of the two additives. Addition of water to the hydrogen sulfide system did not appreciably alter the product yield distribution.

The aqueous ammonium heptamolybdate catalyst precursor was also tested in a semibatch 1-liter autoclave reactor. The reaction conditions in the semibatch autoclave were similar to those in the microreactor with the exception that a flow-through gas was used. The gas rate was 4 scf of H_2 per hour. The feed charge consisted of 500 grams of coal/oil slurry.

The objective of these batch 1-liter tests was to determine the effect of scaling up from batch microreactor tests to semibatch operations (batch liquid, flow-through gas) on conversions and product distributions. These tests were conducted in both catalytic and noncatalytic systems. Figure 2 presents a comparison of the microreactor and 1-liter autoclave reactor product yields from coprocessing. The pitch conversion was similar in both cases. The major difference in the two systems was observed in the asphaltene (defined as heptane-insoluble/THF-soluble fraction) and oil (defined as heptane-soluble) yields. Apparently, the asphaltenes are converted to oil to a much larger extent in semibatch 1-liter reactors than in microreactors. This is observed in both catalytic and noncatalytic systems.

The work-up procedure for the semibatch system includes a distillation step. The total oil product is distilled after the heptane insolubles have been extracted. The distillation step employed a modified ASTM D1160 procedure. Figure 3 includes the results from the distillation of the heptane-soluble products for the semibatch catalytic and noncatalytic runs. The effect of the catalyst is most pronounced on the yield of distillable (C_5-950^oF) oil. A duplicate run for the catalytic case is also presented in Figure 5.

Continuous Unit Operation

The ultimate objective was to develop a dispersed-catalyst system capable of being used in a single-stage continuous operation. Continuous catalytic coprocessing experiments were performed in a computer-controlled 1-liter bench-scale continuous unit shown in Figure 4. A mixture of 30 wt% coal ground to 200 x 0 mesh and 70 wt% Mayan atmospheric tower bottoms (ATB - 650^oF+ boiling material) was injected along with an aqueous ammonium heptamolybdate stream and a hydrogen and hydrogen sulfide gas stream (the H_2S insures that the molybdenum has access to adequate sulfur to be converted to its sulfide form) into a preheater and reactor combination maintained at 2500 psig. Earlier microautoclave studies demonstrated the need for a gradual heat-up of the feed slurry (Cugini and Lett, 1987). Temperature staging of the preheater and reactor was used to provide this gradual heat-up in a continuous system. The residence time in the preheat zone is approximately 20 minutes. The operating conditions used for these runs were the following:

Reactor Temperature:	435^oC
Pressure:	2500 psig
Catalyst Feed Concentration (g Mo/g coal + oil)	0.003
Gas Feed Concentration (vol %):	97% H_2; 3% H_2S
Space Velocity:	0.75 hr^{-1}
Gas Feed Rate:	10 scfh

Slurry Feed Rate: 250 g/hr

The run was continuously operated for 100 hours with no operational problems. The separation scheme used to analyze product distributions was similar to that used for the semibatch 1-liter products. The product gases were sampled using gas burettes and analyzed by gas chromatography. The average material balance over the course of the 100 hours was 96.8%. Table 3 presents product distributions from a 12-hour material balance period. A high yield of distillable product is obtained with the use of catalyst in the system. The insoluble product yield is low, which indicates high conversion of coal to soluble products. The hydrogen consumption is 3.0 wt% of total feed slurry. Coupled with the yield of 80.1 wt% of C_5-950^oF product, the hydrogen utilization efficiency is 26.7 lb distillate per lb H_2.

Catalyst Recovery

To improve the feasibility of PETC's coprocessing scheme, it was felt that a catalyst recovery scheme should be developed. The use of an unsupported molybdenum catalyst would facilitate catalyst recovery because there would be no interferences from the support material, and the recovered form of the catalyst could readily be reused as a catalyst in the process.

The recovery scheme that is being developed is similar in concept to Exxon's recovery scheme for coal liquefaction catalysts (Francis and Veluswamy, 1983). The coprocessing residue is oxidized to separate the carbon from the catalyst-containing mineral matter and to convert the metals in the mineral matter to their oxide form. The resultant ash is extracted with an alkali solution to first solubilize the molybdenum and then solubilize the nickel and vanadium.

An experimental program has been initiated to test the feasibility of this recovery scheme. The first stage of the program was to recover molybdenum from a mixture of coal ash and added metal oxides in a ratio to represent the mixture from a calcined stream of a residue from coprocessing 30% Illinois No. 6 coal and 70% Maya ATB. The composition of this mixture is presented in Table 4. The mixture was calcined at 700^oC to allow for high-temperature interactions between the metals that might occur during the calcining step. The mixture was then extracted with ammonium hydroxide at a series of pH's and temperatures. The results of three catalyst recovery tests are also presented in Table 4. These results indicate that on model systems it is possible to extract 97% of the molybdenum with little contamination by vanadium. More tests are planned to optimize the extraction method on actual coprocessing residues.

CONCLUSIONS

The approach taken to catalytically coprocess a mixture of coal and petroleum-derived residual oil in a single-stage process has been demonstrated successfully. A high-activity unsupported catalyst has been developed that is capable of enhancing coal conversion and distillate yields. Activation of the catalyst has been demonstrated successfully for batch and continuous operations. In a moderate-severity mode of operation, 87 weight percent of the 950°F+ organic material in the slurry feed (Maya ATB and Illinois No. 6) is converted. The hydrogen consumption is about 3 weight percent of the feed.

The catalyst precursor used in this process is ammonium heptamolybdate added directly to the reactor as an aqueous solution. Preliminary results from model compound studies for recovery of the catalyst indicate that a significant fraction of the catalyst (97 percent) can be recovered for reuse.

FUTURE PLANS

The results obtained to date reflect early findings of scale-up from batch to continuous operations of catalytic coprocessing in a single-stage process. The catalyst activation sequence, although successful, has not been optimized. Since the pretreatment of the catalyst played a key role in the ultimate activity of the catalyst, several interdependent investigations will be pursued: (1) the time and temperature effects of preheating in the continuous mode of operation; and (2) the effect of adding promoters to the ammonium molybdate catalyst on coprocessing performance.

A research effort will continue to develop a recovery process for the spent catalyst in the coprocessing residual products. Efforts to date indicate that recovery of catalyst from calcined residues can be performed at very high levels of recovery via an extraction process. Coprocessing residual products will be subjected to calcination and catalytic metals recovery by leaching with an ammonium hydroxide solution. The goal set for the recovery process will be greater than 97 percent recovery of the molybdenum catalyst.

ACKNOWLEDGMENTS

The authors are grateful to Richard G. Lett, Dennis H. Finseth, and Sidney S. Pollack for providing analytical support and several helpful discussions regarding development and interpretation of the coprocessing experiments.

This work was supported in part by the Oak Ridge Associated Universities Graduate Research Program.

REFERENCES

Cugini, A.V., and Lett, R.G., "Microautoclave Studies of Coal/Petroleum Coprocessing," to be submitted for publication as a U.S./D.O.E. Topical Report.

Curtis, C.W., Tsai, K.J., and Guin, J.A., "Catalytic Coprocessing: Effect of Catalyst Type and Sequencing," Ind. Eng. Chem. Res., 26, 12-18 (1987).

Duddy, J.E., MacArthur, J.B., and McLean, J.B., "HRI's Coal/Oil Coprocessing Program: Phase 1," Proceedings of the 11th Annual EPRI Conference on Clean

Fuels, May 7-9, 1986.

Francis, James N., and Veluswamy, Lavanda R., "Recovery of Coal Liquefaction Catalysts," U.S. Patent No. 4417972, November 29, 1983.

Gatsis, J.G., Sikonia, J.G., Nelson, B.J., Luebke, C.P., and Humbach, M.J., "Coal Liquefaction Coprocessing," Proceedings of the DOE Direct Liquefaction Contractors' Review Meeting, November 19-21, 1985.

Greene, M., Gupta, A., and Moon, W., "Update: Lummus Co-Processing Project and Results of Catalyst Maintenance Testing," Proceedings of the 12th Annual EPRI Conference on Fuel Science, Palo Alto, California, May 13-14, 1987.

Lett, R.G., and Cugini, A.V., "Coprocessing Studies," Proceedings of the DOE Direct Liquefaction Contractors' Review Meeting, October 22, 1986.

Shinn, J., Dahlberg, A., Kuehler, C., and Rosenthal, J., "The Chevron Co-Refining Process," Proceedings of the 9th Annual EPRI Contractors' Conference on Coal Liquefaction," Palo Alto, California (1984).

Table 1

ILLINOIS NO. 6
(Burning Star)

Proximate Analysis, wt% (as-received)	
Moisture	4.2
Volatile Matter	36.9
Fixed Carbon	48.2
Ash	10.7

Ultimate Analysis, wt% (moisture-free)	
Carbon	70.2
Hydrogen	4.8
Nitrogen	0.9
Sulfur	3.1
Oxygen (diff.)	9.9
Ash	11.1

Table 2

MAYA ATB
(650°F+)

Ultimate Analysis, wt%	
Carbon	84.5
Hydrogen	10.6
Oxygen	0.3
Nitrogen	0.5
Sulfur	4.0
Ash	0.1
Ni(ppm)	70
V (ppm)	370
950°F-, vol% ASTM D1160	30
Heptane Insols, wt% ASTM D3279	20

Table 3

PRODUCT YIELDS AND CONVERSIONS -- (CAT-8-2)

Yield Structure

Component	Coal + Heavy Oil (Ash-Free) Weight Percent	950°+F (Ash-Free) Weight Percent
C_1-C_4	5.1*	6.9
C_5-950°F	80.1	74.5
950°F+	6.9	8.7
Heptane Insolubles	3.7	4.6
Non-Hydrocarbon Gases	7.2*	9.2
Hydrogen Consumption	-3.0	-3.9

Conversions (Ash-Free Basis)

Component	Weight Percent
950°F+	87
THF Insolubles	95
Heptane Insolubles	92

*Estimated from tail gas sampling.

Table 4

Model Compound Extractions

Model Mixture

Component	Weight Percent
Coal Ash	92.8
V_2O_5	2.8
NiO	0.1
MoO_3	4.3

Molybdenum Recovery

Test	Wt% Mo Recovered As Molybdate	Wt% of V Recovered with Molybdate
1	75	2
2	95	5
3	97	22

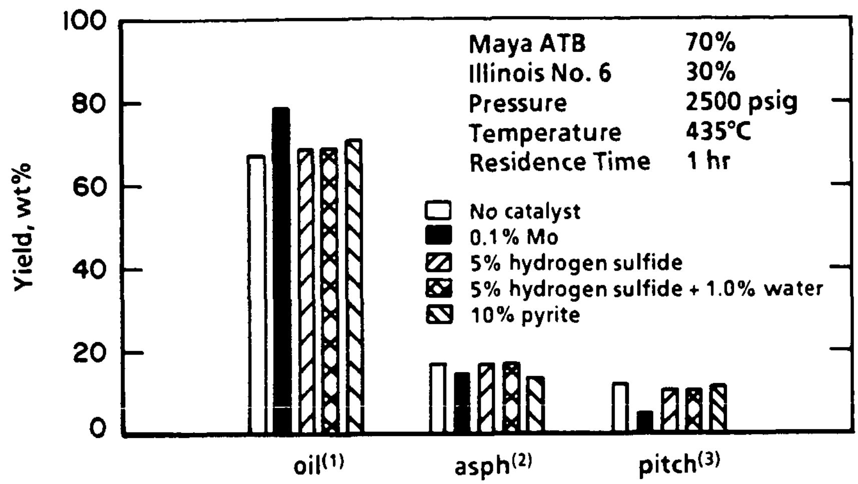

(1) heptane solubles
(2) heptane insoluble/THF soluble
(3) THF insolubles

Figure 1.

MICROAUTOCLAVE PRODUCT YIELDS

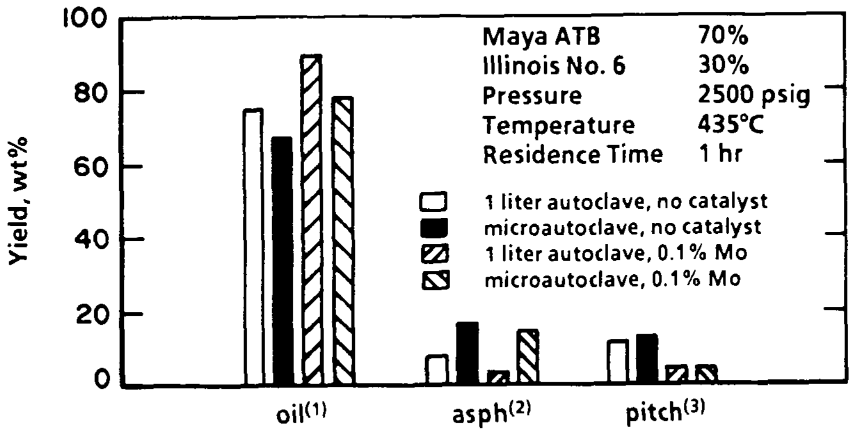

(1) heptane solubles
(2) heptane insoluble/THF soluble
(3) THF insolubles

Figure 2.

COMPARISON OF MICRO- AND 1 LITER-AUTOCLAVE REACTOR SYSTEMS

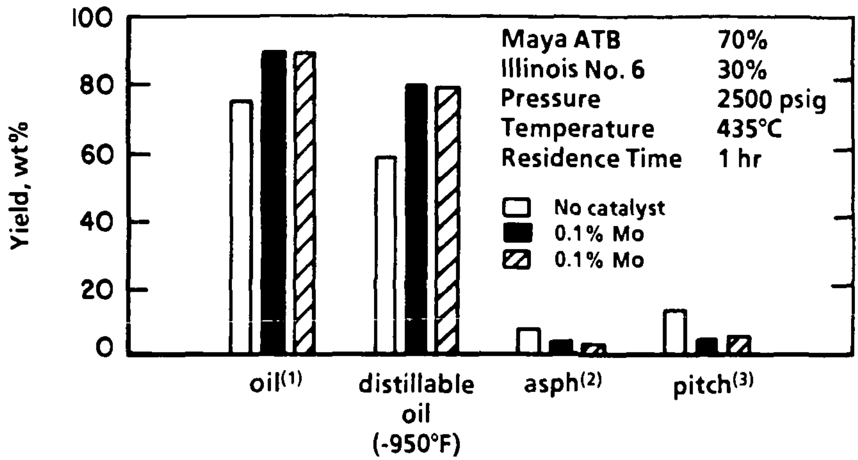

(1) heptane solubles
(2) heptane insoluble/THF soluble
(3) THF insolubles

Figure 3.

BATCH 1 LITER AUTOCLAVE YIELDS

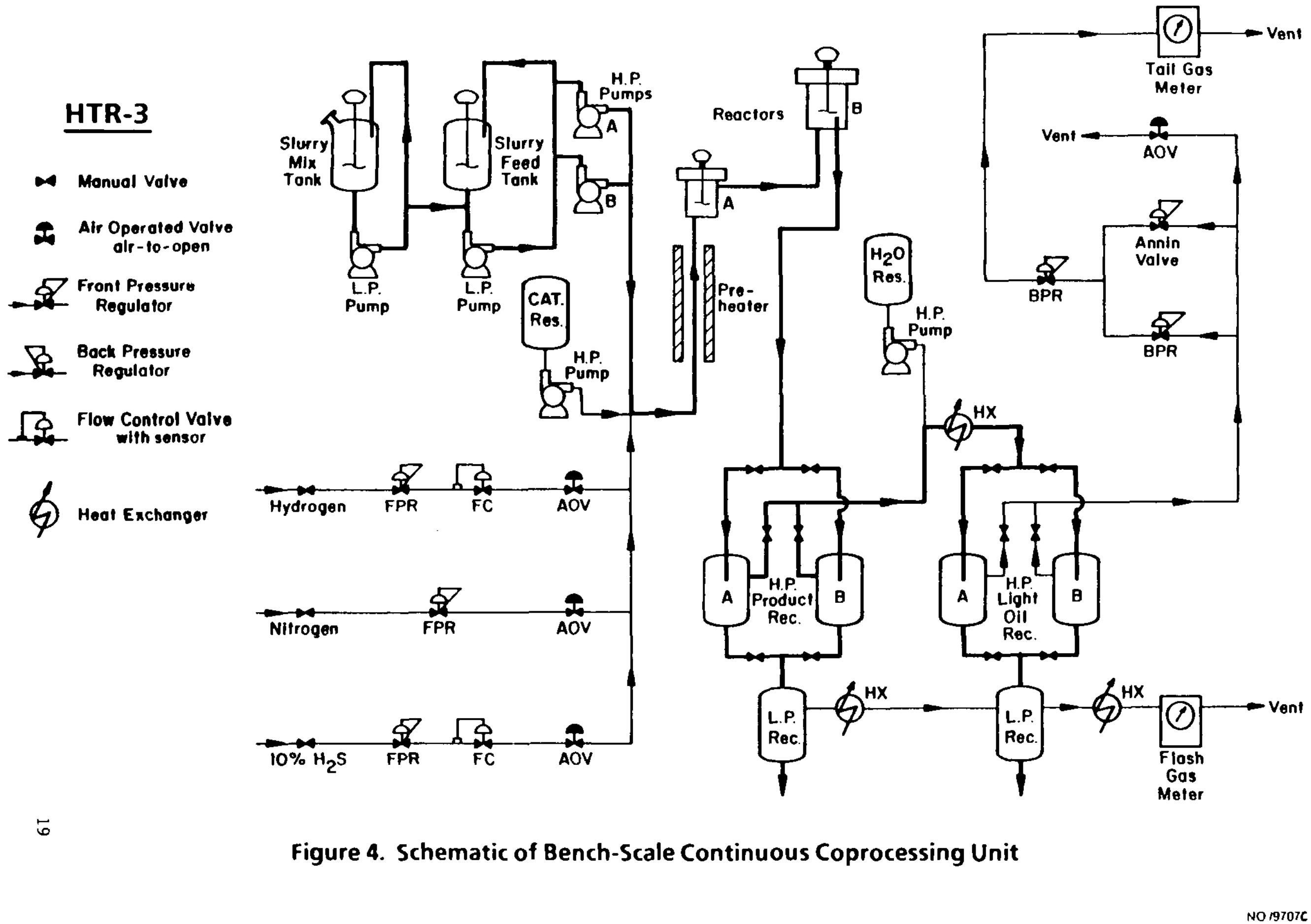

Figure 4. Schematic of Bench-Scale Continuous Coprocessing Unit

THE BEHAVIOUR OF HIGHVALE AND VESTA COALS UNDER CO-PROCESSING CONDITIONS

L.K. Lee and B. Ignasiak

Alberta Research Council
Coal and Hydrocarbon Processing Department
1 Oil Patch Drive, Bag #1310
Devon, Alberta
Canada, T0C 1E0

INTRODUCTION

Co-processing involves the conversion of relatively low-cost coal and heavy oil in the presence of hydrogen to synthetic crudes that can be further upgraded into premium liquid fuels. This alternative coal conversion concept eliminates or significantly reduces the need for solvent recycle and hence offers greater potential for improving economic performance over current direct coal liquefaction technologies.

Alberta is endowed with large reserves of subbituminous coals, bitumen and heavy oils. The combined processing of these feedstocks is attractive for the Alberta scenario. Alberta Research Council has been active in developing the co-processing technology (1,2). Due to the high oxygen and mineral matter contents in Alberta subbituminous coals plus the high sulfur and metal contents in bitumens, special considerations are necessary when processing these feedstocks, for example, removal of oxygen to avoid excessive hydrogen consumption; removal of mineral matter to reduce deactivation of expensive catalysts; or use of less efficient, low-cost disposable catalysts . Alberta Research Council developed a two-stage process which involves a first-stage coal solubilization in bitumen or heavy oil using a mixture of carbon monoxide and steam in the presence of an alkali metal catalyst, followed by a catalytic hydrogenation second-stage (3).

This paper is focused on the use of disposable iron oxide catalysts in co-processing two Alberta subbituminous coal and bitumen feed pairs. Effects of reaction severity, pressure and coal concentration will be discussed.

EXPERIMENTAL

Process Unit

Co-processing experiments were carried out in a two-stage, continuous flow reactor system with a nominal capacity of 2 Kg/h of slurry feed. The reactor system consists of two stirred tanks of one and two litres in volume connected in series. Products were collected over a material balance period of eight hours under steady state conditions. For all experiments reported in this paper, the material balances were within 100 $\pm$ 3%. For comparative purposes, all data were normalized to give 100% recovery by adjusting the weight of the slurry product. Details of the process unit are available elsewhere (4).

Slurry products were distilled according to a modified ASTM D-1160 procedure, followed by extraction using pyridine in a soxhlet apparatus.

Feedstocks

The co-processing characteristics of two feed pairs, Highvale (subbituminous B) / Athabasca bitumen and Vesta (subbituminous C) / Cold Lake bitumen, were evaluated. The two coal samples were obtained from the Alberta Research Council's sample bank.

The Athabasca bitumen sample was a Suncor coker feed (IBP 222°C) while the Cold Lake sample was an atmospheric distillation residuum obtained from the Imperial Oil Strathcona Refinery, Edmonton. Analyses of the coals and bitumen samples are given in Tables 1 and 2, respectively.

Reaction Severity

Previous batch autoclave experiments (5) indicated that iron oxides can be used as effective catalysts to solubilize Alberta coals in petroleum derived solvents at temperatures up to 470°C under a hydrogen atmosphere of about 21 MPa. In order to avoid excessive coking, the continuous flow CSTR experiments were carried out at temperatures below 470°C.

Reaction temperature and space time in both reactors were varied to determine the impact of reaction severity on product yields and qualities. As a first approximation, a simplistic approach was taken by defining a reaction severity index which combined the effects of the temperature (T) and nominal residence time (N. RTime) in a reactor.

$$\text{Reaction Severity (SV)} = [\ (\text{N. RTime}) * \text{EXP}(-E/RT)\ ]_{\text{1st reactor}} + [\ (\text{N. RTime}) * \text{EXP}(-E/RT)\ ]_{\text{2nd reactor}}$$

The activation energy (E) for both stages was assumed to be 1.26×10^5 joules/g-mole (30 Kcal/g-mole). A reference severity index of unity was arbitrarily defined at the condition of 400°C for 60 min.

Figure 1 compares co-processing results obtained at various degrees of reaction severity ($2 < SV < 5$) for the Vesta/Cold Lake pair with moisture-and-ash-free (maf) coal loadings between 27 and 30 wt%. The simplistic, reaction severity index approach gives good correlation with product yields when expressed in terms of maf feed basis. Yields of carbon oxides and hydrogen sulfides are relatively constant over the whole range of conditions studied. Also, as the reaction severity increases the hydrocarbon gas yield increases proportionately, while the pyridine insoluble organic matter (IOM) decreases. Even at the highest reaction severity conditions tested, there was no sign of excessive coke formation, as reflected by the steady decrease in the amount of IOM in the residual solids. These IOM values correspond to coal conversions (measured by pyridine extraction) between 93-99 wt% maf coal, which were found to be in agreement with coal liquefaction results obtained under similar process conditions (7).

With increasing severity distillable oils (IBP-500°C) are formed at the expense of pyridine extractable materials. Using the two-stage CSTR system, a maximum yield of 62 wt% maf feed was obtained at the highest severity tested. Distillable oil yields of as high as 75% maf feed were observed using a tubular reactor system (6).

Comparing product yields from co-processing of the two feed pairs (refer to Figure 1 and 2), the Highvale/Athabasca pair seems to produce more carbon oxides, hydrocarbon gases and IOM, but less distillable oils. These differences which become more pronounced at higher reaction severity conditions, cannot be correlated to the elemental and petrographic analyses as given in Table 1. Although Vesta and Highvale coals have a similar vitrinite content, Vesta coal contains a higher percentage of inertinite and thus is expected to be less reactive. However, conversions of Highvale coal (82-85 wt%) were in fact 10-14 wt% lower than Vesta coal. A similar result was also obtained under the direct coal liquefaction mode (7). On the other hand, the difference in carbon oxides yield from co-processing contradicts previous results obtained for these coals under liquefaction mode (7).

Figures 1 and 2 reveal similar yields of non-distillable, pyridine extractable material for both feed pairs. However, detailed compound class analysis (3) suggests that most of the residual oils occurred in the form of hydrocarbons, resins and asphaltenes with less than 30 wt% as preasphaltenes. The higher preasphaltene content in products from the Highvale/Athabasca pair further confirmed the lower reactivity of this feed pair.

Pressure

Effect of system pressure was studied over a narrow range of 14.2 to 20.7 MPa at two different reaction severities. The low pressure experiments were carried out at a slightly lower maf coal loading of 27 wt%, while the high pressure data were collected using 30 wt% of coal. Considering the slight difference in coal loading, there are no significant effects on product distribution due to the lower operating pressure, as indicated in table 3. However, low pressure operating conditions, which may create long term operating problems, warrant further investigation in a large scale pilot unit.

Coal Concentration

Bitumen is considered a poorer solvent than coal-derived liquids for coal solubilization. In once-through mode operation, the ability of bitumen to solubilize coals may deteriorate as the coal concentration increases. As illustrated in Figure 4, produce yields from co-processing of Highvale/Athabasca under relatively mild severity conditions increase steadily as the coal concentration increases from 0 to 35 wt%. The bitumen-only case gives 58 wt% (feed bitumen basis) of distillable oils. The incremental oil yield at a coal loading of 35 wt% is about 18 wt% on a bitumen feed basis. Translating back to maf coal basis, this is equivalent to 33 wt%, which is 10-15 wt% higher than the typical values when anthracene oil was used as a solvent, under simiiar process conditions. The higher incremental oil yield provides additional incentive for co-processing of coals and bitumen.

CONCLUSION

Co-processing of Alberta Subbituminous coals and bitumen in a two-stage, once-through mode is technically feasible. These results indicate that synergistic effects occur when the Highvale and Vesta coals are processed with Athabasca and Cold Lake bitumen, respectively. Decreasing the system pressure from 20.7 to 14.2 MPa has no significant effect on product distribution. Despite the over simplification of the two-stage CSTR model, good correlations are obtained between product yields and the reaction severity index.

ACKNOWLEDGEMENT

The experimental work reported in this paper was conducted by L. Logan, R. Hawkins, J. Wilson, B. Doherty, and D. Rohatynski. The authors would like to thank Dr. S. Chakrabartty for his comments and reviewing the manuscript. This work was jointly funded by the Alberta Research Council and the Alberta Office of Coal Research and Technology.

REFERENCES

1. E. Boomer and A. Saddington, **Canadian Journal of Research**; 12, p825, 1935.

2. B. Ignasiak, L. Lewkowicz, G. Kovacik, T. Ohuchi and M.P. du Plesis, (Editors: S. Kaliaguine and A. Makay); **Catalysis on the Energy Scene**, Elsevies Science Publishers, B.V., Amsterdam, 1984.

3. B. Ignasiak, T. Ohuchi, P. Clark, D. Aitchison, and T. Lee; **ACS Division of Fuel Chemistry**, 31, No. 4, p200, 1986.

4. L.K. Lee; Alberta Energy and Natural Resource Department / Alberta Research Council (ENR/ARC) Report for Project #34, Final Report for April to September 30, 1985.

5. L. Lewkowicz, R. Lott, S.K. Chakrabartty and B. Ignasiak; ENR-ARC Report, Report # YCLQ-33, 1986.

6. L.K. Lee, D. Aitchison, J. Mendiuk, and G. Kovacik; CCLC Pyrosol Evaluation Program, Phase I Final Report (confidential report), June 1987.

7. L.K.Lee, P.D. Clark, and D.W. Aitchison; ENR-ARC Coal Conversion Research Program, Final Report for 1984/1985, 1, 1986.

Table 1. Typical Properties of Highvale and Vesta Coals

	Highvale	Vesta
ASTM Rank	Subbit. B	Subbit. C
Proximate Analysis (wt%)		
Capacity Moisture	19.6	24.7
Moisture Free Ash	11.4	12.4
Volatile Matter (maf)	39.6	41.9
Fixed Carbon (maf)	60.4	58.1
Elemental Analysis (wt%)		
Carbon	75.0	74.4
Hydrogen	4.3	5.0
Nitrogen	1.1	1.5
Sulfur	0.2	0.6
Oxygen	19.3	18.5
H/C	0.69	0.81
Petrographic Composition (vol%)		
Vitrinite	75.0	73.0
Liptinite	2.1	0.3
Semi-fusinite	22.2	8.9
Inertinite	1.1	17.0

Table 2. Typical Analysis of Feed Oils

	Athabasca Coker Feed	Cold Lake Atm. Bottom
Elemental Analysis (maf)	wt%	wt%
Carbon	82.9	83.2
Hydrogen	10.3	10.3
Nitrogen	0.5	0.9
Sulfur	5.3	5.3
Oxygen (by diff.)	1.1	0.3
H/C	1.49	1.49
Distillation and Extraction		
Moisture	-	0.01
IBP-500°C	29.5	29.2
Residual Oils	69.9	70.7
Residual Solids	0.6	0.05
Compound Class Analysis		
Hydrogen & Resin	79.8	70.5
Asphaltene	18.9	27.2
Preasphaltene	1.3	2.3

Table 3. Effect of Pressure on Co-processing of Vesta/Cold Lake Atmospheric Bottom Using Iron Oxide as Catalysts

	High Severity		Low Severity	
	Case A	Case B	Case C	Case D
Pressure (MPa)	20.7	14.3	20.7	14.2
Temperature (°C)	431/431	431/430	420/419	418/416
Severity Index	3.52	3.90	2.65	2.56
Product Distribution (maf wt% feed)				
C1 - C5	4.53	5.20	3.15	4.08
IBP-200°C	11.14	14.32	7.23	10.43
200-375°C	10.93	16.58	8.54	10.40
375-500°C	31.86	28.76	31.27	29.11
500°C+	36.56	33.81	44.10	42.90
IOM	1.33	1.73	1.76	2.61
H_2 consumed	1.86	2.85	1.65	2.42

Figure 1

Co-processing of Vesta Coal and Cold Lake Atmospheric Bottom

(using dispersed iron oxide as catalyst - bench unit)

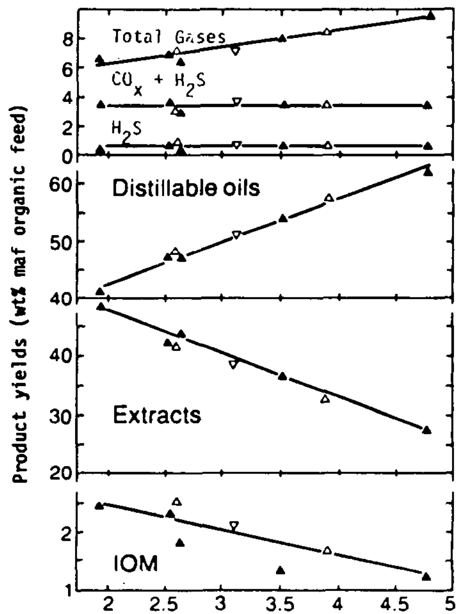

Reaction severity index
Pressure (MPa): Δ, 14.3; ∇, 17.0; ▲, 20.7

Figure 2

Co-processing of Highvale Coal and Athabasca Bitumen (Suncor Coker Feed)

(using dispersed iron oxide as catalyst)

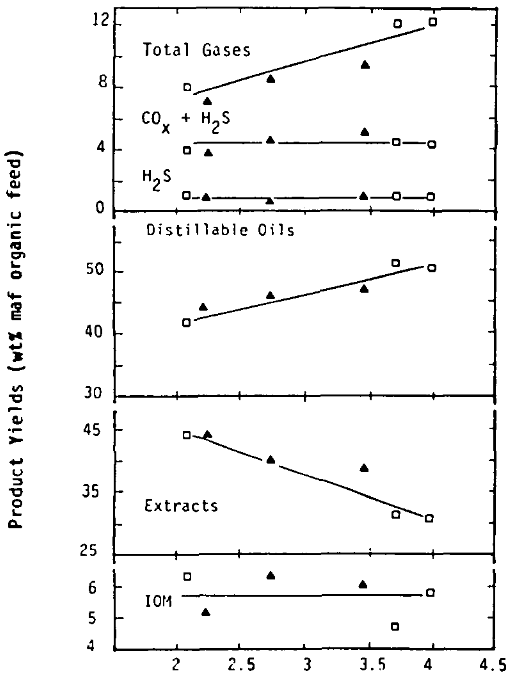

Reaction Severity Index
Coal concentration: □, 30%; ▲, 35% (maf)

Figure 4

Effects of Coal Concentration

- low severity (Highvale Coal/ Athabasca bitumen, iron oxide as catalyst)

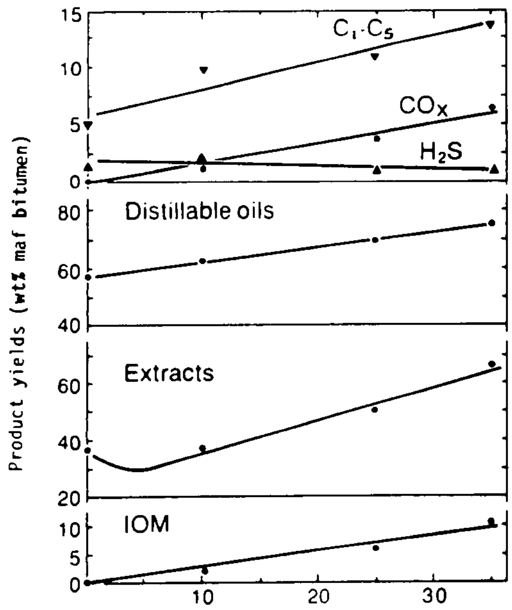

Figure 3

Compound Class Type Distribution of Co-processing Product

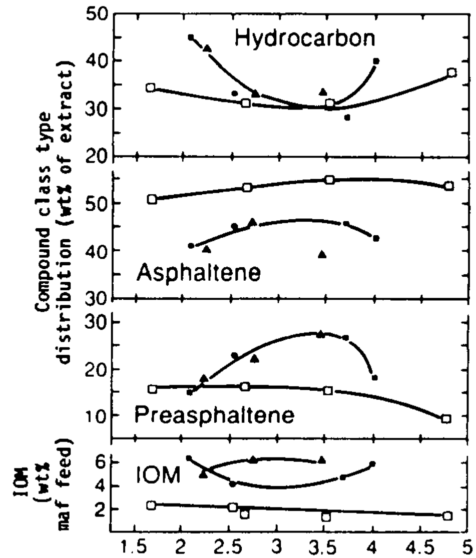

□ Vesta/Cold Lake atm. residuum

▲, ■ Highvale/Athabasca bitumen

COPROCESSING - THE HYDROGENATION OF LIGNITE TOGETHER WITH RESIDUAL OILS

Uwe Lenz, Joachim Wawrzinek *
Axel Giehr**

* Rheinische Braunkohlenwerke AG, D 5000 Köln 41
**Union Rheinische Braunkohlen Kraftstoff AG, D 5047 Wesseling

1 ABSTRACT

The current overflow on the crude oil market must not obscure the fact that world oil resources are limited. Instead, it must be our goal to develop practicable concepts for the conversion of fossil raw materials and optimize their economic viability. The joint development programme of the Rheinische Braunkohlenwerke AG and the Union Rheinische Braunkohlen Kraftstoff AG for the catalytic hydrogenation of fossil raw materials in the liquid phase aims at this goal.

In a continuously operating process development unit extensive investigations have been carried out focussing on:

- conversion of lignite,
- development of catalysts based on lignite coke,
- conversion of heavy residual oils,
- conversion of mixtures of lignite and residual oils (coprocessing).

In this paper the results of these investigations are discussed.

A comparison of lignite liquefaction and coprocessing elucidates the advantage of coprocessing. Thanks to a change in the process route and a yield-improving synergistic effect, coal liquefaction via coprocessing will reach economic viability earlier than the liquefaction of coal alone.

2 RESEARCH AND DEVELOPMENT PROJECTS TO CONVERT FOSSIL RAW MATERIALS

In view of the future situation in the crude oil market where oil less in quantity and quality will be available it is necessary to develop practicable concepts for the conversion of fossil fuels.

In the field of refining, e.g., there are several processes permitting the conversion of heavy residual oils or even extra-heavy crude oils into lower-boiling products. Some of these processes have for quite some time been applied on an industrial scale; they include coking, deasphaltization, and H-oil processes. Limiting factors in respect of process application are the quality of feed oils (content of heavy metals) and/or the quality of by-products (petrol coke).

The process suitable for use in a much wider field of application is the conversion of fossil fuels in liquid-phase hydrogenation; it is based on coal liquefaction according to Bergius-Pier, a process which can look back on many years of application. In our group, e.g., it was used from 1941 to 1964 to process lignite and heavy oil on a commercial scale.

The development programme on which the Rheinische Braunkohlenwerke AG (Rheinbraun) and the Union Rheinische Braunkohlen Kraftstoff AG (Union Kraftstoff) have been cooperating since 1978 and which deals with the hydrogenation of fossil fuels to make high-grade liquid hydrocarbons centres around the following:

- hydroliquefaction of lignite,
- hydroliquefaction of residual oils,
- hydroliquefaction of mixtures of lignite and residual oils (coprocessing),
- development of suitable catalysts based on lignite coke.

In its first stage, i.e. on a process-development scale, we implement the development programme with the aim of

- further developing and optimizing the processes applied from 1941 to 1964,
- determining process data,
- finding out whether hydrogenation of fossil fuels will be economically viable.

Major fields of these projects were and are financially supported by the Federal Ministry of Research and Technology.

In the following, this paper will deal not only with the results obtained in the investigations of coprocessing; in order to facilitate understanding of this subject, it will also discuss the results which are achieved in the investigations of lignite liquefaction, hydrogenation of residual oils, and development of catalysts.

3 FUNDAMENTAL PROCESS DIFFERENCES IN THE CASE OF HYDROGENATION OF COAL, MIXTURES AND RESIDUAL OILS

Between coal liquefaction, on the one hand, and hydrogenation of mixtures and residual oils, on the other hand, there is a major difference in process engineering (Figure 1). Today, conversion of residues and coprocessing are generally operated in a "once-through mode"; contrary to this, coal liquefaction calls for cycling of the slurry oil, and the operating mode preferably used to hydrogenate residual oils in the commercial-scale plants until 1964 was recycling of the cold separator heavy oil and parts of the hot separator sludge. Since recycling is no longer required, coprocessing - contrary to coal hydrogenation - permits a major simplification of the process route. In coprocessing, the mineral oil-derived residual oil acts as slurry oil which is converted into lower-boiling products without any cycling being required.

Due to today's advanced refining technique it is advisable not to recycle the heavy oil produced during hydrogenation, but to hydrocrack it and produce naphtha and gas oil for use in the motor fuel sector or feedstocks for use in petrochemistry.

The liquid-phase process benefits from the "once-through mode"; here, the reaction zone is not filled with cycled heavy oil and, hence, permits full charge with heavy oil.

4 TEST INSTALLATION

SET-UP AND OPERATION OF THE PROCESS DEVELOPMENT UNIT

Figure 2 shows the set-up of the test plant for lignite hydroliquefaction.

This plant is also used to carry out tests on conversion of heavy residual oils and coprocessing.
The plant is designed for fully continuous operation.
The feedstock is predried powdered lignite with a residual water content of up to 12% wt and a maximum grain size of 1 mm and/or oil with an initial atmospheric boiling point of $>$ 510° C.
The reaction pressure of hydrogenation ranged between 150 and 300 bar.
The reactor has a volume of approx. 8 l. Two reactors with an inner diameter of 4.5 cm each are connected in series. The pumps are designed for an hourly

throughput of coal slurry or oils of up to 16 l/hr.

The average availability of the plant was 60% for hydrogenation on the basis of coal while it rose to more than 80% for hydrogenation with residual oil.

5 LIGNITE HYDROLIQUEFACTION

5.1 RESULTS OBTAINED DURING TESTS IN THE PROCESS DEVELOPMENT UNIT

Within the scope of the lignite hydroliquefaction projects we performed, from 1978 to 1983, extensive development work in that process development unit.

In the following, the major results are summarized.

Yields as a function of temperature and gas throughput

In the temperature range under investigation, the oil yields as a function of temperature rise from 41 to 48 parts by weight. The residue portion decreases from 28 to 18 parts by weight, and the amount of hydrocarbon gases produced rises from 13 to 26 parts by weight, each related to 100 parts by weight at a coal throughput, maf, of 0.5 to 0.6 kg/l x hr.

Through an increase in the cycle gas amount of 30% the oil yield rises to approx. 53 parts by weight in the temperature range under investigation, while only some 12 parts by weight (Figure 3) will be obtained as residue.

It has not yet been possible to make definite statements about whether an increase in the amount of cycle gas will also produce higher yields in commercial-scale reactors with different fluid dynamics conditions.

Yield as a function of pressure

The tests in the process development unit have shown that at a pressure of 220 bar and with the same linear flow velocity as at 300 bar - for this, the volume of cycle gas was reduced from 18 to 14 m^3/hr - the oil yield decreases by 3 parts by weight as a result of the lower pressure. The portion of residue increases by the same amount. In the temperature range under investigation, the hydrocarbon gases correspond to the comparative values at 300 bar.

At a pressure of 150 bar and with the same cycle gas velocity as at 300 bar (9 m^3/hr) the process development unit yields an amount of oil which is about 10 parts by weight lower.

Recycling of supercritical fluid (SCF) extract

Thanks to the high extract yields, the supercritical fluid extraction technique produced considerably higher oil amounts and lower portions of residue than would be obtained, if conventional vacuum distillation of the sludge were employed under the same conditions. Figure 4 shows a comparison of the yields.

A final judgement on this technique can only be given when the test results to be obtained in a pilot plant will be on hand.

Sludge recycling

A crucial problem in hydroliquefaction is the formation of $CaCO_3$ containing sediments which give rise to coking.

Since part of the hot separator sludge (approx. 20% of the slurry oil) was recycled into the reaction zone, we were able to prevent cokings and deposits in the reactors of the process development unit; this was due to an improved fluid dynamics resulting from a better "carrying capacity" of the reaction mixture which in turn was caused by a rise in density.

The yields correspond to comparative figures obtained without sludge recycling.

5.2 PROCESS CONCEPT

The process concept of lignite hydroliquefaction consists of the following steps:

- coal drying and slurrying,
- hydrogenation in the liquid phase at pressures between 200 and 300 bar,
- partial cycling of sludge from the hot separator to the slurry oil,
- separation of the remaining hot separator product by way of distillation or supercritical fluid extraction into a solids-free oil for slurrying and a residue for hydrogen production,
- use of H_2S as co-catalyst, and
- coal-oil refining.

The question of whether this process concept can be implemented on a commercial scale has to be cleared up in two development stages, i.e. first in a pilot plant, and then in a demonstration plant where its industrial-scale feasibility and its economic viability are to be verified.

The results we obtained during operation of the process development unit formed a basis for the basic engineering and authority permittance required for a lignite hydrogenation pilot plant. In mid-1983, the competent authority granted the building and operating licences for a plant designed for an hourly coal throughput of up to 25 t (t - tonne) and to be located on the grounds of the Union Kraftstoff.

Due to economic considerations construction of this pilot plant has been postponed because the current price of gasoline produced by lignite hydrogenation is still about two times as high as that of petroleum-derived gasoline.

6 HYDROLIQUEFACTION OF RESIDUAL OILS

Within the scope of the project dealing with residual oil hydrogenation we carried out investigations in the process development unit with the aim of:

- clearing up the mode of action of liquid-phase catalysts and developing a suitable catalyst on the basis of lignite products, and
- determining yields and product qualities when different residual oils are used.

6.1 DEVELOPMENT OF CATALYSTS

From 1948 to 1964 when the commercial-scale liquid-phase plant worked with atmospheric distillation and cracking residues, entrained dust from lignite gasification was used as a base material for developing catalysts. With the addition of ferrous salts this material constituted an efficient and low-priced disposable catalyst.

Since today such or similar products from lignite gasification are either no longer available or occur in such small quantities that are insufficient to meet commercial-scale requirements, tests were made to develop a suitable and low-priced substitution product which is likewise derived from lignite products.

The result we obtained in the extensive research work on catalyst development showed that the following materials are particularly suitable:

- entrained dust from High-Temperature Winkler gasification,
- powdered coke from the rotary-hearth furnace process (rotary-hearth furnace coke),
- steam-activated rotary-hearth furnace coke.

For economical reasons, rotary-hearth furnace coke is preferably used (Figure 5).

The previous tests have shown that the catalysts influence not only the yield structure, but also the performance of the hydrogenation plant. A troublefree long-time performance without any temperature inhomogeneity and coke deposits in the reactors was only obtained when a lignite coke-derived catalyst was added.

Thanks to the successful research work described above we can now provide sufficient quantities of highly suitable and low-priced catalysts for coprocessing and liquid-phase hydrogenation of residual oils.

Mode of action of liquid-phase catalysts

The lignite-based solid matter which is added as catalyst to the liquid-phase process passes slowly through the reactors and is subsequently discharged from the hot separator.

Investigations of this solid matter have shown that due to its surface properties the catalyst used serves as an adsorbent for asphaltenes and carries them out of the reaction zone, thus preventing coking and coke deposits there. We discovered that in this way up to 1% wt of the residual oil fed was discharged along with the catalyst from the process cycle. As electron-microscopical analyses have shown, major part of the catalyst surface is preserved in this process.

Figure 6 compares the X-ray fluorescence analysis of the solid matter isolated from the hot separator sludge with that of powdered coke.

For powdered coke, only the components of lignite ash are indicated. In the electron-microscopical analysis of the solid matter leaving the hot separator, the heavy metals, nickel and vanadium, occur in addition. This is an indication that apart from asphaltenes the liquid-phase catalyst also adsorbs the heavy metal components in the residual oil. Taking-up of the transition metals with hydrocracking activities allows the catalyst to step up its catalytic activity in the liquid phase.

From the catalytic properties of the coke alone, after having been "activated" in the liquid phase and with account taken of the capturing effect on asphaltenes, we can derive the following model representation of the catalyst's mode of action:

- the catalyst on the basis of lignite coke has a hydrocracking effect because of its surface properties and its mineral composition;
- due to the absorption of nickel and vanadium the catalyst on the basis of lignite coke reaches its maximum catalytic activitiy in the liquid phase;
- due to its surface properties the catalyst on the basis of lignite coke acts as an adsorbent on potential coke precursors and carries them out of the reaction zone; thus, it prevents coking and coke deposits there, and

- under the reaction conditions of liquid-phase hydrogenation the catalyst on the basis of lignite coke has a similar fluid-dynamics behaviour to that of the residual oil; it is discharged in an "once-through mode".

6.2 RESULTS OBTAINED WITH DIFFERENT RESIDUAL OILS

The chemical and physical properties of heavy residual oils strongly vary depending on their crude oil origin. Thus, different yields and product qualities are obtained depending on what feedstock is used in liquid-phase hydrogenation of heavy residual oils. Against this background, we conducted an investigation with the object of determining yields and product qualities for a variety of residual oils with most different chemical compositions and, in addition, defining optimum reaction conditions and operating modes in the process development unit.

Figure 7 classifies the different residual oils by their heavy metal contents and the prevailing type of hydrocarbons they contain.

Of the crude oil types classified in Figure 7, we investigated vacuum and visbreaking residues in the process development unit. In doing so, we focussed our activities on the investigation of asphaltene-rich residues since these matters would chiefly be processed in an industrial-scale plant.

The results we obtained in this extensive investigation can be summarized as follows:

- depending on the residual oil used the conversion rates obtained ranged between 70% and 95%;
- under optimized reaction conditions, the oil yields were between 60 and 85% wt; the residue decreased to amounts between 5 and 23% wt; depending on the feedstock, the yield of hydrocarbon gases was 5 to 15% wt;
- under the same reaction conditions, vacuum residues produced higher oil yields than corresponding visbreaking residues; since it was possible to convert visbreaking residues under more severe reaction conditions than vacuum residues, we obtained comparable yield distributions from both products;
- residual oils rich in asphaltene and heavy metals showed a smaller tendency towards coking in the reactors than naphthene- and paraffin-rich residual oils with lower heavy metal contents.

7 COPROCESSING RESULTS

Within the scope of the coprocessing investigations, it was examined whether mixtures of dry lignite and residual oils can be processed under liquid-phase conditions as well.

The tests in the process development unit demonstrated the technical feasibility of coprocessing; in this case, approx. 30% of the vacuum residue was replaced by dry lignite; but almost the same yield distribution was obtained.

Under optimal conditions, coprocessing yielded conversion rates of about 90%. In the temperature range under study and with different reactor throughputs, we obtained oil yields of approx. 80% wt and portions of hydrogenation residue and hydrocarbon gases amounting to approx. 10% each.

In addition it was found that in the case of coprocessing and, in particular, with small reactor throughputs the absolute values of oil yields obtained from the mixture were higher than the comparative amounts in residual oil hydrogenation. It is an unexpected result since with approx. 48% wt the oil yields in conventional lignite liquefaction are much lower than those obtained in residual oil conversion. So, if the oil yields from coprocessing were calculated theoretically, the resulting values would be always lower than those in residual oil hydrogenation. This result is shown in Figure 8.

The bar graph shows yields which were obtained under equal reaction conditions in residual oil hydrogenation, coprocessing and lignite liquefaction.
In the case of coprocessing, we specified not only the figure of the yield distribution determined experimentally in the process development unit, but also the result obtained theoretically.

Figure 8 shows that under the given reaction conditions the oil yield of coprocessing determined experimentally is not only much higher than suggested by the theoretical calculation on the basis of the result obtained in separate hydrogenation of residual oils and coal; in absolute figures, it is even comparable to the oil yield in residual oil conversion.

Due to the oil yields which in practical operation are higher than expected in theory we obtain a desired reduction in the quantities of hydrogenation residue and gaseous hydrocarbons. Since these gases are unwanted products which are formed by using expensive hydrogen, it can be considered another advantage of coprocessing.
The synergistic behaviour was observed over the entire temperature range and with varying reactor throughputs, and it was verified under all reaction conditions. The synergism was all the more pronounced, the smaller the reactor throughput was.
This effect may be due to the heavy metal contents in the residual oil.
The heavy metals can be expected to have a catalytic effect on lignite liquefaction as well. It is also conceivable that lignite or its ash will catalytically act on residual oil hydrogenation.

In the course of our work on coprocessing we determined not only the yield distribution and the quality of the products; furthermore, we critically examined the operating performance of the plant, especially in respect of coke deposits.
During coprocessing no coke deposits were observed in the reactors. Neither did we detect the formation of calcium carbonate-containing sediments known from lignite liquefaction. Obviously, the residual oil which can carry the solids particles away prevents the formation of deposits in the reaction zone which have always given rise to coking. During the above investigations of lignite liquefaction a similar effect was produced by partial recycling of the hot separator sludge.

As already mentioned, coprocessing compared with coal liquefaction alone has the considerable advantage of making slurry oil cycling superfluous.
In coprocessing, the residual oil acts as slurry oil that, on its part, is converted into lower-boiling products. In the case of lignite liquefaction, the portion of cycle oil amounts to some 1.5 t per tonne of dry lignite fed. As an "inert flow" this portion takes up a major part of the reactor volume which in the case of coprocessing can be utilized for further conversion.

This permits higher specific conversion rates relative to the reaction volume. Therefore, coprocessing is expected to reach its commercial viability earlier than coal liquefaction.

Figure 9 shows in quantitative terms how the reaction volume is utilized for lignite liquefaction, hydrogenation of residual oil and coprocessing. The mass flows specified for feed and oil yield are quantities related to the same reaction volume, and thus specific quantities. Two results are given for coprocessing. On the one hand, it is the yield distribution obtained in the process development unit, and, on the other hand, the result achieved by way of theoretical calculation. The oil yield which in practical operation is higher than expected in theory can be attributed to a synergistic cooperation of the components of lignite and residual oils. For the sake of comparison, Figure 9 shows the data of a "two-liquid-phase mode" obtained in two separate plants of the same size for coal liquefaction and residual oil hydrogenation.

The comparison of the relative specific oil yields shown in Figure 9 illustrates the considerable advantage of coprocessing over coal liquefaction alone. In coprocessing, the specific oil yield determined experimentally is 3.5 times higher than in coal liquefaction. In a theoretical calculation, a value of 3.2 is obtained.

When compared with the "two-liquid-phase mode", coprocessing has some advantages as well. For example, the relative oil yield is 3.2 (theoretical) and 3.5 (practical) as against 2.3 in the case of the "two-liquid-phase mode".

Apart from the advantages of coprocessing mentioned before account must be taken of the fact that the quality of the oils produced is slightly inferior to that from residual oil conversion alone. Depending on the boiling range and conversion rate, the oils still contain oxygen of up to about 2% wt. Due to the oxygen content of lignite and the increased formation of gaseous hydrocarbons during lignite liquefaction it is quite understandable that the chemical H_2 consumption in coprocessing is somewhat higher than for residual oil hydrogenation.

In order to corroborate the findings gained so far the coprocessing tests on a process-development scale will be continued within the scope of a follow-up project financially supported by the Federal Ministry of Research and Technology.

8 OUTLOOK

Hydrogenation of residual oil and coprocessing have the advantage of producing an oil yield in a liquid-phase plant of the same size which is about three times higher than in the case of coal hydrogenation alone. This is due to the fact that cycling of slurry oil is no longer required. Almost the entire feedstock can be processed into usable products.

If we compare plant sizes and process steps required for liquid-phase hydrogenation of residual oils from mineral oil processing and those for mixtures of dry lignite and residual oils with hydrogenation of lignite alone, the result will be as follows:

- processing of mixtures of dry lignite and residual oils calls for additional process stages, viz. slurrying and waste water treatment;
- due to a throughput which is about three times higher in coprocessing than in lignite hydrogenation alone, coprocessing permits the use of downstream conversion steps with comparable dimensions to those required for downstream conversion of residual oils;
- thus, coprocessing will call for lower specific capital expenditure than hydrogenation of lignite alone.

Figure 10 gives a qualitative comparison of the product costs arising in lignite hydrogenation, coprocessing and residual oil hydrogenation as a function of the costs arising for the feedstock.

Figure 10 shows that residual oil hydrogenation will reach the threshold of profitability earlier than coprocessing, while hydrogenation of lignite alone which might become a potentially important market for coal in future, will probably take much longer to reach profitability.

In addition, Figure 10 shows that with the relatively expensive residual oil and the relatively low-priced coal coprocessing will involve lower product costs than residual oil hydrogenation.

This expected graduation in time is reflected in the development programme on hydrogenation of fossil raw materials, which has been pursued by Rheinbraun and Union Kraftstoff. As a first step, a liquid-phase hydrogenation plant is planned for residual oil. In a second step, this plant can be extended to permit coprocessing. Coprocessing will allow important experience to be gained which is necessary to take the subsequent third step towards hydrogenation of lignite alone, without requiring great expenditure on a separate pilot or demonstration phase for lignite liquefaction.

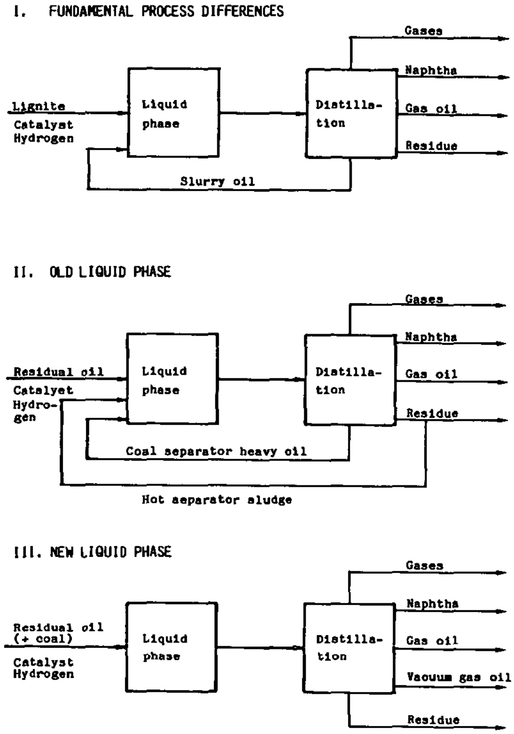

Fig. 1: FUNDAMENTAL PROCESS DIFFERENCES

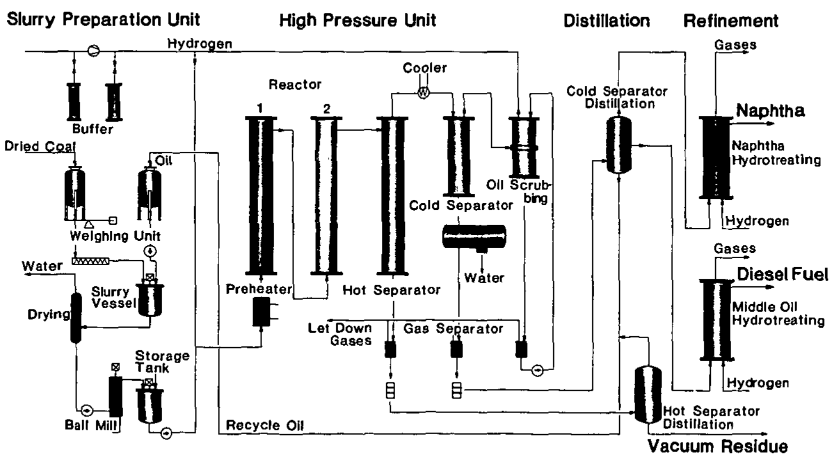

Fig. 2: FLOW SHEET OF THE HVB - TEST PLANT

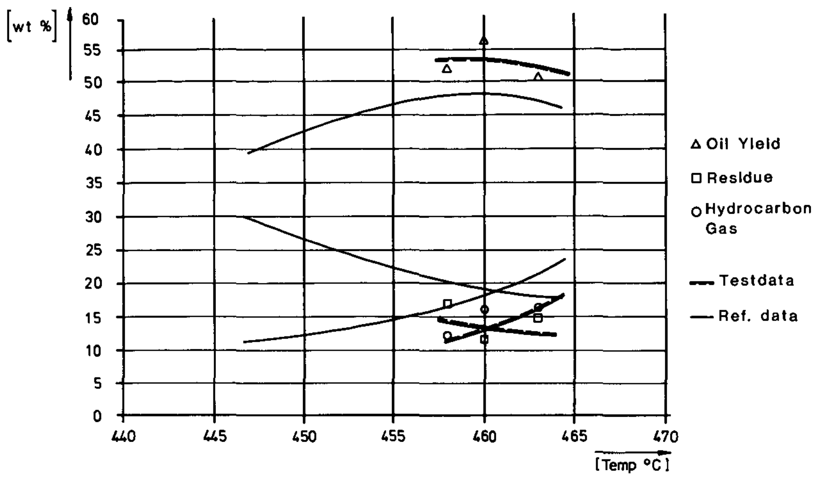

Fig. 3: YIELD AS A FUNCTION OF TEMPERATURE AND GAS INJECTION RATE

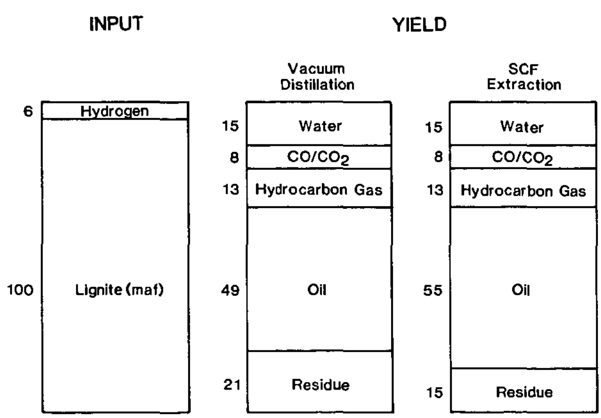

Fig. 4: COMPARISON OF PRODUCTDISTRIBUTION

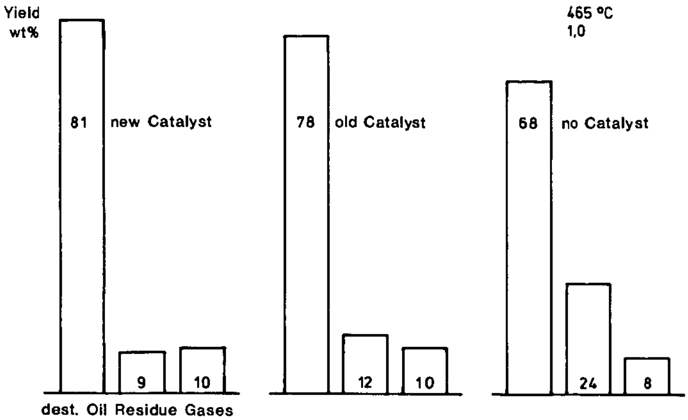

Fig. 5: YIELD STRUCTURE AS A RESULT OF RESIDUAL OIL CONVERSION IN THE PRESENCE OF DIFFERENT CATALYSTS

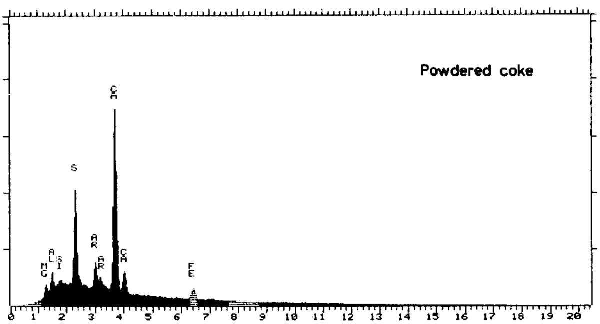

X-ray fluorescence analysis of powdered coke

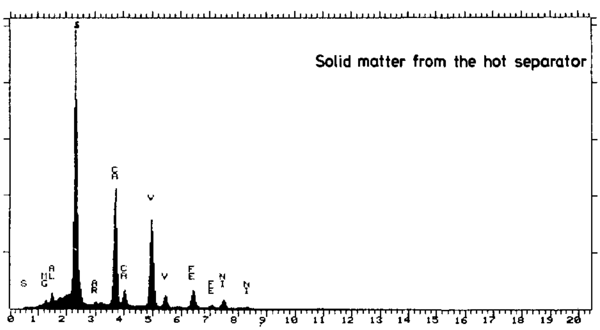

X-ray fluorescence analysis of the solid matter from the hot separator

Fig. 6: X-RAY FLUORESCENCE ANALYSIS

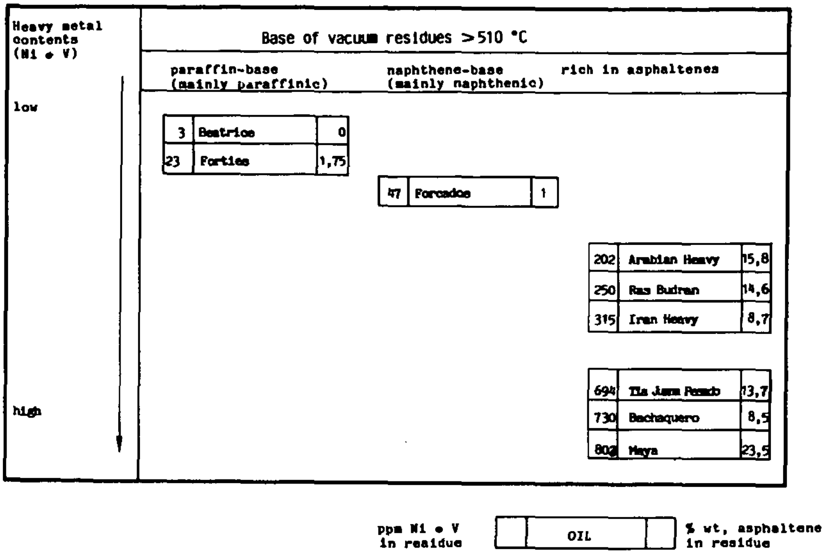

Fig. 7: CHARACTERIZATION OF RESIDUAL OILS

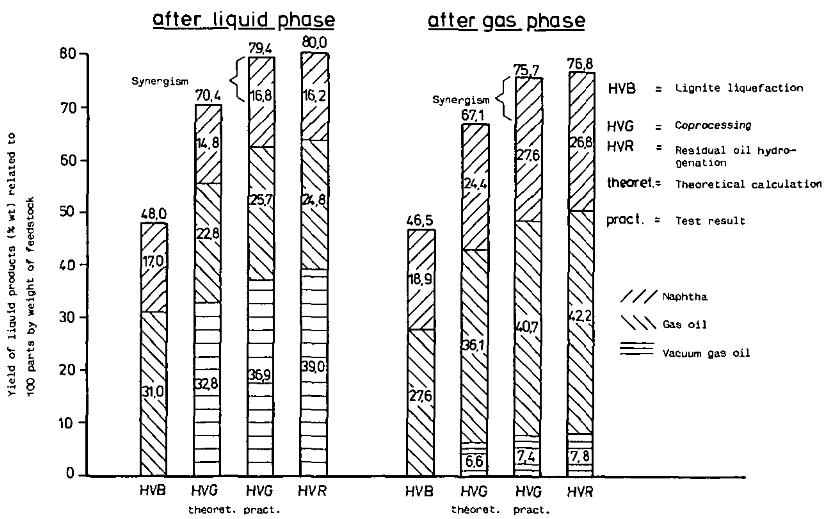

Fig. 8 : OIL YIELDS IN HYDROGENATION OF RESIDUAL OILS , LIGNITE AND MIXTURES OF BOTH

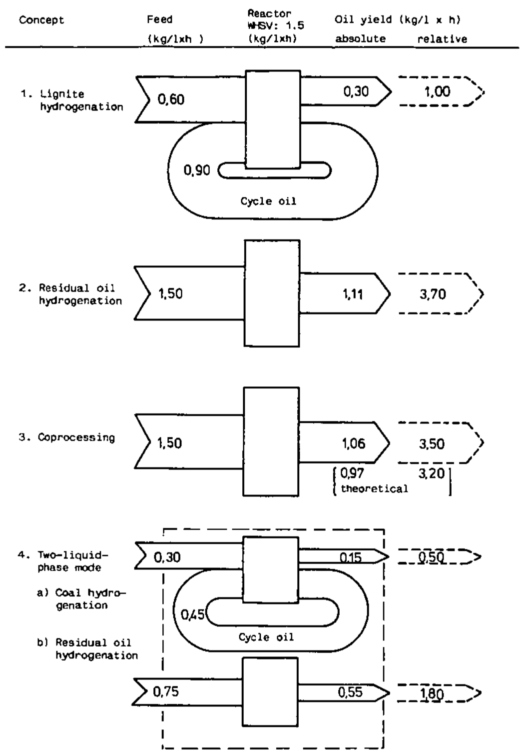

Fig. 9 : PROCESS CONCEPTS

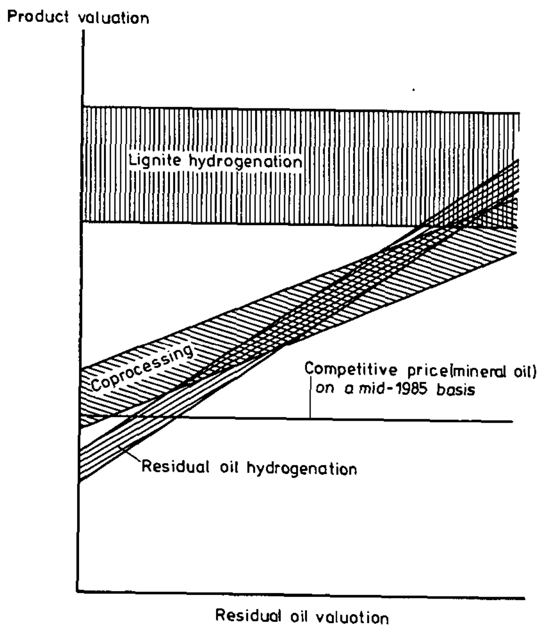

Fig. 10 : PRODUCT COSTS AS A FUNKTION OF FEEDSTOCK COSTS (QUALITATIVE)

THE NEW COPROCESSING PILOT PLANT AT
CANMET'S ENERGY RESEARCH LABORATORIES

J.D. Chase and D.D.S. Liu

Energy Research Laboratory, CANMET
c/o 555 Booth St.
Ottawa, Canada K1A 0G1

I. INTRODUCTION

Canada's large deposits of heavy oil and coal and their proximity warrants the development of coprocessing technology. Coprocessing involves treating a slurry of coal in heavy oil, bitumen or resid with high pressure hydrogen with or without other reducing gas between 400°C and 500°C. Under these conditions coal liquefies and the coal-derived liquids together with the heavy oil hydrocrack to lighter materials.

The advantages of coprocessing over coal liquefaction have been known for some time and and bench-scale research in coprocessing has been underway at CANMET since about 1980. (1,2,3). The bench-scale experiments have indicated a considerable economic potential for the simultaneous processing of coal and bitumen. To develop this process to a stage where it can be evaluated with confidence for further scale-up to demonstration size, the construction of a half-tonne per day pilot plant was initiated.

Whereas the bench-scale facilities are being used to investigate the effect of the process variables on the product yields and quality in short experimental runs, the large pilot plant will be used to solve problems that normally result from long experimental runs lasting up to 60 days. Further, the pilot plant will be able to generate more accurately yield data that is not normally possible with smaller bench scale units, and will enable the production of the much larger quantities of products needed for the detailed assessments required for commercialization.

This paper describes the coprocessing pilot plant which is now being commissioned at CANMET's Energy Research Laboratories.

II. PROCESS DESCRIPTION

(a) Design Basis

- Nominal space velocity of 1.0 reactor volumes/h (1.0 LHSV)
- Feed slurry concentrations of coal from 5 to 50 wt %
- Hydrogen recycle rate of 200 L/h at 15°C (13.9 MPa)
- Pressure capability to 21 MPa (≈3000 psi)
- Reactor temperature to 500°C.

(b) Description of Flow Diagram

The coal from producers will be ground and dried in a new coal preparation unit. This facility handles coal up to 0.63 cm (1/4 in.) in size and up to 60% moisture to produce up to 227 kg/h of dry coal (maximum 10% moisture) at a maximum particle size of 74 ^{e}m (-200 mesh). The dried coal is put in 45 gallon drums with plastic liners and sealed to exclude moisture. The ground coal is then mixed with heated heavy oil in tanks. After mixing with the recycled gas stream containing the the desired concentration of hydrogen, the hot feed slurry is pumped through a preheating section into the reactor which will be maintained at the desired reaction temperature by electrical heaters (Fig.1). The temperature profile in the reactor is measured and controlled by external heaters. Provision has been made for introduction of other process monitors such as pressure transducers and densitometers.

The effluent from the reactor is fed to a high temperature high pressure separator from which a heavy oil product (containing any undissolved coal) is withdrawn. The overhead are then fed to a low temperature-high pressure separator from which a light oil is collected. The gas is then fed to the scrubbing section which removes gaseous hydrocarbons, as well as gaseous nitrogen and sulphur compounds. This scrubbed H_2 stream is then recycled after addition of fresh make-up hydrogen to the recycle gas and then mixed with slurry entering the preheater. Off-gas streams from the product let-down systems will be measured and analyzed.

The feed and the two liquid product streams are weighed continuously, then samples of the product are distilled and analyzed. Considering the flowrates used and the accuracy in measurement, a good mass balance can be expected.

III. PILOT PLANT - ASSEMBLY OF SUB-SYSTEMS

(a) Slurry Preparation Section

The slurry preparation system consists of two tanks, two slurry recirculation pumps and two recirculation loops 4 and 50 m long respectively. The internal pipe size in these loops is 3.81 cm. Since the slurry viscosity is very dependent on temperature, the piping and tanks are equipped with heaters. The length of the larger loop was determined according to the location of the slurry preparation area, i.e., some distance from the main processing area. The high pressure reciprocating feed pump in the process area is fed by part of the recirculating slurry at one end of the large loop. The shorter loop is used for circulating slurry in the other tank when it is not in use, or when the slurry is being prepared from coal and heavy oil. Figure 2 shows a photograph of the slurry area.

Sizing of lines and the power required for recirculating the slurry were estimated for the linear velocity required to prevent settling of coal particles based on Spell's equation (4). The system was designed so that either recirculation pump could be used with either tank in the event of failure during operation. This flexibility along with other characteristics of the long loop make it ideal for the study of mixing phenomena, or in the absence of other data, a means for determining slurry viscosity from known flow and pressure drops.

During slurry preparation, the coal and heavy oil contacting will be done by: (a) an agitator within the tank, (b) recycle flows through the 4 m loop or (c) the use of an eductor within the short loop.

In the coal liquefaction literature interesting rheological behaviour is described where the temperature - viscosity relationship indicates the presence of a gel at certain temperatures (5). Since similar rheological characteristics may be encountered with coal/heavy oil slurries the preheater section has numerous temperature and pressure sensors for monitoring the rheology and flow control (6).

(b) Reactors

The pilot plant has two tubular reactors. One has a 18-L capacity, is 7.62 cm in diameter and is 3.937 m long. The other has a 10-L capacity, is 5.08 cm in diameter and is 4.876 m long. Also there is a 10-L continuous stirred tank reactor (CSTR).

The reactors and separators were designed to accommodate instruments for studying fluid dynamics and for changing reactor geometry. Reactor configuration can be altered to study residence time distributions under various conditions.

The maximum L/D ratio for the tubular reactors is 96. The ratio can be reduced by using one of many holes in the wall as the outlet. The reactors can be connected in various ways for different experiments including multi-step processes. Combinations of CSTR and tubular reactors with various L/D ratios will enable the study of the effect of the degree of mixing on the coprocessing reaction for a wide range of Peclet numbers. Such data are often required to develop or verify scale-up models (7).

The hydrodynamic phenomena of slurry bubble columns at high temperatures and pressures are not well understood. Consequently our experience derived from the use of gamma-ray interrogation techniques during CANMET's development of hydrocracking processes will be applied to coprocessing (8). Figure 3 shows the gamma-ray scanner which will be modified slightly for this new system.

The many thermocouples and sampling systems in the three reactors have resulted in complex instrumentation. This complexity is illustrated in the piping and instrument diagram shown in Fig. 4. The sampling system involves metering control valves and this is seen in the photograph in Figure 5.

(c) Product Separation

It is necessary to separate the products in the reactor effluent. The design of the hot and cold separators was based on experience obtained from hydrocracking of vacuum tower bottoms or bitumen. Although no difficulty is anticipated in the discharge of undissolved coal solids, the efficient removal of solids from reactor effluent is likely to warrant further study. Extra vessels or solids separation equipment can easily be connected to the bottom of the high temperature separator.

The gases from the cold separator initially will be scrubbed by a water and oil scrubber. These scrubbers were designed for investigation of mass transfer. Effective gas clean-up will be required if coprocessing plants are built. Eventually absorbant liquids other than water and oil will be studied.

(d) Gamma-Ray Densitometer

Techniques have been successfully developed for the study of hydrodynamic phenomena in hydrocracking reactors using gamma-ray densitometry. The techniques measure the spatial and temporal void fractions, flow regimes, and bubble size distributions in the reactor (6). These techniques which were developed in our laboratories, contribute to the development, scale-up and successful operation of a large scale Canadian hydrocracking process. The application of gamma-ray densitometry in solid sedimentation is being developed. All of these techniques will be incorporated in the new coprocessing pilot plant. The dotted vertical line in Fig. 4 represents the track for the gamma-ray densitometer.

IV. COMPUTERIZED PROCESS MONITORING SYSTEM

The plan is to have the pilot plant controlled by dedicated controllers. All plant data are collected and stored by a computerized data acquisition and process monitoring system. Field sensors such as thermocouples and pressure gauges are wired to remote processing units (RPU) which perform analogue to digital conversion and translate the sensor output to engineering units. The signals from the RPU are then sent to a plant computer which can display data in various formats including mimics, historical trends and alarm indication. All points are scanned every 10 seconds on average. The plant computer sends all data every minute to the central computer that keeps all the information on a hard disk. Minute and hourly averages are stored for up to 60 days and written every hour to tape. The data stored by the central computer can be recalled for trends, plots and reports. The central system handles data from three separate pilot plants. As a precaution, 60 of the most important points are also recorded on multichannel strip chart recorders. Those points recorded by the computer are shown in Fig. 4 by a circle within a square.

V. REFERENCES

1. Kelly, J.F., Fouda, S.A., Rahimi, P. and Ikura, M. "CANMET Coprocessing: A Status Report", in Proc. of Coal Conversion Contractors Review Meeting, Nov. 14-16, 1984, Calgary, Canada, Editor J.F. Kelly, CANMET, Energy, Mines and Resources, pp. 397-423 (1984).

2. Fouda, S.A., Ikura, M. and Kelly, J.F. "Coprocessing of Canadian Lignites and Bitumen"; Division Report 84-44(OPJ); Preprints of the Spring National Meeting of the A.I.Ch.E., March 24-28, 1985, Houston, Texas.

3. Rahimi, P.M., Fouda, S.A., and Kelly, J.F. "Coprocessing using H_2S as a Promoter", Fuel, Vol. 66, Sept. 1987, 1215.

4. Spells, K.E. Trans. Inst. Chem. Engrs. (London) Vol. 33, No. 2, pp. 79-82, 1955.

5. Thurgood, J.R., Hanks, R.W. and Youngblood, E.L. "The Rheologiocal Characterization of Coal Liquefaction Preheater Slurries", A.I.Ch.E. J., Vol. 28, No. 1, Jan. 1982, p. 111.

6. Liu, D.D.S., Hall, S.S. and Patmore, D.J. "Pulsing Flow through Small Tubes and Orifices: Simulation of Pressure Drop in Hydrocracking Pilot Plant", Submitted to the 38th CSChE. Conference at Edmonton, Alberta, Oct. 2-5, 1988.

7. Levenspiel, O., "Chemical Reaction Engineering", Second Edition Chapter 9, John Wiley and Sons Inc., 1972.

8. Liu, D.D.S., Patmore, D.J., and Lipsett, J.J. "Hydrodynamic Behaviour of Gas-Liquid Two-Phase Flows at Elevated Temperature and Pressures", Proceedings of the 35th Canadian Chemical Engineering Conference at Calgary, Alberta, Oct. 6-9, 1985, p.43.

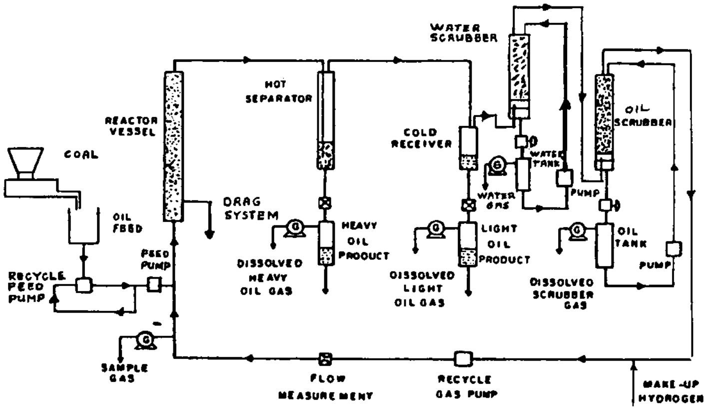

FIGURE 1. SCHEMATIC FLOW SHEET OF COPROCESSING PILOT PLANT

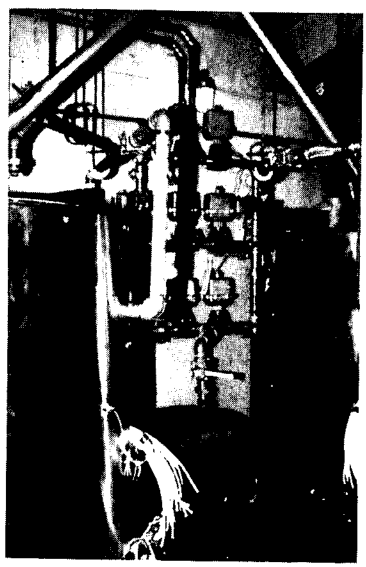

FIGURE 2. PHOTOGRAPH OF SLURRY PREPARATION AREA

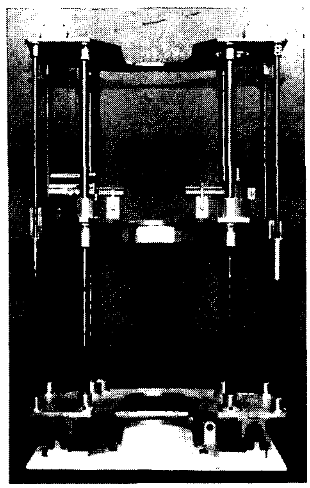

FIGURE 3. GAMMA-RAY SCANNER

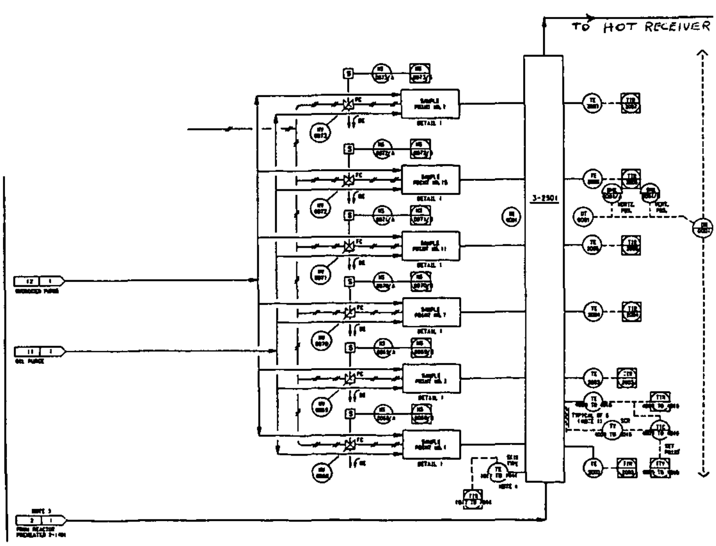

FIGURE 4. PARTIAL P&ID OF TUBULAR REACTOR

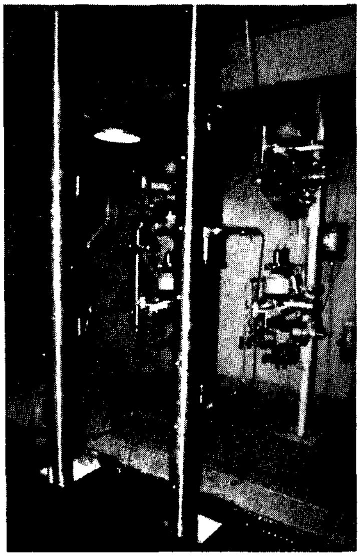

FIGURE 5. PHOTOGRAPH OF TUBULAR REACTOR

BENEFICIATION OF LIGNITE BY OIL AGGLOMERATION AS AN INTEGRAL PART OF COPROCESSING

Michio Ikura[1)] James F. Kelly[1)] and C. Edward Capes[2)]

1) Energy Research Laboratories, CANMET, Energy, Mines and Resources Canada. 555 Booth St., Ottawa, Ontario K1A 0G1

2) Chemical Engineering Section, Division of Chemistry, National Research Council, Montreal Rd., Ottawa, Ontario K1A 0R9

Abstract
The low cost of Canadian low-rank coals makes them prime feedstocks for coprocessing with bitumens and heavy oils. Depending on the coal concentration in the feed slurry, the high ash level in some of these coals can cause operational problems as well as reduce the overall process efficiency and the net liquid product yield. To reduce the ash content in the feed slurry, oil agglomeration can be used for coal beneficiation (deashing) as an integral part of coprocessing technology. However, an optimum integrated approach requires the use of undiluted bitumen or heavy oil feedstocks as a bridging liquid. Also, low-rank coals as well as oxidized higher rank coals often possess a relatively hydrophilic surface. This makes the application of oil agglomeration extremely difficult.

A novel method of beneficiating low-rank coals for coprocessing by oil agglomeration using a part of the feed bitumen for coprocessing has been conceived and developed. This method overcomes the hydrophilic surface problem of low-rank coals and allows the use of undiluted coprocessing feed oils as viscous as vacuum bottoms.

Experimental results on the beneficiation of a Canadian lignite with vacuum bottoms are presented. The efficiency of the process was evaluated in terms of combustibles recovery and ash rejection. The agglomeration of Willowbunch lignite (ash content from 20 to 22 wt % on a mf basis) with Interprovincial Pipe Line (IPPL conventional crude) vacuum bottoms resulted in 51 to 97 wt % combustibles recovery and a corresponding 77 to 42 wt % ash rejection. The effects of vacuum bottoms concentration, operating temperature, and processing time on the beneficiation performance are discussed.

Introduction
Low-rank coals that are often recovered by surface mining are inexpensive and good feedstocks for coal-oil coprocessing. Unfortunately, Canadian low-rank coals are often characterized by their high ash content. For instance, the ash content of Canadian lignites is between 15 and 30%. Most of the low-rank coal deposits in the USA, Australia and other countries also have high ash contents. When such a coal is subjected to coprocessing with heavy oil or bitumen, the high ash content can reduce the net liquid product yields and the overall efficiency of the plant. Also, the handling of process residues with high solids contents may cause operational problems.

An effective route to overcome the high ash problem in the feed coal is coal beneficiation, i.e., deashing of the coal to a certain degree prior to coprocessing. The choice of an appropriate beneficiation process depends on coal rank, composition, surface properties, dissemination of mineral matter, and the end use of the cleaned coal.

Coal beneficiation based on gravity separation of carbonaceous and mineral particles is the most widely used commercial method. However, the efficiency of this technique depends on coal washability, i.e., percentage of mineral matter which can be separated by gravity from various size fractions of coal. For low-rank coals in which mineral particles are often found in a very fine state, beneficiation based on gravity separation may be ineffective.

Selective oil agglomeration, alone or in combination with other methods, may be appropriate for the beneficiation of low rank coals. This technique involves the addition of oil to an aqueous suspension of coal and ash particles. The oil preferentially wets the carbonaceous constituents and causes adhesion of the coal particles by capillary interfacial forces (1). The carbonaceous constituents are agglomerated by oil and recovered from the suspension whereas the ash remains in suspension and is rejected. The oil agglomeration method is based on differences in the surface properties between organic and inorganic matter, the first usually being hydrophobic and the latter hydrophilic. For successful oil agglomeration of coal, the carbonaceous constituents must be less hydrophilic than the ash. As coals decrease in rank from bituminous to subbituminous and to lignite their surface properties become more hydrophilic. This is the major reason that oil agglomeration becomes more difficult for low rank coals (1-3).

The application of selective oil agglomeration to fine coal beneficiation may be especially advantageous if it can be used as an integral part of coprocessing. In coprocessing, coal is ground and mixed with heavy oil to prepare the feed slurry. Normally the feed slurry contains oil and coal at approximately a 2 to 1 ratio. Thus a portion of the heavy oil or bitumen for coprocessing could be utilized for the selective oil agglomeration beneficiation of the feed coal prior to the preparation of the feed slurry (Figure 1). Clean coal particles in the form of agglomerates would then be sent to coal-oil slurry preparation. This integrated process configuration does not result in any additional cost for coal grinding and bridging oil. Also, the overall efficiency and economics of coprocessing will improve by reducing the need for dilution of high ash content residues to permit easier downstream handling.

This paper presents experimental results on a method for lignite beneficiation using vacuum bottoms only as an agglomerating oil. It was shown that at elevated temperatures the vacuum bottoms performed well as a bridging liquid and a hard-to-agglomerate lignite was successfully agglomerated and beneficiated.

EXPERIMENTAL

All beneficiation experiments were carried out using Willowbunch lignite ground to less than 208 um (less than 65 Tyler mesh size). A nominal 500 mL of an aqueous solution containing coal surface conditioner and surfactant was prepared to make approximately a 10% coal suspension. The coal suspension was heated in a closed high pressure mixer to a predetermined temperature and a measured quantity of melted vacuum bottoms was injected into the aqueous solution. High shear mixing (4800-5000 rpm) for 5-20 min was used to create microagglomerates followed by low shear mixing (2000-2300 rpm) for 4-10 min to allow for agglomerates growth. Upon completion of an experiment, the vessel contents were discharged into a vessel filled with water at atmospheric pressure. The agglomerates were then separated over a 100 mesh sieve while the tailings were collected in a dish under the sieve. Residues in the vessel were collected by rinsing with water, then Varsol.

Moisture and ash analyses of lignite samples were carried out prior to oil agglomeration tests in accordance with ASTM procedures. Moisture, ash and oil analyses of agglomerates and tailings were performed at the completion of each run. For the determination of the moisture content of agglomerates, a 2-3 g sample of air-dried agglomerates was weighed, then dried in an oven at 107±3 ^{o}C to a constant weight. For the determination of the ash content of agglomerates, a 2-3 g sample of air-dried agglomerates was weighed, then heated in a closed crucible in a furnace to 750^{o}C and kept at this temperature until no further weight change was recorded.

To determine the ash content of agglomerated lignite on a moisture-oil-free basis, the oil had to be removed from the agglomerates prior to ashing. Since bitumens used for agglomeration of the lignite have high boiling temperatures, they were removed by solvent extraction using toluene. A 3-4 g sample of dried agglomerates was placed in a predried Soxhlet extractor thimble. Upon completion of the extraction, the thimble was dried in a vacuum oven at 90^{o}C to remove any toluene residues. The moisture-oil free lignite sample was then weighed and ashed.

Ash rejection and combustibles recovery were calculated as follows:

$$\text{Ash rejection (wt \%)} = B/(A+B+C) \times 100 \qquad 1)$$

where A, B, and C denote ash in agglomerates, in tailings, and in residues in the agglomeration vessel respectively (all on a moisture-oil-free basis).

$$\text{Combustibles recovery (wt \%)} = (E+F)/(D+E+F) \times 100 \qquad 2)$$

where D, E, and F denote combustibles in tailings, in agglomerates, and in residues in the agglomeration vessel respectively (all on a moisture-ash-free basis).

Tables 1 and 2 give typical ultimate and proximate analyses of Willowbunch (Saskatchewan) lignite and the properties of IPPL vacuum bottoms respectively.

RESULTS AND DISCUSSION

Figure 2 summarizes the effect of vacuum bottoms concentration on the ash rejection and combustibles recovery. The vacuum bottoms concentration was varied from 20 to 64% based on moisture free lignite. When small amounts of vacuum bottoms are used, little agglomeration occurs and the largest part of the ash remains in the tailings. The results in Figure 2 were obtained at 150°C in high and low shear mixing stages. The duration of the high shear mixing was kept at 20 min and that for the low shear mixing was varied between 4 and 10 min.

As the vacuum bottoms concentration is increased from 20 to 40%, combustibles recovery increases from 50 to 93%. However, further increase in vacuum bottoms concentration shows no significant enhancement in combustibles recovery. Ash rejection decreases monotonously with increasing vacuum bottoms concentration.

These results can be explained as follows: When the amount of vacuum bottoms is insufficient for the effective agglomeration of lignite particles in the suspension, the agglomeration is simply incomplete and a large fraction of the lignite particles passes through the 100 mesh sieve with the tailings suspension. As the vacuum bottoms concentration is raised, more vacuum bottoms droplets become available for collision and eventual agglomeration of lignite particles; thus the combustibles recovery further increases. However, at higher combustibles recovery, ash rejection is reduced since there is ash associated with incremental lignite recovery. In addition, an excessive amount of vacuum bottoms in the aqueous suspension results in the formation of emulsion-like agglomerates which contained most of the lignite particles bridged together, as well as a substantial amount of entrapped ash particles. As a result, combustibles recovery is marginally higher but there is an attendant decline in ash rejection.

Figure 3 shows the effect of operating temperature at 40% vacuum bottoms concentration. At 130°C and 140°C, the combustibles recovery was as high as 97.6 to 98.1% at an ash rejection of between 52.5 and 53.1%. The tailings and washings had a clear appearance with very light colored ash settling at the bottom of the tailings collection pan. When the temperature was increased to between 150-160°C, the combustibles recovery slightly decreased to between 94.0 and 95.7% whereas the ash rejection remained essentially constant. This may be explained by the increased viscosity of vacuum bottoms droplets in the suspension. The vacuum bottoms are more viscous at the lower temperature, and when the vacuum bottoms droplets collide, they tend to aggregate resulting in higher combustibles recovery. Because the concentration of suspension is in the order of 10 to 15%, the overall viscosity of the suspension will not change appreciably by the increased vacuum bottoms viscosity. Therefore, it is more advantageous to operate with a vessel temperature as low as practical to promote high combustibles recovery without sacrificing ash rejection. It should be noted, however, that when the temperature of the vacuum bottoms is too low, it becomes impossible to create the fine oil droplets that are needed for oil agglomeration.

Figure 4 shows the effect of processing time used for the high shear mixing. This series of runs was conducted at 150°C and 40% vacuum bottoms concentration. It is seen that high shear mixing for 5-7 min achieved high combustibles recovery and sufficient ash rejection. A further increase of high shear mixing time resulted in a slight decrease of combustibles recovery. This may reflect the fact that some of the microagglomerates were destroyed during prolonged high shear mixing. It was observed that after 3 to 5 min of high shear mixing, the vessel contents had gradually changed from black to gray and then to white. After 7 to 9 min of high shear mixing, a darkening of the vessel contents was observed. Also the appearance of the tailings obtained after 7 min of high shear mixing was clear with mostly white ash settled to the bottom of the tailings collection pan whereas a darkening of the settled particles was observed for the prolonged runs at 9 to 20 min. At 300 min of high shear mixing the combustibles recovery was down to 49.4% and ash rejection increased to 66% indicating unsatisfactory agglomeration. It can therefore be concluded that the present process requires only a very short processing time, and an excessively long mixing time has detrimental effects on the overall agglomeration performance.

CONCLUSIONS

An oil agglomeration technique using vacuum bottoms only as a bridging liquid was developed for low-rank coal beneficiation. It was shown that at elevated temperatures the vacuum bottoms performed well as a bridging liquid and a hard-to-agglomerate lignite was successfully agglomerated and beneficiated. In this work a processing time of 5 to 10 min was sufficient to achieve greater than 90% combustibles recovery and more than 55% ash rejection. The present process is ideally suited for ash reduction in coprocessing feed because it can use a part of the coprocessing feed oil for agglomeration before preparation of the slurry feed to the reactor.

REFERENCES

1) Capes, C.E. and Germain, R.J.; "Selective Oil Agglomeration in Fine Coal Beneficiation", in the "Physical Cleaning of Coal", Editor Liu, Y.A., Marcel Dekker Inc., pp 293-351, 1982.

2) Pawlak, W., Turak, A., Janiak, J., Ignasiak, B., Szymocha, K., Ignasiak, T. and Rodkiewicz, C.,; "Agglomeration of Low Rank Alberta Coals with Bridging Liquids Derived from Indigenous Bitumen and Heavy Oil Deposits", Proceedings of the International Conference on Coal Science, pp 525-528, Sydney, Australia, Oct.28-30, 1985.

3) Capes, C.E., Coleman, R.D. and Thayer, W.L.; "Oil Agglomeration for Fine Coal Processing", Proceedings of 4th International Symposium on Agglomeration, Iron and Steel Society, pp 857-866, Toronto, Canada, June 2-5, 1985.

Table 1 **Ultimate and Proximate Analyses of Willowbunch lignite**

Ultimate analysis (wt %)	
Carbon	52.1
Hydrogen	4.0
Sulphur	0.9
Nitrogen	0.5
Ash	21.5
Oxygen (by difference)	21.0
Proximate analysis (wt % mf)	
Volatile	39.6
Fixed carbon	38.5
Ash	21.0
Sulphur	0.9

Table 2 **Properties of IPPL vacuum bottoms**

General		
Minus 525°C fraction (wt %)		0
Plus 525°C fraction (wt %)		100
Aromaticity		30
Toluene insolubles (wt %)		0.92
Viscosity (cSt)	at 100°C	906
	110	514
	130	184
Elemental analysis (wt %)		
Carbon		86.4
Hydrogen		10.4
Nitrogen		0.43
Sulphur		1.71
Oxygen		0.56

Figure 1
Flowsheet: Oil Agglomeration Beneficiation Integrated with Coprocessing

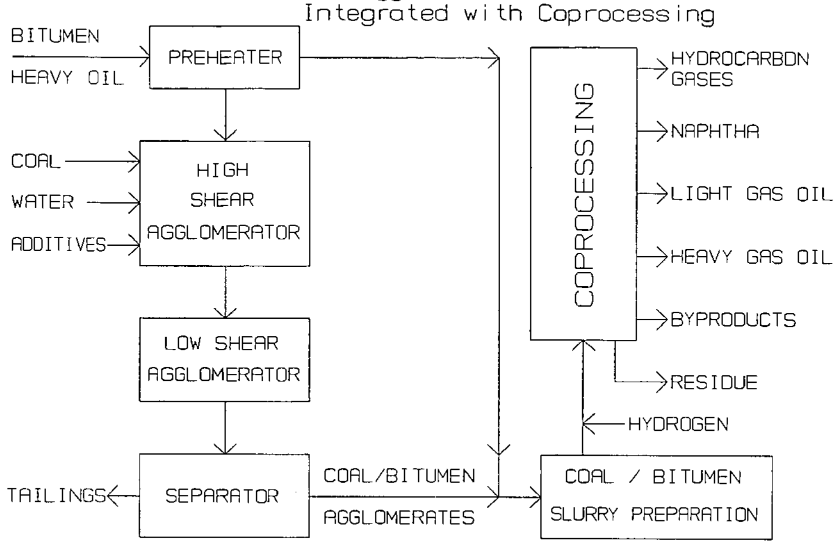

Figure 2
Effect of Vacuum Bottoms Usage

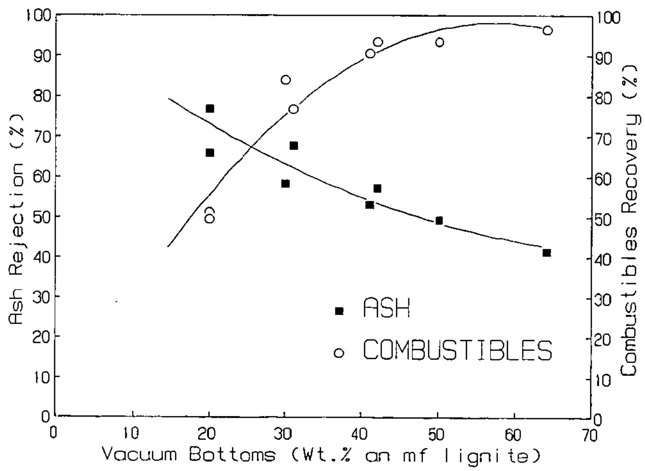

Figure 3
Effect of Operating Temperature

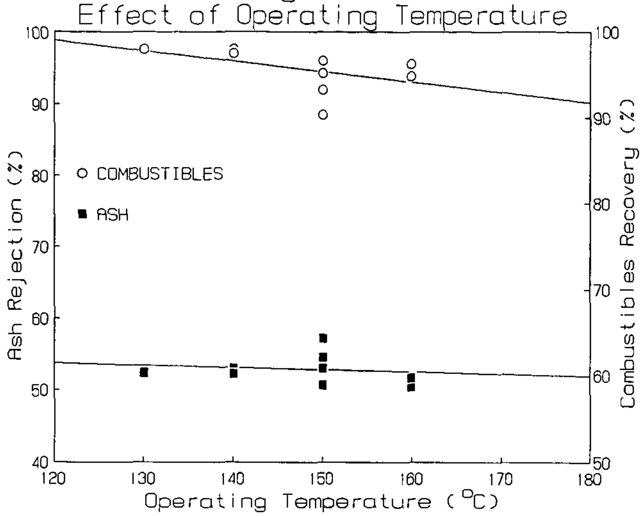

Figure 4
Effect of Processing Time at High Shear Mixing

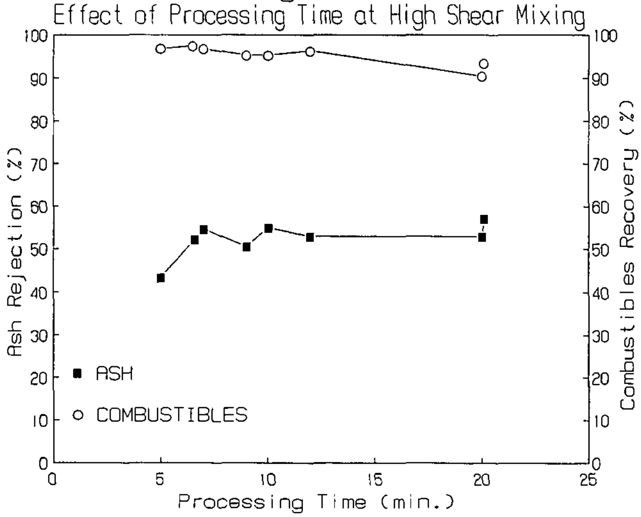

THE CHEMICAL ORIGIN OF SYNERGY IN LIQUEFACTION AND COPROCESSING

Donald F. McMillen, Ripudaman Malhotra,
Doris S. Tse, and S. Esther Nigenda

Department of Chemical Kinetics, Chemical Physics Laboratory
SRI International, Menlo Park CA 94025

INTRODUCTION

The question of possible synergistic effects for coal liquefaction has been raised recently in the context of coprocessing and also in that of straight donor-solvent liquefaction. Synergy is generally defined to occur when the effect of a combination of components exceeds the sum of the effects of the individual components. The existence of such synergism is more difficult to demonstrate in the coprocessing context, because liquefaction of coal alone, that is, in the absence of any other component (e.g., residual oil), is not viable in process terms, and therefore one of the boundary conditions is not available. Synergism can be much more readily assessed in the context of straight liquefaction, where there is always a liquefaction medium, which can be made up of a number of components. This paper specifically addresses liquefaction data, but the conclusions drawn are all equally applicable to coprocessing.

Recently there have been several reports of coal liquefaction illustrating the interactive effect of various components (1-3). We have used these results in conjunction with an improved mechanistic model for coal liquefaction to help shed some light on the chemical origin of such interactive effects. First, it should be noted that the traditional liquefaction mechanism, which ties liquefaction effectiveness to the efficiency with which donor components scavenge fragment radicals formed in the spontaneous thermal scission of the coal structure, cannot easily accommodate interactive effects. On the other hand, such effects would actually be anticipated for mechanisms that are not unimolecular in solvent components, but, in general terms, involve reaction of one component with another to form an intermediate, which then reacts with the coal component. Specifically, we show that the various H-transfer processes that we have hypothesized as leading to bond cleavage by "solvent-mediated hydrogenolysis" clearly fall in the second category of reaction type. As previously discussed by us (4,5), most of these processes require both a hydrogen "donor" species* and an "acceptor" species in order to form the active H-transfer intermediate,

*In the discussion that follows, we use the word "donor" specifically to mean a hydrocarbon, whether aliphatic, alkyl-aromatic, or hydroaromatic, that can contribute a hydrogen atom to a radical or other acceptor. We make this distinction because some of these substances, such as fluorene, are good hydrogen-atom donors in this sense but are <u>not</u> good donor solvents.

a cyclohexdienyl "carrier" radical, which can transfer hydrogen to engender cleavage of even strong bonds.

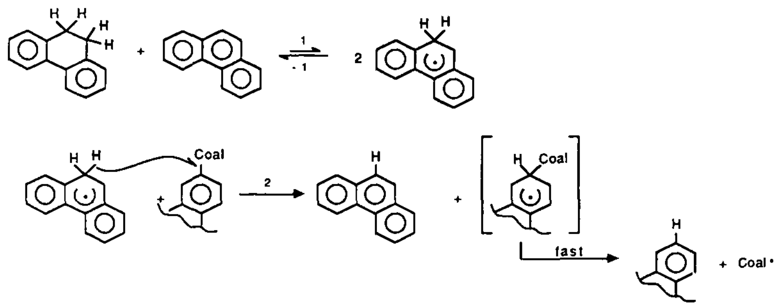

In the following paragraphs, we summarize two of the more recent and more striking examples of synergism. One of these uses only nonhydroaromatic donors and the other hydroaromatic donors. We then discuss, in qualitative terms, how a coal-liquefaction picture that includes strong bond hydrogenolysis mediated by solvent carrier radicals can easily accommodate the liquefaction results. The case involving hydroaromatic solvents is more amenable to mechanistic modeling, and for this case we will compare cleavage rates predicted by the model with the actual liquefaction results. Finally, we extend the mechanistic insight gained in rationalizing the positive interaction among solvent components in coal liquefaction to account for the interactive effects reported for coprocessing.

EXAMPLES OF REPORTED SYNERGY

1. Improvement of Hydroaromatic Solvents by Addition of Non-Donor Aromatic Components

Cassidy and coworkers have very recently published results using a hot-charged, time-sampled autoclave that show substantial increases in oil yield resulting from the replacement of half of the tetralin in the solvent with various aromatics (1). Figure 1 shows the oil yields as a function of time that were obtained when three different PCAH were added to the solvent. Pyrene is clearly the most effective additive, increasing the oil yields by some 30 percentage points at very short as well as longer reaction times. Anthracene and phenanthrene are somewhat less effective, in that order. These changes are remarkable, particularly since the PCAH replaced half of the tetralin, such that the donor content was actually lowered from 50 to 25%! The authors recognized this and evidently took particular pains to assure themselves that the results were reproducible.

These results are parallel to, but more striking than, earlier results of Derbyshire et al., who reported that conversion of an Illinois No. 6 coal (to THF-solubles) in 70% pyrene, 30% tetralin was better than conversion in pure tetralin, at two different hydrogen pressures (2).

2. Aromatic Components Make Accessible Pathways for Bond Cleavage via Solvent-Mediated Hydrogenolysis

The results of Clarke et al. provide a dramatic illustration of the importance of H-acceptor solvent components (3). These workers report that whereas conversion (to quinoline-solubles) of an 84% carbon coal in various perhydro-PCAH was quite poor, it improved slightly when naphthalene was added, and improved quite markedly when PCAH such as phenanthrene or pyrene were added. These results are depicted in Figure 2. The conversion levels achieved with the 3- or 4-ring PCAH (good acceptors) are almost as high as that achieved with octahydropehenanthrene, which is known to be an excellent solvent. The authors also note that only in the presence of the 3- or 4-ring PCAH is there any significant dehydrogenation of the perhydroaromatics. However, in the absence of the PCAH, the perhydroaromatics were observed to undergo cis-trans isomerization, indicating the formation of bridgehead radicals.

RATIONALIZATION IN TERMS OF SOLVENT-MEDIATED HYDROGENOLYSIS

The above results are entirely consistent with (and so far as we know cannot be rationalized without) the mechanistic picture of coal liquefaction that includes solvent-mediated hydrogenolysis of strong bonds by radical hydrogen-transfer (RHT): formation of H-atom "carrier" species from PCAH, followed by H-transfer from these carrier species to ipso- positions on aromatic clusters within the coal structure that bear linkages to other clusters, resulting in hydrogenolysis of these linkages.

Any thermally produced coal radicals can, at a modest rate, abstract aliphatic hydrogens from perhydrophenanthrene or other perhydroaromatics.

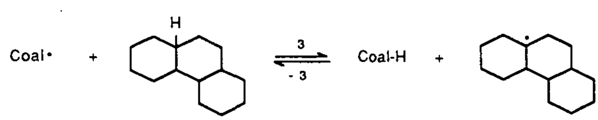

In the absence of any PCAH molecules, which can act as H-acceptors, the cycloalkyl radicals will recapture a hydrogen (reaction -3) or undergo a β-scission of a C-C bond to produce an olefin and a another alkyl radical. β-Scission of a C-H bond leading to free H-atoms, which could engage in further bond cleavages, is estimated to be about 6 orders of magnitude too slow to compete effectively with either of these reactions (6-8). On the other hand, transfer of a hydrogen to a PCAH molecule from the cycloalkyl radicals is comparable to the hydrogen recapture (reaction -3) or the β-scission of a C-C bond.

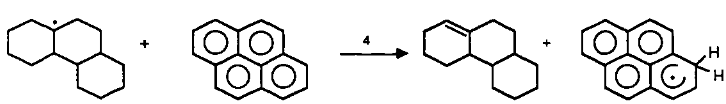

Transfer of a hydrogen to a PCAH molecule produces a cyclic olefin and a cyclohexadienyl radical. These cyclohexadienyl radicals can result in hydrogenolysis of other bonds in the coal structure by RHT (reaction 2). Furthermore, the cyclic olefin has much weakened allylic C-H bonds and the removal of one of these hydrogens ultimately leads to the formation of hydroaromatic structures. Thus, the PCAH molecules can channel the hydrogens available in the perhydroaromatic molecules into useful cleavage reactions.

The above scenario has been borne out more rigorously with the help of a mechanistic numerical model for the case of Cassidy et al. For modeling purposes, we used the cleavage of dinaphthylmethane as a surrogate for those structures in coal that cannot cleave by simple thermolysis under the conditions of reaction, and whose cleavage has to be mediated by the solvent. We modeled the cleavage of dinaphthylmethane with the donor hydroaromatics alone and for cases in which a portion of the hydroaromatic replaced by a non-donor species such as pyrene or anthracene.

Figure 3 shows the computed rates of cleavage resulting from H-transfer (to the ipso position of a naphthalene-X structure) by RHT and free H-additions, as well as the total cleavage rate for a 10:1 dihydrophenanthrene:phenanthrene mixture. Also shown (dark bars) are the rates computed for the case where 10% of the dihydrophenanthrene has been replaced by anthracene. The replacement results in a contribution from a step labeled RHT', that is, H-transfer from the anthracene-derived carrier radical. It also results in a substantial increase in the concentration of, and therefore transfer from, the hydroanthryl radical, and in an increase in the free H-atom contribution, such that the overall increase in cleavage rate is 120%. Examination of the various reactions producing and consuming the hydrophenanthryl radical shows that the increase is mainly due to the rapid formation of AnH·, owing to the very good H-acceptor nature of anthracene. The increased AnH· concentration then results in an increased production of PhenH· through reaction of AnH· with $PhenH_2$. The increase in computed cleavage rate is larger or smaller as the system is poorer or richer, respectively, in "native" acceptor (e.g., phenanthrene). In other words, systems that are "over-hydrogenated," or poorest in acceptors, appear to benefit most from the addition of a good acceptor.

The increased production of PhenH· is in part analogous to the reduction of anthracene by dihydrophenanthrene, which was reported by Billmers and Stein to be catalyzed by the addition of small amounts of dihydroanthracene (9). In both cases a large pool of AnH· radicals produces additional PhenH· by abstraction of H from $PhenH_2$. In the case described by Stein, this pool of AnH· radicals arises because of the very good H-donor quality of the added AnH_2. In the present case, the radical pool increases because of the very good acceptor quality of anthracene itself.

KEY HYDROGEN-TRANSFER REACTIONS IN COPROCESSING

In coprocessing of coals and heavy oils, we have a situation where the heavy oils have a relatively large amount of aliphatic hydrogen that is potentially useful for cleavage of coal structures. We suggest that the PCAH in the coal interact with the aliphatic hydrocarobons in a way very similar to the one we have described the case of coal conversion results in PCAH and perhydro-PCAH reported by Clarke et al. (3), making it possible to utilize the hydrogen from aliphatic compounds. In addition, because petroleum resids contain some amount of polycyclic aromatics (typically as long-chain alkyl aromatics), the benzylic hydrogens on their side chains provide a source of relatively weakly bonded hydrogens that can, along with the coal radicals, serve as initiating sources. Similarly, to the extent that the β-scission breakup of the alkyl chains produces some amount of olefins (even in the presence of H_2), the allylic hydrogens on these olefins will be easily transferred. These aspects of coprocessing chemistry are currently being explored by Bockrath and coworkers using pure hydrocarbons as models for the resids (10). The results of their studies can be expected to provide tests for some of the speculations made here.

SUMMARY

Analysis of synergistic effects of solvent components in coal liquefaction studies indicates that the key chemical features of coprocessing component interaction are:

(1) Coal radicals generate aliphatic radicals from the resid;

(2) The aliphatic radicals can undergo β-scission of C-C bonds to convert the resid, or can transfer a hydrogen to the PCAH to form carrier species capable of engendering hydrogenolysis;

(3) In the presence of gaseous hydrogen, radical abstraction from H_2 adds a propagation step that facilitates the utilization of H_2 for hydrogenolysis.

These reactions allow the hydrogen in the aliphatic resid components, which are known to be poor liquefaction solvent components, to be made available for coal conversion.

Acknowledgment: We gratefully acknowledge the support of the U.S. Department of Energy (PETC), Contract No. DE-FG22-86PC90908.

REFERENCES

1. Cassidy, P. J.; Grint, A.; Jackson, W. R.; Larkins, F. P.; Louey, M. B.; Rash, D.; Watkins, I. D., Proceedings of the 1987 International Conference on Coal Science, Elsevier, 1987, p.223.

2. Derbyshire, F. J.; Varghese, P.; Whitehurst, D. D., Fuel, 1982, 61, 859.

3. Clarke, J. W.; Rantell, T. D.; Snape, C. E., Fuel, 1984, 63, 1476.

4. McMillen, D. F.; Malhotra, R.; Hum, G. P.; Chang, S.-J., Energy and Fuels, 1987, 1, 193.

5. McMillen, D. F.; Malhotra, R.; Chang, S.-J.; Fleming, R. H.; Ogier, W. C.; Nigenda, S. E., Fuel, 1987, 66, xxx.

6. Shaw, R.; Golden, D. M.; Benson, S. W., J. Phys. Chem., 1977, 81, 1716.

7. Kerr, J. A. and Moss, S. J. CRC Handbook of Bimolecular and Termolecular Gas Reactions, Vol. 1, CRC Press, Inc., Boca Raton, Florida, 1981.

8. Benson, S. W., Thermochemical Kinetics, 2nd ed., John wiley and Sons Inc., New York, 1976.

9. Bilmers, R. L.; Griffith, L. L; Stein, S. E., Am. Chem. Soc., Div. Fuel Chem. Prep., 1985, 30(4), 283.

10. Schroeder, K. T.; Bockrath, B. C.; Smith, M. R., "Coprocessing Chemistry," Proceedings of DOE Contractors' Meeting on Direct Liquefaction, Pittsburgh, PA, October 1987, p. 340.

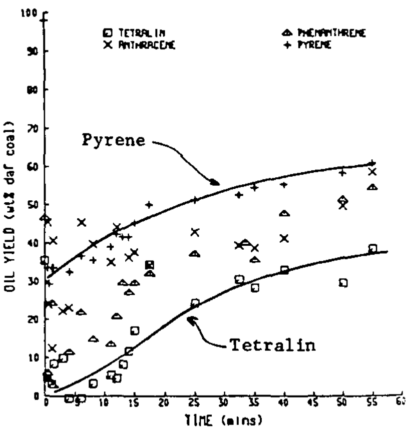

Figure 1: Impact of PCAH addition on liquefaction of Illinois No. 6 coal in tetralin. (Figure from Cassidy et al., Ref. 1)

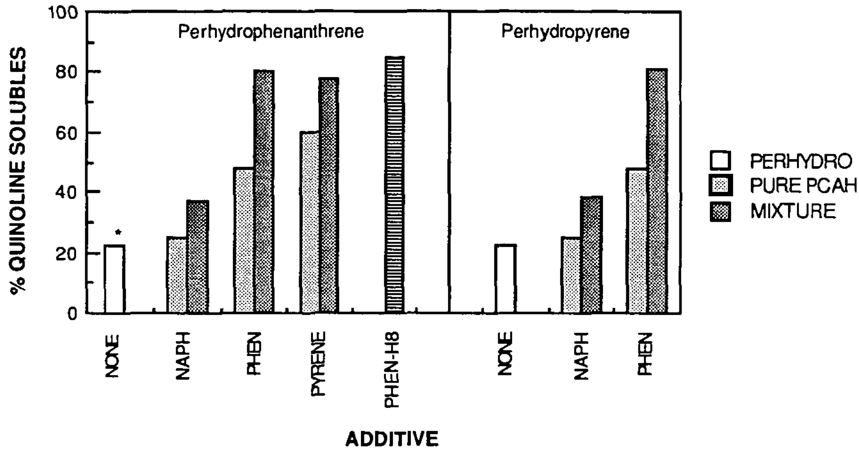

Figure 2. Impact of added PCAH on coal liquefaction in perhydroaromatics. Conversion in 1:1 mixture of perhydroaromatic and aromatic compared with conversion in either pure component. * Upper limit. (Data from Clarke et al., Ref. 3)

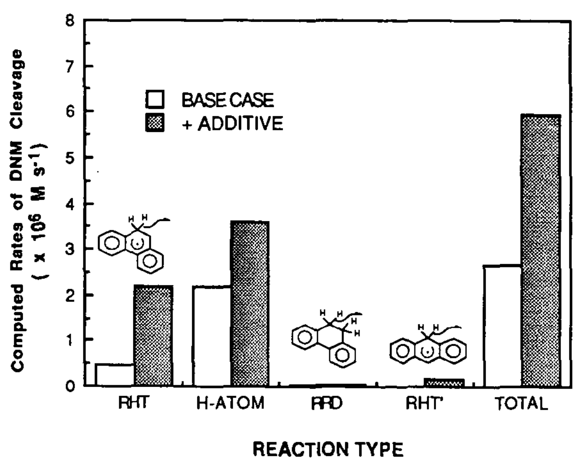

Figure 3: Computed impact of partial replacement of donor with a good acceptor. Base case: $PhenH_2/Phen = 10/1$; additive is 0.3 M anthracene, replacing an equal amount of dihydrophenanthrene.

EVALUATION OF THE INTERACTIVE CHEMISTRY OF COAL-PETROLEUM SYSTEMS USING MODEL AND ACTUAL REACTANTS

Christine W. Curtis and Wook Jin Chung
Chemical Engineering Department
Auburn University, Alabama 36849

The coprocessing of coal with petroleum residuum simultaneously liquefies coal and upgrades petroleum residuum into higher value products. However, coal and petroleum residuum manifest very different chemical properties with coal being more aromatic with a H/C ratio of 0.6 - 0.8 and petroleum residuum more aliphatic with a H/C ratio of 1.4 to 1.6. Although a number of studies have demonstrated the feasibility of coprocessing on the basis of product selectivity and metals reduction (1-8), the interactive chemistry involved between the coal and petroleum materials during coprocessing has not yet been determined.

In this study, the interactive chemistry between coal and petroleum molecules has been examined: first by using model compound types representative of coal and residuum and then by combining the model systems with Illinois No. 6 coal and Maya topped long residuum (TLR). The model systems, composed of naphthalene (NAPH) representing aromatics, 1,4-dimethylcyclohexane (DMC) representing saturated compounds, phenol (PN) representing phenolics, benzothiophene (BZT) representing sulfur compounds, and quinoline (QN) representing nitrogen compounds, were reacted thermally and catalytically using a Shell 324 $NiMo/Al_2O_3$ catalyst. The model systems were reacted individually and then combined together to ascertain the effect of the different components on the thermal and catalytic reactions of the different model systems. Illinois No. 6 coal and Maya TLR were each, respectively, added to the model compound systems and reacted thermally and catalytically.

Experimental

Model Reactions. The model systems, NAPH, DMC, PN, BZT and QN, were reacted as 2 wt% reactant in hexadecane at 350°C with 1250 psi H_2 (cold) for 30 minutes and agitated at 850 rpm. The reactor used was a ~12.3 cc stainless steel vertical tubing bomb with a Nupro fine metering valve for gas introduction. For the catalytic reactions, 0.25 g of presulfided 1/32" Shell 324 $NiMo/Al_2O_3$ extrudates were used. The reaction systems were built in the following manner: NAPH; NAPH and DMC; NAPH, DMC and PN; NAPH, DMC and BZT; and NAPH, DMC and QN. A Varian Model 3700 FID gas chromatograph equipped with a 30 m DB-5 fused silica column was used for analyzing the products from model systems reactions. Para-xylene was used as an internal standard. Product identification was achieved by spiking with authentic compounds and by GC/MS analysis. Gases produced during the reaction were analyzed for hydrogen using a Varian 3700 TCD chromatograph.

Coal and Residuum Reactions. Illinois No. 6 coal (-15 mesh) and Maya TLR were each added individually at 10 wt% to the model compound systems and were reacted under the thermal and catalytic conditions described above. Typical analyses of Illinois No. 6 coal and Maya TLR are detailed elsewhere (5). When residuum was reacted with the model systems, insoluble matter (IM) was produced during the reaction. The IM was recovered by precipitating it from the product mixture by centrifuging and decanting the liquid product mixture. The IM produced during thermal residuum - model systems reactions averaged 8% while that produced during catalytic reactions averaged 5%.

Results and Discussion

In this investigation, each model system produced a number of products from the catalytic reactions. In order to summarize and compare the data, several terms have been defined. These terms are: percent hydrogenation, percent deoxygenation, percent desulfurization, percent denitrogenation, and percent hydrogenolysis. Percent hydrogenation is the number of moles of hydrogen required to produce the observed product distribution from a given reactant as a percentage of the moles of hydrogen required to obtain the most hydrogenated product. Percent deoxygenation is the summation of the mole percents of components not containing oxygen. Percent desulfurization is the summation of the mole percents of the components not containing sulfur. Percent denitrogenation is the summation of the mole percent of the components not containing nitrogen. Percent hydrogenolysis is the mole percents of the components which have undergone cleavage of the carbon-heteroatom bond.

Naphthalene Hydrogenation. NAPH hydrogenation may be represented as a sequential and reversible reaction of NAPH hydrogenating to tetralin followed by hydrogenation to decalin. Thermal reactions of NAPH individually and in combination with other model systems showed no NAPH hydrogenation. Neither the addition of coal nor residuum affected the thermal hydrogenation of NAPH.

Significant hydrogenation of NAPH occurred under catalytic conditions as shown in Table 1. The addition of DMC had no influence on NAPH hydrogenation; however, the addition of the heteroatomic species, PN, BZT, and QN, reduced NAPH hydrogenation with QN giving the most substantial reduction. The addition of Maya TLR and coal to NAPH each produced a substantial reduction in NAPH hydrogenation with residuum being more detrimental than coal under these process conditions. It should be noted that at 350°C not all of the coal was converted to soluble products, thereby reducing its influence on NAPH hydrogenation. Addition of DMC and the heteroatomic species to either the NAPH/Maya TLR or NAPH/coal systems further reduced the hydrogenation of NAPH with the order of influence being QN > BZT > PN > DMC. In terms of being most detrimental to NAPH hydrogenation, the order of model components ranked as QN > BZT > PN > DMC and of coal and residuum ranked as Maya TLR > Coal.

Table 1
Effect of Different Systems on the Catalytic Hydrotreatment of Naphthalene

Systems	Hydrogenation,%
Naphthalene	94.7
Naphthalene/DMC	94.8
Naphthalene/DMC/Phenol	89.0
Naphthalene/DMC/Benzothiophene	75.9
Naphthalene/DMC/Quinoline	32.5
Naphthalene/Coal	57.8
Naphthalene/Resid	39.4
Naphthalene/DMC/Coal	57.0
Naphthalene/DMC/Resid	36.1
Naphthalene/DMC/Phenol/Coal	54.3
Naphthalene/DMC/Phenol/Resid	36.4
Naphthalene/DMC/Benzothiophene/Coal	50.6
Naphthalene/DMC/Benzothiophene/Resid	32.1
Naphthalene/DMC/Quinoline/Coal	17.9
Naphthalene/DMC/Quinoline/Resid	16.3

Phenol Hydrodeoxygenation. PN undergoes deoxygenation to form benzene and further hydrogenation to cyclohexane under hydrogenation conditions. The benzene - cyclohexane reaction is reversible (9). Under thermal conditions, no conversion of phenol was observed. Under catalytic conditions, PN underwent complete hydrogenation and deoxygenation as shown in Table 2. Neither the addition of NAPH and DMC nor coal had any effect on the hydrogenation or deoxygenation of PN. However, the addition of Maya TLR reduced both PN hydrogenation and deoxygenation. The addition of NAPH and DMC to the PN/Maya TLR system moderated the detrimental effect of the residuum.

Table 2
Effect of Different Systems on the
Catalytic Hydrotreatment of Phenol

Systems	Hydrogenation,%	Deoxygenation,%
Phenol	100	100
Phenol/DMC/Naphthalene	100	100
Phenol/Coal	100	100
Phenol/Resid	82.0	82.0
Phenol/DMC/Naphthalene/Coal	100	100
Phenol/DMC/Naphthalene/Resid	88.9	88.9

Benzothiophene Hydrodesulfurization. BZT undergoes hydrogenation to 2,3-dihydrobenzothiophene followed by hydrogenolysis to o-ethylphenol, then hydrogenolysis to ethylbenzene and, finally, hydrogenation to ethylcyclohexane (10). No reaction was observed with BZT under thermal reaction conditions. Under catalytic conditions, two products, ethylbenzene and ethylcyclohexane, were formed in agreement with the literature (9). For the individual BZT catalytic reaction as presented in Table 3, complete desulfurization and ~71% hydrogenation occurred. The addition of the hydrocarbons, NAPH and DMC, as well as coal and Maya TLR reduced the hydrogenation of BZT. In contrast, the residuum only reduced the desulfurization and hydrogenolysis of BZT. The addition of NAPH and DMC to the BZT/Maya TLR system moderated the effect of the residuum by increasing the percent hydrogenation by 3% and both desulfurization and hydrogenolysis to 100%.

Table 3
Effect of Different Systems on the
Catalytic Hydrotreatment of Benzothiophene

Systems	Hydrogenation,%	Desulfurization,%	Hydrogenolysis,%
Benzothiophene	71.2	100	100
Benzothiophene/ DMC/Naphthalene	66.3	100	100
Benzothiophene/ Coal	56.3	100	100
Benzothiophene/ Resid	48.6	96.2	96.2
Benzothiophene/ DMC/Naphthalene/ Coal	55.4	100	100
Benzothiophene/ DMC/Naphthalene/ Resid	51.6	100	100

Quinoline Hydrodenitrogenation. The hydrodenitrogenation of quinoline follows a complicated pathway (11) as shown in Figure 1. In thermal reactions at 350°C, 13% THQ was produced. Neither hydrogenolysis nor denitrogenation was observed. Introduction of NAPH and DMC decreased QN conversion and reduced the amount of THQ produced by half. The addition of coal to the thermal QN reaction blocked conversion of QN to THQ. The addition of NAPH and DMC to the QN/coal system had no effect. The thermal reaction of Maya TLR with QN also prevented any hydrogenation of QN; the addition of NAPH and DMC to the Maya TLR/QN system had no effect.

In the catalytic QN reaction as shown in Table 4, substantial hydrogenation, 79.4%, denitrogenation, 48.9%, and hydrogenolysis, ~50.6%, occurred. The addition of NAPH and DMC to QN increased both denitrogenation, 54.6%, and hydrogenolysis, 56.6%. Both the addition of coal and residuum to QN substantially reduced hydrogenation, denitrogenation and hydrogenolysis. The addition of NAPH and DMC to the QN/coal moderated slightly the effect of coal on denitrogenation and hydrogenolysis. The addition of NAPH and DMC to the QN/resid system increased all three reactions, hydrogenation, denitrogenation and hydrogenolysis, more substantively than the QN/coal system.

Table 4
Effect of Different Systems on the Catalytic Hydrotreatment of Quinoline

Systems	Hydrogenation,%	Denitrogenation,%	Hydrogenolysis,%
Quinoline	79.4	48.9	50.6
Quinoline/DMC/ Naphthalene	79.9	54.6	56.6
Quinoline/Coal	61.0	35.1	39.3
Quinoline/Resid	60.6	34.7	42.5
Quinoline/DMC/ Naphthalene/Coal	61.1	36.6	41.0
Quinoline/DMC/ Naphthalene/Resid	62.8	38.0	47.0

Summary

Thermal hydrogenation reactions at 350°C as performed in this work did not lead to the hydrogenation of any of the model systems except for QN. Combinations of the model systems did not result in thermal chemical reactions among the species except in the case of QN where the addition of hydrocarbons reduced the amount of hydrogenation while coal and residuum totally eliminated it.

In the catalytic reactions, no effect on the hydrogenation of NAPH was observed by the presence of DMC. However, the addition of NAPH and DMC to the reaction systems containing Maya TLR/PN, Maya TLR/BZT, and Maya TLR/QN showed a promoting effect on heteroatom removal (N,S, and O) and hydrogenation of BZT and QN under the catalytic conditions. In the coal system, the addition of NAPH and DMC promoted denitrogenation and hydrogenolysis of QN but did not effect the other reactions. In the QN reaction alone, the promoting effect by the presence of NAPH/DMC on the denitrogenation and hydrogenolysis of QN was observed but the hydrogenation of QN was not affected. The only inhibitor of PN hydrogenation and deoxygenation was Maya TLR whose effect was moderated by the addition of NAPH and DMC. NAPH hydrogenation was inhibited by the addition of all heteroatomic species coal and residuum, with QN and Maya TLR being the most detrimental.

References

1. Monnier, J., "Review of the Coprocessing of Coals and Heavy Oils of Petroleum Oils of Petroleum Origin," Canmet Report 84-5E (March 1984).
2. Moschopedis, S. E., Hawkins, R. W., Fryer, J. F., and Speight, J. G., Fuel, 59, 647 (1980).
3. Moschopedis, S. E., Hawkins, R. W., and Speight, J. G., Fuel Processing Technol., 5, 213 (1982).
4. Rosenthal, J. W., and Dahlberg, A. J., "Two-stage Coal Liquefaction Process with Petroleum-derived Coal Solvents," U.S. Patent No. 4,330, 393 (1982).
5. Curtis, C. W., Pass, M. C., Guin, J. A., and Tsai, K. J., Fuel Scien. and Techno. Intl., 5, 245 (1987).
6. Curtis, C. W., Tsai, K. J., and Guin, J. A., Ind. Eng. Chem. Process Des. Dev., 24, 1259 (1985).
7. Curtis, C. W., Tsai, K. J., and Guin, J. A., Ind. Eng. Chem. Res., 26, 12 (1987).
8. Gatsis, J. G., ACS Fuel Division Preprints, 31, 4, 181 (1986).
9. Weisser, O., and Landa, S., "Sulphide Catalysts, Their Properties and Applications," Pergamon, New York (1973).
10. Patzer, R. R. II, Farrauto, R. J., and Montagna, A. A., Ind. Eng. Chem. Process Des. Dev., 18, 625 (1979); Vogelzang, C. L., Li, G. C., Schuit, A., Gates, B. C., and Petrakis, L. J. Catal., 84, 170 (1983).
11. Satterfield, C. N., and Yang, S. H., Ind. Eng. Chem. Process Des. Dev., 23, 11 (1984).

Acknowledgements

The authors gratefully acknowledge the support of this work by the Department of Energy under Grant No. DEFG-2285PC80502.

Figure 1. Reaction Pathway for Quinoline Hydronitrogenation

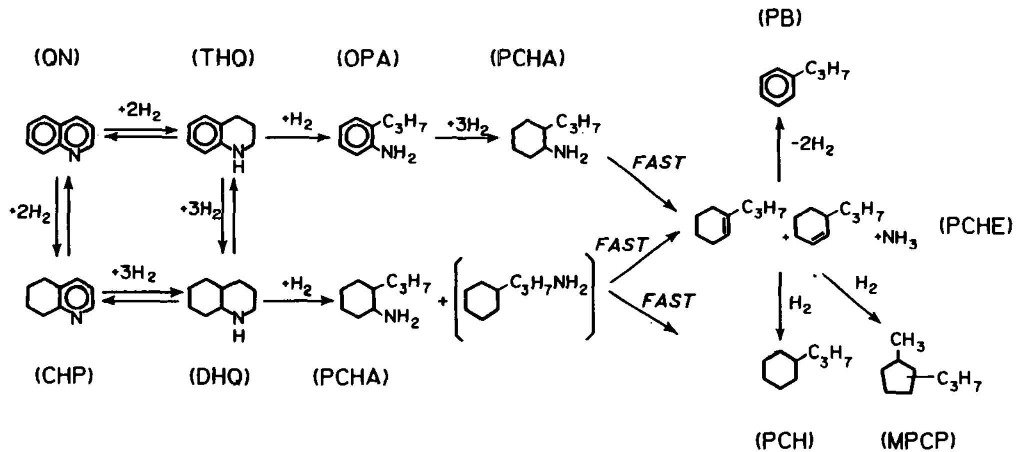

QN – quinoline	PCHA – propylcyclohexylamine
THQ – 1,2,3,4 -tetrahydroquinoline	PB – propylbenzene
CHP – 2,3 - cyclohexenopyridine	PCHE – propylcyclohexene (1,1 or 1,3)
DHQ – *decahyroquinoline (cis and trans isomers)*	PCH – *propylcyclohexane*
OPA – o-propylaniline	MPCP – methylpropylcyclopentane

COAL/OIL COPROCESSING MECHANISM STUDIES

by

Anthony V. Cugini and Richard G. Lett
U.S. Department of Energy,
Pittsburgh Energy Technology Center
P.O. Box 10940
Pittsburgh, PA 15236
and
Irving Wender
University of Pittsburgh
Department of Chemical and Petroleum Engineering
Pittsburgh, PA 15213

ABSTRACT

Initial coprocessing studies, performed to provide a basis for larger scale tests of coprocessing options using batch one-liter autoclave and continuous hydrotreater facilities at PETC, are described. Areas investigated included the response of coal and petroleum resid combinations to processing under thermal hydrotreatment conditions, the means of increasing the conversion of coal, and the nature of resid demetalation effects. The petroleum resids possessed rather low donable-hydrogen capacities, and the interactions between the resids and coals are weak with respect to promoting formation of liquid products under thermal conditions. Maya ATB was superior to Boscan ATB or North Slope VTB for the conversion of Illinois No. 6 coal to liquid or soluble products. The Maya ATB/Illinois No. 6 coal system responded favorably to the addition of low concentrations of a highly dispersed, unsupported molybdenum catalyst. Extensive demetalation of the liquid product was observed and was a function of the amount of coal added. Results obtained using different coal and resid combinations, under thermal and catalytic conditions, and in the presence of various additives, imply that an absorptive mechanism is operative. The primary interactions leading to demetalation appear to be between the metal complexes of the resid and the insoluble carbonaceous coal-derived material. Demetalation of the liquid product was not observed to be dependent on conversion of the organically complexed metal in the resids to inorganic form.

INTRODUCTION

The rapid consumption of conventional light petroleum reserves and the increasing need to refine lower quality petroleum feedstocks have recently prompted serious consideration of technology for coprocessing coal with petroleum resids or heavy bitumens. Coprocessing is attractive as a possible route for introducing the processing of coal in an evolutionary manner into existing refinery infrastructures without immediately incurring the large capital investment associated with other coal liquefaction alternatives.

An experimental program was initiated at PETC to obtain fundamental data on the coprocessing of coal with petroleum resids and to achieve a understanding of the observed "synergistic" interactions between coal and petroleum resid feedstocks.[1-4] This work has focused on coprocessing of Illinois No. 6 bituminous coal and, to a lesser extent, Wyodak subbituminous coal with petroleum resids having widely different properties and coprocessing characteristics. Areas that have been investigated are the response of different coal and resid combinations to processing under thermal hydrotreatment conditions, the means of improving liquid product yields and coal conversions, and the extent and mechanism of liquid product demetalation.

EXPERIMENTAL

Most of the coprocessing experiments were performed with Illinois No. 6 hvBb coal (>100 mesh) from the Burning Star Mine. A few comparative experiments were carried out with Wyodak subbituminous coals from the Clovis Point or Sarpy Creek Mines. The Clovis Point coal was dried before use. Proximate and ultimate analyses of the feed coals are given in Table 1.

Three petroleum resids were employed: North Slope VTB ($950^{o}F^{+}$), Boscan ATB ($650^{o}F^{+}$), and Maya ATB ($650^{o}F^{+}$). Analyses of these resids are presented in Table 2.

Selected experiments also employed a coal-derived thermal resid, pyrite, activated carbon, and kaolin.

Experiments were carried out in 42-mL shaker bomb microautoclave reactors. In the coprocessing experiments, a coal and a resid were added separately to the reactor. Any additive used was introduced after the coal and resid. After pressure testing, the reactors were charged with the reducing gas and slowly heated to run temperature, usually at a rate of ca. $8^{o}C/min$. Heating was achieved by immersion of a bank of five reactors into an electrically heated sand bath. Most experiments were performed with a feed coal concentration of 0-30 wt%, a cold charge pressure of 1200 psig, a reaction temperature of $425^{o}C$, and a reaction time of one hour.

The products were removed from the microautoclave reactors and separated into five fractions for analysis according to the scheme presented in Figure 1. The product work-up scheme minimizes the interactions between solvents and liquid products to reduce product contamination by solvent and product losses associated with solvent removal.

Yields of heptane solubles and THF solubles were calculated on the basis of dry weight of the recovered insolubles. Calculated coal conversions of THF solubles are based on maf coal after correcting for the contribution of the petroleum resid to the THF insolubles found in runs with no added coal.

RESULTS AND DISCUSSION

Effect of Coal Addition

The interaction of the petroleum resids with Illinois No. 6 bituminous coal under thermal-processing conditions was evaluated in terms of yields of heptane solubles, and coal conversions to THF solubles were evaluated as a function of coal addition. A limited number of experiments were performed with the Wyodak coal for comparative purposes.

The observed changes in heptane-soluble yields with increasing addition of coal to North Slope, Boscan, and Maya resid are shown in

Figures 2,3, and 4, respectively. The lower dashed line in these plots indicates the result expected if the coal simply acted as an insoluble diluent. The results for the North Slope VTB in Figure 2 do not deviate significantly from this line. However, an enhanced yield of heptane solubles is obtained with coal addition to both Boscan ATB and Maya ATB, as described by the upper solid curve (actual experimental results) in Figures 3 and 4. The effect is larger for the Maya ATB than for the Boscan ATB.

Interpretation of the enhanced yields requires knowledge of the relative contributions of the coal vs. resids to the heptane-soluble products. Since the petroleum resids are low in oxygen (if dry) and virtually free of phenolic functionality, relative contributions of coal to soluble product fractions can be monitored following the concentration of phenolic OH. As shown in Figure 5, there is a nearly linear increase of phenolic OH in the heptane solubles with coal addition regardless of resid. The data indicate a relatively weak interaction between Illinois No. 6 coal and the three petroleum resids.

Calculated coal conversions of Illinois No. 6 to THF solubles as a function of coal addition to North Slope VTB, Boscan ATB, and Maya ATB are summarized in Figure 6. The experimental results with coal concentrations less than 10 wt% are highly suspect owing to the small quantity of coal and THF insolubles. However, the remaining results indicate decreasing coal conversions to THF solubles with coal addition upon coprocessing with either North Slope VTB or Boscan ATB. In contrast, about 70% coal conversion was achieved in coprocessing with Maya ATB over the entire range of coal additions.

Based upon a number of reports indicating significant improvements in coal conversion by adding H_2S to the initial reducing atmosphere,[5-7] the effect of H_2S addition in coprocessing Illinois No. 6 coal with Boscan ATB and Maya ATB was examined. The results in Table 3 indicate a significant increase (10-15%) in coal conversion to THF solubles with added H_2S. There is also some improvement in the yield of heptane solubles, although the effect is largely masked by the already large contribution to the heptane solubles from the petroleum resid.

The response of the Illinois No. 6 coal and Maya ATB coprocessing system to addition of an active, highly dispersed, unsupported transition metal catalyst is also shown in Table 3. Molybdenum was added directly into the feed slurry in the form of an aqueous (ca. 12 wt%) solution of ammonium heptamolybdate. Hydrogen sulfide was added to the reducing atmosphere to insure rapid conversion of the molybdenum to the sulfide. Using 1.0% Mo gave virtually complete coal conversion to THF solubles and high heptane-soluble yields of ca. 80 wt%. Similar results were obtained using a catalyst concentration of 0.1 wt% Mo.

Metals Removal

One of the most attractive aspects of coprocessing is the potential of processing metal-rich petroleum resids with coal to yield a liquid product of significantly lower metal content. Such resids are currently difficult or impractical to process owing to the detrimental effects of these metals, particularly nickel and vanadium, on conventional upgrading catalysts.[8,9] The role of coal in promoting this demetalation has been investigated by a twofold approach involving monitoring the relative metal (Ni,V) content of the filtered liquid coprocessing products by X-Ray fluorescence and monitoring the organic vanadium (vanadyl) in the insoluble product by electron spin resonance.

Significant reductions in the metal content of the filtered liquid product were obtained in coprocessing a variety of resid and coal combinations. The observed dependence of the metal (Ni + V) concentrations in the feed slurry is summarized in Figure 7. Similar demetalation effects were also found in experiments with Wyodak coal as indicated in Table 4.

The effect of additives other than coal on the coprocessing behavior of Maya ATB was investigated to gain further insight into the requirements for resid demetalation. As shown in Table 5, coprocessing Maya ATB with 30 wt% Illinois No. 6 coal or a high-surface-area activated carbon resulted in liquid products containing only 10-30 ppm vanadium. Similar results have been observed in coprocessing Maya ATB with cellulose chars.[10] In contrast, coprocessing Maya ATB with coal-derived pyrite, which exerts mild catalytic activity but has low surface area, resulted in an enhanced liquid yield but no significant demetalation above that obtained if only the resid is processed. Likewise, no significant demetalation of the liquid product was achieved by the addition of 30 wt% kaolin, which acts as a low-surface-area diluent. Also, the extent of demetalation of the liquid products in experiments with low concentrations of highly dispersed Mo catalyst is similar to that achieved without the added catalyst, although soluble product yields and coal conversion are considerably higher in the catalytic than the thermal-coprocessing experiments.

The experimental data in Table 5 suggest that a sufficient requirement for resid demetalation appears to be a high-carbonaceous insoluble surface area. There is no particular correlation of metals removal with liquid product yields or coal conversion.

The fate of organic vanadium was further investigated by semi-quantitative ESR procedures. Based on elemental analyses, more than 90% of the vanadium in the feed slurry is recovered in the heptane-insoluble product from coprocessing Maya ATB with 30 wt% Illinois No. 6 coal under the conditions used. The ESR analyses of the quadrivalent vanadium in the heptane insolubles from a variety of microautoclave coprocessing experiments are summarized in Table 6. There is no direct relationship between the amount of ESR-observable vanadyl and the degree of demetalation of the heptane-soluble product fractions. In the thermal microautoclave runs, the vanadium associated with the heptane insolubles remains largely in quadrivalent vanadium complexes even under a hydrogen atmosphere. The ESR spectra of the heptane insolubles from coprocessing Maya ATB with coal or activated carbon were remarkably similar. The addition of pyrite as a catalyst yielded a very lossy heptane-insoluble fraction that was not amenable to ESR analysis. Addition of a highly dispersed molybdenum catalyst resulted in a threefold decrease in ESR-observable vanadium in the heptane insolubles. It is reasonable to assume that the reduction reflects conversion of the organic vanadium into inorganic species (sulfides) or other species not observed by ESR. The ESR spectrum of the quadrivalent organic vanadium remaining in the heptane insolubles from the molybdenum-catalyzed run is similar to that obtained in the absence of an added catalyst.

CONCLUSIONS

The observed thermal-coprocessing behaviour of petroleum resids is consistent with their limited compatibility with coal-derived materials and an inability to function as efficient hydrogen-transfer solvents. Under thermal-coprocessing conditions with Illinois No. 6 coal, the coal contribution to the heptane-soluble product was low for each of the three tested and varied in a linear manner with coal addition. This appears to be little more than a thermal extraction. There is evidence, particularly in coprocessing Illinois No. 6 with Maya ATB, for an enhanced yield of heptane solubles from the resid with coal addition. Except in coprocessing experiments with Maya ATB, calculated coal conversion to THF solubles fell with increasing coal addition. Under the conditions used, thermal-coprocessing results for Wyodak subbituminous and Illinois No. 6 bituminous coals were similar with respect to soluble product yields. Overall, the thermal-coprocessing experiments indicate the interaction between coal and petroleum resids is rather weak with respect to promoting the formation of liquid products.

The liquid product yields from thermal coprocessing of coal with untreated petroleum resids are too low to justify a completely non-catalytic approach to coprocessing. A limited improvement, particularly with respect to minimizing the yield of THF insolubles, can be realized by simply adding H_2S to the reducing atmosphere. However, the Maya ATB/Illinois No. 6 coal system responds favorably to addition of low concentrations of active, highly dispersed, unsupported transition metal catalyst. Although no systematic attempt was made to optimize conditions, only a few hundred parts per million of unsupported Mo appear to be necessary to obtain complete conversion to THF solubles and high heptane-soluble yields.

Under thermal-coprocessing conditions in a microautoclave reactor, conversion of organically complexed vanadium to inorganic sulfides or other ESR-unobservable forms occurs to only a limited extent. Minimal catalytic benefit owing to the presence of vanadium in the resid feedstock thus accrues in the absence of an added active hydrogenation catalyst.

Coal addition does facilitate demetalation of the heptane-soluble product from processing petroleum resids. The investigation of the requirements for demetalation in coprocessing indicates that the removal of the resid metals from the soluble product fractions is primarily associated with an interaction of the metal complexes and insoluble carbonaceous components rather than the coal mineral matter. The experimental results strongly suggest that an adsorptive mechanism is initially operative, followed by reactive incorporation of the complexed metal species into the carbonaceous insolubles and by extensive conversion of the metal to inorganic form under appropriate (catalytic) conditions. The primary function of coal is apparently to provide a surface upon which the vanadium species can deposit and undergo further regressive reactions.

ACKNOWLEDGEMENTS

The authors are grateful to Dennis H. Finseth, Bradley C. Bockrath, Daniel L. Cillo, Richard F. Sprecher, and Eugene G. Illig for providing analytical support and several helpful discussions regarding development and interpretation of the coprocessing experiments.

This work was supported in part by the Oak Ridge Associated Universities Graduate Research Program.

REFERENCES

1. Cugini, A.V. "A Review of Coal-Oil Coprocessing Technology". M.S. Thesis, Department of Chemical and Petroleum Engineering, University of Pittsburgh, August, 1985, 91 pp.

2. Shinn, J.H., Dahlberg, A.J., Kuehler, C.W., and Rosenthal, J.W. "The Chevron Co-Refining Process". In Proceedings: Ninth Annual EPRI Conference on Coal Liquefaction (EPRI Report AP-3825-SR), EPRI, Palo Alto, CA, 1985.

3. Miller, R.L. "Use of Non-Coal-Derived Heavy Solvents in Direct Coal Liquefaction". In Proceedings: Tenth Annual EPRI Conference on Coal Liquefaction (EPRI Report AP-4345-SR), EPRI, Palo Alto, CA, 1985.

4. Kelly, J.F., Fouda, S.A., Rahimi, P.M., and Ikura, M. "CANMET Coprocessing: A Status Report". Canada Centre for Mineral and Energy Technology, Energy Research Laboratories, Division Report, DRP/ERL-84-52, September 1984, 41 pp.

5. Lambert, J.M., Jr. "Alternative Interpretation of Coal Liquefaction Catalysis by Pyrite". Fuel 61, 777-778 (1982).

6. Rahimi, P.M., Fouda, S.A., and Kelly, J.F. "Coprocessing Using H_2S as a Promoter". Fuel 66, 1215-1218 (1987).

7. Hei, R.D., Sweeney, P.G., and Stenberg, V.I. "Mechanism of Hydrogen Sulphide Promoted Cleavage of the Coal Model Compounds: Diphenyl Ether, Diphenyl Methane, and Bibenzyl". Fuel 65, 577-585 (1986).

8. Green, D.C., and Broderick, D.H. "Residuum Hydroprocessing in the 80's". Chem. Eng. Prog. 77,(12), 33-39 (1981).

9. Tamm, P.W., Harnsberger, H.F., and Bridge, A.G. "Effects of Feed Metals on Catalyst Aging in Hydroprocessing Residuum". Ind. Eng. Chem., Process Des. Dev. 20,(2), 262-273 (1981).

10. Miller, T.J. "The Role of Coal in the Removal of Metals from Heavy Oils". M.S. Thesis, Department of Chemical and Petroleum Engineering, University of Pittsburgh, 1987, 79 pp.

Table 1. Proximate and Ultimate Analyses of Feed Coals

	Illinois No. 6 (Burning Star)	Wyodak (Clovis Point)	Wyodak (Sarpy Creek)
Proximate Analysis, wt% (As Received)			
Moisture	4.2	6.1	17.7
Volatile Matter	36.9	42.3	31.6
Fixed Carbon	48.2	40.8	38.8
Ash	10.7	10.8	11.9
Ultimate Analysis, wt% (Moisture Free)			
Carbon	70.2	64.4	62.9
Hydrogen	4.8	4.5	3.9
Nitrogen	0.9	1.0	0.8
Sulfur	3.1	0.9	0.9
Oxygen (Diff.)	9.9	17.7	17.0
Ash	11.1	11.5	14.5
Sulfur Forms, wt%			
Sulfate	0.03	0.02	
Pyritic	1.2	0.2	
Organic	1.9	0.7	

Table 2. Properties of Petroleum Resids

	North Slope VTB (950°F+)	Boscan ATB (650°F+)	Maya ATB (650°F+)
Ultimate Analysis (wt%)			
Carbon	86.1	82.5	84.5
Hydrogen	10.6	10.1	10.6
Oxygen	0.7	0.6	0.3
Nitrogen	0.6	0.7	0.5
Sulfur	2.0	5.6	4.0
Ash	<0.1	0.5	0.1
Ni (ppm)	60	120	70
V (ppm)	130	1300	370
°API	8.9	5.7	8.8
850°F$^-$ vol% ASTM D1160	--	19	30
Heptane Insols (wt%) ASTM D3279	4	20	20
$\bar{M}_n$(VPO, pyridine, 80°C)	920	1250	720
H^*_{ar}	0.07	0.08	0.07
f_a	0.38	0.41	0.33

Table 3. Effects of H_2S and Unsupported Mo Catalyst on Coprocessing Illinois No. 6 Coal (30 wt%) and Maya ATB (70 wt%)

Charge Atmosphere					
H_2 (vol%)	H_2S (vol%)	H_2O(wt%) in SLurry	Cat.(wt%) in Slurry	Heptane-Soluble Yield (wt%)	%Coal Conversion to THF Sols
100	0	-	-	68	73
85	15	-	-	72	84
85	15	5	-	74	85
85	15	-	1.0	81	96
90	10	-	0.1	80	95
100	0	-	0.1	76	88

Note. Temperature: 425°C
Residence Time: 1 hr
Charge Pressure: 1200 psig

Table 4. Observed Demetalation of the Filtered Liquid Products from Coprocessing Maya ATB (70 wt%) with Wyodak Subbituminous and Illinois No. 6 Bituminous Coals (30 wt%)

Coal	Coal In Feed Slurry (wt%)	Metals In Filtered Liquid Product (ppm)
Wyodak (Clovis Point)	20	50
	30	20
Illinois No. 6	20	60
	30	10

Note. Temperature: 425°C
Residence Time: 1 hr
Charge Pressure: 1200 psig

Table 5. Effect of Various Additives in Processing Maya ATB

Petroleum Resid	Ill. No. 6 Coal (wt%)	Additive (wt%)	% Heptane Solubles in Product	Vanadium in Liquid (ppm)
Maya ATB	0	-	89	200
Maya ATB	30	-	68	20
Maya ATB	0	Deashed Thermal Resid (30%)	74	10
Maya ATB	0	Activated Carbon (30%)	61	30
Maya ATB	0	Coal-Derived Pyrite (30%)	71	210
Maya ATB	0	Kaolin (30%)	62	230
Maya ATB	30	-	72	20[a]
Maya ATB	30	Mo (0.1%)	80	30[a]

Note. Temperature: 425°C
Residence Time: 1 hr
Charge Pressure: 1200 psig

[a] These runs contained 15 vol% H_2S in the feed gas.

Table 6. Recovery of Organic Vanadium in Heptane Insolubles from Microautoclave Experiments

Feed Slurry Composition			Initial Reducing Gas Composition		Fraction of Feed Slurry Vanadium	
Petroleum Resid	Additive (30 wt%)	Catalyst (0.1 wt%)	H_2 (vol%)	H_2S (vol%)	In Heptane Insols as Vanadyl (ESR)	In Heptane Sols (Elemental Analysis)
Maya ATB	Ill. No. 6	---	100	---	0.9_3	0.05_4
Maya ATB	Activated C	---	100	---	0.9_2	0.06_1
Maya ATB	Pyrite	---	100	---	0.01 (see text)	0.6_9
Maya ATB	Ill. No. 6	---	90	10	0.7_2	0.05_4
Maya ATB	Ill. No. 6	Mo	90	10	0.2_7	0.09_3
Boscan ATB	---	---	99	1	0.4_2	0.4_3
Boscan ATB	---	---	90	10	0.4_9	0.3_8
Boscan ATB	---	---	75	25	0.4_8	0.4_8
Boscan ATB	Ill. No. 6	---	90	10	0.8_2	0.08_8
N. Slope VTB	---	---	100	---	0.1_9	0.6_5
N. Slope VTB	Ill. No. 6	---	100	---	0.5_9	0.07_7

Note. Temperature: 425°C
Residence Time: 1 hr
Charge Pressure: 1200 psig

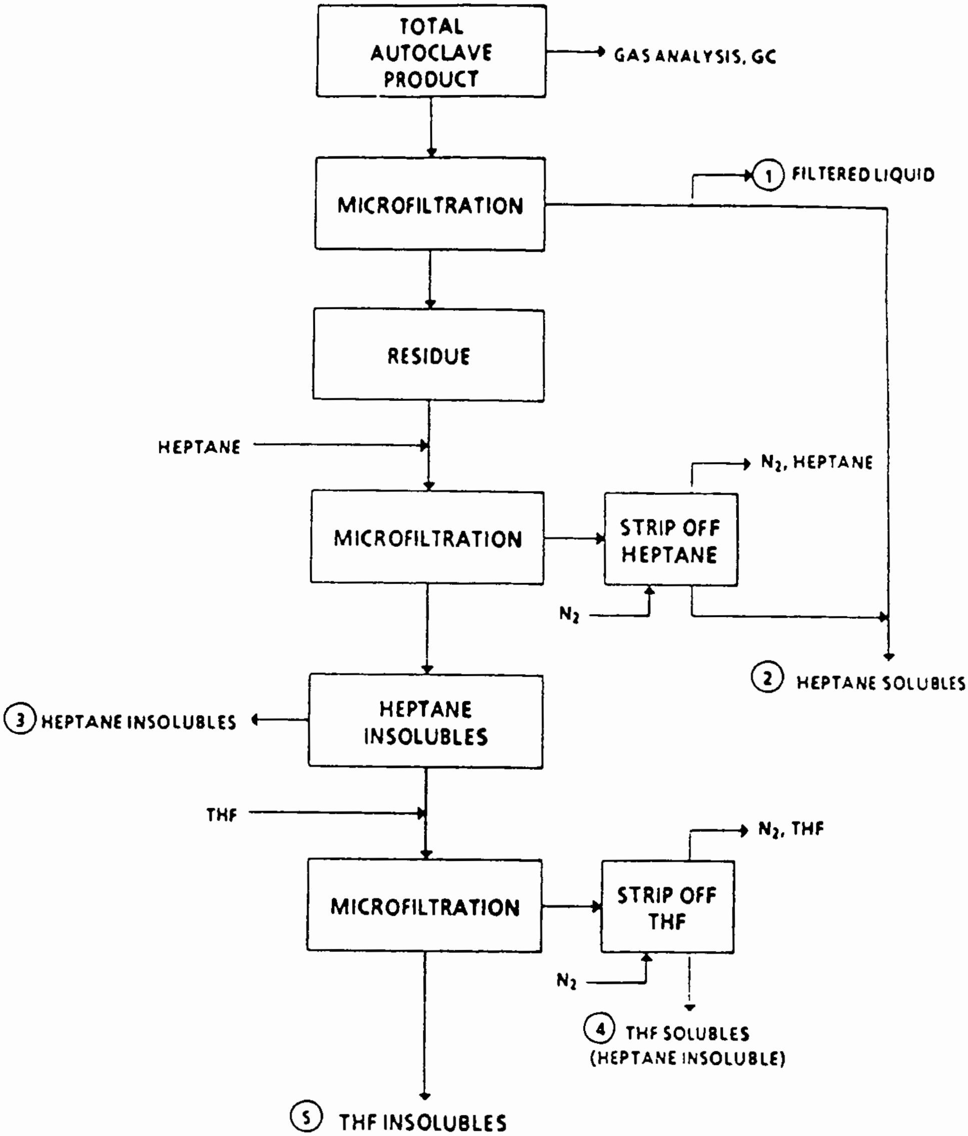

Figure 1. Microautoclave product work-up scheme.

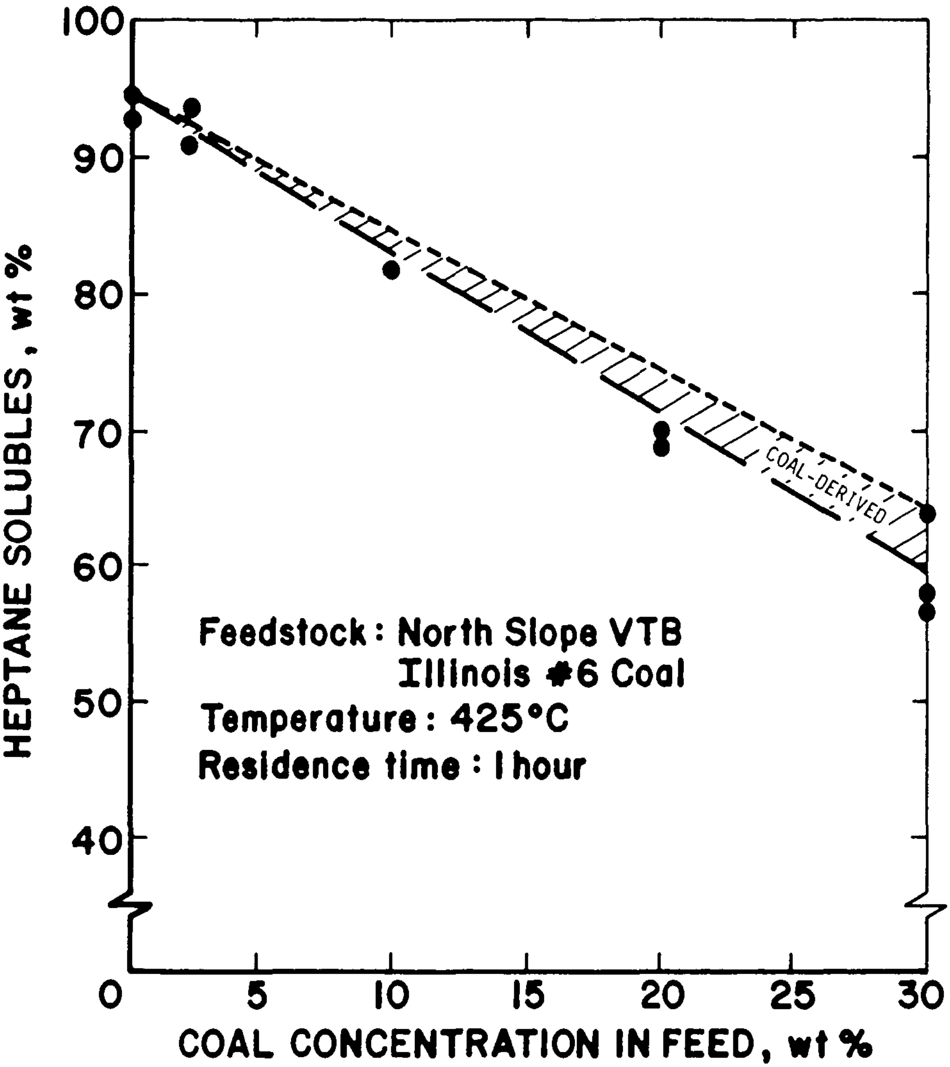

Figure 2. Effect of coal concentration on heptane-soluble yields in coprocessing North Slope VTB with Illinois No. 6 Coal.

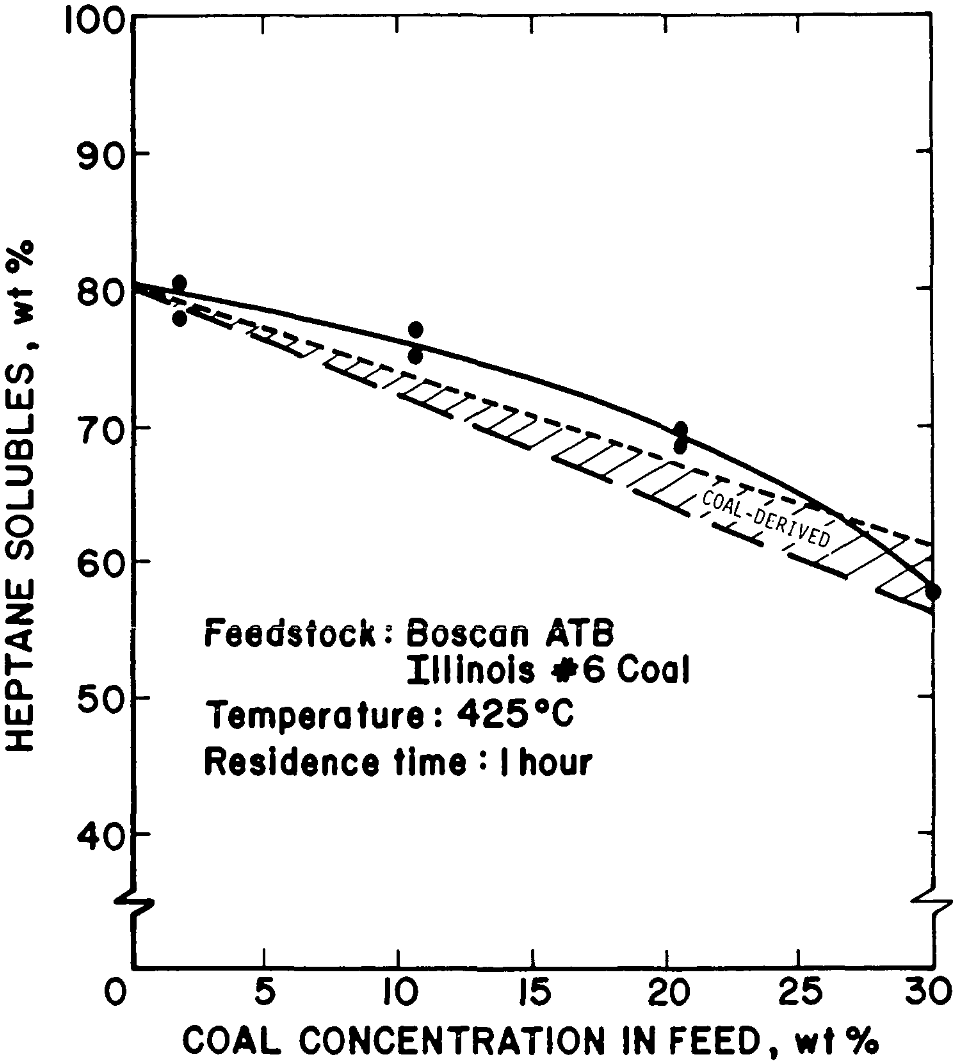

Figure 3. Effect of coal concentration on heptane-soluble yields in coprocessing BOSCAN ATB with Illinois No. 6 Coal.

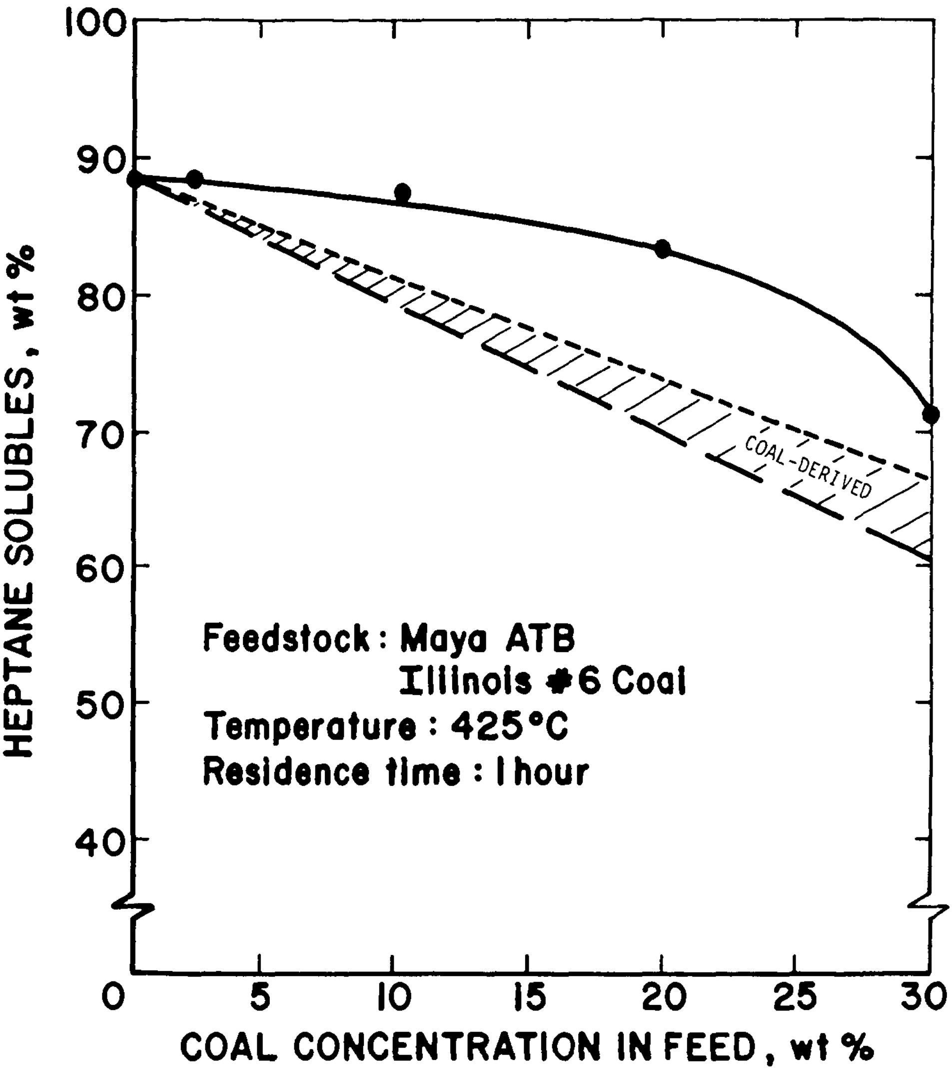

Figure 4. Effect of coal concentration on heptane-soluble yields in coprocessing Maya ATB with Illinois No. 6 Coal.

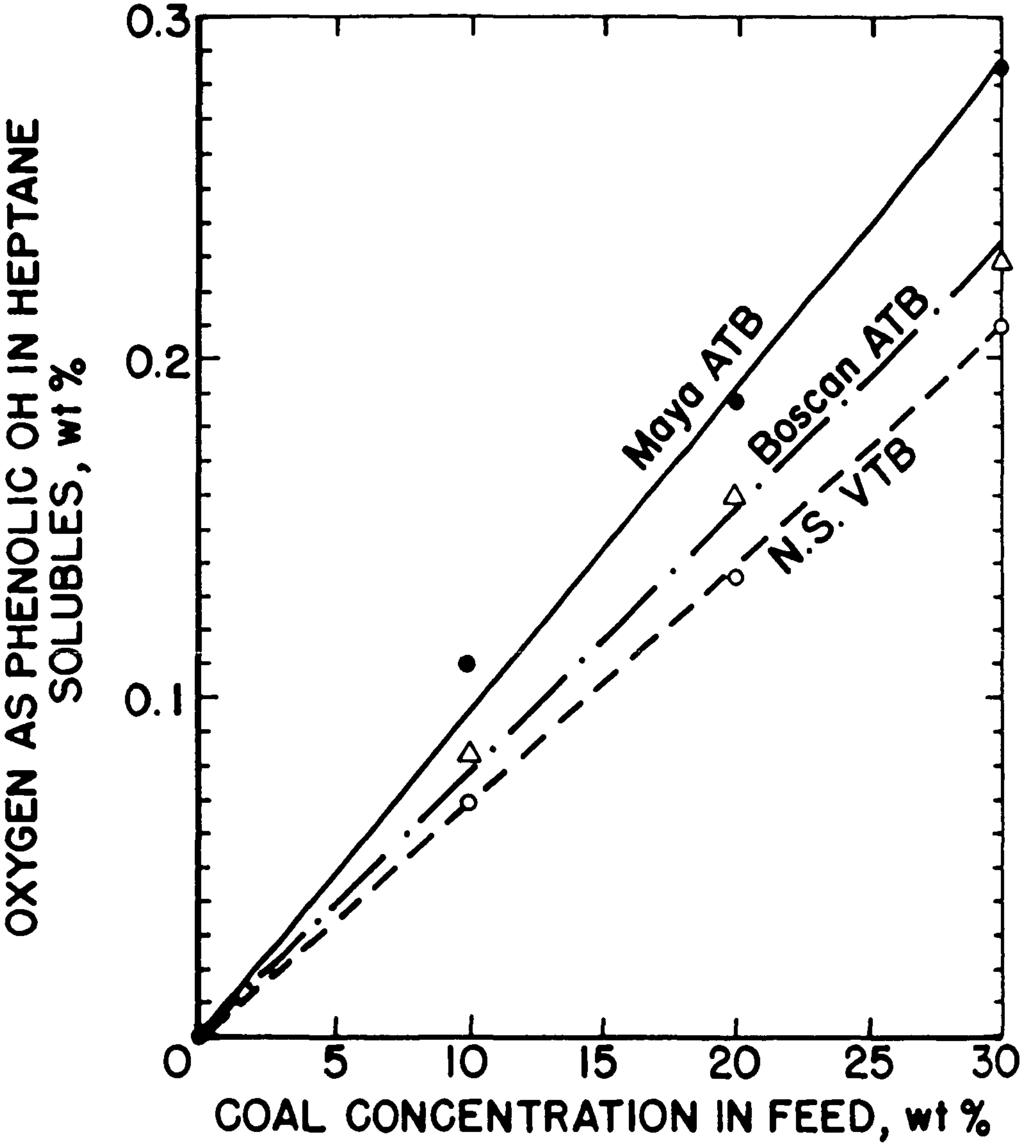

Figure 5. Effect of coal concentration on phenolic OH in the filtered liquid products from coprocessing petroleum resids with Illinois No. 6 Coal.

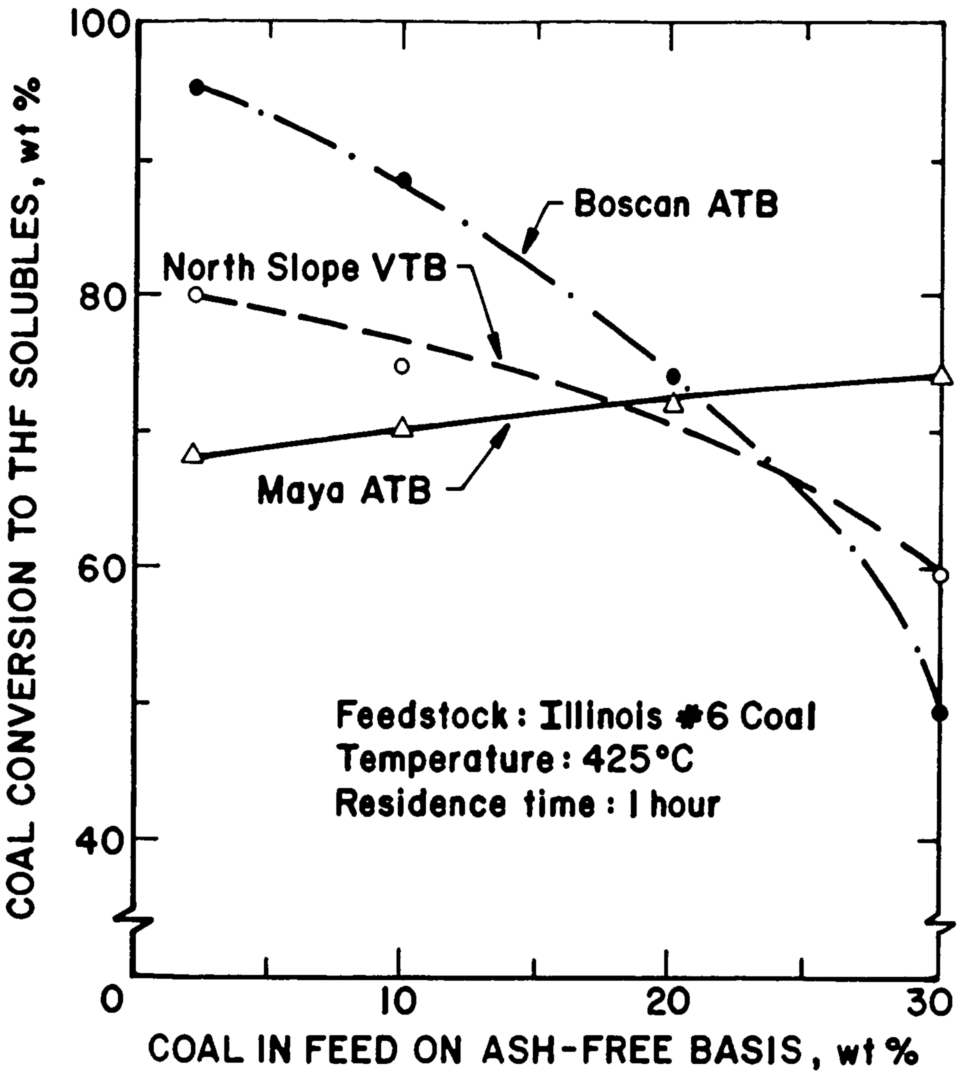

Figure 6. Effect of coal concentration on Illinois No. 6 Coal conversion to THF solubles in coprocessing with petroleum resids.

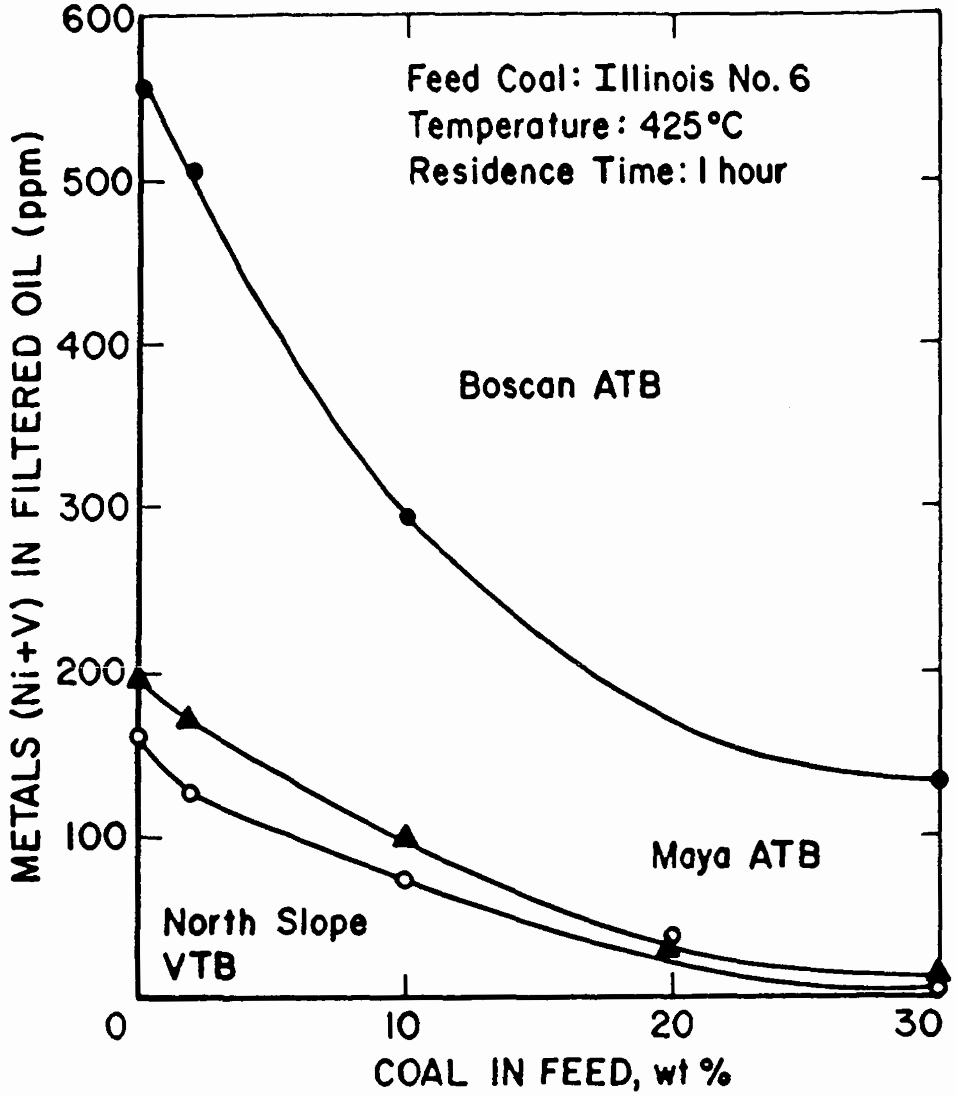

Figure 7. Effect of coal concentration on metals removal.

INTERACTIONS IN THE EXTRACTION STAGE OF TWO-STAGE COPROCESSING.

R. Caygill, T. Flynn, W. Kemp and W. Steedman,
Dept. of Chemistry, Heriot-Watt University, Edinburgh, EH14 4AS.

S. Wallace, C. Jones, M. Burke, K.D. Bartle and N. Taylor,
Dept. of Physical Chemistry, University of Leeds, LS2 9JT.

INTRODUCTION.

In recent years there has been a growing interest in liquefaction processes in which coal recycle solvents are replaced by cheaper petroleum fractions.[1-3] In conventional liquefaction processes there is some evidence that a two-stage process is more advantageous than single stage processes. The Liquid Solvent Extraction (LSE) process of the British Coal Corporation is such a process.[4] Firstly, the coal and solvent are heated in an inert atmosphere before the extract is further upgraded in a second stage involving high pressure hydrogen and a catalyst. The work reported in this paper was undertaken to evaluate the viability of replacing the coal solvent with heavy petroleum fractions in the LSE process.

The results presented here are concerned only with the extraction stage, which in coprocessing is the most important stage. If coal cannot be solubilised to an extractable form poor yields will result however good the upgrading in the hydrocracking stage.

Experimental.

The materials used were Point-of-Ayr (POA) coal and a range of petroleum fractions from various sources. Analytical data are given in Table 1. Samples of coal and petroleum fractions were heated in tubing bombs ($\sim$15 cm^3) with agitation in a fluidised sandbath. Runs were carried out in duplicate. The product was extracted with n-pentane to obtain the % pentane insolubles (% PI). Further extractions were carried out to give the % toluene insolubles (% TI) and quinoline insolubles (% QI).

Table 1 : Analysis of Feed Materials.

		Wt %				
Source	Fraction	C	H	N	S	H/C
Crude "O"	VR > 475°C	85.1	10.5	$\sim$	2.95	1.48
Crude "M"	VR 475°C	86.6	12.5	0.35	0.9	1.73
Forties	VR	87.4	11.1	0.45	0.8	1.52
Arabian Heavy	AR	84.3	11.2	0.3	3.9	1.59
Marguerite Lake	AR	83.4	10.4	0.7	5.0	1.50
POA Coal		84.1	5.2	1.8	1.0	0.74

A small number of extractions were carried out in a 250 ml stirring autoclave with a heating rate of 7C^{o} min $^{-1}$.

The products were extracted with dichloromethane (DCM) and both the soluble and insoluble material was collected and analysed.

Pretreatment of Petroleum Crudes.

Whole crudes were vacuum distilled at 475^{o}C and the residue used in coprocessing runs. Vacuum and Atmospheric residues were used as obtained.

The asphaltene fraction of two petroleum fractions was removed and the deasphaltened samples coprocessed with POA.

Samples of two of the petroleum residues were hydrogenated prior to use at 375^{o}C or 425^{o}C under 80 atm H_2 (cold pressure) with NiMo catalyst.

RESULTS AND DISCUSSION.

Thermal Stability of Petroleum Fractions.

The petroleum fractions were heated alone under a variety of reaction conditions. The extraction yields are shown and compared with those of the untreated fractions in Table 2.

Table 2.

Crude	Reaction conditions	% PI	% TI	% QI
VR-M	-	0	0	0
VR-M	410^{o}C/30 min	2.7	-	-
VR-M	440^{o}C/30 min	5.9		
VR-O	-			
VR-O	380^{o}C/30 min	22.5		
VR-O	410^{o}C/30 min	21.0		
VR-O	440^{o}C/30 min	27.4	15.2	5.4
		23.5	10.0	-
HVR-O	None			
HVR-O	410^{o}C/30 min	11.5	6.4	2.7
VR-FF	None	10.9	-	-
VR-FF	380^{o}C/30 min	11.0	-	-
VR-FF	410^{o}C/30 min	14.9	-	-
VR-FF	440^{o}C/30 min	21.8	4.0	1.0
$(VR\text{-}FF)_{da}$	410^{o}C/30 min	3.3	-	-
AR-ML	None	22.2	-	-
AR-ML	380^{o}C/30 min	19.5	-	-
AR-ML	410^{o}C/30 min	21.4	-	-
AR-ML	440^{o}C/30 min.	24.0	12.3	3.3
AR-ML	410^{o}C/10 min	19.2	-	-
AR-ML	410^{o}C/ 2 h	19.6	7.3	4.0
$(AR\text{-}ML)_{da}$	410^{o}C/30 min	2.2	-	-
H_1ARML	410^{o}C/30 min	8.8	-	-
"	None	0	-	-
H_2AR-ML	None	0	-	-
"	410^{o}C/30 min			
AR-AH	None	15.0	-	-
AR-AH	440^{o}C/30 min	13.6	-	-
AR-AH	440^{o}C/30 min	16.1	4.5	-

In general, higher reaction temperatures resulted in a small increase in PI but more significantly at 440°C TI were formed. Longer reaction times left the PI unaffected but TI and QI were formed.

Untreated hydrogenated fractions were completely soluble in pentane but on heating considerable PI were formed. These hydrogenated petroleum fractions were less thermally stable than the parent fractions.

Effect of Coal/Petroleum Ratio on Extraction Yields.

The extraction yields of compressing runs carried out with a range of coal/petroleum ratios, were measured. During these investigations the reaction conditions were kept constant with a reaction temperature of 410°C and a reaction time of 30 minutes. The results for the coprocessing of VR-FF and AR-ML with POA are shown in Figures 1 and 2 as % insolubles (% INSOL) plotted against % POA in the reaction mix. The dashed lines in the figures indicate the % insolubles that would be obtained if the same quantities of coal and petroleum fractions were heated alone under the same reaction conditions. If the experimental points lie on these lines it suggests that no interactions - either positive or negative - have occurred between the coal and petroleum fractions.

In both Figures 1 and 2 it is observed that the experimental points for PI and TI lie on or close to the dashed lines. However, the points for QI lie below the dashed lines. This suggests that VR-FF and AR-ML help to solubilise the coal to a small extent, possibly by providing aromatic radicals that can act as hydrogen shuttlers.

Coprocessing has led to the formation of preasphaltenes and a decrease in the total insoluble material.

Similar results were obtained with other petroleum fractions although the extent of interactions varied with the nature of the petroleum fraction.

The extent of interaction - the difference between the calculated and experimental values of insolubles - was plotted against the % aromaticity of the petroleum fractions (Figure 3). A maximum interaction is noted around 50% aromaticity for coal loadings of 25% and 50%. It might have been anticipated that the greater the aromaticity of the petroleum fractions, the greater the compatability with coal and so the greater the interaction. The maximum observed at 50% aromaticity might be explained by a concomitant opposing trend. As the % aromaticity of petroleum fractions increases the H/C ratio decreases and so the hydrogen available for shuttling decreases.

Effect of Reaction Temperature.

The effect of reaction temperature on the extraction yields of coprocessing runs is shown in Figures 4 and 5. Coprocessing mixes with 25% loading of POA and either VR-FF or AR-ML were heated at 375°C, 410°C and 425°C for 30 minutes. The trends with reaction temperature depend on the petroleum fraction. VR-FF/POA shows a decrease in oil and gas with reaction temperature whereas the changes in oil and gas for the AR-ML/POA runs are very slight. With both petroleum fractions, the total insoluble material decreased as the reaction temperature was increased from 380°C to 410°C but then increased again as the reaction temperature is raised further. In the AR-ML/POA runs the asphaltene content of the product decreased monotonically with reaction temperature but in the VR-FF/POA reactions the variation is <3%. Preasphaltene content in both reactions increased with reaction temperature.

The variations between the petroleum fractions cannot be explained by differences in their thermal stability. They probably result from the complex interactions involved in the reactions between oil and gas/asphaltene/preasphaltene/total insoluble material.

Despite the differences in levels observed the optimum temperature for coprocessing with both petroleum fractions is $\sim 410^{o}C$.

Effect of Reaction Time.

Coprocessing mixes with 25%, 50% and 75% loadings of POA in AR-ML were heated at $410^{o}C$ for 10 min, 30 min and 2 h. The results are shown in Figures 6, 7 and 8. The effect of long reaction times was to increase the total insoluble material at the expense of the asphaltene and preasphaltene fractions.

The petroleum/coal ratio also affected the levels with reaction time. This can be seen in Figure 9 where % INSOL are plotted against % POA for a reaction time of 2 h. This plot is considerably different from Figure 1. There appears to be a very negative synergistic effect that is greatest at high loadings of coal.

It is apparent that longer reaction times are not advantageous.

Effect of Pretreatment of Petroleum Fractions.

Deasphaltened samples of VR-FF and AR-ML were coprocessed with POA in various ratios at $410^{o}C$ for 30 min. It is clear that the interactions observed with the parent petroleum fractions are no longer present. Particularly notable was the absence of any preasphaltene fraction. The procedure used to prepare these samples removed most of the aromatic material and consequently seriously impaired the ability of the fraction to solubilise the coal.

It was postulated that prior hydrogenation of the petroleum fraction would increase the hydroaromatic content and so increase its ability to donate hydrogen to the coal. The extraction yields for the reactions of hydrogenated VR-0 and AR-ML with POA are given in Figures 12 and 13.

Hydrogenation of VR-0 appeared to have reduced its ability to solubilise coal. All the experimental points lie on the dashed lines. However, the effect of prehydrogenation of AR-ML on its ability to solubilise coal was dramatic. The total insoluble material at 50% POA was reduced to $\sim$15%. This extent of solubilisation is comparable to that of coal solvents.

Extractions in the Autoclave.

The results of % DCMI obtained from coprocessing AR-ML and POA in an autoclave are given in Figure 12. The two values of the % DCMI shown were calculated as follows:

$$\%\ \text{DCMI (min)} = \frac{\text{wt. DCMI}}{\text{wt. mix}} \times 100$$

$$\%\ \text{DCMI (max)} = \frac{\text{wt. DCMI}}{\text{wt. recovered}} \times 100$$

It was observed that the results follow a similar trend to those obtained in tubing bombs with a reaction time of 2 h. A major problem with extraction in the autoclave is that short contact times are not possible.

It was noted from the gc traces of the DCMS product of coprocessing runs that a considerable amount of the lighter material was coal derived. The peaks observed were not simply a combination of those observed from runs involving coal alone and AR-ML alone. Some major peaks were missing while others new to either materials appeared. This potentially very interesting observation, which agrees well with SEC results reported by Wallace et. al.,[5] will be further examined by gc-ms.

Conclusions.

The extraction stage of a two-stage coprocessing operation is very important. Using untreated petroleum fractions, the best coal conversion (d.a.f.) that was achieved was around 30%. This compares poorly with the performance of coal solvents. However, some considerable reaction between the coal and petroleum fractions must take place as indicated by the gc results from autoclave extractions. The greatest promise lies in the result obtained with prehydrogenated AR-ML. The coal conversions (d.a.f.) that resulted with this solvent stream were of the order of 85%. This compares well with the best of coal solvents.

Acknowledgments.

We wish to express our thanks to the Coal Research Establishment, British Coal Corporation, for useful discussions and the gift of materials for this work; and the Commission of the European Communities, who are funding this coprocessing programme under grant no. EM3V-0016-U.K.

References.

1. R. Bloß, R. Bosse and H.H. Oelert, Erdol, Kohle, Erdgas, Petrochemie, 1987, 40(5), 222.

2. C.W. Curtis, J.A. Guin and A.R. Tanner, 1986, DOE Report no. 50793.

3. S.E. Moschopedis and L.G. Helper, Fuel Sci. Tech. Int., 1987, 5(1), 1.

4. G.O. Davies and D.F. Williams, Div. Fuel Chem. Prepr., 1981, 26(1), 67.

5. S. Wallace, K.D. Bartle, M. Burke, N. Taylor, R. Caygill, T. Flynn, W. Kemp, W. Steedman, Third Chemical Congress of North America (in press).

Fig. 1

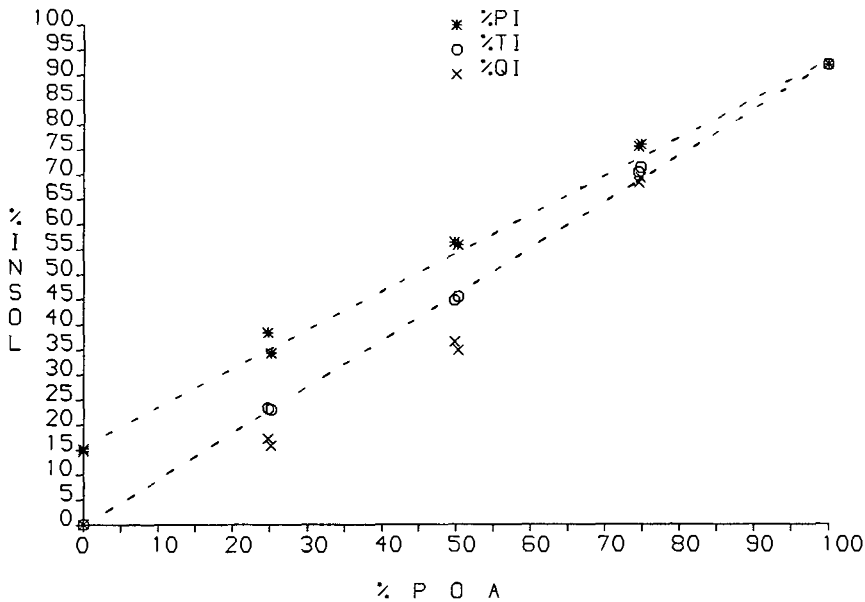

Fig. 2

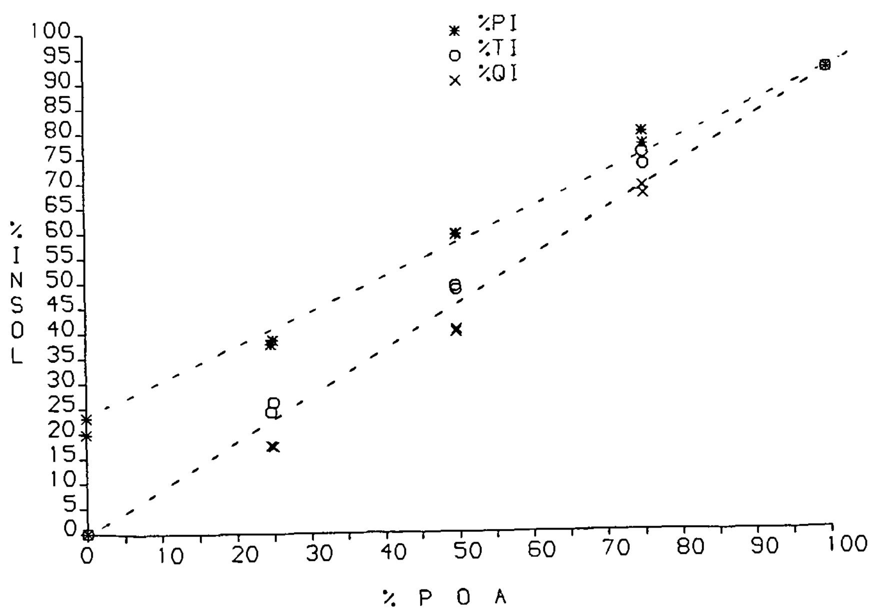

Fig. 3

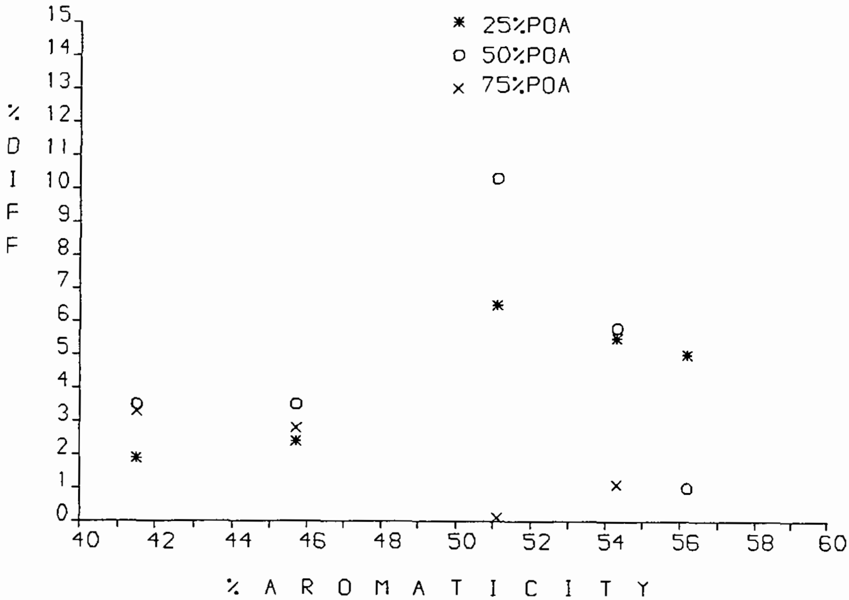

15
14
13
12
11
10
9
8
7
6
5
4
3
2
1
0
% DIFF
40
42
44
46
48
50
52
54
56
58
60
% AROMATICITY
25%POA
50%POA
75%POA

Fig. 4

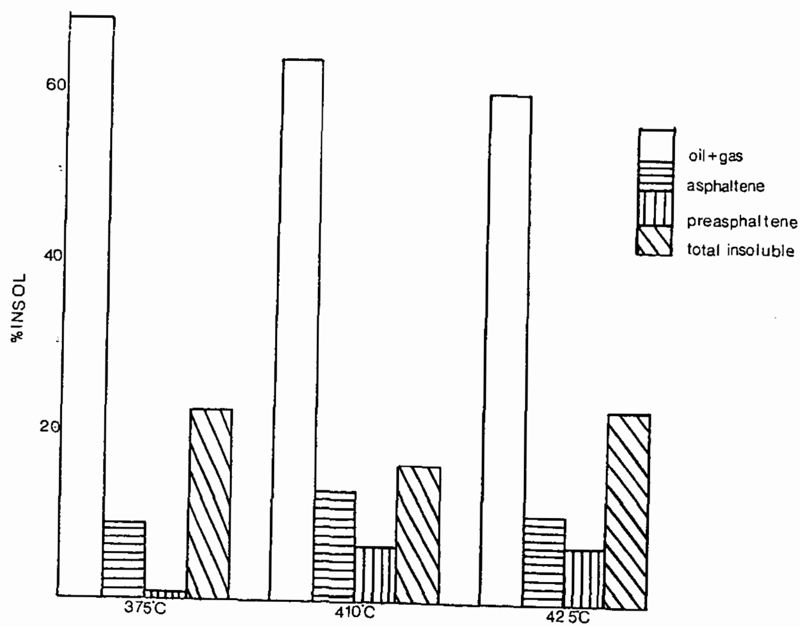

60
40
20
%INSOL
375°C
410°C
425°C
oil+gas
asphaltene
preasphaltene
total insoluble

Fig. 5

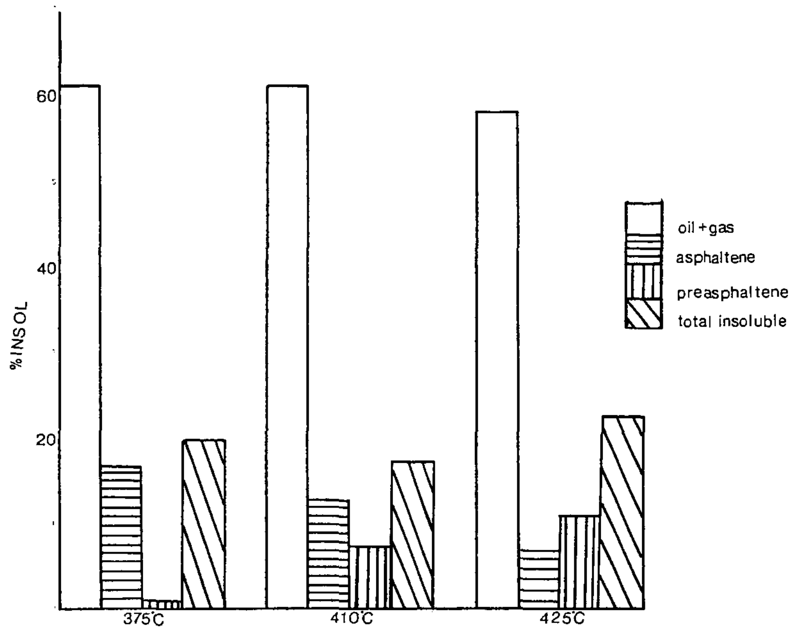

60
40
20
%INSOL
oil+gas
asphaltene
preasphaltene
total insoluble
375°C
410°C
425°C

Fig. 6

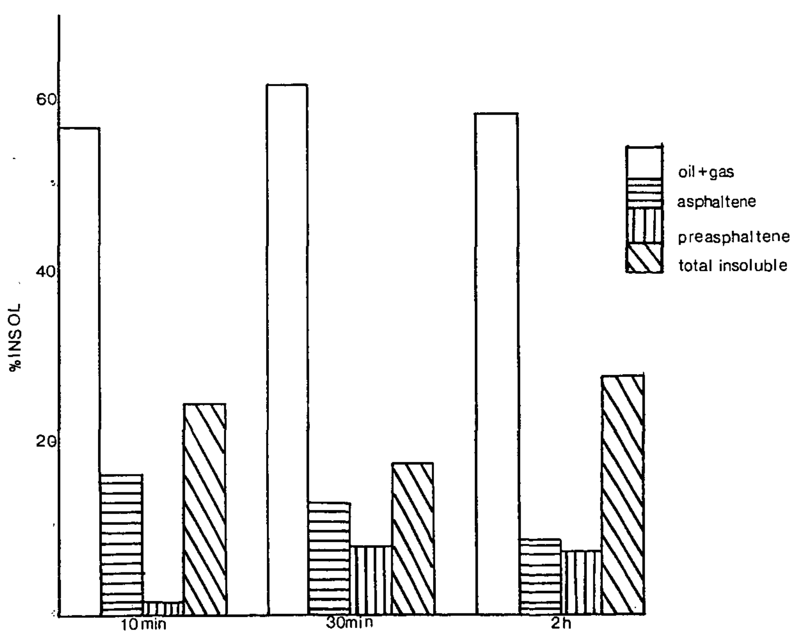

60
40
20
%INSOL
oil+gas
asphaltene
preasphaltene
total insoluble
10min
30min
2h

Fig. 7

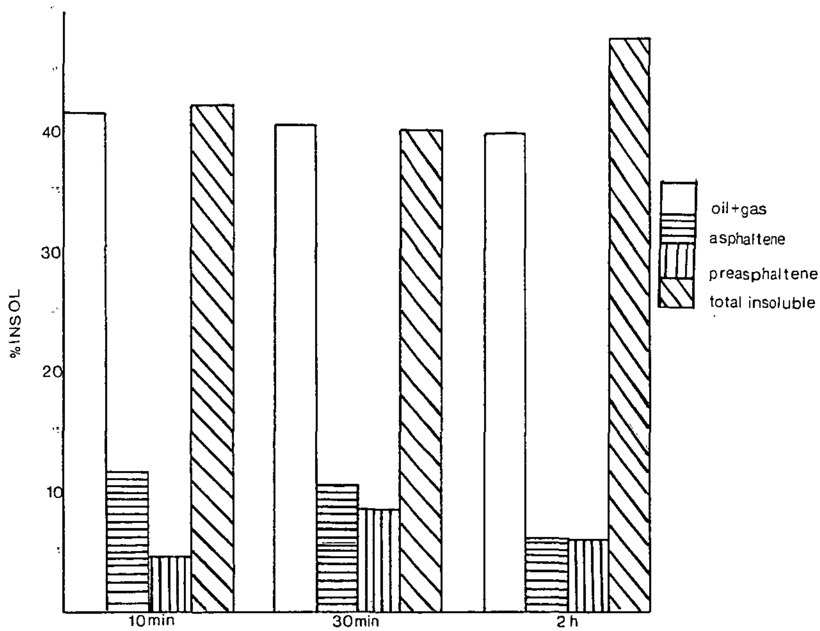

%INSOL
40
30
20
10
10min
30min
2h
oil+gas
asphaltene
preasphaltene
total insoluble

Fig. 8

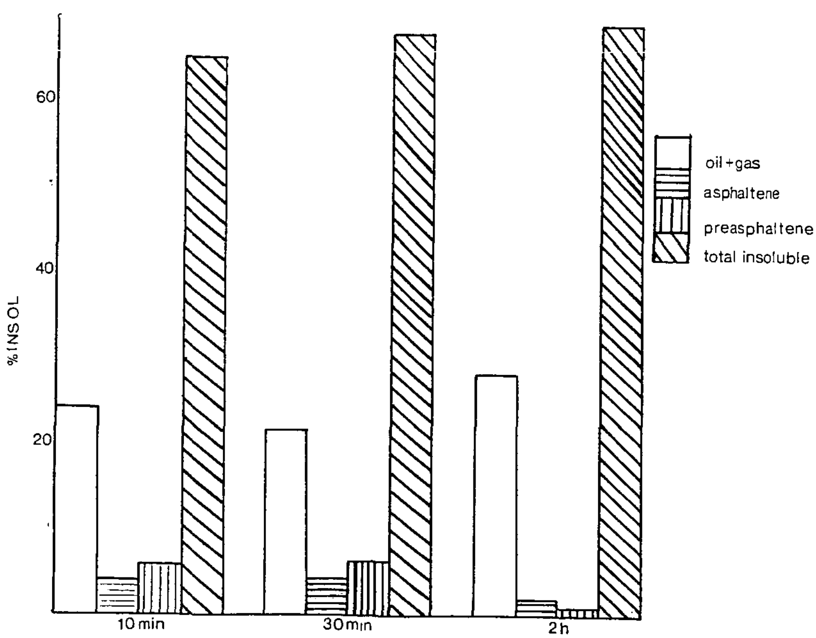

%INSOL
60
40
20
10min
30min
2h
oil+gas
asphaltene
preasphaltene
total insoluble

Fig. 9

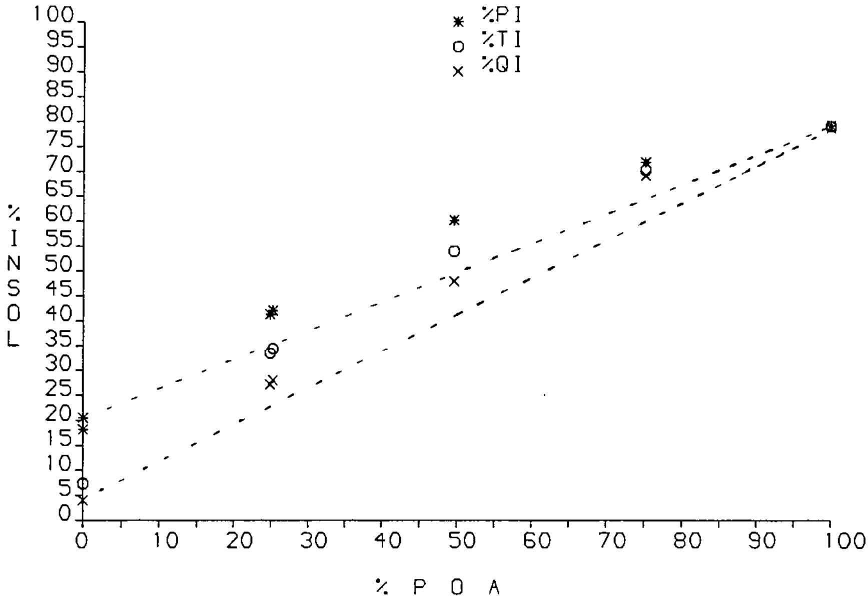

%PI
%TI
%QI
% INSOL
100
95
90
85
80
75
70
65
60
55
50
45
40
35
30
25
20
15
10
5
0
0
10
20
30
40
50
60
70
80
90
100
% POA

Fig. 10

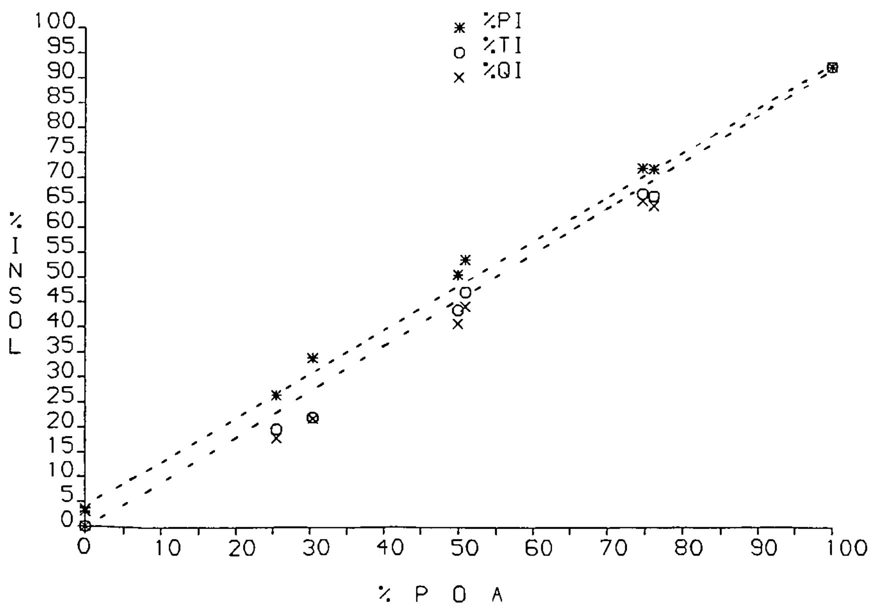

%PI
%TI
%QI
% INSOL
100
95
90
85
80
75
70
65
60
55
50
45
40
35
30
25
20
15
10
5
0
0
10
20
30
40
50
60
70
80
90
100
% POA

Fig. 11

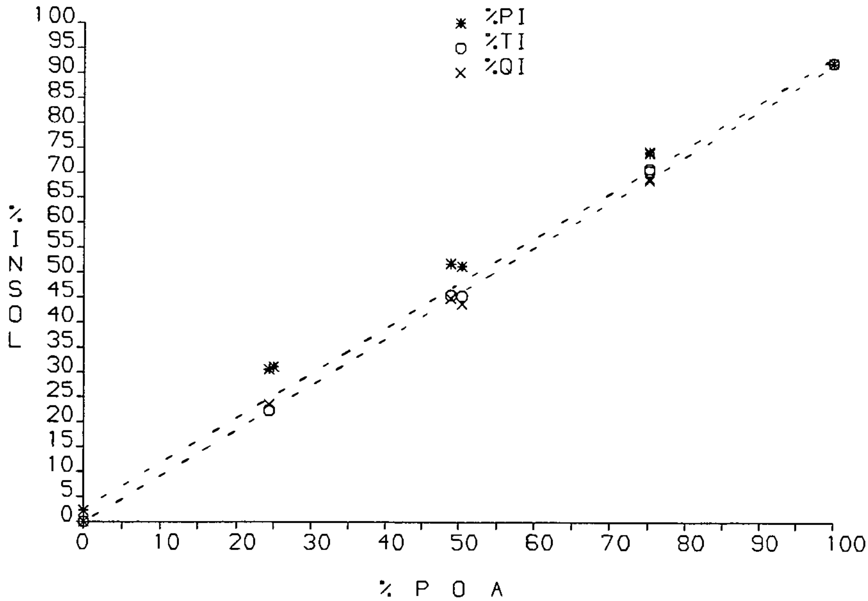
%PI
%TI
%QI
% INSOL
% POA
0
5
10
15
20
25
30
35
40
45
50
55
60
65
70
75
80
85
90
95
100
0
10
20
30
40
50
60
70
80
90
100

Fig. 12

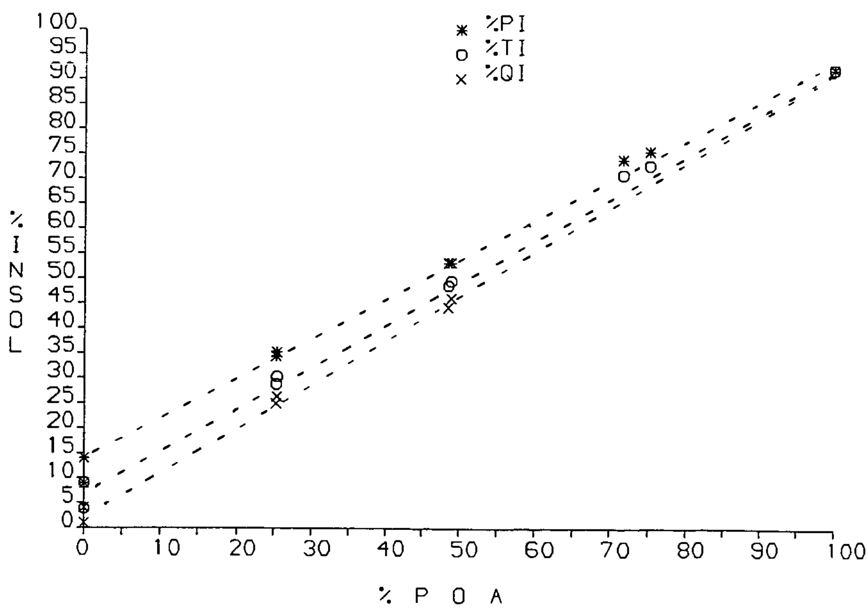
%PI
%TI
%QI
% INSOL
% POA
0
5
10
15
20
25
30
35
40
45
50
55
60
65
70
75
80
85
90
95
100
0
10
20
30
40
50
60
70
80
90
100

Fig. 13

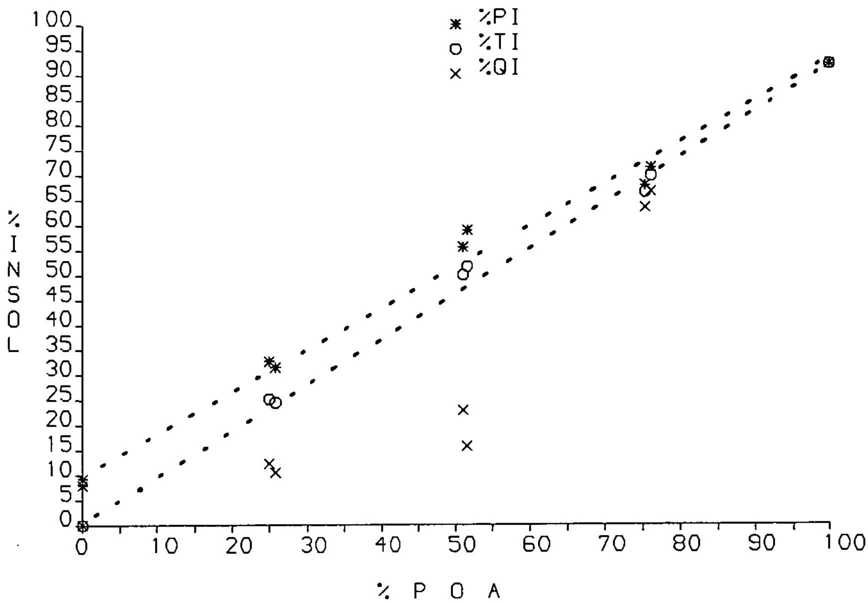
%PI
%TI
%QI
% INSOL
% POA
0
5
10
15
20
25
30
35
40
45
50
55
60
65
70
75
80
85
90
95
100

Fig. 14

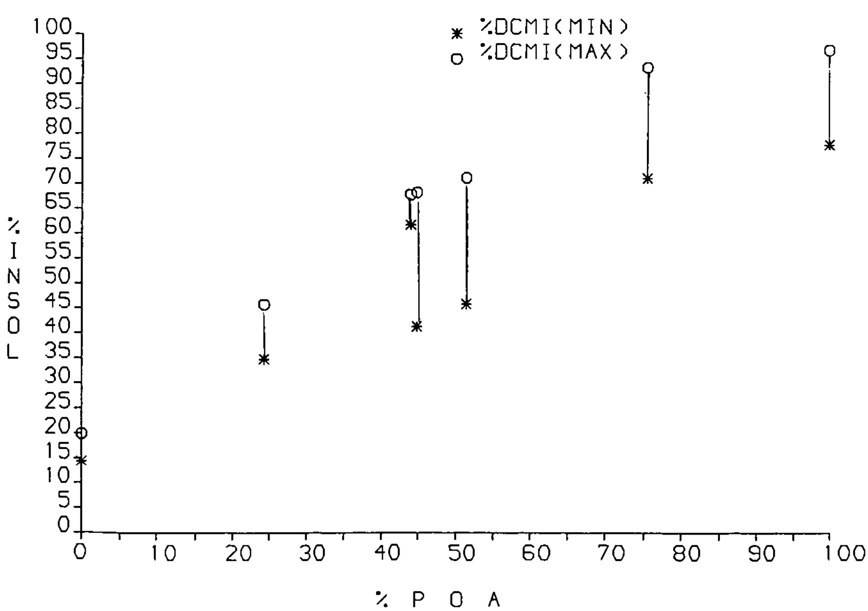
%DCMI(MIN)
%DCMI(MAX)
% INSOL
% POA
0
5
10
15
20
25
30
35
40
45
50
55
60
65
70
75
80
85
90
95
100

COPROCESSING WITH PETROLEUM RESID AND MARTIN LAKE LIGNITE

T.R. Aulich, P.L. Holm, C.L. Knudson and J.R. Rindt

University of North Dakota
Energy and Minerals Research Center
Grand Forks, ND 58202

ABSTRACT

Petroleum resids have traditionally been overlooked as fuel sources despite their significant energy content. These products often contain iron, nickel, and vanadium in concentrations which rapidly deactivate or "poison" hydrogenation catalysts. Reacting petroleum resids with coal under liquefaction conditions or "coprocessing" has been proposed as an economic method for the removal of trace metals. Coprocessing involves the upgrading of a petroleum resid in a reaction with coal. While the resid acts as the liquefaction solvent some of the coal is converted to products, and the unconverted coal acts as a sink for metals. This paper will describe the results of tests to determine the increase in liquid product yields, and the reduction in the concentrations of trace metals achieved by coprocessing Arabian resid with Martin Lake lignite. Four batch-autoclave tests were made using various catalysts and conditions. Distillable products comprising 45-60 wt% of the individual product slurries were found to contain 2-8 ppm nickel and vanadium, and 9-41 ppm iron.

INTRODUCTION

Many petroleum resids contain iron, nickel, and vanadium. These contaminants are found in some resids in concentrations of several hundred parts per million (ppm), and can greatly reduce the value of a resid as a fuel source (1,2). Trace metals in general and vanadium in particular are known to deactivate or "poison" metal-based catalysts used in hydrogenation reactions to upgrade resids (3,4). As a catalyst becomes coated with metals its exposed, active surface area is gradually reduced, resulting in a decrease in catalytic activity (3,5). In order to hydrogenate resids and improve their potential as significant energy sources, trace metals concentrations must be economically reduced to tolerable levels. Several methods for accomplishing this have been studied including "coprocessing" (3,6-14). Coprocessing approaches the upgrading of petroleum resids as a concurrent process with the liquefaction of coal (15-23). While the resid acts as the liquefaction solvent some of the coal is converted to products, and the unconverted coal acts as a sink for metals.

In assessing the feasibility of coprocessing it may be necessary to consider a combination of three parameters rather than one. An ideal coprocessing reaction system would provide a product with minimal trace metals concentrations along with maximum amounts of converted coal and upgraded resid.

REACTION CONDITIONS

Data for this paper were obtained from the analysis of product slurries from four, two-stage batch autoclave tests with Martin Lake lignite and Lummus Arabian resid. Except for varying catalysts, reaction conditions for all four tests were essentially identical and are listed in Table 1.

TABLE 1

COPROCESSING REACTION CONDITIONS

	Test 1	Test 2	Test 3	Test 4
Stage 1				
Residence Time (min)	40	40	40	40
Temp (^{o}C)	368	371	367	372
Pressure (psia)	4100	3875	4400	4370
Pressurizing Gas	CO	CO	CO	CO
Stage 2				
Residence Time (min)	10	10	10	10
Temp (^{o}C)	425	423	433	425
Pressure (psia)	2225	2325	2950	2970
Pressurizing Gas	H_2	H_2	H_2	H_2
Catalyst (both stages)	none	H_2S	Ammonium Molybdate	none

It should be noted that the autoclave tests described in Table 1 were designated as runs N377, N379, N382, and N383 according to documentation procedures established at UNDEMRC. For the purpose of simplifying discussion, throughout this paper the tests will be referred to as Tests 1, 2, 3, and 4, respectively.

Table 2 provides data relating reactants charged and moisture- and ash-free (MAF) coal conversions achieved for each batch autoclave test. The data indicate that coal reactivity was increased by the presence of the catalysts, especially ammonium molybdate. Tests 1 and 4 were performed under nearly identical conditions to provide data on test-reproducibility, but gave substantially different conversions. There is speculation that the higher conversion achieved by Test 4 was influenced by the presence in the autoclave of residual ammonium molybdate from Test 3. A more complete discussion of the test results in reference to product mix, reaction conditions, and catalyst effects can be found in Rindt, et. al. (24).

ANALYSIS OF PRODUCT SLURRIES BASED ON PENTANE-SOLUBILITY

To determine trace metals concentrations in coprocessing products as a function of pentane-solubility, samples of the product slurries from Tests 2, 3, and 4 were separated into pentane-soluble and insoluble fractions. Both fractions, and the raw product slurries from each test were analyzed for iron, nickel, and vanadium using an acid digestion technique. The pentane-soluble fraction of Arabian resid, the raw resid, and raw

Martin Lake lignite were also analyzed according to the same procedure.

TABLE 2

COMPOSITIONS AND RESULTS OF BATCH AUTOCLAVE TESTS

	Test 1	Test 2	Test 3	Test 4
wt as-received coal (g)	134.5	139.6	141.7	142.8
wt MAF coal (g)	93.8	97.8	99.6	100.0
wt solvent (g)	350.5	365.5	372.2	373.7
wt water added (g)	16.7	17.0	18.0	17.4
wt FS* (g)	501.7	522.1	531.9	533.9
% FS that is MAF coal	18.7	18.7	18.7	18.7
wt PS** (g)	472.8	473.9	487.4	464.9
% THFI*** (PS)	11.5	9.7	7.2	11.0
% ash (PS)	4.5	4.4	4.5	4.7
% MAF coal unconverted	35.4	25.3	13.2	29.2
% MAF coal converted	64.6	74.7	86.8	70.8
catalyst	none	H_2S	ammonium molybdate	none

* Feed slurry
** Product slurry
*** Tetrahydrofuran insolubles

Sample sizes ranged from approximately 200 mg for the pentane insolubles, to 600 mg for the pentane solubles, to 1000 mg for the raw product slurries and the resid. The coal sample size was 220 mg. Samples were weighed into 250 mL "Nalgene" plastic containers equipped with screw-on lids. Nitric and hydrofluoric acid were added in 20 and 2 mL amounts, respectively. Lids were placed lightly, as opposed to screwed on the containers, which were then heated in a microwave oven in groups of two, for five minutes on "medium" power. The microwave oven power output was calculated according to a method published by Kingston and Jassie (25), and found to be approximately 330 watts on the medium setting. After cooling, 1 gram of boric and 20 mL of methanesulfonic acid were added to each sample, and the resulting mixtures were heated for 90 minutes at 110°C in the oven of a gas chromatograph. Both heating steps were performed under a hood to safely remove any escaping vapors. The use of methanesulfonic acid is recommended as an effective means of removing metals from porphyrin complexes (26). After vacuum filtration the mixtures were diluted to 100 mL with deionized water and analyzed using inductively-coupled plasma spectroscopy (ICP). Results of the analyses are shown in Table 3.

TABLE 3

METALS CONTENT BASED ON PENTANE-SOLUBILITY

	Fe (ppm)	Ni (ppm)	V (ppm)
Test 2 product slurry	1700	45	91
pentane solubles	0	0	6
pentane insolubles	13000	190	370
Test 3 product slurry	1800	47	70
pentane solubles	17	4	6
pentane insolubles	16000	210	360
Test 4 product slurry	2400	57	100
pentane solubles	46	0	5
pentane insolubles	13000	180	380
Arabian resid raw	56	37	120
pentane solubles	0	8	28
Martin Lake coal	4300	0	24
NBS 8505 certified*	-	-	390
analyzed**	8	57	460
NBS 1634a certified*	31	29	56
analyzed**	27	31	61

* Values certified by National Bureau of Standards.
** Values obtained using described analysis.

The bottom two entries in Table 3 refer to Standard Research Materials provided by the National Bureau of Standards, and were included as a means of determining the accuracy of the analytical method. The standards, NBS 8505, vanadium in crude oil (no values for iron or nickel) and NBS 1634a, trace metals in fuel oil residual, were similar in consistency and color to the coprocessing product slurries. Comparison of NBS certified values with values obtained through analysis suggests that the analytical method may yield an error of up to 18%.

Table 4 compares analytically-obtained metals concentration values for the three product slurries with values obtained using a mass balance calculation. The calculations were done using pentane solubilities and the metals concentration values for the pentane-soluble and pentane-insoluble fractions found in Table 3. As an example, the Test 2 calculated value for vanadium was obtained with the following formula: 74.6%(6) + 25.4%(370) = 98. Comparison of values for iron suggests that something more than analytical error is contributing to the large difference between analyzed and calculated values. One possible explanation may derive from the digestion procedure since the same amount of acid was used to digest all the samples, regardless of weight or iron concentration. Digestion of the pentane-insolubles, which contained high concentrations of iron, was done using a small sample (200 mg). While digestion of the pentane-solubles utilized a larger sample (600 mg), the iron in the samples was much less concentrated. In the case of the product slurry samples, the combination of large sample size (1000 mg) and moderately high iron concentration may have resulted in an incomplete digestion due to an overabundance of iron in comparison to acid.

TABLE 4

COMPARISON OF ANALYZED METALS CONTENT TO MASS BALANCE CALCULATED METALS CONTENT OF PRODUCT SLURRIES (PENTANE SOLUBILITY BASIS)

	Pentane Solubility (%)	Fe (ppm)	Ni (ppm)	V (ppm)
Test 2	74.6			
Analyzed value		1700	45	91
Calculated value		3300	48	98
Test 3	77.4			
Analyzed value		1800	47	70
Calculated value		3600	51	86
Test 4	72.7			
Analyzed value		2400	57	100
Calculated value		3600	49	107

DISTILLATION OF PRODUCT SLURRIES

The effect of coprocessing on trace metals concentrations was also examined as a function of percent product slurry distillable. Vacuum distillations were carried out using Pyrex glassware with T 14/20 joints. Slow flowing water was used as the first stage condenser cooling fluid. A distillation column approximately 20 cm long was used to reduce the chance of non-distilled sample carryover or "bumping". The apparatus was fitted with a fractionating device and operated under a vacuum of about 5 torr as measured with a mercury-filled McLeod Gauge. Product slurry samples of 10 - 25 g were placed into a 30 ml round bottom flask, heated with a mantle, and stirred with a Teflon-coated magnetic stir bar. As heating progressed the system pressure was slowly reduced. In order to minimize the threat of bumping, the sample was stirred vigorously and the distillation column was warmed to 85°C using glass fabric heating tape. Heating the column allowed low-boiling volatile components to remain in the vapor phase instead of condensing and dripping back into the distillation pot. As the system pressure was gradually reduced to 5 torr, the voltage to the heating mantle was gradually increased to 130 volts, a process that took about 30 - 40 minutes.

The first fraction was collected until the temperature in the distillation head reached 120°C, and is identified as the initial boiling point (IBP) to 120°C fraction. Following collection of the first fraction the water flow to the condenser was shut off and the condenser was drained. The remainder of the distillation was carried out using air as the condenser cooling fluid. The second fraction was collected over a temperature range of 120-260°C, and the third fraction was collected over a temperature range of 260°C to the "end point". The end point is defined as the temperature at which one or more of the following conditions exist: 1) the temperature in the head piece remains constant, 2) the temperature in the head piece is consistently falling, or 3) decomposition of the sample is evident (the sample remaining in the pot starts smoking). Two other fractions collected were the cold trap fraction and the pot residue. The cold trap fraction refers to the material collected in the cold trap, which is located between the distillation pot and the condenser, and cooled by a slurry bath of dry ice and 2-propanol. This material is a solid while in the cold trap, but becomes a volatile liquid at room temperature. The pot residue refers to the material remaining in the distillation pot after the end point has been reached and the distillation is complete. This fraction contains a solid phase and a very viscous liquid phase.

ANALYSIS OF PRODUCT SLURRIES BASED ON DISTILLATION CUTS

The technique used for the digestion of the distillates and residues (developed by David J. Hassett at the University of North Dakota Energy and Minerals Research Center) required a sample size of about 1 g. Placement of the sample in a 100 mL Pyrex volumetric flask was followed by the addition of 10 mL Ultrex concentrated sulfuric acid. The flask was then placed on a hot plate and the mixture was heated. When dense white fumes of sulfur trioxide began to appear, a few drops of concentrated Ultrex nitric acid were added to the mixture. The application of heat continued and dense white fumes of sulfur trioxide again began to appear, at which time several more drops of nitric acid were added. This cycle was repeated until the mixture became clear, or no darker than a dilute straw color. A clear solution indicates that the major portion of the organic matter has been oxidized. After cooling, the solution was diluted to 100 mL with deionized water and analyzed by ICP. A sample of Arabian resid was also distilled, digested, and analyzed according to the same procedure, except that only three distillate fractions were collected. Martin Lake coal was prepared for ICP analysis by two separate methods. One sample was digested and the other was ashed. Table 5 displays the results of these analyses.

Comparison of analytically-obtained values with NBS-certified values for NBS 1634a, trace metals in fuel oil residual, helps demonstrate the reliability of the analytical method. As another check on the analysis, Table 6 compares analytically-obtained metals concentration values for the product slurries and resid with values obtained using a mass balance calculation. The mass balance calculation is similar to the calculation used in Table 4 except that distillate percentages rather than pentane solubilities are used to multiply the metals concentration values in Table 6.

TABLE 5

METALS CONCENTRATIONS BASED ON PERCENT PRODUCT SLURRY DISTILLABLE

	wt% product slurry	Fe (ppm)	Ni (ppm)	V (ppm)
Test 1 Prod. Slurry		4200	34	78
Cold trap	9.6	Below	detection	limits
IBP - 120°C	10.3	Below	detection	limits
120 - 260°C	31.7	7	4	4
260 - 275°C	6.2	75	40	40
Residue	42.2	10200	79	150
Test 2 Prod. Slurry		4000	37	81
Cold trap	4.4	Below	detection	limits
IBP - 120°C	13.6	Below	detection	limits
120 - 260°C	27.8	55	4	4
260 - 285°C	13.8	15	6	6
Residue	40.6	10200	99	180
Test 3 Prod. Slurry		4100	39	75
Cold trap	2.2	Below	detection	limits
IBP - 120°C	9.4	Below	detection	limits
120 - 260°C	30.5	12	4	4
260 - 305°C	16.1	7	6	6
Residue	37.3	10800	94	170
Test 4 Prod. Slurry		2700	30	65
Cold trap	2.7	Below	detection	limits
IBP - 120°C	14.6	Below	detection	limits
120 - 260°C	31.8	74	5	5
260 - 285°C	14.1	9	5	5
Residue	36.8	10500	130	260
Resid		1	36	12
120 - 260°C	26.1	1	2	1
260 - 295°C	16.3	26	2	2
Residue	57.6	14	62	19
Coal digested		3900	6	21
Coal ashed		4000	31	22
NBS 1634a analyzed		32	29	58
NBS 1634a certified		31	29	56

Since analyzed and calculated values are in reasonable agreement for Tests 1 - 3 and the resid, the large differences between values for Test 4 are probably due to a measurement error. With the exception of Test 4 the analyzed and calculated values for iron are very close, unlike the values in Table 4.

TABLE 6

ANALYZED METALS CONTENT COMPARED TO MASS BALANCE CALCULATED METALS CONTENT FOR PRODUCT SLURRIES (PERCENT DISTILLABLE BASIS)

	Fe (ppm)	Ni (ppm)	V (ppm)
Test 1			
Analyzed value	4200	34	78
Calculated value	4300	37	67
Test 2			
Analyzed value	4000	37	81
Calculated value	4200	42	75
Test 3			
Analyzed value	4100	39	75
Calculated value	4000	37	66
Test 4			
Analyzed value	2700	30	65
Calculated value	3900	50	98
Resid			
Analyzed value	1	36	12
Calculated value	13	37	12

This may be due to the digestion technique. While the first technique utilized a standard amount of acid for all samples, the amount of acid used in the second technique was individually determined for each sample based on the amount of oxidizable material contained in the sample. Calculated and analyzed values for nickel and vanadium in the resid are much closer than similar values for the product slurries from Tests 1 - 3. This could be because their were fewer chances for analytical error in the resid analysis since only three distillate fractions were obtained, as opposed to five for the product slurries.

COMPARISON OF DIGESTION TECHNIQUES

Table 7 compares analyzed metals concentration values for the product slurries to values that were expected based on feed slurry composition data. All analytical data in Table 7 are the result of analyses using the methanesulfonic acid digestion technique. The metals contents of the coal and resid were used to calculate the total metals content in grams for each slurry charged in the autoclave. By assuming grams metal in feed slurry equals grams metal in product slurry for the three metals, ppm values were calculated based on the weight of total product slurry recovered. Also included in the table is the ratio of expected value to analyzed value for the three metals in each test.

TABLE 7

EXPECTED COMPARED TO ANALYZED METALS CONTENTS BASED ON METHANESULFONIC ACID DIGESTIONS

	Fe (ppm)	Ni (ppm)	V (ppm)
Test 2 expected	1300	29	93
Test 2 analyzed	1700	45	91
expected / analyzed	0.76	0.64	1.02
Test 3 expected	1300	28	99
Test 3 analyzed	1800	47	70
expected / analyzed	0.72	0.60	1.41
Test 4 expected	1400	30	104
Test 4 analyzed	2400	57	100
expected / analyzed	0.58	0.53	1.04

Table 8 also compares analyzed metals contents of the product slurries to expected metals contents based on feed slurry composition data. All analytical data in Table 8 are the result of analyses using the Ultrex acid digestion technique.

TABLE 8

EXPECTED COMPARED TO ANALYZED METALS CONTENTS BASED ON ULTREX ACID DIGESTIONS

	Fe (ppm)	Ni (ppm)	V (ppm)
Test 1 expected	1100	28	15
Test 1 analyzed	4200	34	78
expected / analyzed	0.26	0.82	0.19
Test 2 expected	1200	30	16
Test 2 analyzed	4000	37	81
expected / analyzed	0.30	0.81	0.20
Test 3 expected	1200	29	16
Test 3 analyzed	4100	39	75
expected / analyzed	0.29	0.74	0.21
Test 4 expected	1200	31	16
Test 4 analyzed	2700	30	65
expected / analyzed	0.44	1.03	0.24

The most consistent relationship between analyzed and expected values in either Table 7 or Table 8 is evident in the comparison of ratios for Tests 1 - 3 in the Ultrex acid digestion matrix. Although the analyzed values do not match the expected values, they are reasonably precise and consistent in their variation from the expected values. (Data from Test 4 do not correlate well with data from Tests 1 - 3, but, as previously discussed, it appears likely an error was made, in either the processing or analysis of the Test 4 product slurry.) The ratios displayed in Table 8 indicate that a greater degree of analytical precision is achievable through the use of the Ultrex acid digestion. The consistent variation in analyzed values suggests that a consistently performed step in the reaction process is responsible for the inaccuracy of the analyzed values. The higher than expected analyzed values for iron may be a result of storing the product slurries in metal cans upon their removal from the autoclave.

COMPARISON OF PRODUCT RECOVERY METHODS

Pentane extraction and distillation were compared as methods of recovering the largest product yield with the lowest metals concentrations possible. Table 9 displays metals contents as a function of pentane solubility, along with coal conversions achieved for tests 2, 3, and 4. Pentane solubility and pentane-solubles metals contents are also included for the Arabian resid.

TABLE 9

METALS CONTENT AS A FUNCTION OF PENTANE-SOLUBILITY

	Pentane Solubility (%)	Fe (ppm)	Ni (ppm)	V (ppm)	% MAF coal converted
Test 2	74.6	0	0	6	74.7
Test 3	77.4	17	4	6	86.8
Test 4	72.7	46	0	5	70.8
Resid	80.3	0	8	28	

The data in Table 9 suggest that coprocessing may have potential as a means of reducing nickel and vanadium concentrations in the pentane-soluble fraction of Arabian resid. Since the feed slurries for the autoclave tests contained approximately 72% resid by weight, if no metals were removed during coprocessing, the pentane-soluble fraction of the product slurries should contain about 72% of 28 ppm, or 20 ppm vanadium. (Although this calculation is meaningful, it is not absolutely correct since it does not account for some gas production during the reaction and slight differences in pentane solubilities.)

Table 10 displays metals contents as a function of total product slurry distillable, along with coal conversions for the four tests. Similar data is included for the resid.

TABLE 10

METALS CONTENT AS A FUNCTION OF TOTAL DISTILLATE

	% Distillable	Fe (ppm)	Ni (ppm)	V (ppm)	% MAF coal Converted
Test 1	45	15	7.8	7.8	64.6
Test 2	54	32	3.5	3.5	74.7
Test 3	54	8.7	1.7	1.7	86.8
Test 4	60	41	3.8	3.8	70.8
Resid	42	11	2.0	1.4	

CONCLUSIONS

On the basis of this preliminary study, coprocessing appears to have merit as a means of reducing catalyst-poisoning metals concentrations in petroleum resids. However, in order to properly evaluate coprocessing, coal conversion and extent of resid-upgrading need to be assessed in terms of reaction cost and product value. Also, a larger, more accurate analytical data base is required to validate the metals concentration values.

According to this study, pentane extraction of the product slurry provides a greater usable product yield than distillation, and the pentane-soluble product contains iron, nickel, and vanadium in concentrations comparable to those of the distillate product. However, because of more and greater inconsistencies in data acquired using the methanesulfonic acid digestion, in order to properly compare product recovery methods it would be necessary to analyze a sample matrix based on pentane-solubility using the Ultrex acid digestion.

REFERENCES

1. Nelson, W. L., "Petroleum Refinery Engineering", 4th Edition, McGraw Hill Book Co. Inc., New York, 1958, 783.
2. Abu-Elgheit, M. A., Symposium on Characterization of Heavy Ends in Petroleum, presented before the Division of Petroleum Chemistry, American Chemical Society Meeting, New York, August 23-28, 1981, 912-914.
3. Speight, J. G. Annual Review of Energy, 11, 253, (1986).
4. Narain, N. K., R. E. Tischer, G J. Stiegel, D. L. Cillo, and M. Krishnamurthy, Demetallization of Coal Liquid Residuum; Topical Report, DOE/PETC/TR-86/6, June, 1986.
5. Silbernagel, B. G., and K. L. Riley, "Catalyst Deactivation", B. Delmon and G. F. Fromont, Editors, Elsevier Scientific Publishing Co., Amsterdam, The Netherlands, 1980, 313-321.
6. Rankel, L. A., and L. D. Rollmann, Fuel, 62, 44, (1983).
7. Yan, T. Y., U. S. Patent, 4 369 747, (1983).
8. Yan, T. Y., U. S. Patent, 4 334 976, (1982).
9. Yan, T. Y., U. S. Patent, 4 317 711, (1982).

10. Belinko, K., D. J. Patmore, R. H. Packwood, R. Ranganathan, U. S. Patent, 4 376 695, (1983).
11. VanDriesen, R. P., and L. L. Fornoff, Heavy Oil Upgrading Via Hydrocracking Economics; The Future of Heavy Crude and Tar Sands, International Conference on Future of Heavy Crude and Tar Sands, Caracas, Venezuela, February, 7, 1982, McGraw-Hill Inc., New York, (1984) 1195-1205.
12. Li, T. P., and R. J. Rosscup, U. S. Patent, 3 377 268 (1968).
13. Chakraborty, S., and V. K. Bhatia, Res. Ind., 25, 88, (1980).
14. Erdman, J. G., U. S. Patent, 3 190 829, (1965).
15. Audeh, C. A., U. S. Patent, 4 390 409, (1983).
16. Willson, W. G., C. L. Knudson, and J. R. Rindt, Low Rank Coal Direct Liquefaction; Quarterly Technical Progress Report, October - December, 1986, DOE-FC21-86MC-10637, 2-8.
17. Sendlein, L. V., Cooperative Research in Coal Liquefaction Infratechnology and Generic Technology Development; Quarterly Report, June - September, 1986, DOE-FC22-85PC-80009-T15.
18. Sendlein, L. V., and G. P. Huffman, Cooperative Research in Coal Liquefaction Infratechnology and Generic Technology Development; Quarterly Report, September - December, 1986, DOE-FC22-85PC-80009-T19.
19. Curtis, C. W., J. A. Guin, and A. R. Tarrer, Catalytic Co-Processing: Combined Processing of Coal and Heavy Resids; Final Report, July, 1982 - January, 1986, DOE-PC50793-T14.
20. Curtis, C. W., J. A. Guin, and A. R. Tarrer, Interactive Chemistry of Coal-Petroleum Processing; Progress Report, June - September 1986, DOE-FG22-85PC80502.
21. Lett, R G., and A. V. Cugini, Coprocessing Studies, presented at DOE Direct Liquefaction Contractor's Review Meeting, Pittsburgh, PA, October 22, 1986.
22. Brainard, A., Y. Shah, J. Tierney, I. Wender, A. Joseph, A. Kerkar, S. Ozturk, and A. Sayari, Coprocessing of Coal with Heavy Oils:, Coal Liquefaction: Investigation of Reactor Performance, Role of Catalysts, and PCT Properties; Technical Progress Report, November, 1985, DOE-PC-60054-T9.
23. Kulik, C., Coal-Oil Coprocessing: Phase 1, Project 2657-1; Interim Report, March 1987, Palo Alto, CA, EPRI AP-5101.
24. Rindt, J. R., M. D. Hetland, C. L. Knudson, and W. G. Willson, Direct Liquefaction of Low-Rank Coals; Annual Technical Report, April 1986 - March 1987, DOE-FC21-86MC10637.
25. Kingston, H. M., and L. B. Jassie, Anal. Chem., 58, 2534, (1986).
26. Martin, J., E. Quirke, G. J. Shaw, P. D. Soper, J. R. Maxwell, Tetrahedron, 36, 3621, (1985).

STABLE CARBON ISOTOPE ANALYSIS OF COAL/PETROLEUM COPROCESSING PRODUCTS

R. A. Winschel and F. P. Burke
Consolidation Coal Company, Research & Development
4000 Brownsville Road, Library, PA 15129

ABSTRACT

Coprocessing involves the simultaneous upgrading of coal and petroleum resid by catalytic hydroconversion. To obtain a kinetic/mechanistic description of the process, it is useful if not necessary to be able to distinguish the relative contributions of coal and petroleum to the product mixtures. In this paper, the method of stable carbon isotope ratio analysis is shown to be sufficiently sensitive to determine the relative concentrations of coal and petroleum carbon in coprocessing products. Selective isotopic fractionation does not appear to occur to a significant extent, although additional work is needed to confirm this preliminary conclusion. Application of the method to the coprocessing of Wyodak and Illinois 6 coals with a Lloydminster resid by the Signal Research/UOP process is shown to yield valid results of use in process interpretation and optimization.

INTRODUCTION

A noteworthy recent entry in the list of developing synthetic fuels processes is the concept of coal/oil coprocessing. In coprocessing, a petroleum resid is used as the vehicle to convey coal to a reaction vessel which simultaneously converts the two to distillate mixtures which are either finished products or suitable feeds for more conventional petroleum refinery processes. The incentive for the development of coprocessing lies in its potential to replace a portion of the petroleum feedstock with a lower cost hydrocarbon source while minimizing the recycle requirements which increase the capital costs of a grassroots coal liquefaction plant. To the extent that coprocessing can be integrated with existing refinery capacity, it may find some near-term application if conventional feedstocks are unavailable. A chemical or physical synergy has also been reported by some investigators who observe better results for coprocessing than for the processing of either individual feedstock. An excellent overview of industrial and academic research in the area can be found in the preprints of the American Chemical Society's "Symposium on Coprocessing and Two-Stage Liquefaction" held at the society's Fall 1986 National Meeting (1).

In the development of hydrocarbon conversion processes, it is useful if not essential to be able to describe the hydrogenation, cracking and heteroatom (O,N,S) removal reactions which control product yields and qualities. Ideally, these reactions would be known in sufficient detail to allow a kinetic/mechanistic model to be derived which would assist in data interpretation and process optimization. For coprocessing, the development of such a model is complicated by the presence of two feedstocks greatly different in composition. The ability to distinguish the reactions of the coal and petroleum components of the feed would be a useful tool in process development.

This paper describes the validation and application of the measurement of stable carbon isotope ratios to quantitatively determine the relative concentrations of coal- and petroleum-derived components in coprocessing products. The method relies on the difference between their $^{13}C/^{12}C$ ratios to calculate the ratio of the coal and petroleum carbon in product mixtures containing the two. Since the carbon contents of these materials are typically 85% to 90%, this provides an excellent estimate of the overall mass compositions. The measurement of carbon isotope ratios is standard practice in the petroleum industry and its application is conceptually straightforward. However, several significant questions must be resolved. First, is the method sufficiently precise and are the differences between the carbon isotope ratios of the relevant materials large enough to obtain experimentally meaningful results? Second, does selective isotopic fractionation occur, or do all the products retain the ratio of their individual parent feedstock? Third, do actual applications confirm the utility of the method by providing meaningful process results? The work described in this paper addresses these three questions.

CARBON ISOTOPE RATIOS OF COAL AND PETROLEUM RESIDS

Carbon isotope ratios are determined by quantitatively converting the carbon in a sample to CO_2 and measuring the relative amounts of the isotopically different CO_2 species. The resulting ratio, corrected for oxygen isotopes, is compared to that of a standard material and the result is reported as the relative difference.

$$\delta = \left(\frac{(^{13}C/^{12}C)_{Sample}}{(^{13}C/^{12}C)_{Standard}} - 1 \right) \times 1000$$

The standard used in this work is a Peedee belemnite (PDB)(2), a Cretaceous marine organism whose shell consists of calcium carbonate. Therefore, all ratios are reported relative to PDB. Experimental details have been reported elsewhere (3).

If the carbon isotope ratios of the feedstocks are known and are not identical, the percentage of coal or petroleum carbon, for example, in a coprocessing product can be calculated as

$$\%\ \text{Petroleum Carbon} = \left(\frac{\delta\ \text{Sample} - \delta\ \text{Coal}}{\delta\ \text{Petroleum} - \delta\ \text{Coal}} \right) \times 100$$

This equation requires a sufficient difference between the carbon isotope ratios of the coal and petroleum to be of practical use. Table 1 presents the δ values for the coals and petroleum resids used in the work reported here. Despite the variation in the coal rank from subbituminous (Wyodak) to hvAb (Pittsburgh), the carbon isotope ratios of the coals are essentially the same. By contrast, the resids show a considerable range, although all have absolute values greater than those of the coals. Table 1 also provides the standard deviations, based on at least triplicate analyses, for these feedstocks. These values give a good indication of the intrinsic precision of the analytical method, and are comfortably small relative to the differences between the coal and petroleum resids.

VALIDATION OF METHOD

A critical assumption in the application of this method is that significant isotopic fractionation does not occur. That is, the coal- or petroleum-derived portion of the product mixture must retain the same carbon isotope ratio as the parent feed. Although significant isotope fractionation is not expected (3), some work has been initiated to verify this assumption. In the first test, a light oil, heavy oil and vacuum resid from the LC-Fining of an Arab Heavy crude, supplied by Lummus, were analyzed. The results, shown below, indicate that the products are not substantially different. Comparison to the feed material would have been desirable, but a valid feed sample was not obtained.

LC-Finer Products	$\delta \pm$ Std Dev
Light Oil (600°F$^-$)	-27.01
Heavy Oil (600°F$^+$)	-26.76
Vacuum Resid (975°F$^+$)	-26.86 ±0.11
Average	-26.87 ±0.09

In a second test of isotopic fractionation, a set of petroleum samples, supplied by R. Lett of PETC (DOE) were analyzed. These samples consisted of a Maya atmospheric tower bottoms (ATB) and its heptane soluble and insoluble fractions. The results, below, indicate the insensitivity of the carbon isotope ratio to this type of solubility fractionation.

	$\delta \pm$ Std Dev
Maya ATB	-27.66 ±0.08
Heptane Solubles	-27.66 ±0.08
Heptane Insolubles	-27.28 ±0.07
Average	-27.53 ±0.22

As a further investigation of the possibility of isotopic fractionation, products from the Wilsonville coal liquefaction pilot plant made during operations with Illinois 6 (Burning Star coal) were compared. The results below are for a first-stage vacuum tower distillate (V-178) from Integrated Two-Stage Liquefaction operations and for resids (850°F$^+$) from two different runs. KMV-203 is a heavy deashed thermal resid from Run 245. V-131B is a pasting solvent resid from Run 247.

	$\delta \pm$ Std Dev
V-178	24.14 ±0.03
KMV-203 (Run 245, 850°F$^+$)	23.79 ±0.03
V-131B (Run 247, 850°F$^+$)	23.8 ±0.1
Average	23.91 ±0.20

Again, the product isotope ratios are in good agreement, despite the fact that these products were made during different runs many months apart. The isotope ratios are also in reasonable agreement with the values for Illinois 6 coal given in Table 1, although neither of these Illinois 6 samples was obtained from Wilsonville.

Finally, carbon isotope ratios were determined for two samples of Lloydminster resid provided by Signal Research/UOP. These samples were prepared by distillation of a single feedstock.

Resid	Vol % Overhead (D-1160)	mol wt (amu)	δ
17-R7	5.0	1117	-29.81
18-R8	26.5	755	-29.94

Despite their considerably different boiling ranges, these resids have equivalent carbon isotope ratios.

Although these results are not definitive, they indicate that selective isotope fractionation, at least to a first approximation, is not occurring to a great extent as a result of hydroprocessing, distillation, or solubility fractionation. No gas samples were analyzed, and previous work indicates that selective isotope enrichment of the gas may be significant, particularly at low gas yields (4). However, this effect is not expected to significantly alter the carbon isotope ratios of the distillate and residual liquids which are the main reaction products. While this remains a necessary area for further investigation, the possible effects of selective isotopic fractionation are ignored, with some reason for confidence, in this report.

APPLICATION TO SIGNAL RESEARCH/UOP COPROCESSING RUNS

Signal Research/UOP (UOP) is developing a coprocessing technology that employs a proprietary slurry-phase catalyst in a single-stage reactor. To evaluate the utility of the carbon isotope method in a practical application, a set of four feedstock samples and vacuum overhead and toluene-soluble vacuum bottoms products from sixteen continuous coprocessing runs were obtained from UOP. The toluene-insoluble portions of the vacuum bottoms, containing unconverted coal, ash and catalyst, were removed by UOP specifically to provide samples free of their proprietary catalyst. Reaction conditions and yield data are given in Table 2. Additional data were given elsewhere (3). These data were supplied by UOP. Table 3 gives the carbon isotope analyses and coal carbon as a percentage of total carbon in the vacuum overheads and bottoms, as calculated from the carbon isotope analyses.

UOP made two sets of runs, one with Illinois 6 coal and one with Wyodak coal. All the run periods reported here used a Lloydminster resid designated 18-R8. The carbon isotope data were used to calculate the ratios of coal carbon to total carbon in the two analyzed products. By comparing these values to the percentage of coal carbon in the total feed, it is possible to calculate a "selectivity" as the ratio of the measured percentage of coal carbon to that of the feed mixture. A value greater than one indicates that the given fraction is selectively enriched in coal carbon relative to petroleum carbon; a value less than unity indicates that the fraction is relatively enriched in petroleum carbon. A value equal to one indicates that, per carbon atom, the coal and petroleum respond similarly. Figures 1 and 2 show the selectivities for the runs with Wyodak and Illinois 6 coals. The selectivities are plotted versus vacuum bottoms yields, with increasing vacuum bottoms yields generally representing decreasing processing severity. The results show a clear distinction between the two coals. For the Wyodak coal, the vacuum overheads are consistently enriched in coal carbon, while the bottoms are depleted. This indicates that, per carbon atom, the Wyodak coal is more readily converted to distillate at these conditions than the petroleum resid. The Illinois 6 coal, by contrast, shows little average selectivity for the vacuum overheads, indicating that its carbon conversion to distillate is similar to that of the resid. There is some suggestion in the Illinois 6 data that the vacuum bottoms are depleted in coal carbon at low conversion (high vacuum bottoms yields) and enriched at high conversion. Since coal conversion from toluene insolubles to soluble resid increased with increasing severity, this increase in coal carbon may simply reflect this higher conversion.

Table 4 gives the percentages of coal carbon and petroleum carbon fed which are converted to overhead and bottoms products. These numbers are based on the carbon contents and yields of the products and their relative proportions of coal and petroleum carbon. Comparing the conversions of coal and petroleum carbon to vacuum overheads with reaction temperature (Table 2) by linear regression analysis yields the following results.

<u>Coal Carbon Conversion to Vacuum Overheads</u>

Illinois 6 Coal: % Conv = $-402 + 1.051$ T (°C), $R^2 = 0.89$
Wyodak Coal: % Conv = $-270 + 0.778$ T (°C), $R^2 = 0.81$

<u>Resid Carbon Conversion to Vacuum Overheads</u>

Both Coals: % Conv = $-296 + 0.804$ T (°C), $R^2 = 0.77$

This analysis of the data underscores the significant difference in the coprocessing behaviors of the Wyodak and Illinois 6 coals. By contrast, a single linear equation appears to adequately describe the temperature response of the resid conversion regardless of the coal with which it was coprocessed. These experiments were not specifically designed to demonstrate the effect of temperature in coprocessing, and other reaction conditions were simultaneously varied. However, the results indicate that carbon isotope ratios can be used to independently assess the relative reactions of coal and petroleum in coprocessing. Additional work is required to fully exploit the value of this technique to process development.

The authors are grateful for the assistance provided by Charles Luebke (UOP) and John Gatsis (Signal Research), Marvin Greene (Lummus), Richard Lett (PETC) and Lois Jones and Arnold Taylor (Conoco). This work was performed under U.S. DOE Contract DE-AC22-84PC70018.

REFERENCES

1. "Symposium on Coprocessing and Integrated Two-Stage Liquefaction", Preprints ACS Fuel Chem. Div., Anaheim, CA, September 1986.
2. Craig, H., Geochim. et Cosmochim. Acta, 3, 53-92 (1957).
3. Winschel, R. A., Robbins, G. A. and Burke, F. P., "Coal Liquefaction Process Solvent Characterization and Evaluation - Second Annual Report", DOE Report No. DOE/PC-70018-37, May 1987.
4. Sackett, W. M., Geochim. et Cosmochim. Acta, 42, 571 (1978).

TABLE 1. CARBON ISOTOPE RATIOS OF COPROCESSING FEEDS

Coals	δ %
Illinois 6 (Burning Star)	-24.32 ±0.07
Illinois 6 (UOP)	-24.34 ±0.04
Wyodak (Sarpy Creek)	-24.66 ±0.06
Wyodak (UOP)	-24.36
Pittsburgh (McElroy)	-23.80 ±0.1
Pittsburgh (Ireland)	-23.68 ±0.01
Petroleums	
Lloydminster Resid (17-R7)	-29.81
Arab Heavy Vacuum Resid	-26.21 ±0.28
Athabasca Vacuum Resid	-29.50 ±0.2
Maya Atmospheric Tower Bottoms	-27.66 ±0.08

TABLE 2. OPERATING CONDITIONS, CONVERSIONS, YIELDS AND ANALYSES - UOP COPROCESSING TESTS

	Operating Conditions			Product Yields, wt % of MAF Feed	
Test No.	Resid/MAF Coal wt Ratio	Space Velocity (a)	T, °C	Vacuum Overhead	Soluble Bottoms
Illinois 6 Coal					
16-0915	1.5	B	414	31.6	54.7
14-0905	1.5	B	425	45.1	41.6
15-0907	1.5	B	434	49.0	38.0
4-0513	2	1.25B	425	41.0	45.5
3-0508	2	B	413	32.2	54.3
2-0502	2	B	426	48.0	39.8
6-0522	2	B	431	49.4	36.5
5-0521	2	0.75B	424	45.2	39.7
Wyodak Coal					
10-1111	2	1.25B	427	48.0	34.5
7-1102	2	B	414	42.0	41.0
9-1108	2	B	425	46.6	35.9
8-1107	2	B	426	48.9	35.8
12-1118	2	B	431	53.5	30.9
11-1116	2	0.75B	425	48.5	33.5

(a) Overall space velocity, based on both coal and petroleum. "B" refers to proprietary base conditions.

TABLE 3. CARBON ISOTOPE ANALYSIS - UOP COPROCESSING SAMPLES

Test No.	Carbon Isotope Analyses δ^{13} C, % Vacuum Overhead	Carbon Isotope Analyses δ^{13} C, % Soluble Vacuum Bottoms	Coal Carbon as % of Total Carbon Vacuum Overhead	Coal Carbon as % of Total Carbon Soluble Vacuum Bottoms
Illinois 6 Coal Products				
16-0915	-27.88	-27.93	36.8	35.9
14-0905	-27.61	-27.78	41.6	38.6
15-0907	-27.60	-27.48	41.8	43.9
4-0513	-28.14	-28.13	32.1	32.3
3-0508	-28.11	-28.35	32.7	28.4
2-0502	-28.18	-27.85	31.4	37.3
6-0522	-28.21	-27.88	30.9	36.8
5-0521	-28.19	-27.87	31.2	37.0
Wyodak Coal Products				
10-1111	-27.89	-28.67	36.1	22.3
7-1102	-27.87	-28.86	36.4	19.0
9-1108	-27.88	-28.78	36.3	20.4
8-1107	-27.89	-28.66	36.1	22.5
12-1118	-27.83	-28.58	37.1	23.9
11-1116	-27.95	-28.46	35.0	26.1

TABLE 4. CONVERSION OF COAL AND PETROLEUM CARBON TO VACUUM OVERHEADS - SIGNAL/UOP COPROCESSING

Test No.	% Conversion to Vacuum Overhead Coal Carbon	% Conversion to Vacuum Overhead Resid Carbon
Illinois 6 Coal		
16-0915	30.5	33.6
14-0905	49.3	44.5
15-0907	54.2	48.5
4-0513	42.2	42.8
3-0508	33.6	33.3
2-0502	48.1	50.5
6-0522	48.6	52.3
5-0521	47.6	47.7
Wyodak Coal		
10-1111	60.0	46.9
7-1102	53.6	41.4
9-1108	59.5	45.5
8-1107	61.5	47.9
12-1118	68.8	51.6
11-1116	59.1	48.4

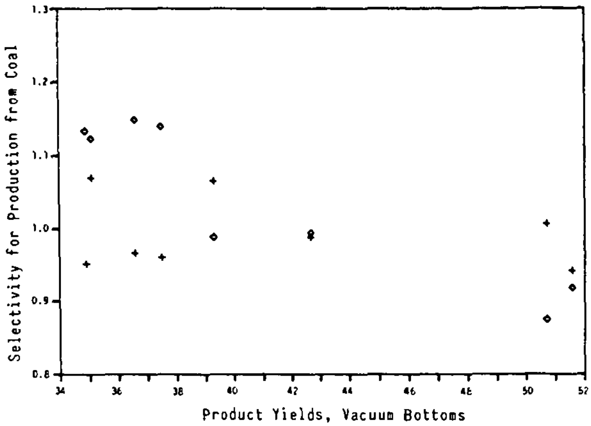

Figure 1. Selectivity vs Vacuum Bottoms Yields, UOP/Signal Research Coprocessing of Illinois 6 Coal, + - Vacuum Overhead, ◇ - Vacuum Bottoms.

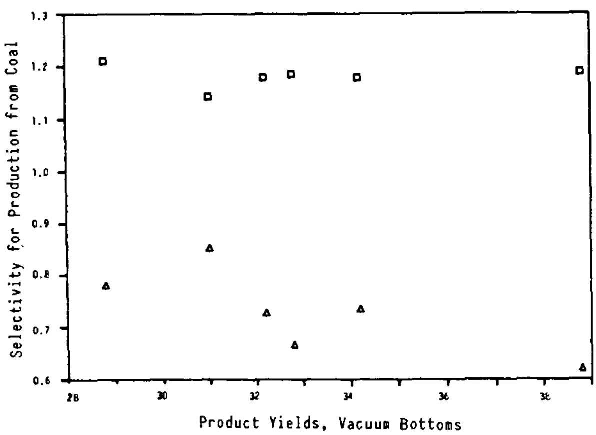

Figure 2. Selectivity vs Vacuum Bottoms Yields, UOP/Signal Research Coprocessing of Wyodak Coal, ◻ - Vacuum Overhead, △ - Vacuum Bottoms.

NATURAL VARIATIONS OF ^{13}C ABUNDANCE IN COAL AND BITUMEN AS A TOOL TO MONITOR CO-PROCESSING

K. Muehlenbachs[1], J.G. Steer[1], A. Hogg[2], T. Ohuchi[3] and G. Beaulieu[3]

[1] Department of Geology, University of Alberta, Edmonton Alberta, T6G 2E3 Canada
[2] Department of Chemistry, University of Alberta, Edmonton Alberta, T6G 2E3 Canada
[3] Coal Department, Alberta Research Council, Devon, Alberta T0C 1E0 Canada

INTRODUCTION

The use of coal to facilitate the generation of transportation grade fuel from bitumen, heavy oil or petroleum resids is a topic of continuing research.(1-3) In order to optimize the upgrading process one needs to know in what proportion each feedstock contributes to each product fraction. Conventional analytical methods are neither able to distinguish the contribution from either feedstock in the synthetic products, nor measure the subtle changes in product character in response to differing process conditions.

The inherent difference in the $^{13}C/^{12}C$ ratio between most coals and bitumen can be utilized as an isotopic tracer to assess the efficacy of co-processing. For example Vesta coal and Athabasca bitumen have sufficiently distinct $^{13}C/^{12}C$ ratios(4) that the measured $^{13}C/^{12}C$ of any product will accurately reflect the proportion of feed incorporated into the product. From the elemental analysis and the $^{13}C/^{12}C$ ratio of the feedstock and products one can calculate the amount of carbon derived from coal (CDC) in each product fraction.(4-5) Analogously the amount of bitumen derived carbon (BDC) can also be independently calculated. In this study the natural variation in ^{13}C concentration was utilized as an isotopic tracer to evaluate co-processing efficiency of a one litre stirred autoclave under differing process conditions. Process variables examined were coal concentration, several iron based catalysts (Fe_2O_3; Fe_2O_3 impregnated with TiO_2, SnO_2, or ZnO and a sludge obtained from a nickel refinery) and temperature.

EXPERIMENTAL PROCEDURE

Coal and bitumen with or without catalyst (3 wt% of Fe, based on daf. coal) were placed in a one litre magnadrive stirred autoclave equipped with an internal cooling coil. The autoclave was pressurized with H_2 (8.6 MPa. ambient temperature) and heated at 8°C per minute to the reaction temperature. The slurry was reacted at operational temperature (±1°C) for 45 minutes. Dried Vesta subbituminous coal (100 mesh) and the +350°C fraction of Athabasca bitumen were used as feeds. The major component fractions of Athabasca bitumen are shown in table 1 and the elemental and isotopic analyses are listed in table 2. Iron based catalysts were prepared by co-precipitation (atomic ratio of 1:1) as described by Tanabe *et al.* (6) The sludge was obtained from Sheritt Gordon's Fort Saskatchewan nickel refining plant (Fe_2O_3 74.1 wt%; Ni 19200 ppm., Co 3580 ppm., Mo 169 ppm.).

Table 1. Component Distribution of Bitumen (+350°C)

Fraction	Wt% Carbon
Distillate	14.9
Maltene	61.5
Asphaltene	23.6
Residue	0.0

Table 2. Elemental Analyses (wt%) of Vesta Coal and Athabasca Bitumen (+350°C)

Fraction	Coal	Bitumen
Carbon	71.6	82.4
Hydrogen	5.0	10.1
Nitrogen	1.7	0.5
Sulphur	1.0	4.9
Ash	17.0	0.7
Moisture	0.7	0.0
$\delta^{13}C$	-26.35	-30.46

† Values expressed in terms of PDB[7]

$\delta^{13}C$ of NBS 22 is -29.81 parts per thousand (ppt.) with respect to PDB.

In experiments involving changes in coal concentration 125 grams of stripped Athabasca bitumen (-350°C fraction removed by distillation) was co-processed with 0, 8, 15, 30 and 60 grams of vacuum dried Vesta subbituminous coal at an operational temperature of 430°C. A second set of autoclave runs was performed in which 125 gram aliquots of stripped bitumen were co-processed with 0,10, and 18 grams of Vesta coal. After reaction, the -300°C fraction was directly removed from the autoclave and trapped by condensation in an ice water trap, distilled to - 177°C then characterized using GC-MS. The influence of iron based catalyst upon coal solubilization was the second process variable examined. Coal (60 grams), stripped bitumen (125 grams), and various catalysts (no added catalyst, Fe_2O_3, Fe_2O_3/TiO_2, Fe_2O_3/SnO_2, Fe_2O_3/ZnO or nickel sludge) were reacted at 430°C. The third process variable examined was the influence of temperature upon co-processing. Three autoclave runs were performed in which 125 grams of stripped Athabasca bitumen were reacted with 60 grams of Vesta coal and Fe_2O_3 catalyst (3 wt% of Fe based on daf. coal weight) at 415°C, 430°C and 445°C.

The following fractions were isolated from the co-processed material: distillate (-524°C), maltene (n-pentane soluble), asphaltene (n-pentane insoluble - toluene soluble), and residue (toluene insoluble). Each product's elemental composition and $^{13}C/^{12}C$ ratio was measured.[4] Product gases were collected and analysed by GC. All the $^{13}C/^{12}C$ ratios were expressed in terms of the $\delta^{13}C$ notation of Craig[7] equation 1:

$$1)\qquad \delta^{13}C = \left(\frac{(^{13}C/^{12}C)_{sample} - (^{13}C/^{12}C)_{ref.}}{(^{13}C/^{12}C)_{ref.}}\right) X\ 1000$$

RESULTS AND DISCUSSION

Mass Balance Calculation

Contrast between the $^{13}C/^{12}C$ ratio of coal and bitumen may be utilized as a natural isotopic tracer to monitor coal or bitumen incorporation into synthetic product fractions. A two end member mixing model [8] can be algebraically derived to calculate the make up of the co-processed products, equation 2.

$$2)\ \%\ \text{COAL INCORPORATION} = \left(1- \frac{\delta^{13}C_{prod} - \delta^{13}C_{coal}}{\delta^{13}C_{bit} - \delta^{13}C_{coal}}\right) \text{X } 100\ \%$$

Two hydroprocessing experiments were performed using only bitumen in order to examine whether any isotopic shift would occur due to processing. Bitumen (125 grams) was processed at 430°C and bitumen (125 grams with 3 wt% Fe_2O_3) was processed at 445°C. Distillate (200°C to 524°C), maltene, asphaltene and residue fractions were found to be enriched (0.16, 0.37, 0.31 and 1.12 ppt. respectively) in ^{13}C relative to unprocessed bitumen fractions.[4] The naptha fraction was enriched in ^{12}C, (table 3). Such measurements serve as blanks and need to be substituted for $\delta^{13}C_{bit}$ in equation 2. In this study the calculated yields of carbon summed over all the fractions is within ±2% of the weight of the original charge.

Table 3: Isotopic Ratio of the Naptha Fraction (-177°C)

0 grams coal	-31.14 ppt.
10 grams coal	-30.99 ppt.
18 grams coal	-30.95 ppt.

† Values expressed in terms of PDB[7]

$\delta^{13}C$ of NBS 22 is -29.81 ppt. with respect to PDB.

Formation of crack gases enriches the residues in ^{13}C but the ^{12}C enrichment in the naptha is enigmatic. Two pathways for ^{12}C enrichment are possible; that large moieties have isotopic heterogeneity, or alternatively that the ^{12}C enrichment may result from a thermal process. Athabasca bitumen has been biodegraded to the stage where many of the original components, i.e. (alkanes and steranes) found in crude oils are no longer present.[9] However C_{27} to C_{29} steranes are released from the asphaltene fraction of Athabasca bitumen by hydropyrolysis[10] suggesting that the asphaltene fraction of bitumen may have incorporated alkanes from the original crude which are released upon thermal degradation. Recent work by Cyr *et al.* [11] indicates that in the highest molecular weight fraction (MW 16900) of Athabasca bitumen the aromatic core of the asphaltene is surrounded by alkyl chains with a mean length of 12. In nondegraded crude oil the alkane fraction is isotopically enriched in ^{12}C relative to the whole crude, while the cycloparaffin and aromatic fraction are relatively uniform.[12] These observations suggest that the observed ^{12}C enrichment of naptha may result from thermal degradation of moieties which have incorporated a portion of the original alkane fraction.

Alternatively, selective enrichment of a low molecular weight product fraction in ^{12}C by C-C bond scission is known to occur.[13-15] Pyrolysis of n-$C_{18}H_{38}$ at 500°C for one hour produced methane enriched in ^{12}C relative to the source by 15 ppt. The C_2 to C_4 gases showed similar but less pronounced enrichment with Sackett[15] suggesting that for C_2,C_3 and C_4 the isotope shift was 1/2,1/3 and 1/4 that of methane respectively.

Effect of Variations of Coal-Bitumen Ratio

Varying amounts of coal were co-processed with bitumen. Coal and bitumen incorporation into a product fraction has been calculated and plotted against the weight% of coal in the slurry, (figures 1,2). Co-processing experiments utilizing coal to bitumen ratios less than 15 wt%, exhibit a noticeable increase in distillate yield (14% to 17%) over and above distillate yields obtained by hydrotreatment of bitumen alone, (figure 1). Graphically there appears to be an antithetic correlation between bitumen-derived distillate and bitumen-derived maltene products. Increased distillate yield corresponds with a decrease in in the bitumen-derived maltene fraction. The shift to a more positive $\delta^{13}C$ value with increasing coal concentration, (table 3), indicates that coal is incorporated into the -177°C naptha fraction. For coal concentrations greater than 8 wt% the BDC incorporated into the maltenes are in excess of the maltene yields obtained from processing of bitumen alone. Increase in the maltene's BDC corresponds with a decrease in the BDC present in the asphaltene fraction. With increasing coal concentration, bitumen's incorporation into the asphaltene fraction decreases . Graphically it is more pronounced for low coal concentrations, (figure 1). Slurry compositions of 8 to 26 wt% coal show only a slight decrease in bitumen incorporation into asphaltenes over the entire range. The isotopically determined BDC yield of the distillate, maltene and asphaltene fractions suggest that the increase in distillate yields for coal-bitumen ratios of 4% to 8% is derived from the thermal degradation of the asphaltene and maltene fractions. The proportion of distillate derived solely from bitumen shows no appreciable change in yield for coal concentration in excess of 15 wt%, (figure 1). Higher coal concentration, however appear to enhance asphaltene conversion to maltene and residue fractions. The increase in bitumen's incorporation into residue parallels a measured increase in coal incorporation into residue, (figure 2). The sharp increase in residue is in part due to polymerization reactions (as evidenced by the increase in the bitumen-derived component of the residue), and in part by coal saturation in the slurry (as evidenced by the three fold increase in the coal-derived residue).

With increasing coal concentration, coal's contribution to each product fraction increases. Calculated yields of distillate (-524°C) solely derived from coal are observed to increase in near linear fashion with coal concentration, (figure 2). Incorporation of coal derived carbon (CDC) into the maltene fraction appears to be largely independent of coal concentration. For coal concentrations of 0 wt% to 15 wt%, a large relative increase in the coal derived proportion of the asphaltene exists. For concentrations in excess of 15 wt%, the amount of coal-derived asphaltenes appear to level off.

The naptha fraction recovered from three co-processing experiments for which 0,10 and 18 grams of Vesta coal were reacted with 137,126 or 126 grams of stripped bitumen was characterized using GC-(P(O)NA column) and GC-MS by means of retention times and library search of compounds. We have now identified, by means of GC-MS, in the naptha fraction of the 10 grams coal co-processing experiment , oxygen and sulphur bearing hydrocarbons; 2-3 dimethlythiophene, 2-4 dimethlythiophene, 2-3-4 trimethlythiophene, 2-3-5 trimethlythiophene, dimethylphenol and methylbenzothiophene.

Effect of Iron Based Catalyst

The effect of select metal oxides catalyst upon coal solubilization was the next process variable examined. The different catalysts affect the make-up of the synthetic liquids, (table 4). In all experiments the weight of feedstocks co-processed was held constant, 60 grams Vesta coal (35.4 grams carbon) and 125 grams of stripped Athabasca bitumen (102.3 grams carbon).

Table 4: Effect of Iron Based Catalyst (CDC, BDC* in grams)

Fraction	Blank		Fe_2O_3		Fe_2O_3/TiO_2		Fe_2O_3/SnO_2		Fe_2O_3/ZnO		Sludge	
	CDC	BDC	CDC	BDC	CDC	BDC	CDC	BDC	CDC	BDC	CDC	BDC
Distillate	7.3	52.7	6.7	46.1	6.5	46.1	7.7	46.1	8.8	54.2	7.6	49.6
Maltene	2.4	22.7	4.0	40.8	2.4	43.7	3.2	44.1	2.8	31.8	2.1	41.2
Asphaltene	9.7	9.5	17.6	11.8	18.7	11.6	13.5	8.7	12.2	11.3	16.5	10.4
Residue	13.5	5.8	5.7	0.2	6.7	0.1	10.4	1.8	10.5	2.2	7.6	0.8
Gas**	2.1	4.4	1.5	4.3	1.3	4.3	1.2	4.3	1.6	4.3	1.0	4.3
% Yield***	98.9	98.1	100.3	100.9	100.6	103.4	101.7	102.6	101.4	101.5	98.3	103.9

* Feeds: 60 g of coal (35.4 g carbon), 125 g of bitumen (102.3 g carbon)

** From GC analysis

*** Based on carbon in the feed

The contribution of both coal-derived carbon (CDC) and bitumen derived carbon (BDC) as calculated from $\delta^{13}C$ mass balance are listed for each product fraction. Isotopically calculated coal and bitumen contribution to the product fraction agree within 98 to 103% of the initial feedstock charge, (table 4).

Distribution of the CDC in both catalyzed and catalyst free experiments for the distillate and maltene fractions ranged from 6.5 to 8.8 grams. and 2.1 to 4.0 grams respectively. These results suggest that CDC incorporation into the maltene and distillate fractions may be largely independent of catalyst. Catalyst showed varying abilities to convert coal to asphaltene. Fe_2O_3 alone or Fe_2O_3/TiO_2 or sludge converted coal more effectively than did Fe_2O_3/SnO_2 to Fe_2O_3/ZnO; 16.5 to 17.6 grams for the former, 12.2 to 13.5 grams for the latter. For bitumen upgrading, large differences in the BDC incorporation into the residue exists. Feedstock bitumen, (table 2) contains negligible toluene insoluble material (residue), so BDC incorporation into the residue fraction must be due to coking. The blank run (no added catalyst) produces both a high coke yield (5.8 grams) and a high distillate yield (52.9 grams). Addition of catalyst strongly inhibited the formation of coke, 0.1 to 0.2 grams with Fe_2O_3 alone or with Fe_2O_3/TiO_2, 0.8 grams with sludge and 1.8 grams to 2.2 grams with Fe_2O_3/SnO_2 or Fe_2O_3/ZnO. Bitumen incorporation into residue appears to be closely related to distillate yield for experiments with added catalyst. The higher the residue yield, the more distillate obtained. Addition of Fe_2O_3/ZnO substantially increased distillate yield (54.2 grams), increased coke yields relative to other catalysts and decreased BDC incorporated into maltene fraction.

Effect of Temperature

Coke inhibition by Fe_2O_3 catalyst upon bitumen upgrading was investigated at three different temperatures, 415°C, 430°C and 445°C. The contribution of CDC and BDC to each product fraction is presented in (table 5). An initial charge of 60 grams of Vesta coal (35.4 grams carbon) and 125 grams of stripped Athabasca bitumen (102.3 grams) were used in all experiments.

Table 5: Effect of Temperature (BDC* and CDC in grams)

	(415°C)		(430°C)		(445°C)	
	CDC	BDC	CDC	BDC	CDC	BDC
Distillate	5.9	37.5	6.7	46.1	11.1	60.4
Maltene	2.5	52.2	4.0	40.8	3.5	18.9
Asphaltene	11.7	13.7	17.6	11.8	13.8	10.8
Residue	12.3	0.1	5.7	0.2	7.2	2.1
Gas**	-	3.6	1.5	4.3	3.0	3.9
% Yield***	90.3	104.5	100.3	100.9	102.4	92.0

* Feeds: 60 g of coal (35.4 g carbon),
126 g of bitumen (103.1 g carbon),
3 wt% Fe_2O_3 (based on daf coal wt.)

** From GC analysis

*** Based on feed carbon

Increasing operational temperatures from 415°C to 430°C increased coal incorporation into the maltene and asphaltene fractions (2.5 to 4.0 grams and 11.7 to 17.6 grams respectively), at the expense of the residue (decreased from 12.3 to 5.7 grams). Little change is observed in the coal derived distillate. At 415°C a large proportion of coal remains unreacted, 12.3 grams of coal derived residue out of an initial coal charge of 35.4 grams. Yields of BDC incorporated into distillate fraction increases with increasing temperature (37.5 to 46.1 grams) while bitumen contribution to the maltene and asphaltene fraction decreased (52.2 to 40.8 grams and 13.7 to 11.8 grams respectively).

Co-processing of bitumen and coal at 445°C generated significantly more distillate, but also more insoluble material. Coal derived distillate increased from 6.7 to 10.4 grams. Whereas coal incorporation into the residue fraction increased from 5.7 to 9.4 grams. The increase in distillate and residue was at the expense of a twofold decrease in CDC in the maltene and asphaltene fractions (4.0 to 1.4 grams and 17.6 to 9.6 grams respectively). With co-processing at 445°C an increase in bitumen's incorporation into distillate was also observed (46.1 to 60.4 grams). Coke formation in terms of insoluble matter (residue) sharply increased from .2 grams (430°C) to 2.2 grams (445°C). Increased distillate and residue yields correspond with a sharp decrease in maltene (40.8 to 18.9 grams). The asphaltene fraction remained nearly constant, 11.8 grams at 430°C to 10.8 grams at 445°C.

CONCLUSIONS

A stable isotope mass balance techniques was used to investigate the efficiency of single stage coal-bitumen co-processing for the solubilization of coal. The results indicate that during co-processing:

1) Uncatalyzed co-processing of coal-bitumen mixtures comprising of 5 to 10 wt% coal enhance bitumen conversion to distillate by 14 to 17%. Concordantly the bitumen derived component of the asphaltene fraction decreases from 32 to 49% with respect to yields obtained in the hydrotreatment of bitumen alone. Coal concentrations of 15 to 26 wt% result in no appreciable increases in distillate over processing of bitumen
2) Increase in coal concentration from 0 to 26 wt% results in a progressive increase in coal incorporation into the distillate, maltene, asphaltene and residue fractions; and that a change in coal concentration from 15 to 26 wt% results in a threefold increase in coal derived residue.
3) In the naptha fraction of co-processing experiment (5 wt% coal) dimethyl thiophenes, trimethyl thiophenes, dimethyl phenol and methyl benzothiophene have been detected using GC-MS. No contrast exists in compound types as determined by GC between coal-bitumen and bitumen only runs. Isotopic mass balance calculations indicate that coal is incorporated into these fractions.
4) Coal incorporation in the distillate and maltene fractions appears to be independent of the iron based catalyst used.
5) Iron based catalyst strongly inhibits coke formation from bitumen and increases coal solubilization into asphaltene fractions.
6) Fe_2O_3/ZnO and Fe_2O_3/SnO_2 increased residue yield from bitumen with respect to Fe_2O_3, Fe_2O_3/TiO_2, and nickel sludge.
7) Sludge from nickel refining can be used as an effective coal solubilization catalyst.
8) Autoclave reaction temperature of 445°C increased bitumen's conversion to distillate by 31% with respect to distillate yield obtained in co-processing at a temperature of 430°C. However a sharp increase in bitumen coking is observed in experiments processed at 445°C.

ACKNOWLEDGEMENTS

The research was partially funded by a grant-in-aid of research from the Alberta/Canada Energy Resources Research Fund, jointly established by the government of Canada and the government of Alberta and administered by the Alberta Office of Coal Research and Technology. The autoclave runs were performed by the Alberta Research Council, Coal Department.

LITERATURE CITED

1) Rahimi, P.M., Fouda, S.A. and Kelly, J.F., (1987), Fuel, 66, p. 1215-1218.
2) Rahimi, P.M., Fouda, S.A. and Kelly, J.F., (1987), Proceedings of the EPRI 12th Annual Fuel Science and Conversion Conference, May.
3) Böller, K. and Oelert, H.H, (1985), Proceedings 1985 International Conference on Coal Science, Sydney, October, p.35-38.
4) Steer, J.G., Muehlenbachs, K., Ohuchi, T., Carson, D., Doherty, B. and Ignasiak, B., (1987), Fourteenth Biennial Lignite Symposium on the Technology and Utilization of Low-Ranked Coals proceedings, May, p. 5 A2-1 to 5 A2-16.
5) Ohuchi, T., Steer, J.G., Muehlenbachs, K. and Carson, D., (1987), 1987 International Conference on Coal Science, 11, p. 379-382.
6) Tanabe, K., Hattori, H., Yamaguchi, T. and Iizuka, T.,(1984). Research on Coal Liquifaction and Gasification published by the Ministry of Education, Science and Culture, Japan, October.
7) Craig H., (1957), Geochim. Cosmochim. Acta., 12, p. 133-149.

8) Steer, J.G., Ohuchi, T. and Muelenbachs, K., (1986), First International Rolduc Symposium on Coal Science, April, p.114-116.
9) Deroo, G., Powell, T.G., Tissot, B. and McCrossan, R.G. (with contributions by P.A. Hacquebard), (1977), Geol. Surv. Can., Bull. 262, p. 136.
10) Fowler, M.G. and Brooks, P.W., (1987), Energy and Fuels, 1, p.459-467.
11) Cyr, N., McIntyre, D.D, Toth, G. and Strausz, O.P., (1987), Fuel, 66, p. 1709-1714.
12) Stahl, W.J., (1978), Geochim. Cosmochim. Acta., 42, p.1573-1577.
13) Friedrich, H.U. and Juntgen, H., (1972), Advances in Organic Geochimestry, Pergamon Press, Oxford, p. 639-646.
14) Sackett, W.M. and Chung, H.M., (1978), Geochim. Cosmochim. Acta., 43, p. 273-276.
15) Sackett, W.M., (1978), Geochim. Cosmochim. Acta., 42, p. 571-580.

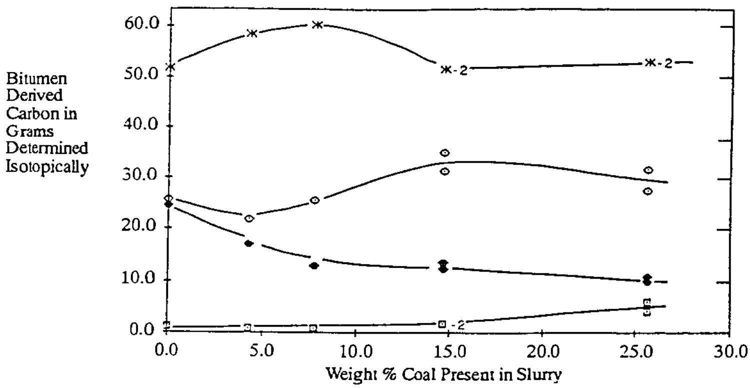

Figure 1 Variation in the isotopically determined amount of bitumen derived carbon incorporated into each synthetic liquid as a function of coal concentration in the slurry. Symbols: ⋇ - Distillate; ⊙ - Maltene; ◆ - Asphaltene; ▫ - Residue.

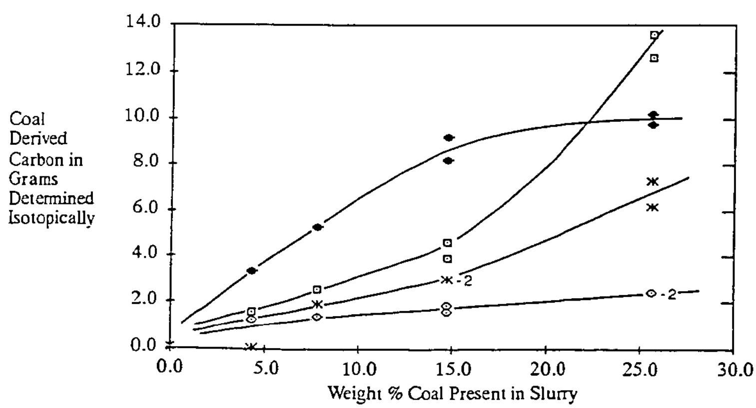

Figure 2 Variation in the isotopically determined amount of coal derived carbon incorporated into each synthetic liquid. Symbols: ⋇ - Distillate; ⊙ - Maltene; ◆ - Asphaltene; ▫ - Residue.

Characterisation of Reactants and Products in Coal-Petroleum Co-processing

S. Wallace, C. Jones, M. Burke, K.D. Bartle and N. Taylor,

Dept. of Physical Chemistry, University of Leeds, Leeds, LS2 9JT.

R. Caygill, T. Flynn, W. Kemp and W. Steedman,

Dept. of Chemistry, Heriot-Watt University, Edinburgh, EH14 4AS.

INTRODUCTION

Over the last few years a number of processes have been developed for the direct liquefaction of coal to distillate fuels. Typically these processes involve thermal degradation of the macromolecular coal structure followed by hydrogenation to stabilise the degraded material and adjust the hydrogen to carbon ratio of the products. One such process, developed by British Coal, is Liquid Solvent Extraction (LSE) (1). This is a two stage process in which coal is firstly digested in a process derived solvent. The resulting coal liquids are then hydrocracked and distilled to give a range of light oil fractions and a residue which is recycled to the extraction stage. Since the solvent stream is generated from the final coal-derived products the extent of hydrocracking has to be limited. In principle this problem could be alleviated by supplementing or replacing the recycle solvent stream with heavy petroleum fractions which are cheap and have a higher H/C ratio than the coal derived solvents.

In this paper we report on the preliminary results from an EEC funded project to examine the viability of incorporating petroleum oils into the existing LSE process. Methods have been developed for the characterisation and assesment of potential solvent streams and also for the determination of product distributions in co-processed mixtures.

SAMPLES AND EXPERIMENTAL

The petroleum samples investigated so far include two atmospheric residues ('A' and'B'), one vacuum residue ('C') and two whole crudes ('O' and 'M'). The crudes O and M were distilled to give vacuum residues boiling $>$ 475°C whilst the three distillation residues were investigated as received.

The distillation residues were characterised by fractionation on silica into saturate, aromatic and polar compound classes (2). The aromatic fractions were further separated into mono, di and poly aromatics on neutral alumina (3). The C-5 and C-7 asphaltene contents of the crudes and residues were also determined. The ^{1}H NMR spectra of all fractions were recorded and form the basis for assessing solvent quality.

Point-of-Ayr (POA) coal was co-processed in two and three component systems containing petroleum fractions and petroleum fractions/anthracene oil respectively under a range of conditions. This work forms a separate part of the project and is discussed more fully in a separate paper by Caygill et al (4).

In order to assess the relative contributions of coal and petroleum derived asphaltenes in the co-processed residue size exclusion chromatography has been used. Briefly, mixtures with differing proportions of coal and petroleum derived asphaltenes were introduced onto an analytical scale PL Gel SEC column with UV detection. From the combined, overlapping, coal and petroleum peak areas a calibration graph was constructed and used to determine the relative contributions of the two asphaltenes to the co-processed residues.

To make a direct comparison between differing solvents a Solvent Dissolving Index was determined for the POA coal. Essentially, the coal was processed in a tubing bomb reactor (420 °C for 60 mins.) using hydrogenated anthracene oil (HAO) as a hydrogen donor solvent. In a series of runs the HAO was progressively diluted with naphthalene thus causing a progressive dilution of hydrogen donors.

RESULTS AND DISCUSSION

Chromatographic analysis of the petroleum residues (eg. atmospheric residue A; Table 1) indicates that they contain a large amount of saturates. Although these materials are generally regarded as not participating in the liquefaction reactions, if present in large quantities they may have an anti-solvent effect and therefore their removal is desirable (5). Whilst removal of n-alkanes is facilitated by the use of urea adduction, removal of branched and cyclic alkanes presents more of a problem.

Table 1
Analytical Data For Atmospheric Residue A

	Total	Asph.	Sats.	Arom.	Polars	
%	-	21.2	13.6	54.3	15.8	-
C	83.3	83.0	86.7	84.0	80.2	80.4
H	10.0	8.25	12.9	10.1	9.6	9.5
N	0.8	1.35	0.3	0.5	1.2	0.7
S	6.4	8.05	0.0	3.8	4.5	5.5
H/C	1.44	1.19	1.79	1.44	1.44	1.42
H_{AR}	6.1	9.3	1.8	8.5	7.5	7.0
$H_{\alpha,2}$	0.5	1.9	0.0	2.0	3.0	1.9
H_{α}	16.0	18.9	6.5	23.6	20.6	16.3
H_{β}	57.3	51.9	63.9	55.3	53.9	56.6
H_{γ}	20.2	18.1	27.8	10.6	15.0	18.2

Removal of asphaltenes from the residues reduces the aromaticity of the remaining material. This is likely to make the remaining n-pentane solubles less suitable as a process solvent. Aromatic species probably participate in hydrogen shuttling reactions and increase radical lifetimes, thus enhancing the probability of radical stabilisation by hydrogen transfer (6). The nature of the aromatic groups in the asphaltene and polar fractions is currently being investigated by electrochemical methods (7).

Figure 1 shows the superimposed SEC traces obtained from a coal liquid and a petroleum derived asphaltene injected onto the column separately. Considerable overlap of the two components is evident and precludes the measurement of coal/petroleum asphalene ratios in co-processed mixtures directly from the chromatogram. However, since the UV detector is more sensitive to coal derived asphaltenes than petroleum derived fractions, the total peak area is dependent on the ratio of the two types of asphaltene in the mixture. Figure 2 shows a plot of peak area verses percentage of coal derived asphaltene for mixtures of different coal and oil derived asphaltenes. It should be noted that, although the asphaltenes were obtained from different sources, all of the points fall broadly on the same straight line. A least squares treatment of the data gives a gradient of 0.100 ± 0.008 %coal/unit area. For individual samples, however, the fit is significantly better (eg. 0.090 ± 0.002 %coal/unit area). Using the plot as a calibration it is possible to estimate the proportions of petroleum and coal derived asphaltene in a co-processed product stream.

Atmospheric residue A was co-processed with Point-of-Ayr coal (48.7% POA/410 °C/30 mins.) and the asphaltenes separated from the product mixture. Using the calibration it was estimated that, of the 8.1% of asphaltene obtained, 62% of it was coal derived. This result agrees well with the findings of Steer et al (8) using isotopic mass balance calculations. The high percentage of coal contributing to the asphaltene is likely arise from the progressive breakdown of the coal structure to preasphaltenes, asphaltenes and then n-pentane solubles thus causing a preferential increase in coal derived species in the high molecular mass fractions.

Figure 3 shows the SDI calibration for POA coal and HAO with naphthalene as a diluent. The horizontal region of the plot indicates that the solvent mixture contains an excess of hydrogen donors. At higher naphthalene concentrations the extraction yield gradually decreases until the minimum extraction is reached at 100% naphthalene (ie no hydrogen donors). The Solvent Dissolving Index is defined as 0 at 100% naphthalene and 20 at the onset of maximum extraction.

In the standard SDI method developed by Clarke et al (9) the test liquefaction solvent is diluted with naphthalene (typically 50%). For the analysis of potential petroleum derived solvents the presence of naphthalene may result in erroneously high dissolving index due to it increasing the average aromaticity of the solvent mix and, therefore, its ability to solubilise the highly aromatic coal derived species.

ACKNOWLEDGEMENTS

This work was supported by the Commission of the European Communities under contract number EN3V/0015-UK. The authors also whish to thank the British Coal Corporation for the supply of samples and permission to publish this paper.

REFERENCES

1) Davies, G.O. Chem. and Ind. **1978**, 15, 560.
2) Marsh, M.K.; Smith, C.A.; Stokes, B.J.; Snape, C.E. J. Chromatography **1984**, 283, 173.
3) Schiller, J.E.; Mathiason, D.R. Anal. Chem. **1977**, 49, 1225.
4) Caygill, R. et al (These Preprints).
5) Winschel, R.A.; Robbins G.A.; Burke, F.P. Fuel **1987**, 66, 654.
6) Derbyshire, F.J.; Whitehurst, D.D. Fuel **1981**, 60, 655.
7) Bartle, K.D.; Gibson, C.; Mills, D.G.; Mulligan, M.J.; Taylor, N.; Martin, T.G.; Snape, C.E. Anal. Chem. **1982**, 54, 1730.
8) Steer, J.G.; Ohuchi, T.; Muehlenbachs, K. Fuel Processing Technol. **1987**, 15, 429.
9) Clarke, J.W.; Kimber, G.M.; Rantell, T.D. Round table meeting 'Chemical and Physical Valorization of Coal', Brussels, 24 Nov, **1983**.

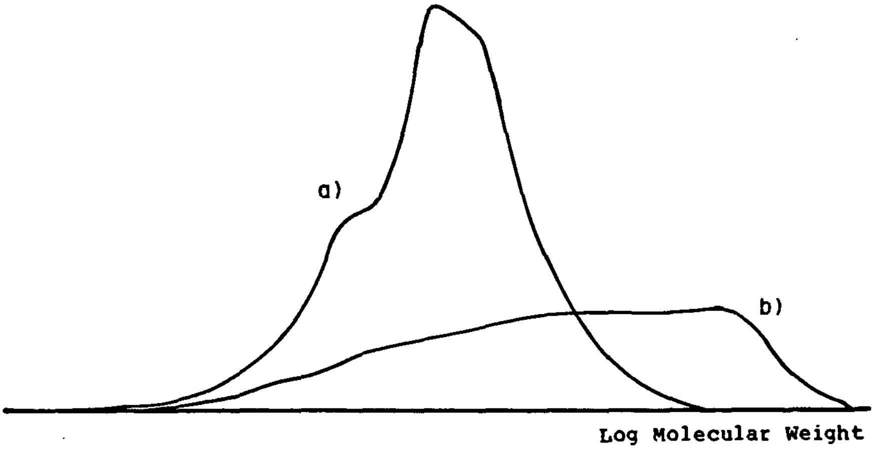

Figure 1. Superimposed SEC Traces from a) Coal Derived and b) Petroleum Derived Asphaltenes.

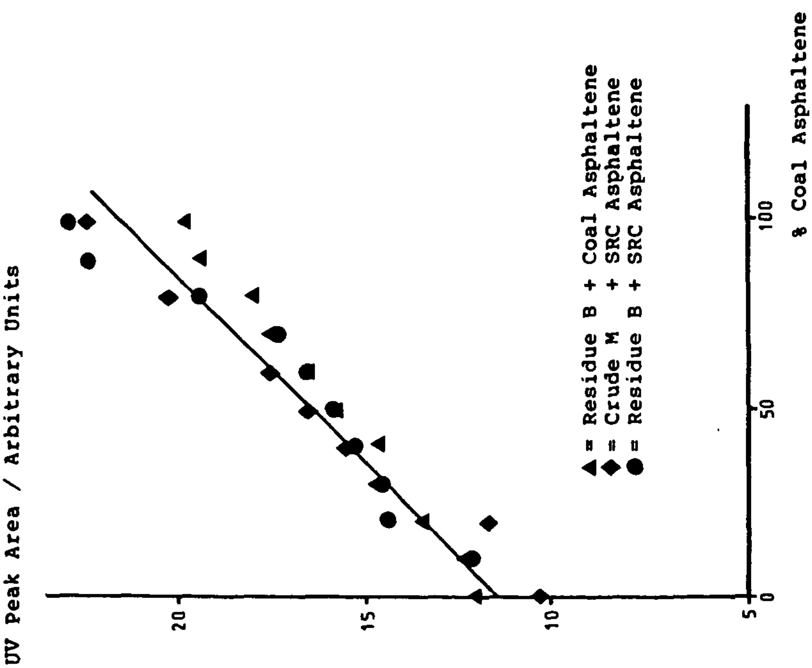

Figure 2. SEC Coal/Petroleum Asphaltene Calibration Plot.

HYDROTREATING OF COPROCESSING DERIVED LIQUIDS

Richard J. Parker, Peter Mohammed and James Wilson

Alberta Research Council
Coal and Hydrocarbon Processing Department
1 Oil Patch Drive, Bag #1310
Devon, Alberta
Canada, TOC 1E0

ABSTRACT

One task of a program, jointly sponsored by Electric Power Research Institute; Hydrocarbon Research, Inc.; Alberta Research Council and Ontario-Ohio Synthetic Fuels Corporation, was to determine the response of various coprocessing derived liquids to hydrotreating. The liquids were collected from an ebullated bed bench unit test performed by HRI. The feedstock was a 1:1 mixture of Ohio No. 5/6 coal and Cold Lake atmospheric resid. The product liquids were separated by distillation into naphtha (IBP to 185°C), distillate (185-343°C) and gas oil (343-470°C).

Scoping tests were performed in a fixed bed hydrotreater to determine suitable conditions for the production of reformer feedstock naphtha and diesel quality distillate. Variables investigated included temperature, pressure and space velocity. A Berty CSTR was employed to measure the kinetics of heteroatom removal from the distillate and gas oil. The resulting products met the specifications for synthetic crude oil feedstocks.

INTRODUCTION

The Alberta Research Council (ARC) has been investigating various coprocessing options to develop a new market for the subbituminous coal reserves and heavy oil/bitumen deposits which are located within the Province of Alberta (1). One promising process option for this purpose is the Hydrocarbon Research Inc., (HRI) coal/oil coprocessing technology which uses hydrocracking over an ebullated bed of supported catalyst to convert coal and heavy oil resids to distillable liquid products (2). In 1985, ARC joined a consortium of Electric Power Research Institute (EPRI), Ontario-Ohio Synthetic Fuels Corporation (OOSFC) and HRI, to develop this technology (Ontario-Ohio Synthetic Fuels Corporation received financial assistance from the State of Ohio, Coal Development Office). Phase I of the program confirmed that both bituminous and subbituminous coals could be converted to high quality liquid synthetic crude oils when coprocessed with heavy oil resids such as Cold Lake atmospheric tower bottoms. Coal conversions exceeded 94% under preferred conditions while distillable oil yields approached 75 wt%.

In 1986, a second phase of the program was initiated with the same contributors. The key objectives of the program were to test alternate feedstocks, to determine catalyst replacement rates and to answer specific questions regarding aspects of the chemistry of the upgrading pathways. One subtask was to investigate processing conditions for the secondary upgrading of distillable oil product fractions. The following paper reports on the activities completed by ARC on the hydrotreating of these coprocessing derived liquids.

EXPERIMENTAL

The distillable liquid product from a bench unit run completed by HRI in their New Jersey facility was separated by distillation into naphtha (IBP-185°C), middle distillate (185-343°C) and a gas oil (343-470°C). The bench unit run was performed on a 1:1 blend of Ohio No. 5/6 coal (dry basis) and Cold Lake atmospheric resid. Properties of these distilled liquids are shown in Table 1. These liquids approached but did not meet specifications set by synthetic crude refiners or ASTM product requirements (diesel, No. 2 fuel oil).

All three fractions were initially hydrotreated in a Berty continuous flow stirred tank reactor (300 ml). Conditions were preselected based on historical data and literature reports. The required specifications for gas oil were met using a presulfided Amocat 1C catalyst. However, all the target specification for naphtha and middle distillations could not be achieved with this catalyst. It was therefore replaced with the more active Shell 324 or Shell 424 catalysts. Even then some target specifications were still unobtainable so the program was completed using a fixed bed reactor.

For the Berty reactor, five hours were allowed for the system to reach steady state. Product was then collected over a 2-3 hour period. Fresh presulfided catalyst (40 g) was charged into the reactor prior to each test. In the fixed bed reactor a two-hour period was adequate to reach steady state. This was followed by a 1 hour yield period. Conditions were then adjusted and the procedure repeated. In this manner, three runs could be completed within a single working day. A single charge of presulfided Shell 424 (50 g) was used throughout the fixed bed tests. Void space was packed with a silicon carbide filler. The operating parameters investigated were temperature, liquid hourly space velocity (LHSV), reported as g feedstock per g catalyst per hour, and hydrogen partial pressure.

Once conditions to produce a naphtha reformer feedstock had been established (Table 2), a production run was performed in the fixed bed hydrotreater. Over a 7 hour yield period, sufficient naphtha (about 0.5 litre) was produced to test the response of this material to reforming. The test unit for the reformer runs was the same fixed bed hydrotreater as had been used in the hydrotreating studies. Three flow rates were subsequently investigated, again in a single day of operation. The catalyst was Cyanamid PR-7, which was predried but otherwise untreated.

RESULTS AND DISCUSSION

The key objectives of the study were to determine suitable conditions for the production of feedstocks which would be acceptable to synthetic crude refineries or conditions to meet ASTM product specifications (No. 2 fuel oil and diesel fuel). The liquid products derived from the HRI coal/oil coprocessing technology are generally superior to those derived from many other upgrading processes. The catalytic conditions in the ebullated bed ensure that a high proportion of the heteroatoms are removed and that substantial hydrogen addition occurs. The conditions required for secondary hydrotreating therefore are less severe than those for most synthetic crude oils. Commercial coking-derived, synthetic crude oils are presently hydrotreated on site to meet pipeline specifications and again at the refinery to meet process specifications. The quality of the ebullated bed products ensures that on site hydrotreating can be eliminated.

The middle distillate and gas oil used in this study already met the sulfur specifications for synthetic feedstocks and fuels without additional hydrotreating. Nitrogen levels were excessive, however, and the cetane number was low (Table 2). Hydrotreating conditions were therefore selected to bring these properties to acceptable levels.

A secondary objective of the programme was to determine kinetic data for the desulfurization and denitrification reactions. However, the conditions were not initially selected for this purpose, so much of the data was within too narrow a range. Also sulfur analyses were highly scattered especially for the Berty reactor. Product samples were routinely flushed with helium gas to remove dissolved hydrogen sulfide but results were often still high. This effect disappeared after two runs with the fixed bed unit, suggesting that the catalyst may have been the source of the interference. These problems were not resolved within the constraints of the program and the data was insufficient to complete a kinetic study.

NAPHTHA

In the fixed bed unit, nitrogen specifications (1 ppm) for production of a reformer feedstock were met whenever the hydrogen pressure exceeded 10.3 MPa (1500 psi) and temperature was greater than 315°C. To reduce the sulfur to the desired level required a minimum of 13.8 MPa and 330°C. The hydrogen consumption was calculated from the hydrogen content of the feed and product; values ranged from 0.4 to 1.0 g/100 g feed (300 - 700 SCF/bbl). The conditions selected for the production run were 13.8 MPa, 345°C and a liquid hourly space velocity of 1.40 hr^{-1}. Conditions were more severe for the Berty reactor but a reformer feedstock could be prepared from this unit.

The naphtha from the production run had over 50% naphthenes which indicated that it should be an excellent reformer feedstock. The conditions in the reformer (Table 2) were adequate to almost completely convert the naphthenes with a moderate gas yield (about 11%). Only two thirds of the naphthenes were converted to the desired aromatics, however, so that these components (43%) were slightly below specifications. Theoretically this would give a low octane number, but the gravity (42°API) was encouragement for a more acceptable research octane number (~99).

MIDDLE DISTILLATE

The end use of this fraction was assumed to be either diesel or No. 2 fuel oil. Nitrogen specifications for synthetic crude were readily obtained in both the fixed bed hydrotreater and Berty reactor. Over 95% of the nitrogen was removed even at 6.9 MPa (Fig. 1). This condition was insufficient to improve the cetane index or reduce the aromatic content to the level ascribed by Sullivan (3) or Kriz (4).

The cetane index reported here is an adapted version of ASTM procedure D-976. This method is based on the true 50% boiling point of the liquid and the gravity. The hydrotreating experiments did not produce sufficient liquid for a true boiling point distillation determination. It was therefore replaced by a simulated distillation. The calculated cetane index of the feedstock by this method was 37.5, similar to that previously published (2) by HRI for this fraction. An engine test gave a cetane number of 32.1 which showed the limitations of the cetane index method. To account for these limitations, a cetane index of 42 was set as the target specification.

The hydrogen pressure had to exceed 10.3 MPa before a significant change in cetane index and aromatic content was achieved. The temperature required was 330°C or higher. A space velocity of 2.0 would meet nitrogen specifications (Fig. 2) but not cetane index. Conditions vary greatly, therefore, dependant upon the end use of the product. The aromatic content of the product as close to 10% at the acceptable cetane index and this satisfied the predicted value of Sullivan. No runs came close to the 4% imposed by Kriz. Hydrogen consumption to make diesel grade product was approximately 1-1.2 g/100 g (700-850 SCF/Bbl) at preferred operating conditions.

GAS OIL

No tests were run on the fixed bed unit with this feedstock. The targetted specifications could be obtained with the Berty reactor. Based on the earlier experience with the naphtha and middle distillate, mild conditions of less than 370°C, 10.4 MPa and LHSV of greater than 2.0 hr^{-1} should provide an acceptable product with either Shell 324 or Amocat 1C in a fixed bed. The requirements for the hydrotreating of gas oil are not highly stringent since it must subsequently be subjected to a cracking process. Up to 70% nitrogen removal was possible at the above conditions. Hydrogen consumption was about 0.7 g/100 g (500 SCF/Bbl).

CONCLUSIONS

Operating ranges for hydrotreating and reforming of coprocessing derived liquid were established. All product fractions met target specifications for a synthetic crude oil feedstock or commercial product.

REFERENCES

1. Energy Alberta 1986, Energy Resources Conservation Board, Calgary, Alberta.

2. Coal/Oil Coprocessing: Phase I, Electric Power Research Institute Report No. AP-5101, March 1987.

3. Richard F. Sullivan and Harry A. Frumkin, "Refining Coal Liquids: Where We Stand", Proceedings American Chemical Society, Division of Fuel Chemistry, April 13-18, 1986.

4. C. Fairbridge and J.F. Kriz, "Hydroprocessing of Coal-Derived Middle Distillate", Fuel Science and Technology International, 4(2), 171-189, 1986.

Table 1

Properties of Coprocessing Derived Liquids

		Naphtha (LO-4749)	Middle Distillate (LO-4750)	Gas Oil (LO-4751)
Carbon	%	83.8	87.1	87.4
Hydrogen	%	13.7	12.1	11.1
Nitrogen	ppm	165	1022	4000
Sulfur	ppm	120	334	1630
API gravity	°	49.7	28.3	17.0
13C aromaticity	%	5	23	30
Distillation	°C			
IBP		57	151	323
50%		131	268	368
90%		177	338	402
FBP		253	387	(470)

Table 2

Product Quality and Reactor Conditions

	Product Quality			Operating Conditions			
				Temperature (°C)	Pressure (MPa)	LHSV (hr^{-1})	Hydrogen Consumption (SCF/Bbl)
Naphtha	Nitrogen (ppm)	Sulfur (ppm)					
Target	1	10					
Berty	1	12		380	10.4	1.0	
Fixed Bed	1	10		330+	13.8	1.4	~500
Reformer	Nitrogen (ppm)	Aromatics (%)	Yield (%)				
Target	1	45(PONA)	--				
Fixed Bed	1	43(PNA)	88	500	1.7	2.0	
Distillate	Nitrogen (ppm)	Aromatics[a] (%)	Cetane Index				
Target	200	10(4)	40[b]				
Fixed Bed	10	10	42	330+	13.8	1.0	700-850
Berty	93	19	38				
Gas Oil	Nitrogen (ppm)	Gravity API					
Target	1200	18					
Berty	1130	18.4		370	10.4	2.0	~500

[a] Carbon 13 NMR

[b] Cetane number

FIGURE 1

Hydrogen Pressure vs Conversion Parameters (345°C)

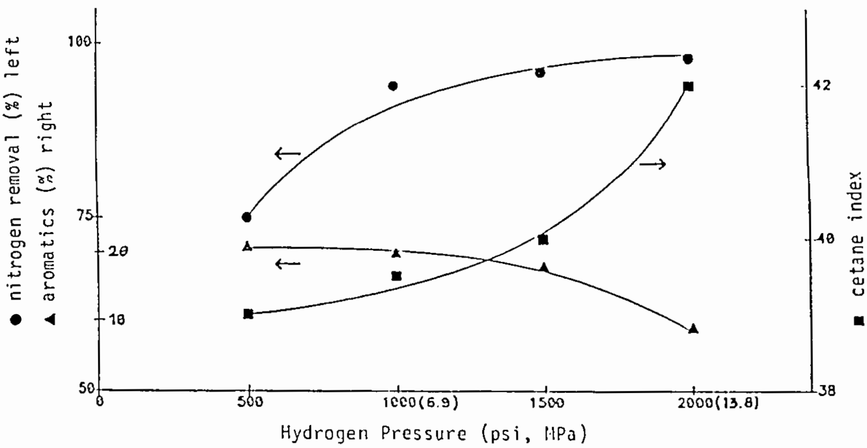

FIGURE 2

Space Velocity vs Conversion Parameters (345°C)

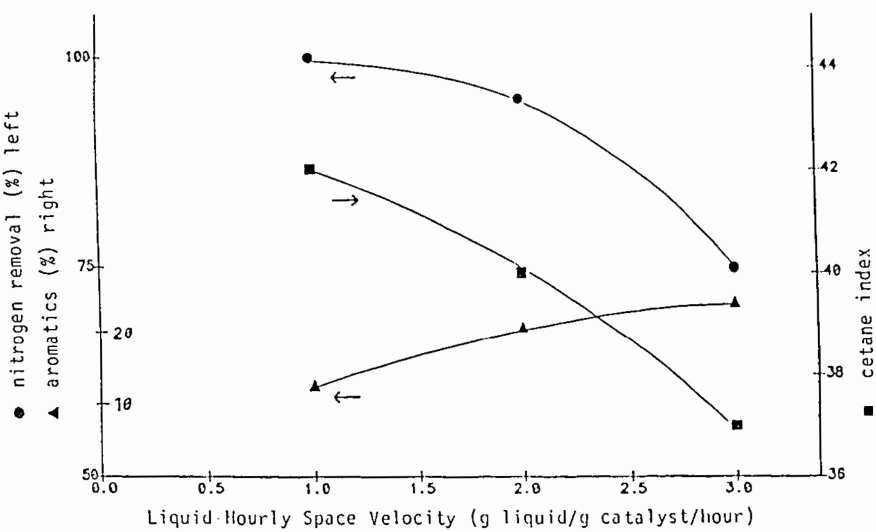

KINETICS OF HEAVY OIL/COAL COPROCESSING

A. J. Szladow, and R. K. Chan
Lobbe Technologies Ltd., Regina, Saskatchewan, S4P 3L7

and

S. Fouda and J. F. Kelly
CANMET, EMR, Ottawa, Canada, K1A 0G1

INTRODUCTION

A number of studies have been reported on coprocessing of coal and oil sand bitumen, petroleum residues and distillate fractions in catalytic and non-catalytic processes (Moschopedis et al., 1984ab, Ignasiak et al., 1984, Kelly et al., 1984, Fouda et al., 1982, MacAurthur et al., 1985, Curtis et al., 1984). The studies described the effects of feedstock characteristics, process chemistry and operating variables on the product yield and distribution; however, very few kinetic data were reported in these investigations. This paper presents the kinetic data and modelling of the CANMET coal/heavy oil coprocessing process.

CANMET has been conducting research and process development work on coprocessing of Canadian heavy oil/bitumen and coal since 1979 including studies of the kinetics and mechanisms of coprocessing. As a continuation of the program, CANMET and Lobbe Technologies undertook a project on mathematical modelling of coprocessing kinetics with emphasis on the development of reaction engineering models for improved process performance and operation. The results of that project were reported in much detail elsewhere (Szladow et al., 1987).

EXPERIMENTAL

The coprocessing experiments were conducted in a continuous-flow stirred-tank coprocessing reactor unit. A detailed description of this unit was given by Fouda et al. (1982). The applied reactor equations were those for CSTR, based on conclusions from the exploratory runs which investigated the effect of impeller speed on the yield of reaction products.

Alberta subbituminous coal and Cold Lake, Alberta, vacuum bottoms (+454°C) were used as the feedstock. The coal was ground to -200 mesh and slurried with heavy vacuum bottoms by mixing about 30 percent of coal and 70 percent of heavy oil (d.a.f. slurry basis). A disposable iron sulphide catalyst was added in the amount of approximately 5 percent on a d.a.f. slurry basis.

The experimental conditions were designed using a Latin Square statistical design at three levels of temperature and space velocity. The range of process conditions included:

Temperature: 400 to 455°C
Nominal Slurry Space Velocity: 0.50 to 1.54 kg/L/hr
Reactor Pressure: 2000 psig
Run Duration: 80 to 180 min.
Total Feed Processed: 402 to 600g
Coal Concentration: 29.71 to 33.38 m.a.f. Wt% feed

The coprocessing products were analyzed for four liquid fractions, solvent soluble and insoluble fractions, gaseous products, hydrogen consumption, and coal and pitch conversion. Distillate products were also analyzed for composition and specific gravity. The residue (+525°C) was analyzed for elemented composition and ash content. A summary of the product definitions and separation procedures is depicted in Figure 1. The percent recovery of the input feed was between 96.40 and 105.02 percent with the mean of 100.78 and standard deviation of 2.84 percent. These accurate mass balances for the product yield facilitated high predictive capabilities of the developed models.

Two different types of models were formulated for predicting the yield structure of coprocessing products: 1) models which had sequential characteristics; and 2) models with parallel characteristics, where most coprocessing products were generated from the initial lumps (Figure 2). In the sequential models, the distillate products always reached a maximum beyond which addition of more hydrogen resulted in generation of C1-C4 hydrocarbon gases. In the parallel models, the yield of distillate products continuously increased - within the range of coprocessing conditions - and the selectivity of products was determined by the relative rates of their formation.

A set of generalized lumped kinetic model equations was derived for an n-component reacting mixture in a stirred-tank reactor:

$$\frac{F^{in}\,(1-\phi)}{(1-\epsilon)\,\rho_P\,V_R}\,(X_{i,o}-X_i) = r_i'$$

where F^{in} = rate of total feed input, kg/hr (d.a.f.)
ϕ = mass fraction of product flashed at reactor T,P
ρ_P = average density of products, kg/L
V_R = reactor volume (to the dip tube), L³
ϵ = gas holdup
$X_{i,o} = F_i^{in}/F^{in}$
$X_i = F_i^{out}/F^{in}$
r_i' = rate of formation (disappearance) for component "i" in terms of fractional conversion, X_i, hr^{-1}

The equations were solved using a Least Square method and the product yield structure for each coprocessing component. The computer algorithms first solved the normal equations developed for the rate parameters, k_{ij}, and later, solved for the rate constant coefficient A_{ij} and E_{ij}. This approach provided information on how the calculated rate constants, k_{ij}, change with the alternative reaction networks. The approach also permitted better understanding of the physical meaning underlying the regressed rate constants and the postulated product yield structures for coprocessing.

A number of studies have been published documenting the pitfalls of using lumped kinetic models for reacting mixtures, in general (Liu et al., 1973, Luss et al., 1971) and for coal liquefaction in particular (Szladow et al., 1981, Prasad et al., 1986). The most common pitfalls reported were the loss of information about the kinetics of individual reactions, different rate expressions for the grouped as opposed to individual species rate equations, little theoretical significance underlying the overall (lumped) activation energies, and the frequent discrepancy between the order of the rate expressions for lumps and for reacting species. Several investigators also showed methods which overcome these difficulties for complex reacting mixtures, (Golikeri et al., 1974, Lee, 1978, Bailey, 1972). These methods were later extended to coal liquefaction (Szladow et al., 1982, Prasad et al., 1986).

Bearing in mind the above limitations of lumped kinetics, the CANMET coprocessing data and product lumping were reviewed to establish whether the product lump definitions were dependent on the severity of the process. The analysis of variance which was performed indicated that product characteristics did not change with the severity of coprocessing reactions. Also, analysis of activation energies for THFI using methods reported by Szladow et al. (1981) showed that one initial lump is sufficient for expressing coal reactivity.

Over twenty different reaction networks were developed and tested based on ANOVA tables and Multiple Classification Analysis of the coprocessing products. A significant number of the networks predicted the coprocessing data structure and met the identified constraints on the rate coefficients. The selection of suitable models was based, therefore, on three criteria:

1. How much of the total variance was explained by the model.
2. How much of the grouped product's variance was explained by the model.
3. How well the model predicts the yields of coprocessing products or how accurate the model is.

First, criterion 1 was used, later, as specific difficulties were addressed, criteria 2 and 3 were reviewed. This approach allowed a systematic evaluation of the models, in conjunction with the interpretation of the rate constants and reaction paths.

Special difficulties were also experienced with modelling preasphaltenes. Figure 3 depicts the effect of temperature on the yield of preasphaltenes. As the temperature increased from 400 to 425°C the yield of preasphaltenes increased; however, the yield of preasphaltenes decreased as the temperature increased from 425 to 450°C, indicating a change in the sign of the temperature coefficient (activation energy). This led us to believe that two mechanisms may be responsible for preasphaltenes formation: one essentially being a chemical reaction mechanism of THFI conversion, with the rates increasing with temperature, and the second representing an adduct formation between preasphaltenes and oils, for which the rate decreases with temperature.

Cronauer et al. (1979) and Sato (1976) reported similar effects for coal liquefaction. They observed a net negative yield of oil at low primary liquefaction products. Our analysis of the CANMET experiment revealed that other coals also exhibit similar "reverse" temperature effects at lower temperatures. At high temperatures, the adduct seemed to disintegrate.

To account for the two opposed mechanisms, one would have to postulate independent rate expressions for chemical reactions and for adduct formation of preasphaltenes. Considering, however, that preasphaltenes constitute only a small fraction of the overall coprocessing products (5 to 10 percent), we decided to retain the parallel structure for preasphaltenes reactions, with only one reaction path leading to its formation. This approach had resulted in somewhat inaccurate modelling of preasphaltenes, but it allowed modelling of the remaining coprocessing reactions.

The final choice of parallel and sequential models is presented in Figure 4. Model 52 has a strong parallel characteristic for the yield of distillate fractions with the prime coprocessing products (light gas oil, naphtha and hydrocarbon gas) constituting the termination lumps for the coprocessing network. Model 61 has sequential characteristics with the exception of the formation paths for the C1-C4 group.

The regressed rate constants for Model 52 and 61 are shown in Table 1. Both models predicted the coprocessing yield data accurately (Figures 5 and 6). The amount of variance explained by the models is shown in Table 2. Model 52 explains 84.4 percent of the total variance. For individual components the variance explained exceeds or is close to the target variance for preasphaltenes, asphaltenes, oils, naphtha and the C1-C4 group. Model 61 explained 81.4 percent of total variance and achieved target variance for THFI, asphaltenes and oils and was close for the C1-C4 group. Interestingly enough, when tested without path #8, Model 61 could not predict the C1-C4 yield accurately.

In the final step, Model 52 was improved by adding two more reaction paths to meet the limiting conditions, i.e., at infinite time distillate fractions should be converted to lighter products (Figure 7). Model 53 explained 90.0 percent of variance, which is very satisfactory, considering the difficulties with modelling preasphaltenes. Model 53 also explained most of the individual component variance except for light gas oil and naphtha.

SUMMARY AND CONCLUSION

A number of reaction networks were evaluated for CANMET coprocessing. The final choice of model was a parallel model with some sequential characteristics. The model explained 90.0 percent of the total variance, which was considered satisfactory in view of the difficulties of modelling preasphaltenes.

The models which were evaluated showed that the kinetic approach successfully applied to coal liquefaction and heavy oil upgrading can be also applied to coprocessing. The coal conversion networks and heavy oil upgrading networks are interrelated via the forward reaction paths of preasphaltenes, asphaltenes, and THFI and via the reverse kinetic paths of an adduct formation between preasphaltenes and heavy oil.

REFERENCES

Bailey, J.E., Chem. Eng. J., 3, 52, 1972.

Cronauer, D.C. and Ruberto, R.G., EPRI Report AF913, 1979.

Curtis, C., Guin, J.A., Pass, M. and Tsai, K.J., Paper presented at Amer. Chem. Soc., Philadelphia, August 26, 1984.

Fouda, S.A., Kelly, J.F. and Rachimi, P.M., ERP/ERL 82-52, CANMET, 1982.

Golikeri, S.V. and Luss, D., Chem. Eng. Sci., 29, 845, 1974.

Ignasiak, B., Lewkowicz, L., Kovacik, G., Ohuchi, T. and Du Pleassis, M.P., "Catalysis on Energy Scene", 595, 1984.

Kelly, J.F., Fouda, S.A., Rachimi, P.M. and Ikura, M., Paper presented at the CANMET Coal Conversion Contractors Meeting, Calgary, November, 1984.

Lee, H.H., AIChE J., 24, 116, 1978.

Liu, Y.A. and Lapidus, L., AIChE, J., 19, 467, 1973.

Luss, D. and Hutchinson, Y., Chem. Eng. J., 2, 172, 1971.

MacAurthur, J., Boehm, F., Liron, A. and Shannon, R.H., Paper presented at 10th Annual EPRI Contractors' Conference on Clean Liquid and Solid Fuel, Palo Alto, Calif., April 23, 1985.

Moschopedis, S. and Ozum, B., Liq. Fuel Tech., 2, 177, 1984a.

Moschopedis, S., Canadian Patent 116586, 1984b.

Prasad, G.N., Witmann, C.V., Agnew, J.B. and Sridhar, T., AIChE J., 32, 1277, 1986.

Sato, S., ACS Div. Fuel Chem., Preprints, 24, 270, 1976.

Szladow, A. and Given P., Chem. Eng. Comm., 19, 115, 1982.

Szladow, A. and Given, P., I&EC, Proc. Des. Dev., 20, 27, 1981.

Szladow, A., Chan, R.K., Tscheng, J., Fouda, S.A., Kelly, J.F., "Mathematical Modelling of Coprocessing Kinetics", Final Report Prepared for CANMET, September, 1987.

Table 1. RATE CONSTANT COEFFICIENTS FOR MODEL 52 , 61, AND 53

Rate Constant	MODEL 52 Ai	Ei	MODEL 61 Ai	Ei	MODEL 53 Ai	Ei
1	1.24E10	33,020	5.33E13	44,040	1.24E10	33,020
2	8.31E23	76,180	5.23E03	12,030	9.11E23	77,730
3	1.84E12	39,030	8.33E08	29,390	1.84E12	39,030
4	1.72E12	40,000	9.48E18	61,030	1.51E12	40,000
5	4.97E17	58,910	5.56E09	31,990	4.17E17	59,610
6	4.06E19	63,400	7.90E06	23,310	4.06E19	63,400
7	7.90E06	23,510	6.53E02	13,860	7.90E06	23,510
8	2.28E14	47,470	1.50E06	55,000	2.28E14	47,470
9	-	-	-	-	3.51E19	66,400
10	-	-	-	-	4.52E16	59,900

Table 2. PERCENT OF VARIANCE EXPLAINED BY MODELS 52, 61 AND 53

	$\sigma(i)$	F(i)[1]	MODEL 52	MODEL 61	MODEL 53
THFI	15.5	92.1	90.4	92.8	91.5
PA	53.5	91.7	96.3	<0	93.1
A	30.6	52.4	54.0	55.3	52.6
OIL	38.1	65.9	95.4	96.6	96.0
HGO 1+2	12.1	94.1	47.2	75.1	90.6
LGO	5.9	98.8	71.5	75.2	78.4
NAPHT	6.1	99.4	91.6	88.4	72.7
C1-C4	10.9	99.7	98.5	98.7	98.9
TOTAL	N/A	92.5	84.4	81.4	90.0

[1] target, based on standard deviations for individual components

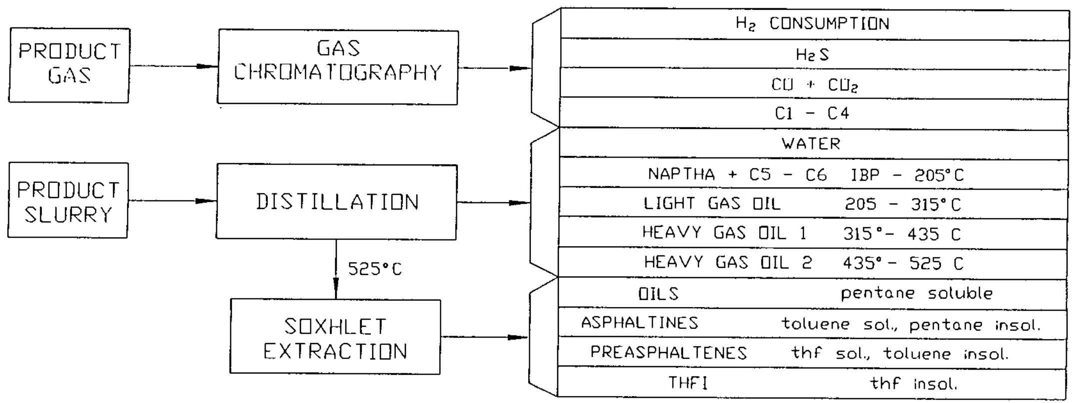

Figure 1. PRODUCT DEFINITION

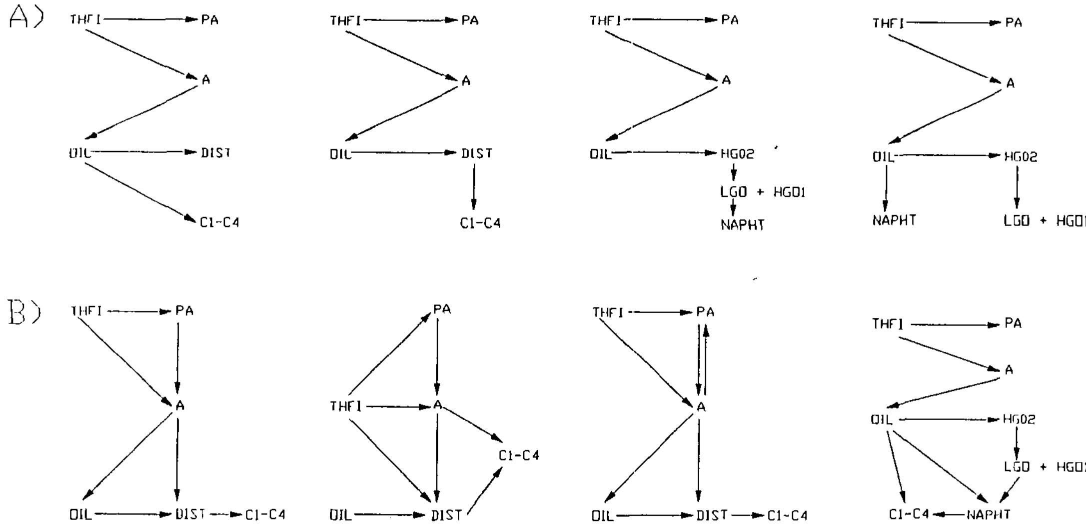

Figure 2. EXAMPLES OF SEQUENTIAL (A) AND PARALLEL (B) KINETIC STRUCTURES FOR COPROCESSING

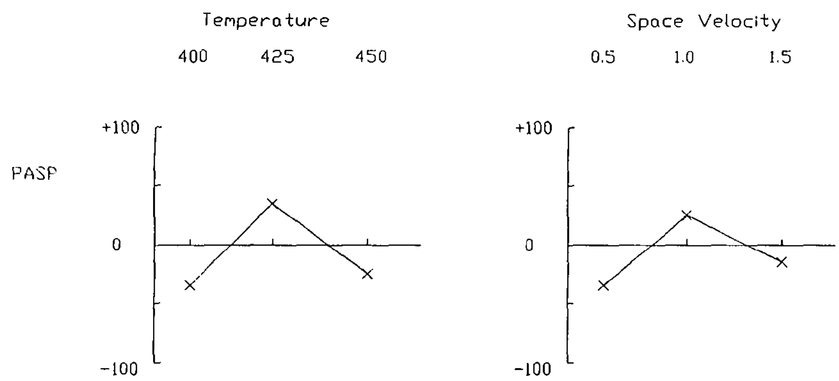

Figure 3. THE EFFECTS OF TEMPERATURE AND SPACE VELOCITY ON PREASPHALTENES COPROCESSING PRODUCTS

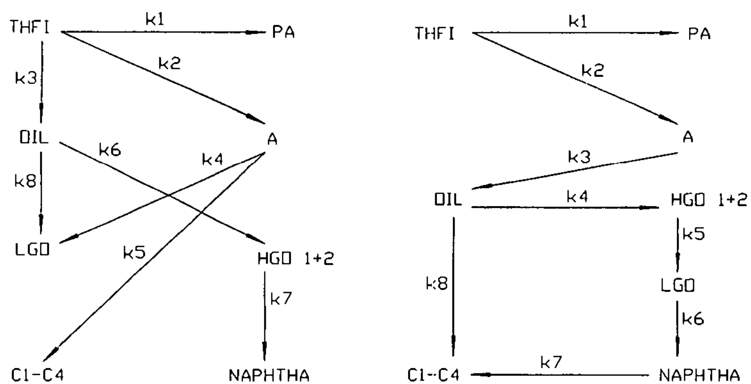

Figure 4. MODELS 52 AND 61

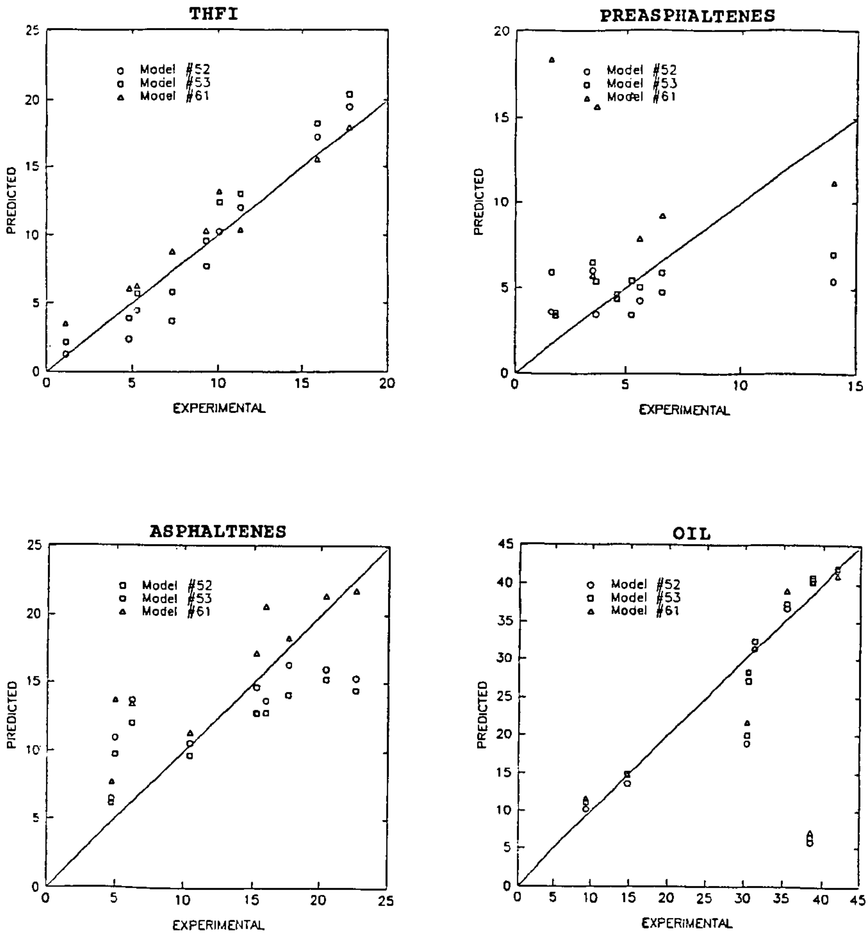

Figure 5. PREDICTED vs EXPERIMENTAL DATA

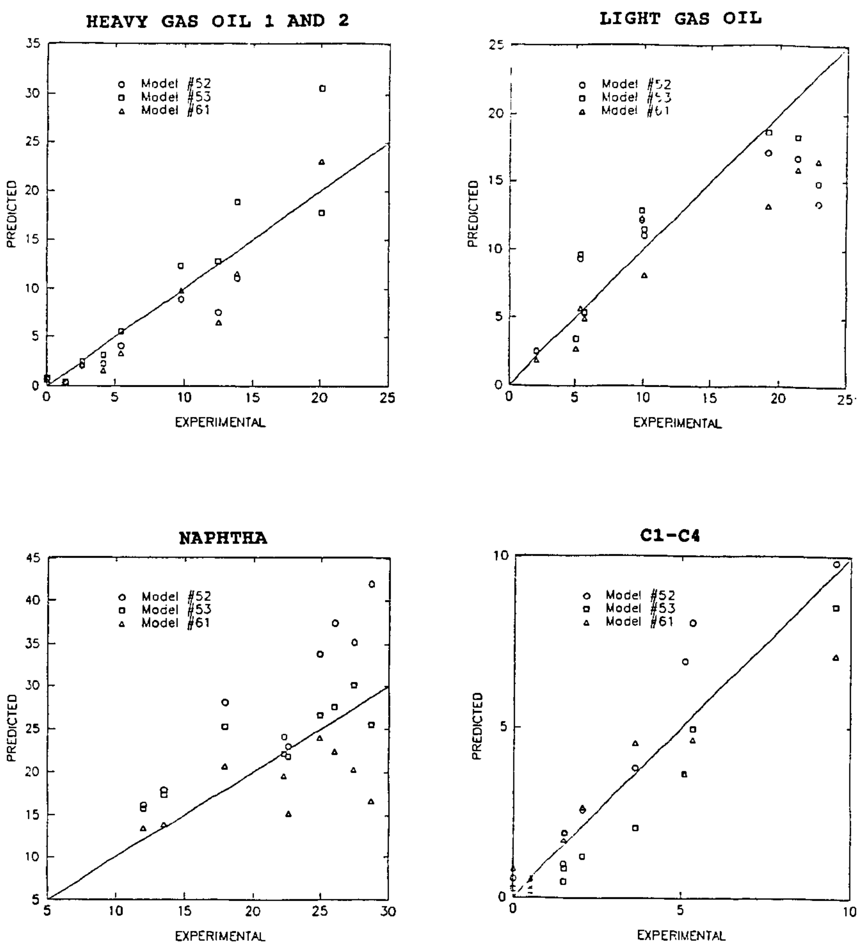

Figure 6. PREDICTED vs EXPERIMENTAL DATA

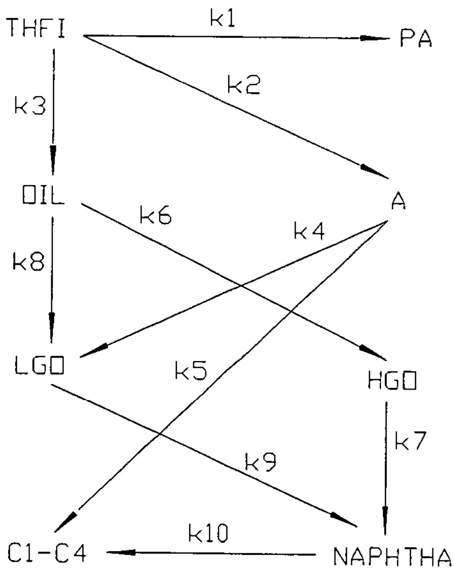

Figure 7. MODEL 53

LOW SEVERITY CO-PROCESSING USING HOMOGENEOUS BASIC NITROGEN PROMOTORS

R.L. Miller, G.F. Giacomelli, and R.M. Baldwin
Chemical Engineering and Petroleum Refining Department
Colorado School of Mines
Golden, Colorado 80401

INTRODUCTION

The possibility of dissolving coal at low severity reaction conditions has intrigued researchers for many years. As early as 1921, Fischer and Schrader (1) reported production of an ether-soluble material by liquefying coal at 350°C using carbon monoxide and water as reducing agent. More recently, other groups including the Pittsburgh Energy Technology Center (2-5), the North Dakota Energy Research Center (6-10), Stanford Research Institute (11-14), Carbon Resources, Inc. (15,16), and the Colorado School of Mines (17-19) have investigated various methods of low severity dissolution. Their efforts have been prompted by the fact that many incentives exist for converting coal at milder conditions than utilized in present day technology. Several of these incentives are listed below:

* Reduced hydrocarbon gas make resulting in reduced feed gas consumption and enhanced hydrogen utilization efficiency

* Suppressed retrogression of primary coal dissolution products resulting in enhanced distillate and residuum product quality

* Production of high boiling residuum which is less refractory and thus amenable to upgrading in a conventional second-stage hydrocracker

* Substitution of less expensive off-the-shelf vessels, piping, and pumps in place of expensive, custom-designed units

* Less severe slurry handling and materials of construction problems as a result of lower operating temperatures and pressures.

In searching for effective coal dissolution promotors to be evaluated at low severity co-processing conditions, we concluded that, based on results from high severity studies, basic nitrogen compounds warranted extensive study. Atherton and Kulik (20,21) summarized data from several high severity liquefaction studies using 1,2,3,4-tetrahydroquinoline (THQ) in which THF coal conversions in the range of 85-100 wt% (MAF basis) were obtained with Wyodak subbituminous coal and Illinois 6 bituminous coal at reaction temperatures of 400°-450°C. However, distillate yields from these experiments were much lower than expected, and nitrogen material balance measurements indicated significant adduction of the THQ into non-distillable products.

Thus, while basic nitrogen compounds appear attractive as coal dissolution promotors, the adduction problem limits their usefulness in high severity co-processing. We hypothesized that utilizing basic nitrogen compounds at lower severity would reduce adduction sharply, but that effectiveness towards promoting coal dissolution would remain high.

Our first low severity co-processing experiments to test this hypothesis were conducted using Wyodak subbituminous coal and either unhydrotreated or mildly hydrotreated shale oil each containing approximately 1.0 wt% heterocyclic basic nitrogen (19). Mild hydrotreatment of the shale oil prior to co-processing greatly improved both liquid yield and THF soluble coal converison. Yield and nitrogen balance results suggested that significantly less adduction of nitrogen compounds in the shale oil occurred at low severity reaction conditions compared with earlier high severity coal/shale oil co-processing experiments.

The success of these preliminary runs provided the incentive to begin a more fundamental study on the use of basic nitrogen compounds to promote coal dissolution and increase distillate yields at low severity reaction conditions. Initial results from model compound studies are reported in this paper.

EXPERIMENTAL PROCEDURE

Kentucky 9 bituminous coal and Wyodak subbituminous coal were used as feed coals in the low severity co-processing experiments. Ultimate analysis data for these coals is presented in Table I. Coal samples were vacuum-dried to less than 1.0 wt% moisture content before use.

Cold Lake atmospheric residuum was used as co-processing heavy oil. Available characterization data for this feedstock, designated A-8, are shown in Table II. Sample A-8 has been extensively studied as a co-processing feed and performs well at low severity reaction conditions (19). The seven model nitrogen compounds listed in Table III were evaluated as coal dissolution promotors. Each compound was ACS reagent grade and was used without further purification. These compounds were chosen to provide a wide range of base strength as measured by aqueous pK_b values. For convenience, the coding system shown in Table III will be used to reference each of the seven model nitrogen compounds.

Runs were completed using either commercial grade hydrogen or carbon monoxide. Each feed gas contained 1.0 mole% krypton used as an inert tracer. Distilled water in an amount equal to 50 wt% of the MAF feed coal was added to runs using carbon monoxide feed gas.

Table IV lists the reaction conditions used in this study. A majority of the runs were completed at the low severity conditions shown. However, for comparison purposes, several runs were also completed at conventional high severity conditions.

Co-processing experiments were performed using a 300 cm^3 Autoclave Magnedrive II batch reactor interfaced to an Apple IIe personal computer for temperature control. The computer was also routinely used for temperature and pressure data acquisition during a run. Reactor heatup time to 330^{o}-$350^{o}C$ reaction temperature was approximately 30 minutes. At the end of a run, water was circulated through cooling coils immersed in the reactor contents, allowing cooldown to temperatures below $200^{o}C$ in less than 20 minutes.

After cooling the reactor to near room temperature, gaseous products were recovered in evacuated stainless steel vessels and analyzed for light hydrocarbon gases and carbon oxide gases using a Carle Model 111H refinery gas analyzer. The krypton tracer concentration was also measured and used as a tie element for determining product gas yields.

The liquid-solid product slurry was removed from the reactor using toluene as a wash solvent and quantitatively centrifuged to separate solids from the liquid product (termed "decant oil"). The residue (termed "centrifuge residue") contained unconverted coal and mineral matter coated with liquid product. Toluene added during slurry recovery and centrifugation was quantitatively removed during distillation. Decant oil samples were distilled to a 454°C endpoint using an ASTM-type microdistillation apparatus. Portions of the centrifuge residue and decant oil 454°C+ residuum were extracted in a Soxhlet extraction apparatus using cyclohexane, toluene, and tetrahydrofuran. Standard elemental analyses for carbon, hydrogen, nitrogen, sulfur and ash content were performed on all liquid and solid product samples. Oxygen content was determined by difference.

Detailed quantitative measurements of individual model nitrogen compounds in 454°C- distillate samples were performed using an HP 5890 capillary gas chromatograph interfaced with an HP 5790B quadrupole mass spectrometer. These data helped provide a measure of nitrogen compound losses by thermal degradation or adduction.

RESULTS AND DISCUSSION

Effect of Model Nitrogen Compound Addition

Low severity co-processing experiments were completed to evaluate the seven model nitrogen compounds listed in Table III as coal dissolution promotors. THF soluble coal conversion results from these runs are shown in Figure 1. The greatest improvement in coal conversion was noted using 1,2,3,4-tetrahydroquinoline (THQ) (N1) and dipropylamine (N2). Addition of piperidine (N4), 4-piperidinopyridine (N5), or diphenylamine (N7) had little effect on the extent of coal dissolution. Similar results were observed using hydrogen gas at low severity reaction conditions.

As shown in Figure 2, addition of each model nitrogen compound significantly influenced the yield of C_4-454°C liquids obtained at low severity liquefaction conditions. Once again, 1,2,3,4-tetrahydroquinoline (N1) and dipropylamine (N2) strongly enhanced process performance, while addition of each of the remaining five nitrogen compounds (N3-N7) reduced the liquid yield obtained. These results are entirely consistent with preliminary nitrogen adduction data showing that neither THQ nor dipropylamine adducted at low severity reaction conditions while approximately 10-15 wt% 4-piperidinopyridine was adducted into the insoluble organic matter fraction.

A comparison of the data presented in Figures 1 and 2 also shows that no direct one-to-one correlation between the levels of coal conversion and liquid yield can be developed. This result has commonly been observed when using nitrogen compounds as conversion promotors, and points out the fact that conversion data alone cannot be used to infer information about liquid yields. Rather, distillations must be performed and used in material balance calculations to provide a direct measure of recoverable liquids.

Effect of Reaction Severity

Figure 3 summarizes coal conversion and liquid yield results from a series of THQ (N1) and dipropylamine (N2) addition experiments using Kentucky 9 coal and hydrogen gas at both low and high severity reaction conditions. Increased reaction severity resulted in a THF soluble coal conversion increase of approximately 22 wt% for the THQ runs, but only about 5 wt% increase for the dipropylamine runs. As shown, the liquid yield was much more sensitive to an increase in reaction severity, with yield increases of about 30 wt% and 53 wt% for the THQ and dipropylamine addition runs, respectively. Much of the increase noted can be attributed to increased cracking of the A-8 heavy oil at high severity conditions.

Preliminary nitrogen balance data for the high severity runs suggested that about half the THQ was adducted into the IOM fraction, and that over 90 wt% of the dipropylamine was cracked to ammonia and propane. In the absence of these losses, liquid yield results for the high severity runs would be higher than shown in Figure 3. Nevertheless, these data substantiate our hypothesis that compounds such as THQ and dipropylamine can be identified which remain effective coal dissolution promotors at low severity co-processing conditions. Improving low severity liquid yields will apparently require a second stage catalytic hydrocracker to process the high boiling residual material produced in the low severity co-processing first stage. Based on previous studies from our laboratory, this residuum should be very reactive and easily converted to distillable liquids.

Effect of Coal Rank and Feed Gas Composition

Additional low severity co-processing runs were completed to study the effects of coal rank (subbituminous vs. bituminous) and feed gas (H_2 vs. CO/H_2O) on the performance of THQ (N1) and dipropylamine (N2) as coal dissolution promotors. Results from these experiments are summarized in Figures 4 and 5. For the Kentucky 9 bituminous coal runs, use of hydrogen and either THQ or dipropylamine slightly improved both coal conversion and liquid yield. Conversely, significantly better Wyodak coal conversion and liquid yield were achieved using CO/H_2O, a result which would be expected based upon aqueous water-gas shift chemistry. Additional coal samples, including several Argonne premium coals will be studied to expand the coal rank relationships shown in Figures 4 and 5.

SUMMARY AND CONCLUSIONS

Results of low severity co-processing experiments completed to date clearly demonstrate the potential for using homogeneous basic nitrogen compounds to promote coal dissolution and increase liquid yields without significant nitrogen losses via adduction or thermal degradation. Both 1,2,3,4-tetrahydroquinoline and dipropylamine significantly improved coal conversion and distillable liquid yields, although, in general, no direct relationship between improvements in conversion and yield structure can be inferred. A comparison of liquid yields from low severity and high severity experiments suggests that a two-stage process consisting of a low severity coal dissolution first stage followed by a second stage catalytic hydrocracker would improve coal conversion and liquid yield while, at the same time, minimizing nitrogen losses via adduction or thermal degradation. Work to evaluate this co-processing concept is currently underway.

ACKNOWLEDGEMENT

The authors wish to acknowledge the financial support of the U.S. Department of Energy under Grant No. DE-FG22-86PC90909.

REFERENCES CITED

1. Fischer, F. and H. Schrader, Brennstoff-Chem., 2, 257, 1921.
2. Appell, H.R., et al., ACS Fuel Chem. Prepr., 20, 1, 58, 1975.
3. Fu, Y.C., and E.G. Illig, I&EC Proc. Des. Dev., 15, 392, 1976.
4. Bockrath, B.C., et al., ACS Fuel Chem. Prepr., 29, 5, 76, 1984.
5. Blaustein, B.D., et al., ACS Fuel Chem. Prepr., 30, 2, 359, 1985.
6. Severson, D.E., et al., ACS Fuel Chem. Prepr., 22, 6, 161, 1977.
7. Severson, D.E., et al., Energy Sources, 6, 173, 1982.
8. Sondreal, E.A., et al., Fuel, 61, 925, 1982.
9. Knudson, C.L., et al., ACS Fuel Chem. Prepr., 26, 1, 132, 1981.
10. Farnam, S.A., et al., ACS Fuel Chem. Prepr., 30, 2, 354, 1985.
11. Ross, D.S., et al., Fuel, 63, 1206, 1984.
12. Ross, D.S., et al., ACS Fuel Chem. Prepr., 30, 3, 94, 1985.
13. Ross, D.S., et al., "Exploratory Study of Coal Chemistry," Final Report for DOE Contract No. DE-AC22-81PC40785, December 1984.
14. Ross, D.S., et al., ACS Fuel Chem. Prepr., 30, 4, 339, 1985.
15. Porter, C.R., and H.D. Kaesz, "The ChemCoal Process for the Chemical Transformation of Low Rank Coal," Thirteenth Biennial Lignite Symposium, Bismarck, North Dakota, May 21-23, 1985.
16. Porter, C.R., et al., in Coal Processing Technology, vol. VII, pp. 135-140, AIChE, New York, 1981.
17. Miller, R.L., and R.M. Baldwin, ACS Fuel Chem. Prepr., 31, 1, 301, 1986.
18. Miller, R.L., and R.M. Baldwin, ACS Fuel Chem. Prepr., 31, 4, 152, 1986.
19. Miller, R.L., "Liquefaction Co-Processing: A Study of Critical Variables," EPRI Final Report for Project No. 2383-1, October 1987.
20. Atherton, L.F., and C.J. Kulik, "Advanced Coal Liquefaction," presented at Los Angeles AIChE Annual Meeting, November 1982.
21. Atherton, L.F., and C.J. Kulik, "Coal Liquefaction Chemistry," presented at Anaheim AIChE National Meeting, May 1984.

Table I

ULTIMATE ANALYSIS OF FEED COALS

Ultimate Analysis, wt% dry basis	Kentucky 9	Wyodak
Carbon	69.7	61.4
Hydrogen	4.7	4.0
Nitrogen	1.4	1.0
Sulfur	4.2	0.7
Oxygen (difference)	9.2	18.6
Ash	10.8	14.3
Total	100.0	100.0

Table II

PROPERTIES OF COLD LAKE ATMOSPHERIC RESIDUUM

Distillate Fraction	Wt%
Water	0.0
177°C-	0.4
177°-260°C	4.1
260°-343°C	4.1
343°-454°C	10.9
454°C+	80.5
Ultimate Analysis, wt% dry basis	
Carbon	84.2
Hydrogen	12.0
Nitrogen	1.0
Sulfur	1.1
Oxygen (difference)	1.7
Ash	0.0
Solvent Solubility, wt%	
Tetrahydrofuran	100.0
Toluene	100.0
Cyclohexane	100.0

Table III

MODEL NITROGEN COMPOUNDS STUDIED

Compound	Aqueous pK_b	Code Symbol
1,2,3,4-tetrahydroquinoline	8.97	N1
dipropylamine	3.00	N2
7,8-benzoquinoline	9.20	N3
piperidine	2.88	N4
4-piperidinopyridine	8.04	N5
5,6-benzoquinoline	10.05	N6
diphenylamine	13.23	N7

Table IV

CO-PROCESSING REACTION CONDITIONS

	Low Severity	High Severity
Reaction Temp. (^{o}C)	344	440
Feed Gas	CO/H_2O, H_2	H_2
Initial Pressure (psig)	850	1000
Maximum Pressure (psig)	1500	2000
Time at Temp. (min)	30	30
Coal/A-8/Nitrogen Compound Feed Ratio	1/1.5/0.5	1/1.5/0.5

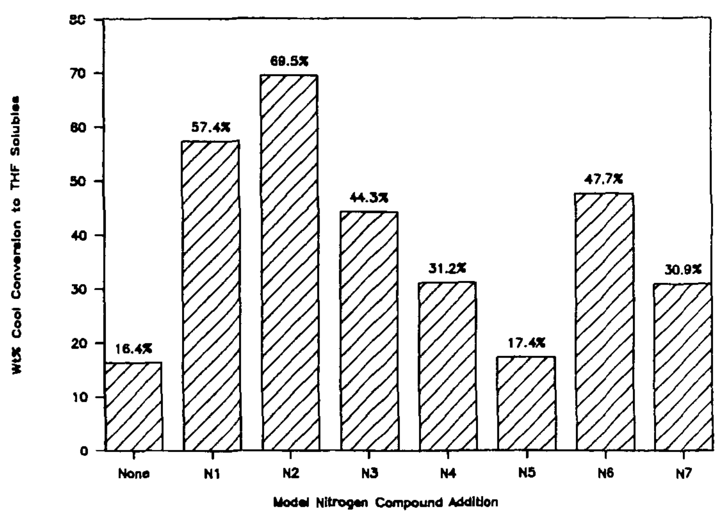

Figure 1. Effect of Model Nitrogen Compound Addition on Low Severity Conversion of Kentucky 9 Coal With Carbon Monoxide Feed Gas

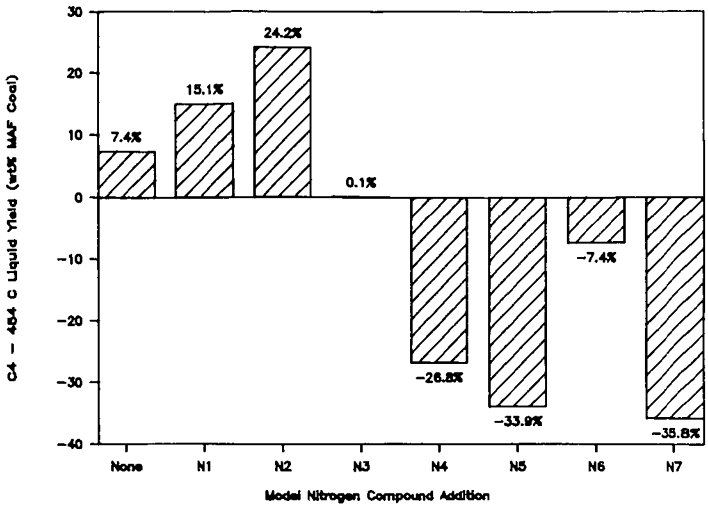

Figure 2. Effect of Model Nitrogen Compound Addition on Distillate Liquid Yield from Low Severity Co-Processing of Kentucky 9 Coal with Carbon Monoxide Feed Gas

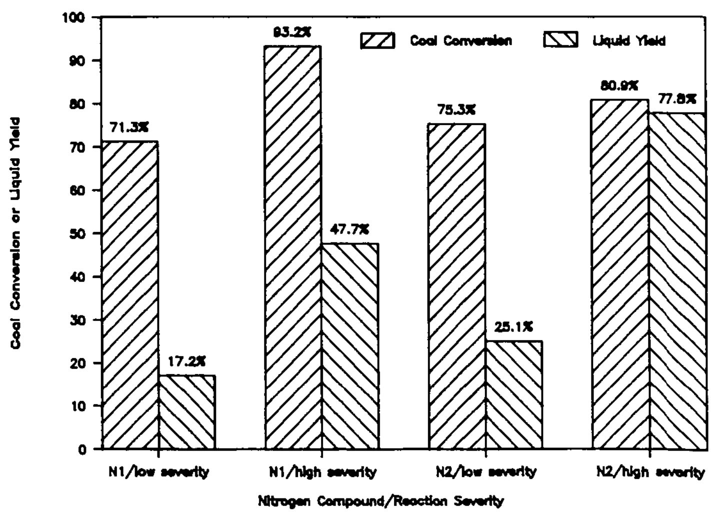

Figure 3. Effect of Model Nitrogen Compound Addition and Reaction Severity on Kentucky 9 Coal Conversion and Distillate Liquid Yield with Hydrogen Feed Gas

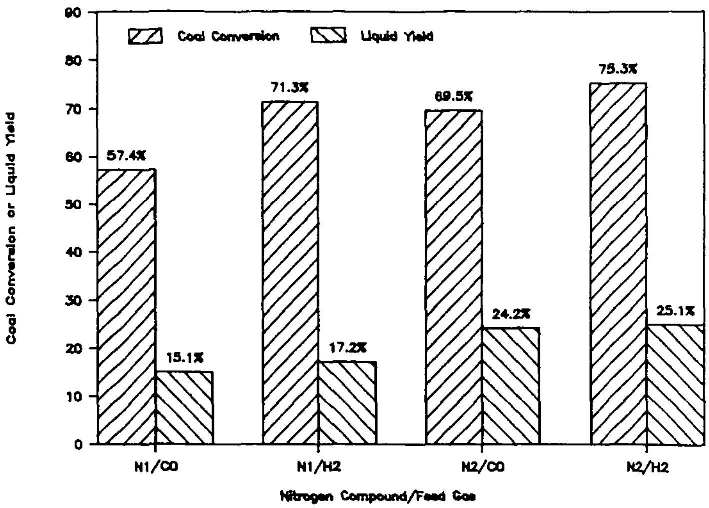

Figure 4. Effect of Model Nitrogen Compound Addition and Feed Gas on Kentucky 9 Coal Conversion and Distillate Liquid Yield at Low Severity Co-Processing Conditions

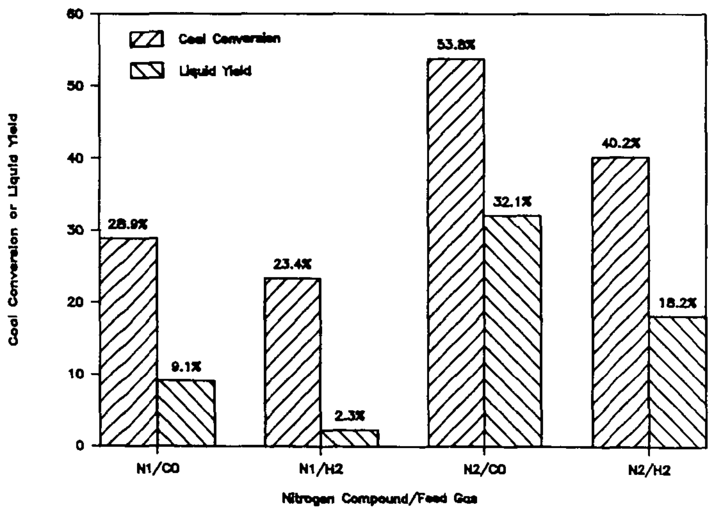

Figure 5. Effect of Model Nitrogen Compound Addition and Feed Gas on Wyodak Coal Conversion and Distillate Liquid Yield at Low Severity Co-Processing Conditions

COPROCESSING COAL LIQUIDS WITH PETROLEUM RESID

Michael M. Schwartz and Albert L. Hensley

Amoco Oil Company
Amoco Research Center
P.O. Box 400
Mail Station H-4
Naperville, IL 60566

ABSTRACT

A series of bench-scale experiments was run to determine the advantages and disadvantages of processing coal liquids with petroleum resid. Standard resid, blends of resid containing 15 and 40% coal-derived liquids (from Wilsonville), plus the neat coal-derived component of the blends were evaluated. The parameters evaluated were: (1) Hydrogen Consumption; (2) Conversions (1000+°F, hydrodesulfurization (HDS), hydrodenitrogenation (HDN), and Ramscarbon removal (HDR)); (3) Catalyst Activity; (4) Unit Operability; and (5) Product Quality (total liquid product plus 360-, 360-650, 650-1000, and 1000+°F fractions).

The major findings are: (1) Hydrogen consumption and HDN increased with increasing coal liquids but HDS and HDR were independent of feed; (2) Coal liquids did not accelerate catalyst deactivation; (3) Unit operability increased with increasing coal-liquids content of the feed; (4) Aromaticity of the 360-, 360-650, and 650-1000°F fractions all increased with increasing coal liquids.

INTRODUCTION

As part of its synfuels development program, Amoco has been doing research to improve the economics of converting coal into liquid fuels using the technique known as direct coal liquefaction.[1-3] Direct liquefaction is a proven technology--used by Germany to produce liquid fuels during World War II. However, it is not economic at the current price of crude oil and there is no current commercial source of coal liquids. The economics of coal liquefaction would improve if existing petroleum refinery units could be used to upgrade coal-derived liquids rather than building a grass-roots facility. The research program described herein was conducted to determine the advantages and disadvantages of processing coal liquids with petroleum resids.

EXPERIMENTAL

Feedstocks

Maya-containing 1000+°F resid blend (Feed A) was chosen as the resid benchmark. Coal-derived liquid (containing about 50% 1000+°F material and designated Feed B) obtained from the Wilsonville, Alabama pilot plant was used to make the blends. The feedstocks containing 15% and 40% coal liquids were designated Feed C and Feed D respectively. The inspections of these feeds are shown in Table I.

Reactor

An automated continuous resid hydroprocessing pilot plant was used. High pressure hydrogen enters through a pressure stepdown and metering device and exits through an outlet pressure control loop so that hydrogen pressure and flow can be controlled within narrow limits. The existing gases pass either into a gas sampling device or through a scrubber and into a wet test meter. Feed is added by a positive displacement pump. Feed and hydrogen flow concurrently upflow through a vertical pipe reactor. The pipe reactor is heated by four independently fired and controlled heating zones. Reactor temperature is measured in a centrally located axial thermocouple well by a travelling thermocouple. Feed exits from the top of the reactor and is collected in either of the following two ways:

1. In normal operation, feed exits through a high pressure gas-liquid separator via a Research Control Valve (RCV) with a control loop that maintains a constant liquid level in the high pressure separator. In this mode, product liquid is collected continuously in a glass bottle at atmospheric pressure.

2. Under some process conditions, solids are formed which plug the RCV making the unit inoperable in that mode. The high pressure receiver is used when high solids conditions are encountered. In this mode, product liquid is held in a heated (about 300°F) Hoke vessel at the system pressure until the vessel is drained and the product is collected (typically every 24 hours).

Reaction Conditions and Sequence of Feedstock Testing

Only feedstock and reactor temperature were varied. Kept constant were liquid feedrate, pressure, and hydrogen flow rate. The feedstock comparison started with a reactor temperature of "base". Sequentially, data were obtained with Feedstocks A (0% coal-liquids), C (15% coal liquids), D (40% coal-liquids), and then with A (0% coal-liquids) again to determine catalyst deactivation. The temperature was then raised to "base + 20°F" continuing with Feedstock A (0% coal-liquids) and then sequentially testing as was done at "base". At the end of the "base + 20°F" test sequence, the program was expanded to also test the 100% coal-liquids feed, Feed B. This experimental program was designated Run 17-258.

RESULTS

Table II shows the average total liquid product inspections for each feedstock in the sequential order the feeds were run; the standard deviation for each inspection is given in parenthesis. The inspections listed in Table II are: °API, percent Shell hot filtration (SHFT), percent hexane insoluble; also percents sulfur, nitrogen, and Ramscarbon.

Table III shows the mass balance data: percent C_1-C_4 gas-make, total hydrogen consumption (SCF/B) and weight percent product recovered. Table IV shows the conversions obtained with each feed, again in the sequential reaction order. Sulfur, nitrogen, and Ramscarbon conversions are the averages for the run period.

Inspections on the 360-, 360-650, 650-1000, and 1000+°F fractions (collected by atmospheric distillation of the 650-°F fractions and vacuum distillation of the 650+°F material) have been obtained for each of the feedstocks after reaction at each temperature. The data from reaction at "base" and "base + 20°F" are shown in Tables V and VI respectively.

Unit Operability

Figure 1 shows the effect of coal-liquids and reaction temperature on SHFT during normal operation through the RCV. Our data clearly show that operability increases with increasing coal-liquids content and the improved operability with added coal liquids is much more pronounced at the higher temperature.

In normal operation, the reaction product continually exits the unit through a separator, the level of which is controlled by a research control valve (RCV). During periods of good operability, flow through the RCV is smooth and the liquid product has a low value for an inspection called the Shell Hot Filtration Test (SHFT). SHFT is a measure of the amount of solids formed. At "base temperature" operation through the RCV was possible with either 0, 15, or 40% coal-liquids giving average SHFT inspections of about 1.2, 0.8, and 0.6, respectively. At "base + 20°F" operability was fine with 15, 40 and 100% coal-liquids resulting in SHFT inspections of 0.8, 0.5, and 0.2, respectively.

In contrast, operation at "base + 20°F" with Feed A was impossible; the RCV plugged and had to be by-passed by using the high pressure receiver. The SHFT inspections of these high pressure receiver products, about 0.88, are lower the the SHFT of 1.2 obtained at "base". Since operability should improve with lower SHFT inspections, the SHFT data obtained from operation with the high pressure separator do not accurately reflect unit operability and cannot be compared with data obtained during operation through the RCV. We do not know why the SHFT inspections are not comparable.

Catalyst Activity

The use of coal liquid-containing feeds had no unusual effect on catalyst activities. Catalyst activity only declined with time on stream at a given temperature, with deactivation increasing with increasing temperature, as would be expected for any feed.

The data for denitrogenation have the lowest experimental error and are used to show our results, but similar trends were followed for sulfur and Ramscarbon reduction.

Figure 2 shows the relative denitrogenation reactivity for each of the feeds in the sequential order which they were run. Relative reactivity is defined as the ratio of 1st-order rate constants to Day 69 for reaction at base and the ratio to day 105 for reaction at "base + 20°F". As is seen, the reactivity of benchmark Feedstock A at "base" was identical before and after running the coal-liquid blends. The reactivity at "base + 20°F" was slightly lower after running the blends, but the decline was very small and is attributed to the expected catalyst deactivation at this temperature and not to the use of coal liquid-containing feeds.

The explanation for the greater denitrogenation of the coal liquids-containing feeds is unknown. One possibility is that the nitrogen-containing compounds in the coal liquids are inherently easier to denitrogenate than those in the petroleum resid. Alternatively, the greater denitrogenation of the coal liquids-containing feeds might simply be a result of their greater amounts of 1000-°F material present (14, 25, and

50% in Feeds C, D, and B, respectively, versus 8% in A); previous studies have shown that ease of upgrading increases as boiling point of the feed decreases.

Conversions and Hydrogen Uptake

The percent conversions of 1000+°F material to 1000-°F material, nitrogen removal, Ramscarbon removal, and sulfur removal for each coal liquid-containing feed plus Feed A at "base" and "base + 20°F" are shown in Figures 3-6 respectively. Conversion of 1000+°F material is calculated (correcting for 1000-°F material in the feed) from one actual distillation of combined product collected over each run period. Nitrogen, Ramscarbon, and sulfur conversions are calculated from inspections of daily products and then averaging the results. Hydrogen uptake is shown in Figure 7. Hydrogen uptake is the average of mass balance calculations taken during each run period.

All conversions with the 15 and 40% blends of coal liquids were always equal to or greater than the conversion with Feed A alone, indicating that no penalty in conversion would result from the addition of coal liquids. Also, the 1000+°F conversions of the blends were higher than those of the straight A and B feeds. This suggests the possibility of a synergistic interaction, but the data do no warrant a definitive statement to that effect. C_1-C_4 gas make appeared independent of feed at each temperature.

Denitrogenation increased with increasing coal-liquids. However, as discussed above, this could have simply been caused by the lower boiling points of these feeds.

Ramscarbon and sulfur conversions were slightly higher at each temperature with the blends than with Feed A, but the differences probably are not statistically significant.

Hydrogen uptake increased with increasing coal liquids at each temperature and hydrogen uptake increased with increasing temperature. This result is expected because the coal liquids are more aromatic than petroleum resid (Feed A) and more hydrogen would go into ring saturation.

Product Quality

Each boiling range fraction got more aromatic and had a lower sulfur content with increasing coal-liquids content at each temperature. These results are illustrated in Figures 8 and 9 which show percent aromatics and percent sulfur in the 650-1000°F cuts, respectively.

The nitrogen contents of the cuts did not show a consistent pattern. The 360-°F cut showed increasing nitrogen with increasing coal-liquids. The 360-650°F fraction showed increasing nitrogen with increasing coal-liquids only at "base". The nitrogen content within the 650-1000°F fraction was the same with each feed at each reaction temperature.

SUMMARY

The purpose of these experiments was to answer the question: "How would the addition of coal-liquids affect resid hydroprocessing?", specifically addressing the topics of unit operability, conversion and hydrogen consumption, catalyst activity maintenance, and product quality.

Our conclusions are:

1. Unit Operability: BETTER
2. Conversions: EQUAL OR HIGHER
3. Hydrogen Consumption: HIGHER
4. Unexpected Effect on Catalyst Activity: NONE
5. Product Quality: MORE AROMATIC, LOWER SULFUR.

REFERENCES

1. Brooks, J. A., R. J. Bertolacini, L. C. Gutberlet, and D. K. Kim, "Catalyst Development for Coal Liquefaction," EPRI Final Report for RP #408-1, -2, November 1979.

2. Mahoney, J. A., J. J. Helstrom, and R. J. Pellet, "Coal Liquefaction Catalyst Development," DOE Final Report for Contract #DE AC 22-79ET-14803, August 1982.

3. Tait, A. M., M. M. Schwartz, and M. A. Pacheco, "Advanced Coal Liquefaction Catalyst Development, DOE Contract Number DE-AC22-81PC40009: Final Report," April 29, 1986.

TABLE I

FEEDSTOCK INSPECTIONS

Percent Coal Liquids:	0	15	40	100
Feedstock Identification:	A	C[a]	D[b]	B[c]
Elemental Analyses				
C, %	84.85	85.38	86.22	88.40
H, %	10.39	10.06	9.55	8.48
S, %	4.04	3.38	2.56	0.26
O, %	1.48	0.83	2.01	1.57
N, %	0.49	0.54	0.59	0.78
Ni, ppm	56	46	34	<2
V, ppm	246	201	152	<2
Ramscarbon, %	18.5	20.1	20.6	22.4
Oil, %	29.3	29.2	29.2	24.8
Resin, %	58.5	56.9	56.5	56.1
Asphaltene, %	12.0	11.5	9.4	4.3
°API	6.8	6.0	4.0	-1.5
% 1000+°F[d]	92	85.6	75	49.5

(a) C = 85% A + 15% B.
(b) D = 60% A + 40% B.
(c) Blend of Wilsonville liquids derived from Illinois No. 6 coal.
(d) By distillation.

TABLE II

RUN 17-258

AVERAGE TOTAL LIQUID PRODUCT INSPECTIONS*

Reaction Temperature	Base				Base + 20°F				
Feedstock Identification	A	C	D	A	A	C	D	A	B
% Coal Liquids in Feed	0	15	40	0	0	15	40	0	100
Sample Days	62–69	72–77	80–84	87–96	99–105	110–119	123–132	136–142	146–152
°API	21.9 (.43)	19.0 (.1)	16.6 (.2)	21.2 (.5)	25.5 (.6)	23.2 (.5)	20.2 (1.0)	25.6 (.5)	10.3 (.4)
S, wt%	0.62 (.03)	0.47 (.05)	0.27 (.01)	0.60 (.03)	0.40 (.04)	0.34 (.02)	0.25 (.04)	0.52 (.04)	0.080 (.027)
N, wt%	0.323 (.025)	0.348 (.031)	0.331 (.015)	0.321 (.016)	0.266 (.023)	0.294 (.013)	0.288 (.025)	0.285 (.010)	0.304 (.014)
Ramscarbon, wt%	7.05 (.04)	7.26 (.30)	6.78 (.18)	7.15 (.15)	3.20 (1.37)	3.02 (1.26)	3.56 (1.11)	4.34 (1.04)	4.66 (.13)
SHFT	1.07 (.52)	0.80 (.35)	0.61 (.30)	1.30 (.31)	0.97[a] (.46)	0.83 (.23)	0.48 (.13)	0.78[a] (.22)	0.15 (.05)
Hexane Insoluble, wt%	3.94 (.35)	4.18 (.55)	3.26 (.14)	4.18 (.27)	2.60 (.61)	2.61 (.24)	2.16 (.21)	2.63 (.12)	1.67 (.2)

*Mean (Standard Deviation)

(a) Sample from high-pressure receiver.

TABLE III

RUN 17-258
MASS BALANCE DATA

Reaction Temperature	Base					Base + 20°F						
Feedstock Identification	A		C	D	A	A	C	D		A		B
% Coal Liquids in Feed	0		15	40	0	0	15	40		0		100
Sample Days	68	72	77	83	92	104	117	131	139	142	147	152
C_1-C_4, %	3.1	3.7	3.8	3.8	4.0	10.0	6.2	5.0	6.0	6.0	7.5	7.5
Hydrogen Consumption, SCF/B	1078	1139	1226	1456	1105	1858	1620	1660	1338	1468	1837	1754
Wt% Product Recovered	100	90	100	97	86	114	101	96	96	100	99	99

TABLE IV

RUN 17-258
CONVERSIONS

Reaction Temperature	Base				Base + 20°F				
Feedstock Identification	A	C	D	A	A	C	D	A	B
% Coal Liquids in Feed	0	15	40	0	0	15	40	0	100
Sample Days	62–69	72–77	80–84	87–96	99–105	110–119	123–132	136–142	146–152
% Desulfurization	85	86	89	85	90	90	90	88	69
% Denitrogenation	32	35	44	32	44	46	51	42	62
% Ramscarbon Conv.	62	64	67	62	83	85	82	77	79
% 1000°+ Conv. by Distillation	—	70.0	71.1	67.5	82.7	88.8	88.9	82.4	77.4

TABLE V

INSPECTIONS OF PRODUCTS AFTER "BASE" HYDROTREATING

Coal Liquids in Feed, %	0	15	40
Feedstock Identification	A	C	D
Run Identification, 17-258-	94	77	84
360°F-, wt%	4.8	4.1	3.9
C, %	82.61	86.04	86.26
H, %	13.95	14.17	14.01
N, ppm	20	212	241
S, %	0.079	0.049	0.022
Paraffins, wt%	54.8	48.0	44.2
Cycloparaffins, wt%	29.0	31.6	34.4
Aromatics, wt%	16.3	20.4	21.4
360-650°F, wt%	24.9	27.7	30.7
C, %	87.25	87.65	87.84
H, %	12.97	12.56	12.07
N, ppm	832	1220	1310
S, %	0.74	0.056	0.034
°API	31.0	30.3	26.6
Paraffins, wt%[a]	30.6	25.3	18.1
Cycloparaffins, wt%[a]	30.5	31.0	31.1
Aromatics, wt%[a]	38.9	43.7	50.8
C-sub-A, wt%[a]	17.2	17.5	23.1
650-1000°F, wt%	37.9	41.5	43.1
C, %	87.48	87.74	88.85
H, %	11.81	11.23	10.87
N, ppm	0.30	0.28	0.32
S, %	0.51	0.41	0.22
°API	19.68	16.53	13.30
Ramscarbon, %	7.30	7.61	5.75
Paraffins, wt%[a]	14.5	12.5	7.8
Cycloparaffins, wt%[a]	31.2	29.5	22.0
Aromatics, wt%[a]	54.3	58.0	70.2
C-sub-A, wt%[a]	25.8	30.6	35.8
Oils, %	70.3	65.1	58.3
Resins, %	28.7	33.0	39.8
Asphaltenes, %	0	0	0
1000°F+, wt%	29.9	25.7	21.7
C, %	87.89	88.38	89.13
H, %	9.96	9.61	9.08
N, ppm	0.61	0.65	0.64
Ni, ppm	22	25	20
V, ppm	6	5	2
S, %	1.18	1.00	0.66
°API	5.24	2.79	0.12
Ramscarbon, %	23.7	29.1	31.6

(a) By Robinson-type mass spectral analysis.

TABLE VI

DISTILLED PRODUCT INSPECTIONS FROM HYDROTREATING AT "BASE + 20°F"

Feed Identification:	A	C	D	B
Run 17-258-	135-139	111-116	122-126	148-151
Coal Liquids in Feed %:	0	15	40	100
360°F-Wt%	9.08	9.0	8.5	5.1
C, %	85.07	81.73	85.32	86.87
H, %	14.41	13.35	14.09	13.17
N, ppm	136	158	222	348
S, ppm	480	238	300	279
360-650°F Wt%	39.51	37.7	38.2	46.0
C, %	86.94	87.19	87.89	88.89
H, %	12.64	12.47	12.11	10.86
N, %	0.132	0.124	0.115	0.137
S, ppm	1250	440	240	50
°API	32.7	32.6	28.4	19.0
Paraffins, wt%[(a)]	30.2	27.7	21.7	4.8
Cycloparaffins, wt%[(a)]	30.7	30.4	30.9	28.8
Aromatics, wt%[(a)]	39.1	41.9	47.4	66.4
C-sub-A, wt%[(a)]	18.0	17.2	20.1	32.4
650-1000°F, Wt%	33.77	43.4	43.9	36.2
C, %	87.33	88.26	88.90	91.14
H, %	11.28	10.65	10.35	8.00
N, %	0.349	0.394	.337	.440
S, %	0.56	0.44	0.276	0.011
API	19.1	13.2	10.7	-1.2
Ramscarbon, %	1.2	2.5	1.8	1.1
Paraffins, wt%[(a)]	15.5	10.8	7.0	--
Cycloparaffins, wt%[(a)]	27.5	22.6	16.7	--
Aromatics, wt%[(a)]	57.0	66.6	76.3	100
C-sub-A, wt%[(a)]	28.8	33.8	41.7	63.1
Oils, %	68.0	61.3	55.9	35.1
Resins, %	31.1	35.7	41.1	62.6
Asphaltenes, %	0.4	0.8	0.4	0.8
1000°F+, Wt%	16.24	9.6	8.3	11.21
C, %	88.23	90.32	89.11	92.25
H, %	8.63	7.91	7.81	6.36
N, %	0.793	0.814	0.592	.206[(?)]
S, %	1.39	.98	.63	.044
Ni, ppm	31	29	26	16
V, ppm	16	7	4	5
°API	-1.5	-5.6	-9.4	-11.4
Ramscarbon, %	34.7	42.5	52.5	49.9

(a) By Robinson-type mass spectral analysis

FIGURE 1

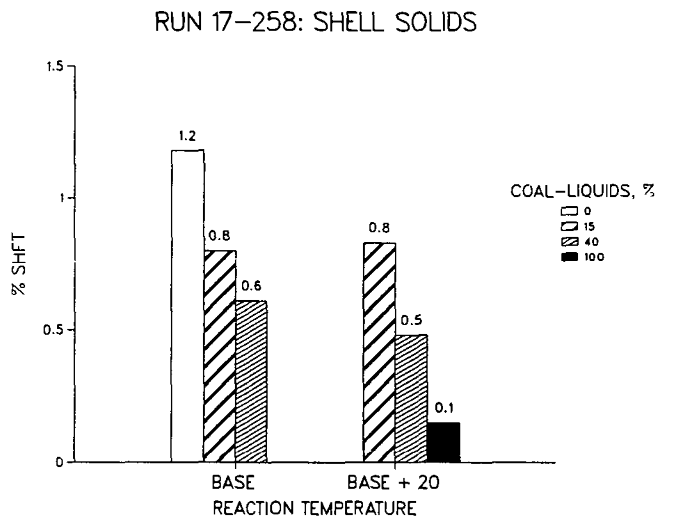
RUN 17-258: SHELL SOLIDS
1.5
1
0.5
0
% SHFT
1.2
0.8
0.6
0.8
0.5
0.1
BASE
BASE + 20
REACTION TEMPERATURE
COAL-LIQUIDS, %
0
15
40
100

FIGURE 2

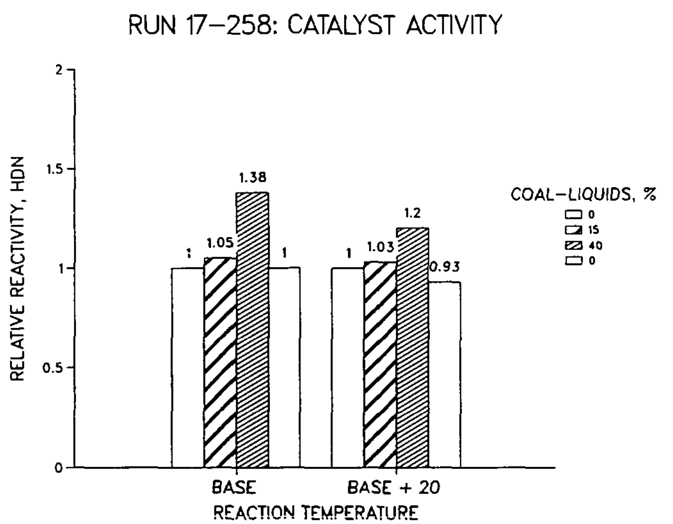

FIGURE 3

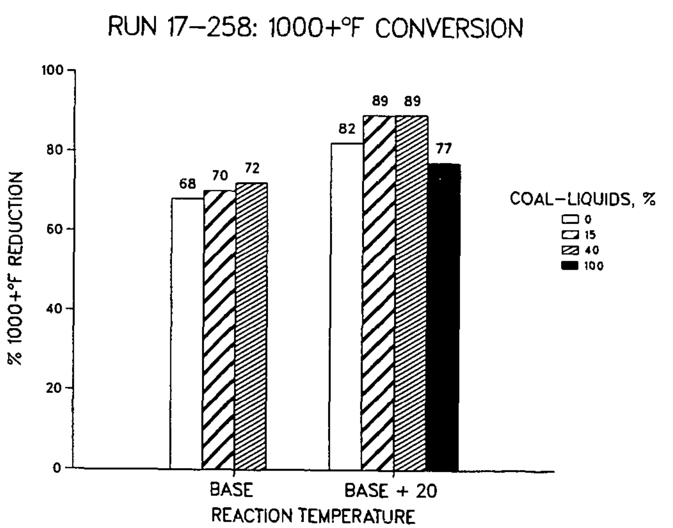

FIGURE 4

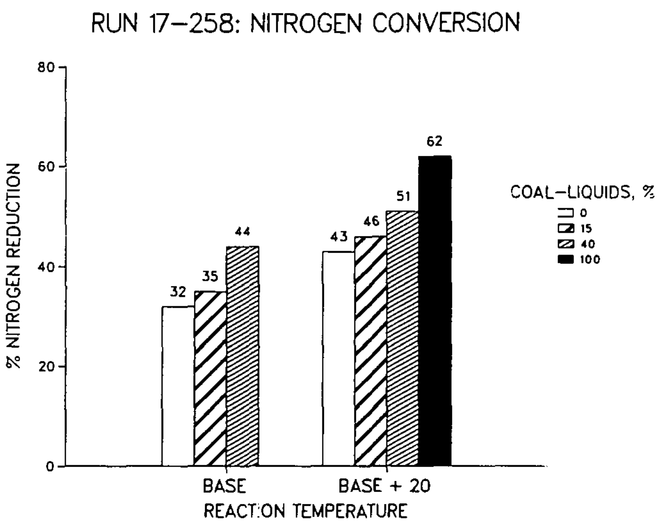

FIGURE 5

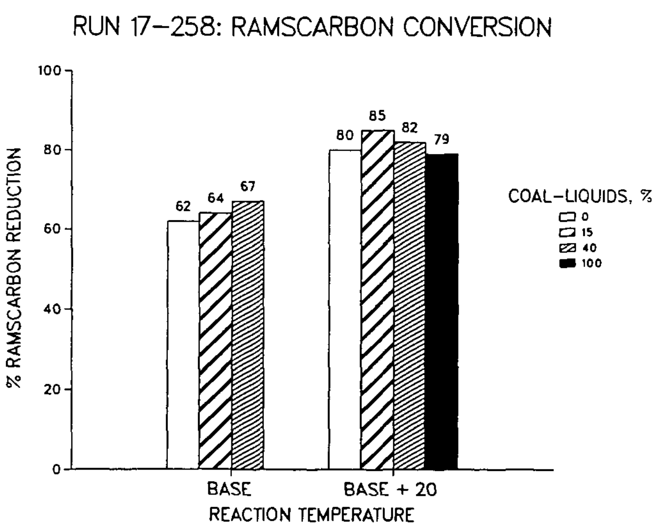

FIGURE 6

RUN 17–258: SULFUR CONVERSION

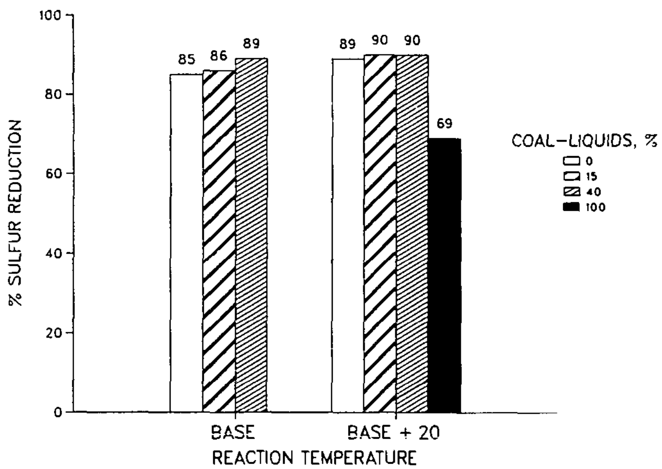

FIGURE 7

RUN 17–258: HYDROGEN UPTAKE

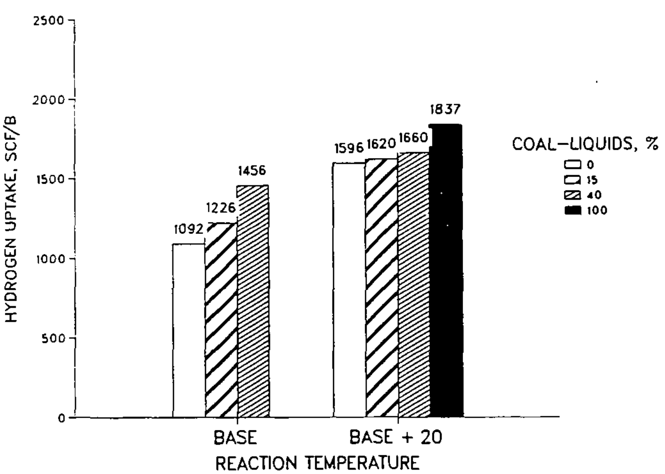

FIGURE 8

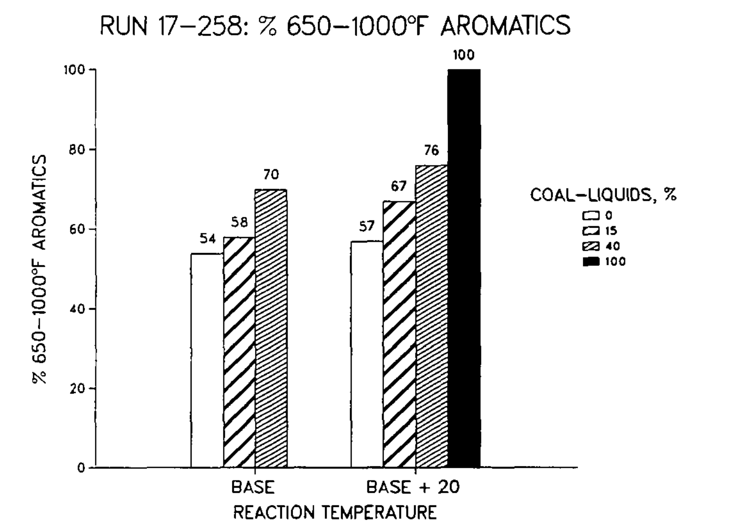

FIGURE 9

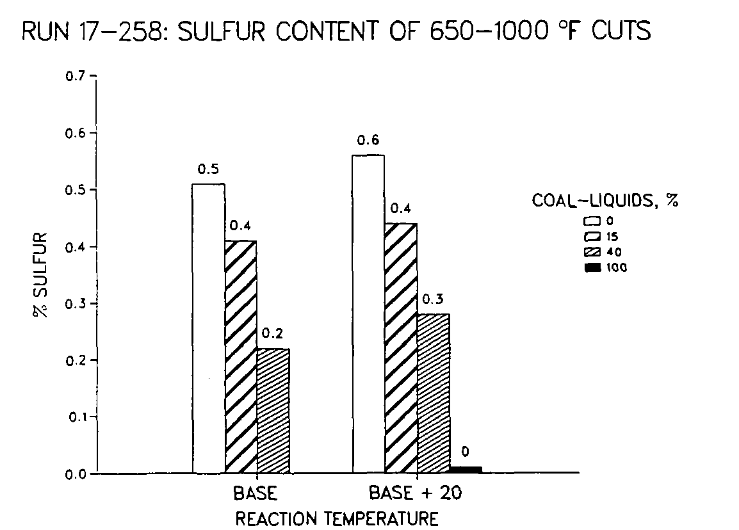

Effect of Coal Concentration on Coprocessing Performance

Safaa A. Fouda, James F. Kelly and Parviz M. Rahimi

CANMET, Energy Research Laboratories
Energy, Mines and Resources Canada, 555 Booth Street
Ottawa, Ontario, Canada, K1A 0G1

Introduction

Coprocessing represents an attractive combination of heavy oil upgrading and coal liquefaction technology. Compared with coal liquefaction, coprocessing eliminates or reduces the use of a recycle oil solvent. This results in a greater proportion of the reactor volume being occupied by upgradable feedstock rather than recycle solvent. The net result is higher effective reactor throughput and lower capital and operating costs. Compared with heavy oil upgrading, coprocessing offers the ability to increase operating margins by replacing expensive oil with lower cost coal. There are also other benefits related to the ability of the added coal to act as an adsorbent for coke formed during the reaction and for heavy metals present in most feedstocks. For some processes and under certain operating conditions there is also the possibility of synergistic effects which results in better process yields (1-2).

In the final analysis the real challenge is to make coprocessing more economically attractive than heavy oil upgrading and this requires a better understanding of the effects that adding more coal to the feed can have on fundamental process behaviour. This paper describes the effects of increasing coal concentration on the coprocessing performance of the CANMET process operating with an Alberta subbituminous coal and Cold Lake vacuum bottoms(CLVB).

Experimental

All experiments were performed with Forestburg subbituminous C coal (from Luscar Ltd.) in minus 200 mesh size(75 μm). The same coal was used to prepare an iron based disposable additive for the process by impregnation with iron sulphate using a water slurry. Coal characteristics are given in Table 1 and those of the oil feed (CLVB, from Imperial Oil Ltd.) in Table 2. Slurry feeds with coal concentrations up to 39.5 wt. % maf coal were prepared by mixing the coal, the additive and the oil to keep the total iron concentration constant at approximately 0.50 wt. % on a maf slurry feed basis.

Coprocessing experiments were carried out in a single stage bench-scale unit which is described elsewhere (3). For comparison purposes, all experiments were performed at 450°C, 13.9 MPa total pressure, 1.0 kg/h·L nominal space velocity and 71.4 g H_2/kg slurry feed(4500 SCF/B). Details of the product workup procedures are also described elsewhere (3).

Results and Discussion

There was a marked difference in process operability in the absence of coal versus its presence in small concentrations even though the same amount of iron based catalyst was used in both cases. Without coal, reactor outlet plugging was experienced and long term operation was not possible. When coal was used, no operational problems were encountered at up to about 40 wt.% maf coal in the slurry feed. This indicates a potential benefit of coprocessing where the coal is used as a carrier or support for a disposable catalyst.

Process Yields

Gross process yields are shown as a function of coal concentration in Figure 1. The addition of about 2-4 wt.% maf coal results in a significant increase in distillate yield. Similar results have also been reported based on isotopic mass balance measurements for an Athabasca atmospheric resid and Vesta subbituminous coal without the use of a catalyst (4). At coal concentrations over the range of most operational interest for coprocessing, the distillate yield is constant and equal to that for the no coal case until a slight drop is observed starting at about 30 wt.% maf coal. These results indicate a potential synergism at lower coal concentrations for a disposable iron based catalyst process of this type. More experimental work needs to be done to determine how this effect is influenced by different catalyst concentrations and other operating parameters such as temperature and space velocity.

Residue yield is almost a mirror image of the distillate yield as would be expected if gas yield is relatively constant as shown in Figure 1. About 30 to 50% of this residue is pentane soluble oil which with a proper solid separation scheme might be extracted for further upgrading to distillate. With more severe operation, residue yields can be lowered to the 20 wt.% range including pentane soluble oils.

Coal and Pitch Conversion

The effect of coal concentration on coal and pitch conversion is shown in Figure 2. The coal conversion data suggests that two different mechanisms are prevalent; one for low coal concentrations and one for higher concentrations starting at about 10 wt.% maf coal. Similar results have been reported when coal-derived liquids replaced a portion of a heavy oil feed (5). This would explain the higher coal conversion values at higher coal concentrations where more coal derived liquids would be available to enhance hydrogen transfer reactions compared with lower coal concentrations where the predominant effect is due to the oil solvent only. For this reacting system, a coal concentration of about 10 wt.% on a maf slurry feed basis is required to observe an enhancement in coal conversion.

Pitch conversion values are directly proportional to residue yields and this accounts for the similar shapes of these curves which are shown in Figures 1 and 2.

Distillate Characteristics

Gross distillate characteristics as a function of coal concentration are shown in Figure 3 . It is apparent that increasing coal concentration in the slurry feed does not decrease the specific gravity or H/C atomic ratio of the overall distillate product. Although the H/C ratio of the product is essentially constant with increasing coal concentration the difference in H/C ratio between slurry feed and distillate product results in a monotonic increase with increasing coal concentration indicating that hydrogen addition reactions are enhanced. This advantage is offset somewhat since with increasing coal concentration the aromaticity of the distillate as determined from ^{1}H NMR and the Brown-Ladner equation is also increasing as shown in Figure 3. However, an increase in aromaticity of the naphtha fraction, would be an advantage for high octane gasoline production obtained by reforming the naphtha.

Metals Removal

The effect of coal concentration on vanadium and nickel removal is shown in Figure 4. Based on these results, which show a considerable amount of scatter, nickel seems to be preferentially removed at lower coal concentrations even though it's concentration in the slurry feed is less than half that of vanadium. As the coal concentration increased, the vanadium and nickel concentration in the slurry feed decreased but as shown in Figure 4 removal of both nickel and vanadium increased. Similar results have been reported for other coals and oil feedstocks (2,6) and this highlights an advantage of coprocessing over other upgrading technologies.

Conclusions

Process operability is improved by the addition of coal. At low coal concentrations in the CANMET process a synergism exists in terms of distillate yields. However, more research needs to be undertaken to determine how other operating parameters affect the degree of potential improvement and if it can be maintained for higher coal concentrations of more interest for commercial operations. The present results indicate that replacing oil with increasing amounts of coal in the feed does not lower the amount of distillate produced up to a coal concentration of about 30 wt.% maf on a slurry feed basis.

Two different mechanisms seem to be operating in terms of coal conversion. For low coal concentrations where the effect of coal derived liquids is negligible, coal conversion decreases with increasing coal concentration. At higher coal concentrations, the presence of coal derived liquids is suggested to result in an increase in coal conversion. Hydrogen addition and metals removal are enhanced with increasing coal concentration but the resulting distillate product becomes more aromatic. This could have significant influence on the type and nature of downstream upgrading to produce marketable products.

References

1. Duddy, J.E., MacArthur, J.B. and McLean, J.B. "HRI's Coal/Oil Co-processing Program", proceedings of the DOE Direct Liquefaction Contractors' Review Meeting, pp304-320, Monroeville, Pa., October 20-22, 1986.

2. Greene, M., Gupta, A. and Moon, W. "Status of the LCI Co-processing Project", proceedings of the EPRI Eleventh Annual Conference on Clean Liquid and Solid Fuels, Palo Alto, California, May 7-9, 1986.

3. Kelly, J.F., Fouda, S.A., Rahimi, P.M. and Ikura, M. "CANMET Coprocessing: A Status Report", proceedings of the Coal Conversion Contractors' Review Meeting, Report SP85-4(ed. James F. Kelly), pp397-423, Calgary, Alberta, November 14-16, 1984.

4. Steer, J., Muehlenbachs, K., Ohuchi, T., Carson, D., Doherty, B. and Ignasiak, B. "Isotopic Constraints on the Efficiency of Liquefaction of Low-Rank Coal", proceedings of the 14 th. Biannual Lignite Symposium on Technology and Utilization of Low-Rank Coals, Dallas, Texas, May 18-21, 1987.

5. Curtis, C.E., Tsai, K. and Guen, J.A., Fuel Processing Technology, 16, pp.71-87, 1987.

6. Lett, R.G. and Cugini, A.V. "Coprocessing Studies", proceedings of the DOE Direct Liquefaction Contractors' Review Meeting, pp362-378, Monroeville, Pa., October 20-22, 1986.

Table 1 - **Characteristics of Forestburg Subbituminous C Coal**

Proximate Analysis (wt.% as received)		Ultimate Analysis (wt.% dry basis)	
Moisture	19.17	Carbon	64.04
Ash	7.68	Hydrogen	3.87
Volatile matter	34.00	Sulphur	0.53
Fixed carbon	39.15	Nitrogen	1.65
		Ash	9.50
		Oxygen(by diff.)	20.41
Metal Content, ppm			
Fe	2379		
Ni	18	Calorific Value	
V	trace	cal/g	4933
		btu/lb	8879

Petrographic analysis, vol.% as received on -200 mesh size	
Vitrinite	92.2
Liptinite	2.6
Inertinite	3.1
Mean reflectance	0.42

Table 2 - **Characteristics of Cold Lake Vacuum Bottoms**

General	
Specific Gravity, 15/15°C	1.038
Conradson Carbon Residue, wt.%	17.1
Pentane Insolubles, wt.%	23.48
Benzene Insolubles, wt.%	0.20
Aromaticity (^{1}H NMR)	34.5
Viscosity, at 80°C, poise	249.12
at 110°C, poise	21.59
Distillation (Spinning Band)	
IBP, °C	420
Distillate (-525°C), wt.%	16.8
Residue (+525°C), wt.%	83.25
Elemental Analysis, wt.%	
Carbon	78.6
Hydrogen	9.3
Sulphur	5.5
Nitrogen	0.6
Ash	0.0
Oxygen (by difference)	5.9
Metal content, ppm	
Fe	18
Ni	93
V	235

Figure 1

Effect of Coal Concentration on Yields

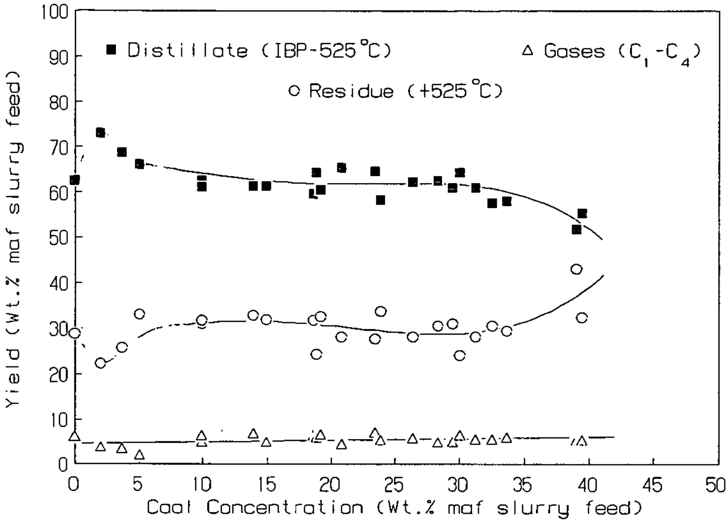

Figure 2

Effect of Coal Concentration on Conversion

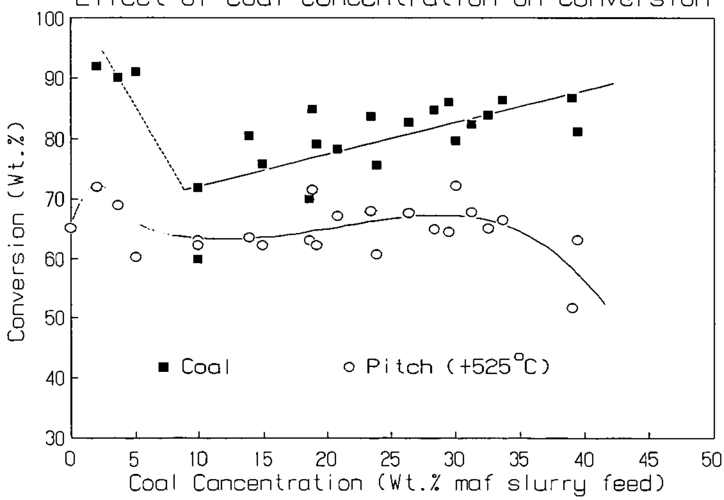

Figure 3
Effect of Coal Concentration on Distillate Characteristics

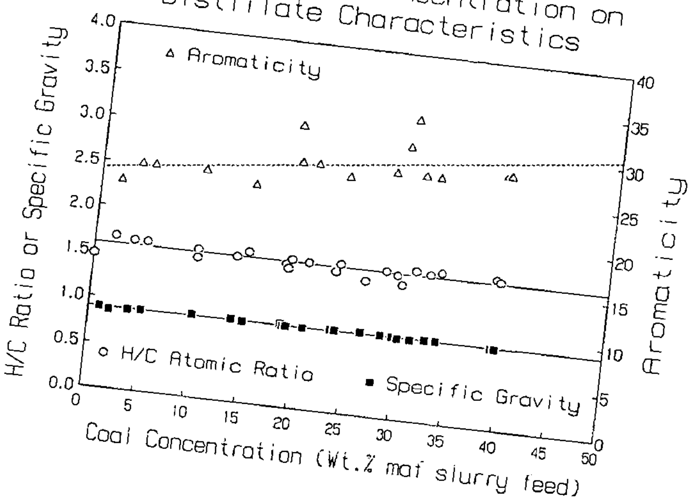

Figure 4
Effect of Coal Concentration on Metals Removal

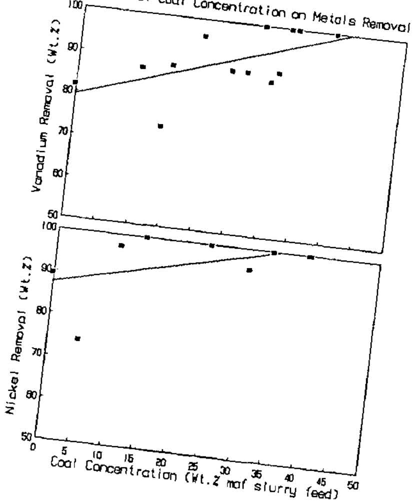

PARAMETER EVALUATION FOR COPROCESSING OF BROWN COAL AND VACUUM RESIDUE FROM PETROLEUM

Henning H Oelert   Richard Bloss   Pei Fang Zhang

Inst.Chemische Technologie und Brennstofftechnik - Universität Clausthal
Erzstraße 18, D 3392 Clausthal, Germany

INTRODUCTION

An increasing share of petroleum short - or vacuum residue (VR) from refining confronted with more heavy crudes is hard to be marketed or upgraded. Coprocessing is the attempt to coreact VR in a hydrogenative and preferable once-through operation together with an appropriate share of a suitable coal especially lignite. A report on this covering the literature till end of 1986 will be published by the European Commission (EC) in 1988 titled "coprocessing".
If the aimed for technology is once-through a limited preevaluation is possible by batch type autoclave experiments especially with respect to parameter influences. This report covers autoclave experiments for one "Rheinische" brown coal and different petroleum refining products including a light vacuum distillate (LSP); a very heavy vacuum distillate (ZYL); the vacuum residue (VR) from one single crude oil and another vacuum residue (VRW) very high in molecular weight.

EXPERIMENTAL

The coal (as reacted) is characterized by analytical data:
moisture 5.9%; ash (wf) 3.6%; volatile matter (dmf) 48.8%; xylene extract 5.8%
And the ultimate analysis (dmf): 68.3% C; 5.6% H; 1.3% S (total); 0.7% N; 24.1% O (diff)
The petroleum derived reactands (solvents) are characterized by basic analytical data:

		LSP	ZYL	VR	VRW
Conradsen carbon (%)		0.04	0.27	21.7	
Asphaltenes (%)		-	-	1.6	2.1
Aromaticity (%)		16	18	50	23
Average molecular weight (VPO)		249	433	897	1410
Ultimate analysis	% C	86.0	86.2	85.4	86.5
	% H	11.6	11.2	9.7	11.4
	% S	1.6	2.4	3.3	1.5
	% N	0.1	0.1	0.4	0.4
	% O (diff)	0.7	0.1	1.2	0.3

For an experiment a coal was slurried in a solvent at a ratio of 1:1.7 and 3.8% red mud and 0.6% Na_2S (refering to coal dmf) were added as catalyst. All experiments were conducted batchwise in a rocking autoclave prepressurized with hydrogen at a set initial pressure. The reactions were controlled for temperature and pressure recorded versus time. Heating and cooling rates were 0.3 K/s. After cooling back to normal temperature products gases (G) were released and analysed by TC-gaschromatography and the hydrogen uptake of the experiment was calculated from gas analysis, water produced (W) and pressure difference before and after the experiment. Non gaseous products were separated and evaluated as raw naphtha (N), medium and heavy oils (O), asphaltenes (A) (precipitated in hexane), and residue (R) (benzene insoluble) all based on feed coal (dmf). For some experiments water was not determined separately and then is contained in the figure for gases. For all solvents forgoing experiments under the same conditions provided the base of correlations for yields of products from only coal.

TEMPERATURE DEPENDENCE

For each feed combination the temperature was screened from 380 to 460°C at set conditions of 9 MPa initial hydrogen pressure and 60 min. residence time. The results are given in Table 1.
The hot system pressure decreases over the residence time for all petroleum derived solvents up to 435°C but already increases at 455°C from stronger cracking reactions in the solvent. Accordingly the hydrogen uptake does not differ or decreases from 435 to 460°C. In total the system pressure is not very much dependent

on the nature of the solvent. The hydrogen uptake in general increases with temperature and no clear dependence on the nature of the solvent exists.
The conversion of coal at 380°C is independent of the nature of solvents at a constant 49 to 50%. At higher temperatures conversion is always highest in the coal derived solvent but heavy vacuum distillates from petroleum provide an almost equal conversion in the range of 410 to 435°C whereas the vacuum residue gives a low conversion independent of the temperature. Heavy solvents obviously do not prevent coking at 460°C under the conditions given. The share of asphaltenes in the products in general decreases at higher temperatures but this then is dependent strongly on the nature of the solvent. In light vacuum distillate the share of coal derived asphaltenes stays below 10% but in heavy distillates it is as high as 17% but then strongly reduced again at temperatures above 430°C. For the vacuum residue at 380°C almost 30% of coal derived asphaltenes exist but then decrease strongly to only 2% at 460°C. It should be noticed, however, that these figures are calculated by difference and that this vacuum residue reacted alone results up to 11% asphaltenes at 410°C decreased to 6% at 460°C. Reacted alone these solvents give less than 3% of asphaltenes at 460°C with the already quoted exception of vacuum residue.
From experiments in petroleum derived solvents the share of product gases in the range of 10 to 13% is almost independent of the nature of solvent and on temperature. Reacted alone these solvents give 5% of gases to the most at 460°C. The higher the temperature the higher is the share of methane in all product gases. There also is a considerable content of carbon dioxide from the destruction of coal but not much influenced anymore by temperature above 380°C.
The share of naphtha in the products for petroleum derived solvents has a maximum at 410°C for vacuum distillates, increases with the boiling range of the solvent, reaches 16% for ZYL-solvent, is much lower for vacuum residue but then increasing with temperature to 11% at 460°C. The total naphtha yield combined from coal and solvent is 40% for ZYL-solvent and 33% for VR-solvent at 460°C.
The total oil yield from coal increases with the boiling range of a petroleum derived distillate solvent to a maximum at 435°C but still increasing to 460°C for the vacuum residue as a solvent. Since no true separation of product oils in shares stemming from coal or solvent is possible a characterization refers to the total product oil. In general an increase in reaction temperature decreases the atomic H/C-ratio of the product oil but still reflects the quality of each feed solvent whereas aromaticity increases with temperature rather independent of the nature of the solvent. At 435°C aromaticities of the total product oil are about 0.35 but are above 0.50 at 460°C. The average molweight of the total product oil at lower reaction temperatures are strongly dependent on the nature of the feed solvent but are equalized at 435°C for distillate solvents to an average of 250 as well as for vacuum residue but then down to 250 only at 460°C.
From recalculations and estimations for a once-through operation for the coal derived solvent the total liquid yield is 73% (M=300) at 460°C, for the vacuum residue as a solvent it is 58% (M=265) at 435°C, and for the most effective petroleum derived solvent it is 78% (M=225) at again 435°C.

RESIDENCE TIME DEPENDENCE

Since 435°C is not the temperature for a maximum gain of total products but obviously significant for the degradation of the brown coal in the mixture residence time variations in between heating-up only and 120 min. are made as presented in Tab. II). The apparent initial system pressure is dependent on the boiling range as well as on the crackability of the solvent but then much higher than from experiments with these solvents alone without addition of coal. This is due to the hydrocarbon gases and the carbondioxide produced from coal and only compensated to some degree from the hydrogen consumption.
The hydrogen uptake shortly after heating up is low and little dependent on the nature of the solvent. After 60 min. residence time it is completely independent of the nature of the solvent. The hydrogen uptake increases for 10 min. only but thereafter is obviously in equilibrium. These results are calculated by difference For these solvents reacted without coal under the same conditions the hydrogen uptake increases four- to sixfold from 0 to 60 min. residence time and thus the data calculated for coal are limited in their evaluation.
For product gases the major component is carbondioxide produced rather spontaneously, thus explaining the small increase of gases with residence time in the range of 10 to 14%. From experiments with only solvents the share of product

gases under the same conditions stays below 2% even at 60 min. residence time. More significant are the differences in produced or retransformed asphaltenes. For short contact times they directly reflect the nature of the solvent. For the light LSP-solvent the asphaltenes derived from coal are rather independent of residence time whereas for the other distillate reach a maximum after 10 min. but then are transfered into oils by about 2% after 60 min. For vacuum residue which reacted without coal gives less than 2% asphaltenes at short contact time the coal derived asphaltenes immediately reach 33% but are transfered into oils by 25% after 30 min.
From the solvents alone reacted without coal under the same conditions the product share of naphtha strongly increases with residence time reaching about 20% after 60 min. The coal derived naphtha is lower, reaches a maximum in distillate solvents after 10-30 min. but is much more dependent on the nature of the solvent. Recalculated for a once through operation this feed combination at 435°C and 30 min. residence time results to a total of 17% naphtha. For vacuum residue only 8% are gained from coal after 30 min. and a recalculated total for the feed combination would be little more than 10%.
More important for the feed combinations are the yields of oil boiling above 200°C as derived from coal. In general it can be stated that the lighter the solvent the higher is the oil yield from coal. The oil yield increases almost steadily with residence time but then data are dependent on the nature of the solvent. The total liquid yield containing naphtha and heavy oils again is the higher the lighter the solvent and is in general increasing with residence time. For the light vacuum distillate as a solvent the total liquid yield from coal of 40% and of 35% for heavy vacuum distillate as a solvent are reached after 60 min. residence time. For vacuum residue as a solvent the influence of time on the total liquid yield from coal is most pronounced. From 3% occuring immediately after heating up it is increased to 26% after 30 min. residence time.
Since no true separation of product oil boiling above 200°C from either coal or solvent is possible, any characterization of oil refers to the total product oil. After heating up only the H/C-ratio of the total product oil is dominated from the solvent with 1.61 for product from LSP-experiments to 1.39 for products from VR-experiments but after 60 min. it is equalized to 1.40 almost independent of the solvent. In accordance the aromaticity of the product oil almost independent of the nature of solvent increases from about 0.26 at heating up to about 0.37 after 60 min. and then is markedly higher than in the solvents themselves. The average molweight (M) of the product oil for each residence time is determinated from the nature of solvent but overproportionally decreased in the experiments with the vacuum residue (initial molweight 900) with M=390 at only heating up but M=250 after 60 min. Recalculated for a once-through operation the total oil yield would be 61% with M=305 for 30 min. residence time from vacuum residue as a solvent and 74% with M=270 for 30 min. residence time from the heaviest vacuum distillate as a solvent.

PRESSURE DEPENDENCE

For comparison set conditions of 435°C and 60 min. residence time were chosen for a variation of initial hydrogen pressure of 6 to 15 MPa. This in the case of 15 MPa initial leads to unrealistic system pressures of up to 42 MPa but are tolerated here for parameter evaluation only. The experiments are limited to two petroleum derived solvents only. The results are presented in Tab. III). The hydrogen uptake increases with initial pressure but rather independent on the nature of solvent and the gas formation is slightly reduced by pressure. For this coal in all solvents conversion increases with increasing initial pressure. For the range of 9-12 MPa initial pressure the coal conversion is the lower the heavier the nature of the solvent applied. For 15 MPa initial pressure the coal conversion might be suppressed if the hot system pressure is too high. Asphaltenes also increase with an increase of the initial pressure but for a given pressure are almost independent of the nature of the solvent. Naphtha formation is improved by a high initial pressure but not very much dependent on the nature of the solvent. For solvent (VR) the oil yield from coal scatters for initial pressures of 9-15 MPa but again is rather independent of the nature of the solvent. About 27% oil yield are gained at maximum in VR. Since no true separation of product oils from coal or solvent is possible an analytical evaluation refers to the total product oil boiling above 200°C. For coal BKR from all solvents the aromaticity of the total product oils is almost constant in a range of 0.35-0.40 against

a solvent aromaticity of about 0.2 and not systematically influenced by pressure or by the nature of the solvent. The strong destruction of coal as well as of heavy residual solvents is reflected from the average molweight (M). In LSP (M=249) the molweight of the total product oil is almost independent of the initial pressure with M=224 for 6 MPa and M=218 for 15 MPa. VR (M=897) comparable data are M=313 at 9 MPa and M=268 at 15 MPa.
Based on a once-through approach recalculated total liquid yields including naphtha under the conditions given and at 12 MPa initial pressure (hot system pressure in the autoclave already above 30 MPa) and is 66% including 18% naphtha and 48% heavy product oil with M=285 in VR.

FEED MIXTURE DEPENDENCE

These experiments are based on a variation of mixtures of the same coal but a different VR-W residue described in the experimental section. The results are presented in Tab. IV) for set conditions of RMPaH_2, 430°C and 30 min. residence time. The system pressure is strongly influenced from the share of coal increasing by 13MPa from 0 to 67% of coal and dominated by CO_2CO and much lesser CH_4 originating from coal. With two exceptions the pressure drops during 30 min. on temperature, however, is almost constant. Hydrogen consumption by reacting VRW is 0.48%. For coal up to about 30% the hydrogen consumption is lower than for VRW. Coal might in part provide hydrogen for radical capping of fragments from VRW. Above 30% coals's hydrogen consumption is increasing from about 0.5% to 0.67% about proportional. The coal conversion is highest at 69% for about 10% of coal, then decreasing but almost constant at about 50% for 30 to 67% of coal.
Product gas formation is strongly increasing with the share of coal and is mainly CO_2 and CO. The total residue increases with the share of coal but the ratio of total residue versus coal share in the feed is about constant. A certain part of the coal does not react under the conditions given, or a part of asphaltenes are included in the residue because the total asphaltene content decreases strongly with an increasing share of coal. The naphtha formation is increasing with the share of coal but then almost constant above 30% of coal in the feed. The high boiling oils are decreasing from more coal in the feed but still above 50% for 30% of coal in the feed. The quality of these high boiling oils are improved from a higher share of coal in the feed. Only VRW or mixed with little coal results to more than 80% of total liquid yield but the quality of the product oil is insufficient with a molecular weight of or above 500. Shares of 30-40% of coal in the feed provide a total liquid yield of 70% with a molecular weight of heavy product oil at or below 400.

Acknowledgements: This work was supported by government grant BMFT-03E-6058B. Mrs R. Bosse provided analytical measurements.

Table I) Dependence on temperature
(9 MPa initial hydrogen pressure; 60 min. residence time)

	Feed	Reaction parameters				
	Solvent	Temperature (°C)	hot pressure beginning	(bar) end	H-up-take %	Conver-sion
1	LSP	380	243	243	0.9	48
2	LSP	410	255	247	1.1	57
3	LSP	435	265	259	1.2	62
4	LSP	460	303	346	1.2	53
5	ZYL	380	230	231	0.7	49
6	ZYL	410	240	230	1.4	63
7	ZYL	435	274	263	1.1	62
8	ZYL	460	279	332	1.1	48
9	VR	380	256	253	0.7	50
10	VR	410	276	255	1.2	50
11	VR	435	291	276	1.1	51
12	VR	460	306	335	1.3	48

continued

	Product distribution (% of feed coal)					
	G	R	A	W	N	O
1	12.1	52.3	8.7	2.1	11.3	14.4
2	12.1	42.9	11.3	3.1	14.9	16.8
3	11.0	37.8	9.1	2.5	9.8	31.0
4	12.6	47.3	4.7	3.0	7.0	26.6
5	10.9	51.1	14.6	3.1	11.4	9.6
6	12.5	37.3	17.3	5.3	15.8	12.9
7	13.8	38.0	13.0	3.8	7.9	24.6
8	13.2	52.0	3.0	4.0	10.5	18.4
9	11.0	50.3	29.2	-	5.0	5.2
10	12.7	49.7	23.7	1.9	6.4	6.8
11	13.4	48.7	8.6	4.0	5.4	21.0
12	12.4	51.6	2.3	4.0	10.6	20.4

All %-results are refering to coal daf. G = gases; R = residue (benzene insoluble); A = asphaltenes (hexane insoluble); W = water; N = naphtha (boiling below 200°C); O = oil

Tab II) Dependence on residence time
(9 MPa initial hydrogen pressure; 435°C)

Feed	Solvent	Residence time (min)	hot pressure (bar) begin.	end	H-up-take %	Conver-sion %
1	LSP	0	276		0.5	42
2	LSP	10	274	274	1.1	54
3	LSP	30	275	274	1.1	57
4	LSP	60	265	259	1.2	63
5	ZYL	0	282		0.3	44
6	ZYL	10	277	275	0.8	56
7	ZYL	30	276	265	1.1	59
8	ZYL	60	274	263	1.1	62
9	ZYL	120	275	263	1.2	59
10	VR	0	287		0.5	46
11	VR	10	289	281	0.8	49
12	VR	30	284	281	1.1	51
13	VR	60	291	276	1.1	51

continued

Product distribution (% of feed coal)

	G	R	A	W	N	O
1	11.0	58.4	8.6	2.7	10.5	9.3
2	14.1	46.0	8.1		14.5	18.4
3	12.0	43.4	7.3	3.1	11.6	23.7
4	11.0	37.8	9.1	2.5	9.8	31.0
5	10.6	56.0	13.7	2.9	8.0	9.1
6	11.6	44.4	14.0	4.4	8.5	17.9
7	12.5	40.7	12.2	4.9	8.2	22.6
8	13.8	38.0	13.0	3.8	7.9	24.6
9	12.7	41.0	10.6	2.1	5.2	29.6
10	10.2	54.4	32.9		2.0	1.0
11	11.2	50.7	17.6	4.3	2.5	14.5
12	13.5	48.7	7.6	5.1	8.2	17.7
13	13.4	48.7	8.6	4.0	5.4	21.0

All %-results are refering to coal daf: G=gases; R=residue (benzene insoluble); A=asphaltenes (hexane insoluble); W=water; N=naphtha (boiling below 200°C); O=oil

Tab III) Dependence on hydrogen pressure
(435°C, 60 min residence time)

Feed		Reaction parameters				
	Solvent	initial H_2-pressure (bar)	hot pressure beginning	(bar) end	H-up take %	Conversion %
1	LSP	60	213	251	0.8	47
2	LSP	90	265	259	1.2	62
3	LSP	120	327	315	1.8	63
4	LSP	150	408	375	1.8	66
5	VR	90	291	276	1.1	51
6	VR	120	361	319	1.5	61
7	VR	150	420	371	1.8	64

continued

Product distribution (% of feed coal)

	G	R	A	W	N	O
1	14.9	52.6	4.2	4.4	8.4	16.3
2	11.0	37.8	9.1	2.5	9.8	31.0
3	14.1	36.9	7.9	3.5	10.0	29.4
4	13.8	33.9	8.7	3.6	10.4	31.4
5	13.4	48.7	8.6	3.1	6.3	21.0
6	11.4	39.1	9.3	3.6	11.2	26.9
7	11.4	36.1	9.0	5.4	14.8	25.1

All %-results are refering to coal daf: G=gases; R=residue (benzene insoluble); A=asphaltenes (hexane insoluble); W=water; N=naphtha (boiling below 200°C); O=oil

Tab IV) Dependence on feed mixture
mixtures of coal and residue VRW without catalyst addition
(conditions 430°C; 12 MPa initial hydrogen pressure; 30 min. residence time)

	Feed %		Reaction parameters			
			hot pressure (bar)		H-up-	Conver-
No	VRW	coal dmf	beginning	end	take % (of coal)	sion of coal %
1	100	0	301	289	0.48	-
2	91	9	312	299	0.35	69
3	83	17	330	317	0.46	55
4	71.5	28.5	360	340	0.56	53
5	61.5	38.5	372	359	0.59	50
6	50	50	389	373	0.64	47
7	33	67	430	392	0.67	50

Product distribution (% of feed)

	G	R	A	W	N	O	M (average mol weight of total heavy oil)
1	0.5	4.5	9.3	-	12.1	74.1	471
2	2.4	3.8	6.9	-	11.3	76.0	520
3	2.6	11.8	7.3	0.9	13.0	64.9	448
4	3.2	17.7	5.8	0.9	21.3	51.7	409
5	4.3	20.7	5.9	2.5	19.2	48.0	373
6	6.3	26.9	2.5	6.7	19.0	39.2	363
7	9.0	33.1	2.1	8.3	19.4	28.7	360

All %-results are refering to total feed (dmf): G=gases; R=residue (benzene insoluble); A=asphaltenes (hexane insoluble); W=water; N=naphtha (boiling below 200°C); O=oil

A NEW PERSPECTIVE ON THE NATURE OF "ORGANIC" SULFUR IN COAL.

Ramani Narayan, Gunnar Kullerud, and Karl V. Wood

Coal Research Center, Purdue University, West Lafayette, IN. 47907.

INTRODUCTION

It is generally assumed that the sulfur in coal is distributed among organic sulfur, sulfatic sulfur, and pyritic sulfur compounds (1). ASTM D-2492 which lists the forms of sulfur in coal also assumes that three forms are present--sulfatic, pyritic, and organic sulfur. The organic sulfur value of coal is derived as the difference between the total sulfur content of coal and the amount of pyritic plus sulfatic sulfur i.e., any form of sulfur that is not pyritic or sulfatic sulfur would be counted as organic sulfur. The **organic sulfur** is generally perceived to occur in covalently bonded C-S compounds like thiophenes, thioethers, and bisthioethers (disulfides) (2,3). **Elemental Sulfur**, which would be accounted for as **"organic sulfur"**, has been mentioned, only in a few references in the literature. Yurovskii (4) in his monumental treatise on 'Sulfur in Coals' provides evidence for the presence of elemental sulfur in coals. Richard, Vick and Junk (5) and White and Lee (6) confirmed the presence of elemental sulfur for several bituminous American coals. In a more recent article, Lee et al (7) report the detection, in a Bevier seam coal, of 3,6-dimethylbenzo(b)thiophene that can be potentially formed by reaction of elemental sulfur with terpenes (Figure 1). Further light on this question was provided by De Roo and Horton (8,9) when they demonstrated that elemental sulfur reacts with simple alkyl aromatics, under mild conditions, to give thiophenic compounds. De Roo (8) showed that such reactions can occur under geochemical settings and conclude that the generation of organic S compounds in petroleum followed this route. Thus, the reaction of elemental sulfur with coal aromatics could, in part, account for the formation of organosulfur compounds found in coal (Figure 2). However, Stock et al.(10) report that pristine coal samples (from the Argonne Premium Sample Coal Bank) are free of elemental sulfur. He suggests that sulfur is not a natural constituent of coal, but that on exposure to air, elemental sulfur, which can account for up to 5% of the total amount of sulfur in the sample, is formed.

In this paper we present a new perspective on the nature of organic sulfur in coal and suggest that the organic sulfur fraction in pristine coal contains sulfur in the form of a **coal-polysulfide complex** (see Figure 3-- an elemental sulfur precursor) which, in some coals, may constitute in excess of 50% of the organic sulfur fraction. Under suitable chemical/biological environments, this sulfur complex would give rise to free elemental sulfur The sulfur, thus set free could get dispersed through the coal matrix and would be present in the amorphous form. The amorphous form arises when sulfur precipitates from solution as a result of chemical-reactions, especially when it first appears in the colloidal state. This sulfur would be insoluble in organic solvents and would not detected by X-ray diffraction.

Experimental evidence using solvent extraction studies (under conditions that will allow the extraction of amorphous sulfur form) and geochemical approaches is presented below supporting the concept of this **new polysulfide sulfur form** in the "organic" sulfur fraction of coal. If this is true, then research and development efforts to remove the so-called organic sulfur components in coal must take into account this factor., especially since the elemental sulfur or the polysulfide sulfur can react with alkyl aromatic structures in coal creating new thiophenic sulfur compounds from which it is very difficult to excise the sulfur.

EXPERIMENTAL

An Illinois No.6 coal (Herrin No. 6 coal from a west central Illinois Underground mine) from the Illinois Basin Coal Sample program (IBCSP, sample No. 1), the corresponding pristine Illinois No. 6 coal from the Argonne Premium Sample Coal Bank and an Indiana bog(reject) coal were selected for extraction studies. Table 1 shows the sulfur analysis for the three coals studied.

TABLE 1

Analysis for Forms of Sulfur in Coals Studied

Coal	Organic %	Pyritic %	Sulfatic %	Total %
IBCSP No.1	3.00	1.20	0.06	4.26
Pristine Coal				
Indiana Bog	3.33	5.20	4.48	13.01

2g of the coal (accurately weighed) were extracted with perchloroethylene solvent at different temperatures and the extract concentrated. The concentrate was diluted to mark in a 25ml volumetric flask and the amount of sulfur determined using GC-MS. The sulfur quantization was carried out using a Finnigan 4000 gas chromatograph/mass spectrometer (San Jose, CA). A 6' x 2 mm i.d. SP2100 on 80/100 Supelcoport chromatographic column was used with a helium flow rate of 35 ml/min. For these analyses, both the column and injector temperatures were held constant at 180°C. The ion source temperature of the mass spectrometer was set at 180°C. The electron energy was set at 70eV and the electron multiplier 1600eV for these analyses. The mass analysis was carried out using multiple ion detection (MID).

In order to quantitate, a standard curve was first obtained using the following series of standards; 0.005% , 0.01%, 0.025%, 0.05%, 0.1%, and 0.5% sulfur. Five microliters of both the standards and samples were injected on-column. The criteria for confirmation of sulfur was two-fold: 1) retention time and 2) relative ratio of the three sulfur ions used in the MID program (m/z 64:192:256; 10:2:1). The standards were run again after the samples to determine the stability/reproducibility of the ion intensities within the mass spectrometer over the total time of the analysis. The peak area of the m/z 64 ion was used in the quantitation.

RESULTS

COAL SAMPLE STUDIES

Perchloroethylene extraction of Illinois Coal

Perchloroethylene is an excellent solvent for solubilizing elemental sulfur. The solubility is ~ 30g S/ 100g Solution as opposed to only 0.066g S/ 100g Solution in Ethyl Alcohol or 2.7g S/ 100g Solution in Acetone. The Illinois Basin Sample Coal Program sample No.1 (-100 mesh) (IBSCP sample 1) was extracted with perchloroethylene at 120°C and the results of three different runs gave an average elemental sulfur content of 1.54% for the coal sample Table 2).

TABLE 2

Elemental Sulfur in Illinois Coals

Coal/Run No.	% Elemental S	Average %	Elemental S as % of Organic S	Elemental S as % of Total S
IBCSP-1 IBCSP-2 IBCSP-3	1.50 1.62 1.50	**1.54**	**51.3**	**36.1**

This means that 51.3% of the so called "organic" sulfur or 36.1% of the total sulfur is present as elemental sulfur. Stock et. al. (10) report that only 2% of the total sulfur in the same type of coal (IBSCP sample 1) was elemental sulfur. However extraction of a pristine Illinois No.6 coal from the Argonne

Sample Coal Bank gave no elemental sulfur within the detection limits used. An Indiana Bog (Reject) coal was extracted with perchloroethylene at different temperatures and as shown in Table 3 there was a 59% increase in the amount of elemental sulfur extracted in going from room temperature to 120°C. The 1.23% elemental sulfur extracted at 120°C amounts to 36.9% of the "organic sulfur" in that coal.

TABLE 3
Effect of Temperature on Sulfur Extraction

Temperature	% Elemental S extracted
Room Temp.	0.78
60°C	1.08
120°C	1.23

Geochemical Approaches

Fresh coal samples from the Minnehaha Mine, Sullivan County, Indiana was used in the study. The method of sampling which was described by Parratt and Kullerud (11) assures that unoxidized specimens are obtained. The samples were divided into approximately equal amounts and placed in ten double polyethylene plastic bags which were sealed airtight and directly transported to storage containers in the Purdue laboratories. One bag was opened within hours upon arrival at the laboratory and its content was exposed its warm, humid air. Oxidation products in the form of a yellowish-brown or ocher colored powder started to form within days, was quite distinct after one week, and occurred in significant amounts after one month. X-Ray powder diffraction charts made on this substance displayed the characteristic reflections of iron-calcium-aluminum sulfates. The color and texture of this substance are similar to those of elemental sulfur. However, the X-ray powder diffraction reflections of sulfur were not observed. The sulfur, if present, may be amorphous.

A number of polished sections were made on material from a second bag and under the reflected light microscope it was noted that pyrite, marcasite and sphalerite make up about 2% of this coal. Pyrite is most common, marcasite much less so and only one or two grains of sphalerite were observed in each section. Sulfates of any form or elementary sulfur were never observed in freshly made polished sections. Four stages of iron sulfide mineralization are distinguishable; framboidal pyrite, marcasite, fibrous pyrite and massive pyrite. Although these sulfides generally are evenly distributed throughout the coal it was possible to localize areas which contained no visible sulfides. Accordingly, fresh samples from a third bag were gently crushed to about 2 mm size and placed in badges of a few grams at a time under the zoom lense of a binocular microscope. It was now possible to quite efficiently separate grains of coal with no visible sulfides. Several grains of this material were next exposed to warm, humid air. Oxidation products again became visible in a few days. The products were the same, but their amounts were much smaller than those which previously were produced under identical conditions in equal time from the original unseparated coal. About one dozen of the coal grains, containing no visible coal, were mounted in low temperature curing epoxy and polished. Less than 0.05% iron sulfide was observed in the polished surfaces under the reflected light microscope. In such grains sporinite is the most common maceral. Vitrinite, cutinite, and resinite are much less common, and fusinite, sclerotinite are the least common. Microprobe analyses were performed on selected sulfide-free areas of polished surfaces of numerous grains. Analyses revealed that sporinite has a sulfur content of about 2.9 to 3.0%, whereas vitrinite, cutinite and resinite contain from 1.1 to 1.4% S and fusinite, sclerotinite contain about 0.25% S (12).

Simultaneous analysis on iron and sulfur in areas where sulfides are not detected in polished sections always gave Fe values of less than 0.1% Fe. The sulfur concentrations cited above reflect the values remaining upon subtraction of the sulfur required to convert all Fe to FeS_2; in other words, it was assumed that all detected iron is present as disulfide. Thus it becomes apparent, that at least in this particular coal, the concentration of the sulfur which we usually refer to as organic is strongly dependent on the type of maceral in which it occurs. Sulfur is,. for instance, almost three times as abundant in sporinite as it is in vitrinite which in turn contains four times as much sulfur as do the typical inertinite macerals.

It is also quite apparent that a significant portion of this maceral sulfur reacts with warm and humid air to produce sulfates and amorphous elemental sulfur. In a series of experiments conducted on the material contained in a fourth sample bag, total sulfur was, by wet chemical analysis on a representative 5 gr sample, found to be 3.2 + 0.2 wt%. The sulfide sulfur determined by separating physically and weighing the sulfides from a representative 1 gr sample gave 1.8% sulfide sulfur after correcting, through polished section study, for remaining unseparated sulfides. Wet chemical analysis of the remaining "pure" macerals, which contain less than 0.05% wt Fe and less than 0.2% A1 accounted for as clay minerals, gave 1.2 + 0.2 wt%. Treatment of these "pure" macerals, which had been crushed as cited above, with warm, humid air produced the ocher colored material. This was carefully removed from the maceral grains. New analysis on a portion of the cleaned maceral grains indicated a sulfur concentration of 0.9 wt%. The remaining portion of the cleaned maceral material was finally treated with distilled water for several days at 60°C on a waterbath. Careful processing involving decanting prior to washing in distilled water, repeated decanting and slow drying at 110°C was followed by a final sulfur analysis. This gave 0.6 wt% S. This would indicate that about 50% of the so-called "organic" sulfur can be removed by exposure of the macerals to hot, humid air and to pure warm water. Conservatively stated: at least a portion of the so-called organic sulfur in coal macerals occurs under chemical conditions which permit it to react with oxygen in the air and with water. The character of the chemical bonds involving this particular sulfur is not know, but at least the generally perceived carbon-sulfur bonds are precluded.

DISCUSSION

Both chemical solvent extraction and geochemical studies strongly indicate that the so called **"organic" sulfur** fraction of coal contains a major sulfur form different from the conventional thiophenic and thioether type structures normally associated with the "organic" sulfur fraction. A **coal - polysulfide complex** as shown in Figure 3 is suggested Under suitable chemical/geochemical conditions, this sulfur complex would give rise to free elemental sulfur. This would account for the fact that no elemental sulfur is detected in the Argonne pristine coal sample, however the not so pristine samples from the IBCSP would undergo reaction to yield elemental sulfur The sulfur, thus set free could get dispersed through the coal matrix and would be present in the amorphous form. Crystalline sulfur (orthorhombic and monoclinic) consist of ring shaped molecules containing eight atoms (Figure 4) and is soluble in common organic solvents like CS_2, and acetone. Amorphous sulfur, on the other hand, results when the ring molecules of sulfur break and successive atoms link together to form a long chain molecule (Figure 4). This would be insoluble in organic solvents and not detected by X-ray diffraction studies. Amorphous sulfur is not stable at temperatures below 160°C and reverts to the crystalline ring-molecule form. **This change, however, is extremely slow at room temperatures and at room temperature, amorphous sulfur remains for years with little change (13).** At temperatures near 100°C the change from amorphous to crystalline sulfur is more rapid, and practically all amorphous sulfur disappears at this temperature in the course of an hour. The amorphous form arises when sulfur precipitates from solution as a result of a chemical reactions, especially when it first separates as a colloidal dispersed system.. This fits in nicely with the 59 % percent increase in elemental sulfur obtained on going from room temperature to 120°C. It may also be the reason why other investigators using x-ray or slovent extractions at or near room temperatures have not observed appreciable amounts of elemental sulfur. The behavior of the amorphous sulfur is further illustrated in the well known **vulcanization of rubber** using sulfur. In this, a part of the sulfur used for vulcanization remains unreacted, and the vulcanized rubber always contains a certain amount of free sulfur. In the hot vulcanization process, the free elemental sulfur is in crystalline and can be readily extracted with hot acetone or carbon tetrachloride. However, if the vulcanization is effected in the cold, the free sulfur is formed in the metastable amorphous modification and is finely dispersed. It is not extractable even, with good sulfur solvents like CS_2

The fact that the **coal - polysulfide complex** can, under appropriate conditions spit out elemental sulfur is supported by observations on model compounds. Thus, Diethyl Xanthogen trisulfide on treatment with moist acetone forms the disulfide and elemental sulfur while, Diethyl Xanthogen tetrasulfide also yields the disulfide and eliminates two sulfur molecules (14) (Figure 5). One fact that needs to be stressed is that a portion of the sulfur contained in higher polysulfides is so loosely bound that they **behave as elemental sulfur** and thus, in many reactions behave like elemental sulfur.

IMPLICATIONS

The existence of **coal-polysulfide complexes** that may yield elemental sulfur and take part in elemental sulfur reactions brings up an important new factor in R&D approaches to removing "organic" sulfur in coal and for coal processing in general. As shown by White and others (6-9) elemental sulfur can react with alkyl aromatics to form thiophene compounds (Figure 2). Our concern is that coal processing operations result in creation of hard to remove covalent C-S bonded structures like the thiophenes from the more easily removable polysulfide type structures. Even more damaging is the fact that thiophenic crosslinks between coal clusters could arise resulting in the creation of a even more intractable macromolecule (Figure 6) that would be more difficult to process.

REFERENCES

1. Shepherd, M. *Electric Power Research Institute Journal*, *10,* 14 (1985).
2. Markuszewski, R., Fan, C. W., Greer, R. T., and Wheelock, T. D. "Evaluation of the removal of organic sulfur from coal." In: *Symposium on New Approaches in Coal Chemistry, American Chemical Society,* Pittsburgh, PA, November 12-14, 1980.
3. Morrison, G. F. "Chemical Desulphurization of Coal," IEA Coal Research, London, Report No. ICTIS/TR15, June (1987).
4. Yurovskii, A. Z., "Sulfur in Coals," English Translation available from the U.S. Department of Commerce, National Technical Information Service, Springfield, VA 22161, U.S.A., No. TT70-57216) (1960).
5. Richard, J. J. Vick, R. D., and Junk, G. A. *Environ. Sci. Technol., 11,* 1084.
6. White, C. M., and Lee, M. L., *Geochemica et Cosmochimica Acta, 44,* 1825 (1980).
7. White, C. M., Douglas, L. J., Perry, M. B., and Schmidt, C. E., *Energy and Fuels, 1,* 222 (1987).
8. De Roo, J., and Hodgson, G. W., *Chem. Geol., 22,* 71 (1978).
9. Horton, A. W., *J. Org. Chem., 14,* 761 (1949).
10. Duran, J. E., Mahasay, S. R., and Stock, L. M., *Fuel, 65,* 1167 (1986).
11. Parratt, R. L., and Kullerud, G., *Mineraliun Deposita, 14,* 195 (1979).
12. Beck, G. U., and Kullerud, G., *Geological Society of America, Abstr., Vol 1982,* 94 (1982).
13. Tuller, W. N., In: *The Analytical Chemistry and Sulfur and its Compounds*, J. H. Karchmer, ed., Wiley-Interscience, chapter 1.
14. Kruse, W , Carl, Illinois Geological Survey, Private Communication.

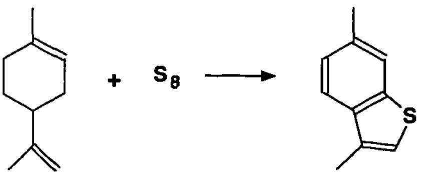

Figure 1. Formation of Thiophenes with Elemental Sulfur. From Ref. 7

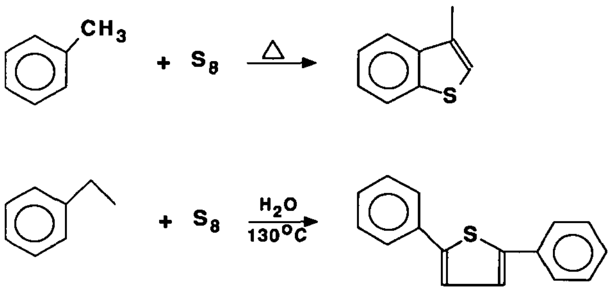

Figure 2. Reaction of Elemental Sulfur with Alkyl Aromatics. Formation of Organosulfur Compounds

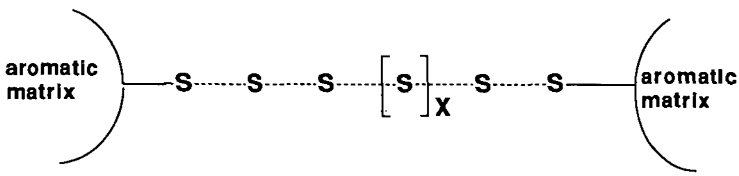

Figure 3. Conceptual Coal-Polysulfide Complex

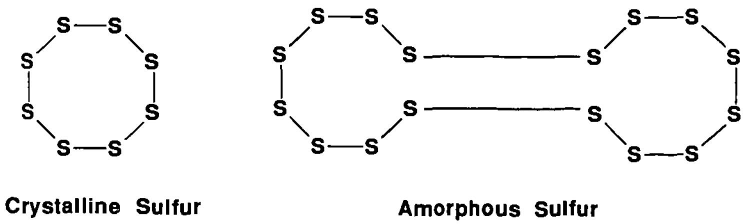

Figure 4. Structure of Crystalline and Amorphous Sulfur

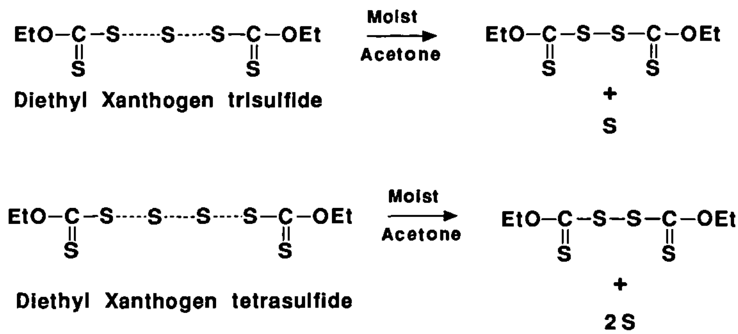

Figure 5. Model Organo-polysulfide Complex Spitting out Elemental Sulfur under Appropriate Conditions

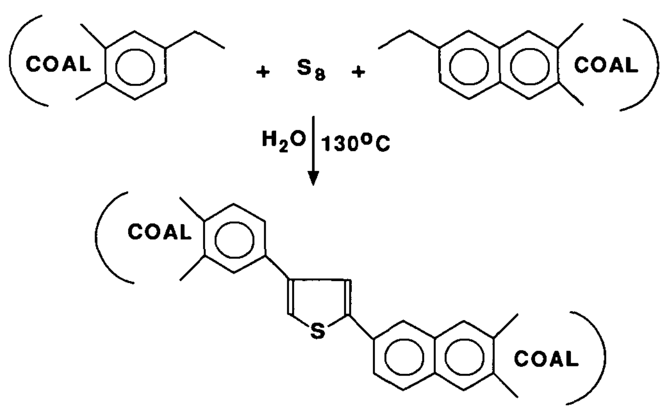

Figure 6. "Crosslinking" of Aromatic Coal Clusters via Thiophenic Bridges

EXAFS Investigation of Organic Sulfur in Coal

G. P. Huffman*, F. E. Huggins*, N. Shah*, D. Bhattacharyya*, R. J. Pugmire**, B. Davis+, F. W. Lytle++, and R. B. Greegor++.

*University of Kentucky, 401 Patterson Office Tower, Lexington, KY 40506; **University of Utah, Fuel Science Department, Salt Lake City, UT 84112; +Kentucky Energy Cabinet Laboratory, Lexington, KY 40512; ++The Boeing Company, Seattle, WA 98124

ABSTRACT

EXAFS spectroscopy is shown to be a very promising technique for investigating the molecular structure of organically bound sulfur in coal and coal derivatives. The current paper presents sulfur K-shell EXAFS results for a number of a maceral separates prepared by density gradient centrifugation and for several biodesulfurized coals. Both the near-edge structure and the radial structure functions exhibit some similarities to dibenzothiophene. However, a broad peak occurs in the XANES region of the coal spectra that is not observed for the molecular structures usually ascribed to organic sulfur in coal. This is believed to arise from resonant photoelectron scattering from second and third nearest neighbor carbon shells and from sulfur bonded to oxygen.

Introduction

Numerous techniques are available for investigating the structure of the inorganic forms of sulfur in coal and coal derivatives. These include ^{57}Fe Mössbauer spectroscopy,[1,2] computer-controlled scanning electron microscopy,[3,4] and x-ray diffraction,[5,6] to mention a few. The development of techniques to determine the structural forms of organic sulfur, however, has proven more difficult. Recently, it has been demonstrated that X-ray absorption fine structure spectroscopy, usually referred to as EXAFS spectroscopy, is a very promising method for investigating the molecular structure of organic sulfur in coal.(7,8) In this article, some recent EXAFS results obtained from maceral separates and other samples containing little or no pyrite are summarized.

Experimental Procedures

EXAFS spectroscopy provides information on the electronic bonding and atomic environment of an element through detailed analysis of the fine structure associated with an X-ray absorption edge of that element. When a synchrotron radiation source is used, individual elements can be investigated at dilute levels (~ 100 ppm to 1%) in complex samples. The current experiments were conducted during a dedicated run at the Stanford Synchrotron Radiation Laboratory using wiggler beam-line VII-3. Electron energies were 3 GeV and beam currents were typically 40 to 80 mA. A Si(111) double crystal monochromator was used to vary the X-ray energy from approximately 100 eV below to 600 eV above the sulfur K-shell absorption edge (2472 eV). To minimize absorption of these relatively soft X-rays, an all helium pathway from the beam pipe to the sample and detector was constructed and thin (6 μm) mylar windows were used wherever possible. The experiments were done in the fluorescent mode, using a fluorescent ionization detector described elsewhere.(9)

Most of the samples examined were maceral separates prepared by density gradient centrifugation (DGC). Discussions of the DGC methods are given elsewhere.(10-12) EXAFS measurements were made on exinite, vitrinite and inertinite separates from coals of several ranks. In addition to maceral separates, several coals from which all pyrite had been removed by biological desulfurization(12) were examined. The EXAFS specimens were prepared in the form of pellets by hydrostatically pressing the coal powder into a boric acid cylinder or, in some cases, adding an epoxy binder.

Results and Discussion

EXAFS spectroscopy determines the electronic structure and atomic environment of an element by analysis of the fine structure associated with an X-ray absorption edge of that element. The spectra are normally divided into two regions. The region within about 20 to 50 eV of the absorption edge is called the X-ray absorption near edge structure, or XANES (see Figures 1 and 2). The peaks and other structure in this region are derived primarily from two sources: photoelectron transitions to vacant, bound levels,(13,14) and low-energy scattering resonances.(15-17) The XANES spectra are quite sensitive to the detailed nature of the electronic bonding and can frequently serve as fingerprints to identify different compounds or types of binding.

The extended X-ray absorption fine structure, or EXAFS, is the oscillatory structure that begins at 30 to 50 eV above the edge and extends to fairly high energies (~ 500 to 1000 eV). These oscillations arise from interference between the outgoing and backscattered photoelectron wave functions. They can be subjected to a Fourier transform analysis to yield a radial structure function (Figure 3) from which interatomic distances and coordination numbers for the atomic neighbor shells of the absorbing atoms can be determined.(18,19)

Typical sulfur K-shell EXAFS data are shown in Figures 1 to 3. The XANES of several standard compounds appear in Figure 1. The zero of energy is taken at the first peak in the differential of the spectrum of elemental sulfur. The first large peak in the XANES, the so-called "white line", probably arises from a transition of the photoelectron from the 1s level to hybridized p levels - 3p/3d-4s for pyrite and 3p/2p for the remaining compounds. The subsequent broader peaks, located between approximately 5 and 30 eV for pyrite and dibenzothiophene (dbt), and from 15 to 40 eV for the sulfur-oxygen bonded compounds, probably arises from low energy scattering resonances.(15-17) It is evident that the increase in valence of the sulfur ions bonded to oxygen in sulfosalicylic acid and ferrous sulfate causes a significant positive shift in the white line and other XANES features.

XANES spectra of several maceral separates from a high volatile bituminous coal (PSOC 733, HVAB, Appale, PA) are shown in Figure 2. The first two peaks, which are relatively sharp, occur at the same locations and have similar intensities to the corresponding peaks in the XANES of dbt. Presumably, they represent s $\Rightarrow$ p transitions characteristic of an aromatically bound sulfur atom. Thianthrene, however, which contains two aromatically bound sulfurs, exhibits only the first of these two sharp peaks, at approximately 3 eV. This could reflect the increase in symmetry of the sulfur sites in thianthrene.

The broad peak at 10-11 eV was observed for all coal specimens examined, but was not present in the XANES of any standard compounds in which S is bonded to C and H. It is in approximately the same location as the strong white line in the XANES of the standard compounds that contain S bonded to O (sulfosalicylic acid and various sulfates). Consequently, sulfur oxidation may be partially responsible for this feature. However, it is seen in Figure 1 and Table I than sulfur-oxygen bonded species also exhibit significant secondary XANES structure between 20 and 30 eV that is not evident in the coal spectra. It seems likely, therefore, that low energy resonant scattering of the photoelectron by second and third neighbor shells may be the primary origin of the broad peak at 10-11 eV. As discussed elsewhere,[15-17] the position of such scattering peaks can be related to interatomic distance. It has previously been noted[16,17] that an ER^2 = constant relation frequently holds for such XANES features, where E is the energy at which the peak occurs and R is the distance from the absorbing atom to the neighbor shell which gives rise to the scattering resonance. Dependent on what reference point the peak energy is measured from, the effect of phase shifts on the E - R relation, and multiple versus single scattering, distances of approximately 2.5 to 4 Å could be compatible with the peak in question. Work is now in progress to establish suitable energy vs. distance calibration curves from analyses of the XANES of various standard sulfur compounds.

Typical radial structure functions (RSF's) produced by Fourier transformation of the EXAFS of maceral separates are shown in Figure 3. It appears that two atomic shells, and possibly three, can be resolved. Assuming that the atoms surrounding the sulfur in coal are primarily carbons, the standard back transform analysis of the RSF peaks was carried out using an empirical S - C phase shift determined from the EXAFS data for dbt. The interatomic distances determined in this manner seem reasonable (Table II).

Conclusions

The current results demonstrate that EXAFS spectroscopy is an excellent method for direct, non-destructive, investigation of the molecular structure of organic sulfur in coal. Future studies will concentrate on development of calibration relationships for interpretation of the XANES, and conducting in situ studies of the changes in sulfur structure resulting from pyrolysis, hydrogenation, and oxidation.

Acknowledgements

This research was sponsored by the Department of Energy under DOE Contract No. DE-FG22-86PC90520, and under DOE Contract No. DE-FC22-86PC90017. The latter contract supports the research program of the Consortium for Fossil Fuel Liquefaction Science. We would also like to acknowledge the staff of the Stanford Synchrotron Radiation Laboratory, sponsored by DOE.

References

1. G. P. Huffman and F. E. Huggins, Fuel 57, 592 (1978).
2. F. E. Huggins and G. P. Huffman, in: Analytical Methods for Coal and Coal Products, Vol. III, Chapt. 50, pp. 371-423, Ed., C. Karr, Jr., Academic Press, 1981.
3. F. E. Huggins, D. A. Kosmack, G. P. Huffman, and R. J. Lee, Scanning Electron Microscopy/1980/I, 531-540, SEM Inc., AMF O'Hare, Chicago, IL.
4. F. E. Huggins, G. P. Huffman, and R. J. Lee, in: Coal and Coal Products: Analytical Characterization Techniques, ACS Symposium Series 205, Ed., E. L. Fuller, Jr., pp. 239-258, Amer. Chem. Society., 1982.
5. R. G. Jenkins and P. L. Walker, Jr., in Analytical Methods for Coal and Coal Products, Vol. II, Chapt. 26, pp. 265-292, Ed., C. Karr, Jr., Academic Press, 1978.
6. C. Prosada Rao and H. J. Gluskoter, Illinois State Geol. Survey Circ. No. 476, 1973, 56 pp.
7. C. E. Spiro, J. Wong, F. Lytle, R. B. Greegor, D. Maylotte, and S. Lampson, Science 226, 48-50, 1984.
8. G. P. Huffman, F. E. Huggins, N. Shah, D. Bhattacharyya, R. J. Pugmire, B. Davis, F. W. Lytle, and R. B. Greegor, in Processing and Utilization of High Sulfur Coals II, Eds. Y. P. Chough and R. D. Caudle, pp. 3-12, Elsevier, 1987.
9. F. W. Lytle, R. B. Greegor, D. R. Sandstrom, E. C. Marques, J. Wong, C. L. Spiro, G. P. Huffman, and F. E. Huggins, Nuclear Instruments and Methods 226, 542-548 (1984).
10. J. Karas, R. J. Pugmire, W. R. Woolfenden, D. M. Grant, and S. Blair, Int. J. Coal Geology 5, 315-338 (1985).
11. R. Keogh, S. Poe, B. Chawla, and B. Davis, in Coal Science and Technology, Vol. II, Eds., J. A. Moulijn, K. A. Nater, and H. A. G. Chermin, Elsevier, 1987, pp. 289-294.
12. Cooperative Research in Coal Liquefaction Infratechnology and Generic Technology Development, Final Report on DOE Contract No. DE-FC22-85PC80009, submitted by the Consortium for Fossil Fuel Liquefaction Science, June 29, 1987.

13. J. Wong, F. W. Lytle, R. P. Messmer, and D. H. Maylotte, Phys. Rev. B 30, 5596-5610 (1984).
14. F. W. Kutzler, C. R. Natoli, D. K. Misemer, S. Doniach, and K. O. Hodgson, J. Chem. Phys. 73, 3274 (1980).
15. F. Sette, J. Stohr, and A. P. Hitchcock, Chem. Phys. Letters 110, 517-520 (1984).
16. A. Bianconi, E. Fritsch, G. Calas, and J. Petiaw, Phys. Rev. B 32, 4292-4295 (1985).
17. F. W. Lytle, R. B. Greegor, and A. J. Panson, "Discussion of XANES: Application to Cu in High T_c Superconductors," submitted to Phys. Rev. B.
18. D. E. Sayers, F. W. Lytle, and E. A. Stern, Phys. Rev. Lett. 27, 1204 (1971).
19. P. A. Lee, P. H. Citrin, P. Eisenberger, and B. M. Kincaid, Rev. Mod. Phys. 53, 769-806 (1981).

TABLE I. Energies (eV) of the first three peaks observed in the XANES of some standard compounds and coal specimens. Peak 1 is the most intense XANES feature.

	Peak 1		Peak 2		Peak 3	
Sample	Position (eV)	Area+ (%)	Position (eV)	Area (%)	Position (eV)	Area (%)
K_2SO_4	11.5	62	15.1	6	17.3	32
thianthrene	3.3	66	9.4	34		
4,4 thiodiphenol	2.5	26	4.1	15	10.7	52
sulfamic acid	9.0	41	11.5	31	18.0	27
sulfosalicylic acid	10.3	83	16.9	17		
dibenzothiophene	2.8	60	4.8	9	8.3	31
2,2 thiodiacetamide	2.6	17	7.8	27	18.5	56
thioacetamide	0.1	42	2.4	13	5.8	46
pyrite	0.9	94	8.9	3	11.8	3
pyrrhotite	-0.5	7	6.8	32	12.0	54
W. KY #9, run 6, biodesul.	2.9	37	5.0	6	11.4	57
W. KY #9, run 5, biodesul.	2.9	32	4.9	4	11.7	64
PSOC 733 (e)	2.8	47	4.9	7	11.3	46
PSOC 733 (v)	2.9	43	4.7	6	11.3	51
PSOC 733 (i)	2.9	41	4.9	3	11.6	56
PSOC 1111 (e)	3.3	41	5.1	23	10.2	36
PSOC 1111 (v)	3.3	39	5.0	24	10.0	37
PSOC 1111 (i)	3.3	43	5.0	24	9.9	33
PSOC 1110 (e)	3.0	46	4.8	20	9.8	34
PSOC 1110 (v)	2.4	26	4.1	9	9.1	73
PSOC 1108S (v)	2.5	21	4.2	9	9.4	78
W. KY #9 (e)	2.9	41	4.8	4	10.8	55
W. KY #9 (v)	2.9	40	5.0	5	10.8	55
W. KY #9 (i)	2.9	35	4.9	1	11.2	64
W. KY #9 (v)	2.9	44	4.9	10	11.2	46
W. KY #9 71095 (v)	2.9	48	4.9	6	11.2	46
W. KY #3 (v)	2.2	38	4.2	5	9.9	57
W. KY #5 (v)	2.2	38	4.1	5	10.3	57
W. KY #6 (i)	2.1	45	4.0	5	10.7	50

*(e), (v), and (i) denote exinite, vitrinite, and inertinite separates prepared by DGC.

+The area percentages are determined by a program developed by one of the authors (R. B. Greegor) that fits the XANES peaks with Lorentzians and the edge step by an arctangent function. The analyses were carried out from -10 to +20 eV.

TABLE II. Distances (Å) from the sulfur atom to its nearest neighbor shells in dibenzothiophene and a variety of coal specimens.

Sample*	Shell 1	Shell 2	Shell 3
dibenzothiophene	1.74	2.71	4.02
W. KY #9, run 6, biodesul.	1.75	2.75	
PSOC 733 (e)	1.75	2.75	4.02
PSOC 733 (v)	1.74	2.74	4.02
PSOC 1111 (e)	1.74	2.74	4.02
PSOC 733 (i)	1.74	2.73	
PSOC 1111 (e)	1.74	2.75	4.05
PSOC 1111 (i)	1.74	2.73	4.02
PSOC 1110 (e)	1.74	2.76	
PSOC 1110 (v)	1.74	2.75	
PSOC 1108S (v)	1.74	2.75	
W. KY #9 (e)	1.78	2.74	
W. KY #9 (v)	1.75	2.74	
W. KY #9 (i)	1.75	2.82	
W. KY #9 (v)	1.75	2.73	
W. KY #9 71095	1.75	2.75	
W. KY #3 (v)	1.75		
W. KY #5 (v)	1.75	2.77	
W. KY #6 (i)	1.74	2.80	

*(e), (v), and (i) denote exinite, vitrinite, and inertinite separates prepared by DGC.

6066P

Fig. 1 — XANES of Sulfur Standards

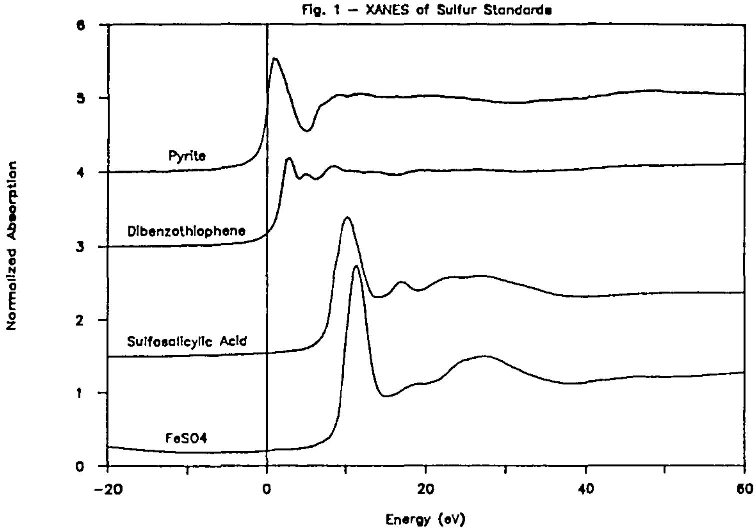

Fig. 2 — XANES of Maceral separates

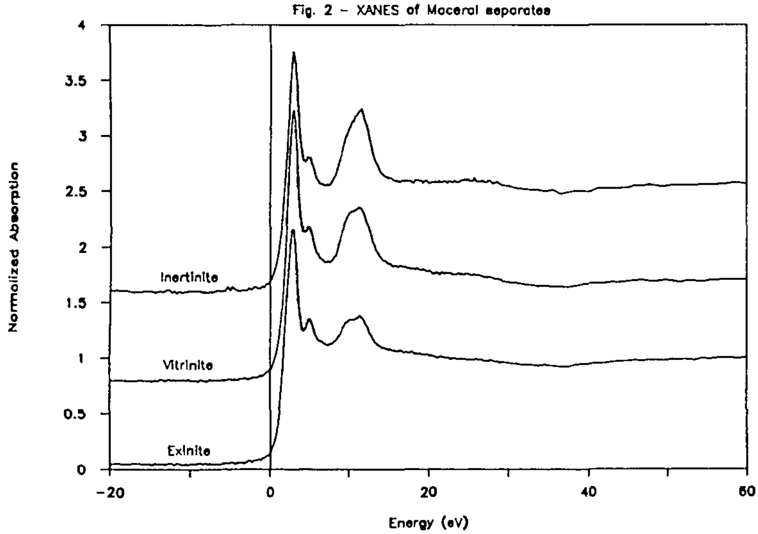

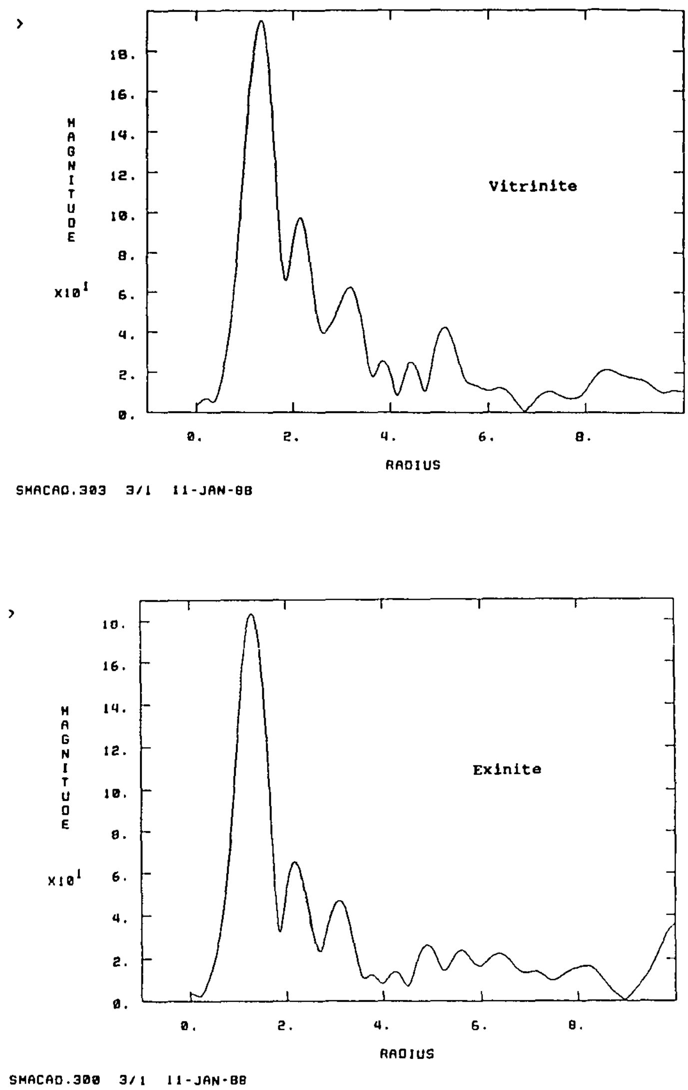

Figure 3. Radial structure functions obtained from the EXAFS of maceral separates from PSOC 733.

DESULFURIZATION OF PURE COAL MACERALS

Edwin J. Hippo* and John C. Crelling**

*Department of Mechanical Engineering and Energy Processes and
** Department of Geology, Southern Illinios University,
Carbondale, IL 62901

The objectives of this study were to modify the present density gradient centrifugation (DGC) techniques for coal macerals (1-6) to obtain 10-20 grams of target maceral concentrates and to determine the reactivity or ease of removing the organic sulfur in the various macerals with supercritical methanol extraction. Although the chemistry needed for this objective is not difficult, the accumulation of 10 to 20 gram quantities of "pure" petrographically verified single maceral concentrates has not been possible until now. The results of recent work (7) have demonstrated that the individual macerals can be separated and verified. The accumulation of much larger quantities than have previously been separated was a problem that has been overcome by pre-concentrating target macerals at their density cut points.

Supercritical fluid extraction of coals has previously been reported as a method in the production of liquid fuel products from coal under mild conditions and as a medium for selective desulfurization of coal (8-11). Alcohols are expected to exhibit greater solubility for polar organic molecules due to hydrogen bonding and dipole attractive forces, also providing the opportunity for chemical reactions during the extraction due to the nucleophilicity of the alcohol oxygen and the tendency to act as a hydrogen donor. In addition, enol rearrangements (12) may play a role in desulfurization.

As previously reported (8-9), different supercritical reaction conditions produced different extents of desulfurization of coals (33.9 - 65.7%). These variable desulfurizations are probably a result of differences in extents of conversion of the pyritic sulfur (to various alteration products, such as pyrrhotite), as well as organic sulfur functionalities (thiophenol, sulfide, and thiophenes) to light gases such as dimethylsulfide, hydrogen sulfide, and methylmercaptons.

EXPERIMENTAL

Maceral Separation

In this research, the DGC technique was modified and improved to obtain larger size samples. This was done in two ways. First, the coal was divided into its natural divisions, lithotypes, which are the easily identifiable natural associations of macerals that make up the coal seam. This can be done (and routinely is being done in the SIU-C Maceral Separation Laboratory) by careful hand-picking, or by centrifugation at a particle size (-100 to -200 mesh) that liberates the lithotypes from each other. Even such similar macerals as pseudovitrinite and normal vitrinite are being successfully separated from each other now in this manner. Second, low frequency maceral phases (those occurring at less than 5% of the whole coal) can be pre-concentrated by centrifugation of bulk quantities (10 grams or more) at the density cut-off points for the target macerals. This procedure results in fractions which are enriched in the target maceral relative to the whole coal and allows relatively larger amounts of pure macerals to be obtained much more easily than starting with the raw coal. These pre-concentrated feedstocks are then subjected to the DGC technique.

Target macerals for this study include sporinite, vitrinite, pseudovitrinite, semifusinite and fusinite. These are the major maceral components which contain significant organic sulfur. Resinite and cutinite were not studied because the abundance of these macerals is low in Illinois coals and they contain relatively low concentrations of organic sulfur.

Desulfurization

The desulfurization of coal by supercritical methanol extraction was carried out in a microautoclave system (11) that consists of a 10cc stainless steel microautoclave linked to a metering valve and a quick disconnect fitting with high pressure tubing. The reactor system is attached to an automatic shaker, which is supported above a fluidized sand bath. The shaker allows the autoclave to be agitated during reaction to ensure uniformity of reaction. The fluidized sand bath is controlled using an Omega temperature controller to ensure temperature stability. The normal charge in the reactor consisted of 1 gram of coal and 2 grams of methanol. After reaction the solid residues were removed from the reactors and ground and then dried in a vacuum oven at 95 degrees Celsius for approximately 90 minutes. The total sulfur was then determined for all the solid residues.

Samples

The three coals used in this study were taken from the Illinois Basin. They include: 1) SIU 1386, from the Herrin No. 6 seam; 2) SIU 647J, from the Brazil Block seam; and 3) SIU 1749, a wash plant mixture of Illinois No. 5 and No. 6. All three coals are high-volatile bituminous in rank with standard vitrinite reflectances of 0.42, 0.49, and 0.79 % respectively. The maceral analysis reveals that coals #1 and #3 are typical midwestern coals composed mainly of vitrinite (82.7 and 85.4 %), while coal #2 has much higher liptinite (11.6 %) and inertinite (22.7%) contents.

RESULTS OF ANALYSIS

Effects of KOH

Prior to standardization the 5% KOH loading was tested against known KOH addition. At low-severity (350 degrees

Celsius, 60 minutes) the presence of KOH shows a slight positive effect on sulfur removal. Under slightly more severe conditions (450-500 degrees Celsius, 30 minutes) the difference between sulfur removal and tests with and without KOH addition increases. The sulfur removals under high-severity conditions (500 degrees Celsius, 60 minutes) shows either no effect or a negative effect of KOH addition. In many cases sulfur removals decrease as reaction times are increased from 30 to 60 minutes. These patterns are independent for the three coals studied and the preparation the coal receives. However, the extent of the reduction is coal dependent. Coal 1 and 2 show a slight reduction in sulfur removal, whereas, coal 3 gives large amounts of sulfur incorporation. This phenomena has been observed previously by Murdie (11). The incorporation is short-lived at moderate-severity and is difficult to pinpoint. At higher severity conditions the degree of incorporation may be permanent. The severe incorporation noted with coal 3 may be experimental coincidence in obtaining the maximum incorporation at the specified temperatures. However, coal 3 did show a consistent linear decrease in sulfur removal as a function of reaction time at 500 degrees Celsius. At 15 minutes reaction time 65% sulfur removal was obtained. At 60 minutes reaction time 6% sulfur removal was obtained. Although incorporation reactions complicate data interpretation, the increase sulfur removals in the presence of KOH were significant enough to standardize on this operation procedure. Thus, most of the data reported is for 5% KOH loadings.

Effects of Sample Preparation

Under mild-severity, micronized coal is less reactive than -60 mesh coal. At moderate-severity the micronized coal tends to be slightly more reactive than the -60 mesh size fraction of the same coal; and at high-severity the micronized coal is substantially more reactive than the -60 mesh size fraction of the same coal.

The data imply that slight oxidation in the fine coal particles retards desulfurization under mild conditions, but mass transport effects are more significant at high- severity. Retardation of sulfur removal under mild desulfurization conditions may be the result of surface oxidation of pyrite particles or oxidation of freshly exposed coal surfaces. The surface oxide on pyrite particles would be expected to be less susceptible to desulfurization at low temperatures. However, at higher temperatures the sulfates would be expected to decompose to SOx. Sulfur incorporation is more likely to occur at elevated temperatures. The micronized particles allow the product less time to react with components on the pore walls than -60 mesh particles. Thus, micronization reduces the chance of incorporation during the process of product diffusion to the bulk gas. Thus, higher sulfur removals can be observed in the micronized samples. On the other hand, when conditions in the bulk gas favor sulfur incorporation, the smaller particle size of the micronized coal will enhance sulfur incorporation.

Figure 1 demonstrates the effect of the trend in sulfur removal as a function of sample preparation. These results are typical of high-severity SME processing and reflect trends in maximum sulfur removal. The data are reported for samples prepared from coal 1, but the trend is also applicable for sulfur removals from coals 2 and 3. Less sulfur is removed from the -60 mesh size fraction than is removed from the micronized coal; less sulfur is removed from the micronized coal than is removed from the micronized/ demineralized coal; and less sulfur is removed from the micronized/demineralized coal than is removed from the micronized/demineralized/ cesium chloride-floated coal. These data reflect trends that are applicable for all process conditions studied at or above 450 degrees Celsius. The patterns are also independent of the sulfur incorporation phenomena. In other words, if sulfur incorporation is observed for a condition, the magnitude of the incorporation appears to be independent of the sample preparation.

Figure 2 shows sulfur removal under 500 degrees Celsius and 60 minutes reaction time for vitrinite and sporinite maceral concentrates of coal 2. Sulfur removal in the vitrinite and sporinite concentrates are substantially higher than sulfur removal in the micronized coal or the sample prepared by a 1.6g/ml floatation process. The vitrinite and sporinite concentrates contain 86% of the total organic sulfur in the coal. Assuming that none of the sulfur in the other macerals is removed, the results on the vitrinite and sporinite concentrates suggests that 65% of the organic sulfur should be removed in the micronized or floated samples. Since both the float and maceral concentrates contain about the same amount of cesium introduced during the preparation process, catalytic desulfurization effects can be eliminated as a cause for the high desulfurization rates in the maceral concentrates. Thus, the data suggests that other macerals inhibit sulfur removal or trap products of the desulfurization process.

Figure 3 depicts sulfur removal of maceral concentrates at milder experimental conditions. Similar trends are observed. Namely, vitrinite and sporinite concentrates evolve more sulfur than whole or floated coals. Thus, sulfur removals in the vitrinite and sporinite occur at a faster rate as well as reaching a higher maximum. Not enough tests have been conducted on the maceral concentrates to judge sulfur incorporation tendencies.

Figure 3 also contains data for one test conducted on the vitrinite concentrate of coal 1 at a high-severity condition. The sulfur removal in the vitrinite concentrate was found to be higher than the sample prepared by sequential micronization, demineralization, and floatation. The difference in sulfur removal between the maceral concentrate and the floated sample is not as great as the equivalent tests on samples prepared from coal 2. However, the vitrinite concentration in coal 1 is substantially higher than in coal 2. Therefore, the float sample from coal 1 would be expected to be similar to the vitrinite concentrate. The 5% lower sulfur removal in the float sample indcates a large sensitivity in sulfur removal with variations in maceral concentration.

CONCLUSIONS

The modified DGC method employing a pre-concentration of macerals at specific density cut-points allows for accumulation of a sufficient quantity of pure maceral concentrates for testing the desulfurization properties of individual macerals. The concentration of 10gm aliquots of pure maceral concentrates represents a new advance in coal separation technology. This is the first time that such large quantities of pure macerals have been segregated by any technique.

The conditions under which samples are tested are extremely critical to the extent of sulfur removal. In general, increased temperature increases desulfurization. Also, sulfur removal increases with longer reaction times. The presence of KOH enhances the rate of sulfur removal. Sulfur can be reincorporated from sulfur-containing gaseous products, and KOH enhances the sulfur reincorporation. Some of the sulfur removal may be retarded by incorporation of products during diffusion of product gases through the pore system of the residual coal. Thus, very fine particle sizes are desirable for chemical desulfurization.

The type of sample preparation affects sulfur removal. In general, particle size reduction increases sulfur removal. Demineralization results in increased sulfur removal in subsequent processing. Variations in sulfur removal due to variations in coal properties are observed for the micronized and demineralized coals.

The demineralized coals contain pyrite. Pyrite is removed by floatation at a 1.6gm/ml solution. Floatation produces a very clean coal that is more reactive than the demineralized coal. For float samples, approximately the same maximum desulfurization level is obtained independent of desulfurization process and coal properties.

The float samples demonstrate that organic sulfur is more amenable to desulfurization than was previously thought.

Since high levels of sulfur removal are obtained during pyrolysis, the sulfur removals reported are not an artifact of sample dilution. Furthermore, either pyrite is less reactive than the organic sulfur or the pyrite (or derived products of pyrite) aid in sulfur incorporation reactions. The results suggest the thermal-chemical desulfurization should be preceded by a thorough physical cleaning that removes both pyrite and other coal minerals.

Finally, the main objective of this study was to investigate the desulfurization behavior of individual coal macerals. The sporinite and vitrinite concentrates are more reactive towards desulfurization processes than any of the other materials that were studied. They also gave the highest desulfurization levels. Since they are more reactive than whole coals or floated samples, the other constituents in the coal matrix must reduce sulfur removals. This phenomena has not been reported previously. It implies that the inertinite macerals may behave in a manner similar to activated charcoal and chemically absorb copious amounts of sulfur during the desulfurization processes. The practical result of this phenomenon is that selection of coals on the basis of maceral composition could be necessary to optimize thermal-chemical desulfurization. Work in this area is continuing at Southern Illinois University at Carbondale.

REFERENCES

1. Gary R. Dyrkacz and E. Philip Horwitz, Fuel, v. 61, No. 1, p. 3-12, (1982).

2. Gary R. Dyrkacz, Carol A. A. Bloomquist, and Peter R. Soloman, Fuel, v. 63, p. 536-542, (1984).

3. Gary R. Dyrkacz, Carol A. A. Bloomquist, and Ljiljana Ruscic, Fuel, v. 63, p. 1166-1174, (1984).

4. Gary R. Dyrkacz, Carol A. A. Bloomquist, and Ljiljana Ruscic, Fuel, v. 63, p. 1367-1374, (1984).

5. Gary R. Dyrkacz, C. A. A. Bloomquist, L. Ruscic, and E. Philip Horwitz, in: Chemistry and Characterization of Coal Macerals, Randall E. Winans and John C. Crelling, eds., American Chemical Society Symposium Series 252, American Chemical Society, Washington, D. C., (1984).

6. Jirina Karas, Ronald J. Pugmire, Woolfenden Warner, David M. Grant, and S. Blair, Int. Jour. Coal Geol., v. 5, p. 315-338, (1985).

7. Crelling, John C., Proceedings of the 1987 International Coal Science Conference - IEA, Coal Science and Technology II - Elsevier, Amsterdam, p. 119-122, (1987).

8. J. W. Chen, C. B. Muchmore, T. C. Lin, and K. E. Tempelmeyer, Fuel Processing Technology, v. 11, p. 289-295, (1985).

9. C. B. Muchmore, J. W. Chen, A. C. Kent, and K. E. Tempelmeyer, Fuel Division Preprints, 188th National Meeting, American Chemical Society, Miami Beach, Florida, (1985).

10. E. J. Hippo, N. Murdie, J. W. Chen, C. B. Muchmore, and A. C. Kent, Fuel Processing Technology (in press).

11. N. Murdie, E. J. Hippo, W. Tao, C. Muchmore, and A. Kent, Fuel Processing Technology (in press).

12. R. T. Morrison and R. N. Boyd, in: Organic Chemistry, 2nd edition, Allyn & Bacon, Inc., Boston, Massachusetts, (1966).

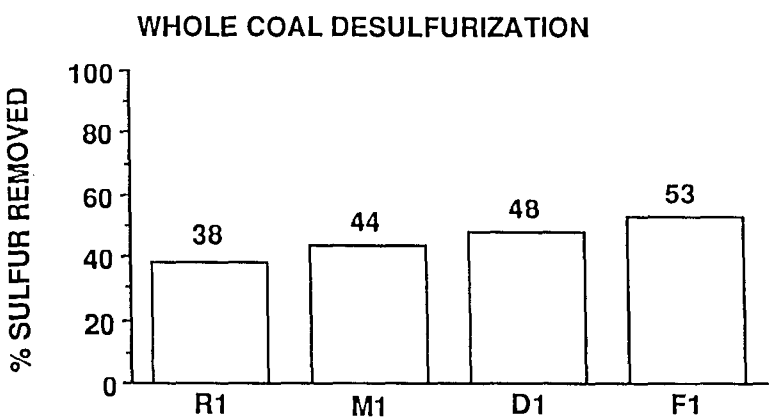

Figure 1. Typical results from a single coal sulfur removal with supercritical methanol extraction at 450 degrees C for 30 minutes showing the effects of pretreatment of the sample. (R = raw, M = micronized, D = micronized and demineralized, F = micronized, demineralized, and floated at 1.6 gm/ml.)

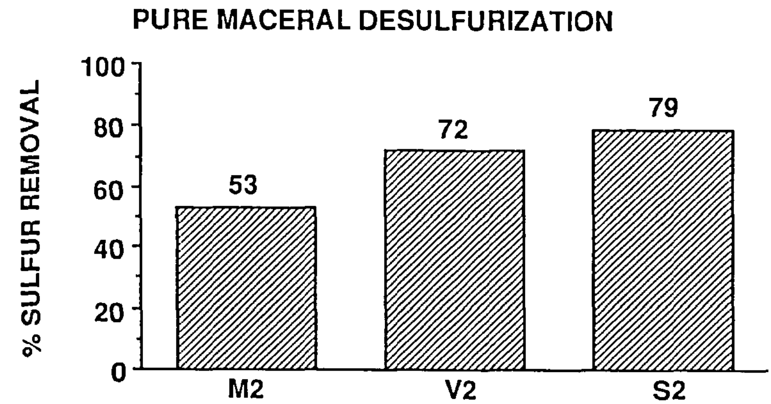

Table 2. Results of sulfur removal with supercritical methanol extraction (SME) on pure maceral fractions from the same coal sample at 500 degrees C for 60 minutes. (M = micronized coal, V = vitrinite, S = sporinite.) It should be noted that the high sulfur removals represent the removal of organic sulfur. Pyritic and sulfate sulfur have been removed earlier.

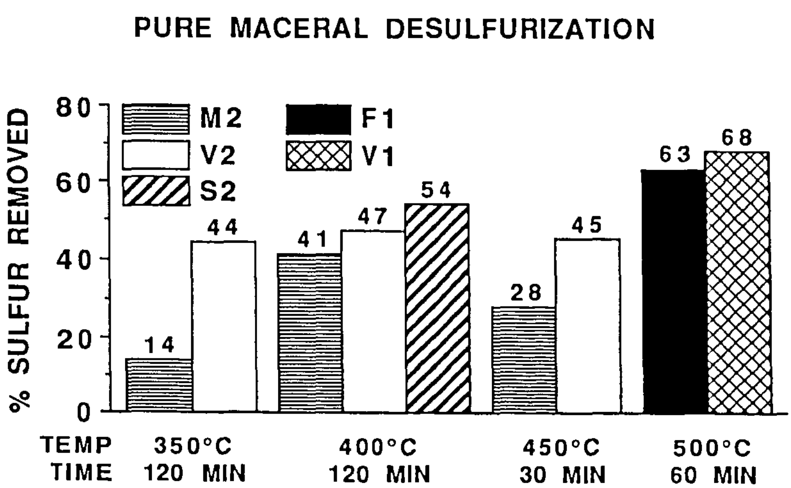

Table 3. Results of sulfur removal with supercritical methanol extraction on pure maceral concentrates. In all cases more sulfur is removed from the macerals than the micronized and/or floated coal. (M2 = micronized coal #2, V2 = vitrinite from coal #2, S2 = sporinite from coal #2, F1 = floated coal #1, and V1 = vitrinite from coal #1.)

SUPERCRITICAL DESULFURIZATION RATES OF WHOLE AND TREATED COALS.

E.J. HIPPO, W. TAO, D.P. SARVELA, C.B. MUCHMORE, AND A.C. KENT

DEPARTMENT OF MECHANICAL ENGINEERING AND ENERGY PROCESSES,
SOUTHERN ILLINOIS UNIVERSITY, CARBONDALE, IL 62901.

Introduction

Growing concern over the environmental effects of acid rain has resulted in increased interest in development of precombustion removal of sulfur from coal. Most coals are not in compliance with the recent requirements which call for reduction of sulfur emissions from various fuel sources. Under proposed guidelines, even low sulfur, western bituminous coals require some cleaning to meet new source standards of 1.2 lb. of SO_2 per million Btu's and 90% reduction in sulfur content of the coal on a concentration basis.

Typically, Illinois Basin coals contain more sulfur than coals from other coal bearing regions. In order for typical Illinois coals to meet EPA guidelines, some organic sulfur must be removed, in addition to most of the pyritic sulfur. Almost all Illinois coals contain greater than 1% organic sulfur, with most containing more than 2% [1].

The Department of Mechanical Engineering and Energy Processes at Southern Illinois University is developing a desulfurization process to remove both organic and inorganic sulfur from coal without deleteriously affecting key combustion properties [2]. This process employs alcohols under supercritical conditions. The coal/alcohol mixtures produce a clean solid product with an acceptable sulfur content, a high Btu gaseous product and coal derived liquids.

Supercritical fluid extraction of coals has been reported previously, as a method for the production of liquid fuel products from coal under mild conditions, and as a medium for selective desulfurization of coal [2-4]. Alcohols are expected to exhibit greater solubility for polar organic molecules because of hydrogen bonding and dipole attractive forces. They also provide the opportunity for chemical reactions during the extraction because of the nucleophilicity of the alcohol oxygen and the tendency to act as a hydrogen donor. In addition, enol rearrangements [5] may play a role in desulfurization.

As reported previously [4], different supercritical reaction conditions produced different extents of desulfurization of coals (33.9-65.7%). However this work concentrated on Illinois Coals. The variable desulfurizations probably result from differences in extents of conversion of the pyritic sulfur (to various alteration products, such as pyrrhotite), [4] as well as organic sulfur functionalities (thiophenol, sulfide, and thiophene) to light gases such as dimethylsulfide, hydrogen sulfide and methylmercaptons. Although the exact mechanism of the methanol/sulfur functionality reactions are not known, the reactions are believed to be complex, involving hydrogen donation by the alcohol, as well as nucleophyllic substitutions.

The overall objective of this study was to gain a better understanding of the supercritical alcohol/coal desulfurization process. Initial development of the supercritical desulfurization process utilized a batch reactor system [4]. Recently, microreactor system has been developed, which is similar to tubing bombs developed by Neavel [6], for coal liquefaction studies. This new system has several advantages over the batch reactor system and approximates more closely the operating conditions of the continuous reactor. Using the microreactor system, the heating and cooling times were reduced compared with those required for the batch reactor. This reduction of heating and cooling time, from 60-120 minutes in the batch reactors to 2-3 minutes in the microreactors, is anticipated to give a better understanding of the reaction kinetics under supercritical conditions. The microreactors are designed to provide a uniform temperature within the reactor and allow precise measurements of temperature. Previous optical characterization of the batch reactor residues suggested that mass and/or heat transfer resistance might be present in the batch system [4].

This paper describes the desulfurization of various coals in supercritical methanol. The objective of the study is to determine the effect of coal properties and treatment of coals on desulfurization rates in supercritical methanol. The effects of KOH addition on desulfurization rates is discussed. Other treatments such as physical cleaning and acid demineralization are reported in an associated paper [7].

Experimental

The eight samples studied in this investigation were obtained from the Argonne Premium Coal Sample Bank. The analysis are reported in Table 1. These samples ranged in rank from Lignite to Low Volatile Bituminous and ranged in Sulfur contents from 0.5 to 5.0% on a dry basis. The values reported in Table 1 were calculated from as received basis as reported by Dr. Vorres, the manager of the sample bank.

For some experiments, the coal was treated with KOH. In these experiments, the coal was soaked overnight in a 5% KOH solution of alcohol.

The reaction of coal with methanol was carried out using a microautoclave system. The apparatus consisted of a 10 cc. stainless steel microautoclave linked to a metering valve and a quick disconnect fitting by high pressure tubing. The reactor system was attached to an automatic shaker supported above a fluidized sand bath. The shaker allowed the autoclave to be agitated during reaction to ensure uniformity of reaction. The fluidized sand bath was temperature stability. Pressure was monitored by and Omega pressure transducer connected to the reactor through a two way valve.

Supercritical Reaction

The microautoclaves were first flushed with nitrogen to remove any oxygen present. The reactors were then charged with coal (1 g.) and methanol (2 g.). Further pressurized flushings with nitrogen were carried out to ensure the removal of oxygen after the microautoclave had been sealed. The valve was opened after successive flushed to release the pressurized nitrogen. The charged microreactors were then attached to an automatic shaker held above a sand bath, as shown in Figure 1. The fluidized sand bath was the raised, so as to fully submerge the reactor in the fluidized sand, which had been preheated to the desired temperature. The shaker was then switched on for the desired reaction time (30, and 60 minutes).

Following reaction, the sand bath was lowered and the reactors removed from the shaker. The reactors were vented by slowly opening the metering valve. After the valves had been opened fully for approximately one minute, the reactors were then quenched in a water bath.

The solid residues were removed from the reactors, ground, and then dried in a vacuum oven at 95^{o}C for approximately 90 minutes. The reactors were cleaned after each run, using acetone in an ultrasonic bath to remove tarry residues. Total sulfur analysis was carried out on all of the solid residues. Desulfurization can be calculated on a concentration or weight basis. The results in this paper are reported on a concentration basis. A concentration basis would be used by the EPA if the 90% removal requirements were to be applied. The weight basis is useful in in understanding sulfur incorporation and coal vaporiztion. The two basis can be calculated as follows:

%S Removed(conc.) = (%S Raw Coal - %S Product)/ %S Raw Coal
%S Removed(wt. %) = (wt. S Raw Coal - wt. S Product)/ wt. S Raw Coal

DESULFURIZATION OF COALS OF VARIOUS RANKS

Desulfurization results obtained on the Argonne Premium samples are listed in Table 2. The coals are listed in approximate rank order from left to right. Results are listed for a moderately severe temperature of 400 C, and a high severity temperature, 450^{o}C. Reaction times of 30 and 60 minutes were studied. Results are also listed for tests conducted with and without KOH present.

In general, desulfurization results decrease from left to right indicating a tendency for sulfur to be less removable as rank increases. For example,the data listed for no KOH, 400^{o}C, and 30 minutes of reaction time shows that the sulfur removal in the lignite is an order of magnitude greater than for the low volatile bituminous coal. This relationship can be seen in Figure 1. Since more weight loss is obtained in the lower rank coals, the relationship is more pronounced when the weight percent basis is used. The scatter in the data shown in Figure 1 also decreases when data are viewed on the weight percent basis. However, there is some variability in the relationship within the high volatile rank range even when weight factors are taken into account. Muchmore et al[3] have reported that the Organic to pyritic sulfur ratio has an effect on desulfurization of Ill.

basin coals and Hippo et al[7] have reported that physical cleaning increases subsequent desulfurization response. Thus variation in total sulfur, pyritic to organic sulfur ratio, and mineral content and composition might explain some of the observed variations.

Results from the tests conducted at 400°C at 30 minutes reaction time yield information on rates of sulfur removal. Two additional factors need to be considered. These factors are the maximum desulfuriztion obtainable and the selectivity of the sulfur removal. Although the test conducted thus far can not answer these questions entirely, they do shed light on the problems each coal has in obtaining the desired 90% removal level. For example the lignite coal yielded a 70-75% reduction in sulfur on a concentration basis and 85-89% reduction on a weight basis for the 450°C tests without KOH addition. But, this was obtained at 48% weight loss. Energy balances have not been conducted, but the 48% weight loss must represent a significant loss of energy to the vapor phase. This is not necessarily a detriment since the liquid in gases could be sold after they were cleaned. But, the weight loses complicate the analysis of the data and the determination of the optimum desulfurization conditions.

For 5 of the eight coals examined, the maximum sulfur removal in the absence of KOH occurred at 450°C and 30 minutes of reaction time. The other three coals yielded higher sulfur removals on a concentration basis at 400°C. The difficulty in specifying conditions at which maximum sulfur removals will occur arises from many factors. The major factor is that sulfur removals on a concentration basis can decrease with increase reaction time and temperature. Examples of this can be seen throughout Table 2. The decrease in the sulfur removal can occur for two reasons. One, incremental weight loses results in low selectivity towards additional sulfur removal and an increase in the selectivity toward hydrocarbon removal. For example, results at 450°C for 30 and 60 minutes reaction time in the absence of KOH for coal 6 shows a decrease in the concentration of sulfur removed even though on a weight basis the total sulfur removal has increased from 35 to 39%. The second reason for decreases in the sulfur removal on a concentration basis is due to incorporation of sulfur as has been reported previously[8]. For example, at 60 minutes of reaction time for 400°C and 450°C in the presence of KOH; coal 5 decreases in sulfur removal from 43% t0 -2% on a concentration basis. The weight % sulfur removed also decreases from 45% to 3%.

Both of these factors appear to be somewhat dependent on coal rank. The low rank coals appear to be more susceptible to loss of sulfur removal due to loss of selectivity than the high rank coals. For example the subbituminous coal in the absence of KOH shows a decrease in the sulfur removal at 450°C between the 30 and 60 minutes of reaction time despite an increase in the total sulfur removed. Furthermore when the lower rank coals show some decrease in the total weight of sulfur removed; it is usually small in magnitude. The higher rank coals show the exact opposite trend. When a decrease in sulfur removal on a concentration basis is observed it is always as a result of a decrease in the weight of sulfur removed. In addition as rank increases, the relative amount of sulfur that is incorporated back into the coal residue increases. Thus, Rank appears to be one factor that influences selectivity of the sulfur removal and the incorporation of the sulfur.

The above observation may be the result of the experimental conditions employed. As has been reported previously, the extent of the sulfur incorporation is extremely condition sensitive[8].In addition, equilibrium considerations may be dominant in the system. If so, then total sulfur in the vapor phase might contribute to the sulfur incorporation. Other factors might include the composition of the minerals present and the reactions that the minerals undergo during the extraction process. Pyrite and other minerals might catalyze the incorporation phenomena. The incorporation might be temporary as observed by Murdie et al[8] or at the high severity the incorporation may be permanent. The cause of the incorporation is not understood. It may be associated with phase changes reducing the solubility of the sulfur compounds in the supercritical vapor, or it may be due to the reaction of sulfur compounds in the bulk vapor phase with coal radicals created by the thermal processing of the coal. At mild severity the sulfur may remain active towards removal but at high severity the incorporated sulfur may crosslink and become inactive toward the alcohol.

EFFECT OF KOH ADDITION

The effect of KOH can also be seen in Table 2. At almost every condition KOH increases sulfur removal. The few results where KOH does not increase sulfur removal is where extensive sulfur incorporation is noted. Since KOH does not effect the global activation energy[8],the increase sulfur removals must be due to physical effects. One possibility is that KOH may function as a crosslinking agent. This is supported by the well known tendency of KOH to reduce fluidity, agglomeration, and swelling. Or KOH may serve as a cracking catalysts providing increase amounts of sulfur sites for reaction. In order to have no effect on the activation energy, the cracking reaction must be much faster than the sulfur removal reactions. This idea is supported by the large effects that KOH has on coals 5 and 6. The data also suggest that KOH plays a role in the incorporation of sulfur. The extent of sulfur incorporation is much greater in the presence of KOH. This may be simply that KOH provides a larger concentration of sulfur compounds in the vapor phase at the conditions that incorporation occurs. Or, the KOH may play a direct role in adding sulfur to coal free radicals and thus providing a higher probability for sulfur to be affixed by crosslinking.

CONCLUSIONS

This study has shown that:

1) Desulfurization is rank dependent.
2) Other coal properties effect desulfurization.
3) KOH increases sulfur removal and sulfur incorporation.
4) Maximum desulfurization is difficult to access.
5) Sulfur removal is condition dependent.
6) Sulfur removal selectivity varies throughout the process.
7) Optimization for maximum selectivity and removal requires an understanding of sulfur incorporation kinetics and mechanism as well as removal mechanisms and kinetics.

References

1. U.S. Bureau of Mines, Content: Part 1. The Eastern States, U.S. Bureau of Mines Information Circular No. 8980 (1975).

2. J.W. Chen, C.B. Muchmore, T.C. Lin, and K.E. Templemeyer, Fuel Processing Technology, 11, 289-295 (1985).

3. C.B. Muchmore, J.W. Chen, A.C. Kent, and K.E. Templemeyer, Preprints, 188th National Meeting, American Chemical Society, Miami Beach, Florida (1985).

4. E.J. Hippo, N. Murdie, J.W. Chen, C.B. Muchmore, and A.C. Kent, Desulfurization of Illinois Coal, Fuel Processing Technology, 17, pp.85-102, (1987).

5. R.T. Morrison and R.N. Boyd, In Organic Chemistry, 2nd Edition Boston Massachusetts: Allyn & Bacon, Inc. (1966).

6. R.C. Neaval, Fuel, 55, 237 (1976).

7. E.J. Hippo, and J.C. Crelling, (Preprints from this symposium).

8. N. Murdie, E.J. Hippo, W. Tao, A.C. Kent, and C.B. Muchmore, Fuel Processing Technology,(In Press).

9. E.J. Hippo, J.C. Crelling, D.P. Sarvela, and J. Mukerjee, PROCESSING AND UTILIZATION OF HIGH SULFUR COALS II, Y.P. Chugh, and R.D. Caudle, eds, Elesvier Science Publishing Co. Inc.,N.Y.,New York.

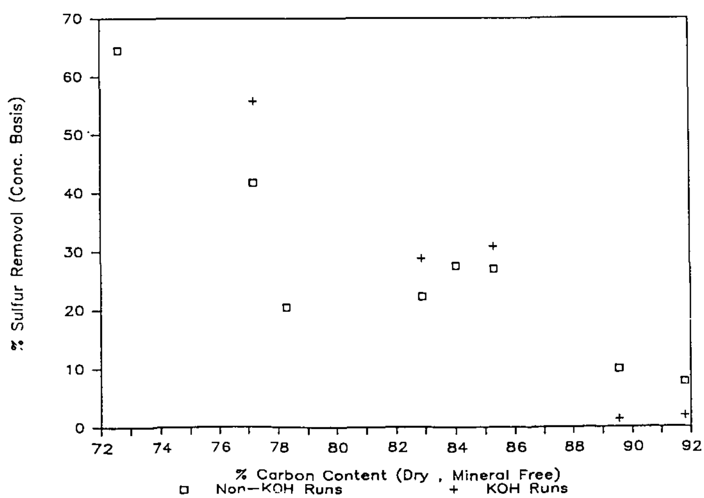

Figure 1. DESULFURIZATION IS A FUNCTION OF RANK: The data in the graph is for supercritical methanol extraction at 400^{0}C and 30 minutes reaction time.Both KOH and Non-KOH runs indicate that sulfur is difficult to remove as rank increases.

TABLE I

Properties of Coals* Used in Supercritical Methanol Extraction Tests

COAL	UPPER FREEPORT	WYODAK	ILL NO.6	PITTSBURGH NO.8	POCAHONTAS NO.3	BLIND CANYON	LEWISTON STOCKTON	BEULAH ZAP
SAMPLE NO.	1	2	3	4	5	6	7	8
(dry)								
ULTIMATE ANALYSIS								
CARBON	75.46	69.35	65.2	75.6	86.6	74.1	65.1	67.15
HYDROGEN	4.72	2.42	4.82	5.34	4.48	5.7	4.38	7.89
NITROGEN	1.40	1.05	1.19	1.49	0.93	1.30	1.03	0.92
SULFUR	2.49	0.66	5.05	2.25	0.61	0.59	0.70	0.78
OXYGEN (by diff.)	2.83	17.57	6.04	5.88	2.48	13.65	8.98	16.73
PROXIMATE ANALYSIS								
ASH	13.10	8.95	17.7	9.44	4.90	4.68	19.81	6.53
VOLATILE MATTER	27.6	33.95	30.92					
SULFUR FORMS								
SULFATE	0.01	0.007	0.008	0.01	0.003			
PYRITE	1.98	0.12	2.78	1.39	0.178			
ORGANIC	0.50	0.54	2.26	0.85	0.427			
CALORIC VALUE	13,362	11,646	10,290					
MINERAL MATTER**	15.73	10.17	21.31	11.32	5.62	5.40	22.5	7.5

*Properties of Argonne Coals Supplied by Karl Vorres except Sulfur Contents which were determined at SIUC.

**PARR Formula.

TABLE II

DESULFURIZATION OF ARGONNE PREMIUM SAMPLE COALS IN

SUPERCRITICAL METHANOL

Coal No.		8	2	3	6	7	4	1	5
Rank		Lignite	Sub-bit	High Vol	High Vol	High Vol	High Vol	Med Vol	Low Vol
REACTION CONDITIONS									
TEMPERATURE ^{0}C	TIME MIN.								
NO KOH ADDITION									
400	30	65	42	22	21	28	27	10	8
400	60	74	47	21	8	30	32	24	17
450	30	75	50	28	19	34	24	29	3
450	60	70	48	26	14	32	28	33	7
KOH ADDITION									
400	30		56	29			34	1	10
400	60		61	28	56		32	24	45
450	30		42	35	72		32	37	19
450	60		54	30	66		12		3

THE CONVERSION OF ORGANIC SULFUR IN COAL TO SULFATE USING PERCHLORIC ACID

Chris W. McGowan, Kimberly Qualls Cates, and Richard Markuszewski*
Department of Chemistry, Tennessee Technological University,
Cookville, Tennessee 38505, and
*Ames Laboratory, Iowa State University, Ames, Iowa 50011

ABSTRACT

Based upon our previous research in which the variable oxidizing power of perchloric acid ($HClO_4$) was used to determine directly the organic sulfur in coal, it was hoped that this property of $HClO_4$ could be also used to determine different forms of organic sulfur in coal. This preliminary investigation into the usage of $HClO_4$ to delineate between various organic sulfur forms was based on model compounds. Dibenzothiophene, benzothiophene, diphenyl sulfide, 2-naphthalenethiol, dibenzyl disulfide, and dioctyl sulfide were oxidized in a Bethge apparatus with $HClO_4$ of varying concentration and boiling point. To insure complete sulfur recovery, gases produced during the reaction were captured in a trap containing hydrogen peroxide. Sulfate was then measured nephelometrically, after precipitation as barium sulfate, in the residual $HClO_4$ solution and in the peroxide trap. No appreciable amount of sulfate was measured for the aromatic compounds until a temperature of 170°C or higher was reached. However, for dibenzyl disulfide and dioctyl sulfide, large amounts of sulfate were measured in the trap, even at lower temperatures. The volatility of these two compounds may be a contributing factor in their high conversion to sulfate.

INTRODUCTION

A method for the direct determination of the sulfur forms in coal has been developed which takes advantage of the selective oxidizing ability of perchloric acid (1). In that method, sulfate sulfur was extracted from a coal sample with a boiling perchloric acid solution having a boiling point of 120°C. At the boiling point of 120°C, perchloric acid is a non-oxidizing acid. If any sulfidic sulfur was present, it was converted to hydrogen sulfide and absorbed in the trap containing 15 percent hydrogen peroxide. The residue from the 120°C reaction was reacted with a perchloric acid solution at a boiling point of 155°C. At this temperature, perchloric acid begins to have some oxidizing power (2). Thus, pyritic sulfur was converted to sulfate and a sulfur-containing gas which was trapped in hydrogen peroxide. The residue from the 155°C reaction was reacted with a 9:1 mixture of concentrated perchloric and phosphoric acids boiling at 205°C. At this temperature, perchloric acid is a powerful oxidizing agent (2), converting organic sulfur to sulfate and a sulfur-containing gas which was trapped in hydrogen peroxide. Total sulfur was determined by reacting another coal sample with the 9:1 mixture of perchloric and phosphoric acids. Sulfate was determined turbidimetrically in the perchloric acid solution and in the peroxide trap after precipitation as barium sulfate. Sulfur recoveries were good and the results for sulfur forms compared well with the results obtained using the ASTM procedure (3) on the same coals. The development of this method was based on a series of perchloric acid oxidations performed on coal-derived pyrite and the Charming Creek coal from New Zealand in which almost all of the sulfur was organic (4).

The present study was undertaken for two reasons. The first was to further validate that organic sulfur was not oxidized appreciably at 155°C. The second reason was to investigate the possibility of delineating between various organic sulfur forms by taking advantage of the considerable variation in the oxidizing ability of perchloric acid. It was hoped that different sulfur functionalities would react at different temperatures above 155°C to produce sulfate and/or sulfur-containing gases. To attain these objectives, several sulfur-containing organic compounds were oxidized with perchloric acid solutions ranging in boiling point from 155°C to 203°C (concentrated perchloric acid). The model compounds subjected to oxidation were dibenzothiophene, benzothiophene, diphenyl sulfide, 2-naphthalene-thiol, dibenzyl disulfide, and dioctyl sulfide.

EXPERIMENTAL

Dibenzothiophene, benzothiophene, diphenyl sulfide, 2-naphthalene thiol, and dioctyl sulfide were obtained from Aldrich Chemical Company. Dibenzyl disulfide was obtained from Columbia Chemical Company. All reagents were used as received. All reactions were run in a modified Bethge apparatus described previously by McGowan and Markuszewski (4). The Bethge apparatus was designed to maintain a constant boiling mixture. The system was fitted with a trap containing 15 percent hydrogen peroxide to collect sulfur-containing gases and convert them to sulfate.

A Note on Safety. The use of perchloric acid alone as an oxidizing agent for organic materials always poses a hazard. In this study, all reactions were performed in a hood and behind an explosion shield. For each sample, reactions were performed at the lower temperatures first. For reactions at 203°C, small samples were reacted to minimize the possibility of an explosion. In the course of this study, a small fire occurred during the reaction of a 0.3-mL sample of dioctyl sulfide at 190°C and for a 0.1-mL sample of dioctyl sulfide reacted at 203°C. The fires were contained in the reaction vessel and no glassware was broken. The authors recommend that extreme care be taken any time perchloric acid alone is used as an oxidizing agent for organic materials.

Reaction Procedure. For the oxidations, the following procedure was followed. A perchloric acid solution was added to the Bethge apparatus and the boiling point adjusted to the desired temperature. By varying the initial amount of perchloric acid solution added, a final volume of approximately 50 mL was obtained. The perchloric acid solution was allowed to cool. In the case of dibenzyl disulfide and dioctyl sulfide, the 9:1 mixture of perchloric acid and phosphoric acid was used instead of only concentrated perchloric acid for the reaction at 205°C. A weighed sample of the solids or a pipetted sample of the liquids was placed in the Bethge apparatus. The mass of the liquid samples was calculated by using handbook densities. A gas absorption bottle containing 100 mL of 15 percent hydrogen peroxide was attached to the top of the Bethge apparatus. Nitrogen was used as the purge gas. The reaction vessel was heated to the stable reaction temperature, and the reaction was allowed to proceed for 1.5 hrs. After the heat was removed, the system was purged for an additional 30 min. with nitrogen. The solution in the absorption bottle was boiled to insure oxidation of all the sulfur to sulfate and to reduce the volume to approximately 25 mL. The solution was transferred to a 50-mL volumetric flask and diluted to mark. After cooling, the perchloric acid reaction mixture was filtered. The filtrate was transferred to a 250-mL volumetric flask and diluted to mark.

Sulfate in the trap and the filtrate was determined by precipitation with barium and spectrophotometric measurement of the turbidity of the resultant barium sulfate suspension. The procedure used was described by Markuszewski et al. (5) and modified by McGowan and Markuszewski (4). Since some of the filtrates contained a solid material, the solutions were allowed to sit at least overnight and the sample used in the analysis was pipetted from the supernatant liquid. Since most of the filtrates were also colored, the absorbance of the sample without barium chloride added was measured and subtracted from the absorbance of the test solutions. In the case of analysis of the filtrates, perchloric acid was added to the standards to approximate the acid concentration of the filtrates.

RESULTS AND DISCUSSION

The results for the oxidation of model compounds in which the sulfur is attached directly to an aromatic ring appear in Tables 1-4. The results were very similar. Only insignificant amounts of sulfate were measured in products from the reactions carried out at 155°C. For the reactions at 170°C, a significant amount of sulfate was measured for 2-naphthalenethiol, while the remaining aromatic compounds still produced only insignificant amounts. With increasing temperature, the amount of measured sulfate increased linearly, and sulfur recovery was complete for the reactions carried out at 203°C. For the aromatic materials, most of the sulfate was found in the filtrate as the temperature increased above 170°C.

Table 1. Results for the oxidation of dibenzothiophene (Theoretical=17.4% sulfur)

Boiling Point (°C)	Sample Weight (g)	Sulfur in Trap (% Samp.)	Sulfur in Filtrate (% Samp.)	Total Sulfur (% Samp.)	Sulfur Recovered (% of Theor.)
155	0.3062	0.09	0.30	0.39	2.2
170	0.3095	0.00	0.00	0.00	0.0
180	0.3129	2.23	0.18	2.41	13.8
190	0.2956	1.43	7.05	8.48	48.7
203	0.2956	2.21	15.29	17.50	100.5

Table 2. Results for the oxidation of benzothiophene (Theoretical=23.9% sulfur)

Boiling Point (°C)	Sample Weight (g)	Sulfur in Trap (% Samp.)	Sulfur in Filtrate (% Samp.)	Total Sulfur (% Samp.)	Sulfur Recoverd (% of Theor.)
150	0.5024	0.46	0.27	0.73	3.1
155	0.4993	0.59	0.34	0.93	3.9
170	0.5000	0.16	0.44	0.60	2.5
180	0.5065	1.21	6.07	7.28	30.4
190	0.5000	2.53	11.80	14.33	60.0
203	0.0623	3.68	19.70	23.38	97.9

Table 3. Results for the oxidation of diphenyl sulfide (Theoretical=17.2% sulfur)

Boiling Point (°C)	Sample Weight (g)	Sulfur in Trap (% Samp.)	Sulfur in Filtrate (% Samp.)	Total Sulfur (% Samp.)	Sulfur Recovered (% of Theor.)
150	0.3354	0.34	0.28	0.62	3.6
155	0.3354	0.09	0.44	0.53	3.1
170	0.3354	0.00	0.00	0.00	0.0
180	0.3354	1.91	1.55	3.46	20.1
190	0.3354	2.12	6.86	8.98	52.2
203	0.1115	1.40	14.60	16.00	92.9

Table 4. Results for the oxidation of 2-naphthalenethiol (Theoretical=20.0% sulfur)

Boiling Point (°C)	Sample Weight (g)	Sulfur in Trap (% Samp.)	Sulfur in Filtrate (% Samp.)	Total Sulfur (% Samp.)	Sulfur Recovered (% of Theor.)
155	0.3118	0.13	0.00	0.13	0.7
171	0.3022	1.67	0.80	2.40	12.0
180	0.3138	2.63	8.52	11.15	55.8
190	0.2961	1.98	11.74	13.72	68.6
203	0.0996	1.24	20.67	21.91	109.6

The results for the oxidation of compounds in which the sulfur was attached to an aliphatic carbon appear in Tables 5 and 6. For these compounds, significant amounts of sulfate were found in the peroxide traps for reactions at all the temperatures tested. For dibenzyl disulfide, 87-108% of the theoretical amount of sulfur was recovered at

155-205°C. Over 80 percent of the sulfur contained in dibenzyl disulfide was found in the gas trap for every reaction except that at 205°C. Lesser amounts of sulfate were measured for reaction products from dioctyl sulfide. For the reactions at 155°C and 170°C, the peroxide traps had foul, nauseating odors. This suggested that the sulfur-containing gases trapped were thiolic in nature and did not exist as an oxidized form of sulfur. The implication is that oxidation occurred on the carbon portion of the molecule, forming smaller, more volatile organosulfur compounds which escaped and were subsequently trapped. This was especially true for dibenzyl disulfide, containing the reactive benzyl carbon. The amounts of sulfate measured in the filtrates for dioctyl sulfide were similar to the amounts measured for the aromatic compounds. For dibenzyl disulfide, lesser amounts of sulfate were measured in the filtrate.

Table 5. Results for the oxidation of dibenzyl disulfide (Theoretical=26.0% sulfur)

Boiling Point (°C)	Sample Weight (g)	Sulfur in Trap (% Samp.)	Sulfur in Filtrate (% Samp.)	Total Sulfur (% Samp.)	Sulfur Recovered (% of Theor.)
155	0.3099	21.78	0.86	22.64	87.3
170	0.3068	22.16	1.17	23.90	90.0
181	0.3050	22.20	2.18	24.38	93.8
190	0.3000	22.33	3.43	25.76	98.8
205	0.1090	9.48	18.82	28.30	108.8

Table 6. Results for the oxidation of dioctyl sulfide (Theoretical=12.4% sulfur)

Boiling Point (°C)	Sample Weight (g)	Sulfur in Trap (% Samp.)	Sulfur in Filtrate (% Samp.)	Total Sulfur (% Samp.)	Sulfur Recovered (% of Theor.)
155	0.2526	3.72	0.00	3.72	30.0
170	0.2526	4.08	0.00	4.08	32.9
181	0.2526	6.02	2.97	8.99	72.5
190	0.2526	7.24	4.34	11.56	93.2
205	0.0842	1.41	12.56	13.97	112.6

Benzothiophene, diphenyl sulfide, and 2-naphthalenethiol were soluble in perchloric acid, giving clear solutions. Only very small amounts of char formed during the reactions at 170°C to 190°C. The odor of naphthalene was noted in the filtrates of the reaction of 2-naphthalene-thiol at 170°C and 180°C. A black char formed during the reaction of dioctyl sulfide at 155°C, 170°C, and 180°C. The color of the filtrates from the above reactions ranged from yellow at 155°C to orange and brown at 170°C and 180°C, respectively, and back to clear at 203°C.

During the oxidation of dibenzyl disulfide, a purplish-black, gummy solid, representing from 60 to 90 percent of the sample mass, formed at temperatures from 155°C to 190°C. The color of the filtrates indicated that some new compounds were formed at temperatures below 203°C. The filtrate was orange-pink at 155°C, light orange at 170°C, orange with a green tint at 181°C, dark brown at 190°C, and colorless at 203°C.

Dibenzothiophene was insoluble in perchloric acid, and unreacted dibenzothiophene was recovered from reactions carried out at 180°C and below. A different, yellow solid was formed at 190°C. This solid material was analyzed by Fourier transform infrared spectroscopy and mass spectrometry. Three series of compounds were identified in the solid. The major series consisted of chlorinated dibenzothiophene sulfones containing from one to seven chlorine atoms. A second series consisted of chlorinated dibenzothiophenes containing from one to eight chlorine atoms. A minor series of chlorinated compounds for which the base was dibenzothiophene plus three oxygen atoms was also indicated. No solid was recovered from the reaction carried out at 203°C.

CONCLUSIONS

Aromatic sulfur compounds are not oxidized to sulfate or a sulfur-containing gas by perchloric acid having boiling points of 170°C or lower. At higher temperatures, aromatic sulfur compounds apparently are oxidized by perchloric acid first to sulfones and chlorinated sulfones, then to sulfonic acids and finally to sulfate. Volatile sulfur-containing gases are not produced by this oxidation sequence. However, for aliphatic sulfur compounds, the carbon portion is apparently oxidized at lower temperatures, resulting in the formation of volatile sulfur-containing compounds which are trapped in hydrogen peroxide.

For analysis of a coal containing aliphatic sulfur near the end of a chain, it is possible that some of the sulfur measured after reacting the coal at 155°C could be due to organic sulfur, thus causing a positive error in the measurement of pyritic sulfur. However, during previous oxidation reactions of several different coals, no odor has ever been noted around the trap of the reaction carried out at 155°C, indicating that this possibility is probably low. Since a difference has been noted in the oxidation of aromatic sulfur and aliphatic sulfur compounds, the possibility of distinguishing between the two forms exists, and further investigation is warranted.

ACKNOWLEDGEMENT

Ames Laboratory is operated for the U. S. Department of Energy by Iowa State University under Contract No. W-7405-ENG-82. The Ames Laboratory portion of this work was supported by the Assistant Secretary for Fossil Energy through the Pittsburgh Energy Technology Center.

LITERATURE CITED

1. McGowan, C. W. and R. Markuszewski, "Direct Determination of Sulfate, Sulfide, Pyritic, and Organic Sulfur in a Single Sample of Coal by Selective, Step-Wise Oxidation with Perchloric Acid," Fuel, in press.

2. Smith, G. F., "The Dualistic and Versatile Reaction Properties of Perchloric Acid," Analyst, 80, 16 (1955).

3. "1982 Book of ASTM Standards," Part 26, Method D-2492, American Society for Testing Materials, Philadelphia, PA.

4. McGowan, C. W. and R. Markuszewski, "Fate of Sulfur Compounds in Coal During Oxidative Dissolution in Perchloric Acid," Fuel Process. Technol. 17, 29 (1987).

5. Markuszewski, R., B. C. Wheeler, R. S. Johnson, and C. C. Hach, "Rapid Dissolution of Coal for Analysis for Sulfur, Iron, and Other Elements," Am. Chem. Soc. Fuel Chem. Preprints, 28, 292ff. (1983).

DESULFURIZATION OF COAL BY PHOTO-OXIDATION

Virendra K. Mathur and Susan Murphy

Department of Chemical Engineering
University of New Hampshire
Durham, NH 03824

Abstract

Desulfurization of coal by oxidative methods has been investigated by several workers. These techniques primarily involve selective oxidation of organic sulfur to sulfoxide and sulfones, followed by thermal decomposition of the oxidation product.

In this study, photo-oxidation of sulfur in coal is investigated. Finely divided coal samples, suspended in solvent(s), are exposed to radiation using ultraviolet and xenon lamps. The coal samples are next subjected to hydrolysis to remove the oxidized sulfur from the coal matrix. The effect of wave length, light intensity, slurry concentration, and duration of exposure is studied. The maximum desulfurization achieved is about 42%.

Introduction

The U.S. has about one-third of the world's known coal reserves. But coal is difficult to mine, expensive to transport and heavily polluting. The pollution is mainly due to the presence of mineral matter (ash) and sulfur which gives rise to the formation of fly ash and sulfur dioxide. Fossil energy research, development, and demonstration strategy is to develop a wide variety of coal utilization techniques that are clean, efficient and conserve resources. Industry can then choose promising processes which will eventually be commercialized. However, there is one serious limitation to increased consumption of coal namely, sulfur dioxide pollution caused by its direct combustion. There is still a need for an efficient and inexpensive coal desulfurization technique which utility companies could readily use. In this paper, desulfurization of coal using a photo-oxidation technique is discussed.

Scientific Rationale for Photo-Desulfurization of Coal

Coal is a complex mixture of organic and inorganic compounds in which the organic matrix comprises most of the coal weight. Organic coal matrix can be viewed as a complex macromolecular structure containing the classical organic functional groups such as carbonyl and hydroxyl, aromatic and heterocyclic ring units, and aliphatic bridges. The organic sulfur in coal can be categorized into one of the functionalities such as thiol, sulfide, disulfide, thiophene, benzothiophene, and dibenzothiophene.

Desulfurization of coal has been investigated by several workers (1,2). They have used techniques such as oxidation (3-6), chlorinolysis (7-8), electrolysis (9), etc. All these methods essentially oxidize sulfur in coal. There are other methods reported in the literature involving hydrogenolysis, hydrolysis, etc. It is observed that among the organic sulfur functionalities, removal becomes increasingly difficult in the order thiolic $<$ sulfide $<$

disulfide < thiophenic < benzothiphenic < dibenzothiophenic. As the complexity of the sulfur containing functionality increases the selectivity of desulfurization, without affecting the rest of the coal matrix, becomes difficult. For example, the selectivity of hydrodesulfurization is reduced whenever the n-electrons of sulfur are in resonance with π-electrons as in the cases of thiophene, benzothiophene, etc. This leads to competing hydrogenolysis of the carbon-carbon bonds since the energies of carbon-sulfur and carbon-carbon bonds become practically identical due to resonance (10). It has been reported that atmospheric weathering leads to desulfurization of coal which can be due to the combined effect of air oxidation and photo-oxidation. However, the authors have not presented any mechanism or photonic role for this process (6).

It has been suggested that accompanying the oxidation of the sulfur to sulfone, the bond energy between the carbon and the sulfur is reduced on the average by 5.2 kcal/mole for aliphatic sulfides and by 11.8 kcal/mole for aromatic sulfides and thiophenes. Thus, the selectivity of decomposition at the sulfur-carbon bond is increased (3).

Oxidative desulfurization of coal has been studied by several workers (1-8). These methods primarily involve two steps: (1) selective oxidation of organic sulfur to sulfoxide and sulfones as shown below and (2) thermal decomposition of the oxidation product expelling sulfur dioxide.

$$\text{-S-} \xrightarrow{(O)} \underset{\substack{\| \\ O}}{\text{-S-}} \xrightarrow{(O)} \overset{\substack{O \\ \|}}{\underset{\substack{\| \\ O}}{\text{-S-}}}$$

Photo-oxidation of Sulfur in Coal

No work is reported on the photochemical oxidation of coal. It is important to understand how the coal molecule would react in the presence of light and air. Coal due to its strong absorption of the entire visible spectrum has black color. It is also well known that coal has a complex aromatic structure with polyaromatic nuclei capable of absorbing light in the visible region. Attached to these are the sulfur atoms. The n-electrons on sulfur can resonate with the aromatic π-cloud. Hence, in the presence of light the n,π^* transition is also feasible which would affect the bonding properties of sulfur. This might lead to either electron deficient sulfur linkage or formation of diradical or free radicals. Due to the complexity of coal structure it is difficult to theoretically predict the exact course of reaction from the excited state.

There is enough literature evidence that oxygen in air attacks the organic sulfur compounds photochemically (11). Extending the mechanism of photo-oxidation of sulfur compounds to coal, two courses of reaction can be predicted. One of them could be the formation of free radical/diradical center at sulfur from the excited coal molecule and subsequent oxidation and hydrogen abstraction leading to oxidized sulfur functionalities such as sulfonic acid. The second one would be the attack of sulfur center by excited molecular oxygen, namely, singlet oxygen, if the reaction conditions are conducive to the production of singlet oxygen. Either of these mechanisms would cause the formation of sulfoxides, sulfones or sulfonic acids depending upon the reaction conditions. Hence, it is safe to predict that the organic sulfur functionalities in coal could be oxidized in the presence of oxygen and visible light.

By this photo-oxidation treatment the sulfur in coal would remain in an oxidized form. The next step would then be to eliminate the oxidized sulfur from the coal matrix. This can be achieved by subjecting the photo-oxidized coal to hydrolysis. This procedure is reported to be used in other chemical desulfurization techniques also. It is envisaged that most sulfur removed by this technique as sulfonic, sulfurous or sulfuric acid or their derivatives would be organic in nature (12).

Experimental Set-up and Procedure

Finely crushed coal is suspended in 95% ethanol and kept agitated by bubbling oxygen at such a rate that the coal particles are not allowed to settle down. Also, oxygen bubbling would facilitate the removal of sulfur by oxidation. The coal slurry is subjected to photolysis in an internally lighted reaction vessel. In some experiments methylene blue is used as a sensitizer for the production of singlet oxygen. The photo-oxidized coal is washed thoroughly with ethanol to remove the dye and the ethanol is separated by centrifugation. Next, the coal is dried at 110°C for 8 hours. A portion of the photo-oxidized coal is subjected to hydrolysis either in boiling water or by refluxing with solutions of HCl or NaOH. Reference coal is also hydrolyzed with water, acid or base under the same conditions employed for photolyzed coal in order to study the effect of photolysis. The samples are analyzed for their sulfur contents.

In a second set of experiments, coal samples suspended in solvent(s), are exposed to high intensity light using an apparatus as shown in Figure 1. The other details remain the same as for experiments conducted in an internally lighted reaction vessel.

Results and Discussions

Details of the experimental conditions and results are presented in Table I through Table III. Effect of wave length on sulfur reduction is presented in Table I, showing a photonic advantage of about 35% when coal samples are exposed to radiation of wavelength 254nm as compared to 23% for 300-600nm. In both cases coal samples are subjected to hydrolysis in 1N NaOH medium. It is to be noted that same % sulfur reduction is obtained for water hydrolysis at 254nm. On the other hand, a photonic advantage of only 5% is achieved when coal samples are exposed to wave length 300-600nm and subjected to water hydrolysis.

Effect of methylene blue, as a sensitizer, on sulfur reduction when added to coal samples suspended in 95% alcohol and exposed to wave length 300-600nm is presented in Table II. No change in sulfur reduction is observed.

Effect of light intensity on sulfur reduction in coal is presented in Table III. The coal samples are suspended in water, 1N NaOH, and 95% alcohol and exposed to xenon light (800 watts) for 4 hours duration. Coal slurry is maintained at 8.3%. In spite of this high slurry concentration the photonic advantage is observed to be 16.5%, 22.5%, and 20.5% for water, 1N NaOH, and 95% alcohol, respectively, It may also be noted that coal samples are exposed for 4

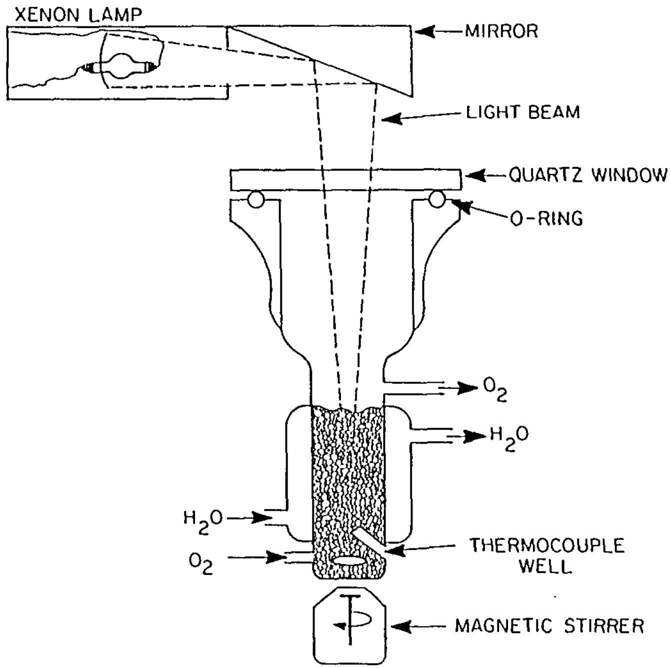

FIG. 1 HIGH INTENSITY PHOTOREACTOR ASSEMBLY

Table I

Effect of Wavelength on Sulfur Reduction

Parameters	S.N. 1	S.N. 2	S.N. 3	S.N. 4
Coal	Ill#6 Bituminous	Ill#6 Bituminous	Ill#6 Bituminous	Ill#6 Bituminous
Slurry Concentration	2%	2%	2%	2%
Particle Size	44 micron	44 micron	44 micron	44 micron
Solvent	95% ethanol	95% ethanol	95% ethanol	95% ethanol
Reactor	internal	internal	internal	internal
Sensitizer	none	none	none	none
Radiation	300-600nm	254nm	300-600nm	254nm
Light Intensity	450 watts	100 watts	450 watts	100 watts
Reaction Time	16 hr	16 hr	16 hr	16 hr
Hydrolysis Duration	reflux 8 hr	reflux 8 hr	reflux 8 hr	reflux 8 hr
Hydrolysis Medium	water	water	1N NaOH	1N NaOH
	% Sulfur Reduction			
Dark Hydrolysis	6.1%	6.1%	6.5%	6.5%
Light Hydrolysis	11.5%	41.9%	30.0%	41.8%
Photonic Advantage	5.4%	35.8%	23.5%	35.3%

hours only. An experiment is also conducted with light intensity of 450 watts using the internal photo-reactor (S.N.4) for coal slurry of 8.3% exposed for 4 hours duration. A photonic advantage of only 10% is obtained. An advantage of using high intensity light is clearly observed.

Conclusions

The results of this study show that there is a reduction in sulfur of about 24% when coal particles are subjected to 300-600nm radiation. It is also observed that coal slurry concentration can be increased and time of photolysis reduced at high intensity light exposure. The use of ultraviolet light (254nm) shows higher sulfur reductions compared to when coal samples are exposed to radiation of wavelength 300-600nm.

Acknowledgment

This study was funded by the Solar Energy Research Institute, U.S. Department of Energy, Golden, Colorado 80401. The use of high intensity photoreactor assembly at the Department of Chemistry, University of Houston, Houston, TX is also gratefully acknowledged.

References

1. R.A. Meyers, "Coal Desulfurization", Marcel Dekker, Inc., NY, 1977.

2. R.C. Eliot (Ed.), "Coal Desulfurization Prior to Combustion", Noyes Data Corporation, 1978.

Table II

The Effects of Methylene Blue on Sulfur Reduction (12)

Parameters	S.N. 1	S.N. 2	S.N. 3	S.N. 4	S.N. 5	S.N. 6
Coal	Ill#6 Bituminous	Ill#6 Bituminous	Ill#6 Bituminous	Ill#6 Bituminous	Ill#6 Bituminous	Ill#6 Bituminous
Slurry Concentration	2%	2%	2%	2%	2%	2%
Particle Size	74 micron	44 micron	44 micron	44 micron	44 micron	44 micron
Solvent	95% ethanol	95% ethanol	95% ethanol	95% ethanol	95% ethanol	95% ethanol
Reactor	internal	internal	internal	internal	internal	internal
Sensitizer	Methylene Blue	Methylene Blue	Methylene Blue	none	none	none
Radiation	300-600nm	300-600nm	300-600nm	300-600nm	300-600nm	300-600nm
Light Intensity	450 watts	450 watts	450 watts	450 watts	450 watts	450 watts
Reaction Time	16 hr	16 hr	16 hr	16 hr	16 hr	16 hr
Hydrolysis Duration	reflux 6 hr	reflux 6 hr	reflux 6 hr	reflux 8 hr	reflux 8 hr	reflux 8 hr
Hydrolysis Medium	water	1N HCl	1N NaOH	water	1N HCl	1N NaOH
			% Sulfur Reduction			
Dark Hy rolysis	4.5%	14.9%	4.2%	6.1%	6.9%	6.5%
Light Hydrolysis	12.0%	17.4%	27.8%	11.5%	9.1%	30.0%
Photonic Advantage	7.4%	3.4%	23.7%	5.4%	2.2%	23.5%

Table III

Effect of Light Intensity on Sulfur Reduction

Parameters	S.N. 1	S.N. 2	S.N. 3	S.N. 4
Coal	Ill#6 Bituminous	Ill#6 Bituminous	Ill#6 Bituminous	Ill#6 Bituminous
Slurry Concentration	8.3%	8.3%	8.3%	8.3%
Particle Size	44 micron	44 micron	44 micron	44 micron
Solvent	water	1N NaOH	95% ethanol	95% ethanol
Reactor	High Intensity	High Intensity	High Intensity	internal
Sensitizer	none	none	none	none
Radiation	Xenon	Xenon	Xenon	300-600nm
Light Intensity	800 watts	800 watts	800 watts	450 watts
Reaction Time	4 hr	4 hr	4 hr	4 hr
Hydrolysis Conditions	reflux 8 hr	reflux 8 hr	reflux 8 hr	reflux 8 hr
Hydrolysis Medium	1N NaOH	1N NaOH	1N NaOH	1N NaOH
		% Sulfur Reduction		
Dark Hydrolysis	6.5%	6.5%	6.5%	6.5%
Light Hydrolysis	23.0%	29.0%	27.0%	16.2%
Photonic Advantage	16.5%	22.5%	20.5%	9.7%

3. A. Attar, and W.H. Corcoran, Ind. Eng. Chem. Prod. Res. Dev., 17(2), 103 (1978).

4. D.J. Boron, and S.R. Taylor, Fuel, 64, 210 (1985).

5. L. Lomlpa-Krzymien, Fuel, 61, 871 (1982).

6. D. Chandra, J.N. Chakrabarti, and Y.V. Swamy, Fuel, 61, 204 (1982).

7. N.P. Vasilakos, and W.H. Corcoran, Fuel, 62, 1112 (1983).

8. N.P. Vasilakos, and C. Gage, Fuel, 65, 593 (1986).

9. S. Lalvani, M. Pata, and R.W. Coughlin, Fuel, 65, 122 (1986).

10. A. Attar, and W.H. Corcoran, Ind. Eng. Chem. Prod. Res. Dev., 16 168 (1977).

11. K. Gollnick, "Advances in Photochemistry", ed. W.A. Noyes, Jr., G.S. Hammond, and J.N. Pitts, Jr., Interscience Publisher, NY, 1968, Vol. 6, pp. 109-111.

12. V.K. Mathur, and U. Govindarajan, Am. Chem. Soc., Div. Fuel Chem. 1987, 32(4), 313.

MIGRATION OF SULFUR BETWEEN ORGANIC AND INORGANIC PHASES DURING HYDRODESULFURIZATION PROCESSES[1]

Lois V. Dunkerton*[2], Keith C. Hackley[3], John B. Phillips[2], Somenath Mitra[2], Sanjiv Mehrotra[2], and Asutosh Nigam[2]

Department of Chemistry and Biochemistry, Southern Illinois University at Carbondale, Carbondale, Illinois 62901, and
Illinois State Geological Survey, 615 E. Peabody Drive, Champaign, Illinois 61820

The co-occurrence of organic sulfur and iron sulfides in high-sulfur coal and their interrelationships are suggested to play an important role in the design and effectiveness of methods for precombustion desulfurization. The mobility and interconversion of pyritic and organic sulfur forms can be both advantageous as well as disadvantageous. Iron catalysts have been reported to exhibit high activity in coal gasification (4). More extensive studies have been done regarding the role of iron sulfides in hydroliquefaction in which pyrite is transformed to pyrrhotite and H_2S which will catalyze hydroliquefaction around 380°C (5). Studying this phenomena in more detail, with coal model compounds, showed that 316 stainless steel was a radical scavenger in the H_2S promoted radical chain cleavage of the model compounds, while pyrrhotite and pyrite decreased the reaction rate to a lesser extent (6-9). The formation of sulfur-containing organic compounds during hydrogen sulfide promoted liquefaction leading to reduction of overall desulfurization is undesirable. This is especially disadvantageous if either inorganic sulfur or easily desulfurized organic sulfur compounds are converted to less easily desulfurized thiophenic sulfur. The identification of organosulfur compounds in coal using reductive, oxidative, or metallic reagents continues to be studied with the obvious limitations in distinguishing original coal structures from secondary products formed during reactions of organic compounds with minerals, especially during pyrolysis conditions (10-18).

In the course of investigation of the non-isothermal hydrodesulfurization of model organic sulfur compounds in a coal-like environment with and without troilite, it was found that some of the non-thiophenic sulfur from the organic compounds was absorbed by troilite (1). This observation suggested that during hydrodesulfurization the organic sulfur had migrated to the inorganic phase. As the temperature was raised, more H_2S evolved from the sample with troilite, suggesting reevolution by pyrrhotite to trolite conversion.

The purpose of this study was to use isotopic labeling to determine the mechanism of incorporation of sulfur into troilite. One possibility, as suggested by the formation of pyrrhotite confirmed by Mössbauer spectroscopy, is that the H_2S produced from the organic compound was transferred to the inorganic phase, and then as the temperature was raised, H_2S evolution occurred from the troilite. Another possibility was that a direct reaction between the troilite and the organic compound took place, forming an intermediate followed by H_2S evolution from this intermediate as the temperature was raised. The fate and H_2S evolution profile from the labeling of the mobile organic sulfur group has been studied in an effort to distinguish possible mechanisms and demonstrate the role of troilite in this process.

MATERIALS

Two ^{34}S labeled compounds 2-(thiomethyl)dibenzothiophene (2) and 4-(thiomethyl)-dibenzothiophene (3) were prepared from dibenzothiophene (1) using our previously reported methods as shown in Scheme 1 (19). Compounds 2 and 3 gave spectral data in agreement with their structural assignments, including high resolution mass spectral confirmation. Compound 2 gave m/z 232.0179 for $C_{13}H_{10}{}^{32}S^{34}S$ (calculated 232.0181) and compound 3 gave m/z 232.0140.

EXPERIMENTAL

The coal-like mixture was prepared by grinding together 8 mg of compound 2 or 3 and 60 mg of charcoal (previously degassed by heating to 680°K *in vacuo*) with or without 80 mg of troilite. The mixture was placed in a pyrex tube placed in a furnace. Hydrogen was passed through the tube at a flow of 55 mL/min while heating at 3°/min from 523°K to 700°K. The evolving gases were analyzed for the ratio of $H_2{}^{32}S$ to $H_2{}^{34}S$ as the temperature was raised using a quadrupole mass spectrometer attached to a split off the gas outlet. The residue was extracted with CH_2Cl_2 to recover the organic desulfurized compound, 2- or 4-methyldibenzothiophene and the remaining residue subjected to the combustion-precipitation sequence previously reported for isotopic analysis of coal pyrolysate chars (1,20).

RESULTS AND DISCUSSION

The hydrodesulfurization of 2-(thiomethyl)dibenzothiophene(2) with and without troilite gave a total H_2S evolution profile as a function of temperature shown in Figure 1. The major process producing H_2S was the desulfurization of the thiomethyl group occuring between 523°K and 600°K while the thiophenic group began to slowly desulfurize around 725°K. In the presence of troilite, the total H_2S evolution was similar, except less evolved between 523°K and 550°K, while slightly more evolved between 550°K, and 600°K. The amount of $H_2{}^{34}S$ evolved from 2 is expected to follow the same profile between 523°K and 550°K. If some $^{34}H_2S$ migrated into the troilite, then at the higher temperatures, as the H_2S reevolved from the pyrrhotite, the $H_2{}^{34}S$ would be diluted by isotopic mixing, resulting in decreased $H_2{}^{34}S$ evolution relative to $H_2{}^{32}S$ evolution. A corresponding increase in the ^{34}S isotopic composition of the char would then be expected. If no mixing occured, the $H_2{}^{34}S$ evolution profile would be expected to follow the same pattern as the total H_2S, with no increase found in the char.

REFERENCES

1. Part 2. For part 1 see Dunkerton, L. V.; Mitra, S.; Phillips, J. B.; Smith, G. V.; Hinckley, C. C.; and Wiltowska, T. *Fuel* **1988** *67*, 000.
2. Southern Illinois University.
3. Illinois State Geological Survey.
4. Ohtsuka, Y.; Tamai, Y; and Tomita, A. *Energy and Fuels* **1987** *1*, 32-36.
5. Trewhella, M. J.; and Grint, A. *Fuel* **1987** *66*, 1315-1320.
6. Hei, R. D.; Sweeney, P. G.; and Stenberg, V.I. *Fuel* 1986 *65*, 577-585.
7. Sweeney, P.G.; Stenberg, V.I.; Hei, R. D.; and Montano, P.A. *Fuel* **1987** *66*, 532-541.
8. Yokoyama, S.; Yoshida, R.; Narita, H.; Kodaira, K.; and Markawa, Y. *Fuel* **1986** *65*, 164-170.
9. Doughty, P.W.; Harrison, G.; and Lawson, G. J. *Fuel* **1986** *65*, 937-944.
10. Boudou, J.P.; Boulegue, J.; Maléchaux, L.; Nip, M.; deLeeuw, J.W.; and Boon, J. J. *Fuel* **1987** *66*, 1558-1569.
11. Chen, P.; and Chen, W. *Fuel* **1986** 65,1305-1309.
12. Chakrabarity, S. K.; Iacchelli, A. *Can. J. Chem.* **1986** *64*, 861-864.
13. La Count, R. B.; Anderson, R. R.; Friedman, S.; and Blaustein, R. D. *Fuel* **1987** *66*, 909-913.
14. Clark, P. D.; Dowling, N.I.; Hyne, J. B.; and Lesage, K. L. *Fuel* **1987** *66*, 1353-1357.
15. Buchanan, A. C. III; Dunstan, T. D. J.; Douglas, E. C.; and Poutsma, M. L.; *J. Am. Chem. Soc.* **1986** *108*, 7703-7715.
16. White, C. M.; Douglas, L. J.; Perry, M. B.; Schmidt, C. E. *Energy and Fuels* **1987** *1*, 222-226.
17. Calkins, W. H. *Energy and Fuels* **1987** *1*, 59-64.
18. Johnson, D. E. *Fuel* **1987** *66*, 255-260.
19. Dunkerton, L. V.; Barot, B. C.; and Nigam, A. *J. Heterocyclic Chem.* **1987** *24*, 749-755.
20. Liu, C. L.; Hackley, K. C.; and Coleman, D. D. *Fuel* **1987** *66*, 683-688.

Scheme 1

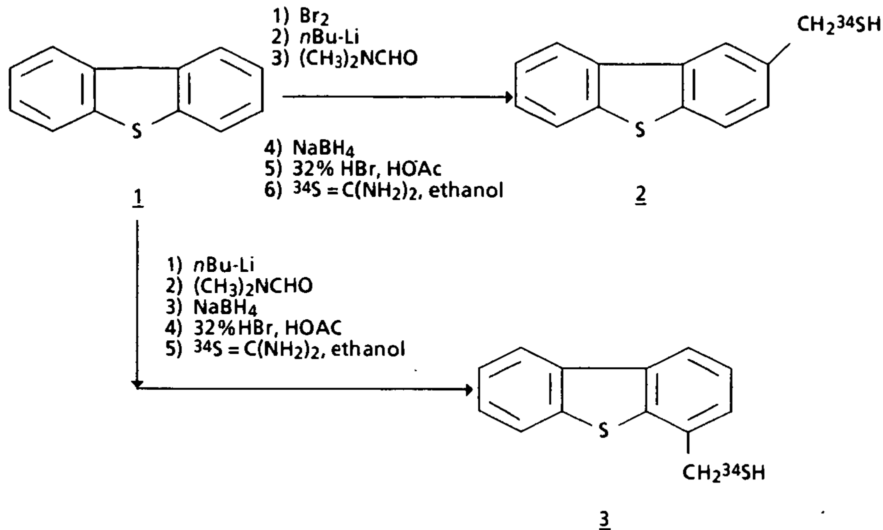

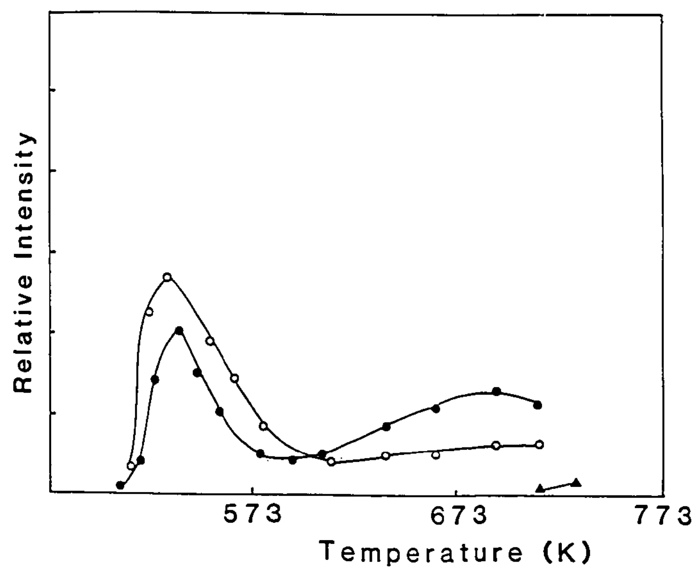

Figure 1. Rate of H_2S evolution as a function of temperature for compound 2 and dibenzothiophene at a heating rate of 3°K/min: O, compound 2 without troilite; ●, compound 2 with troilite; ▲, dibenzothiophene without troilite.

HYDRODESULFURIZATION OF A SPANISH LIGNITE

Ana B. Garcia-Suarez and Harold H. Schobert

Fuel Science Program
Department of Materials Science and Engineering
The Pennsylvania State University
University Park, PA 16802

The objective of this work is to investigate catalytic hydrodesulfurization (HDS) reactions of lignite under mild conditions. The reactions are conducted in a single stage in the absence of a donor solvent. The lignite being studied is Mequinenza (Spanish) lignite, which has the exceptionally high sulfur content of 12.9% (daf basis). Most of the sulfur in this lignite is present as organic sulfur, the organic sulfur content being 11.6% daf. Since about 90% of the total sulfur is organic, physical coal cleaning methods designed to remove pyritic sulfur are not applicable to this lignite.

On a commercial scale, the role of a hydrodesulfurization operation would be, ideally, to remove the sulfur as H_2S leaving a desulfurized coal or char having a heating value comparable to that of the feedstock. Under the HDS reaction conditions the formation of some hydrogen-rich liquids is inevitable; these liquids could be used either directly or after a second HDS step as raw materials for petrochemical processes. Our research was not primarily concerned with the process development, but rather focused on the chemistry of the HDS reactions of the lignite.

Transition metal catalysts, particularly containing cobalt, molybdenum, nickel, or tungsten, have been widely used in coal and coal liquids processing at high temperature and high pressure conditions, both with and without donor solvents. Sulfides of these metals have activity as hydrodenitrogenation and HDS catalysts. For example, the HDS activities of molybdenum and cobalt/molybdenum sulfide catalysts have been investigated for HDS of thiophenes (1,2). Currently there is extensive interest in HDS catalysts using both alumina and carbon supports (3-8). Zinc chloride has also been shown to catalyze the removal of sulfur from coal-derived compounds (9).

There appear to be no current studies of coal HDS in the absence of donor solvent. In the absence of a solvent, supported heterogeneous HDS catalysts could not be used. Consequently, we have impregnated the lignite with catalyst precursors which subsequently form the active catalysts, dispersed throughout the lignite, at reaction conditions. Collateral research at Penn State has explored the use of dispersed catalysts and absence of solvent for liquefaction (e.g., 10,11) but as far as we are aware the work reported here is the first such study for the principal purpose of HDS.

EXPERIMENTAL

The Mequinenza lignite samples were obtained from the Instituto Nacional del Carbon y Sus Derivados, Oviedo, Spain. On a daf basis the lignite contains 64.81% C, 5.72% H, 12.93% S. The forms of sulfur (dry basis) were 1.17% pyritic, 0.20% sulfate, and 9.20% organic. The ash content was 20.40% (dry basis). The lignite samples were crushed to -60 mesh in a glove box under oxygen-free nitrogen and subsequently vacuum freeze dried to less than 1% moisture. The dried samples were stored under nitrogen.

The general procedure for catalyst impregnation was to dissolve the requisite quantity of the catalyst precursor (a water-soluble salt of the desired metal) in sufficient distilled water to give a water:coal ratio of 1:1. A slurry of the lignite in this solution was stirred for at least two hours. After stirring, the excess water was removed by vacuum freeze drying to less than 1% moisture. Normally, enough lignite for a complete series of experiments would be impregnated in one batch and stored under nitrogen. For experiments with molybdenum, the catalyst precursor was ammonium tetrathiomolybdate, which was prepared by bubbling H_2S through an aqueous solution of ammonium heptamolybdate for 30 minutes.

HDS reactions were conducted in microautoclave reactors (tubing bombs) of 25 - 30 ml capacity. The reactors were pressurized with hydrogen and immersed in a preheated fluidized sand bath. The reactors were oscillated vertically through 2.5 cm at 200 cycles/min for the desired reaction time. For this work initial (cold) hydrogen pressures of 1000 and 1500 psi, reaction temperatures of 250 - 350°C, and reaction times of 0.5 - 4.0 hr were used.

After reaction, the yields of CO, CO_2, C_{1-4} hydrocarbons and H_2S were determined by GC. The reactor contents were washed with solvent (chloroform, tetrahydrofuran (THF), and ethanol were tested) into an alundum thimble and extracted under nitrogen in a Soxhlet apparatus for 20 - 24 hr. Solvent was removed from the extracts in a rotary vacuum evaporator. The extracts and insoluble residue were dried in a vacuum oven for 18 - 20 hr at 100°C before weighing. Yields of extract and insoluble residue were directly determined; total gas make was calculated by difference.

RESULTS AND DISCUSSION

Total Sulfur Removal

To establish a set of baseline conditions, a set of standard conditions was established using ammonium tetrathiomolybdate catalyst precursor, 1000 psi H_2 pressure, 0.5 hr reaction time, and THF as the extraction solvent. The catalyst loading was equivalent to 1% by weight of molybdenum. The results obtained with these conditions at five temperatures are summarized in

Table 1 below.

TABLE 1. Results of HDS with Standard Test Conditions, dry basis

Temp., °C	Conversion	Extract	H_2S Yield	Total S Removed
250	12.8%	12.6%	-	9.57%
275	13.8%	13.6%	-	13.1%
300	20.8%	19.1%	0.18%	23.9%
325	38.0%	33.0%	1.4%	47.7%
350	68.1%	53.6%	7.1%	77.2%

A marked shift in the reaction chemistry occurs in the temperature range of 300 - 325°C. First, below 300° the catalyst has essentially no effect on the reaction. For example, in reaction at 275° without catalyst impregnation but at otherwise identical reaction conditions, a conversion of 10.3% and total sulfur removal of 16.2% were observed; these results are very close to those shown in Table 1 for the catalytic experiment. By contrast, at 350° in the absence of catalyst, the conversion is only 33.7% and total sulfur removal, 48.1%. Two alternative explanations may be proposed to explain these observations: The active form of the catalyst, which is presumed to be molybdenum disulfide, may not yet have formed from the precursor at the relatively low temperature reaction conditions. Alternatively, the MoS_2 catalyst may not be active for HDS in this system below 300°.

A second aspect of the change in reaction chemistry at the higher conditions is the form in which sulfur is ultimately being removed from the system. At or below 300° essentially all of the sulfur is removed in the form of organosulfur compounds which are taken out with the extract. At the higher temperatures, most of the sulfur is removed as H_2S. Specifically, at 350° 84% of the sulfur lost from the lignite appears as H_2S, whereas at 300° only 7% (of a smaller total amount of sulfur removed) appears as H_2S. In a reaction at 350° in the absence of catalyst, the proportion of the sulfur removed as H_2S is 33%.

In this system at temperatures above 300°, the catalyst is performing two roles. First, it facilitates the breakdown of the coal structure, as shown by the higher extract yields in the catalytic vs. non-catalytic experiments. Second, it facilitates HDS, as shown by the much higher proportion of the total sulfur removed being lost as H_2S in the catalytic experiments (e.g., 84% vs 33% at 350°). There are two mechanisms by which the total HDS may be proceeding under these conditions. One possible mechanism is the direct reaction of hydrogen with sulfur functional groups in the lignite to form H_2S. The second is the liquefaction of the lignite to form sulfur-rich liquids which then undergo a subsequent HDS in situ to produce the H_2S. (A third option is that both mechanisms are proceeding simultaneously.) At present we do not have enough data to suggest which, if either, is the predominant mechanism.

Catalyst Screening

Although a 77% reduction in total sulfur is encouraging, the reaction conditions, particularly the temperature, needed to achieve this reduction are severe. Thus it is of interest to evaluate other potential catalysts to determine whether greater sulfur reduction, lower reaction temperatures, or both, are possible. This section is a brief review of results obtained with dispersed catalysts other than the standard MoS_2.

Cobalt and cobalt/molybdenum. The catalyst precursor for cobalt was $Co(NO_3)_2$; for the cobalt/molybdenum system, a solution of cobalt acetate and molybdenum oxalate. At 300°, 1000 psi H_2, and 0.5 hr reaction time the results show slight improvement compared to the MoS_2 and non-catalytic systems. The results are summarized in Table 2. The catalyst loadings were 1% Mo and 0.6% Co by weight daf, which gives equal atomic amounts of the two metals.

TABLE 2. HDS by Cobalt and Cobalt/Molybdenum Catalysts, 300°C, 1000 psi H_2, 0.5 hr; dry basis.

Catalyst Precursor	Conversion	Extract	Total S Removed
None	17.7%	15.7%	26.7%
$(NH_4)_2MoS_4$	20.8%	19.1%	23.9%
$Mo(C_2O_4)_2$	27.1%	23.3%	28.9%
$Co(NO_3)_2$	25.8%	23.5%	28.7%
$Mo(C_2O_4)_2/Co(OAc)_2$	24.3%	23.9%	25.9%

Tungsten sulfide. The precursor was ammonium tetrathiotungstate. The catalyst loadings were 1.9 and 5.7% by weight daf, giving the same tungsten loading in the lignite as would be equivalent on an atomic basis to 1 and 3% by weight Mo. At 300°, 1000 psi H_2 and reaction time of 1 hr, the conversion and extract yield were both below the values obtained under the same conditions without catalyst: conversions of 16.0 vs 19.1% and extract yields of 13.0 and 16.7%, respectively. However, reaction in the presence of the tungsten sulfide catalyst generally gave the highest concentrations of hydrogen sulfide in the gaseous products. At the reaction conditions of 300°, 1000 psi H_2 and 1 hr, the gas yields were 3.1% for molybdenum sulfide catalyst and 3.0% for the tungsten sulfide, but the hydrogen sulfide in these gases was 1.05 and 3.0%, respectively, essentially a three-fold increase. These results suggest that the mechanism of tungsten sulfide catalysis may be different from that of molybdenum sulfide. We plan further work with tungsten sulfide in both hydrodesulfurization and liquefaction studies.

Zinc chloride. The results obtained at 275°, 1000 psi H_2 and 2 and 4 hr residence times are very similar to those obtained under the same conditions using molybdenum sulfide catalyst (with comparable metal loadings on an atomic basis). Under these conditions the only advantage of the zinc chloride catalyst in comparison to molybdenum sulfide is that the zinc chloride does not introduce additional sulfur into the system, though of course the introduction of chloride may be undesirable in its own right. Mobley and Bell found that zinc chloride promotes desulfurization of aliphatic sulfides and disulfides via H_2S evolution (9). In our work, the H_2S formation in the presence of zinc chloride catalyst was of the same magnitude as from experiments without catalyst addition. There are several explanations for this observation. The organosulfur groups in the Mequinenza lignite may be of the aromatic sulfide, thiophene, or benzothiophene type, which are not susceptible to hydrocracking at our reaction conditions in the presence of zinc chloride. The liberated sulfur may react with the zinc to produce zinc sulfide, which would remain with the THF-insoluble residue. Also, our experiments were at temperatures about 50° below other work done with this catalyst (9).

CONCLUSIONS

It is possible to achieve significant reduction in the sulfur content of this remarkable lignite by HDS in the presence of a molybdenum sulfide catalyst at temperatures of 350°. A distinct change in HDS chemistry occurs around 325°. Below that temperature, most of the sulfur removed from the lignite is removed as organosulfur compounds in liquid products, whereas at 325° and above most of the sulfur is removed as H_2S. The use of zinc chloride and cobalt or cobalt/molybdenum catalysts did not appear to offer any significant advantages over the use of molybdenum sulfide. In terms of total sulfur reduction, the same is true of tungsten sulfide. However, the fact that tungsten sulfide catalysis significantly increases H_2S formation relative to comparable experiments with molybdenum sulfide suggests that the chemistry of HDS over tungsten sulfide is worthy of further investigation.

ACKNOWLEDGEMENTS

Dr. Garcia-Suarez was supported by a postdoctoral fellowship provided by the Spanish Research Council (CSIC). The authors are also grateful for financial support for the experimental work provided by The Pennsylvania State University Cooperative Program for Coal Research.

LITERATURE CITED

1. Derbyshire, F. J.; de Beer, V. H. J.; Abotsi, G. M. K.; Scaroni, A. W.; Solar, J. M.; Skorovanek, D. J. Applied Catalysis 1986, 27, 117.

2. de Beer, V. H. J.; Derbyshire, F. J.; Groot, C. K.; Prins, R.; Scaroni, A. W.; Solar, J. M. Fuel 1984, 63, 1095.

3. Mochida, I.; Sakanish, K. Y.; Fuditsu, H. Fuel 1986, 65, 1090.

4. Yoshimura, Y.; Sato, T.; Shimada, H.; Nishimida, A. Fuel Sci. Technol. 1986, 4, 621.

5. Fairbridge, C.; Farnand, B. Fuel Sci. Technol. 1986, 4, 225.

6. Eichs, J. J.; Hallenbeck, L. E.; Lucarelli, M. A. Fuel 1985, 64, 440.

7. Krichko, A. A.; Maloletnev, A. S.; Yulin, M. K.; Arifulin, A. S.; Zaidman, N. M.; Milova, L. P. Khim. Tver. Top. 1983, 17, 78.

8. Conti, L.; Botteghi, C.; Mansani, R. Fuel 1984, 63, 1414.

9. Mobley, D. P.; Bell, A. T. Fuel 1980, 59, 507.

10. Stansberry, P. G.; Lin, R.; Terrer, M. T.; Lee, C. W.; Davis, A.; Derbyshire, F. J. Energy and Fuels 1987, 1, 89.

11. Derbyshire, F. J.; Davis, A.; Lin, R.; Stansberry, P. G.; Terrer, M. T. Fuel Proc. Tech. 1986, 12, 1986.

Using X-ray Methods to Evaluate the Combustion Sulfur Minerals and Graphitic Carbon in Coals and Ashes

David L. Wertz and Leo W. Collins

Department of Chemistry and Center for Coal Product Research, University of Southern Mississippi, Hattiesburg, MS 39406 USA

INTRODUCTION

Coals are complex mixtures of vastly different materials whose combustion kinetics may well exhibit symbiotic effects. Although the sulfur oxide gases produced during the combustion of coals may have a variety of sources, they are frequently caused by the thermal degradation of inorganic minerals to produce "acid rain"; i.e.,

$$CaSO_4(s) + R\text{-}H + H_2O \rightarrow CaCO_3(s) + SO_2(g) + H_2S(g) \quad 1)$$

$$CaCO_3(s) \rightarrow CaO(s) + CO_2(g)$$

or

$$FeS_2(s) + O_2(g) \rightarrow FeS(s) + Fe_2O_3(s) + SO_2(g) \quad 2)$$

Since many of the minerals involved either as reactants or products in coal combustion produce well defined x-ray powder diffraction (XRPD) patterns, the fate of these minerals may be followed by measuring the XRPD patterns of combustion products.

Coal 1368P, a coal with an unusually high pyrite (FeS_2) fraction, has been the subject materials in our investigations of the fate of the inorganic minerals during combustion. These studies include measuring the fate of pyrite and of graphitic carbon in coal 1368P under varying combustion conditions. The results discussed below were obtained by standard XRPD methods (1).

EXPERIMENTAL

The analysis of coal 1368P, as furnished by PSOC (2), is provided in Table I along with some specialized information which resulted from our x-ray analysis.

Table I. A Definition of Coal 1368P

A. Rank: high volatile bituminous A	
B. Proximate Analysis:	
Ash:	16.7% (a)
Fixed Carbon:	40.0%
Volatile Matter:	37.1%
Moisture:	6.2%
C. Ultimate Analysis	
Carbon:	60.3%
Hydrogen:	4.4%
Nitrogen:	1.4%
Sulfur:	9.6% (FeS_2)
Oxygen:	1.3% (SeO_2)
D. Results of USM X-ray Measurements	
μ^*:	17.2 cm^2/g by XRA
minerals in ash:	Fe_2O_3 and SiO_2 by XRPD
major elements:	Fe, S, and Si by XRF

(a) The ash weight is not necessarily the minerals fraction in the non-combusted coal.

Each finely powdered sample of coal 1368P was combusted in a Lindberg Single Zone Furnace which approximates a stoker furnace. Each coal sample was weighed prior to and after combustion to determine its mass loss. Each partially combusted product was finely powdered and then loaded into our automated x-ray diffractometer. An x-ray powder diffraction pattern was obtained by measuring the counts accumulated in a ten second interval collected at increments of $d2\Theta = 0.05°$.

RESULTS AND DISCUSSION

The x-ray powder diffraction patterns of several partially combusted products from coal 1368P are shown in figure 1. These products were produced by one minute combustions with no air flow through the combustion chamber and at several different combustion temperatures. Key diffraction peaks characterizing quartz (Q), pyrite (P), hematite (H), and troilite (T) are indicated, as is the large, broad hump due to the amorphous material(s) in each sample.

QUARTZ PEAK. Previous results have shown that the 3.343 Å peak of quartz is not measurably affected by the mild combustion conditions used in these experiments (3), so this peak has been used as a reference in the interpretation of each XRPD pattern. The increase in the intensity of the quartz peak indicates an increase in the abundance of quartz, which is due to the removal of the volatile and moisture fractions from the coal (4). Shown in Table II is the intensity of the quartz peak measured in the XRPD patterns shown in figure 1.

Table II. Absorption Corrected Intensity of the 3.343 Å Quartz Peak Measured in the XRPD Patterns of the Combustion Products

Combustion Temperature	Peak Area
coal	2183
400	2545
600	2762
800	3326
1000	4072
1200	4017
1400	3809 (a)

(a) Thermal degradation may be beginning to occur at this temperature.

Comparison of the areas of the quartz peaks in the XRPD patterns may be used to calculate the loss of the volatile components during each partial combustion. Shown in Table III is kthe mass loss caused by each combustion protocol calculated from our XRPD analysis and compared to the mass loss measured by normal gravimetric methods. The excellent agreement indicates that the XRPD patterns are sufficiently accurate to use for the semi-quantitative analysis of the pyrite and of the graphitic carbon in the combustion products of coal 1368P.

Table III. Mass Loss Caused by Combusting coal 1368P for One Minute With Zero Air Flow

	Mass Loss	
Combustion Temperature	Gravimetric	Our XRPD
400	17.1%	16.6%
600	20.9%	21.0%
800	35.3%	34.4%
1000	44.8%	46.4%
1200	46.1%	45.6%

By using the ratio of the intensity 2.40 Å pyrite peak/intensity 3.34 Å quartz peak the pyrite abundance in each sample may be determined without the necessity of adding an "external standard" to each combustion sample. Using the graphitic maximum/quartz peak ratio allows a similar determination of the graphitic carbon retained in each combustion product. The uncertainty in each analysis is ±5%.

PYRITE ANALYSIS. Although several of the diffraction peaks characterizing FeS_2 are in themselves suitable for the analysis methods we have developed, the 2.40 Å peak is not, in these complicated XRPD patterns, overlapped by diffraction peaks due to other materials. For that reason the 2.40 Å peak has been used in the subsequent analyses as a measure of the weight fraction of pyrite in the combustion products. Shown in figure 2 are the ratios of the 2.40 Å pyrite peak intensity/3.34 Å quartz peak intensity in each combustion product for which both the air flow and the temperature were varied. From the measurement of the pyrite peak in each combustion product, the percent pyrite reacted may also be calculated (fig. 2). These data indicate that the thermal degradation of pyrite begins at $T > 600°C$, with all of the pyrite reacted at $T = 1200°C$.

GRAPHITIC CARBON ANALYSIS. Shown in figure 3 is the ratio of the area under the broad amorphous maximum which measures the graphitic carbon (5) to the quartz peak area in each mixture. Also shown is the percent graphitic carbon reacted for each of the combustion products. These data indicate that only a small portion of the graphitic carbon reacts, even under the most severe combustion conditions employed in these experiments.

CONCLUSIONS

By using quartz in a sample of the powdered coal as the "internal reference" and our XRPD ratio method, the fate of pyrite and of graphitic carbon in combustion processes may be determined. These XRPD data may be manipulated to minimize the ratio of reacted pyrite/reacted graphitic carbon by measuring the pyrite and graphitic carbon retained in each combustion product.

The same XRPD data may be used to determine the combustion conditions at which the volatile and mositure fractions of the coal are completely removed and to evaluate the quality of the combustion product for commercial usage.

REFERENCES

1. McCarthy, G. J., Powder Diffraction, 1 (1986) 50.
2. Pennsylvania State Office of Coal Research.
3. Wertz, D. L., Collins, L. W. and Froelicher, F., "Advances in X-ray Analysis, Vol. 31, Plenum Press (1988) in press.
4. Ohtsuka, Y., Tamai, Y., and Tomita, A., Energy and Fuels, 1 (1987).
5. Wertz, D. L., Powder Diffraction, 1988, submitted for publication.

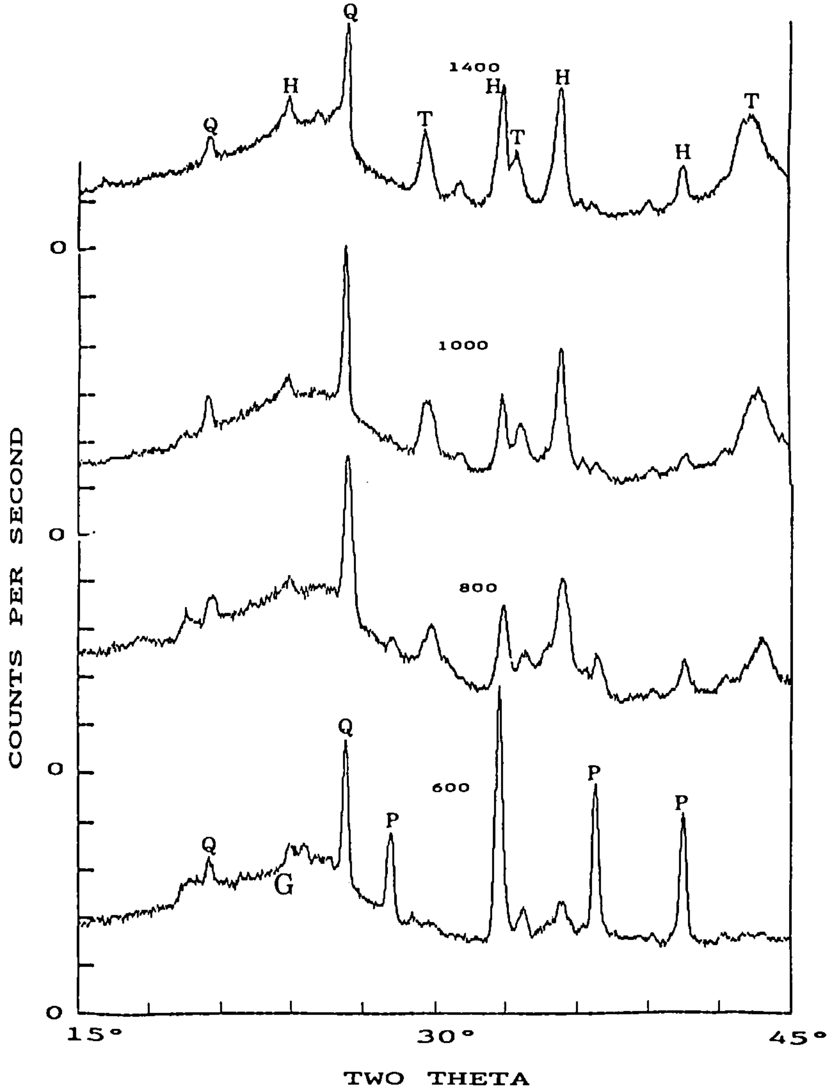

COUNTS PER SECOND
TWO THETA
15°
30°
45°
0
0
0
0
1400
1000
800
600
Q
H
Q
T
H
T
H
H
T
Q
Q
G
P
P
P

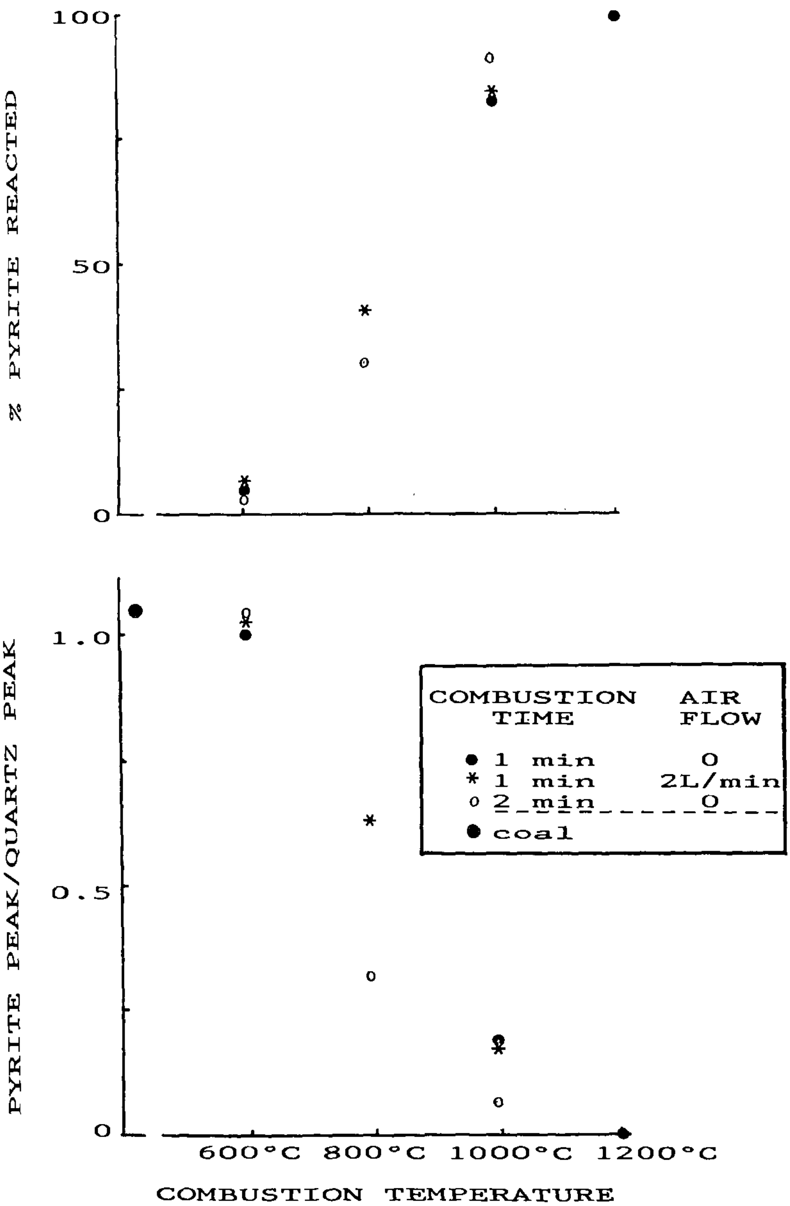
100
50
0
% PYRITE REACTED
1.0
0.5
0
PYRITE PEAK/QUARTZ PEAK
COMBUSTION TIME
AIR FLOW
1 min 0
1 min 2L/min
2 min 0
coal
600°C 800°C 1000°C 1200°C
COMBUSTION TEMPERATURE

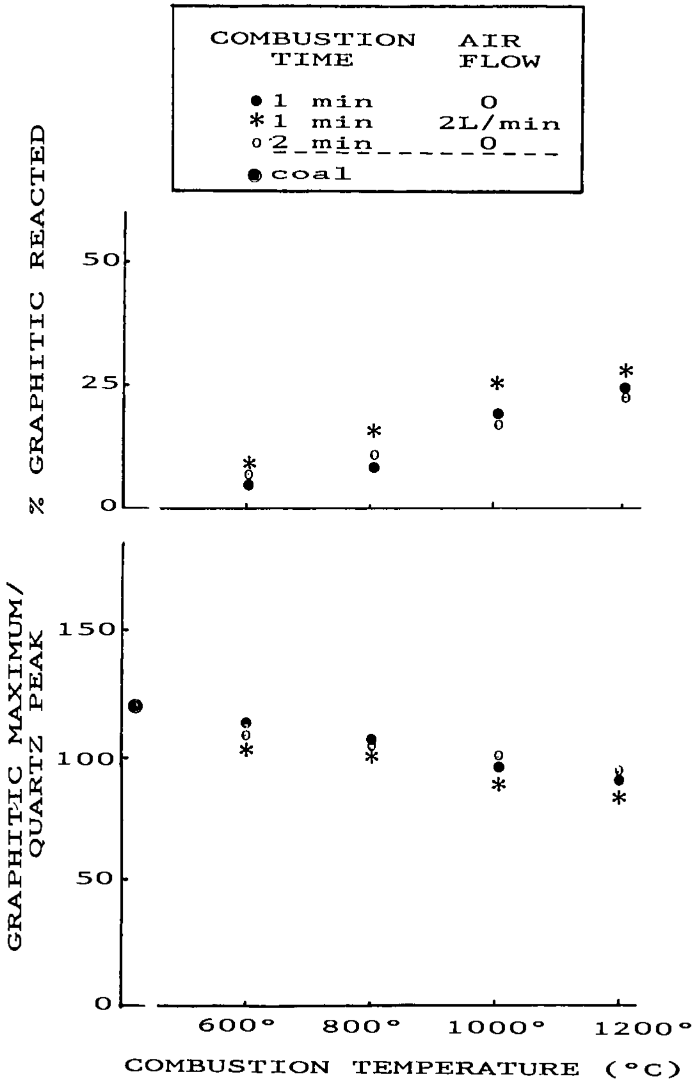
COMBUSTION TIME
AIR FLOW
1 min
0
1 min
2L/min
2 min
0
coal
% GRAPHITIC REACTED
50
25
0
GRAPHITIC MAXIMUM/ QUARTZ PEAK
150
100
50
0
600°
800°
1000°
1200°
COMBUSTION TEMPERATURE (°C)

INFLUENCE OF COAL TYPE AND PYROLYSIS TEMPERATURE ON SULFUR DISTRIBUTION IN PRODUCTS DURING DEVOLATILIZATION

M. Rashid Khan
U.S. Department of Energy
Morgantown Energy Technology Center
P.O. Box 880
Morgantown, WV 26507-0880

ABSTRACT

During coal devolatilization, the coal sulfur is distributed into solid, liquid, and gaseous products depending on the type and quantity of the coal sulfur and the processing conditions (e.g., temperature, pressure, and heating rate) used. In this study, a series of coals was devolatilized at a relatively low temperature in a fixed-bed reactor in an inert atmosphere. The distribution of sulfur in solid, liquid, and gaseous products was monitored. Influence of peak devolatilization temperature on sulfur distribution in products was determined for a high-volatile bituminous coal (Pittsburgh No. 8). The sulfur content of the pyrolysis liquids generated at 500°C correlate well with the total coal sulfur. The total sulfur of the char can be correlated with the pyritic sulfur content of the coal. Total gaseous sulfur content (sum of H_2S and COS) increases with the increase in pyritic or organic sulfur of coal but direct correlations are poor. An increase in pyrolysis temperature increases the total gaseous sulfur yield. Based on sulfur distribution data for about 25 coals, models have been developed to correlate the sulfur yield in products with the total sulfur of the feed coal.

INTRODUCTION AND OBJECTIVES

A fundamental understanding of the physical and chemical transformations of coal sulfur which occur during pyrolysis is essential for effective utilization of the large reserve of coal available in the United States (1). Work at the Morgantown Energy Technology Center (METC) demonstrated that a relatively high-quality liquid fuel (low sulfur, high H/C) can be produced by low-temperature devolatilization of coal (2,3). Coal devolatilization is a key step in various conversion processes including gasification, combustion, and liquefaction. The organic and inorganic constituents of coal (including sulfur) undergo significant changes during devolatilization. The extent of these changes depend on the peak pyrolysis temperature, heating rate, gas atmosphere, and most importantly, coal type. The objective of this study was to investigate the distribution of coal sulfur into gaseous, liquid, and solid products that occurs during devolatilization of coal of various types.

BACKGROUND

Influence of Coal Type on Sulfur Evolution

Numerous factors influence the mechanisms of sulfur release during the pyrolysis of coals of various types. Some excellent reviews on the sulfur chemistry of coal are available (4-11). However, with the exception of a few limited studies (10,12,13), relatively little has been reported on the influence of coal type on sulfur release during devolatilization, especially at relatively low temperatures (500 to 600°C). This temperature region is where significant changes in coal structure occur. Furthermore, very few correlations between the sulfur in coal and its distribution in the products and evolution rates are available in the literature.

It is generally accepted that three forms of sulfur occur in coal (8,14): (a) organic sulfur (an integral part of coal structure), (b) pyritic and/or marcasites (generally discrete particles or "lumps"), and finally, (c) sulfates (as salts of calcium or iron). Sulfates are not usually present in large quantities in raw coal. However, significant amounts can be formed if the coal has been weathered (i.e., oxidized). The type and distribution of organic sulfur vary widely in a complex manner in different coals. Roughly 40 to 70 percent of the organic sulfur of a coal is in thiophene structure (and its derivatives). The remaining 30 to 60 percent is present as thiols (R-SH), sulfides (R-S-R'), and disulfides (R-S-S-R'). Thiophenes are hetero-aromatic compounds with the sulfur as part of an aromatic ring. In an aryl sulfide, the sulfur is linked to an aromatic ring. In cyclic sulfides, the sulfur is part of a nonaromatic ring. Sulfides are usually present as aryl sulfides, cyclic sulfides, and aliphatic sulfides in a ratio of 3:2:1, respectively (5,6). For high-rank coals, disulfides are not believed to be a significant portion of the total sulfur (5). The amount of thiols is substantially higher in lignites and high-volatile coals than in low-volatile coals (5). The coalification process appears to cause the organic sulfur to change from -SH through R-S-R' to thiophene by cyclization reactions. In summary, the bonding of the organic sulfur with the coal structure varies with the coal rank. The greater rigidity of sulfur present in the higher rank coals renders the sulfur more stable during heat treatment.

The amount of volatile matter evolved during pyrolysis also influences the sulfur evolution process (12). The volatile matter yield of the lower rank coals (hvAb or lower) is significantly higher than that of the higher rank coals. The lower rank coals with higher volatile matter content will retain less sulfur in the residue (by fixation of sulfur by organic or inorganic coal constituents) than the higher rank coals. Finally, the indigenous mineral matter present in coal (particularly calcium and iron compounds) may react and fix sulfur species in the solids during devolatilization.

Transformation of Coal Sulfur During Heat Treatment

The pyrite present in a coal decomposes to ferrous sulfide and sulfur when heated in an inert atmosphere by the following reaction: $FeS_2 \longrightarrow FeS + S$ (Reaction 1, Table 1). This transformation begins at 450 to 500°C and is essentially complete at 850°C. At elevated temperatures, the pyrite may be reduced by carbon (Reaction 3 of Table 1). Examples of reactions of pyrite with hydrogen (donated by coal), CH_4, or $CaSO_4$ are shown by the Reactions (4), (5), and (6), respectively (Table 1).

Most aliphatic sulfur compounds decompose appreciably at about 500°C. Diethyl sulfides begin decomposition at ~400°C to form H_2S and mercaptans. Aliphatic and benzylic sulfides, mercaptans, and disulfides lose H_2S between 700 and 800°C. Aromatic sulfides and mercaptans are relatively stable (5) and yield H_2S and CS_2 only at a relatively high temperature (800°C). Examples of the reactions of organic sulfur are summarized in Table 1.

Yergey, et al. (15), performed nonisothermal kinetic studies on sulfur evolution in hydrogen at a relatively slow heating rate (1 to 100°C/min). They developed a kinetic scheme to describe the H_2S evolution in hydrogen. Stinnet, et al. (16), applied the principle of free energy minimization and used the NASA chemical equilibrium code (CEC) to predict the composition of the fixed-bed exit gases, including the sulfur species. In 1932, Snow (13) investigated the conversion of coal sulfur at various peak temperatures in the presence of different gases and reported that first traces of H_2S could be observed at a temperature as low as 200°C. Calkins (10) studied the conversion of coal and model organic sulfur in a rapidly heated fluid-bed reactor.

EXPERIMENTAL

A fixed-bed reactor (slow heating rate organic devolatilization reactor, SHRODR) was used to generate pyrolysis liquids at 500° C. More details on this reactor system and the experimental procedures are available (2,3). A range of feedstocks (primarily coal, but also oil shale, and tar sand) was devolatilized in this reactor. In this study only the coal data were considered. Most coal samples were supplied by

TABLE 1. A Summary of Possible Reactions Involving Sulfur Compounds During Coal Devolatilization

---

<u>Inorganic</u>

- $FeS_2 \xrightarrow[500°C]{inert} FeS + S \longrightarrow$ Nonvolatile S Compounds (1)

  $S \xrightarrow[(coal\text{-}H)]{} H_2S + (coal)$ (2)

- $FeS_2 \xrightarrow[1{,}000°C]{(coal\ C)} CS_2 + 2\ FeS + (Coal) \longrightarrow 2\ Fe + CS_2$ (3)

- $2\ FeS_2 \xrightarrow[230°C]{H_2} Fe_2S_3 + H_2S \xrightarrow[280°C]{H_2} 2\ FeS + 5\ H_2S \xrightarrow[370°C]{H_2} 2\ Fe + 2\ H_2S$ (4)

- <u>Similar Reactions</u> are possible between CO and FeS_2

- $4\ FeS_2 + CH_4 \xrightarrow[500°C]{} CS_2 + 4\ FeS + 2\ H_2S$ (5)

- $CaSO_4 + FeS_2 + H_2O \longrightarrow CaO + FeS + 2\ SO_2 + H_2$ (6)

<u>Organic</u>

-  $\xrightarrow[>450°C]{H_2}$ C=C-C=C + $H_2S \xrightarrow{H_2} C_4H_{10} + H_2S$ (7)

  (Thiophene)

- 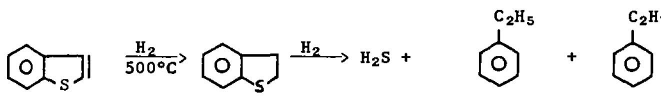 (8)

  (Thionaphthene)

- 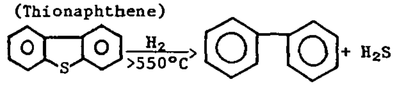 (9)

  (Dibenzothiophene)

- 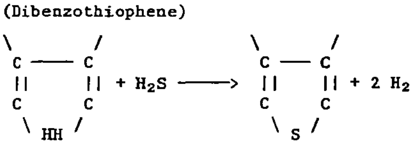 (sulfur fixation reaction) (10)

- 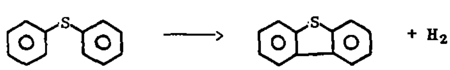 (cyclization reaction) (11)

  Diphenyl Sulfide Dibenzothiophene

---

the Penn State/DOE coal data bank (17). Sample preservation and avoidance of air oxidation of the samples were key considerations in this investigation as reported previously (18-22). Availability of fresh (well-preserved, not weathered) samples was the criterion used for sample selection. Some coal samples utilized by Given, et al. (22), for an investigation on direct liquefaction were selected in this study for comparison with our pyrolysis studies. Primarily bituminous coals were used in this study as these are known to yield the highest liquid product during pyrolysis (1,2). All samples were prepared and handled in an inert atmosphere.

About 25 coal samples, mostly in the high-volatile range, were investigated in this study. The carbon content of the samples ranged between 70 and 80 percent (daf) while the oxygen content ranged from less than 2 to over 20 percent. The sulfur content of these coals varied widely from < 0.5 to over 6 percent (of dry coal). The sulfur type in the feedstocks and the distribution of the sulfur in selected products are provided in Table 2. The Statistical Analysis System (SAS) program developed by the SAS Institute (24) was used for data analysis.

RESULTS AND DISCUSSION

Influence of Coal Type on Sulfur Distribution in Products

A summary of the distribution of coal sulfur to the gaseous, liquid, and solid products resulting during pyrolysis at 500°C is presented by the following equations:

$$\text{Total sulfur in gas} = 0.31 \times S_{coal} \quad [R^2 = 0.93,\ F = 425,\ P = 0.0001] \tag{1}$$

$$\text{Total sulfur in tar} = 0.06 \times S_{coal} \quad [R^2 = 0.85,\ F = 175,\ P = 0.0001] \tag{2}$$

$$\text{Total sulfur in solid} = 0.61 \times S_{coal} \quad [R^2 = 0.98,\ F = 1476,\ P = 0.0001] \tag{3}$$

The above correlations show that for our data set, about 61 percent of the coal sulfur appears in the char while 31 percent of the coal sulfur appears in the gaseous products (sum of H_2S and COS). Only a small portion of the coal sulfur (6 weight percent) evolve as the total sulfur of the pyrolysis liquids. This is partly because a relatively small portion of coal (5 to 25 percent) is converted to liquids during pyrolysis. The water evolved during pyrolysis contains relatively insignificant amounts of dissolved sulfur species.

The R^2, F- and P-values for the models are also summarized with the equations. R^2, the coefficient of determination, measures how much of the variation in the dependent variable can be attributed to the model (i.e., independent variable), rather than to random error. R^2 has been calculated using the regression program of SAS (R^2 for the no-intercept version was redefined by SAS, Reference 24).

The F-value is the ratio of the mean square for the model divided by the mean square error. It is a test of how well the model as a whole (after adjusting for the mean) accounts for the behavior of the dependent variable. P is the significance value or probability of obtaining at least as great an F value, given that the hypothesis is true. When $P < 0.05$, the effect is usually termed "significant." For more details on these statistical terms, see Reference 24.

The total gaseous sulfur yield (i.e., sum of H_2S and COS), the major gaseous sulfur products evolved during pyrolysis of coal, can be correlated with the feed dry coal sulfur (Figure 1A). The solid line represents the regression fit through the data. The dotted lines represent 90th percentile confidence limits for the mean predicted values.

TABLE 2. Sulfur Contents of the Coals and the Distribution of the Sulfur in Products (Tar, Char, and Gases)

		Sulfur Content, Coal				Products (Wt. %, Dry)		Products (Wt. %, Dry Coal)	
Coal	Rank	Total	Pyritic	Organic	Sulfate	Tar Total	Char Total	H_2S	COS
PSOC 123	hvAb	0.68	0.06	0.61	0.01	0.72	0.45	0.201	0.035
PSOC 181	SubA	0.58	0.04	0.54	0.00	0.54	0.45	0.067	0.025
PSOC 267	hvAb	1.96	0.02	1.89	0.05	0.78	1.00	0.487	0.096
PSOC 275	hvAb	2.14	1.41	0.73	0.00	1.17	2.46	0.503	0.098
PSOC 296	hvAb	0.98	0.91	0.07	0.00	0.73	0.91	0.436	0.034
PSOC 306	hvAb	2.05	1.21	0.83	0.01	1.54	1.72	0.559	0.083
PSOC 355	hvAb	2.77	2.12	0.63	0.02	1.02	2.27	0.605	0.177
PSOC 375	hvAb	1.11	0.38	0.68	0.05	0.90	1.20	0.415	0.060
PSOC 1109	hvCb	1.82	0.78	0.71	0.33	0.75	2.02	0.348	0.073
PSOC 1313	mvb	5.65	4.52	0.98	0.51	2.57	4.23	1.040	0.231
PSOC 1323	hvBb	4.10	1.47	2.29	0.34	2.39	3.10	1.491	0.216
PSOC 1448	hvAb	0.46	0.04	0.41	0.01	0.22	0.36	0.190	0.028
PSOC 1449	hvAb	1.64	0.53	1.09	0.02	0.55	2.08	0.560	0.103
PSOC 1469	hvAb	0.79	0.26	0.51	0.02	0.46	0.56	0.236	0.051
PSOC 1470	hvAb	2.50	1.88	0.58	0.04	--	--	--	--
PSOC 1471	hvAb	1.04	0.22	0.79	0.03	0.55	0.73	0.468	0.074
PSOC 1472	hvAb	0.85	0.28	0.55	0.02	0.38	0.62	0.406	0.031
PSOC 1473	hvAb	0.63	0.08	0.53	0.02	0.30	0.49	0.207	0.025
PSOC 1475	hvAb	0.98	0.32	0.64	0.02	0.41	0.67	0.300	0.049
PSOC 1481	hvAb	4.82	3.20	1.42	0.20	2.10	3.88	1.061	0.248
PSOC 1492	hvCb	4.35	1.82	2.50	0.03	2.24	3.20	1.325	0.222
PSOC 1499	hvAb	0.67	0.02	0.65	0.00	0.34	0.53	0.278	0.061
PSOC 1502	hvCb	0.51	0.15	0.36	0.00	0.25	0.40	0.229	0.051
PSOC 1504	hvAb	0.77	0.04	1.21	0.02	0.41	0.54	0.284	0.088
PSOC 1517	hvAb	1.92	0.70	1.21	0.01	0.41	1.89	0.779	0.131
PSOC 1520	SubC	1.21	0.05	1.15	0.01	0.50	1.08	0.401	0.043
PSOC 1523	hvAb	0.71	0.02	0.69	0.00	0.53	0.48	0.373	0.054
PSOC 1524	hvAb	1.85	1.39	0.44	0.02	0.81	1.81	0.571	0.046
PITT No. 8	hvAb	1.99	0.34	1.08	0.13	0.72	1.77	0.359	0.067
OHIO No. 6	hvCb	2.91	--**	--	--	0.88	2.46	0.462	0.229
WELLMORE No. 8	hvAb	1.23	--	--	--	0.43	0.95	0.507	0.051
AMAX*	hvAb	0.91	--	--	--	0.35	0.58	0.316	0.038

* Physically/chemically cleaned by AMAX process. Kentucky Hazard coal.
** Not available.

A single, variable model (total coal sulfur) was used to predict the sulfur yield. The predicted and experimental H_2S and COS are compared in Figures 1B and 1C. The following equations describe the yields of these gaseous species:

$$[H2_2S] = S_{coal} \times 0.259 \; [R^2 = 0.91,\ F = 319,\ P = 0.0001] \quad (4)$$

$$[COS] = S_{coal} \times 0.050 \; [R^2 = 0.94,\ F = 504,\ P = 0.0001] \quad (5)$$

In these equations $[H_2S]$ and [COS] signify weight percent of coal sulfur as H_2S and COS in the products. The combined amount represented by Equations 4 and 5 agrees with the amount represented by Equation 1. Additional two-variable models (including the total sulfur and organic sulfur) facilitated improved predictions of the experimental results. These results will be discussed in a separate communication.

The sulfur content of the pyrolysis tar (weight percent) can be predicted based on the coal sulfur (weight percent dry coal) as shown in Figure 2A. The following equation describes this prediction:

$$S_{tar} = 0.467 \times S_{coal} \; [R^2 = 0.946,\ F = 522,\ P = 0.0001], \quad (6)$$

where S_{tar} equals weight percent sulfur in tar, and S_{coal} equals weight percent sulfur in dry coal.

The finding shows that the pyrolysis liquids contain less than half as much sulfur as the parent coal (for the same amount of fuel by weight).

The correlations between the pyritic, organic, or sulphatic sulfur in the coal and the sulfur content of the tar were poor.

The char sulfur (weight percent char) can be correlated with the sulfur content of the parent coal (weight percent dry coal), as shown in Figure 3A. The total char sulfur content (weight percent of char) can be correlated somewhat with the pyritic sulfur content of the parent coal (Figure 3B). The greater the pyritic sulfur content of the coal, the larger the char sulfur. From a thermodynamic standpoint, pyrite is unstable above 450°C. Not all pyrite is decomposed at 500°C even when a long residence time (~ 40 min) is maintained at a temperature above the pyrite decomposition temperature. This finding suggests that the kinetics of pyrite decomposition and reaction strongly influences the amount of sulfur liberation. The sulfur content of the char can be predicted based on the feed coal sulfur (dry basis). The following equation represents this relationship:

$$S_{char} = S_{coal} \times 0.81 \; [R^2 = 0.975,\ F = 1192,\ P = 0.0001], \quad (7)$$

where S_{char} = sulfur content of char (weight percent), and S_{coal} = sulfur content of coal (weight percent).

Influence of Peak Pyrolysis Temperature on Sulfur Distribution in Products

To investigate the influence of the peak devolatilization temperature on sulfur evolution during coal pyrolysis, Pittsburgh No. 8 coal was pyrolyzed to various peak temperatures. Data on the influence of the peak pyrolysis temperature on product distribution and quality have been reported (2,3). This coal contained about 2 weight percent sulfur (dry basis). The correlation coefficient between the total gaseous sulfur content (summation of COS and H_2S, expressed as the weight percent of dry feed coal sulfur) with the pyrolysis temperature (between 400 and 725°C) was 0.99 (Figure 4). The general regression model [GLM] of SAS provided the following relationship on sulfur yield for the temperature range 400 to 725°C:

$$\text{Total S in gas} = (0.00103) \times (\text{Temp, in°C}) \; [R^2 = 0.99,\ F = 234,\ P = 0.0006] \quad (8)$$

An increase in temperature resulted in an increase in the sulfur content of the tar (expressed as weight percent of the feed dry coal sulfur). As one would expect, the total and pyritic sulfur content of the char decreased as the peak heat treatment temperature increased. In contrast, the char organic sulfur content increased (data not shown) with an increase in the heat treatment temperature. The influence of peak pyrolysis temperature or heating rate on the sulfur distribution in products for additional coals will be addressed in future studies.

SUMMARY AND CONCLUSIONS

The results of this study demonstrate that the total gaseous sulfur (H_2S + COS) generated during coal pyrolysis can be correlated with the total coal sulfur. Furthermore, total coal sulfur could be utilized to predict the yields of H_2S or COS species individually. Correlations between the feed coal sulfur and char or tar sulfur have been obtained. The char sulfur could be correlated somewhat with the pyritic sulfur content. However, correlations between sulfur type (organic, pyritic, or sulfatic sulfur) with sulfur content in the products were generally poor. Multivariate analysis will be performed in the future to understand the role of sulfur type (e.g., pyritic, organic, or sulfatic sulfur) on their distribution.

The essence of this investigation is the development of a number of correlations for relating the distribution of coal sulfur into solid, liquid, or gaseous products occurring during pyrolysis. It is shown that about 61 percent of coal sulfur appears in the char while about 31 percent of coal sulfur appears as gaseous products when coal is pyrolyzed at a relatively low temperature (500°C). With an increase in the peak devolatilization temperature, however, the gaseous sulfur yield increases monotonically for the Pittsburgh No. 8 coal at the expense of char sulfur.

REFERENCES

1. Khan, M. R., and T. Kurata. (1985). "The Feasibility of Mild Gasification of Coal: Research Needs." DOE/METC-85/4019, NTIS/DE85013625, 73 pp.
2. Khan, M. R. (1987). Production of High-Quality Liquid Fuels from Coal by Mild Pyrolysis of Coal-Lime Mixtures. Fuel Science and Technology International, 5(2), pp. 185-231.
3. Khan, M. R. (1987). Coal Devolatilization at Mild and Severe Conditions, Int. Conf. on Coal Science, IFA, Elsevier 1987, p. 647.
4. Attar, A., and W. H. Corcoran. (1977). "Sulfur Compounds in Coal." Ind. Eng. Chem. Prod. Res. Dev., Vol. 16, No. 2, pp. 168-170.
5. Attar, A., and F. Dupuis. (1979). Preprint Am. Chem. Society, Div. of Fuel Chem., 24(1), 166.
6. Attar, A. (1978). "Chemistry, Thermodynamics, and Kinetics of Reactions of Sulfur in Coal-Gas Reactions -- A Review," Fuel, Vol. 57, April, pp. 201-212.
7. Attar, A., W. H. Corcoran, and G. Gibson. (1976). Preprints Div. Fuel Chem., ACS, 21(7), pp. 106.
8. Given, P. H., and W. F. Wyss. (1961). "The Chemistry of Sulfur in Coal." The British Coal Utilization Research Association, Monthly Bulletin, Vol. XXV, No. 5, May, pp. 165-179.
9. Reid, E. E. (1958). Organic Chemistry of Divalent Sulfur, 2, Chemical Publg. Co.: New York.
10. Calkins, W. M. (1987). "Investigation of Organic Sulfur-Containing Structures in Coal by Flash Pyrolysis Experiments," Energy and Fuels, 1, pp. 59-64.
11. Desikan, P., and C. H. Amberg. (1963). "Catalytic Hydrodesulfurization of Thiophene," Canadian Journal of Chemistry, Vol. 41, pp. 1966-1970.
12. Cernic-Simic, S. (1962). "A Study of Factors that Influence the Behavior of Coal Sulfur During Carbonization," Fuel, Vol. 41, No. 2, March, pp. 141-151.

13. Snow, R. D. (1932). "Conversion of Coal Sulfur to Volatile Sulfur Compounds During Carbonization in Streams of Gases," Ind. Eng. Chem., Vol. 24, No. 8, August, pp. 903-909.
14. Speight, J. (1983). The Chemistry and Technology of Coal, Marcel Dekker, Inc.
15. Yergey, A. L., F. W. Lampe, M. L. Vestal, A. G. Day, G. J. Fergusson, W. H. Johnston, J. S. Snyderman, R. H. Essenhigh, and J. H. Hudson. (1974). "Nonisothermal Kinetics Studies of the Hydrodesulfurization of Coal," Ind. Eng. Chem., Pro. Des. Develop, Vol. 13, No. 3, pp. 233-240.
16. Stinnett, S. J., D. P. Harrison, and R. W. Pike. (1974). "Prediction of Sulfur Species Distribution by Free Energy Minimization," Environmental Science and Technology, Vol. 8, No. 5, May, pp. 441-444.
17. Penn State/DOE Coal Data Bank. Office of Coal Research, Penn State University, University Park, Pennsylvania, 16802.
18. Khan, M. R. (1987). Energy and Fuels, 1(4), pp. 366-376.
19. Khan, M. R. (1987). 193rd ACS Petroleum Division Chemistry Preprint 1987, Denver, Colorado, April.
20. Khan, M. R. (1986). Proceedings, *19th Oil Shale Symposium*, Colorado School of Mines, Golden, Colorado, pp. 139-148.
21. Khan, M. R., and R. G. Jenkins. (1985). Fuel, 64(2), pp. 189-192.
22. Khan, M. R., and R. G. Jenkins. (1985). Fuel, 64(11), pp. 1618-1622.
23. Given, P. H., et al. (1982). Fuel, 61(10), p. 971.
24. User's Guide, Fifth Edition, SAS Institute. Raleigh, North Carolina.

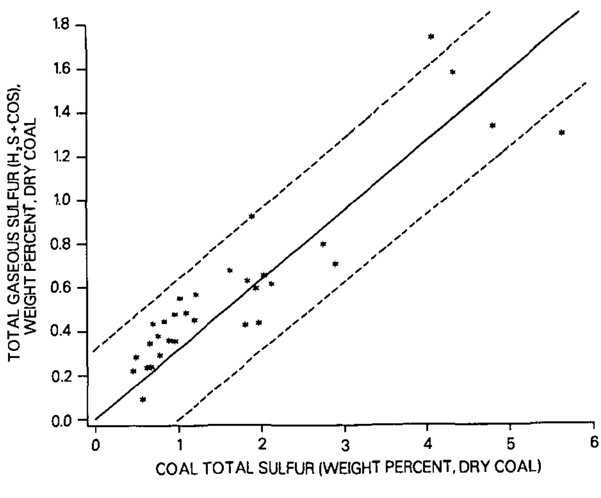

Figure 1A. The relationship between the total gaseous sulfur with the feedstock sulfur content (weight percent, dry coal). The solid line represents the regression through data. The dashed lines represent 90th percentile confidence limits for the mean predicted values.

2B:1-20-88:rd:5a

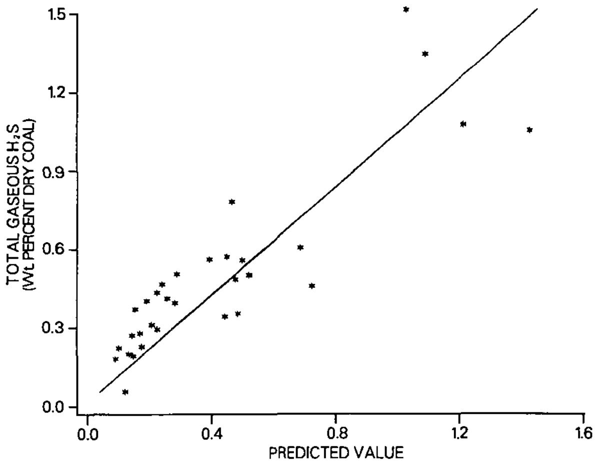

Figure 1B. A comparison between the predicted and actual H_2S yield. The prediction was based solely on the sulfur content of the coal (weight percent, dry coal).

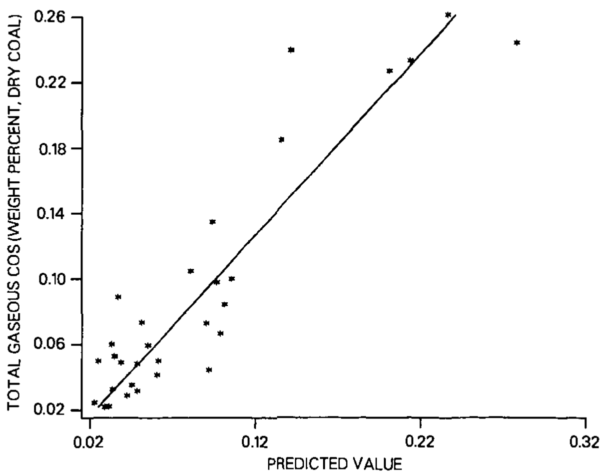

Figure 1C. A comparison between the predicted and actual COS yield. The predictions was based on feed sulfur content (weight percent, dry coal).

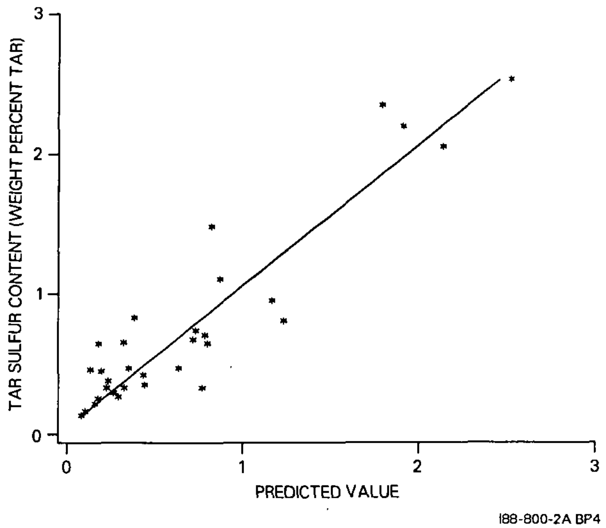

Figure 2. A comparison between the predicted and measured sulfur content of the pyrolysis tar (weight percent of tar). The prediction was based on coal sulfur (weight percent dry coal).

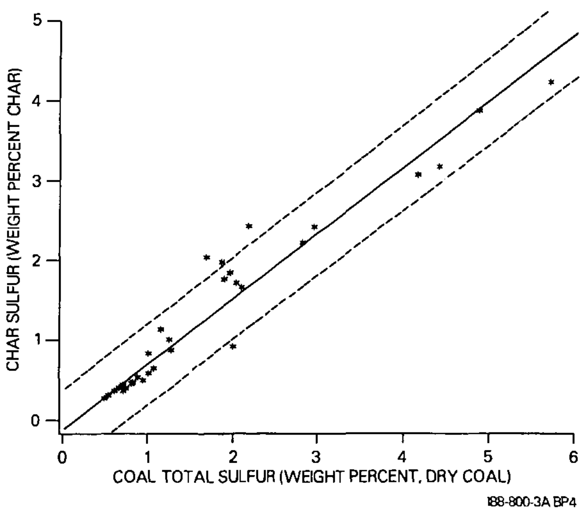

Figure 3A. The comparison between the char sulfur content (weight percent char) with the feed coal sulfur content (weight percent, dry coal). The solid line represents the regression through the data. The dashed lines represent 90th percentile confidence limits for the mean predicted values.

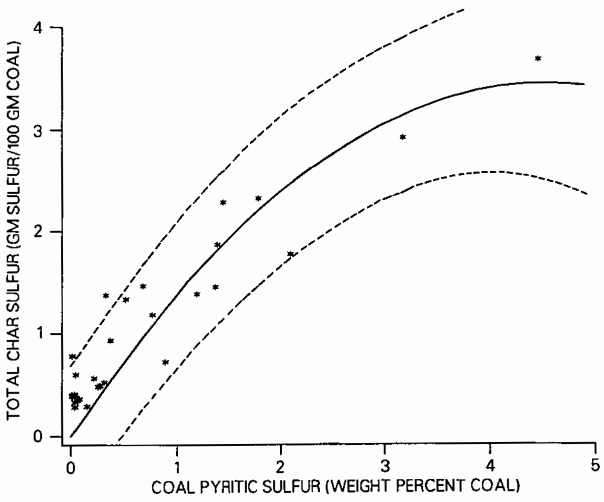

Figure 3B. A relationship between the char sulfur content (weight percent char) with the pyritic sulfur content (weight percent, dry coal). The solid represents the regression through the data. The dashed lines represent 90th percentile confidence limits for the mean predicted values.

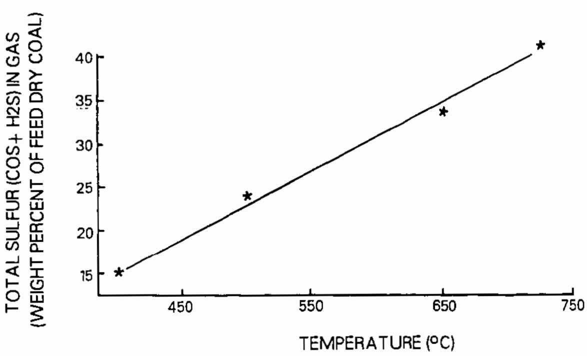

Figure 4. Influence of peak pyrolysis temperature on total gaseous sulfur yield (H_2S + COS) as a function of temperature.

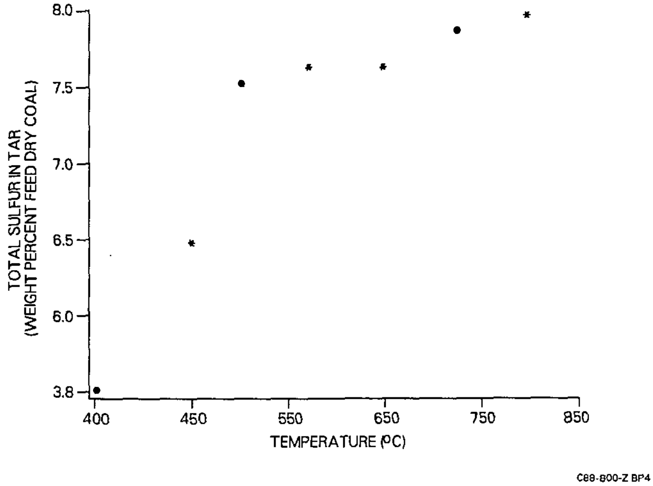

Figure 5. Influence of peak pyrolysis temperature on tar sulfur content (weight percent of tar).

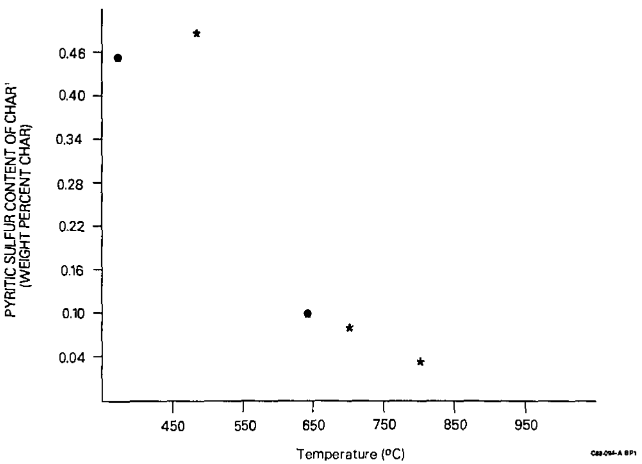

Figure 6. Pyritic sulfur content in char prepared at various peak temperatures.

2B:1-20-88:rd:5a

Distribution of Sulfur During Coal Pyrolysis in a High Pressure Entrained-Flow Reactor

Mohammad Fatemi-Badi, Alan W. Scaroni and Robert G. Jenkins

The Pennsylvania State University
Combustion Laboratory
405 Academic Activities Building
University Park, PA 16802

Introduction

An understanding of the fundamental and interrelated processes involved in coal pyrolysis/gasification is essential in order to advance gasification technologies. Therefore, it is necessary to generate data on the effect of coal properties and operating conditions on coal devolatilization behavior under conditions similar to those in advanced-concept gasifiers; typically, a high-temperature and high pressure environment for entrained coal particles.

The thermal decomposition of raw coal produces solid char/coke plus some liquid (tar) and gaseous products.(1) Tars are vapors at the pyrolysis temperature, but are usually heavy liquids or solids at room temperature. The chars, which usually account for between 30-70% of the original coal, consist mainly of carbon, along with small amounts of H, O, N and S as well as the ash which results from the mineral matter. The quantity and quality of the char, tar and gases produced during pyrolysis depend on the chemical and physical properties of the coal (i.e. coal type, particle size, etc.) as well as on the pyrolysis conditions (i.e. temperature, pressure, etc.).(1)

Due to the environmental impact of the emission of SO_2 during combustion, pre-combustion processing may be necessary to reduce the sulfur content of so-called "high sulfur coals". Desulfurization of coal prior to combustion can be achieved by one or more of the following methods.(2-4) 1) Advanced physical cleaning -- this method involves a variety of approaches (i.e. froth flotation, float-sink, etc.) for reduction of pyrite in the coal based on the differences between the density of pyrite (5.0g/cm^3) or marcasite (4.87 g/cm^3)(5) and the organic matrix (1.2-1.5 g/cm^3).(6) 2) Chemical coal cleaning -- based on the concept of breaking the chemical bonds of the organic sulfur by exposing the coal usually to molten chemicals such as sodium hydroxide. 3) Conversion of the coal to low-sulfur liquid and gaseous fuels -- based on liquefaction and gasification technologies.

According to the literature, there are three commonly recognizable forms of sulfur in coal: sulfate, pyrite and organic sulfur. Although the distribution of various forms of sulfur is less often determined than the total sulfur, their presence can have a significant effect on coal utilization. However, the degree to which the sulfur can be reduced and/or removed from the coal by the above techniques is strongly dependent on the forms of sulfur present in the coal. Therefore, accurate analytical data on the forms of sulfur is a requirement for improving removal processes.

Pyrolysis has been used by some researchers to study the behavior and distribution of sulfur in coal.(7-12) Some investigators have also used pyrolysis in order to study the chemistry and kinetics of reactions involving sulfur-containing compounds in coal.(13-15) The purpose of the current work was to determine the distribution of the total sulfur between the products of pyrolysis (tars and chars) and the various forms of sulfur in the chars from pyrolysis of a subbituminous coal in a high pressure entrained-flow reactor.

Experimental

A schematic diagram of the entrained-flow reactor used in this study is shown in Figure 1. This reactor is capable of subjecting pulverized coal particles to temperatures and pressures as severe as 1373 K and 1000 psig, respectively. It is also equipped with a computerized data aquisition system for rapid data collection and monitoring of the experimental conditions. The operating principle and procedure have been described elsewhere.[16,17]

Pyrolysis experiments were performed on pulverized and sized samples, ~57 μm mean diameter, of Montana Rosebud Subbituminous coal at 1189 K, 100-900 psig applied N_2 pressure and 0.1-1.7s residence time. The collectable products of pyrolysis, both solid and the material trapped on the filter, were extracted in conventional Soxhlet apparatus using tetrahydrofuran (THF) as the solvent. The extracted material represented the tars from pyrolysis while the THF insoluble material represented the char. The gaseous products from pyrolysis were analyzed qualitatively and quantitatively at steady-state operation by an on-line Carle gas chromatograph capable of monitoring the following gases: H_2, N_2, O_2,H_2S, CO, CO_2, CH_2, C_2H_4, C_2H_6, H_2O, SO_2, and C_3+C_4 hydrocarbons. An infrared gas analyzer was used to continuously monitor the CO concentration in the outlet gas stream. This was needed to determine when steady state operation had been reached.

Proximate analyses were performed on the raw coal and the chars using a Leco MAC-400 analyzer. Ultimate analyses were also performed on raw coal, chars and tars using a Leco CHN-600 analyzer. Total sulfur contents of the raw coal, tars and chars were determined by a Leco SC-132 sulfur analyzer. Sulfate and pyritic sulfur in the raw coal and the chars were determined according to the American Society for Testing and Materials (ASTM) standard procedure D-2492.[18] Organic sulfur for the raw coal and chars was calculated by subtracting the percentage sums of sulfate and pyritic sulfur from the total sulfur. Higher heating values were measured for both the raw coal and the chars using a Parr model 1241 adiabatic bomb calorimeter. Full analyses of the Montana Rosebud coal are shown in Table 1.

Coal particle residence times in the furnace were determined using a computer flow model. The governing equations have been discussed elsewhere.[16,17] Weight loss due to the coal devolatilization was calculated by using ash as a tracer. Tar yields (~5-15%) were measured from the total amount of THF solubles collected and expressed as weight percent of coal (daf) fed into the reactor. Total gas yields were calculated from the difference between the weight loss and tar yield.

Results and Discussion

Pyrolysis results on weight loss, tar and gas yields and gaseous compositions have been reported and discussed in detail elsewhere.[16,19,20] Total and forms of sulfur (daf) for the raw coal and selected chars from pyrolysis of Montana Rosebud coal at 1189 K, 100-900 psig applied N_2 pressure and 0.3-1.7s residence time are shown in Table 2. Total sulfur analyses of the corresponding tars are also shown in Table 2.

A comparison of the total sulfur (daf) contents of the chars and tars (Table 2) clearly indicates that the sulfur in the chars is always higher than the sulfur in the tars produced from the pyrolysis experiments. In most cases the sulfur content of the tars was about 50% lower than the sulfur content of the corresponding char and the raw coal. It was observed that as the residence time of pyrolysis increased, the sulfur content of the tar increased, as shown in Figure 2.

The reason for the increase in the sulfur content of the tar with increasing pyrolysis residence time might be the higher rate of decomposition of pyrite in the coal and the secondary reactions between the decomposition product and the tar molecules in the gas phase. This is supported by the data in Figure 3. As can be seen, the pyritic sulfur content of the chars decreases as the pyrolysis residence time increases.

It has been shown by Given et al.[21] and others that pyrites decompose between 724-773 K. The produced ferrous sulfide and free sulfur (S^{2-}) then react with the organic matrix of the tars and chars by crosslinking according to the following reactions.[14,22]

$$FeS_2 \xrightarrow{723 - 773\ K} FeS + S^{2-} \quad (1)$$

$$S^{2-} + C{=}C \longrightarrow -\overset{\displaystyle S}{\overset{|}{C}} - C - \quad (2)$$

The effect of pressure on the pyritic sulfur content of the chars produced from pyrolysis of Montana Rosebud subbituminous coal is shown in Figure 4. As the pressure increases, the pyritic sulfur content of the chars increases. This indicates that increasing the pyrolysis pressure reduces the rate of the pyrite decomposition reactions.

Reductions in the total sulfur content of the coal were calculated according to the following equation:(10,12)

$$\%S_t = \left\{ (S_t)_{Raw\ Coal} - [(S_t)_{Char} \times (char\ yield)]/(S_t)_{Raw\ Coal} \right\} \times 100$$

The effect of residence time on the percent reduction in total sulfur is shown in Figure 5. As the pyrolysis residence time increases, the percent reduction in sulfur content of the coal increases, meaning a higher reduction in total sulfur can be achieved by increasing the pyrolysis residence time. This is supported by the data in Figure 2. The decrease in pyritic sulfur with increasing residence time is most likely the reason behind the increase in the percent reduction in the total sulfur content with increasing pyrolysis residence time.

The effect of pressure on the percent reduction in the total sulfur content of the coal is shown in Figure 6. It was observed that as the pyrolysis pressure increased, the percent reduction in the total sulfur content decreased. In other words, increasing the pyrolysis pressure reduces the percent total sulfur reduction. This behavior is probably due to the fact that increasing the pyrolysis pressure reduces the decomposition of pyrite, Figure 4, which in turn affects the overall percent reduction in the sulfur content of the chars.

It has been reported that H_2S is the dominant sulfur-containing species produced by high-temperature (>1073 K) pyrolysis.(14,15,22) H_2S is the result of desulfurization reactions between the H_2, generated by the decomposition of the coal matrix during pyrolysis, and pyrites according to the following equations:

$$FeS_2 + H_2 \longrightarrow FeS + H_2S \quad (3)$$

$$FeS + H_2 \longrightarrow Fe + H_2S \quad (4)$$

However, some of the produced H_2S reacts with the tars and chars as soon as they are formed and becomes organically bonded to the products. This is due to the availability of active carbon sites in the chars produced during devolatilization of the coal matrix, and in the reactive organic species formed during secondary cracking reactions of the tars. This is supported by the fact that the secondary cracking reactions of the tars increase as the pyrolysis residence time increases, and the data in Figure 2, which indicate that as the pyrolysis residence time increases the total sulfur in the tars increases.

Conclusions

Based on the information available in the literature and the data presented here on the pyrolysis of Montana Rosebud subbituminous coal the following can be concluded:

1) Total sulfur in the tars produced during pyrolysis is residence time dependent.

2) Forms of sulfur in the chars produced from pyrolysis revealed that pyritic sulfur is most affected by the pyrolysis conditions (residence time and pressure).

3) A higher percent reduction in total sulfur can be acheved by increasing the pyrolysis residence time.

4) Increasing the pyrolysis pressure reduces the percent total sulfur reduction.

5) The dominant species from the decomposition of pyrite in the coal at high-temperatures is H_2S. However, some of the evolved H_2S reacts with the chars and tars, especially at higher residence times.

References

(1) Normand, M.L., "Heterogeneous Kinetics of Coal Char Gasification and Combustion," Prog. Energy Comb. Sci., Vol. 4, 1978, pp. 221-270. (Pergamon Press Ltd., Great Britain).

(2) United States Department of Energy, "America's Clean Coal Commitment," Report, Office of Fossil Energy, DOE/FE-0083, 1987.

(3) Bullard, C.W., "Processing and Utilization of High Sulfur Coal," Coal Science and Technology, Elsevier Science Publisher, Amsterdam, 1985, pp. 117-137.

(4) Friedman, S. and Werzinski, R.P., J. Eng. for Power, 1977, p. 361.

(5) Weast, R.C. (Ed.), CRC Handbook of Chemistry and Physics, 63rd ed., 1982-83.

(6) Van Krevelen, D.W. and Schuyer, J., Coal Science, Elsevier, Amsterdam, 1957.

(7) Sunha, R.K. and Walker, P.L., Jr., Fuel, Vol. 51, 1972, p. 329.

(8) Hamrin, C.E., Jr., and Maa, P.S., Fuel, Vol. 54, 1975, p. 288.

(9) Campbell, J.H., Fuel, Vol. 57, 1978, pp. 217-221.

(10) Guruz, G.A., Fuel Processing Technology, Vol. 5, 1982, pp. 183-201.

(11) Cleyle, P.J., Caley, W.F., Stewart, I. and Stirling, G., Fuel, Vol. 63, 1984, pp. 1579-1582.

(12) Ibarra, J.V., Miranda, J.L. and Perez, A.J., Fuel Processing Technology, Vol. 15, 1987, pp. 31-43.

(13) Mudar, R.E., in "Chemistry of Coal Utilization," Suppl. Vol. (Ed. H.H. Lawry), Wiley, New York, 1963, p. 634.

(14) Attar, A., Corcoran, W.H. and Gibson, G., Preprints, Div. Fuel Chem., Am. Chem. Soc., Vol. 21, No. 7, 1976, p. 106.

(15) Attar, A., Fuel, Vol. 57, 1978, pp. 201-212.

(16) Fatemi, M., Scaroni, A.W., Lee, C.W. and Jenkins, R.G., Preprints, Div. Fuel Chem. Am. Chem. Soc., Vol. 32, No. 3, 1987, pp.117-124.

(17) Jenkins, R.G. and Scaroni, A.W., Proceedings of the Sixth Annual Gasification Contractors Meeting, DOE/METC-86/6043, 1986, pp. 171-181.

(18) Annual Book of ASTM Standards, Vol. 5.05, American Society for Testing and Materials, Philadelphia, PA,1986.

(19) Jenkins, R.G. and Scaroni, A.W., Proceedings of the Seventh Annual Gasification and Gas Stream Cleanup Systems Contractors Review Meeting, DOE/METC-87/6079, Vol. 2, 1987, pp. 542-547.

(20) Fatemi, M., Scaroni, A.W., Lee, C.W. and Jenkins, R.G., Proceedings, Fourth Annual Pittsburgh Coal Conference, 1987, pp. 767-778.

(21) Given, P.H. and Jones, J.R., Fuel, Vol. 45, 1966, p. 151.

(22) Maa, P.S., Lewis, C.R., Hamrin, C.E., Jr., Fuel, Vol. 54, 1975, p. 62.

Table 1.

Characteristics of Montana Rosebud Subbituminous Coal

Proximate Analysis	(wt%, dry)
Moisture	--
Ash	10.31
Volatile Matter	36.50
Fixed Carbon	53.19
Ultimate Analysis	
Ash	--
Carbon	83.89
Hydrogen	3.72
Nitrogen	1.38
Total Sulfur	1.12
Oxygen (by diff.)	9.89
Forms of sulfur	
Pyritic	0.217
Sulfatic	0.092
Organic	0.814
Total	1.123
Heating Value (Btu/lb, daf)	**13929**

Table 2.

Sulfur Analyses of the Tars and Chars From Pyrolysis of Montana Rosebud Subbituminous Coal at 1189 K, 100-900 psig N_2 Pressure and 0.3-1.7s Residence Times.

	Total Sulfur (wt%, daf)		Forms of Sulfur (wt%, daf)		
Sample(a)	Tar	Char	Pyritic	Sulfatic	Organic(b)
Raw Coal	--	--	0.217	0.092	0.814
100-0.3	0.54	0.92	0.209	0.101	0.608
100-1.0	0.82	1.16	0.098	0.079	0.983
100-1.7	0.97	0.88	0.044	0.073	0.766
178-0.3	0.75	1.17	0.220	0.132	0.822
178-1.0	0.70	0.89	0.121	0.154	0.608
178-1.7	0.97	0.99	0.008	0.076	0.902
309-0.3	0.51	1.01	0.144	0.119	0.748
309-1.0	0.90	0.96	0.125	0.120	0.709
309-1.7	1.02	1.18	0.021	0.166	0.989
530-0.3	0.40	0.84	0.272	0.151	0.520
530-1.0	0.68	1.17	0.190	0.142	0.833
900-1.0	0.62	1.42	0.304	0.162	0.954

(a)Pressure-Residence Time
(b)By Difference

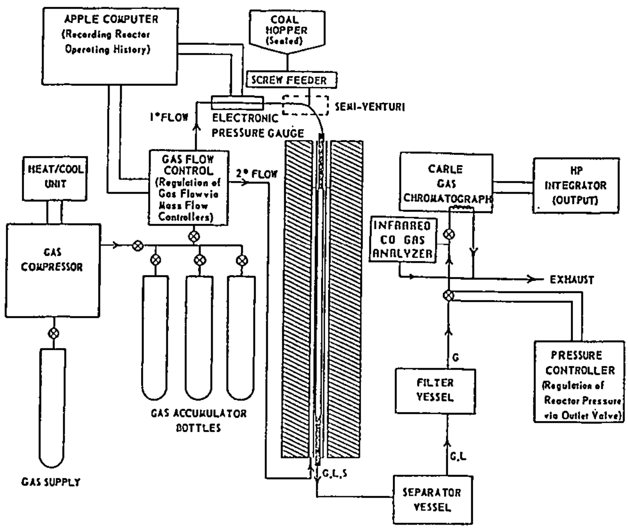

Figure 1. Configuration of High Pressure Entrained-Flow Reactor

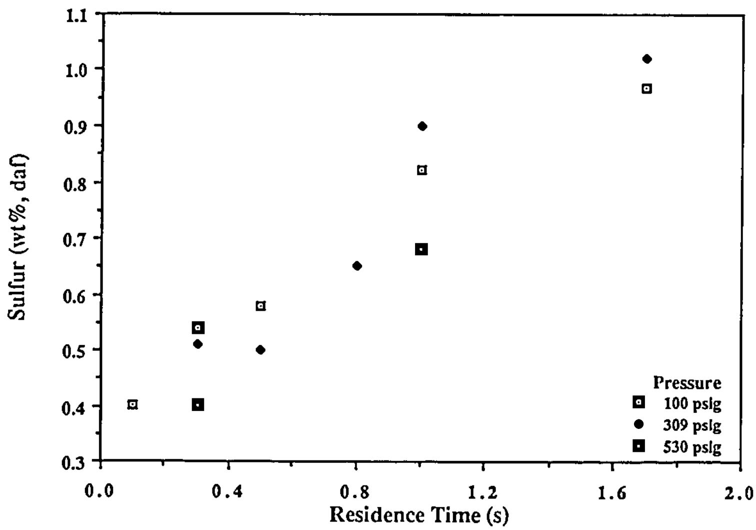

Figure 2. Effect of Residence Time on Total Sulfur (daf) of Tars from Pyrolysis of Montana Rosebud Coal at 1189 K

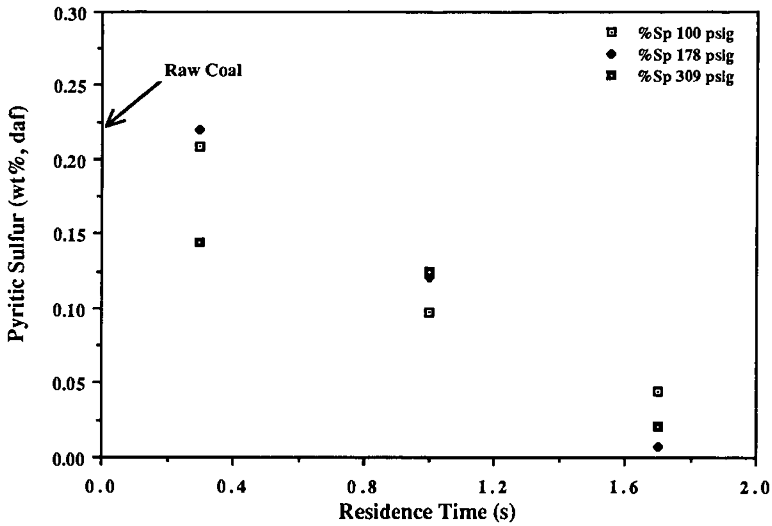

Figure 3. Effect of Residence Time on Pyritic Sulfure of the Chars from Pyrolysis of Montana Rosebud Coal at 1189 K

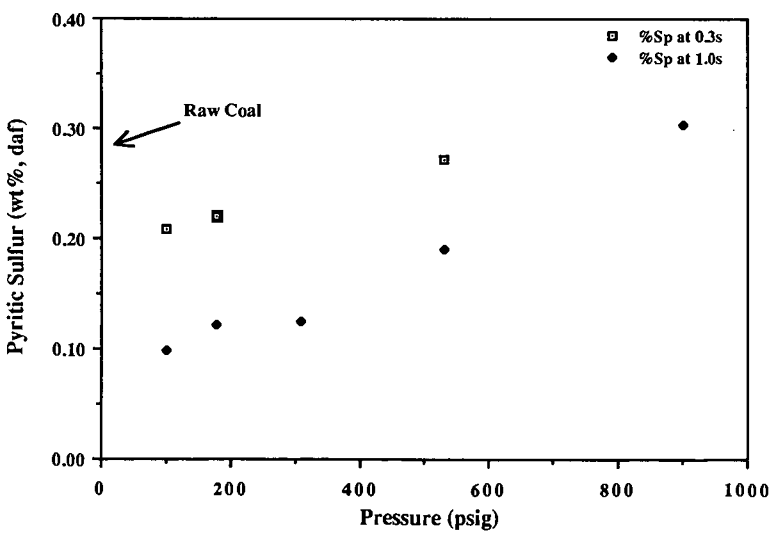

Figure 4. Effect of Pressure on Pyritic Sulfur of the Chars from Pyrolysis of Montana Rosebud Coal at 1189 K

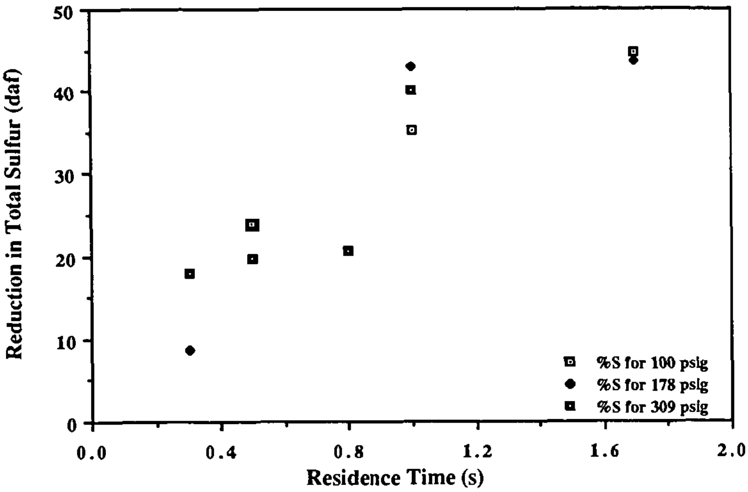

Figure 5. Effect of Residence Time on Percent Reduction in the Total Sulfur of Montana Rosebud Coal Pyrolyzed at 1189 K

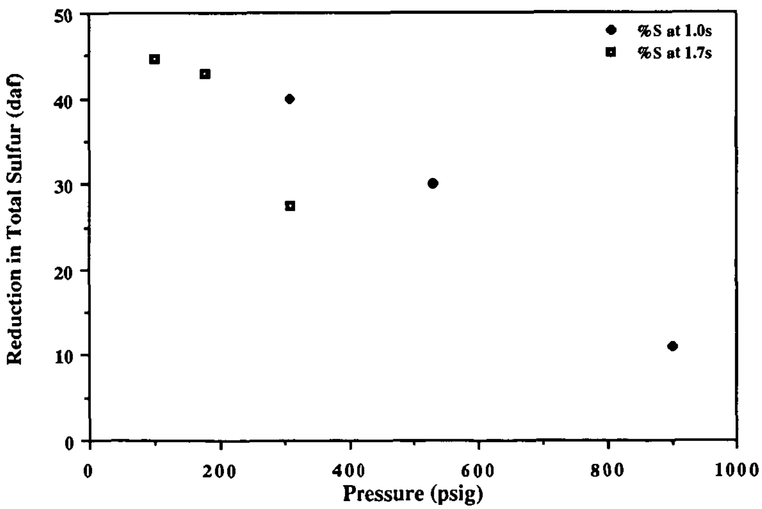

Figure 6. Effect of Pressure on Percent Reduction in the Total Sulfur of Montana Rosebud Coal Pyrolyzed at 1189 K

EVOLUTION OF SULFUR GASES DURING COAL PYROLYSIS

M. S. Oh, A. K. Burnham, and R. W. Crawford

Lawrence Livermore National Laboratory, Livermore, CA, 94550

1. Introduction

The yields and rates of evolution of sulfur gases depend not only on pyrolysis conditions but also on the coal itself (1). The organic/inorganic forms of sulfur, as well as the secondary reactions of sulfur gases with solids and with other pyrolysis-generated gases, play an important role. Monitoring the time- and temperature-dependent evolution of sulfur-containing gases provides insight into the sulfur chemistry affecting evolution profiles (1,2). Programmed-temperature studies of sulfur gas evolution often have been limited to H_2S. In some cases, all sulfur gases have been studied collectively by reducing or oxidizing them to H_2S or SO_2 (3,4). Recently, Calkins (5) studied the evolution of individual sulfur species from a Pyroprobe using Gas Chromatograph/Mass Spectrometer (GC/MS) and from isothermal flash pyrolysis. Boudou et al. (6) also identified some individual sulfur gases from isothermal pyrolysis using a Curie-point reactor in combination with MS, GC, and GC/MS.

In this study, we monitored the real-time evolution of sulfur gases during slow-heating pyrolysis via a triple quadrupole mass spectrometer (TQMS). We also monitored the evolution of hydrocarbon gases, water, and carbon oxides. We compared the evolution profiles of sulfur gases and related them to the rank of the coal, the organic and inorganic sources of sulfur in each coal sample, and the evolution of other pyrolysis-generated gases. We also studied the extent of secondary reactions by varying the pyrolysis conditions.

2. Experimental

A schematic of the experimental set-up is shown in Fig. 1. Coal was pyrolyzed in a 1.5-cm-i.d. quartz tube, placed in a 1.9-cm-i.d. three-zone furnace. The control thermocouples for the top and bottom zones were embedded in the furnace wall, while the thermocouple for the mid-zone was placed between the furnace wall and the reactor. Another thermocouple was inserted into the center of the coal-sand bed, and the average bed temperature was calculated from the wall and the center temperatures. Coal particles were diluted with quartz sand to prevent the bed from being plugged because of softening and agglomeration of coal. Coal was then heated from 25°C to 900°C at a heating rate of 4.5°C/min.

To examine the effect of secondary reactions on the observed products, we varied the amount of coal from 0.5 to 2.5 g and the argon flow rate from 34 to 169 cc/min. Compared to our reference conditions of 0.5 g and 34 cc/min, the experiment with sample size of 2.5 g and 34 cc/min argon flow represents a five-fold increase in pyrolysis gas partial pressure at nearly constant gaseous residence time. For the experiment in which both the sample size and argon flow were increased, gaseous partial pressures remained constant, but the gaseous residence time decreased.

To monitor the evolution of water and naphtha, including thiophenes, we heated all the parts, from the pyrolyzer to the TQMS. A constant flow of argon swept volatiles to a glass wool trap that was placed in an oven at ~130°C to condense high boiling liquid products (tar). All transport lines from the trap to the TQMS were maintained at T > 140°C.

In the TQMS operation, both normal mass scans (ms mode) and daughter ion scans (ms/ms mode) were used in all experiments. Details of the TQMS and the ms and ms/ms mode operation were described elsewhere (7). Table 1 summarizes the parent/daughter pairs for sulfur gases we monitored. All gases in Table 1, except H_2S and SO_2, are calibrated using analyzed commercial standards with the concentration levels about 200 ppm. We used a 981-ppm standard for H_2S, and SO_2 was not calibrated.

We chose eight Argonne premium coal samples for our work because of their diverse properties, high quality, and wide-spread use by other researchers. Among the eight coals, we studied in detail two coals with the highest and the lowest sulfur contents. Illinois No. 6 high volatile bituminous coal (ILHVB) had the highest sulfur content (5.4%), while Blind Canyon Seam high volatile bituminous coal (BCHVB) had the lowest (0.5%). The properties of these two coals, provided by Argonne National Laboratory or obtained from literature (8), are shown in Table 2. Samples were stored under nitrogen and we saw no aging effects. Sulfur gases from other coals are discussed qualitatively based on the data obtained from pyrolysis in a stainless steel reactor. In those experiments with the stainless-steel reactor, the main goal was to study hydrocarbon gases under well-defined temperatures.

3. Results

The TQMS has the sensitivity, selectivity, and speed to monitor the real-time evolution of individual species in a complex pyrolysis gas mixture. We monitored H_2S and CH_3SH in both ms and ms/ms modes, while other sulfur gases were monitored only in ms/ms mode which was necessary to differentiate them from hydrocarbon gases of the same molecular mass. For H_2S and CH_3SH, $m/z = 34$ and 48 in ms mode are free of hydrocarbon interferences because $m/z = 34$ and 48 are rare fragments of hydrocarbons. However, $m/z = 48$ has to be corrected for SO_2 fragments when SO_2 is abundant.

For all eight coals, there are three temperature regions at which sulfur gases evolve under the given time-temperature history. Although the exact temperature of the maximum rate of evolution (T_{max}) varies with the coal, the three regions are roughly < 200°C, 400°C-500°C, and 500°C-600°C.

At temperatures lower than 200°C, the only sulfur gas observed was SO_2. Low temperature evolution implies the existence of loosely bound, trapped, or adsorbed SO_2. However, SO_2 evolution seems to be very sensitive to pyrolysis conditions. More low-temperature SO_2 was detected as the ratio of coal to sweep-gas flow rate was increased. Experiments with a 316-stainless-steel reactor showed no SO_2 at this temperature region, suggesting a reaction of SO_2 with the stainless steel.

Figure 2 shows evolution profiles of eight other sulfur gases between 200 and 800°C from two coals, ILHVB (solid lines) and BCHVB (dotted lines). Because of the low sulfur content of BCHVB, only four major sulfur gases were detected. Most of the organic pyrolysis reactions occur between 350 and 500°C. While all gases have a peak in this temperature region, H_2S, COS, and CS_2 have a second peak between 550 and 600°C. While the high temperature source is clearly pyrite decomposition, the lower temperature source is more complicated.

Figure 3 compares the evolution profile of four organic sulfur compounds with the corresponding hydrocarbons. The sulfur compound precedes its corresponding hydrocarbon in all cases. While T_{max} for CH_4 is substantially higher than those for other hydrocarbons, methanethiol is evolved at approximately the same temperature as the other thiols.

The evolution profiles in Fig. 2 are similar to those reported previously for Green River shale. Burnham et al. (2) noted that most of the H_2S evolved in the 550°C region could be shifted to the 400-450°C range if pyrolysis occurs under self-purging conditions (no auxiliary gas sweep). To explore this effect and other secondary reactions, we conducted two additional experiments on ILHVB coal. Table 3 compares the amounts of sulfur gases evolved under our standard conditions to those evolved from experiments representing higher product partial pressure (P_{vol}) at similar residence time and shorter gaseous residence time (t_{res}). The amounts of H_2S formed in the two temperature regions show no clear changes with these variations in conditions. The only observable effects are increased COS generation in the 550°C range at shorter t_{res} and changes in the amounts of CS_2.

In Fig. 4, we report T_{max} for H_2S and hydrocarbons from the experiments with a stainless-steel reactor. Even though some aspects of the sulfur-gas profiles were affected by reactions with the steel, Fig. 4 shows that T_{max} for H_2S depends on coal rank. The increase in T_{max} of the low temperature peak with the rank is greater than a similar increase in T_{max} for total organic volatiles (total ion current minus Ar, CO_2, CO, H_2O, and H_2S). T_{max} for the high temperature H_2S peak shows more scatter, so the trend is not as clearly present as the low temperature H_2S peak. However, Whelen et al. (9) also observed an increase in T_{max} of both COS peaks with maturity in Type III kerogens, which suggests that our high temperature trend is real.

4. Discussion

An obvious goal is to be able to relate the amounts and kinds of various sulfur components to the sulfur composition of the original coal and the processing conditions. The results in this paper provide only a small fraction of the information needed to achieve that goal. However, we have made significant progress.

The sulfur evolution profiles at temperatures between 400 and 500°C are a poorly defined combination of organic pyrolysis reactions and pyrite reactions. The source of sulfur can be both sulfur in the organic matrix as well as pyritic sulfur. Coal-matrix sulfur, especially in high volatile bituminous coals, exists as sulfides and thiophenes (4,5). Thus, sulfides and thiophenes are probably primary products of pyrolysis or products of tar cracking. Thiophenes are very stable at $T < 500°C$, so they are not likely to go through gas phase secondary reactions. Hydrocarbon gases such as acetylene are also known to react with pyrite to form thiophenes (1). However, we found that, for Green River shale, removal of pyrite by acid treatment (7) and doping low-sulfur shales with pyrite (10) had negligible effects on the amount of thiophenes generated.

In contrast, H_2S and thiols can be generated by pyrite reactions. Pyrite decomposition is a strong function of grain size, gas environments, and pyrolysis conditions (2,11). Although the H_2S evolved below 500°C from well-swept fine particles can be attributed to organic sulfur (7), it can be shown from other data (2,7,12) that about two-thirds of the H_2S evolved below 500°C from Green River shale under self-purging conditions comes from pyrite. Unfortunately, we did not see any clear effect of pyrolysis conditions on H_2S formation reactions in ILHVB, as shown in Table 3. Apparently our range of conditions was too small to see the marked differences between gas sweep and self-purging conditions observed previously for Green River shale (2,13). We are also investigating other explanations for our observation, such as the effect of pyrite grain size and crystal structure.

Attar (1) indicated that organic matter can react with pyrite at temperatures as low as 250°C. The important reactions can be summarized in Reaction 1.

$$FeS_2 + \text{Organics} \longrightarrow FeS + H_2S + R\text{-}SH, \qquad (1)$$

As implied in Reaction 1, the major source of hydrogen in H_2S formation reaction at these temperatures is probably hydrocarbons and hydrocarbon radicals both in condensed and gas phases. H_2S and thiols are also likely to be involved in secondary reactions. For example,

$$R + H_2S \longrightarrow R'\text{-}SH \qquad (2)$$

$$R\text{-}OH + H_2S \longrightarrow R'\text{-}SH + H2O \qquad (3)$$

For thiols, the gas phase secondary reactions may dominate, because the rate of evolution maximizes when H_2S evolution maximizes.

The results in Figure 2 show that only a few of the sulfur-containing compounds (H_2S, COS and CS_2) are related to high-temperature pyrite reactions. Near 600°C, the evolution of hydrocarbon gases from pyrolysis, except CH_4, is essentially completed. Other pyrolysis gases available at this temperature are CO, CO_2, H_2O, and H_2, of which the amounts are affected by char gasification, mineral dehydration, water-gas shift reaction, and carbonate mineral decomposition where possible. For the coal with high pyritic sulfur such as ILHVB, sulfur gases at this temperature are mainly from pyrite decomposition. Pyrite decomposes rapidly at temperatures above 550°C, and H_2S is the major product of pyrite decomposition. In our experiments, the source of hydrogen is probably H_2, H_2O, and hydrogen in char; but the relative importance of each hydrogen donor is not yet clear.

Reactions to form COS and CS_2 can be both gas-solid and gas phase secondary reactions. The pyrite reactions are:

$$FeS_2 + CO \longrightarrow COS + FeS \qquad (4)$$

$$FeS_2 + \text{coal C} \longrightarrow CS_2 + FeS + \text{coal} \qquad (5)$$

$$4FeS_2 + CH_4 \longrightarrow CS_2 + 4FeS + 2H_2S \qquad (6)$$

In his review, Attar (1) claimed Reactions 4 and 5 are slow at $T < 800°C$. However, Taylor et al. (14) found that the rate of formation of COS from the reaction of pyrite and 1% CO in argon was significantly fast even at 500°C. Calkins (5) suggested Reaction 6 takes places at $T > 800°C$, so it may also be slow at the temperatures of interest here.

Examples (15) of the possible gas phase reactions at this temperature are:

$$H_2S + CO \longrightarrow COS + H_2 \qquad (7)$$

$$H_2S + CO_2 \longrightarrow COS + H_2O \qquad (8)$$

$$2H_2S + CO_2 \longrightarrow CS_2 + 2H_2O \qquad (9)$$

$$H_2S + COS \longrightarrow CS_2 + H_2O \qquad (10)$$

$$2COS \longrightarrow CS_2 + CO_2 \qquad (11)$$

Reaction 10 is known to occur at temperatures between 350 and 900°C, and Reaction 11 is slow but reaches a maximum at 600°C (16). Calkins's (5) observation of CS_2 formation at $T > 850°C$ at the expense of H_2S indicates that Reactions 9 and 10 are possible. Our observation of the decrease in CS_2 and the increase in COS yields at 550°C as t_{res} decreases supports Reactions 10 and 11. This observation also agrees with our previous results for Green River shale which found greater yields of COS from vacuum pyrolysis than in a self-purging reactor (7). Some of the sulfur from pyrite decomposition may also be trapped in the organic matrix (17).

We didn't detect elemental sulfur (S_2 and S_3), nor did Boudou et al. (5) find elemental sulfur from isothermal pyrolysis of non-oxidized coal. In our study, the parent/daughter pair of 64/32, which could either be SO_2 or S_2, had a very weak signal.

Because the evolution of sulfur gases always precedes that of hydrocarbon gases, organic sulfur components in coal, in general, seem to be more readily released during pyrolysis than non-heteroatom hydrocarbons. Lester et al. (18) made the same observation in their study with model compounds, although they found sulfur compounds and hydrocarbons evolve nearly simultaneously from coal in a chemical shock tube in which the coal residence time was 1.2-1.5 ms. We also find that T_{max} for H_2S and hydrocarbons both increase with the rank. The same trend is also seen for thiols and thiophenes. The increase in T_{max} for hydrocarbons with rank reflects coal becoming more carbonaceous with rank.

4. Conclusion

We studied the evolution of individual sulfur species during coal pyrolysis. Sulfur dioxide is the only sulfur gas that evolves at $T < 200$ °C, and all organic sulfur gases as well as COS, CS_2, and H_2S are found at 400-500°C, the temperature range of pyrolysis. The decomposition of pyrite at ~550°C produces H_2S, COS, and CS_2. Both gas-solid reactions and gas-phase secondary reactions are responsible for sulfur gas formation. The evolution of sulfur gases precedes that of hydrocarbon gases.

References

(1) Attar, A. Fuel 1978, 57, 201-212.
(2) Burnham, A. K.; Bey, N. K.; Koskinas, G. J. Oil Shale, Tar Sands, and Related Materials, ACS Symposium Series, 163, 1981, 61-77.
(3) Attar, A.; Dupuis, F. Prepr. Pap.-Am. Chem. Soc., Div. Fuel Chem. 1978, 23(2), 44-53.
(4) La count, R. B.; Anderson, R. R.; Friedman, S.; Blaustein, B.D. Prepr. Pap.-Am. Chem. Soc., Div. Fuel Chem. 1986, 31(1), 70-78.
(5) Calkins, W. H. Energy & Fuels 1987, 1, 59-64.
(6) Boudou, J. P.; Boulegue, J.; Malechaux, L.; Nip, M.; De Leeuw, J. W.; Boon, J. J. Fuel 1987, 66, 1558-1569.
(7) Wong, C. M.; Crawford, R. W.; Burnham, A. K. Anal. Chem. 1984, 56(3), 390-395.
(8) Wert, C. A.; Tseng, B. H.; Hsieh, K. C.; Ge, Y. P. Prepr. Pap.-Am. Chem. Soc., Div. Fuel Chem. 1987, 32(3), 250-259.
(9) Whelan, J. K.; Solomon, P. R.; Deshpande, G. V.; Carangelo, R. M. Energy & Fuels 1988, 2, 65-73.
(10) Fadeff, S. K.; Burnham, A. K.; Richardson, J. H. Organic and Pyritic Sulfur Determination in Oil Shale 1983, Lawrence Livermore National Laboratory, Livermore, CA, UCID-19751.
(11) Maa, P. S.; Lewis, C. R.; Hamrin, C. E. Jr. Fuel 1975, 54, 62-69.
(12) Singleton, M. F.; Koskinas, G. J.; Burnham, A. K.; Raley, J. H. Assay Products from Green River Oil Shale 1986, Lawrence Livermore National Laboratory, Livermore, CA, UCRL-53273 Rev. 1.
(13) Wong, C. M.; Crawford, R. W.; Burnham, A. K. Prepr. Pap.-Am. Chem. Soc., Div. Fuel Chem. 1984, 29(3), 317-321.
(14) Taylor, R. W.; Morris, C. J.; Crawford, R. W.; Miller, P. E. Internal Report, 1985, Lawrence Livermore National Laboratory, Livermore, CA.
(15) Gmelin Handbach der Anorganischen Chemie, 8th Ed., System No. 14, Part D 5, 1977, Springer-Verlag, Berlin, Heiderberg, 4.
(16) Ferm, R. J. Chem. Rev. 1957, 57, 621-640.
(17) Cleyle, P. J.; Caley, W. F.; Stewart, I.; Whiteway, S. G. Fuel 1984, 63, 1579-1582.
(18) Lester, T. W.; Polavarapu, J; Merklin, J. F. Fuel 1982, 61, 493-498.

Table 1. Parent/Daughter Mass Combination Employed in Sulfur Gas Identification.

	Sulfur Species	Parent/Daughter Mass
H_2S	Hydrogen Sulfide	34/32 or 34
CH_3SH	Methanethiol	48/45 or 48
COS	Carbonylsulfide	60/32
C_2H_5SH	Ethanethiol	62/29
$(CH_3)_2S$	Dimethylsulfide	62/47
SO_2	Sulfur Dioxide	64/48
CS_2	Carbon Disulfide	76/32
C_3H_7SH	Propanethiol	76/42
C_4H_4S	Thiophene	84/45
$CH_3C_4H_4S$	Methylthiophene	97/53

Table 2. Elemental Analysis and Sulfur Forms (MAF basis) of Illinois No.6 Seam High Volatile Bituminous Coal (ILHVB) and Blind Canyon Seam High Volatile Bituminous Coal (BCHVB).

	ILHVB	BCHVB
% C	77.7	77.9
% H	5.7	6.0
% N	1.4	1.4
% O[a]	9.8	14.2
% Total S	5.4	0.5
Sulfur Forms:		
% Org. S	2.4	0.38[b]
% Pyrite	3.0	N.A.
% Sulfate	0.01	N.A.

a. By difference.
b. Ref. 8.

Acknowledgments

We gratefully acknowledge Ken Foster's contribution to pyrolysis experiments, Armando Alcaraz's contribution to operation of TQMS, and Robert W. Taylor and Thomas T. Coburn for helpful discussion and reading the manuscript. This work was performed under the auspices of the U.S. Department of Energy by the Lawrence Livermore National Laboratory under Contract No. W-7450-Eng-48.

Table 3. Yields (STP cc/g coal) of Sulfur Gases under Different Pyrolysis Conditions.

Sweep Gas Flow Rate (cc/m):		34	34	169
Coal Sample Size (g):		0.52	2.54	2.58
Sulfur Species		Std. Run	High P_{vol}	Shorter t_{res}
H_2S	1st Peak	4.800	6.161	5.503
	2nd Peak	8.230	8.702	9.113
	Total	13.030	14.863	14.616
COS	1st Peak	0.057	0.071	0.067
	2nd Peak	0.110	0.138	0.254
	Total	0.167	0.209	0.321
CS_2	1st Peak	0.017	0.019	0.002
	2nd Peak	0.087	0.040	0.036
	Total	0.104	0.059	0.038
CH_3SH		0.202	0.221	0.184
C_2H_5SH		0.031	0.036	0.029
$(CH_3)_2S$		0.006	0.006	0.005
C_3H_7SH		0.007	0.009	no data
C_4H_4S		0.022	0.020	0.023
$CH_3C_4H_4S$		0.076	0.072	0.089

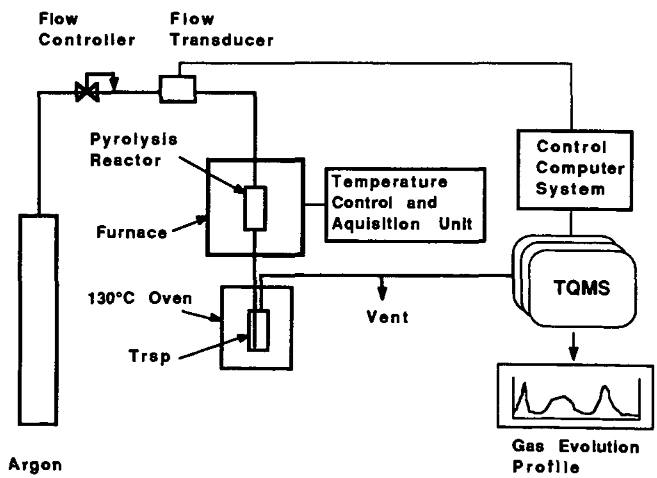

Fig. 1. Schematic of experimental set-up for gas evolution studies.

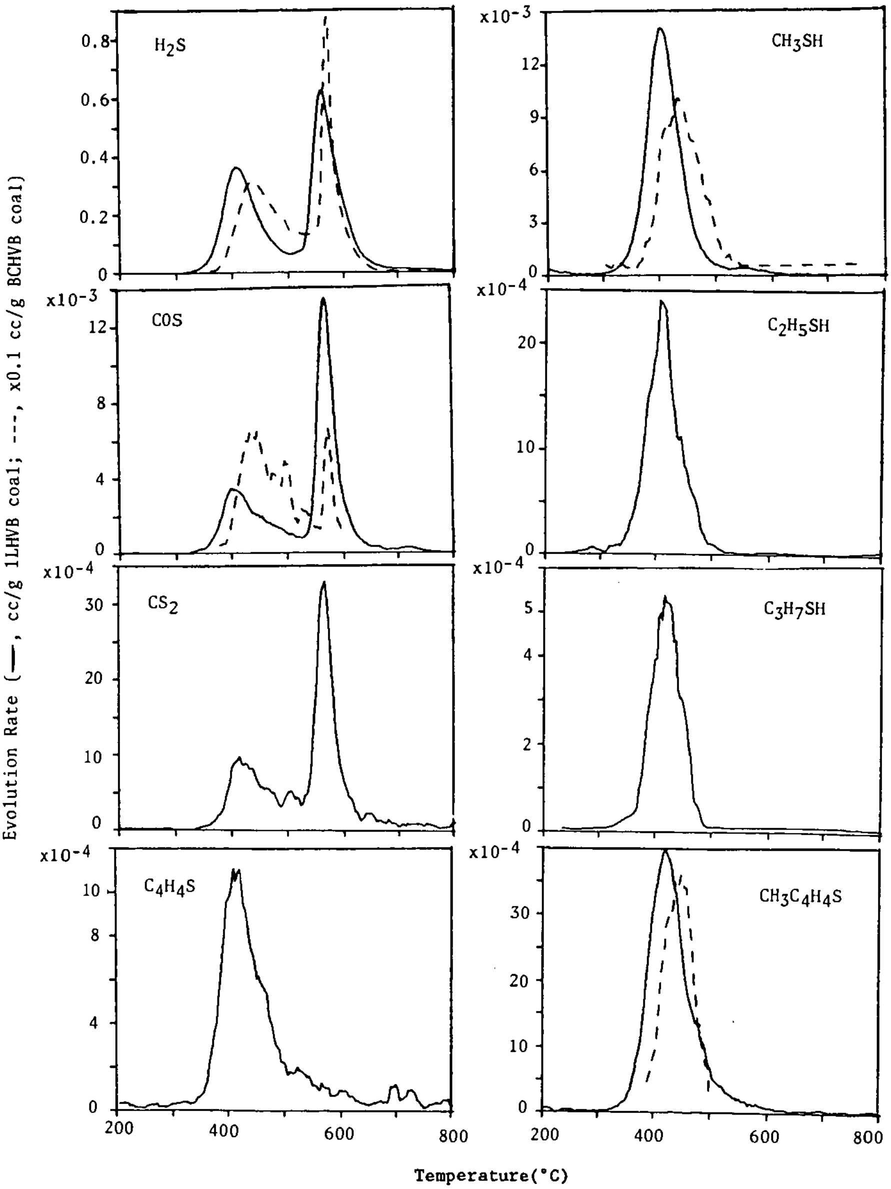

Fig. 2. Evolution profiles of eight sulfur gases.

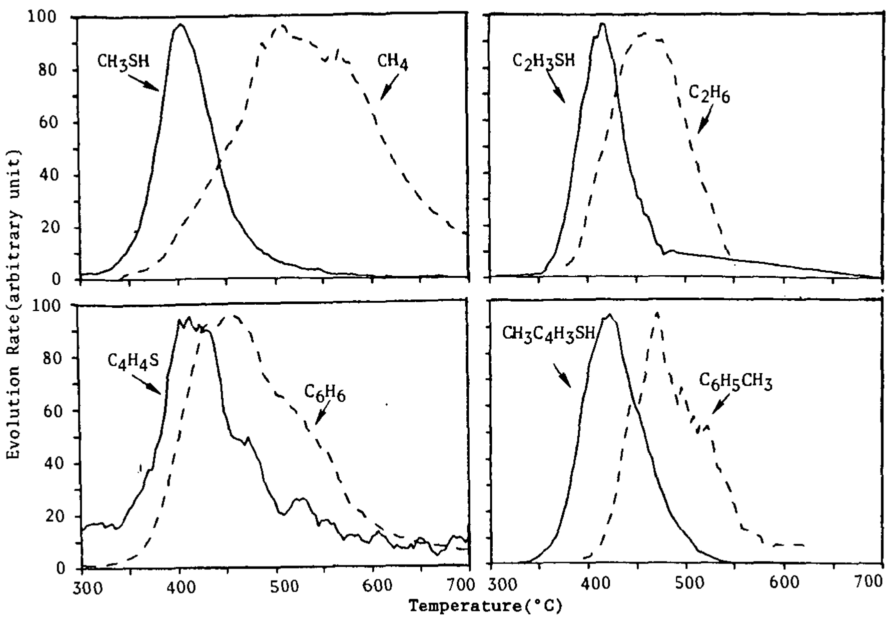

Fig. 3. Comparison of sulfur gas evolution with hydrocarbons.

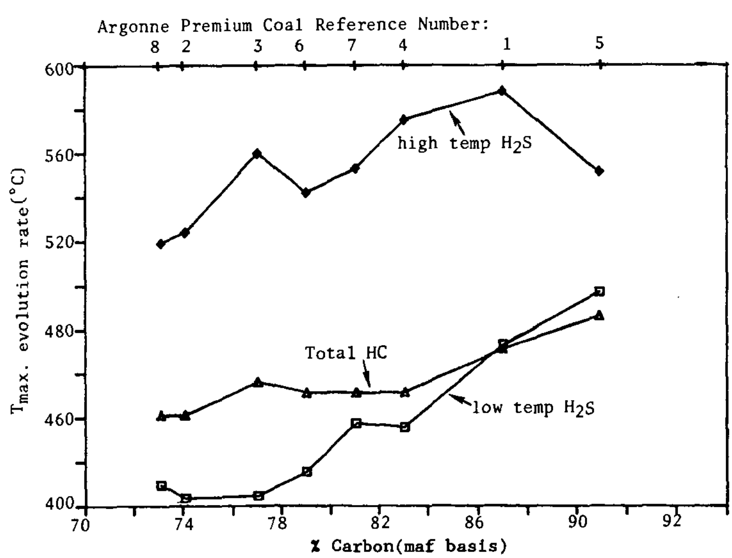

Fig. 4. Variation of T_{max} for H_2S and total hydrocarbon gases and naphtha (HC) with coal rank

SEPARATION OF CO_2 AND H_2 MIXTURES USING REACTIVE ION EXCHANGE MEMBRANES

by

J. Douglas Way and R. Lane Hapke
SRI International
Chemical Engineering Laboratory
Menlo Park, CA 94025.

Introduction

Currently, the most widely used method for producing hydrogen is steam reforming of methane. The volatility in the price of natural gas has created increased interest in finding alternative feedstocks for the manufacture of hydrogen. Thus, it is appropriate at this time to conduct research which has the best opportunities for reducing H_2 production costs from coal gasification.

Bartis and Marks (1984) have identified low energy separation processes such as membranes as a key research opportunity in reducing capital and operating costs and hence the H_2 production costs. They state that technical improvements in gas separation could lead to production cost reductions of 15 to 20 percent. Figure 1 is a block flowsheet of a process to produce hydrogen from synthesis gas. There are two points in the process where gas separation processes take place. Acid gases must be removed from the gas stream after gasification and prior to the shift reaction. This separation step prevents sulfur poisoning of the shift catalysts and maximizes hydrogen production from the shift reaction. The second gas separation occurs after the shift reaction. CO_2 must be removed from the product stream to produce high purity H_2.

Membrane Separations

The use of membrane separations for the gas separation processes described above is an area deserving special attention because of its great potential for low capital cost and energy efficiency (Matson et al., 1983). A membrane process could theoretically separate a binary mixture reversibly, and therefore consume only the minimum work to accomplish the separation. The implicit simplicity and energy

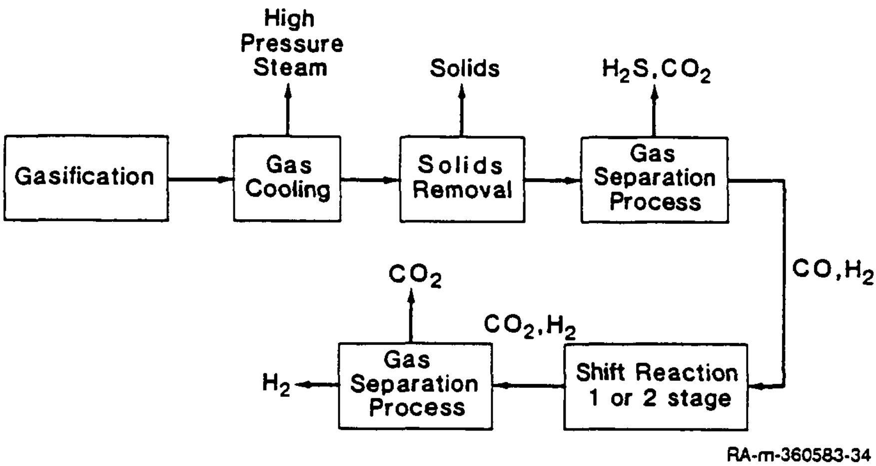

FIGURE 1 BLOCK FLOW DIAGRAM OF HYDROGEN PRODUCTION FROM SYNTHESIS GAS

efficiency of membrane processes have stimulated basic and applied research for many years.

The selective removal of CO_2 from mixtures of H_2, CO, and other gasification products using membranes depends on the appropriate choice of the membrane material. Many glassy polymers commonly used in commercial gas separation membranes are more permeable to H_2 than CO_2. The ideal separation factor, $\alpha(H_2/CO_2)$ for commercial asymmetric cellulose ester membranes is 2.2 (W. R. Grace, 1986) while the value for the polydimethylsiloxane/polysulfone composite membranes is 2.3 (Henis and Tripodi,1980). Due to the large diffusivity of H_2 in typical glassy polymer materials the permeability coefficient (product of the diffusivity and solubility) of H_2 is greater than that of CO_2. While diffusivity controls the selectivity in glassy polymers, in rubbery polymers such as polydimethylsiloxanes (PDMS) or PDMS copolymers the solubility of penetrant gases controls the selectivity. In this case, the selectivity of the rubbery polymer membranes is reversed, and the membranes are more permeable to CO_2 than to H_2. The ideal separation factors (CO_2/H_2) are 4.9 and 4.6 for PDMS and PDMS/polycarbonate copolymers, respectively (Robb, 1968; General Electric, 1982). A separation factor of 6.4 was measured using a commercial GE PDMS membrane with a 50/50 mole % CO_2/H_2 feed gas mixture at ambient conditions. The measured CO_2 permeability was 2310 Barrer (1 Barrer=10^{-10} $cm^3(STP)cm/cm^2 \cdot s \cdot cm$ Hg) which is within 7% of the pure component value (General Electric, 1982). However, the H_2 permeability was 359 Barrer, only 70% of the pure component value. This observation could be explained if the H_2 solubility, and therefore the permeability, during the mixture experiment is lower than the pure component value due to the presence of CO_2 in the membrane.

Facilitated Transport Membranes

Liquids and solvent swollen ionomer membranes can also be used as membrane materials (Ward and Robb, 1968; LeBlanc et al., 1980; Way et al., 1987).

Incorporation of a complexation agent in these membranes can enhance the flux of a reactive species through a process known as facilitated transport. Way et al. (1987) have demonstrated facilitated transport of CO_2 through water-saturated perfluorosulfonic acid ion exchange membranes (IEMs) containing monopositive ethylene diamine as a counterion.

Ion exchange membranes containing EDA were prepared using the method of Way et al. (1987) using nominal 30 μm NE-111 perfluorosulfonic acid membranes. The experimental NE-111 membranes have an equivalent molecular weight of 1100 g/eq and are not available commercially. Preliminary transport measurements were performed at 25 °C and 1 atm to determine the CO_2 and H_2 permeabilities of the NE-111 IEMs. The pure component CO_2 permeability was 145 Barrer, in good agreement with the value of 146 Barrer previously reported by Noble et al. (1988). The H_2 permeability was 21.2 Barrer, corresponding to an ideal separation factor of 6.84 for the NE-111 IEM. The ideal separation factor for water, calculated by determining the ratio of permeability coefficients, is 17.2 at 25 °C and 1 atm (Kohl and Riesenfeld, 1985; Cussler, 1984). A possible explanation of the lower separation factor for the water-swollen IEM is that H_2 may diffuse through both the water containing cluster-channel network phase of the IEM (Gierke, 1977) and the fluorocarbon polymer phase. Further experiments will be performed to determine the permeability and separation factor for mixtures of CO_2 and H_2 using water as a solvent.

Selectivity improvements may be obtained by preparing facilitated transport IEMs using polar organic solvents such as propylene carbonate which are used commercially in physical absorption processes for removing CO_2 from gas mixtures. Propylene carbonate has the property that CO_2 is 121 times more soluble than H_2 at ambient conditions (Kohl and Riesenfeld, 1985). Assuming that the ratio of the diffusion coefficients (CO_2/H_2) in propylene carbonate is the same as water, an ideal separation factor (CO_2/H_2) of approximately 50 can be calculated.

Summary

Liquids and rubbery polymers are good candidate membrane materials for the separation of CO_2 from mixtures with H_2 because the solubility selectivity controls the separation that can be obtained. Facilitated transport IEMs containing monopositive ethylene diamine counterions have been shown to be selectively permeable to CO_2 over H_2. Transport measurements will be conducted to determine the influence of feed gas mixture composition, pressure, temperature, and solvent on the CO_2 and H_2 permeabilities and separation factor.

Acknowledgement

The authors would like to ackowledge the support of the Dept. of Energy Morgantown Energy Technology Center for this work under subcontract NB773000707471 to DOE Contract No. DE-AI21-86MC23120, with special thanks to Ms. Lisa A. Jarr. We would also like to acknowledge Dr. Louis L. Burton of E. I. duPont de Nemours & Co., Inc., for supplying developmental forms of perfluorinated ion exchange membranes.

References

Bartis , J. T., and L. S. Marks, "Technical Evaluation and Systems Analysis of Hydrogen Production from Coal," Final Report for DOE Contract No. DE-AP21-84MC02159 (August, 1984).

Cussler, E. L., *Diffusion: Mass Transfer in Fluid Systems*, Cambridge University Press, Cambridge (1984).

General Electric Membrane Products Operation, General Electric Permselective Membranes Product Literature, 1982.

Gierke, T. D., "Ionic Clustering in Nafion Perfluorosulfonic Acid Membranes and Its Relationship to Hydroxyl Rejection and Chlor-Alkali Current Efficiency," Proc. Electrochemical Society Meeting, Atlanta, GA,1977.

Grace Membrane Systems, Performance Specifications, 1986.

Henis, J. M. S., and M. K. Tripodi, U. S. Patent 4,230,463 (1980).

Kohl, A. L., and F. C. Riesenfeld, *Gas Purification*, 4th Edition, Gulf Publishing Co., Houston (1985).

LeBlanc, O. H., Ward, W. J., Matson, S. L., and S. G. Kimura, "Facilitated Transport in Ion Exchange Membranes," *J. Mem. Sci.*, **6**, 339-343(1980).

Matson, S. L., Lopez, J. and J. A. Quinn, "Separation of Gases With Synthetic Membranes," *Chem. Eng. Sci.*, **38**, 503-524(1983).

Noble, R. D., Pellegrino, J. J., Grosgogeat, E., Sperry, D., and J. D. Way, "CO_2 Separation Using Facilitated Transport Ion Exchange Membranes," *Sep. Sci. Tech.*, accepted for publication, 1988.

Robb, W. L., "Thin Silicone Membranes-Their Permeation Properties and Some Applications," *Ann. N. Y. Acad. Sci.* **146**, 119-137(1968).

Ward, W. J., W. L. Robb, "Carbon Dioxide-Oxygen Separation: Facilitated Transport of Carbon Dioxide Across a Liquid Film," *Science*, **156**, 1481(1967).

Way, J. D., Noble, R. D., Flynn, T. M., and E. D. Sloan, "Liquid Membrane Transport: A Survey," *J. Mem. Sci.*, **12**, 239-259(1982).

SEPARATIONS OF OLEFINS AND HETEROCYCLIC ORGANIC COMPOUNDS BASED ON REVERSIBLE COMPLEXATION REACTIONS.

Carl A. Koval,[1] Steven Drew,[1] Terry Spontarelli,[1] Richard D. Noble,[2] Departments of Chemistry and Biochemistry[1] and of Chemical Engineering,[2] University of Colorado, Boulder, CO 80309

While numerous biological processes utilize membranes that contain transporting agents (carriers) to separate molecular and ionic permeates, the potential of synthetic membranes for separations in commercial processes has not been fully realized. In principal, the phenomenon of facilitated transport (FT) in membranes, which relies on the reversible formation of a permeate:carrier complex, can provide selective and efficient separations. Recently, membranes and thin films derived from ion exchange materials have received considerable attention with respect to their structural, physical and chemical properties. We report the facilitated transport of 1-hexene and 1,5-hexadiene between two decane phases separated by thin, hydrated membranes (ca. 25 μm). The flux of olefin across the membranes is enhanced by factors of several hundred when silver ions are exchanged for sodium ions.

Flux measurements were made using a two compartment cell arranged vertically and separated by the membrane which was held in place with o-rings and a clamp. The surface area of the membranes exposed to the solution was 1.8 cm^2. Both compartments of the cell contained decane (20 mL) that had been saturated with water and were mechanically stirred to provide efficient mass transport to and from the membrane. The lower compartment contained either 1-hexene or 1,5-hexadiene (0.1 M). After the cell was assembled, aliquots (1 μL) of the solution were removed periodically with a syringe from the upper compartment and injected into a gas chromatograph. The GC response for the olefins was monitored continuously by the injection of standards.

For membranes in the Na^+-form, the flux of olefin across the membrane was quite low, but stable for over two days. Transport rates were much higher for the membranes in the Ag^+-form. In both cases, plots of concentration of olefin in the upper compartment vs. time were linear. This indicates a constant flux of olefin across the membrane which can be readily calculated from the slopes: $J_{Na+,hexene} = 2.4 \times 10^{-13}$, $J_{Ag+,hexene} = 1.1 \times 10^{-10}$, $J_{Na+,hexadiene} = 4.0 \times 10^{-13}$ and $J_{Ag+,hexadiene} = 1.8 \times 10^{-10}$ (all J's in mol cm^{-2} sec^{-1}).

We attribute the enhanced olefin flux for the Ag^+-form of the membrane to the reversible complexation of the olefins with silver ion:

$$Ag^+ + \text{olefin} \rightleftharpoons Ag(\text{olefin})^+.$$

Formation constants for these complexes have been reported for 1-hexene (K = 860 M^{-1}) and 1,5-hexadiene (K = 1850 M^{-1}) in 1 M aqueous $AgNO_3$. Assuming that the enhanced fluxes are due to facilitated transport associated with the mobility of the $Ag(olefin)^+$ complex, facilitation factors, F, can be calculated as the ratio of the olefin flux for the Ag^+-form to the flux for the Na^+-form. From the fluxes calculated above, $F_{hexene} = 460$ and $F_{hexadiene} = 450$.

Synthetic fuels derived from coal liquids, tar sands or oil shale contain a wide variety of nonvolatile chemical compounds containing nitrogen and sulfur. Many of these compounds display mutagenic or carcinogenic activity. Therefore, these classes of compounds are undesirable pollutants which must be removed from fuels and other related hydrocarbon products.

We are exploring a novel process for the selective removal of organic nitrogen and sulfur compounds (R-N and R-S) from hydrocarbon phases. The process is based on electrochemically modulated chemical complexation. The complexing agents are water-soluble derivatives of Fe metalloporphyrins. A porphyrin (P) is a tetradentate macrocyclic ligand. Metalloporphyrins have numerous biological functions including the transport of oxygen. The metal ions in metalloporphyrins bind other molecules (ligands) in addition to the porphyrin itself. These bonds are perpendicular to the plane of the porphyrin so the bound molecules are referred to as axial ligands. Reversible reactions between metalloporphyrins and organic compounds containing nitrogen and sulfur are the basis for this separation process. In general, these complexation reactions have greater equilibrium constants when the metals are in the +2 oxidation state as opposed to the +3 state. Interconversion of the Fe(III) and Fe(II) states in metalloporphyrins is a kinetically facile process at metal electrodes. By applying relatively mild potentials, we can achieve the cyclical process:

cathode: $\mathrm{Fe(III)P + e \longrightarrow Fe(II)P}$

$\mathrm{Fe(II)P + R\text{-}N \text{ or } R\text{-}S \longrightarrow Fe(II)P(RN \text{ or } RS)_{1 \text{ or } 2}}$

anode: $\mathrm{Fe(II)P(RN \text{ or } RS)_{1 \text{ or } 2} \longrightarrow Fe(III)P + e^{-} + R\text{-}N \text{ or } R\text{-}S.}$

The reactions described above can be incorporated into a staged electrochemical separation process. Results for the removal of isoquinoline and pentamethyene sulfide from iso-octane and the subsequent concentration of these compounds is a second (waste) hydrocarbon phase will be presented.

REMOVAL OF HYDROGEN CHLORIDE FROM HIGH TEMPERATURE COAL GASES

Gopala N. Krishnan, Bernard J. Wood, and Gilbert T. Tong

SRI International
333 Ravenswood avenue, Menlo Park, CA 94025

Vijendra P. Kothari

U.S. Department of Energy, Morgantown Energy Technology Center
3600 Collins Ferry Road, Morgantown, WV 26505

Introduction

The chlorine content of U.S. coals ranges from 0.01 to 0.5%, and some coals in U.K. contain as high as 1.0% chlorine.[1] This element is present in the coal mainly as alkali chlorides, but it also occurs as oxychlorides of calcium and magnesium.[2] During coal gasification or combustion, these chloride species are converted to HCl vapor. Concentrations of HCl vapor in coal gas have been found in the range 1 to 500 ppm.[3] The presence of HCl in the coal gas can lead to corrosion of metallic and ceramic components of the gasifier, attack gas turbine components and to poisoning of molten carbonate fuel cell electrodes.

Morgantown Energy Technology Center, as the U.S. Department of Energy's lead center for coal gasification and gas stream cleanup technology, has been concerned for some years with the purification of coal-derived gases for a range of applications including gas turbine, fuel-cell, and combined-cycle power generation. Removal of harmful impurities from the coal gas stream at elevated temperatures (>500°C) is necessary for achieving high thermal efficiency in such applications. Although the tolerance to HCl level of fuel cells has not been determined accurately, it is typical to specify that fuel cell feedstocks should contain no more than 1 ppm HCl. Similar requirements may be necessary in turbine applications. Currently available processes for removing HCl vapor operate at relatively low temperatures (T < 300°C) and thus they are not suitable for use with hot coal gases (T > 500°C). This paper presents the results of a laboratory-scale evaluation conducted at SRI International to determine the effectiveness of naturally occurring minerals and commercially available sorbents to remove HCl vapor from simulated coal gas streams at temperatures from 550° to 650°C.[4]

The thermodynamic stability and the volatility of the solid chloride products were the major criteria in selecting the nature of the sorbent. Alkaline earth chlorides, generally, are less volatile than alkali metal chlorides and transition metal chlorides. However, the calculated equilibrium partial pressure of HCl over alkali metal chlorides were calculated to be lower than those over alkaline earth compounds (Table 1). In considering these two factors, along with availability in a natural form, sodium carbonate based sorbents were judged to be superior to other compounds.

Table 1

EQUILIBRIUM PARTIAL PRESSURES OF HCl AND METAL CHLORIDES AT 900 K IN PRESENCE OF A SIMULATED COAL GAS

Parent Compound	Product chloride (MCl)	Equilibrium Partial Pressure (atm) HCl	MCl
Na_2CO_3	NaCl	1.5×10^{-6}	3.5×10^{-6}
K_2CO_3	KCl	3.0×10^{-6}	8.0×10^{-6}
$BaCO_3$	$BaCl_2$	2.2×10^{-5}	1.5×10^{-11}
$CaCO_3$	$CaCl_2$	9.5×10^{-4}	2.8×10^{-9}
$SrCO_3$	$SrCl_2$	1.5×10^{-4}	2.2×10^{-11}

Materials, Apparatus, and Experimental Procedures

Three naturally occurring minerals and a commercially available sorbent were selected for evaluation. The tested minerals were nahcolite ($NaHCO_3$), shortite ($Na_2CO_3 \cdot 2CaCO_3$), and dawsonite ($NaAl(OH)_2CO_3$). The mineral samples were pelletized and calcined at 600°C. During calcination the minerals decomposed as follows:

$$2\ NaHCO_3 \rightarrow Na_2CO_3 + H_2O + CO_2$$

$$Na_2CO_3 \cdot 2CaCO_3 \rightarrow Na_2CO_3 \cdot CaCO_3 + CaCO_3$$

$$NaAl(OH)_2CO_3 \rightarrow NaAlO_2 + CO_2 + H_2O$$

The natural minerals are characterized by low specific surface areas and high levels of active sodium components (Table 2). The commercial sorbent was Katalco Chloride Guard 59-3, manufactured by Katalco Corporation, Oakbrook, IL. This product is sold to remove chloride vapor from natural gas and light hydrocarbon feedstocks. The sorbent contains a proprietary active sodium compound impregnated on a porous alumina support and shows a very high specific surface area with a low level of active sodium component.

Table 2

PROPERTIES OF SORBENTS

Sorbent	Bulk density ($g.cm^{-3}$)	Surface area ($m^2 \cdot g^{-1}$)	ASC[1] (wt% Na)
Katalco Chloride Guard 59-3	0.76	247.0	4.7
Shortite	1.46	0.25	15.0
Nahcolite	0.65	1.2	40.3
Dawsonite	0.59	2.3	16.5

[1]ASC = Active sodium component expressed as wt% sodium.

The reactivities of the selected sorbents toward HCl vapor were evaluated in a thin bed, microreactor (Figure 1) under isothermal conditions. A simulated coal gas of composition 22% H_2, 34% CO, 7% CO_2, 36% H_2O, 1% He and 300 ppm HCl was used as a feedstock. The gas mixture was prepared by metering and blending the individual components using mass flow controllers. Glass or PTFE tubing was used to minimize adsorption or interaction of HCl vapor on the tube walls. Glass walls exposed to the HCl stream containing steam was kept heated to 180°C. The gaseous effluent leaving the sorbent bed was analyzed for HCl by reacting it with a 0.5 M $NaHCO_3$ buffer solution and measuring the dissolved $[Cl^-]$ with a chloride ion selective electrode. The cumulative concentration of the $[Cl^-]$ was calculated using the Nernst equation and the instantaneous partial pressure of HCl vapor in the reactor effluent was calculated by differentiating the cumulative chloride concentration with respect to time.

Results and Discussion

The reaction of the sorbent with HCl vapor yielded solid NaCl as the product:

$$Na_2CO_3 + HCl \rightarrow 2NaCl + CO_2 + H_2O$$

The rate of reaction with the sorbents was rapid initially, but it decreased with time onstream. Even at a space velocity of 5×10^4 h^{-1}, initial residual HCl vapor levels of about 1 ppm were attained with all the tested sorbents (Figure 2). The rate of removal of HCl and the chloride uptake capacity of the sorbents were found to be a functions of the level of its active sodium component (ASC) and its surface area (Table 3). Calcined nahcolite and dawsonite, with their high ASCs and moderate surface

Table 3

CHLORIDE UPTAKE CAPACITIES OF THE TESTED SORBENTS

Sorbent	Chloride capacity (wt%)	
	525°C	650°C
Katalco Chloride Guard	7.1	4.3
Shortite	4.4	4.6
Nahcolite	52.5	52.5
Dawsonite	21.9	18.0

areas had high chloride uptake capacities. The chloride capacity of shortite was the smallest of the sorbents tested because of its low surface area in spite of its high ASC level. The capacity of Katalco Chloride Guard 59-3 was limited by the ASC level, although its surface area was very high.

In the range of 525° to 650°C, the temperature had only a small effect on the rate of HCl removal by shortite and nahcolite. Similarly, their maximum chloride uptake capacities were not affected by temperature. However, for Katalco Chloride Guard and dawsonite the uptake capacity at 650°C was less than at 530°C. Since these sorbents contain alumina, it is likely that at 650°C, the interaction of the active sodium component with the alumina present in the sorbent decreased their reactivity with HCl vapor.

Under the experimental conditions used, with very high surface area sorbents such as Katalco Chloride Guard, the rate of chloride uptake was controlled initially by gas phase mass transfer. Mass transfer calculations indicated that the rate of HCl vapor transfer from the gas phase (300 ppm) to the surface of Katalco Chloride Guard sorbent at 525°C would be about 2×10^{-6} $mole \cdot g^{-1} \cdot s^{-1}$ which compared favorably with the measured initial rate of 1×10^{-6} $mole \cdot g^{-1} \cdot s^{-1}$ at that temperature. At longer exposures, the rate became limited by pore diffusion. Effectiveness factor calculations indicated that pore diffusion could control the rate of chloride uptake with Katalco Chloride Guard once the external areas have been reacted. This rate limitation was confirmed when larger particles were found to react more slowly than smaller particles[4] in the size range of 0.05 to 0.5 cm. Rate control by other mechanisms such as chemical reaction at the interface or diffusion through the chloride product layer became predominant only when the sorbent was nearly saturated.

To determine the rate control mechanism with moderate surface area sorbents such as nahcolite, small quantities (0.1 g) of nahcolite were exposed to the gas mixture at a space velocity of 1 x 10^5 h^{-1} for various periods of time and the accumulated chloride in the solid was measured. Because of the small quantity of the sorbent and the large flow rate, the concentration of HCl vapor and the composition of the sorbent across the bed could be assumed to be nearly constant. The results of these experiments indicated that the rate of HCl reaction with nahcolite was limited initially by mass transfer. However, beyond an initial period, chemical reaction at the interface controlled the rate through a major portion of the sorbent active life time as indicated by a linear correlation between the log of the unreacted fraction (1-x) of the sorbent and time (Figure 3). This behavior is to be expected because of the relatively fewer number of micropores in a moderate surface area material in comparison with a high surface area material. Hence, the shift from mass transfer limited rate to chemical reaction limited rate would occur earlier with nahcolite than with Katalco Chloride Guard. After about 80% of the nahcolite sorbent has been reacted, the rate control appears to be limited by diffusion through a chloride product layer as indicated by the non linear behavior in log (1-x) vs. time plot.

Bench-scale experiments were also conducted with these sorbents at the Institute of Gas Technology, Chicago, IL.[5] The rate of chloride uptake was calculated from the analysis of the chloride content of the spent sorbent as a function of the bed depth. The results of bench-scale experiments were in general agreement with the laboratory-scale experiments although the HCl removal rate and the chloride capacities were somewhat lower than found in the laboratory-scale experiments. This may be due to the large particles used in the bench-scale study. Impurities such as H_2S and trace metals did not affect significantly the rate of HCl removal or the chloride capacities of the sorbents.

A preliminary economic analysis was performed at SRI to determine the cost of HCl removal from hot coal gas.[4] The cost of using Katalco Chloride Guard was estimated to be too high (~$0.02/kWh) for use as throwaway sorbent. In contrast, the annual operating cost for the use of nahcolite was estimated to vary from $0.0017 to $0.0031/kWh depending on whether the gasifier is oxygen-blown or air-blown. In this annual operating cost, the capital investment and the capital recovery components are major cost factors whereas the cost of nahcolite sorbent and its chloride capacity have only a small impact.

Conclusions

The reaction of HCl vapor with calcined sodium-carbonate based natural minerals and synthetic sorbents is rapid and the HCl vapor concentration can be reduced to about 1 ppm level in coal gas in the temperature range of 525° to 650°C. The rate of reaction is controlled initially by the rate of mass transfer from the gas phase to the surface of the sorbents. At later times the rate is controlled by diffusion through micropores in high surface area sorbents and by chemical reaction in moderate and low surface area sorbents. The presence of H_2S and trace metal impurities did not affect significantly the performance of the sorbents. The cost of HCl removal using naturally occurring mineral, nahcolite, is very low.

Acknowledgment

The authors wish to acknowledge the U.S. Department of Energy, Morgantown Energy Technology Center for support of this work under contract No. DOE-AC21-84MC21167.

References

1. W. H. Ode, "Coal Analysis and Mineral Matter" in *Chemistry of Coal Utilization*, supplementary volume, edited by H.H. Lowry, John Wiley and Sons, New York (1963).

2. T. L. Iapalucci, R. J. Demski, and D. Bienstock, "Chlorine in Coal Combustion", Reports of Investigation No. 7260, U.S. Bureau of Mines, (May 1969).

3. TRW, "Monitoring Contaminants in Coal Derived Gas for Molten Carbonate Fuel Cells", Final Report to Argonne National Laboratory under contract No. 31-109-38-6108, DOE/METC/82-44 (May 1981).

4. G. N. Krishnan, G. T. Tong, B. J. Wood, and N. Korens, "High Temperature Coal Gas Chloride Cleanup for Molten Carbonate Fuel Cell Applications", Report No. DOE/MC21167-2080 (November 1986).

5 G. L. Anderson and F. O. Berry, "Chlorine Removal from Hot Coal Gas," Report to SRI International by Institute of Gas Technology under contract No. C-11317 (April 1986). (see Appendix C of Reference 4).

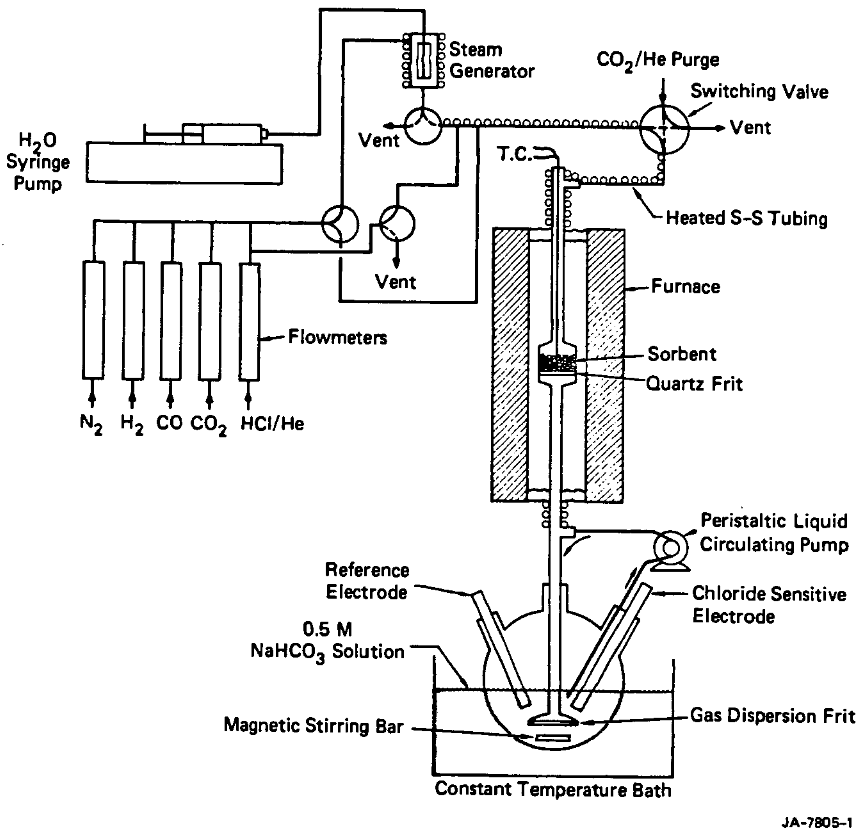

Figure 1. Schematic diagram of thin bed reactor for studying HCl removal.

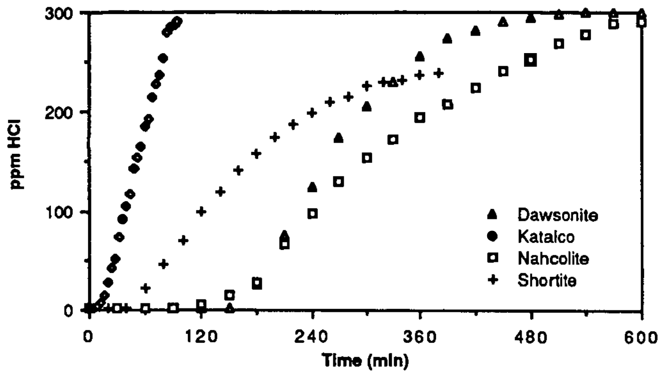

Figure 2. Examples of HCl Breakthrough Curves for Various Sorbents at 525°C
Sorbent quantity - Dawsonite = 0.4 g; Nahcolite = 0.2 g
- Katalco = 0.23 g; Shortite = 1.0 g

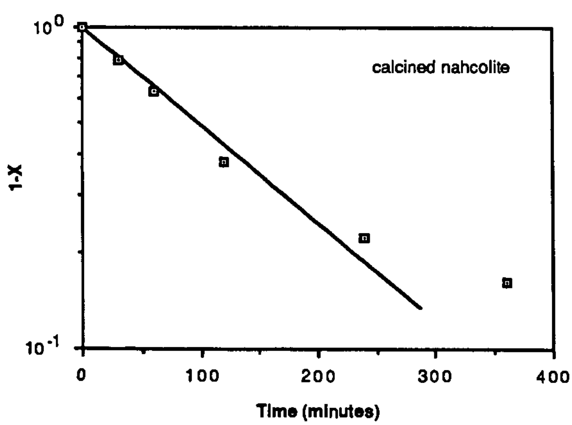

Figure 3 Plot of logarithm of unreacted fraction with time

REMOVAL OF H_2S FROM COAL-DERIVED GASES

by

S. Lynn, R.M. Hix, D.W. Neumann, S.F. Sciamanna, and C.A. Stevens
Department of Chemical Engineering
University of California, Berkeley, CA 94720

Introduction

When coal is gasified most of the sulfur is converted to H_2S and must be removed before the gas can be used either as a fuel or as synthesis gas. The UCB Sulfur Recovery Process (UCBSRP) is being developed as a general method for removing H_2S from gases. The H_2S is absorbed in a polyglycol ether, then reacted in the liquid phase with SO_2 to form marketable elemental sulfur and water. The process allows high specificity and flexibility; H_2S can be reduced to the part-per-million level or below in the presence of CO_2 and the other components of gasified coal. The CO_2 may be left in the original gas stream or it may be co-absorbed and recovered as a separate, sulfur-free product. The process thus has application both to syngas and hydrogen production from O_2-blown gasifiers and to power production using an air-blown gasifier.

Process Configurations

Figure 1 shows a flowsheet for the UCBSRP in a configuration that gives maximum selectivity for H_2S removal. In the primary absorber H_2S is removed primarily by physical absorption. The stream of solvent leaving the absorber is nearly saturated with all of the components of the gas being treated. A water wash at the top of the primary absorber prevents loss of solvent vapor in the treated gas.

Most of the solvent stream leaving the primary absorber then enters a reactor/crystallizer that operates at the pressure of the primary absorber. A second solvent stream containing SO_2 is metered into the same reactor at a rate that keeps the SO_2 content within the reactor a few percent above stoichiometric relative to the H_2S. (It is necessary to have an excess of one reactant or the other in each reactor to avoid excessive reactor volumes and the need for highly precise reactor control.) A clarified overflow from the SO_2-rich reactor is pumped back to the primary absorber. This solvent stream has been completely freed of its H_2S content but is still saturated with respect to the other components in the gas being treated in the primary absorber. The net co-absorption of these other gas components (such as CO_2) is thus kept quite small and the effective selectivity for H_2S is of the order of 50 to 100. The SO_2 content of this solvent stream, although low, provides a chemical enhancement for the absorption of the H_2S on the upper trays of the primary absorber to facillitate meeting very stringent H_2S specifications in the treated gas. (The temperature in the primary absorber is high enough to prevent precipitation of the sulfur formed by this reaction. Not shown in

- - - - -

For presentation at the symposium "Separation Processes for Coal Conversion"
Toronto Meeting, American Chemical Society, June, 1988.

Figure 1, to avoid clutter, is provision for cooling both reactor/crystallizers with cooling water so that the solvent is sub-saturated in sulfur at all other points in the system.)

The underflow from the SO_2-rich reactor carries the sulfur and water formed in the reaction between H_2S and SO_2. The flow of this stream is sized to keep the water content of the solvent from exceeding 5% and is directly proportional to the rate of H_2S removal - - the flow will typically be about 10% of the total flow of solvent through the primary absorber. Sufficient H_2S-rich solvent, from the primary absorber, is added to the stream to leave a small excess of H_2S after all of the residual SO_2 has reacted. This stream is then flashed to atmospheric pressure in the settler/surge tank.

The sulfur made in the process forms a slurry in the underflow from the surge tank. The sulfur is recovered and washed in a centrifuge. In most cases about one-third of the sulfur will be burned in the furnace to make the SO_2 needed in the process. The energy recovered in the waste-heat boiler will usually supply and perhaps exceed the energy required by the process.

The overflow streams from the surge tank and the centrifuge are combined and sent to the solvent stripper. Boiling most of the water out of the solvent provides a stripping vapor that also removes unreacted H_2S and co-absorbed gases such as CO_2 from the solvent. Most of the solvent leaving the solvent stripper is used in the SO_2 scrubber where it absorbs the SO_2 from the combustion gas leaving the furnace. The SO_2 content of this solvent is nil, and hence the SO_2 content of the stack gas leaving the scrubber can readily be reduced to the part-per-million level. The remainder of the solvent from the stripper is sent to the primary absorber, where it prevents loss of SO_2 in the treated gas.

Figure 2 shows a process configuration suitable for removing and recovering one or more components (in addition to the H_2S) from the gas being treated, such as removing CO_2 from a synthesis gas ahead of a shift reactor in a process for producing hydrogen. The operation of this process is identical to that described above in many respects. It differs as follows:

At the bottom of the primary absorber is a short section in which much of the H_2 and CO are stripped from the solvent. The stripping gas is obtained by a partial flash of the solvent immediately downstream of the primary absorber. Most of the H_2S-rich solvent stream leaving the flash drum, together with a controlled flow of SO_2 solution, enters an SO_2-rich reactor. The pressure of the SO_2-rich solvent stream is reduced in stages (only two are shown) to about one atmosphere. The off-gas from each stage is recompressed to the pressure desired for the CO_2 product and is contacted with neat solvent to remove traces of SO_2, then washed with water to recover solvent vapor. For the case shown, in which a high degree of CO_2 removal is not required, clarified H_2S-free solvent from the atmospheric flash can be pumped directly back to the primary absorber.

As in the flow configuration designed for high H_2S selectivity, the sulfur and water formed in the reaction are conveyed out of the last SO_2-rich reactor in a stream that is rendered H_2S-rich with by-passed H_2S solution. As before, the flow of this stream is proportional to the rate of sulfur production.

Lynn, et al. (1987) compared conventional technology to the UCBSRP for removing H_2S from the recycle gas of a crude oil residuum hydrodesulfurization unit. The UCBSRP has the potential for significantly reducing both the capital and operating costs because of the reduction in the number of processing steps and in utilities consumption. Lynn and Sciamanna (1988c) found a similar advantage for the UCBSRP for treating natural gas to remove H_2S, water and C_{3+} hydrocarbons.

Gas and Sulfur Solubilities in Process Solvents

The solubilities of H_2S, SO_2, CO_2, propane, butane and sulfur in a variety of glycol ethers have been measured as a function of temperature. Water, a product of the reaction, reduces these solubilities. These results have been reported by Demyanovich and Lynn (1987) and by Sciamanna and Lynn (1988a and 1988b).

Reaction Kinetics

The reaction between H_2S and SO_2 in glycol ethers is relatively slow when uncatalyzed. However, as reported by Neumann and Lynn (1986), tertiary aromatic amines are effective catalysts and reduce the time required for nearly complete reaction to a few seconds.

Corrosion Studies

Corrosion studies were performed by submerging metal coupons half way in a solution of H_2S or SO_2 in a glycol ether. To make the system as corrosive as possible, the solvent was a mono-ether (which is also an alcohol) and sulfur and water were added in concentrations twice (or greater) those encountered in the process. The exposure was carried out for three successive 20 to 30-day periods at each temperature. Table 1 shows the corrosion rates observed.

Table 1: Corrosion Rates of Steels in Process Solutions.

	MEASURED RATES AND CONDITIONS *		
Metal	SO_2: @ 100°C	@ 120°C	H_2S: @ 150°C
Carbon Steel	0.6	1.7	0.05
304 Stainless	0.7	1.5	0.02
316 Stainless	1.3	4.8	0.01

* Mils/year in diethylene glycol methyl ether, 5% H_2O, saturated with sulfur, 50 - 100 psi gas pressure.

Since 60^oC is the maximum temperature at which SO_2 is present (outlet of the SO_2 absorber), carbon steel and 304 and 316 stainless steels should corrode at rates much less than 1 mil/year (0.02 mm/yr) under all process conditions.

Sulfur Crystallization

A major potential advantage of the UCB Sulfur Recovery Process is the purity of the crystalline sulfur that is produced. The sulfur crystallizes from solution both as a result of cooling and as a result of chemical reaction between H_2S and SO_2. In the former case the degree of supersaturation is relatively low because the solubility of sulfur in the solvent varies only a few grams per liter over the temperature range of interest. A substantially higher concentration of sulfur can result from the chemical reaction.

The crystallizer consists of a well-stirred 2-liter vessel. Hot saturated feed enters at the top, and the vessel walls are cooled. Cold effluent exits at the bottom of the vessel as a sulfur/solvent slurry. A sample of the effluent slurry is collected when the system is at steady-state and the size distribution of the sulfur crystals is determined. analysis.

Gas Absorption with Chemical Reaction

Tray efficiency data are needed for two process situations. In one, H_2S at very low concentration is being absorbed by a chemically reactive solution of SO_2. In the other, gaseous SO_2 in the low parts-per-million concentration range is absorbed by lean process solvent. Both are of interest because one wishes to effect very stringent sulfur removal with the UCBSRP. The equipment consists of a single seive tray (or section of packed column) placed in a test section through which gas and liquid streams pass. Murphree tray efficiencies are determined from the mass balances and previously obtained solubility data.

Work Required for Proof-of-Concept

The crystallizer is being modified to incorporate crystal size classification to retain smaller crystals and produce a product of larger size. Sulfur will be produced by chemical reaction. Data obtained for absorption of H_2S enhanced by the presence of SO_2 in the solvent will be used to develop a model that incorporates the reaction kinetics work done previously.

A computer model that simulates all of the unit operations in the process is operational and facillitates process synthesis for specific applications. It will be used to evaluate and further refine the process configurations shown in Figures 1 and 2 for the purification of hydrogen derived from gasified coal.

Acknowledgement

This work was supported by the Assistant Secretary for Fossil Energy, Office of Coal Utilization, Division of Surface Coal Gasification, of the U.S. Department of Energy under contract DE-AC03-76SF00098.

References

Demyanovich, R.J. and Lynn, S. **1987**. Vapor-Liquid Equilibria of Sulfur Dioxide in Polar Organic Solvents. *I&EC Research* **26** 548.

Lynn, S., Neumann, D.W., Sciamanna, S.F., and Vorhis, F.H. 1987. A Comparison of the UCB Sulfur Recovery Process with Conventional Sulfur Recovery Technology. *Environmental Progress* **6** 257.

Neumann, D.W. and Lynn, S. **1986**. Kinetics of the Reaction of H_2S and SO_2 in Organic Solvents. *I&EC Proc. Des. & Dev.* **25** 248.

Sciamanna, S.F. and S. Lynn, **1988**. Sulfur Solubility in Pure and Mixed Organic Solvents. *I. & E.C. Research* (in press).

Sciamanna, S.F. and S. Lynn, **1988**. Solubility of Hydrogen Sulfide, Sulfur Dioxide, Carbon Dioxide, Propane and n-Butane in Polyglycol Ethers. *I. & E.C. Research* (in press).

Sciamanna, S.F. and S. Lynn, **1988**. An Integrated Process for Simultaneous Desulfurization, Dehydration, and Recovery of Hydrocarbon Liquids from Natural Gas Streams. *I. & E.C. Research* (in press).

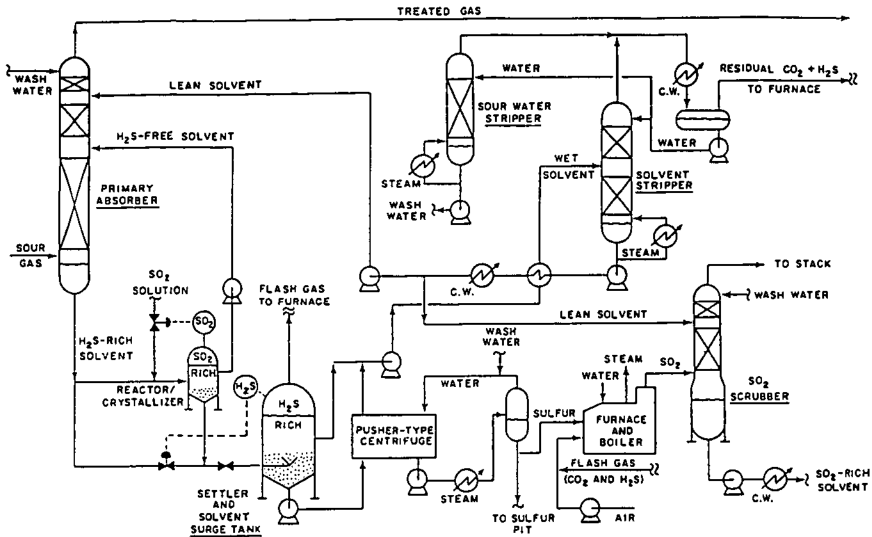

Figure 1 H_2S-Selective Process.

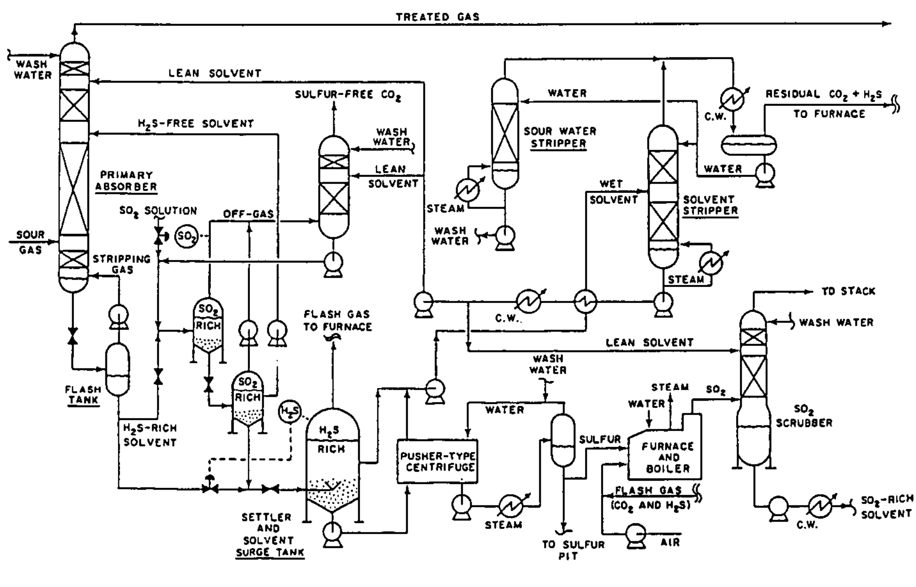

Figure 2 Co-Absorption Process.

SORBENT-BASED RECOVERY OF SULFUR FROM REGENERATION TAIL GASES

S. K. Gangwal and S. M. Harkins
Research Triangle Institute, Research Triangle Park, NC 27709

T. P. Dorchak, Morgantown Energy Technology Center, Morgantown, WV 26507

The U.S. Department of Energy (DOE), Morgantown Energy Technology Center (METC) is sponsoring research on advanced methods for controlling contaminants for hot coal gas streams of integrated gasification combined-cycle (IGCC) systems.(1) The programs focus on hot gas cleanup technologies that match or nearly match the temperatures and pressures of the gasifier, cleanup system, and power generator. The purpose is to eliminate the need for expensive heat recovery equipment and to avoid the efficiency losses associated with fuel gas quenching. DOE/METC has originated the Gasification Island concept for IGCC systems, which combines temperature and pressure matching, modular shop fabricated construction, and steam and air integration of the gasifier and turbine. Figure 1 illustrates the simplified IGCC system that can be achieved with hot gas cleanup. For the control of sulfur in the coal gasifier gas, DOE/METC continues to conduct and to sponsor work toward the development of a zinc ferrite absorption process. Absorption capacity of the zinc ferrite is highest at temperatures of 800 to 925 K compatible with the operation of a fixed-bed gasifier turbine system.

The hydrogen sulfide laden fuel gas passes through a fixed bed of zinc ferrite, in the form of 3/16-inch extrudates, which absorbs sulfur up to 25 percent of its weight. The clean gas contains less than 5 ppm, well below New Source Performance Standards (NSPS) and also enhances corrosion and erosion protection for the downstream turbine. The sulfided sorbent is regenerated with a dilute typically less than 2 percent oxygen containing gas. The oxygen content of the regenerator gas is limited to avoid overheating and sintering the sorbent due to the highly exothermic oxidation of the sulfide to sulfur dioxide. The tail gas from the regeneration process must be further processed to remove the sulfur and recover it in an environmentally acceptable manner in a salable or readily disposable form.

This paper will discuss the results of experimental/theoretical research on two novel process concepts for elemental sulfur production from regeneration tail gases. Both concepts utilize a highly efficient sodium/aluminum (Na/Al) based SO_2 sorbent at elevated temperatures (800 to 1,000 K) and pressures (1 to 3 MPa). One concept involves sulfation of the Na/Al sorbent with the tail gas followed by regeneration with reducing gas to produce a suitable Claus plant feed. The other concept aims for single step sulfur production by reacting the tail gas with a small quantity of raw coal gasifier product gases over the sorbent.

The first concept is schematically shown in Figure 2. The SO_2 in the tail gas is absorbed onto the Na/Al sorbent and the hot diluent is recycled for regenerating zinc ferrite. The sulfated Na/Al sorbent is then regenerated using a small side stream of the coal gasifier gas. The resulting concentrated sulfur stream at elevated temperature and pressure containing from 10 to 50 percent H_2S is a suitable feed for a Claus plant for elemental sulfur recovery.

The preparation of the Na/Al sorbent follows from Beinstock et al. at the U.S. Bureau of Mines for the removal of SO_2 from combustion flue gases.(2) Further development in this study has produced a sorbent as strong 1/16 inch to 1/8 inch extrudates with greater structural integrity, reactivity, capacity, and mechanical strength.(3) Enhancement of these properties is believed to be necessary for successful application at high temperature and pressure conditions.

The sorbent has been tested at atmospheric pressure as well as elevated pressures to demonstrate the potential of the concept shown in Figure 2. Atmospheric pressure tests have been carried out using both a fixed-bed reactor system and a thermogravimetric reactor (TGR) system. Tests have been conducted at 800 to 975 K with a tail gas containing 1 to 2 percent SO_2. These conditions are representative of zinc ferrite regeneration tail gas. Atmospheric pressure tests have shown that the sorbent can absorb SO_2 up to 40 percent of its weight. The sorbent can be regenerated while maintaining a crush strength greater than 13.5 N/mm over 20 sulfation/regeneration cycles. In atmospheric pressure fixed-bed tests, the sorbent demonstrated high efficiency in absorbing SO_2 by reducing it from 2 percent to less than 10 ppmv. This essentially "zero" prebreakthrough level of SO_2 was maintained for over 2 hours at a space velocity of 2000 h^{-1}. Approximately 30 percent by weight SO_2 was absorbed prior to 100 ppm SO_2 breakthrough. Regenerations of the sorbent with coal gasifier gas and hydrogen in separate tests produced H_2S rich gas streams containing up to 16.4 and 60 percent H_2S, respectively.

Elevated pressure TGR tests have recently been initiated to evaluate sulfation and regeneration kinetics that could be used to predict fixed-bed sorbent performance at elevated pressure. Figure 3 compares the atmospheric pressure sulfation rate to sulfation rate at 2.5 MPa. As can be seen, the overall SO_2 absorption capacity as a function of time is significantly higher at 2.5 MPa. This indicates that it will be possible to sulfate a fixed-bed of the sorbent to significantly greater levels at elevated pressures than at atmospheric pressure, prior to breakthrough. Following completion of measurement of elevated pressure sulfation/regeneration kinetics, a fixed-bed absorption/regeneration model will be developed to predict sorbent capacity at breakthrough in fixed-bed reactors. Bench-scale tests will then be carried out to demonstrate the concept at elevated pressures.

Elemental sulfur has been observed on the surface of the sorbent following sulfation/regeneration cycles. Also significant amounts of elemental sulfur elutes from the sorbent after breakthrough has been achieved during sulfation. This has suggested a second concept for direct recovery of elemental sulfur from regeneration tail gases which if successful would result in significant reduction of the burden on the Claus plant. Ideally this concept (shown schematically in Figure 4) may allow the complete elimination of the Claus plant. A thermodynamic analysis of potential sulfur forming reactions of H_2, SO_2, CO, H_2S, CO_2, and steam indicates that 96 to 98 percent of the SO_2 can be potentially converted to elemental sulfur at 800 to 1,000 K and 2.5 MPa. A few bench-scale tests will be carried out in the future to assess the potential of this concept.

References

1. U.S. Department of Energy, "Hot Gas Cleanup for Electric Power Generation Systems," Morgantown Energy Technology Center, DE86006607, May (1986).

2. Bienstock, D., J. H. Field, and J. G. Myers, Bureau of Mines, Department of Investigations, 5735, PB 192542 (1961).

3. Gangwal, S. K., S. M. Harkins, and M. C. Woods, "Disposal of Off-Gases from Hot Gas Desulfurization Processes," Yearly Technical Status Report, Contract No. DE-AC21-86MC 23260, to be published (1987).

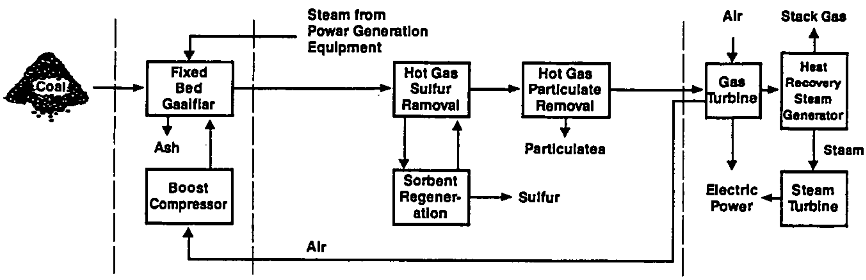

Figure 1. Gasification island concept for IGCC systems.

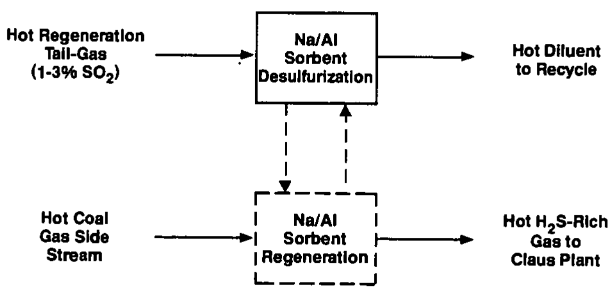

Figure 2. High temperature regeneration tail-gas treatment.

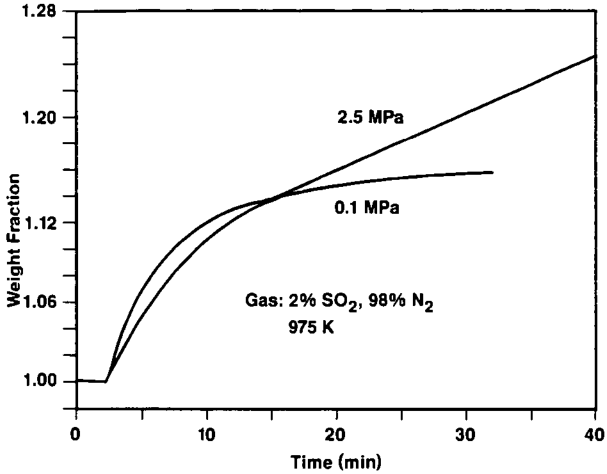

Figure 3. Effect of pressure on sorbent sulfation rate.

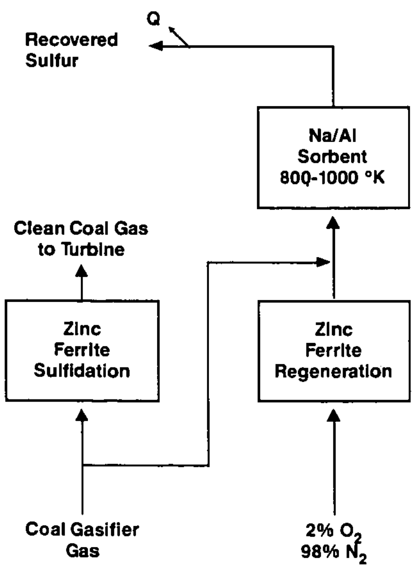

Figure 4. Direct recovery of sulfur from regeneration tail-gas.

SEPARATION OF GAS MIXTURES BY TRANSITION-METAL COMPLEXES

M. A. Lilga, R. T. Hallen, D. A. Nelson

Battelle, Pacific Northwest Laboratory
P.O. Box 999
Richland, WA 99352

INTRODUCTION

The selective separation or purification of gases, especially hydrogen and CO, is highly desirable in processes utilizing product gas from coal gasification. However, gas separation is a difficult and energy intensive process. The development of new and innovative methodologies to selectively and efficiently separate specific gas components from mixed-gas streams would significantly reduce the cost and complexity of product gas production and processing. For example, efficient H_2 separation from synthesis gas could make coal an attractive future source of H_2 for use as a fuel or chemical feedstock. In addition, this technology could have a significant impact on processes not directly associated with coal gasification in which hydrogen is lost in a waste stream. These processes include ammonia manufacture, reduction of metallic oxide ores, and hydrogenation of fats and oils. Thus, wide-ranging applications exist for hydrogen separation and recovery technologies.

Current separation technologies are inefficient or non-selective. For example, recovery of H_2 from Pressure Swing Adsorption is on the order of 80%. PSA is ineffective with feeds containing less than 50% H_2. The COSORB™ process for CO recovery is highly moisture sensitive, requiring removal of water from feed streams. Membranes are inherently energy efficient but systems, such as PRISM™, cannot separate H_2 from CO_2.

The Pacific Northwest Laboratory (PNL) is examining transition-metal complexes as selective agents for the separation of syngas components from gas mixtures. Transition-metal complexes are known which react reversibly with gases such as H_2, CO, O_2, and CO_2. This reversible binding can be used to transfer the gas from a region of high partial pressure to a region of lower partial pressure. The selectivity of transfer is determined primarily by the selectivity of the metal in binding a specific gas. The nature of the ligands surrounding the metal has a large influence on the selectivity and reversibility and we have successfully used ligand modification to prepare complexes that have improved properties for H_2 or CO binding. Applications of metal complexes to gas separation and two specific examples of metal complexes under study will be discussed.

APPLICATION OF METAL COMPLEXES TO GAS SEPARATION

Two gas separation systems which take advantage of selective, reversible gas binding by transition-metal complexes are absorption/desorption and facilitated transport membrane systems. A two-column apparatus used at PNL is shown in Figure 1 and its operation is illustrated for CO separation. Inlet gas containing CO enters the bottom of the absorber column and encounters a counter-current flow of solution containing a metal complex. Non-reactive feed gases exit the top of the absorber while CO is transported to the stripper column in the form of a CO/metal complex. Heat and an inert stripping gas release the CO from the metal complex in the stripper column. CO product gas exits the top of the stripper column and volatilized solvent is condensed and returned to the system. The solution containing regenerated metal complex is recycled to the top of the absorber column and the cycle begins again. This apparatus is similar to that used in the COSORB™ process and allows for continuous gas separation. Any gas could be separated from a feed stream by this process assuming an appropriate metal complex/solvent system specific for that gas is available. Potential drawbacks include the relatively large amounts of carrier required and the interference of solubility of undesired gases in the solvent.

Immobilized liquid membrane systems, in which the metal complex acts as a facilitated transport agent, offer the potential for high selectivity and increased flux. This type of system is illustrated in Figure 2 for H_2 separation. The driving force to separation is a pressure gradient across the membrane. Hydrogen entering the membrane on the high pressure side reacts with a metal complex. The metal/hydrogen complex diffuses across the membrane where H_2 is released in the H_2-lean environment and product H_2 leaves the membrane and is removed. A concentration gradient drives the metal complex back across the membrane and more H_2 is bound the continue the cycle. The function of the metal complex is to act as a specific carrier for H_2 and serves to increase the effective H_2 concentration in the membrane relative to the undesired gases. Thus, selectivity for H_2 is high, allowing the use of thinner membranes resulting in a greater flux. Permeability and selectivity in these systems are expected to be significantly greater than for dry or liquid-wetted membranes.

PALLADIUM COMPLEXES

Palladium dimer complexes were evaluated for their ability to reversibly bind CO (Equation 1). Kinetic and thermodynamic data for these complexes (X = NCO, Cl,

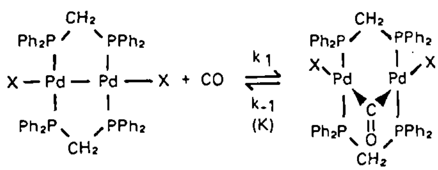

1)

Br, I) indicate that halide substitution greatly influences the binding of CO (1). For example, the equilibrium constant, K, for CO binding follows the order NCO > Cl > Br > I where K for the NCO complex is approximately 300 times that of the iodide complex. This difference in equilibrium constant is primarily due to differences in k_{-1}, the rate of CO dissociation.

Specificity for CO is high. Gases including CO_2, N_2, H_2, O_2 and ethylene do not interfere with CO binding. H_2S was found to react in a novel way to release H_2 according to Equation 2 (2).

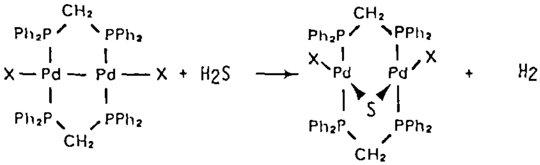

2)

Equilibrium data for the bromide complex indicated suitable reversibility over the temperature and CO pressure ranges of interest. This complex was chosen for bench-scale experiments in the absorber/stripper system shown in Figure 1 (3). Presence of the complex enhances transfer of CO by an order of magnitude and the system functions to separate CO from N_2. With a five-component mixture (CO, CO_2, H_2, CH_4, and N_2) a combination of chemical complexation of CO and the solubility of CO_2 and CH_4 in the solvent resulted in significant transfer of these gases to the stripper. Little H_2 was transferred and an H_2-rich gas stream was produced indicating the potential of this system for H_2 separation from a low-btu gas mixture. A cost analysis indicated that the initial costs of palladium were not necessarily prohibitive but to compete with existing technology the lifetime of the complex must be at least one year.

CHROMIUM COMPLEXES

The reaction of H_2 with $[CpCr(CO)_3]_2$ (Cp = cyclopentadienyl, C_5H_5) was reported by Fischer, et al. (4,5) to occur at 70°C and 150 atm H_2 to afford the monomeric hydride complex $CpCr(CO)_3H$. It has also been reported that the pure monomeric hydride complex evolves H_2 when heated to 80°C, its melting point. Our initial objective was to determine the temperature and H_2 pressure conditions required to carry out the reversible H_2 binding in solution (Equation 3).

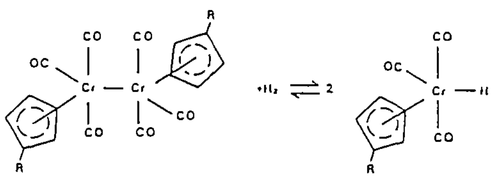

3)

Derivatives of the complex were also prepared to study the effects of electron-withdrawing groups on the cyclopentadienyl ligand (R = CO_2CH_3) on Equation 3. Our investigation has demonstrated that the reaction of H_2 with $[CpCr(CO)_3]_2$ is much more facile than previously reported. At 10 atm and room temperature, the reaction is complete before a spectrum can be taken. This dimer is found to react with 1 atm H_2 slowly at room temperature but faster at 65°C, reaching completion in 0.5 hours. Regeneration to the extent of about 5% can be achieved by heating to 100°C for 2 hours. H_2 is rapidly lost upon photolysis, however, CO is also lost and an inactive complex is formed. The substituted complex shows similar activity for H_2 binding but regeneration appeared to be easier with 10% conversion at 90°C after two hours. Regeneration may be difficult because it involves a bimolecular process in which two chromium centers interact. It is possible that regeneration will be improved by linking the cyclopentadienyl groups together, since hydrogen formation would then be unimolecular.

CONCLUSIONS

Selective transition-metal complexes can enhance gas transport in gas separation processes. Properties of complexes can be tailored by chemical modification of the ligand environment to improve binding characteristics. As a result, high selectivity for specific gas components is attainable. In addition, complexes need not be prohibitively expensive.

ACKNOWLEDGMENT

This research was supported by the U.S. Department of Energy, Morgantown Energy Technology Center under contract DE-AC06-76RLO 1830.

REFERENCES

(1) Lee, C. L.; James, B. R.; Nelson, D. A.; Hallen, R. T. *Organometallics*, 1984, *3*, 1360.

(2) James, B. R.; Lee, C. L.; Lilga, M. A.; Nelson, D. A. U.S. Patent 4 693 875, 1987.

(3) Lyke, S. E.; Lilga, M. A.; Ozanich, R. M.; Nelson, D. A. *Ind. Eng. Chem. Prod. Res. Dev.*, 1986, *25*, 517.

(4) Fischer, E. O. *Inorg. Synth.*, 1963, *7*, 136.

(5) Fischer, E. O.; Hafner, W.; Stahl, H. O. *Z. Anorg. Allgem. Chem.*, 1955, 282, 47.

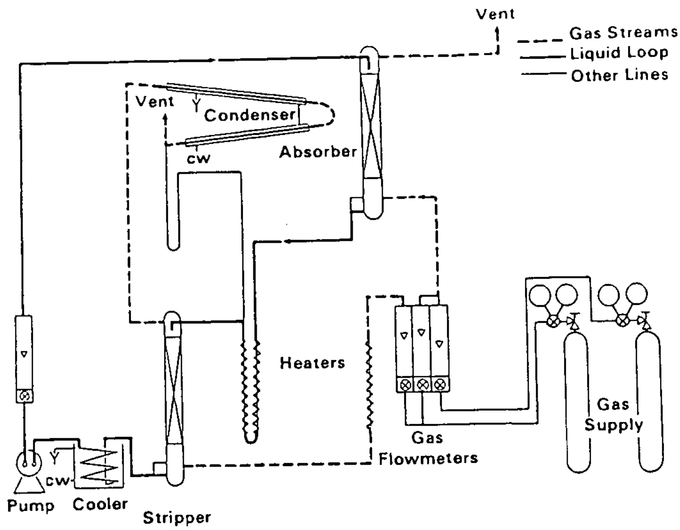

FIGURE 1. Absorber/Stripper Apparatus

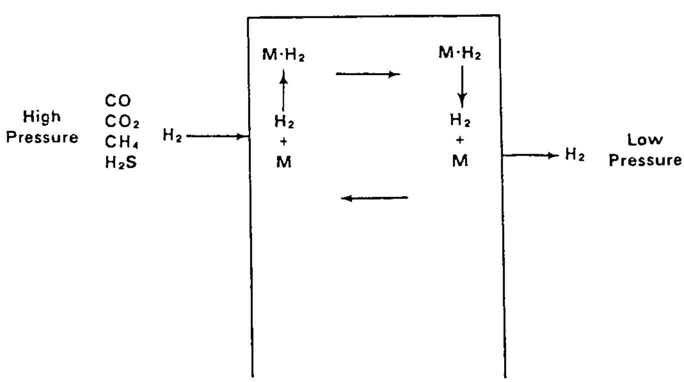

FIGURE 2. Facilitated Transport of H_2 by a Membrane Containing a Dissolved Metal Complex

The Removal of Impurities from Hot Coal-Derived Gas by Filtration

by

T. Grindley and R. G. Logan
U.S. Department of Energy
Morgantown Energy Technology Center
Morgantown, WV 26505

At the Morgantown Energy Technology Center (METC) of the U.S. Department of Energy, an effort is underway to clean hot coal-derived gas to a sufficient purity for combustion in heat engines and other applications. Experiments were conducted in which the hot product gas, raw and desulfurized, from a fluid-bed coal gasifier was filtered at temperatures up to 1,600°F, pressures up to 250 psig, and flow rates up to 2,500 scfh. Particulate and condensate samples were collected at the inlet and outlet of the filters and analyzed for 10 metals which are common constituents of coal ash. The results were used to determine how filtration of particles from a gas stream at high temperatures affected metal concentrations in the gas. In general, the removal efficiency for the metals correlated with the particulate removal efficiency.

Introduction

Under the Advanced Environmental Control Technology Program established in 1979 by the Department of Energy (1), Morgantown Energy Technology Center has been actively engaged in the development of technology necessary to control contaminants from coal gasification that are deleterious to gas turbines and hazardous to the environment. A significant part of this effort has been concerned with particulate and trace metal, particularly alkali metals, removal from the hot gas streams. Three hot gas filtration devices developed in the program by contractors were tested at METC to determine their performance in an actual hot gas stream produced by a small-scale, fluid-bed gasifier (2). The three devices were a Westinghouse ceramic cross-flow filter, an Acurex ceramic bag filter, and an electrostatic precipitator developed by Denver Research Institute. Details of the design of these devices and results of the work to date have been reported in a series of contractor review meetings (3-9).

Although the principal purpose of this series of tests was to measure the particulate removal efficiency of the hot gas filters at temperatures up to 1,850°F, they afforded the opportunity to also measure the concentration of 10 metals, which are common constituents of coal ash, in the gas stream. Specifically, it was desired to determine whether removal of particles from a coal gas at temperatures up to 1,850°F would affect the downstream concentration of trace species of metals such as sodium and potassium. The results of the experiment are reported in this paper.

Experimental

The low-Btu coal gas used during these tests was produced by METC's advanced concepts fluid-bed gasifier. The gasifier was designed to operate with a wide range of coals at pressures of 200 to 1,000 psig and temperatures up to 1,900°F. The gasifier is used as a source of low- to medium-Btu gas for use in testing downstream components and analytical instrumentation.

During these tests, the gasifier was operated at 400 psig with Montana Rosebud subbituminous coal, air, and steam to produce a gas of the following average composition:

N_2:	38.0 Percent	CO_2:	10.0 Percent
H_2O:	17.0 Percent	CH_4:	3.5 Percent
H_2:	17.0 Percent	H_2S:	0.3 Percent
CO:	13.5 Percent		

Approximately 300 feet of insulated pipe separated the gasifier from the cleanup device test area. Heat loss and particle dropout in the pipe resulted in a gas temperature and solids loading that were lower than that required for the tests. Thus, a methane-fired heater was used to increase the temperature to the desired range (1,400° to 1,850°F), and a pressurized, screw-type particle feeder was used to feed particles into the gas stream up stream of the test device. These particles were obtained from a cyclone on the gasifier and had the same composition as the entrained particulate. The rate of particulate addition was varied depending on the amount already in the gas and the requirements of each test. Typically, the added particles were approximately 10 to 40 percent of the total at the inlet of the test devices. After exiting the cleanup device, the gas was cooled to remove condensibles, metered, and then incinerated.

Tests conducted with the Westinghouse and Acurex filters lasted 250 hours each. The test of the DRI electrostatic precipitator was terminated after approximately 50 hours because of a mechanical failure. During 50 hours of the Acurex filter test, the coal gas was desulfurized prior to particulate removal. This was accomplished using METC's hot gas desulfurization unit which uses a zinc ferrite ($ZnFe_2O_4$) sorbent to remove gaseous sulfur species. This device typically removes greater than 99 percent of the sulfur in the gas and produces gas streams with sulfur concentrations of less than 10 ppm (8). The configuration of the various components of the test system are shown in Figure 1.

Particulate sampling probes were positioned at various points in the system to characterize the performance of each device. To measure the solids loading of the gas produced by the gasifier, a sampling probe was placed in the gas line after the primary cyclone. Sampling probes were installed before and after the hot gas desulfurization unit to determine if this device removed particles from the gas stream or if zinc ferrite bed material was being lost by attrition.

The data reported here were collected at the inlet and outlet of the particulate removal test devices. The inlet probe was positioned downstream of the particle feeder, but upstream of the test device. The outlet sampling system was designed to filter the total system flow exiting the test device.

Sampling System Design

The inlet sampling probe was constructed of 1/4-inch stainless steel tubing with either a 0.035- or 0.049-inch wall thickness. The tip of the probe was beveled approximately 1/4 inch. When the probe was operated isokinetically, approximately 3 to 5 percent of the total process flow was sampled. The probe was positioned in a process pipe elbow with the probe tip approximately 6 inches upstream of the start of the bend.

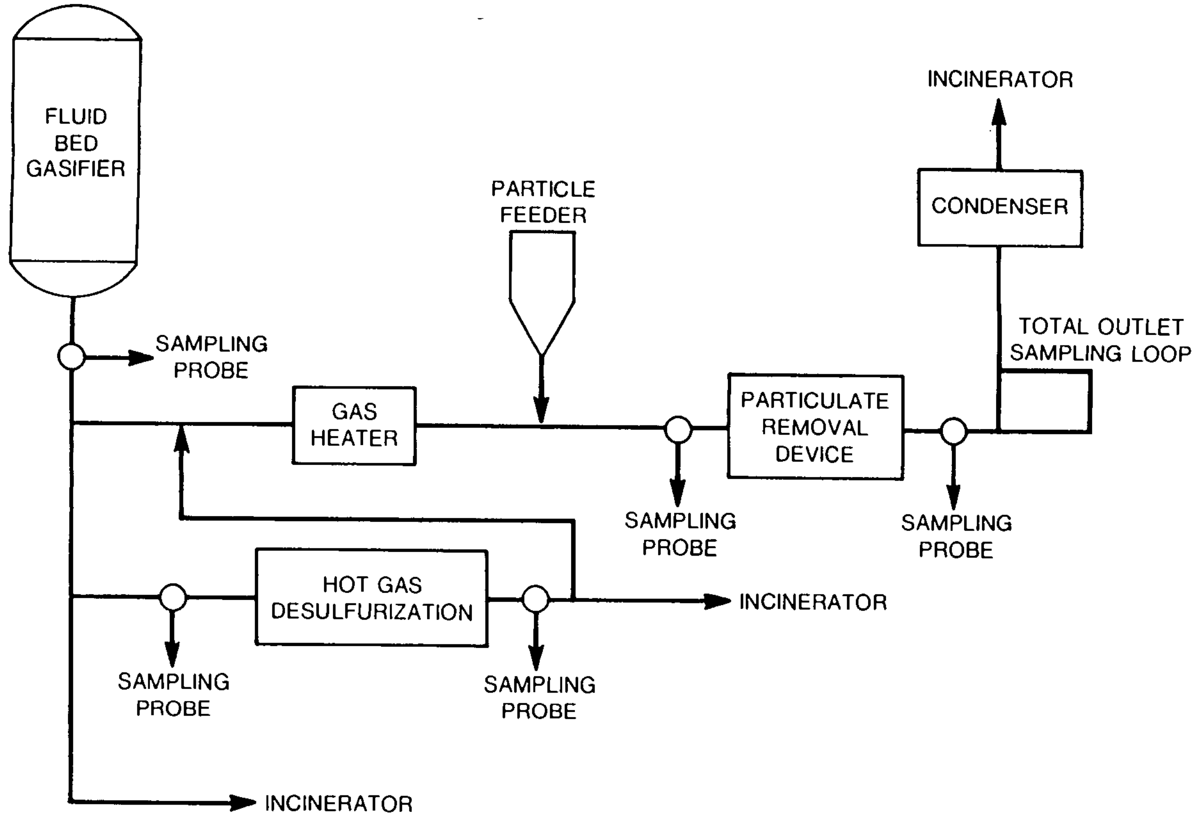

Figure 1
System Components

A-86-046-001 BP1-86

Figure 2 shows the inlet sample line configuration. The particulate samples were collected using 1.37- by 3.94-inch (35- by 100-millimeter), rounded bottom, alundum ceramic extraction thimbles (Norton No. 6406). The thimbles are designed to withstand temperatures up to 2,600°F, and pressure drops of up to 100 psi. The entire sampling line and gate valves were wrapped in high-temperature heating tapes, insulation, and a high-temperature glass cloth (Colombia Fiberglass). The heating tapes, controlled by digital temperature controllers (Omega Model No. CS4001KF), were maintained at 1,000°F. It was necessary to use an alternative heating method for the thimble holders because of their high mass. An 8-foot by 1/8-inch heating rod (ARI Industries, Inc.) was coiled around the elongated section of a thimble holder by means of metal hose clamps. The heating rods were powered from variable autotransformers set at 100 to 120 volts. The gas temperature at the downstream end of the thimble holders was typically 350° to 400°F for the inlet samples and 700° to 800°F for the outlet samples.

Approximately 30 feet of 3/8-inch stainless steel tubing separated the thimble holder from the flow monitoring system. This was necessary because of the shortage of available space in the test device area. The flow monitoring system consisted of a cooling coil, a condensate trap, and a flowmeter (rotameter). Condensate samples were collected in a 1-liter, stainless steel sampling cylinder (Hoke No. 8LD1000).

The flowmeter, a temperature indicator and a pressure gauge were located between two 1/4-inch needle valves. By adjusting these valves, the desired flow could be maintained at a known pressure and temperature. After metering, the gas was exhausted to an incinerator.

To take a particulate sample, the probe, gate valves, and thimble holder were first heated for 1 hour. Just prior to starting sample collection, the probe was purged with nitrogen for 3 to 5 seconds. The gate valves were opened and then the needle valves on the flow monitoring system were adjusted to set the sample gas flow rate. Sampling times were typically 1 to 2 hours.

After sample collection was completed, the thimble holders were disconnected and allowed to cool before removing the loaded thimble. The condensate was drained and measured so that the contribution of water vapor to the total gas flow could be calculated. The 30-foot section of tubing between the thimble holder and the flow monitoring system was purged with steam and nitrogen after each sample to remove residual condensate from the tubing walls. This was added to the condensate sample.

Figure 3 depicts the configuration of the total outlet sampling system. The sampling system was designed as a bypass loop from the main gas line. The entire gas flow was filtered using two thimble holders in parallel and then the gas was cooled to condense water vapor. The sample loop was isolated by gate valves (Vogt No. 821) upstream and downstream of the thimble holders. The sample loop and thimble holders were insulated and heated as described previously. The condensate was collected in stainless steel vessels which were drained before and just after each outlet sampling. The weight of the condensates was recorded so that the contribution of water vapor to the total gas flow could be calculated. Metal concentrations in the condensate could also be translated into equivalent total gas concentrations.

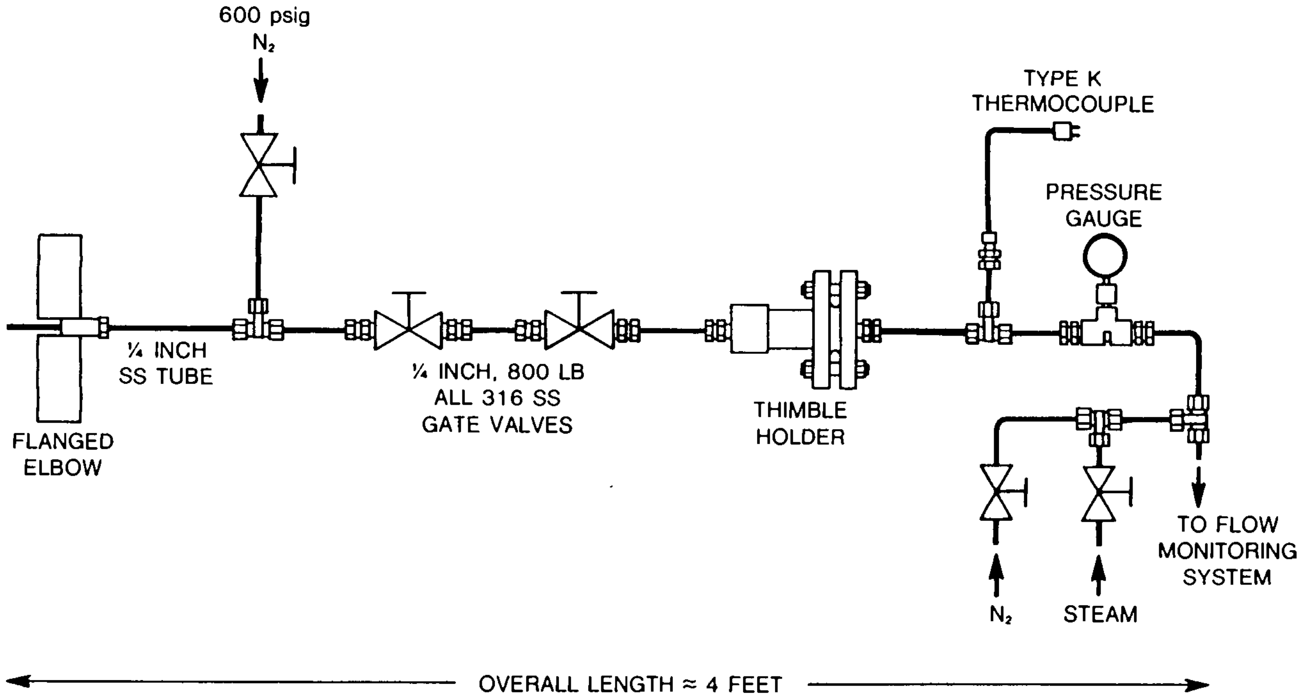

Figure 2
Sampling Probe Configuration

A-86-046-002 BP1-86

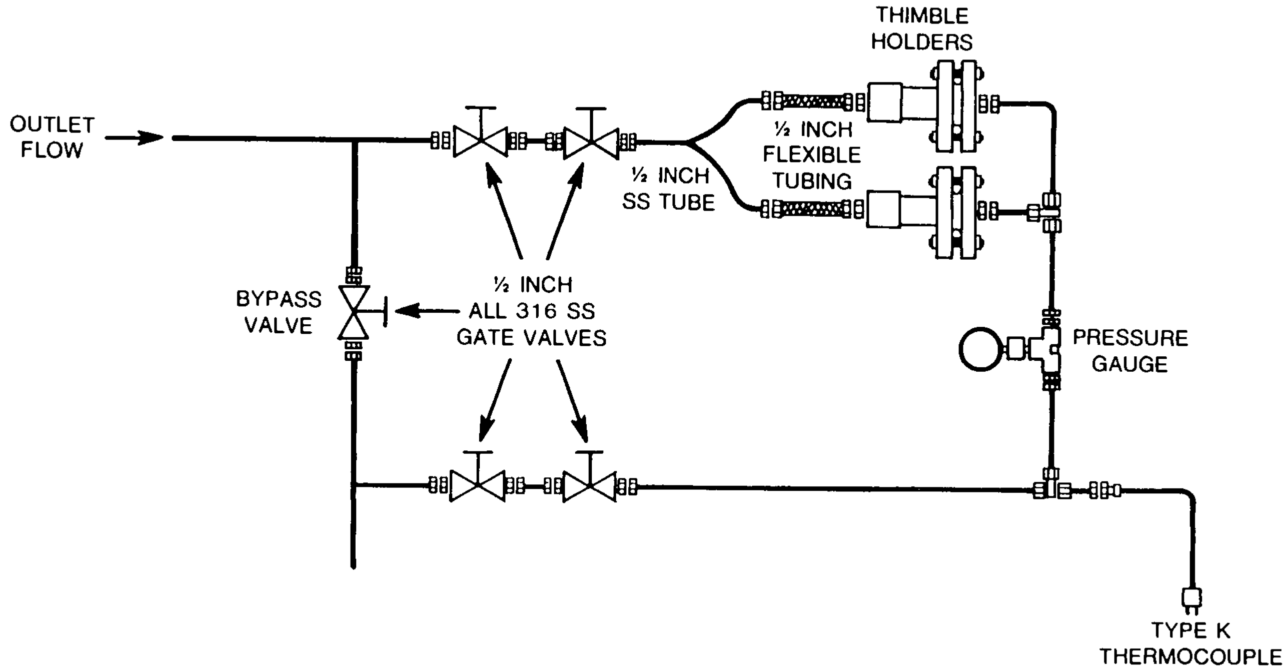

Figure 3
Total Outlet Sampling Configuration

A-86-046-004 BP1-86

Sample Preparation

Thimbles were heated in an oven at 250°F for approximately 30 minutes, cooled in a desiccator, and weighed on an analytical balance prior to being loaded into a thimble holder. After collecting a particulate sample, the thimble holders were extremely hot and were allowed to cool for approximately 30 minutes. The holder was then taken apart and the thimble removed. The thimble, containing the particulate sample, was placed in an oven at 250°F for approximately 45 minutes. After cooling, the thimble was weighed again. The difference in the initial and final weights was taken to be the weight of particles on the thimble. Typically, a small fraction of the particles escaped around the edge of a thimble while in the holder. These particles were collected together with the condensates and filtered out using Gelman Metricel, 47-millimeter, 0.45-micron, Type GA-6 filters under vacuum. The sample was then dried in an oven, cooled in a desiccator, and weighed. This weight was added to the weight of particles collected on the thimble to yield a total sample weight. Portions of the particles collected in the thimbles were submitted for particle size, ultimate, and metals analyses. Particles filtered from the condensates were not used for the chemical analyses because of the possibility that leaching had affected their composition. Particle size analyses were performed using a Model No. TAII Coulter Counter. The pH of the condensates was adjusted to $\leq$ 2.0 by addition of nitric acid, and stored in polyethylene bottles.

The solid and condensate samples were analyzed for 10 metals using a Perkin-Elmer Model 5000 atomic absorption spectrophotometer and a Spectrametrics, Inc., direct plasma atomic emission spectrometer. A lithium metaborate fusion was performed on the solid samples in order to generate a liquid for these analyses.

Data Analysis

As described in the experimental section, the concentrations of the metals in the gas stream were obtained by measuring their amounts in the particles and condensate collected utilizing sampling devices at the inlet and outlet of the test devices, and relating them to the quantity of gas which had flowed through the devices. In the course of the tests, 18 sets of inlet/outlet samples were taken for the Westinghouse ceramic cross-flow filter, 23 for the Acurex fabric bag filter, and 10 for the Denver Research Institute electrostatic precipitator.

The performance of the 3 filters are summarized in Table 1, which gives the average particulate loading of the inlet and outlet gas together with the calculated removal efficiency and the mean particle diameter. The average ultimate analyses of the particulate samples are detailed in Table 2, and Table 3 gives the average gas concentrations of particles, ash, and 10 metals. The calculated values of removal efficiency are also included.

Generally, the Westinghouse filter had the highest particulate removal efficiency followed by the Acurex and DRI filters. Removal efficiency tended to increase with inlet particle loading. The Westinghouse filter tended to result in a lower outlet particle loading than the Acurex or DRI filters because of its higher particulate removal efficiency.

Statistical analysis of the data indicates that, though not strong, there is a correlation between particulate removal efficiency and each of the metal removal efficiencies. The metal removal efficiencies significantly are some

2 to 6 percentage points lower, on average, than the particulate removal efficiency. This cannot be accounted for by gasification of carbon in the particulate on passing through the filters, for a similar result is obtained when compared with the ash removal efficiencies. This may be due to a higher metals concentration in the smaller particles passing through the filters.

A particularly interesting result is that metal removal efficiencies could not be shown to be dependent on operating conditions which varied in the ranges: temperature -- 800° to 1,600°F; pressure -- 140 to 250 psig; and flow rate -- 1,300 to 2,500 scfh. This is especially important for the case of the alkali metals, sodium and potassium, since it is speculated that, at higher temperatures and lower pressures, these relatively volatile species might pass more readily through the hot gas filters.

The average measured removal efficiency for the metals varied slightly among themselves. This is shown in Table 4. In Table 5, the metal concentrations are expressed as the average percentage of the total sum of the ten metals for both the inlet and outlet. These data show that there was an enrichment of Ca in the outlet gas. This was most apparent during the Westinghouse test during which the average Ca concentration increased from 20 percent of the total of the metals at the inlet to 28 percent of the total at the outlet. The source of this enrichment was believed to be the refractory lining of the piping. This assertion is supported by the fact that after the Westinghouse test, the original refractory was replaced with a new refractory that was rated for a higher temperature. Subsequently, during the Acurex and DRI tests Ca enrichment of the outlet gas continued but to a lesser degree. The outlet gas was enriched in Mg and alkalis as well, but to a lesser degree than Ca. These metals are also components of the refractory. The composition of the two refractories is shown in Table 6.

During 50 hours of the Acurex filter test, the hot gas to the filter was first desulfurized by passage through a fixed bed of zinc ferrite (8). The resulting gas tended to have a lower particulate loading comprising smaller size particles. No particulate was added to the gas stream during this period. However, the particulate removal efficiency during this period did not differ significantly from test periods when raw gas was utilized. Nor was it found that the particulate was enriched in zinc, which might have been a consequence of attrition or vaporization of the zinc ferrite bed. The only metal which showed a significant difference in removal efficiency during the test using desulfurized gas was nickel. The efficiency during the desulfurization test was lower.

TABLE 1. CHARACTERIZATION OF PARTICLES IN THE HOT COAL GAS STREAM

	Average Inlet Loading (mg/scf)	Average Outlet Loading (mg/scf)	Average Particulate Removal Efficiency %	Standard Deviation Removal Efficiency %	Average Inlet Mean Diameter (micron)	Average Outlet Mean Diameter (micron)
WESTINGHOUSE (18 samples)	65.91	0.86	98.15	1.42	9.76*	7.50**
ACUREX (23 samples)	64.38	1.91	95.59	4.38	8.76	7.00
DENVER RESEARCH INSTITUTE (10 samples)	72.36	5.03	93.29	4.25	8.84	8.70

* Inlet particulate size data available for 11 samples.

** Outlet particulate size data available for 10 samples.

TABLE 2. ULTIMATE ANALYSIS OF PARTICULATE SAMPLES

Filter	Location	Average Weight Percent				
		Ash	C	H	N	S
ACCUREX	Inlet	34.34	60.12	0.49	0.51	0.83
	Outlet	37.63	59.59	0.37	0.42	0.69
DRI	Inlet	39.34	55.10	0.38	0.69	1.20
	Outlet	38.18	56.94	0.30	0.69	0.85
WESTINGHOUSE	Inlet	34.61	58.22	0.53	0.88	1.36
	Outlet	39.94	55.47	0.44	0.87	1.36

TABLE 3. REMOVAL OF PARTICLES AND METALS FROM HOT COAL GAS

		Average Inlet Concentration (ppm)	Average Outlet Concentration (ppm)	Removal Efficiency (%)
WESTINGHOUSE	Particles	2,365.37	30.87	98.7
	Ash	742.00	12.40	98.3
	Al	105.27	1.75	98.3
	Ca	58.93	1.89	96.8
	Cr	2.62	0.07	97.3
	Cu	1.40	0.04	97.1
	Fe	91.09	2.29	97.5
	K	8.85	0.25	97.2
	Mg	21.08	0.46	97.8
	Na	4.62	0.12	97.4
	Ni	2.44	0.08	96.7
	Zn	0.84	0.03	96.4
ACUREX	Particles	2,310.50	68.55	97.0
	Ash	718.00	23.80	96.7
	Al	89.99	3.09	96.6
	Ca	48.51	2.40	95.1
	Cr	1.08	0.06	94.4
	Cu	1.53	0.04	97.4
	Fe	76.11	2.82	96.3
	K	8.89	0.47	94.7
	Mg	18.22	1.09	94.0
	Na	3.06	0.22	92.8
	Ni	0.61	0.05	91.8
	Zn	0.60	0.04	93.3
DRI	Particles	2,596.90	180.55	93.0
	Ash	969.00	57.7	94.0
	Al	173.61	23.59	86.4
	Ca	46.36	5.88	87.3
	Cr	0.92	0.10	89.1
	Cu	0.73	0.08	89.0
	Fe	113.89	12.80	88.8
	K	21.40	2.12	90.1
	Mg	15.50	2.49	83.9
	Na	5.75	0.72	87.5
	Ni	3.53	0.60	83.0
	Zn	0.62	0.06	90.3

TABLE 4

AVERAGE REMOVAL EFFICIENCIES FOR EACH METAL IN ORDER OF DECREASING EFFICIENCY

Metal	Number of Samples	Average Efficiency (%)
Al	50	93.89
Fe	51	93.73
Cr	51	93.21
K	51	92.83
Cu	51	92.37
Zn	51	91.89
Na	51	91.56
Ca	51	91.05
Mg	51	90.92
Ni	51	89.52

TABLE 5. AVERAGE INLET AND OUTLET PERCENT METAL COMPOSITIONS

Metal	Location	Average Metal Composition (% of Total of Ten Metals) Acurex	DRI	Westinghouse	Average
Al	Inlet	35.50	46.16	32.30	36.46
	Outlet	27.73	42.72	25.22	29.78
Ca	Inlet	22.01	12.88	20.02	19.52
	Outlet	25.56	15.51	28.09	24.48
Cr	Inlet	0.64	0.26	1.45	0.85
	Outlet	0.87	0.47	1.15	0.89
Cu	Inlet	1.14	0.21	0.69	0.79
	Outlet	0.62	0.63	0.57	0.60
Fe	Inlet	27.18	28.15	31.78	28.99
	Outlet	25.43	23.10	30.14	26.64
K	Inlet	3.22	5.13	3.01	3.52
	Outlet	4.12	4.81	4.01	4.22
Mg	Inlet	8.19	4.34	7.39	7.15
	Outlet	10.24	8.49	7.07	8.78
Na	Inlet	1.28	1.49	1.69	1.47
	Outlet	4.20	1.92	1.91	2.94
Ni	Inlet	0.41	1.21	1.33	0.89
	Outlet	0.70	1.95	1.35	1.18
Zn	Inlet	0.44	0.18	0.35	0.36
	Outlet	0.52	0.41	0.50	0.49

TABLE 6. PIPELINE REFRACTORY COMPOSITIONS*

Test	Al_2O_3 %	SiO_2 %	Fe_2O_3 %	TiO_2 %	CaO %	MgO %	Alkalis %
Westinghouse[1]	13.95	30.29	5.34	0.14	35.39	8.81	2.92
Acurex, DRI[2]	38.61	31.48	5.38	1.50	19.54	0.79	1.41

* Plibrico Company Laboratory Report.
[1] Refractory maximum temperature rating was 1,500°F.
[2] Refractory maximum temperature rating was 2,000°F.

Conclusions

Analysis of inlet and outlet particulate samples in a hot coal gas stream passing through three different filtration devices indicates that 10 metals, commonly occurring in coal ash, were removed from the gas stream in proportion to the particulate removal. This remained true up to a temperature of 1,600°F, even for relatively volatile metals such as sodium and potassium. Metal removal efficiencies could not be shown to be dependent on operating conditions for temperatures up to 1,600°F, pressures up to 250 psig, and flow rates up to 2,500 scfh. The efficiency of removal of the metals was slightly less than the particulate removal efficiency, suggesting an enrichment of the metals in the smaller particles escaping through the filter.

References

1. Advanced Environmental Control Technology Program. Morgantown Energy Technology Center. 1981. Report No. DOE/METC/SP-187.

2. Evaluation of Three High-Temperature Particle Control Devices for Coal Gasification. Gas Cleaning at High Temperatures. The Institution of Chemical Engineers Symposium Series No. 99. R. J. Dellefield and R. C. Bedick. 1986.

3. High-Temperature, High-Pressure Particulate and Alkali Control in Coal Combustion Process Streams. K. E. Markel, Ed. 1981. Report No. DOE/MC/08333-167.

4. Second Annual Contractors' Meeting on Contaminant Control in Hot Coal-Derived Gas Streams. K. E. Markel, Ed. 1982. Report No. DOE/METC/82-47.

5. Third Annual Contractors' Meeting on Contaminant Control in Hot Coal-Derived Gas Streams. K. E. Markel, Ed. 1983. Report No. DOE/METC/84-6.

6. Fourth Annual Contractors' Meeting on Contaminant Control in Hot Coal-Derived Gas Streams. K. E. Markel, Ed. 1984. Report No. DOE/METC-85/3.

7. Fifth Annual Contractors' Meeting on Contaminant Control in Coal-Derived Gas Streams. D. C. Cicero and K. E. Markel, Eds. 1985. Report No. DOE/METC-85/6025.

8. Sixth Annual Contractors' Meeting on Contaminant Control in Hot Coal-Derived Gas Streams. K. E. Markel and D. C. Cicero, Eds. 1986. Report No. DOE/METC-86/6042.

9. Seventh Annual Contractors' Meeting on Gasification and Gas Stream Cleanup Systems. M. R. Ghate and K. E. Markel, Eds. 1987. Report No. DOE/METC-87/6079.

7B:4-28-87:dc:5b

OPPORTUNITIES FOR MEMBRANE SEPARATION PROCESSES IN COAL GASIFICATION

R.W. Baker, C.-M. Bell, I. Pinnau and J.G. Wijmans

Membrane Technology and Research, Inc.
1360 Willow Road, Menlo Park, CA 94025

The separation of hydrogen from synthesis gas is a major cost element in the manufacture of hydrogen from coal. Separation of these gases by membranes is an alternative technique that is still largely unexplored and that could offer substantial cost savings. We have been developing membranes for this application at Membrane Technology and Research, Inc. Most of this work has been supported by the U.S. Department of Energy.

There are three opportunities for membrane separation in the production of hydrogen from coal:

(1) The separation of hydrogen from carbon monoxide before the shift reactor.

(2) The separation of hydrogen from carbon dioxide and hydrogen sulfide after the shift reactor.

(3) The separation of hydrogen from nitrogen after the acid gas removal in an air-blown gasification process.

After reviewing polymer permeability data available in the literature or obtained at MTR, two polymers were selected for membrane development work:

(1) <u>Poly(etherimide)</u> for the separation of hydrogen from nitrogen and from carbon monoxide.

(2) <u>Poly(ether-ester-amide)</u> for the separation of hydrogen sulfide and carbon dioxide from hydrogen.

After characterizing the membrane properties of relatively thick (20-50 μm) films, we concentrated on fabricating asymmetric and composite ultrathin high-performance membranes. Asymmetric or composite ultrathin membranes in which the permselective layer is on the order of 0.5- to 1.0 μm-thick are required if usefully high membrane fluxes are to be obtained. The membranes were then tested with pure gases and gas mixtures.

POLY(ETHERIMIDE) MEMBRANES

The properties of the poly(etherimide) membranes are summarized in Figure 1. As shown, these membranes are extremely permeable to hydrogen compared to nitrogen and carbon monoxide. Poly(etherimide) membranes would, therefore, be most suitable for these separations. Poly(etherimide) is a tough, high-melting polymer. We have shown that the membranes maintain their desirable selectivity properties at temperatures in excess of 90°C. Membrane selectivity for gas mixtures is also essentially independent of feed gas composition, as the results in Figure 1 show. The membranes have been fabricated into continuous rolls of flat-sheet membranes and into hollow fibers.

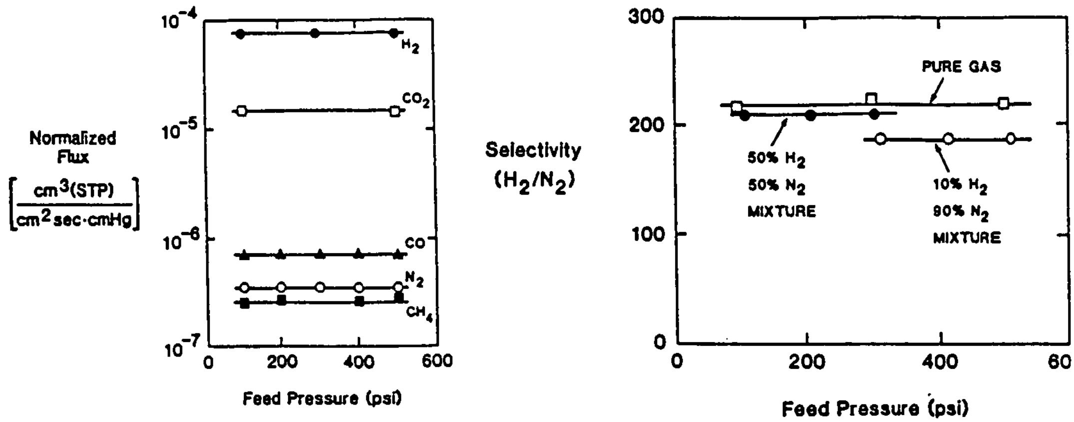

Figure 1. Normalized fluxes and selectivities of poly-(etherimide)/poly(dimethylsiloxane) composite membranes as a function of feed pressure. Temperature: 25°C.

POLY(ETHER-ESTER-AMIDE) MEMBRANES

Poly(ether-ester-amide) membranes are extremely selective for carbon dioxide, compared to other gases, as the data in Figure 2 show. Thus, these membranes are most suited to the separation of carbon dioxide from hydrogen/methane/nitrogen mixtures. Based on data from pure gases, a carbon dioxide/hydrogen selectivity greater than 10 would be expected. With gas mixtures, plasticization of the membrane by carbon dioxide lowers the selectivity to between 7 and 8. This mixed gas selectivity is lower than the pure gas selectivity, but still much higher than other polymeric membranes.

We have fabricated these poly(ether-ester-amide) membranes into spiral-wound membrane modules and tests with these modules are underway.

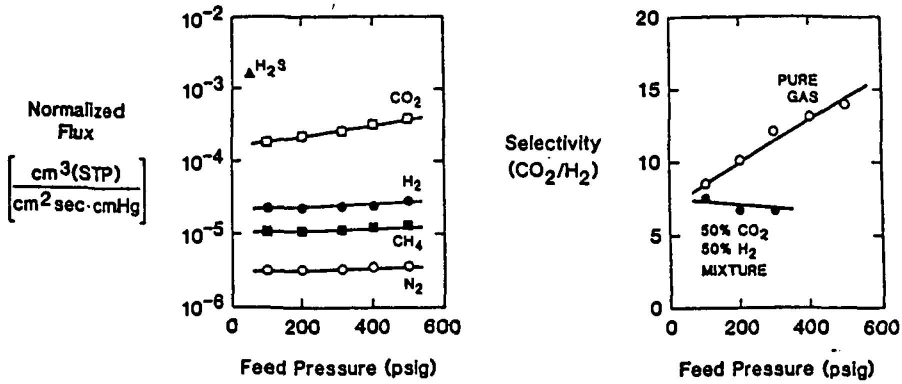

Figure 2. Normalized fluxes and selectivities of poly-(ether-ester-amide) composite membranes as a function of feed pressure. Temperature: 25°C.

STUDIES OF CATALYTIC UPGRADING OF LOW-SEVERITY
LIQUEFACTION PRODUCTS FROM LOW-RANK COALS

Edwin S. Olson, John W. Diehl and Ramesh Sharma

University of North Dakota Energy and Mineral Research Center
PO Box 8213 University Station
Grand Forks, ND 58202

Introduction

The optimal liquefaction conditions for low-rank coals appear to be the use of a two stage process, where relatively low temperatures (380^{o}) are used in the first stage because of the higher reactivity of low-rank coals and the tendency to coke at higher temperatures. This low-severity product can then be subjected to a secondary upgrading process to give a better fuel product. Much of the carboxylate groups of the coal are decarboxylated in the first stage, thus the second stage reaction involving catalytic hydrogenation does not waste much hydrogen on reactions with the evolved carbon dioxide. Transformations of the numerous oxygen functional groups of the low-rank coals occur during both the low-severity and the hydrotreating steps along with the depolymerization and other conversions, and the objective of our studies is to understand these transformations on a quantitative basis and correlate with the other liquefaction parameters, such as yields, changes in molecular weight distributions, and changes in hydroaromatic groups.

This paper is concerned with the catalytic hydrotreatment of a low-severity product obtained from the liquefaction of a Wyodak subbituminous coal in tetralin solvent at $384^{o}C$ (1 hour) in carbon monoxide plus hydrogen sulfide. The low-severity product was separated into two fractions, a methylene chloride soluble fraction and methylene chloride insoluble fraction. The results from second stage liquefaction of the methylene chloride soluble fraction under various conditions will be reported here. This fraction comprised the major portion of the low-severity product. The second stage reaction used the same solvent as the first stage. This solvent was chosen because it does not contain oxygen and is a simple system whose products, naphthalene, decalin, methylindan, butyl benzene and dimers, can be easily distinguished in the reaction products. Two reaction temperatures ($425^{o}C$ and $450^{o}C$) were used in the high severity treatments. Runs for one or two hours were conducted. Hydrogen pressure was another variable during these investigations, although all reactions contained the same amount of the sulfided Co-Moly catalyst.

Experimental

In a typical run, methylene chloride solubles (20 g including tetralin solvent) obtained from the low-severity Wyodak liquefaction in tetralin and 0.80 g of sulfided Co-Moly catalyst (AMOCAT) were sealed in a 75 ml tubing bomb. The tubing bomb was evacuated and pressurized with 300 or 400 psi of hydrogen, if needed in the test. The tubing bomb was lowered into a fluidized bed sand bath maintained at the desired temperature (425^{o} or 450^{o}C). The bomb was heated with constant agitation for the desired time (1 or 2 hrs). At the end of the reaction, the tubing bomb was removed from the sand bath, cooled to room temperature and slowly depressurized. The raw product slurry obtained on opening the tubing bomb was transferred to a beaker with methylene chloride and was separated into various product fractions.

The following products were obtained from the product work-ups of the high severity liquefaction product slurry (1):

1) methylene chloride insolubles
2) pentane insolubles
3) low-boiling (less than 160^{o}C/1.4 torr) distillate (mainly solvent, see below)
4) high boiling (160-240^{o}C/1.4 torr) distillate (contains some solvent and dimers, see below)
5) vacuum bottoms (nondistillable material)

The conversion was calculated as the conversion of the pentane insoluble fraction of the low-severity material to pentane soluble material during the high severity liquefaction, and these data are given in Table 1. Of course this conversion is not the only description of reaction progression of interest. The product yield (coal-derived material) in the distillates is also very important. Also of interest is the retrograde reaction which results in methylene chloride insoluble material.

The product distillate yields were then calculated by subtraction of the solvent (tetralin, naphthalene, and decalin) from the low-boiling distillate yield and adding this to the result obtained by subtraction of the the solvent-derived dimers (bitetralin, binaphthyl, naphthyltetralin, etc.) from the high boiling distillate yield. The solvent distillate yields are a combination of the amounts of tetralin, naphthalene, decalin in both distillates plus the solvent-derived dimers in the high boiling distillate.

The volatile products were characterized by GC-FID and GC/FTIR/MS, the nonvolatile products were characterized by photoacoustic FTIR, solid state or solution ^{13}C NMR and weight average molecular weight determinations (low angle laser light scattering photometry).

Results and Discussion

Conversions

The data summarized in Table 1 reveal that the degree of conversion is dependent on several factors. The reaction at 425^{o}C for one hour with no hydrogen present gave a conversion of only 30%. Raising the processing temperature to 450^{o} for the same time and with no hydrogen pressure increased the conversion to 84%. Also increasing the contact time from one hour at 425^{o} to two hours (no hydrogen) increased the conversion to 78%. In the tests with 400 psi of hydrogen, the conversions increased to 66% at 425^{o}C for one hour and to 92% at 450^{o} for one hour. The two hour reaction under hydrogen (charged to 300 psi, run one hour, recharge to 300 psi, run another hour) gave 80% conversion. Thus the conversion is directly proportional to the reaction temperature, the reaction time, and the added hydrogen pressure.

Another interesting feature of the high severity reactions was the solvent conversion, that is tetralin to naphthalene as a result of hydrogen donation to the coal-derived material. The tetralin to naphthalene ratios in the products from high severity treatments were calculated from the GC/FID determinations of the volatile material (low boiling distillate plus a very small amount in the high boiling distillate) and compared with the ratio initially present in the low-severity product. These ratios are also reported in Table 2. The initial tetralin/naphthalene ratio in the low-severity product was 27, indicating the relatively low hydrogen consumption in the low-severity reaction.

The high severity reactions changed the tetralin/naphthalene ratios significantly. The reaction at 425^{o} for one hour without added hydrogen gave a ratio of 3.31. This corresponds to the formation of 3.7 g of naphthalene (24 mmoles) or transfer of 48 mmoles of H_2 from the tetralin to the coal material during the reaction. Increased reaction time further decreased the ratio (to 2.76). Raising the temperature to 450^{o} for one hour, with no hydrogen added, dropped the ratio even more to 2.06, which indicates that more hydrogen is transferred to the coal fragments at higher temperatures and is consistent with the more extensive conversion which was observed at the higher temperature. When molecular hydrogen was added to the reaction mixture (425^{o}, one hour, 400 psi H_2), the ratio of tetralin to naphthalene was somewhat greater (4.16) than that observed when no hydrogen was added (3.31). Longer reaction times with hydrogen present similarly gave higher ratios (2.51) than those reactions with no hydrogen present (2.76), but lower ratios than the one hour reactions. Thus the tetralin/naphthalene ratios for the high-severity ratios are inversely proportional to the reaction temperature and the reaction time and directly proportional to the hydrogen present. These results are in agreement with the conversion percentages, that is the higher the conversion, the more hydrogen was transferred.

Methylene chloride insoluble product

The methylene chloride insoluble material isolated from the reaction products consisted of the added Co-Moly catalyst plus only about 1% of material derived from the starting low-severity material. The insoluble material was studied using photoacoustic FTIR spectroscopy and was found to contain both alkyl and aromatic groups. This material may be the product of retrograde or cross-linking reactions of the some of the macromolecules of the low-severity product which occurred during the catalytic high severity reaction. Although it cannot be described exactly as coke, since it has alkyl groups, the retrograde reaction which produces these small amounts may be similar to that described as "coking."

Since the amount of this material is insignificant even in reactions at 450^{o}C with no hydrogen pressure, the soluble low-severity product is not likely to be the source of the coked material obtained during some liquefaction experiments with whole coals. More likely the source is the more aromatic and less soluble part of the coal which continues to donate hydrogens to the more soluble portions until it becomes the coke.

Pentane insoluble product (Methylene chloride soluble)

The decrease in the amount of the pentane insoluble fraction in going from the low-severity material to the high severity product has been discussed above in terms of the conversion of the reaction, which was shown to be highly dependent on the conditions chosen for the high severity reaction. The question of interest here is how did the structure and properties of the recovered pentane insoluble fraction change in comparison with the pentane insoluble fraction of the starting low-severity material, as a result of the high severity liquefaction carried out under different conditions

The changes in the molecular weights of the coal macromolecules during second stage processing of this methylene chloride soluble fraction from low-severity liquefaction of Wyodak was investigated by static low angle laser light scattering (LALLS) photometry in tetrahydrofuran solvent. This product was nondistillable and nonvolatile. Rayleigh scattering factors were measured for the dilute THF solutions of the pentane insoluble products and corrected by means of the Cabannes factors which were determined for each of the solutions used. The corrected Rayleigh factors gave a linear reciprocal scattering plot ($KC/\bar{R}_{\theta iso}$ versus C) with an r^2 of 0.99. The weight average molecular weight of the pentane insoluble fraction of the starting low-severity material was 5.6 x 10^5 daltons. The weight average molecular weight of the pentane insoluble material recovered from the high severity treatment in tetralin solvent at 425^{o}C for one hour in the absence of added hydrogen was 6.27 x 10^6 daltons, a significant increase over that observed for the pentane insoluble fraction of the starting Wyodak low-severity product. An increase in molecular weight was also observed for the pentane insoluble fractions recovered from the high severity treatment of Big Brown lignite in work done earlier (2). There may be two reasons for the increase. First, a selective reaction of the lower molecular weight material during the heating a 425^{o}C would have changed the distribution to a higher molecular weight. Second, the liquefaction reactions may involve some retrograde or polymerization reactions which would increase the molecular weight distribution of this fraction.

The pentane insoluble material recovered from the high severity reaction at 425^o for one hour with hydrogen (400 psi) gave a weight average molecular weight of 4.06 x 10^6. Again this value is larger than that of the starting pentane insoluble material, indicating either the change in distribution by preferential reaction of lower molecular weight material or retrograde reactions were occurring. The main difference between this material and that isolated from the high severity reaction carried out without hydrogen is that the amount of pentane insoluble material obtained in the presence of hydrogen is much smaller, possibly as a result of minimization of the retrograde reaction by the molecular hydrogen.

Further characterization of the pentane insoluble fractions were carried out using photoacoustic-FTIR and solid state ^{13}C NMR spectroscopy. FTIR spectra of the fractions recovered from the high severity reactions when compared with that of the low-severity fraction showed an increase in the aromatic absorptions at 1600 cm^{-1}. The carbonyl absorptions in these products were insignificant. The increase in aromatics was confirmed by the NMR spectra. The low-severity material showed an aromatic carbon to aliphatic carbon ration of 1.47. This ratio was 3.25 in the pentane insoluble fraction from the reaction at 425^o for one hour in tetralin in the presence of 400 psi of hydrogen. The ratio was even higher in the product of the reaction at 425^o for 2 hours in the absence of hydrogen (3.84). These NMR data for the various fractions show that there is a preferential solubilization of the aliphatic material. Two explanations are possible. First, aliphatic material may be cleaved from the aromatic clusters of the coal macromolecules. Second, the more aliphatic members of the distribution of macromolecules may be preferentially degraded during the high-severity liquefaction. The higher ratio for the reaction in the absence of hydrogen as compared with that for the reaction in the presence of hydrogen may be explained in several ways.

First, aromatics may be converted to hydroaromatics in the presence of hydrogen. Second, alkyl radicals formed in the thermal degradations may be converted to alkanes by trapping with molecular hydrogen when present or by reacting with coal structures which result in formation of aromatics in the absence of hydrogen.

Solvent-derived distillate

The low boiling distillates obtained from low-severity treatment of Wyodak in tetralin and the high-severity treatments under various conditions were characterized using GC/MS. The low-severity low boiling distillate consisted mainly of tetralin and naphthalene (T/N ratio = 27) along with small amounts of decalin and methylindan. No significant amounts of solvent-related dimers were found in the low-boiling distillates. The coal derived material in this distillate is discussed separately below.

The high boiling distillate (160-240^{o}C/1.4 torr) consisted of small amounts of tetralin and naphthalene and the dimers (bitetralyl, binaphthyl, naphthyltetralin, naphthyldecalin, etc.) derived from the solvent in addition to the coal-derived material. Some of these dimers were present in the distillate from the methylene chloride soluble fraction of the low-severity material. The amounts of this material formed from the solvent was greatest at the lower (425^{o}) temperatures when no hydrogen was present and was the least at the high temperatures with or without hydrogen pressure.

Product distillate

A small fraction of the low boiling distillate consisted of coal derived material such as phenols, alkanes and arylalkanes. The volatile material in the high boiling distillate fraction which was derived from the low-severity product was mainly n-alkanes plus the usual variety of 1 to 4-ring aromatics (unsubstituted and alkyl substituted). Substantial amounts of diphenyl ethers and dibenzofuran were found.

The coal-derived product was only 1% of the amount of the low boiling distillate of the methylene chloride soluble fraction of low-severity material but was 2/3 of the high boiling distillate of the low-severity material. The sum amounted to 33% of the mass of the methylene chloride soluble low severity material. As a result of the high severity treatments, the amount of distillable product increased in all cases; the highest yield was obtained for the 450^{o}C reaction with hydrogen, where 81% of the total liquefaction product was the distillate.

Vacuum bottoms

The vacuum bottoms are the undistillable materials left after distillation of the pentane solubles at 1.4 torr. The amounts of the vacuum bottoms obtained from the low-severity product of Wyodak was 0.56 g/batch or 15.6% of the total coal-derived material in the low-severity product. The amounts of vacuum bottoms increased slightly for the high-severity treatment at 425^{o}C with or without added hydrogen. However, raising the reaction temperature to 450^{o}C resulted in decreased amounts of vacuum bottoms.

The vacuum bottoms were characterized using infrared spectroscopy, molecular weight determinations, and proton-decoupled solution ^{13}C NMR in deuterated chloroform. Both the infrared spectra and the solution NMR spectra indicate that the vacuum bottoms obtained from the high severity liquefactions are more aromatic than the distillates, but not nearly as aromatic as the pentane insoluble fractions discussed above. The bottoms obtained from the reaction at 450^{o}C with no hydrogen added had an aromatic carbon to aliphatic carbon ratio of 1.73.

The vacuum bottoms fractions contained some material which sublimed at 0.25 torr and 250^{o}, but the remainder exhibited large Cabannes factors and large Rayeigh scattering, giving molecular weights of 10^5 daltons.

Conclusions

The low severity methylene chloride soluble product consists of a high molecular weight pentane insoluble fraction, a high molecular weight vacuum bottoms fraction and one third distillable oils. This material was converted by the high severity conditions into a product consisting of small amounts of a higher molecular weight pentane insoluble fraction, a high molecular weight vacuum bottoms fraction, and an increased amount of a distillable oil product. The relatively small amount of the high molecular weight aromatics in the distillate or volatiles may be a consequence of the absence of very large polycondensed aromatic clusters in the low severity product. When the macromolecules are cleaved they go all the way to small molecular weight species. A similar distribution was observed in the Wyodak ITSL product reported by Moroni (3).

Acknowledgements

Financial support of this work was provided by the US Department of Energy under Contract No. DOE-FE21-86MC10637. The assistance of Michael L. Froehlich in obtaining solid state NMR spectra is gratefully acknowledged.

References

1. Olson, E.S. Quarterly Report of Investigations, UNDEMRC, Oct. to Dec. 1987.
2. Olson, E.S. Direct Liquefaction Contractor's Review Meeting, Pittsburgh PA (Oct. 6-8, 1987); Abstracts, p.32.
3. Moroni, E.C., ACS Division of Fuel Chemistry, Preprints, (1987) 32(1), 611-616.

TABLE 1

#	Reaction Conditions	Products (in gms)				Conversion (%)	
		PI	Prod. Dist.* (%)**	B	Total	(PI → PS)	T/N Ratio
1.	Starting Material (L,S)	1.60	1.05 (33.0)	0.56	3.21	--	27.0
2.	425-1-0H_2	1.10	1.27 (43.0)	0.57	2.94	30.00	3.26
3.	425-2-0H_2	0.33	1.76 (63.0)	0.73	2.84	78.7	2.76
4.	425-1-400H_2	0.52	1.27 (50.8)	0.71	2.50	66.40	4.16
5.	425-1+1-300+300	0.31	1.66 (62.64)	0.68	2.65	80.1	2.51
6.	450-1-0H_2	0.24	1.67 (69.87)	0.48	2.39	84.50	2.06
7.	450-1-400H_2	0.15	2.23 (81.10)	0.37	2.75	92.0	3.40

* Wt %: does not include low boiling phenolic products (<60°C at 1.4 torr)

** % of total coal-derived products.

PI = Pentane Insolubles

PS = Pentane Solubles

B = Vacuum Bottoms

T/N = Tetralin/Naphthalene

L.S = Low Severity

UPGRADING OF COAL DERIVED OIL BY INTEGRATING HYDROTREATMENT TO THE PRIMARY LIQUEFACTION STEP

Ulrich R. Graeser, Rolf Holighaus
VEBA OEL Entwicklungsgesellschaft mbH, D-4650 Gelsenkirchen-Hassel

Klaus D. Oohms, Josef Langhoff
Ruhrkohle Oel und Gas GmbH, D-4250 Bottrop

The Bottrop Coal Liquefaction Project

The coal liquefaction project in the Coal Oil Plant in Bottrop, West-Germany, pursued the following targets:

- Demonstration of the improved Bergius-Pier hydrogenation technology on a technical scale
- Testing and further development of process-related and mechanical components
- Identification of environmental impact
- Development of design data base for a commercial unit and
- Generation of technical and operational know how.

The Pilot plant in Bottrop with a capacity of 200 t maf coal/day was erected in order to meet these targets.

The project was initiated in late 1977. After the engineering and construction phase, the plant came on stream in November 1981 and was operated up to May 1987.

The plant was layed out for

300 bar pressure,
475 - 490 °C reaction temperature and
the use of red mud as catalyst.

The project was pursued jointly by RUHRKOHLE AG and VEBA OEL AG. It was from the very beginning supported substantially by the State Government of Northrhine Westfalia and starting from 1984 also by the Government of the Federal Republic of Germany.

The initial process configuration is shown in Fig. 1. In this project phase the program focussed on the primary conversion of coal, using liquid phase hydrogenation reactors. This procedure yielded a raw oil from coal in the boiling range of naphtha and mid distillate, which was highly aromatic and had high contents of oxygen and nitrogen compounds. Secondary upgrading processes were applied in process development units, in order to convert the primary products into marketable fuels, e.g. gasoline, heating oil, kerosene and diesel fuel. Each of the different upgrading routes included severe hydrotreating as first step.

For this reason, the hydrotreating reactors were in 1986 directly linked to the primary conversion system as shown in the simplified flow scheme (Fig. 2). Contrary to the first mode of processing in which the net product fractions - naphtha and middle distillate - were subjected to upgrading processes in separate units, the total vaporised effluent from the liquid phase reactors including the vacuum gasoil fraction is in the integrated alternative fed to the hydrotreating stage, the so called "gasphase reactors". The new configuration makes use of the complete heat content of the LP reactor effluent and supplies reaction heat from the hydrotreater for the preheating of the fresh coal slurry, improving in this way the complete heat-exchange system thanks to the lower amount of external preheating fuel required. A further advantage of the integrated mode consists of the use of the high pressure of the first step and the secondary upgrading. Only a slightly higher pressure drop over the whole plant - caused by the additional equipment - has to be surmounted in the recycle gas compression.

The fact that the vacuum gasoil fraction from the coal liquids, which is in any case used as slurry oil for the fresh coal, was in the integrated process hydrotreated and hydrogen-enriched caused a large feed-back so the first process step and led to essential improvements in the performance, as described below.

Results

The total operating time of the plant for the coal liquefaction program amounted to more than 28.000 hours. During this time, appr. 166.000 t of coal were converted. Hard coal from the Ruhr Area, such as "Westerholt Coal" or "Prosper Coal", was usually used as feed. However, for comparison with competitive technologies, the program also included a batch of 4.000 t of Illinois No. 6 coal. The process mode with integrated hydrotreating was demonstrated for appr. 2.300 h with a total amount of 18.000 t of processed coal from the Westerholt mine. Fig. 3 compares the yield structures of the two processing modes. Due to the improved quality of the slurry oil, higher oil yields - 57,9 wt-% on maf coal against 50,6 wt-% - were obtained with substantially lower catalyst requirements, lower gas formation and lower amounts of hydrogenation residues.

The effect of integrated hydrotreatment on the sulfur- and nitrogen content of the liquid products is very high (Fig. 4) and leads from a raw oil to the expected refinery feedstock resp. blending component.

In addition, hydrotreatment adds hydrogen to the liquid products, which results in lower densities, aromaticities and higher heating values. The corresponding data for naphtha, middle distillate and vacuum gasoil - used as slurry oil - are listed in the following table:

Tab. 1: Comparison of product qualities

		Naphtha		Middle Distillate		VGO	
		LPH	Int. hydrotr.	LPH	Int. hydrotr.	LPH	Int. hydrotr.
C	(wt-%)	83.1	87.1	86.2	88.4	88.7	88.4
H	(wt-%)	11.8	13.6	9.3	11.9	8.1	11.7
C/H		7.0	6.4	9.3	7.4	11.0	7.6
Aromatic carbon	(wt-%)	29	14	59	21	67	20
Gravity	(kg/m^3)	813	722	979	912	1066	955
Lower heating value	(MJ/KG)	40.2	42.7	39.1	41.3	38.9	40.8

As mentioned above, the new slurry oil quality provided various improvements for the whole process. The hydrotreated vacuum gasoil made it possible to operate the liquid phase hydrogenation section at more moderate conditions. In addition to smaller catalyst requirements, it was possible to reduce the reaction temperature in the liquid phase reactors for 10 - 15 K, which was finally the reason for the lower gas formation and the resulting reduction in the specific overall hydrogen consumption.

While the initial hydraulic conditions in the slurry preparation, the slurry feed system and the preheating section were maintained, the lower density and viscosity of the slurry oil enabled a considerable increase of the coal concentration in the slurry from 40 % to more than 50 %, as well as a raise of the total coal throughput.

As the integrated mode of operation condenses only hydrotreated products instead of the raw materials, the phenol load in the process water stream which is separated from the condensate is reduced to zero. This makes the process water treatment much easier.

A further advantage obtained by the integration of hydrotreatment into the liquefaction process which deserves mentioning is the availability of the reaction heat from the hydrotreater for the whole process. This led to a new concept for the preheating section, shown in principle in Fig. 5. In the original concept, the mixture of slurry and hydrogenation gas is heated in a series of heat exchangers and has to get the required final temperature by passing a gas-fired preheater. This system was very sensitive against deposit and coke formation, especially at the high temperatures prevailing in the preheater tubes. After the integration of the hydrotreating section it was possible, by adding adequate heat-exchanger capacity, to preheat the total amount of slurry together with a small volume of hydrogenation gas - necessary to prevent coking - to an extent that made the us of an additional preheater superfluons. The lacking heat requirement was introduced into the system by overheating the main stream of hydrogenation gas in a separate line by heat exchange and the use of the preheater capacity. With this concept preheater fouling is no problem anymore. To conclude it can be said that the direct connection of the hydrotreating step to liquid phase hydrogenation provided a large improvement for the whole process and yielded products which can be directly fed to refinery streams. The naphtha fraction can be introduced into a refiner/reformer system producing high octane premium-grade motor fuel. The middle distillate fraction may be used as blending component for light heating oil or graded up to diesel fuel by means of ignition accelerators.

Current Use of the Bottrop Plant

The coal liquefaction program in the pilot plant in Bottrop was terminated in May 1987 at a level of technical development and know how which enables the operating companies to design and operate such plants on a commercial scale. The increase in know how which could have been gained from a further continuation of the program would not have justified the financial effort.

However, to keep the technical and operational know how alive and to maintaining the availability the plant for future coal liquefaction requirements, the two companies decided in agreement with the supporting authorities involved to modify the plant for the conversion of vacuum residues from refineries by means of the VEBA-Combi-Cracking process which has the same technological roots as coal liquefaction. The process principle in comparison to that of coal liquefaction is shown in Fig. 6.

The plant capacity for residue conversion amounts to 3.500 bpd of vacuum residue. At a conversion rate of 92 % the productive amounts for:

900 bpd naphtha
2.400 bpd middle distillate and
600 bpd vacuum gasoil

After revamping in the remainder of 1987 the plant was recommissioned in January 1988 with its new feedstock. It is aimed that the future operation will be performed under commercial terms and conditions.

The specific equipment for coal liquefaction is preserved and can at any time be reactivated for coal liquefaction or even coprocessing.

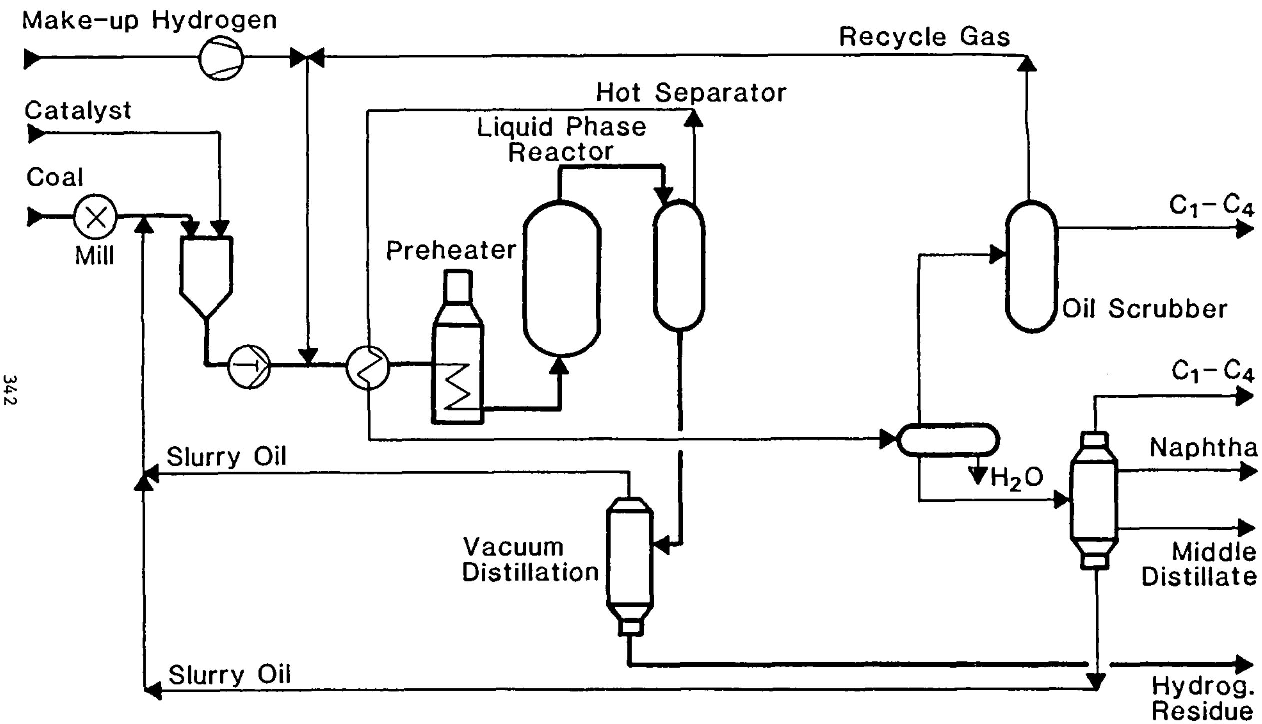

Fig. 1: Liquid Phase Hydrogenation - Initial Process Configuration

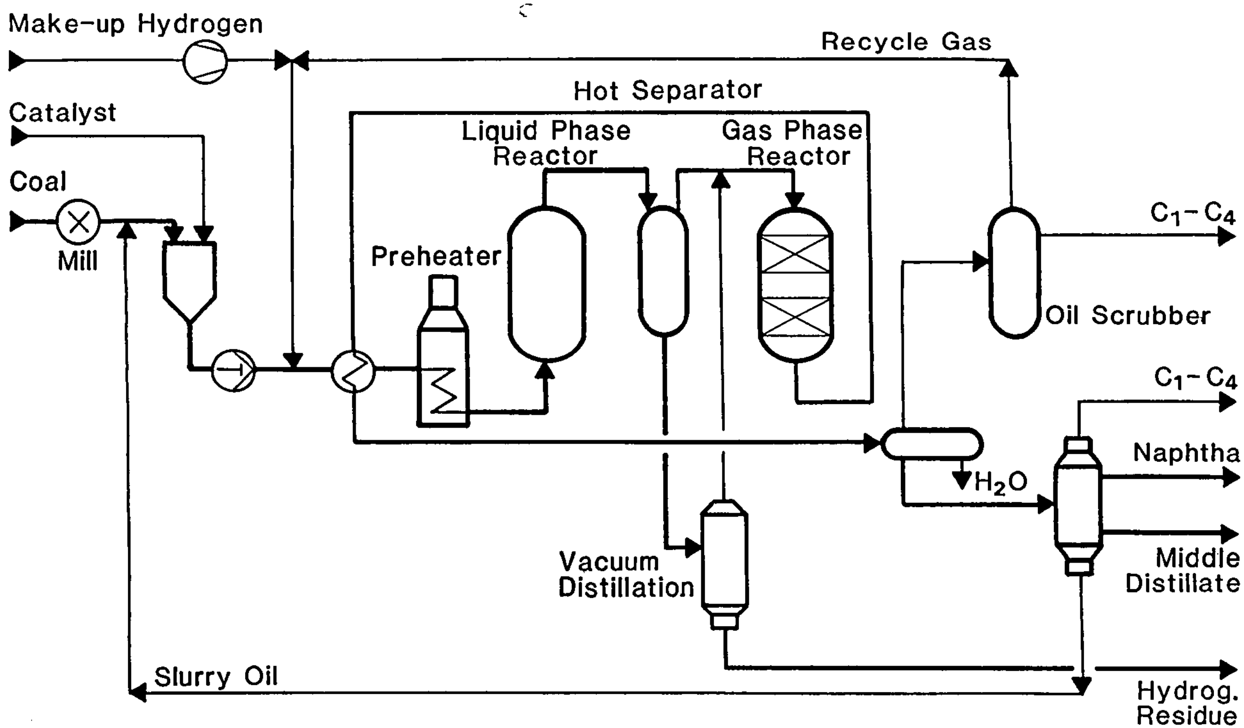

Fig. 2: Liquid Phase Hydrogenation with Integrated Hydrotreatment

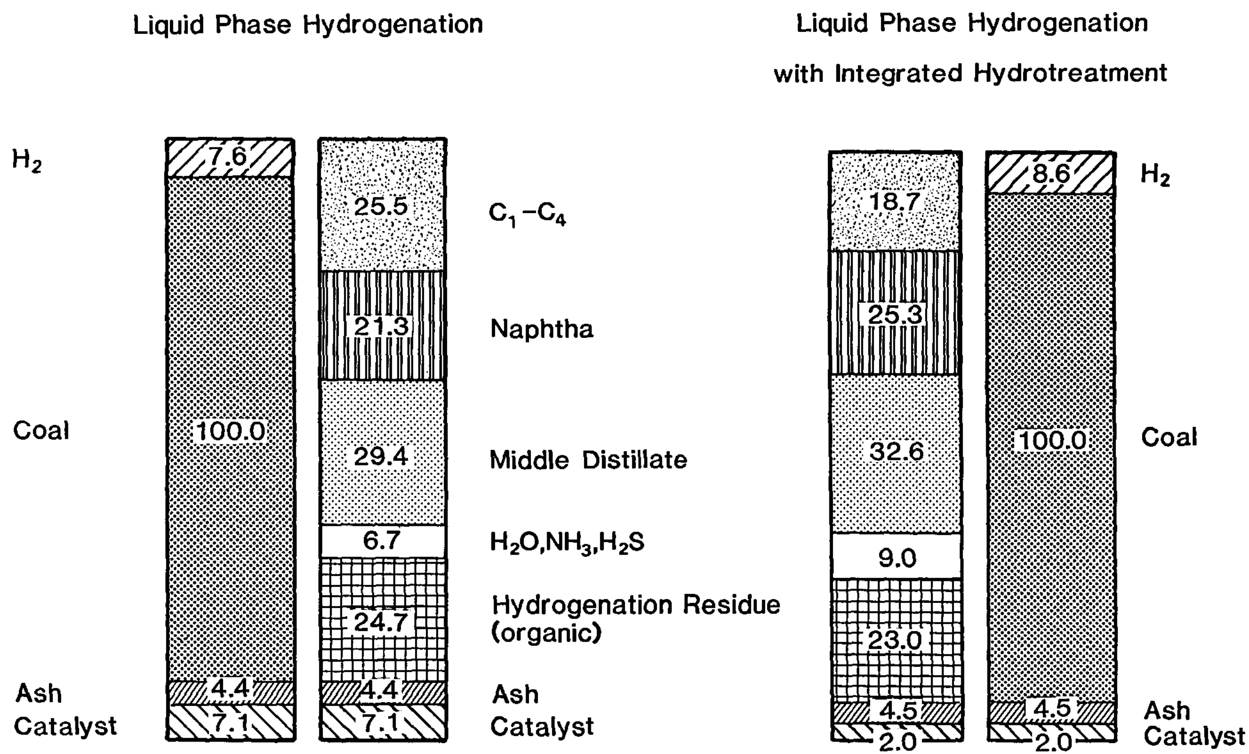

Fig. 3: Comparison of the Yield Structures for the two Process modes

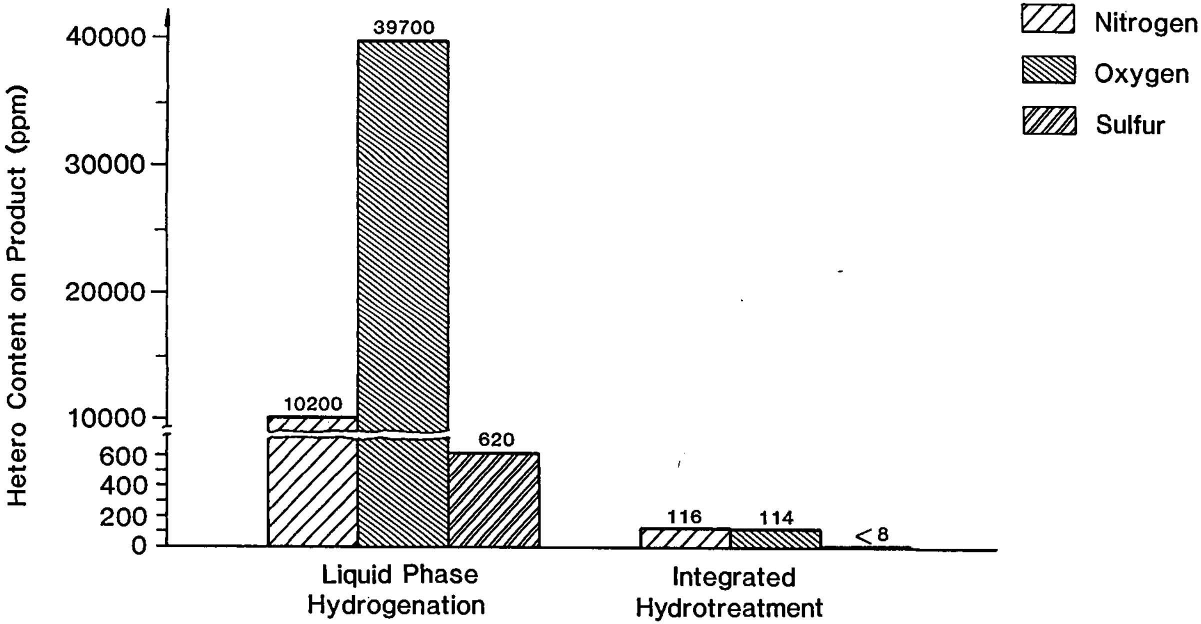

Fig. 4: Hetero Content in Liquid Products

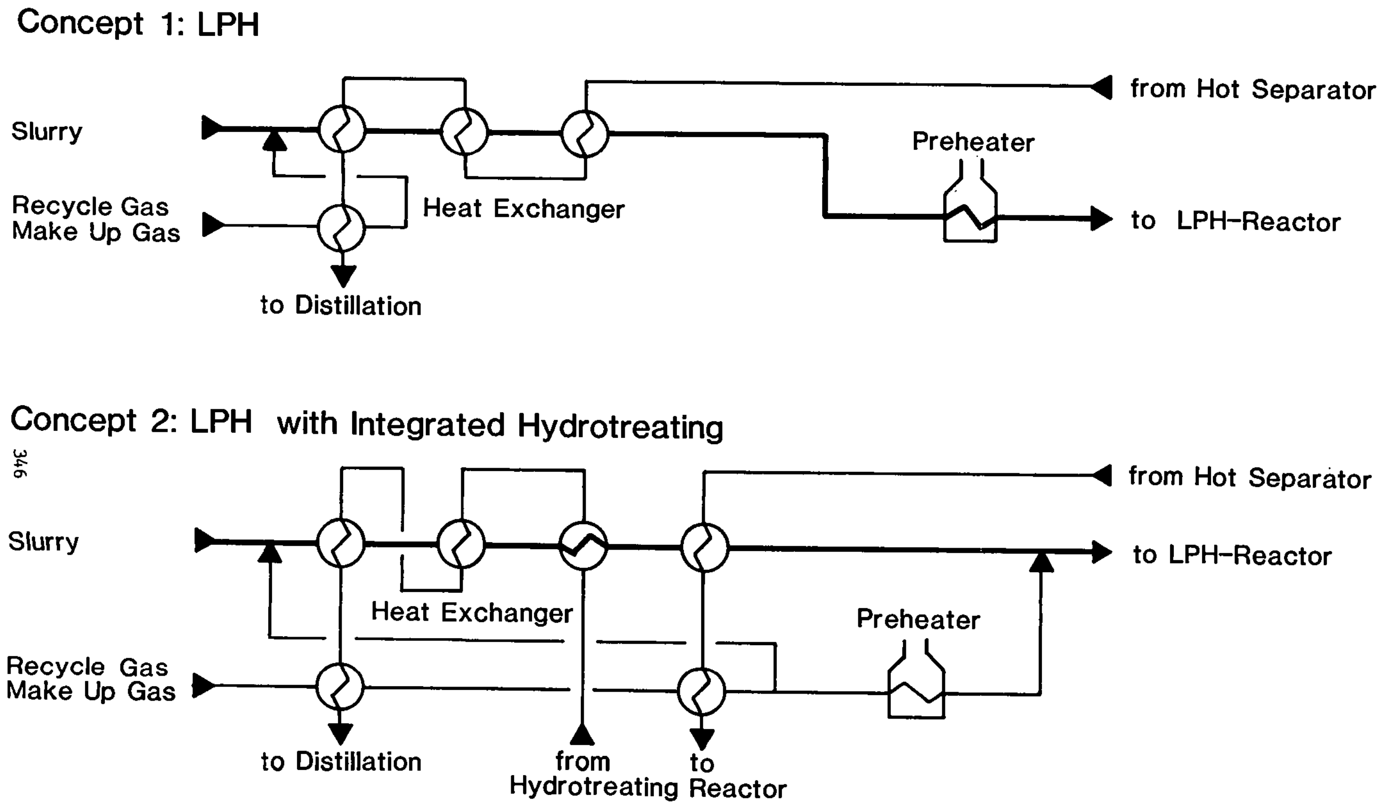

Fig. 5: Preheating Section

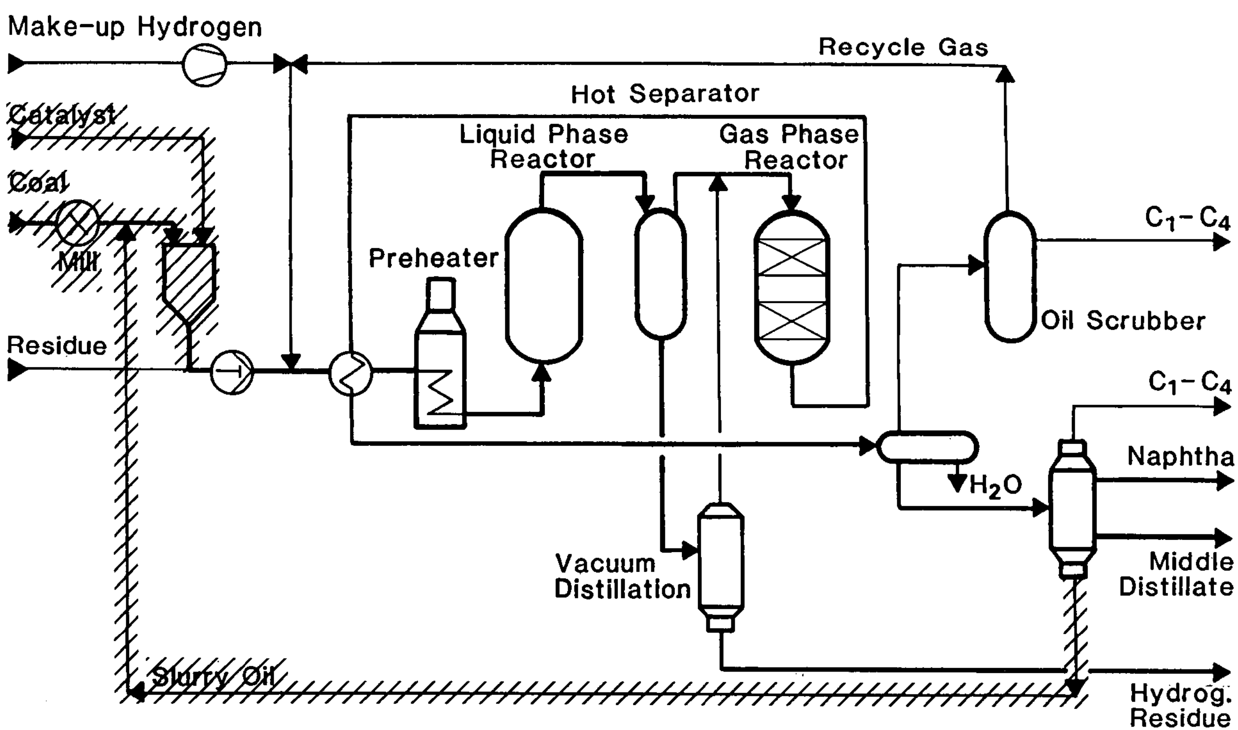

Fig. 6: Coal Liquefaction Plant Bottrop - Residue Conversion Mode

PERFORMANCE OF HYDROUS TITANIUM OXIDE-SUPPORTED CATALYSTS IN COAL-LIQUIDS UPGRADING

by

D. L. Cillo, D. N. Smith, J. A. Ruether,
U.S. Department of Energy,
Pittsburgh Energy Technology Center,
P.O. Box 10940, Pittsburgh, PA 15236,
and
H. P. Stephens and R. G. Dosch,
Sandia National Laboratories,
Albuquerque, NM 87185

ABSTRACT

Experimental tests were performed in a continuous-flow hydrotreating unit at Pittsburgh Energy Technology Center to evaluate the performance of hydrous titanium oxide-supported (HTO) catalysts as hydrotreating catalysts for use in two-stage coal liquefaction. Catalysts containing either a combination of Co, Ni, and Mo as the active metal components or Pd as the active metal component were tested with representative hydrotreater feed stocks from the Wilsonville Advanced Coal Liquefaction Research and Development Facility. Catalyst performance evaluation was based on desulfurization and denitrogenation activity, the conversion of cyclohexane-insoluble material, and hydrogenation activity during 100-hour reactor runs. Results indicated that the HTO catalysts were comparable to a commercial Ni/Mo-alumina supported catalyst in the areas evaluated.

INTRODUCTION

Personnel from the Pittsburgh Energy Technology Center (PETC) have been collaborating with researchers at Sandia National Laboratories (SNL) to further development of the novel hydrous titanium oxide-supported (HTO) catalysts for use in the hydrotreatment of coal-derived liquids. The HTO materials were originally developed at SNL for use as precursors for ceramic materials[1] and as ion-exchange materials for the decontamination of aqueous nuclear waste streams.[2] The properties of these materials, including high surface areas and ion exchange capacities, chemical stability, variable Bronsted acidities, and the ability to apply them in thin films, have led to investigations related to their performance as catalysts in a variety of chemical systems.[3-5] They have also been applied to coal-oil coprocessing,[6] coal hydropyrolysis tars.[7]

The HTO catalysts containing either Co, Ni, and Mo (CoNiMo-HTO) as the active metal components or Pd (HTO-Pd) as the active metal component were tested in a continuous-flow hydrotreater at PETC for possible use as hydrotreating catalysts in the second stage of the integrated Two-Stage Liquefaction process. The PETC has been testing catalysts used in the hydrotreater of the Wilsonville Advanced Coal Liquefaction Research and Development Facility (ACLRDF). Such areas as the effect of catalyst pore size distribution,[8] the effect of active metals loading,[9] and the determination of the thermal component of residuum hydrogenation[10] have been studied. The objective of this study was to ascertain if the HTO catalysts could be used to hydrotreat a typical two-stage liquefaction feedstock material containing coal-derived residuum. Catalyst performance was based on comparison of the desulfurization, denitrogenation, hydrogenation, and cyclohexane-insoluble conversion activities of the HTO catalysts with those of a commercial alumina-supported Ni/Mo-alumina catalyst (Shell 324M) that has been used widely in these types of applications.

Experimental

A typical Two-Stage Liquefaction process[11] consists of a thermal liquefaction first stage, followed by a solvent-deashing step, and a subsequent catalytic-hydrotreating stage (Figure 1). The feedstock for the work described herein came from the Wilsonville ACLRD Facility and consisted of a distillate vehicle from the thermal first stage (designated V-178) and the deashed residuum (WSRC) from the solvent-deashing step. These were supplied to PETC from the Wilsonville ACLRD Facility and have been documented elsewhere.[10,11] Typical analyses of these materials are presented in Table 1. The feedstock used in these experiments consisted of a 1:1 mixture of V-178 and WSRC. The hydrous titanium oxide-supported catalysts were prepared from an HTO-Na material by ion exchange of the Na with Co, Mo, Ni, and Pd from aqueous solutions of their salts. The HTO-Na was prepared by hydrolyzing the product of a reaction between tetraisopropyl titanate and a methanol solution of NaOH. Detailed preparation procedures have been described elsewhere.[3-5]

The HTO catalysts remain in the form of a low-tap-density powder (0.3 g/cm^3) through the ion exchange step used to load the active metals. For this application, the ion-exchanged powders were pressed into discs, which were subsequently crushed and screened to -10/+20 mesh to minimize diffusion effects in comparing the HTO catalysts with the Ni/Mo-alumina catalysts. The latter were obtained as 1/32-inch extrudates. The as-prepared HTO catalysts are calcined prior to use to remove the volatiles (15 to 25 wt %), which consist primarily of water along with small amounts of alcohols. This calcination can be done either in the reactor or in an external furnace before the catalysts are loaded into the reactor. A density change accompanies calcination of the hydrous titanium oxide-supported catalyst, so that bed shrinkage during calcination in a system that utilizes constant catalyst volumes must be compensated for in loading the catalyst bed. In either case the material was calcined in a nitrogen atmosphere using a temperature of 100°C to remove the bulk of the volatiles and a final one-hour soak at 375°C for the CoNiMo-HTO catalysts and at 300°C for the HTO-Pd catalysts.

Sulfiding of the CoNiMo-HTO catalyst was done in the reactor with a hydrogen gas stream containing 10 vol% hydrogen sulfide for five hours at 390°C. The Ni/Mo-alumina catalyst was activated by heating in the same manner. The HTO-Pd catalyst did not require sulfiding prior to use.

Compositions and some physical properties of the catalysts used in this work are presented in Table 2. Two HTO-Pd catalysts are listed because there was a significant difference in the way the materials were prepared. The difference involved the acidification step used to increase the Bronsted acidity of the support; phosphoric acid was used in the preparation of HTO-Pd1, but sulfuric acid was used in the preparation of HTO-Pd2. The use of different acids resulted in variations in surface area, as well as the expected compositional changes.

Two experiments of 100-hour duration using the CoNiMo-HTO catalyst and two experiments of 100- and 700-hour duration using the Ni/Mo-alumina catalyst were completed. The reaction conditions (temperature, pressure, and volume hourly space velocity) were kept the same for both catalyst systems and are presented in Table 3. The reaction conditions used with the HTO-Pd catalysts were the same as those given in Table 3 with the following exceptions. The run using the HTO-Pd1 catalyst was intended to be a 100-hour run but was terminated at 42 hours owing to a power failure. The duration of the run with the HTO-Pd2 was 100 hours; however, the run temperature was held at 320°C for at least 24 hours, and the temperature was then raised to 370°C and finally to 390°C during the course of the run.

RESULTS AND DISCUSSION

The average run results of tests using the CoNiMo-HTO and Ni/Mo-alumina catalysts are presented in Table 4. There were sufficient variations in the slurry feed rate of the continuous-flow unit to cause the volume hourly space velocity to vary, thus precluding a detailed comparison of the catalyst activities. In examining the data in Table 4, it is apparent that there are significant differences in the results of the two CoNiMo-HTO 100-hour runs. This may be because two different batches of catalyst were used, but it is more likely due to variations in the space velocity during the runs. Differences of the same magnitude are observed when comparing the 100-hour Ni/Mo-alumina run with the first 100 hours of the 700-hour Ni/Mo-alumina run. Since these runs did not use different batches of catalyst, the variations in the results are probably due to a variable space velocity. The differences between the average results of the first 100 hours of the 700-hour Ni/Mo-alumina run and those of the final 500 hours of the 700-hour run are due to catalyst deactivation. These differences are not as great as those seen when comparing the initial 100 hours of both Ni/Mo-alumina runs. However, there appear to be trends in the data that allow for a qualitative comparison of the HTO and Ni/Mo-alumina catalyst systems using the average activities calculated over the duration of the runs specified in Table 4.

The CoNiMo-HTO catalyst appears to be similar in overall activity to the Ni/Mo-alumina system (Shell 324M). Hydrogenation activity, as measured by the change in the hydrogen-to-carbon atomic ratio (H/C) of the product as compared to the feed, was on the order of 10% for each catalyst. The range of conversions of cyclohexane-insoluble material to cyclohexane-soluble material and the desulfurization activity of the two catalytic materials also appear to be comparable. The denitrogenation activity of the CoNiMo-HTO catalyst was somewhat lower than that of the Ni/Mo-alumina catalyst based on the 100-hour tests. However, when the level of denitrogenation of the CoNiMo-HTO is compared to the "lined-out" activity of the Ni/Mo-alumina catalyst at 700 hours, both catalysts seem to have similar activities. The activity of the Shell 324 Ni/Mo-alumina catalyst is known to "line out" after approximately 200 hours under the conditions used in these runs. Long-term runs, i.e., 700 hours, with the CoNiMo-HTO catalyst are needed before a more definitive comparison can be made.

One would expect that a noble metal such as palladium would be an ineffective catalyst under the conditions described herein owing to sulfur and nitrogen poisoning. However, batch tests indicated that the HTO support seems to provide some protection to the Pd against sulfur poisoning and that the degree of protection increased with increasing temperature. The Pd catalyst, HTO-Pd1, used in the initial test, which was done under conditions in Table 3, deactivated early in the run. Table 5 shows that the most sensitive indicator of this was the change in H/C atomic ratio of the product with respect to the feed. Conversions of cyclohexane- and pentane-insoluble materials also decreased somewhat while the desulfurization activity appeared to remain relatively constant. The run was prematurely ended at 42 hr owing to a power failure.

The second test of a HTO-Pd catalysts used a material that was considerably different both in composition and in surface area (Table 2). Batch testing indicated that the palladium hydrous titanium oxide-supported catalyst was active at lower temperatures, and consequently, the operation of the continuous-flow unit was altered with respect to reaction temperature as described previously where the temperature was increased stepwise from 320°C to 390°C throughout the course of the 100-hour run. All other experimental conditions were the same as those given in Table 3. At the time this paper was written, the only analytical results available for this run were the H/C ratios given in Table 6. As can be seen, the HTO-Pd2 experienced a decrease in hydrogenation activity during the first 19 hours at 320°C. Increasing the run temperature restored the activity to that observed during the initial 7 hours of the run, and the hydrogenation activity appeared to be increasing during the final 24 hours of the run at 390°C.

CONCLUSIONS AND RECOMMENDATIONS

The experimental results indicate that HTO-supported catalysts such as CoNiMo-HTO are capable of achieving catalytic activities similar to those of a Ni/Mo-alumina catalyst (Shell 324M), which is considered to be as good as any commercial catalyst for this particular application. A HTO-Pd catalyst also showed considerable promise for this application. Both HTO-supported materials must be subjected to further research before definitive comparisons can be made with other catalyst systems.

Previous testing of the Ni/Mo-alumina system has shown that only moderate increases in catalytic activities can be achieved by manipulating the average pore size distribution and pore structure of the alumina support. Since no attempt has been made as yet to modify or optimize the physical properties of HTO supports, there may be potential for significant improvements in these materials.

ACKNOWLEDGMENTS

The authors would like to acknowledge the work of the Gilbert-Commonwealth operating staff at PETC for making the continuous-flow-hydrotreating runs at PETC, and the Coal Science Division at PETC for their cooperation and work in the analysis of the products in a timely fashion.

A portion of this work supported by the US DOE at Sandia National Laboratories under contract DE-AC04-76DP00789.

DISCLAIMER

Reference in this report to any specific commercial product, process, or service is to facilitate understanding and does not necessarily imply its endorsement or favoring by the United States Department of Energy.

REFERENCES

1. Dosch, R.G.; Headly, T.J.; Hlava, P.F. **1984**, J. of American Ceramic Society, 67, 354.
2. Dosch, R.G. **1981**, Sandia National Laboratories Report No. SAND 80-1212.
3. Stephens, H.P.; Dosch, R.G. **1987**, Studies in Surface Science and Catalysis: Preparation of Catalysts IV, 31, 271.
4. Stephens, H.P.; Dosch, R.G.; Stohl, F.V. **1985**, Ind. Eng. Chem., Prod. Res. Dev., 24(1), 15.
5. Dosch, R.G.; Stephens, H.P.; Stohl, F.V. **1985**, U.S. Patent 4 511 455.
6. Monnier, J.; Denes, G.; Potter, J.; Kriz, J.F. **1987**, Energy and Fuels, 1, 332.
7. Bolton, C.; Snape, C.E.; Stephens, H.P. **1987**, Prepr., ACS Div. of Fuel Chem., 32(1), 617.
8. Cillo, D.L.; Stiegel, G.J.; Tischer, R.E.; Krastman, D. **1987**, U.S.DOE Report No. DOE/PETC/TR-87/8.
9. Tischer, R.E.; Stiegel, G.J.; Cillo, D.L.; Narain, N.K. **1986**, U.S.DOE Report No. DOE/PETC/TR-86/1.
10. Technical Progress Report: Run 242 with Illinois No. 6 Coal, **1983**, Document No. DOE/PC/50041-19, July, Contract No. DE-AC22-82PC50041 and Technical Progress Report: Run 243 with Illinois No. 6 Coal, **1984**, Document No. DOE/PC/50041-31, February, Contract No. DE-AC22-82PC50041.
11. Stiegel, G.J.; Lett, R.G.; Tischer, R.E.; Cillo, D.L.; Narain, N.K. **1987**, Canadian Journal of Chem. Eng., 65, 82.

Table 1. Representative Analysis of Feed Materials

	RESIDUUM (WSRC)	VEHICLE (V-178)
Elemental Analysis, wt%		
Carbon	88.6	88.3
Hydrogen	6.8	9.8
Nitrogen	1.3	0.4
Sulfur	0.6	0.3
Moisture, wt%	0.1	0.1
Ash, wt%	0.3	< 0.01
Specific Gravity, 60°F/60°F	1.19	1.01
Solvent Analysis, wt%		
Toluene insolubles	12.1	< 0.02
Asphaltenes*	47.8	4.9
Oils** (by difference)	40.1	94.9

* Toluene soluble, pentane insoluble
** Toluene soluble, pentane soluble

Table 2. Physical Properties and Composition of Catalysts After Calcining

	Shell 324M	CoNiMo-HTO	HTO-Pd1	HTO-Pd2
BET surface area, m^2/g	161	245	116	320
Pore Volume, cm^3/g	0.427	0.310	*	*
Average Pore Diameter, Å	106	39	*	*
Cobalt, wt%	-	0.9	-	-
Nickel, wt%	2.5	1.1	-	-
Molybdenum, wt%	13.0	10.6	-	-
Palladium, wt%	-	-	5.4	7.5
Phosphate, wt%	-	-	17.5	-
Sulfate, wt%	-	-	-	4.5

* Not determined

Table 3. Reaction Conditions for Shell 324M NiMo and CoNiMo-HTO Runs

Pressure	2000 psig
Temperature	390°C
Catalyst charge	80 cm^3
Target hourly space velocity	0.6 cm^3 resid /cm^3 cat
Hydrogen gas feed rate	8 scfh
Slurry feed rate	114 g/hr
Feedstock	WSRC/V178 weight ratio = 1/1

Table 4. Results of Reactor Runs using CoNiMo-HTO and Shell 324M Catalysts

CATALYST	CoNiMo-HTO	CoNiMo-HTO	Ni/Mo-alumina		
			Shell 324M	Shell 324M	Shell 324M
Test duration, hr	100*	100	100	(100)**	200-700
Variation of space velocity	0.49-0.65	0.59-0.74	0.46-0.84	0.57-0.60	0.56-0.63
Percent change in H/C atomic ratio	10	7	9	10	9
Conversions, wt% cyclohexane	73	57	71	58	54
Desulfurization, wt%	85	76	85	71	52
Denitrogenation, wt%	22	20	40	23	16

* The catalyst was contacted with kerosene at room temperature prior to this test, and a carbon residue was left on a portion of the catalyst. This was not planned and did not seem to affect catalyst performance.
** First 100 hours of the 700-hour test

Table 5. Hydrotreating Results Using HTO-Pd1 Catalyst

Time, hr	10	22	35
Percent change in H/C atomic ratio	12	11	3
Conversions, wt%			
cyclohexane	77	78	68
pentane	60	58	56
Desulfurization, wt%	75	75	75

Table 6. Hydrogenation Activity of HTO-Pd2

Operating Conditions temp., °C	time, hr	Change in Atomic H/C ratio, percent
320	7	7
320	10	4
320	19	2
320	23	3
	27 temp. change	
370	35	4
370	36	3
370	45	5
	50 temp. change	
390	63	8
390	67	7
390	73	8
390	85	8
390	91	9
390	98	8

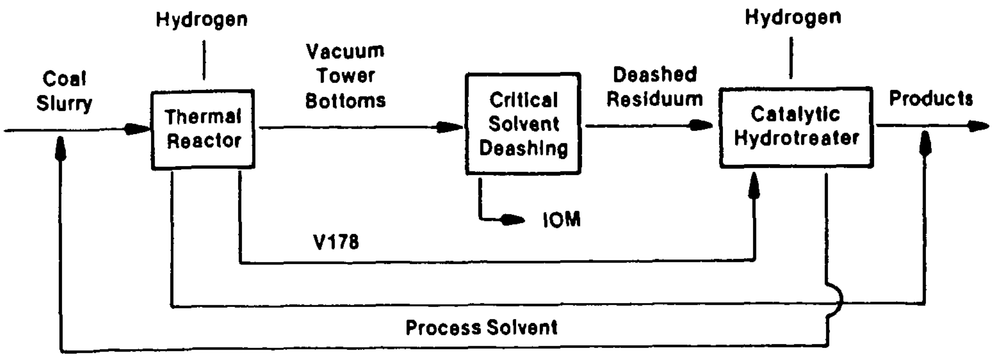

Figure I. Typical Two-Stage Liquefaction Process

HEAVY OIL UPGRADING USING HALIDE CATALYSTS IN A BUBBLING MICROAUTOCLAVE

A. Chakma, E. Chornet, R.P. Overend
Université de Sherbrooke, Sherbrooke, Québec, Canada, J1K 2R1

and

W. Dawson
Energy Research Laboratories, CANMET, Ottawa, Ontario, Canada, K1A 0G1

ABSTRACT

Athabasca bitumen has been treated with halide catalysts under a continuous flow of H_2 in a 15 mL microautoclave. The H_2 was bubbled through the liquid using a microporous steel grid. $ZnCl_2$, CuCl and $ZnCl_2$/CuCl mixtures, with and without tetralin, were used as catalysts. The experimental conditions were: 13.8 MPa operating pressure, 1 L_{STP}/min as H_2 flowrate, 425-450°C and 30 min as reaction temperature and time respectively. $ZnCl_2$ has been found effective for converting asphaltenes into maltenes while lowering the coke formation with respect to the uncatalyzed reaction. The addition of tetralin to the reaction mixture minimized coke and gas formation.

INTRODUCTION

Bitumen and heavy oil upgrading has been the subject of many investigations since the early thirties (1). Present industrial technologies such as delayed coking or fluid coking result in the formation of large amounts of coke (up to 22% of the feed) (2). This decreases the yield of valuable liquid products. Whereas coke derived from petroleum in general may find a variety of uses, the high sulphur content of the coke produced from Canadian oil sands bitumen such as Athabasca bitumen, precludes its use (3).

Hydrocracking of Athabasca bitumen has proven to yield 10-15% higher liquid distillate product than conventional coking processes (4). Catalysts are required for effective removal of sulphur and nitrogen and to improve liquid yields. Coke is also formed during hydrocracking, although significantly less than in coking. However, this creates operational problems such as reactor fouling and catalyst poisoning. Coke formation increases with temperature (5,6) and decreases with hydrogen partial pressure (5). Addition of coal and coal-based catalysts has been claimed to reduce coke formation (7).

Coke formation from oil sands bitumen is believed to be related to its high asphaltene content (2). Dickie and Yen (8) have studied structures of asphaltenes from various sources and postulated that asphaltene aggregates are made of planar sheets of condensed aromatic rings, saturated carbon chains and a loose net of naphthenic rings. Therefore, polynuclear aromatic hydrocarbons may be considered as possible constituents of asphaltene and catalysts which are effective in hydrocracking polynuclear aromatic compounds should also be effective in asphaltene hydrocracking.

Molten halide salts have been found to be excellent catalysts in the hydrocracking of the polynuclear (9,10) and alkyl substituted polynuclear aromatic hydrocarbons (11). Zielke et al. (9) have shown the superiority of molten $ZnCl_2$ catalysts over conventional hydrocracking catalysts for pyrene, coal and coal extract and subsequently carried out continuous hydroliquefaction of subbituminous coal in molten $ZnCl_{2(12)}$.

Herrmann et al. (13) carried out a comparative study of Fe, $ZnCl_2$ and $ZnCl_2$-promoted Fe catalysts for hydrocracking of Athabasca bitumen. They found $ZnCl_2$ to be the most active, to produce less hydrocarbon gas and significantly less sulphur in the liquid product. Nomura et al. (2) studied hydrocracking of Athabasca asphaltene over molten $ZnCl_2$-KCl-NaCl mixtures with and without an additive of some transition metal chlorides and found a mixture of $ZnCl_2$-KCl-$NaCl_5$ to give higher asphaltene conversion (60% pentane soluble) and small amounts of coke (3.7% benzene insoluble). Based on this information we decided to carry out systematic experiments to investigate the hydrocracking of Athabasca bitumen with molten $ZnCl_2$, CuCl and their mixtures with and without tetralin. This latter hydrogen donor compound was added to rapidly transfer H and then prevent coke formation by recondensation of the hydrocracked radicals.

FEEDSTOCK AND REAGENTS

Athabasca bitumen produced by hot water process from mined oil sands of the McMurray stratigraphic unit by Suncor Inc. and obtained from the Alberta Research Council was used as the feedstock. Table 1 summarizes the relevant properties of the bitumen.

All the reagents used were of ACS reagent grade. Tetralin and $ZnCl_2$ were purchased from Aldrich Chemicals, Milwaukee, WI.: CuCl was purchased from Anachemia Ltd., Montreal and hydrogen was purchased from Liquid Carbonic Inc., Montreal.

EQUIPMENT

Traditionally laboratory scale hydrocracking experiments have been carried out in stirred autoclaves (13) and rocking autoclaves (2). However, the fluidodynamic conditions in these traditional autoclaves are considerably different from those of an industrial hydrocracker because industrial hydrocrackers operate under continuous flow conditions.

To simulate industrial conditions as closely as possible we used a bubbling microautoclave system of our own design. A schematic diagram of the experimental setup is shown in Fig. 1. It consists of a 15 mL bubbling microautoclave, water cooled condenser, gas collection assembly, molten salt heating bath, cooling water bath, connecting tubings, and instrumentation. The bubbling microautoclave is the heart of the experimental setup and is equipped with a microporous steel grid, through which gas can be dispersed.

The gas collection assembly was specially designed to collect all the gases. It consists of two 75 L tanks, capable of withstanding pressures up to 20 psig. The contents can be mixed thoroughly by means of two built-in stirrers. In addition a pump can transfer the contents from one tank to another and vice versa thereby facilitating intermixing the contents of both.

EXPERIMENTAL PROCEDURE

The microautoclave was filled with about 7 g of bitumen for the non-catalytic experiments plus desired amounts of catalysts for the catalytic experiments. $ZnCl_2$ and CuCl were oven dried at 100°C for about 3 h prior to use to eliminate any moisture. The microautoclave was then completely sealed. Hydrogen was then bubbled through the microporous grid and the system pressure was raised to the desired pressure (13.8 MPa). The hydrogen flowrate (1 L_{STP}/min) was established by a pre-calibrated mass flow meter (Brooks Instruments, Model 5850). The microautoclave was then plunged into the preheated molten salt bath heater and the previously evacuated gas collection assembly was started. The temperature of the microautoclave contents was monitored constantly by an electronic temperature indicator (Analogic, Model AN2572). It usually took about 5-7 min to reach the desired reaction temperature (425°-450°C). Experiments were carried out for 30 min after reaching the reaction temperature. The microautoclave temperature was carefully controlled as follows: when it exceeded the desired reaction temperature by 2°C, the autoclave was partially withdrawn momentarily from the molten salt bath to reduce the temperature to the reaction temperature. In this manner it was possible to stay within ±3°C of the desired temperature.

At the end of the experiment, the microautoclave is quickly immersed into the cooling water bath while the hydrogen is continued. When room temperature is reached (25°C), which takes about 1-2 min, the gas flow is stopped. The gas remaining in the system is then evacuated into the gas collection assembly.

ANALYTIC PROCEDURE

The gases were well mixed in the gas collection assembly for about 1 h, then analyzed by a gas chromatograph (Hewlett Packard, Model 5890) equipped with a Porapak Q and a Molecular Sieve column in series.

The microautoclave was weighed before and after the experiment and the difference gave the quantity of gas formed plus any entrainment. Usually entrainment was negligibe as the condenser was purposely overdesigned and was filled with metal springs. Most of the gases were thus condensed and returned to the microautoclave.

The microautoclave was then cleaned thoroughly with dichloromethane. Dichloromethane insoluble products were filtered, dried in an oven at 100°C and weighed. When catalysts were used, the dichloromethane insoluble material was washed with hot water in an ultrasonic bath. $ZnCl_2$/CuCl remaining in the dicholoromethane insoluble material (except those chemically combined) were thus removed. The solvent was then evaporated in a rotary evaporator (Buchi, Rotavapor RE121). n-Pentane in 1:50 ratio was then added and the mixture placed in an ultrasonic bath for 15 min. It was left for 24 h before n-pentane insolubles, termed as asphaltenes were filtered. The asphaltenes were then dried in a vacuum dessicator, weighed and collected. n-Pentane was evaporated from the filtrate in the rotary evaporator and the remaining yellowish material, termed as maltenes, was collected.

RESULTS

The experimental conditions and product analysis in terms of coke (dichloromethane insolubles), asphaltene (pentane insolubles), maltenes (pentane solubles) and gas are summarized in Table 2. The following observations are made.

The amount of coke and gas increase, in general, with reaction temperature (see expts. 1,5,8 for the non-catalytic and expts. 2,6,9 for the catalytic runs). Both the asphaltene and the maltene fractions appear to decrease with temperature for the range studied (see expts. 1,5,8).

Addition of $ZnCl_2$ decreases the asphaltene, coke and gas fractions whereas it increases the maltene fraction with respect to the uncatalyzed reaction. The asphaltene fraction decreases whereas the maltene fraction increases with increased $ZnCl_2$ as can be seen from expts. 1-4,5-7, and 8-11. The gas fraction initially decreases with respect to the uncatalyzed reaction but increases with additional $ZnCl_2$. Although there is some scatter in the data the coke content also appears to decrease somewhat with $ZnCl_2$.

Addition of tetralin results in decreased gas and coke fractions as can be seen by comparing expts. 1, 12-14. The asphaltene fraction also decreases somewhat whereas the maltene fraction increases. CuCl also has some catalytic activity towards heavy oil cracking, but its reactivity is lower than that of $ZnCl_2$. Addition of CuCl to $ZnCl_2$ lowers the coke content of the product, but decreases the reactivity towards asphaltene cracking as can be seen by comparing expts. 7, 17 and 18.

Some observations on the performance of the bubbling microautoclave with respect to conventional stirred autoclaves are worth mentioning. Our results were compared with those of Herrmann et al. (13), carried out under somewhat similar conditions with Athabasca bitumen. A substantial difference in the quantity of gas formed was noted. In the present case it ranged from 15 to 23 wt % for runs carried out at 440°C and 450°C. In the case of Herrmman et al. (13) it was about 6 wt %. This is probably an indication of improved cracking in the microautoclave. We attribute this to a homogeneous distribution of temperatures and gas throughout the fluidized system and to the absence of hot spots on the walls.

CONCLUSIONS

Athabasca bitumen has been hydrocracked in a bubbling microautoclave with molten halide catalysts. $ZnCl_2$ has been found to be an effective catalyst for the conversion of asphaltenes into maltenes and gases. Since $ZnCl_2$ is in the liquid state under hydrocracking conditions it may be used as a homogeneous catalyst for the hydrocracking of bitumen and heavy oils. The addition of tetralin reduces gas and coke formation but a substantial amount is required to significantly reduce coke.

REFERENCES

1. Pruden, B.B., Canadian J. of Chem. Eng., 56, 277-280, 1978.
2. Nomura, M. Terao, K. and Kikkawa, S., Fuel, 60, 699-702, 1981.
3. Speight, J.G. and Moschopedis, S.E., Fuel Proc. Tech., 2, 295-302, 1979.
4. Chandra Sekhar, M.V. and Ternan, M., Fuel, 58, 92-98, 1979.
5. Pruden, B.B., Logie, R.B. Denis, J.M. and Merrill, W.H., CANMET Report 76-33, 1976.
6. Khulbe, C.P. Pruden, B.B. and Denis, J.M., Laboratory Report ERP/ERL 77-79(J), 1977.
7. Ranganathan, R. Pruden, B.B. and Denis, J.M., CANMET Report 77-62, 1977.
8. Dickie, J.P. and Yen, T.F., Anal. Chem., 39, 1847, 1967.
9. Zeilke, C.W., Struck, R.T., Evans, J.M., Costanza, C.P. and Gorin, E., Ind. Eng. Chem. Process Des. Dev., 5, 158-164, 1966.
10. Nakatsuji, Y., Kubo, T., Nomura, M. and Kikkawa, S., Bul. Chem. Soc. Japan, 51, 618-624, 1978.
11. Nakatsuji, Y., Ikkaku, Y., Nomura, M. and Kikkawa, S., Bul. Chem. Soc. Japan, 51, 3631-3634, 1978.
12. Zeilke, C.W., Klunder, E.B., Maskew, J.T. and Struck, R.T., Ind. Eng. Chem. Process Des. Dev., 19, 85-91, 1980.
13. Herrmann, W.A.O., Mysak, L.P. and Belinko, K., CANMET Report 77-50, 1977.

Table 1

Select properties of Athabasca bitumen

API gravity	10.1	Density	0.999 g/mL
Viscosity, 25°C	42000 cP	Ash	0.48 wt %
Carbon	83.77 wt %	Hydrogen	10.51 wt %
Nitrogen	0.37 wt %	Sulphur	4.75 wt %
Oxygen	0.88 wt %	Vanadium	200 ppm wt
Nickel	75.5 ppm wt	Asphaltene	16.1 wt %
Pitch (524°C+Fraction)	53.7 %	Coke	0.57 wt %
		Maltene	83.33 wt %

Table 2

Summary of the experimental conditions and product analyses

Expt. #	Temp. °C	Catalyst %	Cat. Conc. wt %	Coke wt %	Asphaltene wt %	Maltene wt %	Gas wt %
1	450		-	8.4	8.6	60.1	22.9
2	450	$ZnCl_2$	1.5	5.5	8.2	66.0	20.2
3	450	$ZnCl_2$	10	6.3	4.4	67.7	21.6
4	450	$ZnCl_2$	25	2.8	2.4	72.3	22.5
5	440	-		4.8	10.4	66.7	18.1
6	440	$ZnCl_2$	1.5	3.8	8.3	69.9	18.0
7	440	$ZnCl_2$	10	4.1	3.2	72.1	20.6
8	425	-		3.6	11.7	67.0	17.7
9	425	$ZnCl_2$	1.5	3.2	9.1	74.7	12.9
10	425	$ZnCl_2$	10	4.0	4.7	78.9	12.4
11	425	$ZnCl_2$	25	1.6	4.0	77.7	16.7
12	450	Tetralin	25	4.6	6.5	68.1	20.8
13	450	Tetralin	50	3.8	5.2	73.9	17.1
14	450	Tetralin	100	2.7	5.4	76.5	15.4
15	440	CuCl	1.5	6.7	7.2	67.9	18.2
16	440	CuCl	10	5.9	6.3	69.8	18.0
17	440	$ZnCl_2$+	10				
		CuCl	1.5	3.6	6.1	70.0	20.3
18	440	$ZnCl_2$+	10				
		CuCl	4.5	3.4	5.2	72.4	19.0

* values are wt % of feed.

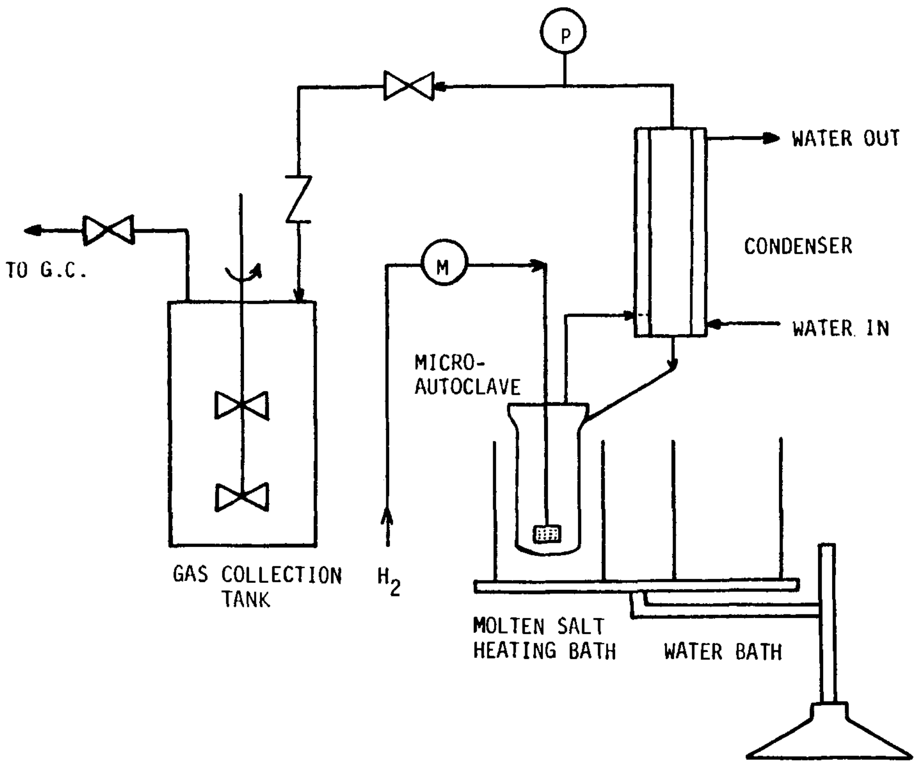

Figure 1. Schematic diagram of bubbling microautoclave.

PROCESS OPTIONS FOR EXTINCTION RECYCLE CONVERSION OF HEAVY OILS IN CATALYTIC TWO STAGE LIQUEFACTION

A. G. Comolli, E. S. Johanson, J. B. McLean, T. O. Smith

Hydrocarbon Research, Inc.
(A subsidiary of DynCorp)
P. O. Box 6047
Lawrenceville, New Jersey 08648

ABSTRACT

Hydrocarbon Research, Inc. (HRI) is developing a Catalytic Two-Stage Liquefaction (CTSL) Process which converts coal to distillate liquid products. A particularly attractive feature of the process that has been demonstrated recently using two bituminous coal feedstocks (Illinois No. 6 and Ohio No. 5/6 coals) is the capability to achieve extinction conversion of heavy oil products (heavy vacuum distillate and soluble residuum oil) through integration of coal cleaning, product solids separation, and selective recycle. Yields of distillate oils of up to five barrels per M.A.F. ton of coal have been achieved. Elimination of heavy oils of boiling points above 700-750°F greatly simplifies downstream processing requirements. Several process configuration options and the resulting yield distributions are discussed.

INTRODUCTION

Hydrocarbon Research, Inc.'s (HRI) Catalytic Two-Stage Liquefaction (CTSL) Process features two close-coupled catalytic ebullated-bed reactor stages in series, with the first stage at a lower temperature than the second stage, so as to optimize the hydrogenation/conversion functions of the two stages. The process has been under development, sponsored by the U. S. Department of Energy (DOE), since 1982. This paper summarizes the status of the program and discusses the results of the most recent operations in HRI's continuously operated bench-scale unit which demonstrated extended operations with virtually complete elimination of residual oil and/or heavy vacuum gas oils from the net products of the operation. Upgrading studies by Chevron[1] have correlated upgrading costs directly with product oil end points and emphasized the need to eliminate the heavy vacuum gas oil products. Recently completed economic studies by HRI have shown a product cost benefit for the extinction mode of operation.[2] Such modes of operation were demonstrated for Illinois No. 6 and Ohio No. 5/6 bituminous coals.

PROCESS DESCRIPTION

The key feature which distinguishes the CTSL Process from other single- or two-stage liquefaction processes is the use of a relatively low temperature (<800°F) in the first-stage reactor which contains an effective hydrogenation catalyst. In this stage, coal is largely converted at a controlled rate by dissolution in the recycle solvent, allowing catalytic hydrogenation reactions, necessary to maintain solvent hydrogen-transfer capability and stabilize the liquefaction products, to keep pace with the rate of coal conversion. The second stage operates at more severe conditions, but not as severe as required in a single-stage mode such as in the H-Coal® Process, and it completes the job of coal conversion with the additional conversion of high boiling primary liquefaction products to high quality distillates. Overall, the CTSL Process obtains higher yields of better quality distillate products than obtained in competing technologies.

BENCH UNIT DESCRIPTION

Process development studies have been conducted in HRI's continuously operating two-stage Bench Unit, schematically shown in Figure 1. The operation is sustained with the net feed of only coal and hydrogen, with recycled solvent recovered from the contemporary gross products leaving the reaction system, by the distillation and filtration means indicated in Figure 1. The immediate recovery and recycle of solvent is a true prototype of full scale operations and facilitates the interpretation of the operating results, by avoiding the problems of batch and once-through experimental modes. There is an on-line sampling system for the slurry leaving the first stage, so that the effectiveness of each of the two stages can be assessed.

An important factor in process performance is the nature of the solvent that is recycled. Figure 1 includes a schematic summary of the modes of adjusting solvent composition. First, slurry product from the reaction system is distilled at atmospheric pressure to eliminate from the solvent pool middle distillate oils for which there is little incentive to submit to further processing by recycling to the liquefaction reactors. The atmospheric bottoms slurry can be recycled directly or further modified for recycle, either by a solids removal method, here pressure filtration although alternative methods are feasible, or by vacuum distillation which provides heavy vacuum distillate for incorporation in the recycle solvent pool. In the bottoms extinction demonstration operation summarized in this report, the atmospheric still was operated with a stripping gas to give a middle distillate endpoint (atmospheric still overhead going to product pool) and solvent pool IBP such that the solvent pool was virtually completely eliminated by undergoing further secondary reactions in the liquefaction reactors.

Bench unit scale of operations during the development program has been approximately 50 pounds per day. Scale up of the results from reactor systems of this size to plant scale has proven satisfactory for the H-Oil® and H-Coal® Processes, which employ the ebullated-bed reactor system used in the CTSL Process. The bench unit operations use a single charge of catalyst which is used in an extended operation, up to thirty days in some cases, without augmentation. This is in contrast with anticipated application to plant scale where, because of the convenience of the ebullated-bed system, a portion of the catalyst is to be replaced on a daily basis, so as to maintain a constant catalytic performance, while holding the reactors at a fixed temperature. Again, the interpretation of the bench scale results in projection of the amount of catalyst replacement required on a plant scale has proven to be satisfactory. The catalyst used in the operation described in this report is a commercially available hydrodesulfurization catalyst, one of several which have performed equally well.

DEMONSTRATION RUN PARAMETERS

The bottoms extinction operations showed that a sustained operation could maintain a product distribution eliminating the highest boiling constituents from the product pool. This mode requires that all such materials leaving the reactor be recycled to the reactor system. A portion of these high boiling oils are mixed with product solids (unreacted coal and ash), in the filter cake for these operations, and for inclusion in the solvent recycle pool these oils must be separated from the solids. For these experiments the filter cake was washed with low-boiling aromatic solvent, and the extracted oils were returned to the solvent pool after distilling off the solvent. Since this solvent washing operation had some handling and processing inefficiencies, some of the solvent range material was not available for recycle and was rejected as a net product of the operation. The bottoms extinction objective is limited only by the engineering problems of the recovery for recycle of solvent range material.

To reduce the scale and cost of the solvent/solids separation operations it is desirable to process feed of relatively low ash content. To this end for the demonstration operation, the available mine-washed coal was further cleaned by heavy-media washing which reduced the ash content by approximately half. Table 1 gives, for Illinois coal, the analyses for the as-received mine-washed coal and the heavy-media washed coal used in the demonstration run. Table 2 gives these analyses for the Ohio coal. The CTSL results with heavy media washed coal are not appreciably different from those using mine-washed coal, as shown in Table 3 which compares the CTSL results for the two types of feed in process development operations using the same operating conditions. The principal difference in the results is 3% higher coal conversion with the heavy-media washed feed, with the increased conversion appearing as light and middle distillate product. This higher coal conversion is ascribed to the removal, along with the ash, of a portion of the most difficult to convert portion of the coal. The bottoms extinction mode is as feasible for the mine-washed feed as for the heavy-media-washed feed. The selection between these alternatives is an economic-engineering judgment involving the costs of product solids separation and the feasibility of alternative uses for the high ash reject from the heavy-media washing operation.

The vacuum gas oil extinction mode of operation consisted principally of unfiltered atmospheric still bottoms along with sufficient vacuum gas oil, obtained by vacuum distillation of the balance of the atmospheric still bottoms, to achieve extinction of the vacuum gas oil components. Here, too, the atmospheric still was operated with stripping gas to give a solvent pool IBP such that the vacuum gas oil component would be eliminated. Because of the reduction of the proportion of residual oil in the recycled solvent pool there would be a net production of residual oil from the operation, which would be withdrawn from the process as a vacuum bottoms slurry in combination with the unreacted coal and ash.

With the normal catalyst activity decline, operating conditions were adjusted so as to maintain the bottoms or gas oil extinction objectives. To this end, the temperatures of the two stages were increased progressively during the runs. Figure 2 summarizes the reactor temperature changes during the bottoms extinction demonstration run using Illinois No. 6 coal. Here, between the seventh day and the twenty-fifth day of the run, during which the bottoms extinction objectives of the run were attained (see below), the first-stage temperature was increased by 15°F and the second-stage temperature was increased by 20°F. Nominally, in a plant scale operation with daily replacement of catalyst, any level of performance obtained during the run could be maintained using the temperatures holding at that stage of the run and an appropriate rate of catalyst replacement that would maintain the catalyst activity holding for the particular stage of the operation. Also, during the run there was a progressive adjustment in the cut point between the atmospheric overhead withdrawn as product and the solvent recycle component being extincted, as summarized in Figure 3. This cut point was increased by about 80°F over the interval of the run during which the extinction objective was maintained. Nominally, such an adjustment of the cut point is not necessary to maintain the extinction objective, but without this adjustment in cut point greater changes in reactor temperatures would have been necessary in maintaining the extinction objective at a constant distillate product end point.

A comparison of the process options investigated highlighting the cut point differences is presented in Table 4.

OPERATING RESULTS WITH ILLINOIS COAL

The operating results for the demonstration operation in the bottoms extinction mode with Illinois coal are summarized in Table 5. The results are the average values for the seventh through twenty-fifth days of the run during which bottoms extinction objectives were maintained. Recycle solvent inventory corrections based on actual analysis were included. Figures 4 through 8 summarize day-by-day some details of the product distribution during the run, illustrating the degree to which minimum bottoms yields were maintained. Over this interval of the run, during which the endpoint of the atmospheric overhead product averaged 750°F, the yield of C_4-750°F distillate product averaged 77.2 W % of M.A.F. coal (corresponding to 5 barrels/ton of M.A.F. coal), with 1.0 W % yield of heavier distillates boiling to 975°F, and 2.7 W % yield of residual oil. Table 5 also summarizes the results of a comparable conventional CTSL operation with the heavy-media washed coal in which the 650-750°F boiling range material was included in the solvent recycle.[3,4] The change in the composition of the solvent recycle lowered the yield of 750°F$^+$ oils plus residuum from 19.6 W % of M.A.F. coal to 3.6 W %. Some of this change is due to the higher reactor temperatures used in the extinction mode operation, but other experimental work has shown that less than one-half of the difference is associated with the change in temperatures.

Figure 4 shows that the yield of C_4-End Point(about 750°F) product scattered around the average value during the seventh through twenty-fifth days of the run. Figure 5 displays a similar pattern for the 975°F$^+$ residual oil yield, and Figure 6 for the yield of heavy distillate to 975°F retained in the solvent recycle pool. Figure 7 shows an increase in coal conversion of about 1.5 W % over this interval of the run. Figure 8 shows an increase in C_1-C_3 hydrocarbon gas yield of about 2.5 W %.

OPERATING RESULTS WITH OHIO COAL

The operating results for the demonstration operations with Ohio No. 5/6 bituminous coal in the bottoms extinction mode and in the gas oil extinction mode are summarized in Table 6. These two types of operation were demonstrated in a single run, in which the bottoms extinction mode was used for the first ten days, and the vacuum gas oil extinction mode for the balance of the operations up to twenty-two days. The stage temperatures were progressively increased during these operations, similarly to the pattern used for the Illinois coal operations, with the reactor temperatures being increased by about 20°F over the interval of the run during which the extinction objectives were attained.

The bottoms extinction operation with Ohio coal maintained a 975°F$^+$ residual oil yield of 1.8 W % of M.A.F. coal. However, the yield of 750-975°F gas oil was somewhat higher, averaging 8.5 W %. Since there was virtually complete elimination of the 750-975°F fraction in the subsequent vacuum gas oil extinction operation, there is probably no barrier to equivalent extinction in the bottoms extinction mode. The shortfall in performance in this specific operation was probably due to too low a cut point between the atmospheric still overhead product and solvent recycle pool, at 700°F. It is probable that with this cut point raised by 25-50°F, there would have been essentially complete extinction of the 750°F$^+$ materials, with a total yield of C_4-750°F distillate product of about 77 W % of M.A.F. coal. This is similar to the yield in this mode of operation with Illinois coal. Beyond this consideration of the heavy gas oil extinction, the greatest difference from the Illinois coal results is about 2 W % higher yield of unconverted coal for the Ohio coal.

The vacuum gas oil extinction operation with Ohio coal gave a yield of 750-975°F gas oil of 0.2 W % of M.A.F. coal. For this operation, the yield of 975°F$^+$ residual oil was 14.1 W %, which would be taken off as a vacuum bottoms slurry along with the unreacted coal and ash. Such a slurry would have a composition of 61% residual oil, 21% unconverted coal, and 18% ash, and could be pumped for internal use as fuel or as raw material for hydrogen manufacture. The yield of C_4-750°F distillate was 65.1 W % of M.A.F. coal for this operation.

RESULTS AND CONCLUSIONS

- Heavy oil extinction recycle has been demonstrated for vacuum gas oil and vacuum gas plus residual oil for bituminous coals.
- Up to five barrels of distillate liquid product per ton of moisture ash free coal feed was produced. These yields are the highest demonstrated continuously for a direct liquefaction process.
- Increased liquid yields and reduced process separation costs were achieved through deep cleaning of bituminous feed coals.
- The distillate yields from Ohio coal are equivalent to those from Illinois coal at similar extinction recycle operating conditions.

ACKNOWLEDGEMENT

The experimentation summarized in this paper was sponsored by U.S. Department of Energy (DOE), Contract No. DE-AC22-85PC80002, under the direction of Dr. Edgar Klunder, DOE Project Manager.

REFERENCES

1. Sullivan, R. F., et al, "Transportation Fuels From Direct-Liquefaction Products". Division of Fuel Chemistry of the American Chemical Society, Anaheim, California, September 1986.

2. Abrams, L. M., A. G. Comolli, G. A. Popper, C. Wang and G. Wilson, "Catalytic Two-Stage Liquefaction Process - Illinois Coal Conceptual Commercial Plant Design and Economics". Department of Energy Topical Report prepared under Contract No. DE-AC22-85PC80002, to be issued February - March 1988.

3. McLean, J. B., A. G. Comolli, E. S. Johanson and T. O. Smith, "Demonstration Results for Illinois No. 6 Coal". DOE Direct Liquefaction Contractors' Conference, Pittsburgh, Pennsylvania, October 1987.

4. Comolli, A. G., E. S. Johanson, J. B. McLean and T. O. Smith, "Process Variable Studies and Residual Oil Extinction Recycle in Catalytic Two-Stage Liquefaction". DOE Direct Liquefaction Contractors' Review Meeting, Monroeville, Pennsylvania, October 1986.

TABLE 1

ILLINOIS COAL FEED ANALYSIS

SOURCE: ILLINOIS No. 6, BURNING STAR No. 2 MINE

	MINE-WASHED	HEAVY MEDIA CLEANED
PROXIMATE, W % DRY		
Fixed Carbon	51.5	54.1
Volatile Matter	38.2	40.4
Ash	10.3	5.5
ULTIMATE, W % DRY		
Carbon	70.4	73.9
Hydrogen	4.5	4.9
Nitrogen	1.4	1.5
Sulfur	3.6	2.8
Ash	10.6	5.8
Oxygen (Difference)	9.5	12.1
PETROGRAPHIC, V %		
Total Reactives	88.2	91.5
Total Inerts	11.8	8.5
Fusinite	1.9	0.3

TABLE 2

OHIO COAL FEED ANALYSIS

SOURCE: OHIO No. 5/6, CRAVAT COAL COMPANY

	MINE-WASHED	HEAVY MEDIA CLEANED
PROXIMATE, W % DRY		
Fixed Carbon	56.1	50.6
Volatile Matter	43.9	43.4
Ash	8.5	4.0
ULTIMATE, W % DRY		
Carbon	73.1	77.5
Hydrogen	4.8	5.0
Nitrogen	1.5	1.6
Sulfur	2.9	2.1
Ash	8.5	4.0
Oxygen (Difference)	9.2	9.8
PETROGRAPHIC, V %		
Total Reactives	88.0	90.4
Total Inerts	10.8	7.8
Fusinite	1.1	1.8

TABLE 3

OPERATING RESULTS BENCH UNIT CTSL OPERATIONS WITH MINE-WASHED AND HEAVY MEDIA WASHED ILLINOIS COAL

	WASHED	
COAL PREPARATION	Mine	Heavy-Media
ASH IN COAL FEED, W %	10.55	5.33
RUN	18	19
DAYS ON STREAM, Average	8	9
Reactor Temperatures, °F		
First Stage, Average	750	750
Second Stage, Average	810	810
End Point of Atmospheric Overhead Product, °F	670	664
PRODUCT DISTRIBUTION, W % OF M.A.F. COAL		
C_1-C_3 in Gases	5.9	6.2
C_4-390°F Naphtha	17.2	19.0
390-650°F Distillates	32.9	35.7
650-975°F Distillates	19.2	18.5
975°F$^+$ Residual Oil	8.3	8.3
Unconverted Coal	7.0	4.0
Water	11.7	11.7
H_2S, NH_3, CO_X	5.0	4.3
Total (100 + H_2 Reacted)	107.2	107.7
Total C_4-975°F	69.2	73.2
Distillate Yield Bbls/Ton	4.2	4.7

TABLE 4

COMPARISON OF PROCESS OPTIONS EVALUATED

	Product					
Illinois No. 6 Coal Runs	Vacuum Gas-Oil	Residual Oil	Clean Coal	Solids Rejection	W % Distillate	Distillate End Point
I-10/11 - Demonstration	Yes	Yes	No	VSB	60	975°F
I-13 - Process Variable	No	No	No	DS		
I-27 - Demonstration	No	No	Yes	DS	77	750°F
Ohio No. 5/6 Coal Runs						
0-1 - Demonstration	No	No	Yes	DS	70	700°F
	No	Yes	Yes	VSB	65	700°F

VSB = Vacuum Still Bottoms
DS = Dry Solids

TABLE 5

EXPERIMENTAL RESULTS OF CONVENTIONAL AND EXTINCTION MODES OF CTSL BENCH UNIT OPERATIONS WITH ILLINOIS COAL

MODE	CONVENTIONAL	EXTINCTION
RUN	19	27
DAYS ON STREAM, Average	14	16
Reactor Temperatures, °F		
First Stage, Average	750	761
Second Stage, Average	810	817
End Point of Atmospheric Overhead Product, °F	656	749
PRODUCT DISTRIBUTION, W % OF M.A.F. COAL		
C_1-C_3 Hydrocarbons	6.8	8.3
C_4-390°F Naphtha	18.9	20.3
390-650°F Distillates	32.4	37.5
650-750°F Distillates	9.1	19.5
C_4-750°F Distillates	60.4	77.3
750-975°F Distillates	11.0	1.0
975°F$^+$ Residual Oil	9.5	2.7
Unconverted Coal	3.8	3.3
Water	11.2	10.8
H_2S, NH_3, CO_X	4.6	4.2
Total (100 + H_2 Reacted)	107.3	107.6

TABLE 6

EXPERIMENTAL RESULTS OF BOTTOMS AND VACUUM GAS OIL EXTINCTION CTSL BENCH UNIT OPERATIONS WITH OHIO COAL

MODE	BOTTOMS EXTINCTION	VACUUM GAS OIL EXTINCTION
RUN	0-2	0-2
DAYS ON STREAM, Average	7	18
Reactor Temperatures, °F		
First Stage, Average	753	764
Second Stage, Average	806	819
End Point of Atmospheric Overhead Product, °F	702	697
End Point of Vacuum Gas Oil Product, °F	---	975
PRODUCT DISTRIBUTION, W % OF M.A.F. COAL		
C_1-C_3 in Gases	7.9	10.1
C_4-390°F Naphtha	19.1	18.8
390-650°F Distillates	36.8	38.1
650-975°F Distillates	14.6	8.1
C_4-750°F Distillates	70.5	65.1
750-975°F Gas Oil	8.5	0.3
975°F$^+$ Residual Oil	1.8	14.1
Unconverted Coal	5.2	4.8
Water	10.0	9.0
H_2S, NH_3, CO_X	3.5	3.4
Total (100 + H_2 Reacted)	107.4	106.7
Distillate Yield, Bbls/Ton	4.3	4.0

Note: $C_4$975°F Yield, 79% equal to 5:1 Bbls/Ton

FIGURE 1

EBULLATED-BED BENCH UNIT 227

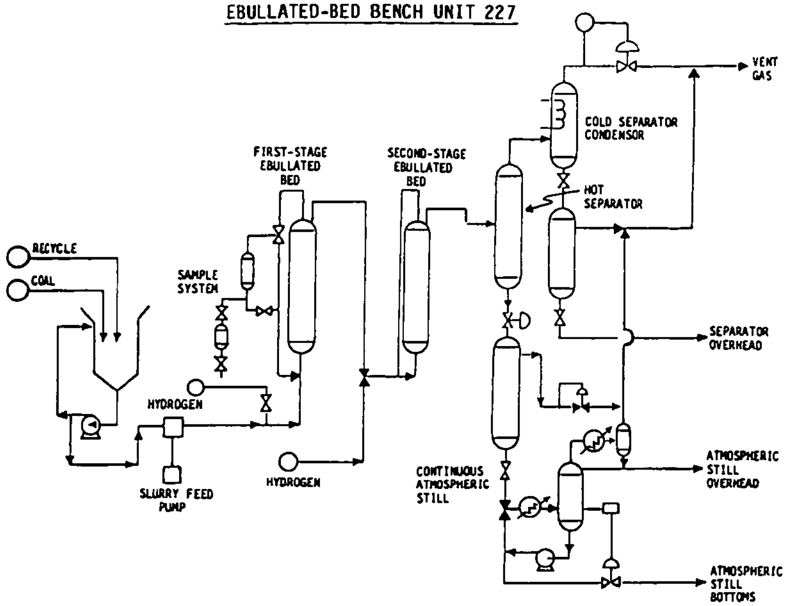

BENCH UNIT - RECYCLE PROCEDURES

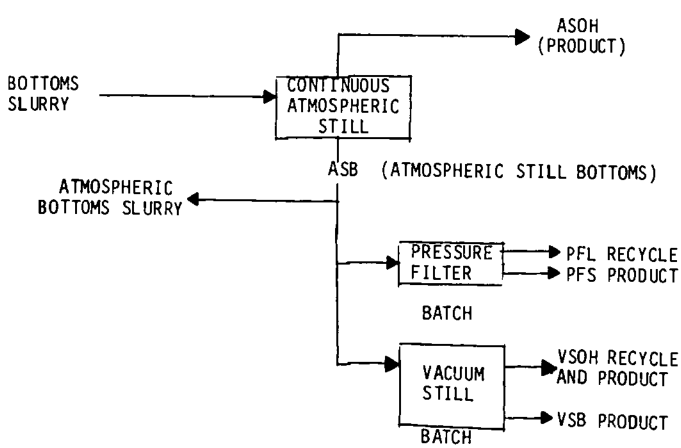

FIGURE 2

REACTOR TEMPERATURES

CTSL DEMONSTRATION OPERATION WITH ILLINOIS COAL

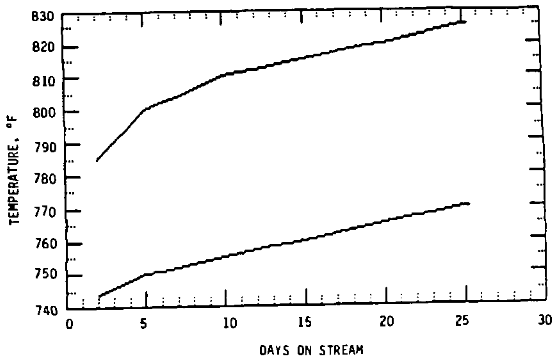

FIGURE 3

ATMOSPHERIC STILL CUT POINT

CTSL DEMONSTRATION OPERATION WITH ILLINOIS COAL

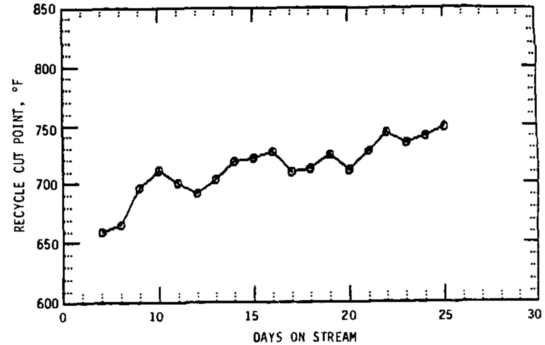

FIGURE 4

C_4-END POINT DISTILLATE YIELDS

CTSL DEMONSTRATION OPERATION WITH ILLINOIS COAL

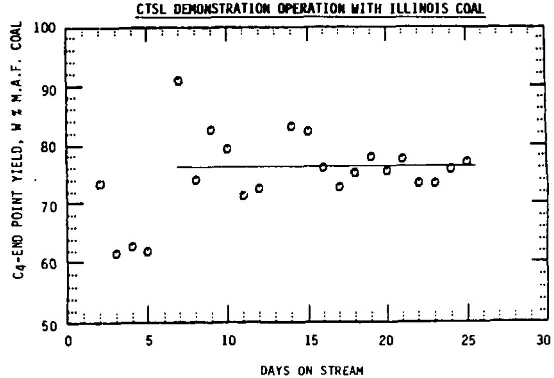

FIGURE 5

975°F+ YIELD

CTSL DEMONSTRATION OPERATION WITH ILLINOIS COAL

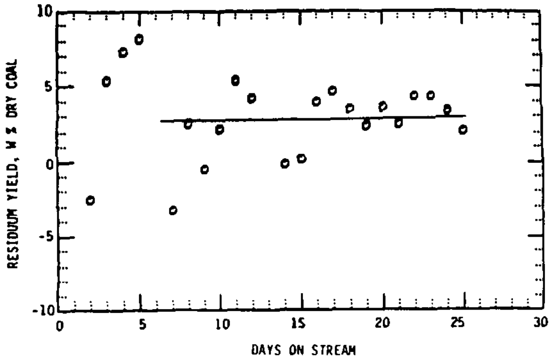

FIGURE 6

END POINT PLUS DISILLATE YIELD

CTSL DEMONSTRATION OPERATION WITH ILLINOIS COAL

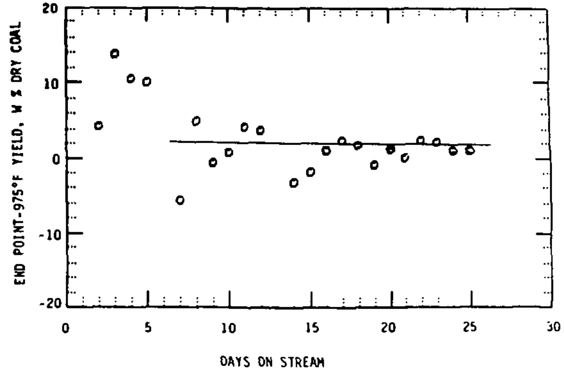

FIGURE 7

COAL CONVERSION

CTSL DEMONSTRATION OPERATION WITH ILLINOIS COAL

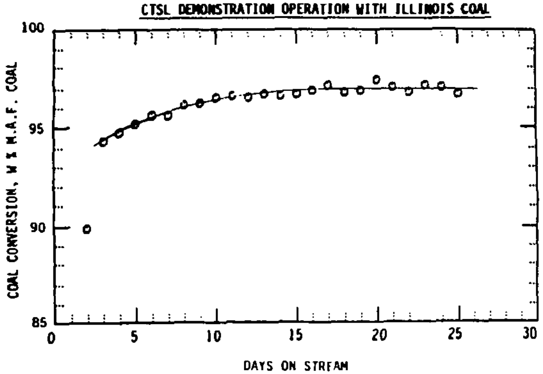

FIGURE 8

C_1-C_3 YIELDS

CTSL DEMONSTRATION OPERATION WITH ILLINOIS COAL

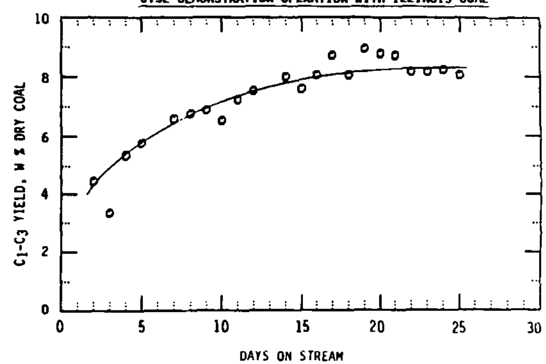

ACTIVITY AND SELECTIVITY OF MOLYBDENUM CATALYSTS IN COAL LIQUEFACTION REACTIONS

Christine W. Curtis and Joan L. Pellegrino
Chemical Engineering Department
Auburn University, Alabama 36849

During coal liquefaction, coal fragments forming a liquid product with reduced heteroatom content. Coal can be considered to be a large network of polynuclear aromatic species connected by heteroatoms and alkyl bridging structures. Predominant heteroatoms contained in coal are sulfur, oxygen, and nitrogen. Predominant alkyl bridges are methylene and ethylene structures. The purpose of this work is to evaluate how effectively three different molybdenum catalysts promote reactions involving heteroatom removal and cleavage of alkyl bridge structures. The reactions studied include: hydrogenation (HYD), hydrodeoxygenation (HDO), hydrodesulfurization (HDS), hydrodenitrogenation (HDN) and hydrocracking (HYC).

Both model and coal liquefaction reactions were performed to test the activity and selectivity of three different molybdenum catalysts. The three catalysts used were molybdenum naphthenate, molybdenum supported on gamma alumina (Mo/Al_2O_3) and precipitated, poorly crystalline molybdenum disulfide (MoS_2). The model compounds, chosen to mimic coal structure, on which the effectiveness of the catalysts for the model reactions was tested were: 1-methylnaphthalene, representing aromatic hydrocarbons, for hydrogenation; 1-naphthol, representing oxygen containing compounds, for deoxygenation; benzothiophene, representing sulfur containing compounds, for desulfurization; indole, representing nitrogen containing compounds, for denitrogenation; and bibenzyl, representing alkyl bridging structures, for hydrocracking. Catalytic reactions of combinations of reactants were performed to simulate a complex coal matrix. Thermal and catalytic coal liquefaction reactions were performed using Illinois No. 6 coal with anthracene as a solvent. The efficacy of the catalysts was determined by comparing the product and compound class fractions obtained from the liquefaction reactions.

Molybdenum Catalysts. All the catalysts used in this study have the element Mo (molybdenum) as the active metal component complexed with sulfur in a MoS_x form. Mo naphthenate is a thermally decomposable, hydrocarbon-soluble organometallic compound which was dispersed directly in the reaction mixtures. The catalytic species was generated in situ. Bearden et al. (1) postulates that at elevated temperatures and pressures inherent to coal liquefaction the metal naphthenate is converted to the active form by thermal decomposition. The active form is postulated to be MoS_2 (2,3) which is formed during pretreatment with H_2S or sulfur present in the feedstock. The Mo naphthenate used in this study was obtained from Shepherd Chemical consisting of ~6% Mo. The active form of the catalyst was generated in situ by introduction of excess sulfur to the reaction mixtures.

The Mo/Al_2O_3 used in this study was Amocat 1B obtained from Amoco. The active form was generated by presulfiding. The surface area of this material was 212 m^2/g.

Precipitated MoS_2 was prepared by the method of Chianelli and Dines (4) by precipitating MoS_2 from an ethyl acetate solution of $MoCl_4$ and Li_2S followed by annealing in H_2S. Precipitated MoS_2 exhibits a poorly crystalline "rag" structure (5), consisting of several stacked and highly disordered S-Mo-S layers. The layers have unusual flexibility in terms of number of dimension of the stacks and increased ability to intercalate organic species (5-7). Despite its poorly crystalline structure, precipitated MoS_2 exhibits an X-ray diffraction pattern similar to that of highly crystalline hexagonal MoS_2 (7). The synthesis of precipitated MoS_2 was confirmed by X-ray diffraction in this work. The surface area of precipitated MoS_2 was 42 m^2/g.

Experimental

Model Reactions. Model reactions were performed in horizontally mounted stainless steel tubing bomb reactors of ~20 ml volume. The model compounds and solvent, hexadecane, were obtained from Aldrich. All compounds of less than 99% purity were recrystallized before use. Model compound reactions were performed at 380°C with 1250 psig H_2 (cold) for 25 minutes and were agitated at rates greater than 800 cpm. For the individual reactions, the reactants were charged at 2 wt% in n-hexadecane; for the reactions with combined reactants, each component was introduced at 1 wt% giving 5 wt% reactant solutions. The reaction products were analyzed using a Varian 3700 FID chromatograph with a DB-5 fused silica capillary column. Para-xylene was used as internal standard. Catalyst, if used, was added in the individual reactant experiments at 1500 ppm Mo/g of reactor charge and in the combined reactions at 3500 ppm Mo/g of reactor charge. Elemental sulfur was added only to those reactions involving Mo naphthenate at a ratio of 2.5 to 1 sulfur to Mo by weight. Thermal reactions with excess sulfur were also performed to determine the independent effects of sulfur on reactant activity. Sulfur was added in the thermal reactions at a sulfur to Mo ratio of 2.5 to 1, calculated by assuming Mo would have been present at a loading of 1500 ppm/g reactor charge for the individual reactions.

Coal Liquefaction Reactions. Coal liquefaction reactions were performed thermally and catalytically with all three molybdenum catalysts in ~50 ml stainless steel horizontal reactors. The reactor charge was 0.5g coal with 0.5g anthracene as solvent and 1250 psig H_2 (cold). Reactions were performed at 425°C for 30 minutes at an agitation rate of 850 rpm. The catalyst loading was 3500 ppm Mo/reactor charge; 0.01g of sulfur was used for the Mo naphthenate reactions.

The liquid and solid products were separated by sequential washing with methylene chloride-methanol (9:1 v/v) solution (MCM) and tetrahydrofuran (THF). The separation produced three fractions: MCM solubles (MCMS), MCM insolubles-THF solubles (THFS) and THF insolubles or ash-free insoluble organic matter (IOM). The MCMS fraction was further fractionated by the chromatographic method of Boduszynski (8) into compound class fractions: hydrocarbons (HC), nitrogen heterocycles (NH), hydroxyl aromatics (HA) and polyfunctional compounds (PC). The HC fraction was further analyzed for anthracene and its hydrogenation products using the same GC analysis procedure as the model systems.

Results and Discussion

A sequence of reactions was performed with each model which included thermal reactions, thermal reactions with excess sulfur, and catalytic reactions using Mo naphthenate, Mo/Al_2O_3, and precipitated MoS_2. The product distributions achieved from the model reactions were summarized using several defined terms. The terms are: (1) percent hydrogenation which is the number of moles of hydrogen required to achieve the obtained product distribution as a percentage of the moles of hydrogen required for the most hydrogenated product; (2) percent hydrogenolysis which is the summation of the mole percent of components resulting from carbon-carbon and carbon-heteroatom bond cleavage; (3) percent desulfurization which is the summation of the mole percents of components not containing sulfur; (4) percent hydrodeoxygenation which is the summation of the mole percents of components not containing oxygen; (5) percent hydrodenitrogenation which is the summation of the mole percents of components from which nitrogen has been removed; and (6) percent hydrocracking which is the summation of the mole percents of components resulting from the breakage of an alkyl bridge structure.

Hydrogenation of 1-Methylnaphthalene. Hydrogenation of 1-methylnaphthalene proceeds through two pathways, both culminating in the production of decalin. 1-methylnaphthalene can either be hydrogenated to methyltetralins (tetrahydromethylnaphthalenes) followed by demethylation to naphthalene and further hydrogenation, or demethylated initially forming naphthalene and its hydrogenation products, tetralin and decalin (9-11).

Under thermal and thermal with sulfur conditions, essentially no hydrogenation of 1-methylnaphthalene occurred as presented in Table 1. Under catalytic conditions, Mo naphthenate produced the highest conversion of 1-methylnaphthalene among the three Mo catalysts, yielding major products of 5-methyltetralin and 1-methyltetralin. Conversion to hydrogenated naphthalenes was not observed with any of the Mo catalysts, although small quantities of naphthalene were produced. Very little hydrogenolysis of the methyl group was observed, indicating that these Mo catalysts were not selective for cleavage of the carbon-carbon bond.

Table 1
Activity and Selectivity of Mo Catalysts in Model Compound Systems

	Thermal	Thermal with Sulfur	Mo Naphthenate	Mo/Al_2O_3	$P\text{-}MoS_2$*
1-Methyl-Naphthalene					
Hydrogenation, %	0.7±0.3	0.8±0.6	31.3±0.8	13.5±0.6	7.6±0.5
Hydrogenolysis, %	0.4±0.1	0.5±0.1	1.6±0.4	0	0
1-Naphthol					
Hydrogenation, %	28.5±4.0	10.6±2.7	53.1±0.6	41.0±0.3	46.1±0.6
Deoxygenation, %	38.5±1.7	17.4±3.3	100.0	100.0	100.0
Benzothiophene					
Hydrogenation, %	1.3±0	1.1±0.1	51.9±0.5	51.0±0.2	51.1±0.1
Hydrodesulfur-ization,0	1.4±0.1	1.2±0.1	100.0	100.0	100.0
Indole					
Hydrogenation, %	1.6±0.5	1.1±0.2	35.6±4.3	22.6±0.1	8.2±1.6
Hydrodenitro-genation, %	0	0	18.6±4.7	11.9±0.1	2.0±0.8
Hydrogenolysis, %	1.7±1.0	0.5±0.2	69.6±5.4	38.2±0.5	10.4±5.0
Bibenzyl					
Hydrogenation, %	2.7±0.1	1.7±0.1	2.3±0.2	1.9±0.3	1.8±0.01
Hydrocracking, %	4.8±0.3	2.7±0.1	3.8±0.3	3.2±0.1	3.2±0.1

*$P\text{-}MoS_2$ - precipitated MoS_2

Hydrodeoxygenation of 1-Naphthol. Two reaction pathways for the hydrodeoxygenation of 1-naphthol are available, one in which 1-naphthol is hydrodeoxygenated and then hydrogenated to tetralin and decalin and one in which 1-naphthol is hydrogenated without removal of oxygen forming 5,6,7,8-tetrahydro-1-naphthol and 1-tetralone (12).

Significant thermal hydrogenation of 1-naphthol which followed both reaction pathways was observed. When sulfur was added, a marked inhibition of naphthol hydrogenation activity was obtained (Table 1), although the reaction still proceeded through both reaction pathways. In the catalytic reactions (Table 1), considerably more hydrogenation of 1-naphthol was observed. However, the catalytic hydrogenation proceeded through only one reaction pathway, the one involving immediate removal of the hydroxyl group with the major product being tetralin. All three Mo catalysts completely deoxygenated 1-naphthol; however, differences were observed in their ability to hydrogenate the deoxygenated 1-naphthol. Mo naphthenate was most active for hydrogenating 1-naphthol, followed by precipitated MoS_2 and then Mo/Al_2O_3.

Hydrodesulfurization of Benzothiophene. The reaction pathway for benzothiophene involves first hydrogenation to the dihydro form, then ring cleavage at the carbon-sulfur bond and finally hydrodesulfurization releasing H_2S (10,11,13,14).

Sulfur had no effect on thermal reactions of benzothiophene which was only slightly reactive without a catalyst present (Table 1). The thermal reactions formed the products, dihydrobenzothiophene and ethylbenzene, in small quantities. In the catalytic reactions, complete desulfurization was achieved with all of the Mo catalysts, producing primarily ethylbenzene and a minor product of ethylcyclohexane in all cases. Similar results have been observed over $CoMo/Al_2O_3$ catalysts (13). The hydrogenation activity of all of the catalysts was also nearly equivalent (Table 1).

Hydrodenitrogenation of Indole. The reaction pathway for indole hydrodenitrogenation proceeds by hydrogenation of the five-membered ring, followed by ring cleavage, removal of NH_3 and then hydrogenation to a six-membered ring alkane (15).

Thermal reactions of indole showed nearly 6% conversion primarily to dihydroindole. The addition of sulfur to thermal indole reaction had little or no effect on indole reactivity. The catalytic reactions yielded substantially more hydrogenation and hydrodenitrogenation of indole (Table 1). Mo naphthenate proved the most selective for denitrogenation of indole, with the major products being o-ethylaniline and ethylcyclohexane, with minor products of dihydroindole and ethylbenzene. Neither complete denitrogenation nor hydrogenation was achieved with any of the catalysts. The ranking for denitrogenation selectivity among the three catalysts was Mo naphthenate > Mo/Al_2O_3> P-MoS_2.

Hydrocracking of Bibenzyl. The reaction pathway for the hydrocracking of the ethylene bridge in bibenzyl can either proceed by cleaving the carbon-carbon bond of the bridge structure forming toluene or by cleaving the bond between the aromatic ring carbon and the ethylene bridge, forming ethylbenzene and benzene. Under proper conditions, these hydrocracked products can be further hydrogenated (16).

Hydrocracking of bibenzyl only occurred to a small degree both thermally and catalytically. For all cases, percent hydrocracking was ~3% (Table 1). Products observed in most cases were minor amounts of ethylbenzene, ethylcyclohexane, toluene and benzene.

Combined Reactant Reactions. Reactions were performed thermally and catalytically with solutions composed of 1 wt% of all five model compounds in order to simulate the interaction among the different functionalities in a coal liquefaction system. Combined thermal reactions resulted in an increase of indole conversion to indoline and a decrease in the reactivity of 1-naphthol compared to the individual reactions.

Catalytic reactions performed with Mo naphthenate revealed the same trend as the thermal reactions but to a much greater degree. Complete conversion of indole was observed as well as complete deoxygenation of 1-naphthol; however, significant inhibition of the hydrogenation products of 1-naphthol was observed. Also, a decrease in hydrogenation of 1-methylnaphthalene and in bibenzyl hydrocracking was observed compared to the individual reactions. Since increased catalyst loading was used for the combined reactions, individual reactions with indole were performed with increased Mo loading of 3500 ppm Mo per g of reactor charge to ascertain the effect of increased catalyst loading compared to additional reactants. The same trends were observed as stated above, with small increases in inhibitive effects.

Reactions performed on combined solutions with Mo/Al_2O_3 exhibited different trends. The inhibitive effects noted with Mo naphthenate were reversed with Mo/Al_2O_3. Increases were achieved in the hydrogenation products of 1-methylnaphthalene and 1-naphthol, with the same corresponding conversion of indole as observed with the Mo naphthenate reactions.

Reactions performed with precipitated MoS_2 on the combined solutions yielded results similar to that of Mo naphthenate, but to a lesser degree. Hydrogenation of 1-methylnaphthalene and 1-naphthol products was inhibited as was hydrocracking of bibenzyl. An amplification of indole conversion was also observed.

Coal Liquefaction Reactions. A series of coal liquefaction reactions was performed to assess the activity and selectivity of the three Mo catalysts for the conversion of Illinois No. 6 coal to soluble products. Final assessments of selectivity and activity were based upon the production of the different solubility fractions and compound classes described in the Experimental section. Hydrogenated products of the solvent, anthracene, were also analyzed to assess the percentage of hydrogenation achieved during the reaction.

Thermal reactions of Illinois No. 6 coal yielded a coal conversion of 62%. The product distributions of gas, MCMS, THFS, and IOM, given in Table 2, indicate low thermal gas production and appreciable IOM after reaction. Much higher coal conversion was produced during the catalytic reactions as shown in Table 2. Mo naphthenate achieved 92% coal conversion; Mo/Al_2O_3 yielded 90%, and precipitated MoS_2 converted much less at 79%.

Production of THFS ranged from 22% thermally to 31% with Mo/Al_2O_3. The production of THFS was generally related to an increase or decrease in the amount of the MCMS fraction. The lowest production of THFS was generated by Mo naphthenate at 17% which was accompanied by the highest production of MCMS, ~48%. The largest production of THFS was obtained with Mo/Al_2O_3, which also exhibited a relatively high MCMS fraction, 40%. Mo/Al_2O_3 was not as effective as Mo naphthenate in converting THFS to MCMS. Precipitated MoS_2 produced low THFS at 21% and a MCMS of 37% which was comparable to Mo/Al_2O_3 but was not as effective for overall coal conversion.

Table 2
Product Distribution from Coal Liquefaction Reaction

Weight Percent

Product Fraction	Thermal	Mo Naphthenate	Mo/Al_2O_3	P-MoS_2
Gas	8.7±3.3	28.2±4.3	19.6±1.7	20.2±0.9
MCMS				
HC	11.5±1.8	24.0±1.0	16.6±0.1	15.0±0.7
NH	3.9±1.2	4.6±1.4	6.1±0.1	5.0±0.1
HA	8.1±2.0	8.8±0.2	9.7±0.5	10.8±2.3
PC	8.4±0.5	9.5±0.6	7.5±0.4	6.3±1.4
THFS	21.6±5.2	16.5±0.9	30.9±0.3	21.4±2.8
IOM	37.8±3.8	8.4±3.8	9.6±1.9	21.3±0.3
Coal Conversion, %	62.2±3.8	91.6±3.8	90.4±1.9	78.7±0.3

Comparisons of the compound class separations given in Table 2 indicate that Mo naphthenate produced the largest percentage of hydrocarbons (HC) at 24%. The other catalysts yielded less, ~17% with Mo/Al_2O_3 and 15% with precipitated MoS_2. The nitrogen heterocyles (NH) were 4% thermally and in the presence of a catalyst increased only slightly to 6%. The same trend was observed with hydroxyl aromatics (HA) with thermal production at 8% and increasing to 11% with the precipitated MoS_2 catalyst. The increase in the NH and HA fractions in the catalytic reactions was due to increased coal conversion and MCMS production, yielding more nitrogen heterocycles and hydroxyl aromatics soluble and analyzable.

The relative differences in the NH and HA fractions of the catalytic reaction can be seen more easily by examining the average results on a MCMS basis as given in Table 3. A general trend could be seen for Mo naphthenate and Mo/Al_2O_3, where the catalysts produced the NH and HA fractions on a proportionate basis, although the former produced less overall of the two fractions. P-MoS_2 produced a different distribution with the HA fraction produced being disproportionately higher than that of the other catalysts and the NH fraction being lower than Mo/Al_2O_3 but not as low as Mo naphthenate. These compound class distributions indicated that precipitated MoS_2 was more selective for denitrogenation than for deoxygenation.

Table 3
Compound Class Fractions from Coal Liquefaction Reactions on a MCMS Basis

Compound Classes, Wt% on MCMS Basis	Thermal	Mo Naphthenate	Mo/Al_2O_3	P-MoS_2
HC	36.1±4.0	51.3±1.7	41.7±0.2	40.4±0.2
NH	12.2±2.6	9.8±3.2	15.1±0.1	13.5±0.4
HA	25.3±3.5	18.7±0.3	24.3±1.3	29.1±4.9
PC	26.4±3.0	20.2±1.1	18.9±0.5	17.0±4.6

Polyfunctional compound (PC) decreased smoothly from thermal conditions at 26% to catalytic with precipitated MoS_2 at 17% on a MCMS basis. These results are best interpreted in terms of the HC fraction. The increase of HC to 51% for Mo naphthenate was a result of the reduction of all the other classes, NH, HA and PC. Mo/Al_2O_3 followed the same patterns but only produced ~42% HC. Precipitated MoS_2 yielded 40% HC which was produced more from denitrogenation than from deoxygenation.

In terms of the greatest selectivity for hydrocarbon production, hydrodeoxygenation and coal conversion to soluble products,the catalysts can be ranked as Mo naphthenate > Mo/Al_2O_3 > P-MoS_2. However, for hydrodenitrogenation selectivity of greatest impact was Mo naphthenate > P-MoS_2 > Mo/Al_2O_3.

Anthracene Hydrogenation. Anthracene hydrogenation during coal liquefaction ranged form 33% under thermal conditions up to 41% for Mo naphthenate reactions (Table 4). Reaction products resulting from anthracene hydrogenation included dihydroanthracene (DHA), hexahydroanthracene (HHA) and octahydroanthracene (OHA). Some cracking of anthracene was observed, from 4 to 6 mole percent, with the cracked products being in the boiling point range for naphthalene and its derivatives. Reactions with Mo/Al_2O_3 produced the highest level of cracking. The percent hydrogenation of the solvent remained within a deviation of 3 mole percent for all catalysts with only slight variations in product distributions.

Table 4
Anthracene Hydrogenation in Thermal and Catalytic Coal Liquefaction Reactions

Reaction	Hydrogenation, %
Thermal	33.0±0.7
Mo Naphthenate	41.1±2.7
Mo/Al_2O_3	36.1±2.3
$P-MoS_2$	40.1+1.2

Summary

The oil-soluble Mo naphthenate was the most effective catalyst for reactions involving hydrogenation, deoxygenation and denitrogenation. Effective hydrocracking was not achieved with any of the catalysts involved. Roughly equal activity for desulfurization was observed for each Mo catalyst. Reactions containing model compounds representative of the five reactions studied, experienced interactive effects which included hydrogenation and hydrocracking inhibition and increased reactivity of nitrogen compounds in the presence of Mo naphthenate and precipitated MoS_2. These inhibitive effects were reversed to promotional effects in the presence of Mo/Al_2O_3.

Mo naphthenate was also the most effective catalyst for overall coal conversion and the production of MCMS fraction and hydrocarbons. This catalyst also proved most effective for denitrogenation and deoxygenation. Mo/Al_2O_3, while exhibiting comparable coal conversion as Mo naphthenate, produced less MCMS and hydrocarbons. Precipitated MoS_2 showed the least propensity for coal conversion, but did exhibit somewhat better selectivity for denitrogenation than did Mo/Al_2O_3. The anthracene hydrogenated thermally and catalytically forming hydroaromatic species. Hydrocracking of anthracene was observed in all reactions, with those using Mo/Al_2O_3 producing the most.

References

1. Bearden, R., Jr.; Aldridge, C. L. U. S. Patent 4,134,825 (1979).
2. Kottenstette, R. J. Sandia Report No. SAND-82-2495, Energy Abstracts 22936 (1983).
3. Bockrath, B. C. "Mechanisms of Coal Liquefaction" Quarterly Report for the Period Ending June 30, 1981, Pittsburgh Energy Technology Center, November 1981.
4. Chianelli, R. R.; Dines, M. B. Inorganic Chemistry, 17, 2758 (1978).
5. Chianelli, R. R.; Prestidge, E. B.; Pecoraro, T. A.; De Neufville, J. P. Science, 203, 1107, (1979).
6. Chianelli, R. R. Catalysis Reviews - Science and Engineering, 26, 361 (1984).
7. Chianelli, R. R. Journal of Crystal Growth, 34, 239 (1976).
8. Boduszynski, M. M.; Hurtubise, R. J.; Silver, H. F. Analytical Chemistry, 54, 375 (1982).
9. Vamos, E., Siklos, P., Pozsgai, T. Periodica Polytechnica, 16, 253 (1972).
10. Sonada, R.; Ohmae, T. German Potent, German Offen. 2,229,844 (1973) as cited in Chem. Abstracts, 78: 97381.
11. Patzer, R. R. II; Farrauto, R. J.; Montagna, A. A. Industrial and Engineering Chemistry Process Design and Development, 18, 625 (1979).
12. Vogelzang, C. L.; Li, G. C.; Schuit, A.; Gates, B. C. Petrakis, L. Journal of Catalysis, 84, 170 (1983).
13. Odebunmi, E. O.; Ollis, D. F., Journal of Catalysis, 80, 65 (1983).
14. Schlosberg, R. H.; Kurs, A. Journal of Catalysis, 80, 65 (1983).

15. Stern, E. W. Journal of Catalysis, 57, 390 (1979).
16. Conklin, K. M.; Bell, A. T. U. S. Department of Energy Report LBL-4440, Energy Research Abstracts, No. 15400 (1975).

Acknowledgements

The authors gratefully acknowledge the Department of Energy and the Consortium for Coal Liquefaction Science for support of this work under Contract No. UK-RF-42181687.

ORIGINS AND REACTIONS OF ALKLYS AND ALKANES IN DIRECT COAL LIQUEFACTION

ENEO C. MORONI

U.S. Department of Energy, FE-25 GTN, Washington, D.C. 20545

INTRODUCTION

Recent analytical methods have attempted to unveil the nature of the aliphatic part of the molecules present in coal structures, and, with some approximation, they were successful in determining the origins and the size distribution of the alkyl chains and of the linear hydrocarbons. The abundant presence of alkyl groups have been observed among the products of thermal and donor solvent dissolution reactions of various coals. While the analytical determination of alkyls presence in the products of coal conversion and the speculation of their original status in the coal matrix have been extensively studied, their roles in the various reactions occurring in coal liquefaction have not received adequate attention by the research community. In particular, the high severity of operation used in the experimental research works for so many years and, regrettably, even in present research works, has precluded the determination of the role of each of the reactive components existing in the coal structure or formed in various stages of coal liquefaction. In addition, there is a scarcity of information on the role of each of the reactive species and their effect on the reactivity of the other components of coal and coal liquids.

It is commonly accepted that beneficial results are obtained in coal liquefaction by the programmed or staged temperature approach(1), and, currently, this experimental mode has become popular with many researchers.

For a more fundamental approach in coal liquefaction there is an opportunity to study the reactions occurring at the low temperature ranges, say 250-380^{o}C, for each of the reactive components, or each group of components present in coal or formed in the initial stages of liquefaction, which can be related to the most significant beneficial effects observed in the staged temperature experiments.

By increasing the reaction temperature to above 380-400^{o}C, the researcher must be aware that he or she is approaching the threshold separating the predominance of hydrogenation reactions of aromatic compounds at the lower temperatures from those of dehydrogenation of hydroaromatic compounds which occurs at the higher temperatures.

This paper, presently in the form of a communication to be complemented by the oral presentation and expanded for publication in Energy and Fuels, intends to present some of the reactions involving alkyl groups as well as formation of alkanes, which might have important roles in coal liquefaction. The paper has the additional objective to stimulate the research community to undertake a more systematic research approach in liquefaction which ought to separate the many reactions occurring at the lower temperature range from the subsequent reactions occurring at the higher temperatures. The latters are profoundly affected by the way the former are carried out.

INITIAL STAGES OF COAL LIQUEFACTION

In coal liquefaction experiments, in which coal is slurried in a solvent and heated up to promote coal dissolution, reactions are observed to start at 250-280^{o}C with evolution of mainly CO_2, particularly evident in low-rank coals. A large conversion of CO_2 to methane has been observed when the reaction off-gas is in the presence of hydrogen pressure and hydrogenation catalysts, and by increasing the reaction temperature from 300^{o} to 380^{o}C. This undesirable reaction consumes hydrogen and creates obvious confusion if one desires to determine accurately the methane derived from the cleavage of methyl groups from the coal structure, at the same or subsequent higher temperatures. Up to date most researchers in coal liquefaction have neglected this occurrence, and, for that matter, to provide full material balances. At the same temperature range in which CO_2 converts to methane, there are other reactions involving the isomerization of alkylphenols. These reactions occur in the presence of gamma-alumina, and perhaps of clays present in the coal mineral matter, such as, montmorillonites and illites. By increasing the reaction temperature above 350^{o}C, alkylphenols isomerize to the more thermally stable meta-position. The thermal removal of the hydroxyl groups from meta-alkylphenols is much harder than from the ortho-alkylphenols.

The importance of removing the hydroxyl groups has been emphasized by this author in a previous paper(2), because of the substantial benefits it provides in both liquefaction stage and in the subsequent upgrading stage. An example cited in that paper was the cleavage of the oxygen bridge in diphenyl ether, very often used as model compound reaction related to coal liquefaction according to recent literature, in which the oxygen bridge is cleaved at lower severity if an alkyl group is present in one of the ring, and, in particular, if it is located in ortho-position to the oxygen.

This seems to be in agreement with the fact that oxygen moieties have been removed with ease at much lower severity of experimental conditions in coal liquefaction than from oxygen-containing model compounds commonly used by researchers in this field. This fact would confirm that alkyl groups and, for that matter, other groups which are present in the ring structure of coals, are playing an important role in the initial stages of coal liquefaction. But, given the preponderance of oxygen moieties and the hydrogenation environment required, the predominant feature in coal liquefaction is the dominance of phenolic chemistry.

SUBSEQUENT LIQUEFACTION STAGES

At higher severity of operations, the phenolic chemistry is still dominant in coal liquefaction, because of the conversion of phenol-precursors to phenols. In the 400-450^{o}C temperature range, transalkylation reactions occur as polyalkylated phenols are able to donate alkyl groups to the non- or less-alkylated phenols, in the presence of clay catalysts(3). At hydropyrolysis temperature range of 600-1000^{o}C, oxygen in the aromatic rings and hydroxyl groups of phenols were found to strongly enhance the methane yield(4), decarbonylation being the key initial step.

At one point in coal liquefaction perhaps the active oxygen moieties will be practically removed, and other functional groups will probably emerge as the critical reactive species. However, little is known of the reactions involving alkylated cyclic compounds containing nitrogen and sulfur in the ring. It is believed that the chemistry of alkyl polycyclic aromatics, or hydroaromatics, ought to have a more influential role in the upgrading and refining steps. The selection of the proper catalyst and the experimental conditions in these steps appear to affect the reactions involving alkyl groups, such as, isomerization, transalkylation and "paring" reactions(5).

CONCLUSIVE REMARKS

The abundance of various oxygen moieties and alkyl groups in coals, revealed by current sophisticated analytical devices, signifies that they are a critical part of coal reactivity and consequently are having a major effect on the initial stages of coal liquefaction and very likely in the upgrading and refining steps.

Little is known about the homogeneous chemical reactions which, during liquefaction, bring about the reaction of either the removal of each of these groups, or condensation reactions, that is, coupling for the phenols and cyclization for large alkyl groups. Even less known is the effect of one group on the other, and the combined effect on other critical reactions in coal liquefaction.

This communication lists some of the reactions known from unrelated past works which, it is felt, could be profitably pursued in future coal liquefaction research. An amplified version of this communication will be covered during the oral presentation, and a more detailed and complete set of data will be published in Energy and Fuels.

REFERENCES

1. Derbyshire, F.J., et al. (1986). Temperature-Staged Catalytic Coal Liquefaction, FUEL, 65, p. 1233, and references cited therein.

2. Moroni, E.C., Coal Liquefaction and Upgrading Benefit from Heteroatom Removal. Proceedings of the 1987 International Conf. on Coal Science, Maastricht, The Netherlands, October 26-30, 1987, p. 351, and references cited therein.

3. Neuworth, M.B., Moroni, E.C., and DelBel, E., Selectivity of Transmethylation of High Boiling Cresylics. U.S. Patent 3,417,149, December 17, 1968.

4. Gobarty, M.L., and Maa, P.S., A Critical Temperature Window for Coal Hydropyrolysis, Am. Chem. Soc., Div. Fuel Chem. Preprints, 31,(4), 5, 1986, and references cited therein.

5. Sullivan, R.F., et al. A New Reaction That Occurs in Hydrocracking of Certain Aromatic Hydrocarbons. JACS, 83, 1156 (1961).

The Macromolecular Structure of Coal- Its Relationship to Diffusion and Reaction Processes in Coals

Eric M. Suuberg, Yoshi Otake, and Seetharam Deevi
Division of Engineering
Brown University
Providence, R.I. 02912

INTRODUCTION

Recently, a considerable amount of attention has been directed at understanding how the macromolecular structure of coal influences its reaction behavior. The fact that coal must have a macromolecular structure has been recognized for some time, and has been embodied in many of the "classic" models of coal structure(e.g. refs. 1-5). The recognition that coals will behave accordingly naturally accompanied the development of these models. Van Krevelen[2] and Kreulen[6] recognized the colloidal nature of coals and used this to explain many important features of their behavior. Wolfs et al.[7] demonstrated that that certain polymeric substances were good analogs for coal, with respect to pyrolysis behavior. This work remains the cornerstone for many of the sophisticated models of coal pyrolysis behavior today. The development of models of fluidity has long been based on "depolymerization" as a key step (e.g. ref.8). And of course extraction of soluble material from coal has been understood for many years as the segregation of small soluble components from an insoluble matrix which can also be broken down to some extent by thermal decomposition.[9]

What has changed in recent years is mainly the level of understanding of the macromolecular structure of coal, and the number of tools (mostly borrowed from the polymer field) used to study that structure. The review by Green et al.[10] has summarized much of the historical development of the coal macromolecular concept, as it exists today, and discusses many of the tools that have been applied in studying the problem.

The present paper is concerned mainly with some rather specific aspects of the problem of characterization of the macromolecular structure of coals, and their relationship to key reaction processes and physical properties.The main characterization technique used throughout this work is solvent swelling[11], as has been used extensively in recent years to characterize the extent of crosslinking in coals[12-16]. This classic technique was originally developed for examination of extents of crosslinking in polymers. The simplest relationship that embodies the essence of the technique is the Flory-Rehner equation, a relationship between the molecular weight between crosslinks in a polymer (M) and the extent to which the polymer is volumetrically swollen by a particular solvent (Q):

$$M = -\left[\frac{\rho_c Ms}{\rho_s}\right]\left[\frac{(1/Q)^{1/3}}{\ln\,[1-(1/Q)] + (1/Q) + \chi(1/Q)^2}\right]$$

where ρ_c is the density of the original coal, ρ_s is the density of the solvent, M_s is the molecular weight of the solvent and χ is the solvent-network interaction parameter. The measurement of χ is difficult, as is its estimation for specifically interacting solvents such as pyridine. Values range between 0.3 and 0.6 for typical pairs of solvents and coals. It has been suggested that the Flory-Rehner equation does not hold particularly well for coals, which are highly crosslinked rigid networks[12,13]. Its use here is only illustrattive, and more sophisticated approaches have been developed[17,18]; unfortunately these other approaches require more information about the structure of the coal- namely, the molecular weight of repeat units within the coal structure. Since such information is not readily available at present, this will tend to restrict somewhat the use of these more sophisticated approaches. For the purposes of modeling transport and reaction processes in coals, detailed information about the structure will not always be necessary, and progress can be made without having the exact form of the structure-swelling relationship available. It is in this light that the present results are presented.

The present paper considers two entirely different aspects of the relationship between macromolecular structure and reactivity and transport in coals. The first aspect concerns the reactions of crosslinking in coals during thermal treatment. This topic has been previously explored using the solvent swelling methodology[15,16]. Here the work is extended to consider how the colloidal structure of coal is affected by moisture removal, and by further heating. The second aspect concerns the diffusive transport of solvent species in coals, and the activation energies for such processes.

EXPERIMENTAL

The analyses of the coals examined in this study are provided in Table 1. Except where otherwise noted, the coals were ground and sieved to the size range 53-88μm. Special care was given to the lignites to avoid any more drying than necessary while processing. The first four samples in Table 1 were judged to have dried to only a limited extent since mining, and all were crushed in-house from large lumps. To prevent drying, these four samples were stored at 100% relative humidity conditions, at room temperature, by suspending the samples above a large reservoir of clean water, in a sealed container. It is of course difficult in practice to maintain truly 100% relative humidity conditions in such a manner, particularly if the chamber must be occasionally opened for sample removal. There was consequently a small difference in measured moisture contents between bed-moist samples (which are effectively immersed storage samples) and those used in this study. The difficulty in characterizing the initial moisture contents of immersed samples was what prompted us to use this slightly different storage method. Related sample storage and characterization information concerning these lignites can be found elsewhere[19].

Thermal treatments of the samples were always performed under inert gas (high purity helium or nitrogen), to avoid any possible role of oxidation in the results. The thermal treatments were performed in either standard tube furnaces, in which the samples were normally heated at low heating rates (a few tens to hundreds of degrees per minute) or in a wire mesh type of apparatus, in which small amounts of sample are contained in the folds of a stainless steel wire grid that is heated at rates of order 1000K/sec.

Solvent swelling measurements were performed largely as described in other studies[20]. In the present case, however, the measurements were performed in small tubes of a few millimeters inner diameter and less than 5 cm in length. This technique permitted such measurements to be made with modest quantities of sample, provided that the sample and solvent is frequently stirred during the first phases of the swelling process. This technique gives reproducibility comparable to that for the standard technique with large tubes. A major reason for the difference between the standard solvent swelling techniques and those employed here stems from a concern about measuring accurately rates of swelling. In the second part of this paper, results will be given for activation energies of diffusion processes in coals, which were determined from timed swelling experiments. In the cases in which rate data were of interest, the swelling experiments were performed in thermostatted baths. The small diameter of the tubes and the frequent mixing of the contents with a small stirrer assured good heat transfer between the environment and the sample. In order to determine the height of the column of coal at any particular time (and thus the volumetric swelling ratio), the samples were "quenched" by immersion in an ice bath, and were quickly centrifuged in a high speed centrifuge, with cooling. The centrifugation takes only about ten minutes, during which time, because they are cooled, the samples swell negligibly.

RESULTS AND DISCUSSION

THE CROSSLINKING BEHAVIOR OF COALS DURING DRYING AND PYROLYSIS

Some aspects of this problem have been discussed previously, both in connection with the drying behavior of lignites[19] and the pyrolysis behavior of various ranks of coal[15,16]. This work has been extended in order to understand more fully how the macromolecular structure is altered during these processes.

At the outset, it is important to note that all ranks of coal have a colloidal structure, that will shrink and swell in response to imbibation of a solvent. The most common "solvent" is water, in that it is naturally present in all ranks of coal at the time of mining. The shrinkage and swelling behavior of lignites and brown coals in response to moisture loss and gain, respectively, has been quantitatively studied[19,21]. In these earlier studies, it was noted that the extent of shrinkage was closely related to the amount of moisture lost from the lignite- to a crude approximation, the extent of shrinkage was calculable assuming the the water lost from the coal had a specific volume of 1cc/g. This is why measurements of BET surface area (or any of the other usual measurements of porosity) often reveal so little micro- and transtitional porosity in lignites-- the porosity essentially collapses as the samples are being dried for examination by the usual porosity determination methods.

More recently, we have extended the examination of drying phenomena to include a much wider range of ranks. Figure 1 shows the volumetric shrinkage of coals ranging from lignite up to bituminous in rank, and surprisingly, a very good linear correlation exists between the volumetric shrinkage and moisture content throughout the entire range. The actual correlation is:

$$\%\text{Shrinkage} = 0.94(\%\text{Moisture Loss}) -0.6$$

Thus it is apparent that colloidal swelling behavior is observed with water as a "solvent" even in ranks up to bituminous. This menas that this entire range of ranks is subject to the same qualitative kinds of uncertainty in porosity characterizations as are lignites. To be sure, the effects are not nearly as large in bituminous coals, but there is no question that porosity does collapse upon drying.

It has been shown that the shrinkage that accompanies drying of lignites is to some extent irreversible. Typically, only about 80% of the shrinkage is recoverable[19]. The question is, what determines the extent of irreversiblity of shrinkage? There are apparently some processes that occur, presumably on a molecular level, that prevent full reswelling of the coal, once it is rewet. This raises a general question of how coals crosslink during thermal treatments of any kind. We have explored some aspects of this problem by performing solvent swelling measurements on thermally treated coals. The results on one set which was heated slowly in a tube furnace is shown in Table 2. Several features may be noted in Table 2. First, coals that are still wet generally do not swell to as great an extent in pyridine as do coals that are dried at ordinary conditions. This is easily understood in terms of the network having already swollen to a significant extent in water. The fact that pyridine is able to swell it as much as it does is evidence of its stronger interaction with the lignites, relative to water with the lignites. Tetrahydrofuran (THF), on the other hand, is only a marginally better solvent for these lignites than water itself, as indicated by the modest swelling of wet coals in this solvent. There appears to be no constant ratio of swelling in pyridine to swelling in THF, nor is there a constant ratio of swelling in THF compared to that in water; this makes the point that even in fairly similar coals of identical rank, such as in this set of North Dakota lignites, the individual interactions of solvent and coal are rather important in determining swelling behavior.

The swelling ratio of a wet coal in pyridine is related to the swelling ratios of room temperature dried coals in pyridine. If the pyridine swelling ratio of a wet sample is multiplied by the ratio of (water) wet to dry volume of the lignite, the actual swelling ratic of the dry sample in pyridine may be estimated, i.e. there is no evidence of co-operative swelling effects involving pyridine and water.

The samples that are heated directly to 373K from a wet state obviously crosslink to a much lesser degree than do the samples that were first dried, and then heated. This is evidence that there are crosslinking processes that must occur at temperatures at least as low as 373K, and in the absence of oxygen from the atmosphere. Further, the processes are apparently strongly promoted by the absence of moisture during heating. The carboxyl contents of the lignites have been measured directly by barium exchange after reaction under these conditions, and in no case was a reduction greater than 10% seen in increasing the drying temperature from 373K to 473K. Together, this information suggests that the decarboxylation reactions that have been postulated to determine crosslinking in high temperature processes[15] (and which has received support from modeling work[22]), may be supplemented by another process that is promoted by the absence of water during the initial phases of the heating process. For comparison, high heating rate pyrolysis behavior is shown in Figure 2. The illustrated behavior is fairly typical of all of the lignites, whether dried or undried, except as noted below. The experiment in this case consisted of heating a wet lignite at a rate of roughly 1000K/sec to a peak temperature, shown as the abcissa value, and then immediately cooling at a rate of about 300K/sec. It can be seen that the extent of crosslinking remains much lower at much higher temperatures in these rapid heating experiments.There is, however, still a slight tendency to crosslink at temperatures below about 625K. Above about 650K, all the lignites show a tendency to depolymerize, shown as an increase in solvent swelling tendency, and coinciding with the onset of the tar formation process. A similar observation has recently been independently reported[23]. The swelling ratio decreases rapidly beyond about 700K, as the crosslinking reactions occur rapidly in this temperature range. It was in this temperature range that the decarboxylation reactions were thought to dominate. The directly determined decrease in carboxyl content did, in the one case studied, exactly equal the amount of CO_2 formed in the temperature range up to 900K. The mechanism of the decarboxylation, and more importantly, how it participates in the crosslinking process reamains unknown. Again, the absence or presence of water had no effect on these higher temperature mechanisms, except in one sample. This may not be surprising in view of the fact that the water should have evaporated by the time these high temperatures are attained. However, earlier pyrolysis results for the Beulah lignite did show an effect of predrying even at high heating rates[15].

In addition to the effects of thermal treatment noted above, 373K drying was also noted to considerably decrease the rate of diffusion into coals, compared to the rate of diffusion into room teperature air-dried samples. The rate of swelling of even a low moisture bituminous coal, such as Powhatan was decreased by a factor of two by 373K drying (i.e. standard ASTM conditions). The ultimate swelling ratio was however unaffected by the drying. This suggests that physical crosslinking of some kind is promoted by the drying procedure, but may be reversed if the solvent is strong enough. This reversible crosslinking is also noted in the lignite samples, and is distinct from the irreversible crosslinking that occurs above 373K, or in some cases, even at 373K.

ACTIVATION ENERGIES FOR DIFFUSION

The above discussion of the effects of crosslinking has pointed up how crosslinking may affect the diffusion process in coals. As part of an effort to characterize better the diffusion of solvents and large molecules through the bulk of the coal (as opposed to through pores), we have made measurements of diffusion rates of various solvents by tracking solvent swelling as a function of time. The process of diffusion in the bulk of a crosslinked macromolecular material is generally an activated process, meaning that the diffusion coefficient varies according to: $D=D_0\exp(-E/RT)$. Very good recent studies of the diffusion process, unde conditions similar to those of interest here have shown the process to actually be of the "Case II" type; i.e. relaxation controlled[14,18]. There is not space here to go into the details of the process.

The process of diffusion has been studied at temperatures from 298Kup to 318K, with pyridine, tetrahydrofuran and water as diffusants. Various ranks of coal, and heat treated coals have been examined. Selected results are given in Table 3. Several features are important to note. First, there is a large difference in activation energies between the different ranks of coal, and between different solvents. Heat treatment seems to have the expected effect- not only does the diffusion become slower at all temperatures, but the activation energy increases, presumably as the structure becomes more rigid, and the vibrational conformations necessary to allow for solvent molecules to pass become ever less probable. The value of activation energy is felt to depend more upon the size of the penetrant species, and less upon the specific interactions of the coal and the solvent molecule. Note that the activation energy for THF is considerably lower than that for pyridine, however the rate of swelling in pyridine is more than an order of magnitude higher than in THF at room temperature, and the extent of swelling is also much higher in pyridine.

CONCLUSIONS

This paper has, in a very brief manner, touched upon two different aspects of how the macromolecular structure of coal relates to important physical and chemical phenomena. The studies continue as of this writing, on both of the above topics. The utility of straightforward techniques of characterization of macromolecular structures, such as solvent swelling, cannot be underestimated as important contributors to the more complete understanding of complex processes and phenomena in coals.

ACKNOWLEDGEMENT

The support of the USDOE through grants DE-FG22-85PC80527 and DE-AC18-84FC10617 is gratefully acknowledged.

REFERENCES

1. Fuchs,W. and Sandhoff, A.G., I&EC,34,567 (1942).
2. Van Krevelen, D.W.,Coal, Elsevier, 1961.
3. Given,P.H., Fuel,39,147 (1960).
4. Hill, G.R. and Lyon,L.B., I&EC,54, 36 (1962).
5. Wender,I., ACS Div. Fuel Chem. Prepr.,20(4), 16,(1975).
6. Kreulen,D.J.W., Fuel,25, 104 (1946).
7. Wolfs, P.M., Van Krevelen,D.W., and Waterman, H.I., Fuel,39, 25 (1960).
8. Fitzgerald,D., Fuel,35, 178 (1956).
9. Kiebler,M.W., in Chemistry of Coal Utilization, Vol. I., H. Lowry, Ed.,Chapter 19, Wiley, 1945.
10. Green,T.,Kovac,J., Brenner,D., and Larsen, J.W., in Coal Structure, R. Meyers, Ed., Chapter 6, Academic Press, 1982.
11. Flory,P.J. and Rehner,J. J.Chem.Phys.,11 ,521 (1943).
12. Larsen,J.W. and Kovac, J., ACS Symp. Ser. No. 71, 36 (1978)
13. Lucht, L.M. and Peppas, N.A. ACS Symp. Ser. No. 169, 43 (1981)
14. Peppas,N.A. and Lucht,L.M.,Chem. Eng. Comm.,37,333 (1985); also Energy &Fuels,1,56 (1987); Barr-Howell et al., Chem.Eng. Comm.,43,301 (1986); Ritger and Peppas Fuel,66,815 (1987).
15. Suuberg, E.M., Lee,D., and Larsen, J.W., Fuel,64, 1668 (1985).
16. Suuberg, E.M., Unger,P.E., and Larsen, J.W., Energy & Fuels,1, 305 (1987).
17. Kovac,J., Macromolecules,11,362 (1978).
18. Peppas,N. Lucht, L., Hill-Lievense,M., Hooker,A., DOE Final Tech. Report DE-FG22-80PC3022, US Dept. of Energy, 1983.
19. Deevi, S. and Suuberg, E.M., Fuel,66,454 (1987).
20. Green, T.K., Kovac,J. and Larsen, J.W., Fuel,63, 935 (1984).
21. Evans,D.G., Fuel,52, 186 (1973).
22. Solomon, P.R., Hamblen, D.G., Carangelo, R.M., Serio, M.A., and Deshpande, G.V., Comb. &Flame in press.
23. Solomon,P.R.,Hamblen,D.G.,Deshpande,G.V., and Serio,M.A., 1987 Int. Conf. Coal Sci. (J.Moulijn et al., Eds.) p 601, Elsevier,1987.

Table 1-Coals Studied

sSAMPLE	C	H	N	S	ASH	O	Moisture
Beulah lignite[a]	65.6	3.6	1.1	0.8	11.0	17.9	26.0
Freedom lignite[a]	63.5	3.8	0.9	1.4	6.1	24.3	27.9
Glenn Harold lignite[a]	61.1	4.4	0.8	0.4	7.4	25.9	28.9
Gascoyne lignite[a]	60.9	4.2	0.6	1.4	8.2	24.7	30.7
Beulah lignite[b]	65.9	4.4	1.0	0.8	9.7	18.2	32.2
Texas lignite (PSOC1036)[c]	61.5	4.7	1.4	1.3	12.5	18.5	31.8
Belle Ayr Subbit.	69.3	4.4	1.0	0.5	10.3	14.5	30.3
Big Brown Subb.(PSOC785)[c]	62.8	4.6	1.1	1.1	12.6	17.8	27.8
Montana Subbit.(PSOC837)[c]	57.8	4.3	0.8	0.7	11.9	24.6	17.0
Pittsburgh No.8 (HVBit.)[b]	74.2	4.1	1.4	2.3	13.2	4.8	1.7
Bruceton HVBit.[d]	80.4	5.3	1.6	1.0	4.6	6.7	1.7
Powhatan HVBit.	72.3	5.1	1.5	3.6	9.7	7.8	1.1

•All results on a dry weight percent basis, except moisture which is ASTM value on an as-received, bed moist basis.
•Oxygen by difference.
a- Grand Forks Energy Research Center lignite sample bank.
b- Argonne National Laboratory Premium Coal Samples.
c- Pennsylvania State University Coal Sample Bank.
d- U.S. Bureau of Mines Standard Sample.

Table 2- Effect of Drying and Thermal Treatments on Solvent Swelling of Lignites

Condition	Beulah	Freedom	Gascoyne	Glenn Harold
Wet	1.48/1.08	1.62/1.00	1.33/1.07	1.60/1.18
0% R.H.,300K,24hrs	2.20/-	2.01/-	1.90/-	2.10/-
0%R.H.,300K, 30days	2.22/1.28	2.06/1.33	2.10/1.32	2.14/1.32
Wet, dried at 373K,1hr	2.34/-	2.50/-	2.05/-	2.47/-
Dry,then 373K,1hr	2.0/1.34	1.70/1.35	1.68/1.38	1.81/1.33
", then 473K, 1hr	1.43/1.25	1.66/1.28	1.54/1.29	1.75/1.22
", then 573K, 1 hr	1.22/1.16	1.45/1.15	1.50/1.06	1.50/1.15
", then 573K, 2 hr	1.14/1.10	1.30/1.12	1.42/1.06	1.45/1.13

•All values are volumetric swelling ratios, given as:
(pyridine volumetric swelling ratio/tetrahydrofuran volumetric swelling ratio).
•0% R.H. refers to drying over concentrated sulfuric acid, a 0% relative humidity environment. Samples marked "dry" were initially dried in this manner at room temperature, prior to thermal treatment.

Table 3- Activation Energies for Diffusion in Coals

Coal	Treatment	Activation Energy (kcal/mol)
Beulah (Argonne Sample)	Air dried, 1day	18.0
" "	Air dried, 3days	17.9
" "	Vacuum dried, 298K	19.4
" "	Vacuum dried, 373K	21.5
Montana Subbit.	Air dried	18.1
Pitts. No. 8	Vacuum dried, 373K	12.6
Bruceton HVBit.	Vacuum dried, 373K	13.
Bruceton HVBit.	Vacuum dried, 373K	8.8 (THF)

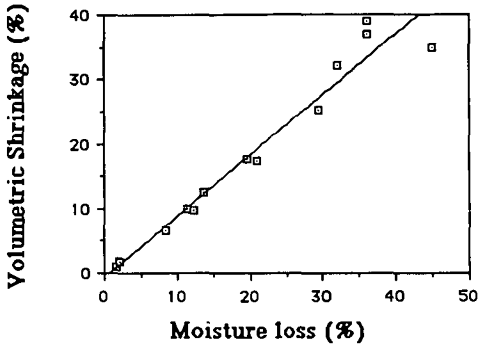

Figure 1. Volumetric Shrinkage of coals during room temperature drying.

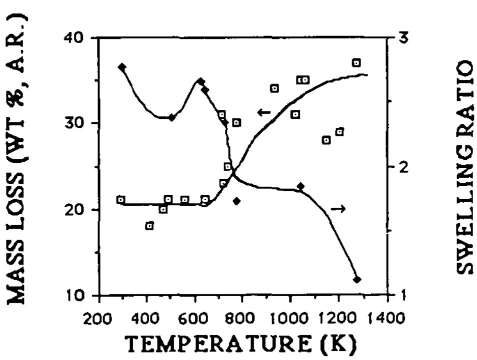

Figure 2. Mass loss and pyridine solvent swelling behavior of "wet" Freedom lignite, rapidly pyrolyzed under non-isothermal conditions to indicated peak temperatures.

INTERRELATIONSHIPS BETWEEN COAL ANALYSIS, COAL CONVERSION AND COAL STRUCTURE

Dennis Finseth and Bradley Bockrath
U.S. Department of Energy
Pittsburgh Energy Technology Center
P.O. Box 10940
Pittsburgh, PA 15236

Models for the average structure of a coal and for its chemistry both rely heavily on analyses that are subject to considerable errors. In addition to these analytical problems, it is often true that our notions concerning the "reasonableness" of a chemical reaction of a coal are influenced by our conception of what an average structure for that coal looks like. This picture of an average structure for a coal was in turn probably influenced by analytical results obtained for extracts and/or products of "mild" reaction conditions. These two factors -- the weakness of analytical techniques for solid coal, and the somewhat circular dependence of our concept of coal structure on coal chemistry -- present problems for studies of both coal structure and coal chemistry. The development of improved analytical techniques for solid coal as well as for characterization of coal chemistry, is very important to any improvement in our real knowledge of coal and its significant fuel- processing chemistry. Several projects at PETC have focused on improvement of our ability to characterize solid coal and its fundamental chemistry during direct liquefaction.

A large number of average structural models for specific coals have been published, and many describe in some detail how the structure was derived (1). The input data include elemental analyses (C,H,N,O,S), possibly an aromaticity from 13C NMR, and often some characterization data on extracts or mild-reaction products. It is emphasized by everyone who publishes an average structure that the structure is only a statistical entity and is not meant to represent the organic structure of a coal on a molecular scale. Although we are repeatedly cautioned, it is easy to let our thought processes concerning chemistry be influenced by such attractive (seductive) visual representations. It is worthwhile to look at the potential errors in the data used for generation of an average structure or for describing a chemical reaction of coal.

Determination of the elemental composition of coal is routinely accepted as a starting point for describing a coal's structure; however, the distinction between organic and inorganic forms can lead to problems. The recent paper by Ehmann et al. (2) reviews the well-documented problems associated with determination of organic oxygen in coals. This problem is in part related to the lack of an accurate analytical method for the determination of water. Because of the sequence of steps in a total elemental analysis of coal, residual water remaining after drying translates directly into errors in both organic oxygen and organic hydrogen. Similarly, the accepted method for determination of organic sulfur is by difference (3) and thus contains a significant coal-specific uncertainty related to the dispersion of pyritic sulfur in the coal. The rather bleak picture is that there is significant uncertainty in three of the five major elements in the organic structure of coal.

The composition of coal extracts is a very important input to construction of coal models; however, this extract rarely appears explicitly in average structural models that focus on representing the insoluble matrix of a coal structure. The amount of extractable material that is truly soluble, so that it can be analyzed by modern techniques, is usually rather small (5-15%). Inference of an overall coal structure from the 5% of its composition that can be analyzed is always fraught with difficulties. The yield of extract can be raised significantly by a variety of thermal and chemical means; however, these extracts may be criticized as being too substantially transformed to be meaningful for coal structural studies. How would a reviewing organic chemist react if the identification of an organic solid was accomplished by analyzing the sample as a THF extract after heating to 300°C with 10% water and 15% added mineral matter?

Bulk spectroscopic analyses of coal that are capable of yielding direct structural information on the solid are infrared (IR) and nuclear magnetic resonance (NMR). Infrared spectroscopy is always capable of yielding qualitative information, but quantitation has proven elusive. The solid-state CP^{13}C NMR spectra of coal can provide very useful structural information; however the question of what fraction of the total carbon is being observed is still being debated (4). If the ^{13}C aromaticity is determined on a nonrepresentative fraction of the total carbon, our picture of the average structure of a coal may be seriously in error.

Investigation of chemical reactions involving coal is rendered very uncertain by our problems in analyzing the coal itself. It is difficult to describe the chemistry of an organic reaction when the nature of the starting material is uncertain. An improved understanding of the fundamental chemistry of direct liquefaction is an ongoing area of interest at PETC. This goal requires development of analytical techniques appropriate to the coal liquefaction system. One approach has been application of CP-MAS-^{13}C NMR techniques for measurement of net hydrogenation. By combining this measurement with material balance information, it is possible <u>in principle</u> to determine the relative amounts of hydrogen consumed in hydrogenation, bond cleavage, and heteroatom removal.

The analysis of a variety of liquefaction systems using this hydrogen utilization approach has led to several conclusions: (1) under conventional liquefaction conditions, the net hydrogen consumed in hydrogenation of aromatic components is often small, (2) significant changes in "conversion" measured by solvent solubility can be accomplished with virtually no <u>net</u> hydrogen chemistry, and (3) analytical methods for analysis of slurries of coal and vehicle oil are a major limitation to the improvement of our understanding of coal conversion chemistry. A typical hydrogen utilization profile for a coal conversion experiment conducted at 380°C is shown in Table 1.

The conversion of coal to THF solubles was in excess of 80% in this experiment. Although the experiment indicates an >80% "conversion", all of the numbers in Table 1 may be nonsignificant because of experimental error. A major potential contributor to the experimental error in both heteroatom removal and total hydrogen consumption is the inability to accurately determine water in coal. If 1 wt % molecular water exists in the "dry coal" the analytical method conventionally used for direct oxygen and hydrogen determinations translates this water content into an error of -2 H/ 100C in the coal and would also result in a significant overestimation of the amount of organic oxygen in the slurry. This sensitivity of organic hydrogen and organic oxygen to the accuracy of the water determination indicated to us a need for improved confidence in the coal moisture analysis. A recently completed study of the water content of a variety of coal samples, both from the Argonne sample bank and from coals typically used for liquefaction research, indicates that the problem may be significant, especially for air-dried (or mildly air oxidized) samples (5). This study used an isotope exchange procedure that is capable of determining water that is not volatile under conditions of the ASTM procedure. The method does not require removal of the water from the coal to obtain an analysis. It is hoped that this method will provide a more accurate evaluation of the water content of a coal, which in turn will improve the accuracy of organic oxygen and hydrogen determinations.

Another significant uncertainty in discussions of coal chemistry is the measurement of the hydrogen within the slurry that is available in hydroaromatic structures. Such structures as the hydropyrenes have repeatedly been shown to be very effective in enhancing coal conversion. However, the content of such materials in complex heavy recycle vehicles, not to mention coal, is not easily determined. The content of multi-ring hydroaromatics in a coal structure is very important in establishing the amount of <u>internal</u> hydrogen readily available for participation in thermolytic reactions. Catalytic dehydrogenation of coal and vehicle has been used as a measure of this available hydrogen. We have attempted to use this technique coupled with NMR measurement of the aromaticity change on dehydrogenation to better understand the source of the hydrogen in such experiments. Conversion of a hydroaromatic to an aromatic with H_2 generation should conform to the following stoichiometry:

$$1\left(\begin{matrix}\text{Hydroaromatic}\\ \text{Carbon}\end{matrix}\right) \xrightarrow{\text{CAT}} 1\left(\begin{matrix}\text{Aromatic}\\ \text{Carbon}\end{matrix}\right) + \tfrac{1}{2}\ H_2\ (g)$$

Thus it should be possible to plot change in moles of aromatic carbon versus moles of hydrogen gas produced and obtain a slope of 2 (moles of carbon aromatized per mole H_2 produced). An example of such a system, the Pd catalyzed dehydrogenation of the bitumen gilsonite, is shown in Figure 1. Gilsonite was chosen because of its apparent high hydroaromatic content and its complex composition. The slope indicated in Figure 1 is near enough to the theoretical value for classical hydroaromatic dehydrogenation to conclude that the approach may be workable. This very simple analysis is applicable to complex systems and has potential for providing quantitative information relevant to coal conversion chemistry. If condensation of aromatics is the dominant source of the hydrogen gas generated, then a slope near zero might be expected because condensation should not affect the carbon aromaticity, f_a. If the hydrogen produced from hydroaromatic dehydrogenation is subsequently consumed by some unspecified bond cleavage chemistry within the liquefaction system, a slope greater than two would be expected. This technique has some promise for investigating internal redistribution of hydrogen in coal- vehicle slurries at mild temperatures.

Another example of a well-accepted concept in coal chemistry that is difficult to study directly is the role of free radicals in the thermal chemistry of coal. The existence of a huge reservoir (~10^{19} spins/g) of stable radicals in coal itself complicates the direct observation of the effects of the incremental transient of thermolytically produced radicals via ESR(6). An alternative method for observing the radical involvement in complex systems is to introduce into the system a nonintrusive chemical probe molecule sensitive to the presence of radicals. This approach attempts to circumvent our inability to directly monitor the formation and destruction of reactive free-radical species in coal with any reliability. The hope is that the appropriate probe will be selectively sensitive to the population of coal radicals that are directly involved in conversion. Recent work at PETC has used the equilibration of cis- and trans-decalin as a probe of the time-averaged steady-state concentration of radicals in complex coal liquefaction systems. A greater steady-state concentration of radicals results in a more rapid conversion of pure cis-decalin to the equilibrium mixture of cis and trans isomers. In this chemical-probe approach, only a small amount of a pure compound is added to the liquefaction feedstock. Because the chemistry of complex liquefaction systems is not likely to be perturbed by a small amount of additive, the chemical probe method has the potential to yield more relevant information than that from investigation of reactions in which a model compound is the sole or the predominant reactant. The decalin isomerization probe has been used to determine the steady-state concentration of free radicals in coal liquefaction using heavy petroleum resid as vehicle.

Conclusions

Studies of the net chemistry of direct liquefaction have focused attention on a number of analytical deficiencies that limit our confidence in describing coal chemistry and/or coal structure. The most obvious analytical limitations are the accuracy of the ^{13}C f_a value, which allows us to quantitatively assess the hydrogenation of aromatics, and the accuracy of the water determination in coal, which determines the accuracy of subsequent measurement of organic oxygen and hydrogen. These concerns are, of course, not new, but it is important that they be kept firmly in mind so that research aimed at resolving our analytical deficiencies can go on simultaneously with our investigations of the relevant chemistry of liquefaction and the structure of coal.

References

1. Heredy, L.A., and Wender, I., Am. Chem. Soc., Div. Fuel Chem. Preprints, 25(4), 1980.

2. Ehmann, W.D., et al., Fuel 65, 1563-70, 1986.

3. Bureau of Mines Bulletin No. 638, p. 11, 1967.

4. Hagaman, E.W., Chambers, R.R., and Woody, M.C., Anal. Chem., 58(2), 387-394, 1986.

5. Finseth, D., Am. Chem. Soc., Div. Fuel Chem. Preprints, 32(4) 260-263, 1987.

6. Sprecher, R.F., and Retcofsky, H.L., Fuel, 62, 473-476, 1983.

Table 1.

	Hydrogens per 100 Carbons of Slurry
Hydrogenation	1
Heteroatom Removal	1
Gas Production	0
Matrix Bond Cleavage	2
Total Hydrogen Consumption	4

Conditions: Feed = Illinois No. 6 coal (4g) + SRC II HD (7g)
Temperature = 380°C
Reaction Time = 20 minutes
Catalyst = Molybdenum (as ammonium heptamolybdate), 0.006g
Gas = H_2, 2000 psi

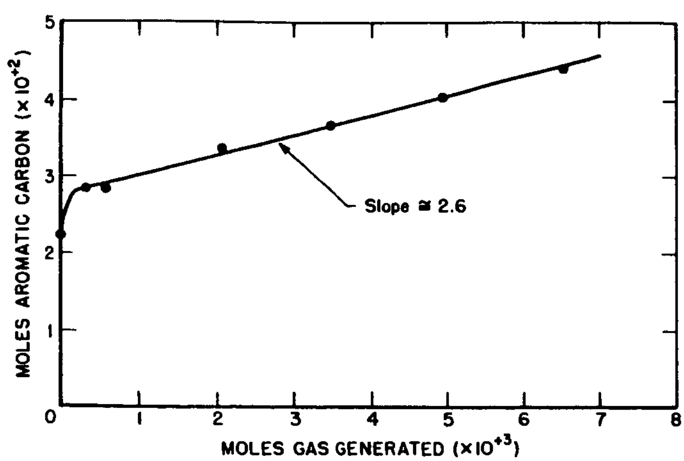

Figure 1. Relationship between change in aromaticity and gas generation on catalytic "Dehydrogenation" of gilsonite.

THE MACROMOLECULAR STRUCTURE OF BITUMINOUS COALS: MACROMOLECULAR ANISOTROPY, AROMATIC-AROMATIC INTERACTIONS, AND OTHER COMPLEXITIES

John W. Larsen
Department of Chemistry
Lehigh University
Bethlehem, PA 18015

and

Exxon Research and Engineering Co.
Route 22E, Clinton Township
Annandale, New Jersey 08801

INTRODUCTION

A homogeneous piece of vitrinite containing no mineral matter has two organic phases. One of these consists of a crosslinked macromolecular network and the other is a soluble family of macromolecules having a very broad molecular weight distribution. The network is held together by covalent bonds as well as by non-covalent interactions. There is abundant evidence for an important role of hydrogen bonds in the macromolecular structure and growing evidence for an important role for dipole-based interactions between the aromatic groups.[1-4] These same non-convalent forces are important in binding the extractable phase to the insoluble network. This paper deals with the way the macromolecules pack together in the solid and especially the role that the aromatic-aromatic interactions play in the packing of the macromolecular segments.

Evidence for the Existence of Non-covalent Interactions and their Geometry

Hydrogen bonds in coals can be observed directly in the IR spectra of coals. The disruption of coal-coal hydrogen bonds by organic bases has also been directly observed spectroscopically.[2] Coals swell much more in solvents which are strong hydrogen bond acceptors than they do in very similar material without hydrogen bonding capabilities[1]. There can be no doubt but that hydrogen bonds between different parts of the coal network exist and can be broken by external reagents and presumably can re-arrange within the coal provided the conditions are right. There is an enormous literature on the geometry of hydrogen bonding. For our purposes, it is simple enough to state that the hydrogen will lie on a line collecting the two nuclei which serve as the terminus for the non-covalent interaction.

Attractive interactions exist between aromatic units due to London dispersion forces.[5] There have been a number of calculations on various systems, but since they are very time consuming, they emphasize small molecules, particularly benzene-benzene interactions.[6] In addition, there are experimental studies of gas phase complexes, complexes in biological systems and also crystal structures of PNA systems.[7] In small rings, the most favorable interaction occurs when the rings are at right angles to each other in a T-shaped configuration. Face-to-face parallel stacking is repulsive at all distances. This is not surprising since one is bringing two electron clouds into increasingly close proximity. As the ring size grows larger, there is a tendency to move off of the perpendicular somewhat, but the parallel stack remains repulsive.[6] In crystal structures where there is the necessity for filling space, a "herringbone" pattern is adopted which preserves both the "T" interactions and provides a packing geometry which is space filling.

In an amorphous polymer network like coals, we anticipate a compromise between the thermodynamic driving force for "T" configuration interactions between aromatics and a packing which efficiently fills space. It is not easy to predict what the outcome will be. Hirsch's X-ray data are quite explicit in identifying some parallel stacking in coals but it is impossible to compare the frequency of this geometry with that of a perpendicular orientation of aromatics.[8]

Orientation of Aromatics with Respect to the Bedding Plane

It is often assumed by coal scientists that the aromatic systems in coals both have a strong tendency towards parallel alignment and tend to align parallel to the bedding plane. While there is clear X-ray evidence for some tendency towards parallel stacking, the evidence for alignment of aromatic rings parallel to the bedding plane is much more tenuous. In Hirsch's classical papers, he provides evidence for the alignment of aromatic systems parallel to the bedding plane in an anthracite coal but states that "the degree of preferred orientation is small in the low rank coals and increases with rank, particularly in the anthracite region".[8]

The other factor which comes into play is the striking anisotropy in coal mechanical properties. Coals are much stronger perpendicular to the bedding plane than parallel to the bedding plane.[9] This is a significant factor in mine design but it has not heretofore been determined whether the mechanical anisotropy was an inherent property of the material or was due to the cleats and cracks which form whenever a piece of coal is hacked from a seam.[9]

The alignment of aromatic structures in coals with reference to the bedding plane was investigated using Fourier transform IR dichroism with photoacoustic detection. A solid disk of coal was cut and the bedding plane accurately determined. This was placed in the photoacoustic detector of an IBM FTIR and spectra obtained using plane polarized light indexed to the bedding plane. Spectra were obtained at 45° intervals moving in a 360° circle. To verify that the instrument was operating properly, a crystal of acrylamide was oriented in the IR instrument and the dichroic spectra obtained. From these spectra, we could accurately back-calculate the known bond angles in the oriented single crystal. Based on these calculations, we estimate that our error is $\pm$ 3°. Dichroic spectra of Ill. No. 6 coal and acrylamide are shown in Fig. 1. In none of the coals was any alignment of the organic structures parallel to the bedding plane detected.

We have applied ^{13}C NMR using oriented samples in a single crystal probe as well as optical birefringence to some of these coals. Both of these techniques indicate a net orientation of the aromatic rings of about 1.5°, within the experimental error of the IR measurements. Our conclusion is that the organic groups in coals are essentially randomly arranged.

To probe the mechanical anisotropy, a series of coal thin sections were swollen under a microscope and the swelling measured on photographs of the thin sections.[7] Features on the thin section were identified, these features being connected by lines which would run either parallel to or perpendicular to the bedding plane. The coal is wet with a solvent and as it expands it was photographed and the movement of these features measured on the photographs, directly giving linear expansions. These data were obtained for six coals and are shown in Fig. 2. For all coals and solvents, the swelling is highly anisotropic. The coals expand much greater perpendicular to the bedding plane than they do parallel to the bedding plane. The mechanical anisotropy of coals must be a direct consequence of their macromolecular structure.

We are faced with an apparent contradiction in that coals have randomly oriented groups on a molecular level but are mechanically anisotropic on a larger scale. There are two possibilities. There may be a random coil network with a non-random distribution of branch points, the branch points occurring more frequently parallel to the bedding plane than perpendicular to it. Another possibility is a coal structure which features an array of sheets dividing and twisting and eventually achieving an individual group random orientation while maintaining a bulk structure anisotropy under stress.

Such structures have been proposed for amorphous carbons and recently for a low-rank coal based on X-ray data.[10]

Reversible Association of the Coal in the Macromolecule

As if this was not sufficient structural complexity, the coal is not at an equilibrium configuration when removed from the mine to atmospheric pressure and is capable of undergoing a number of internal re-arrangements.[7] A plot of linear expansion during solvent swelling parallel to and perpendicular to the bedding plane for several coals vs. time is shown in Fig. 3. Both of these coals show excess expansion both parallel and perpendicular to the bedding plane, that excess occurring at different times. The existence of the swelling excess was first noted by Peppas and ascribed to a metastable state caused by the slow motion of the coal macromolecular segments.[11] We agree with his interpretation.

When the solvent is removed from the coal, the solid which remains has a somewhat different shape than the starting coal did: it is higher perpendicular to the bedding plane and not quite as wide. Subsequent swellings of this material are totally reversible, always returning to the same shape and size. Wetting the coal with the solvent, allowing it to expand, and then contracting it by removing the solvent lets the coal macromolecular segments find the equilibrium positions to which they will return again and again as the process is repeated. The configuration of coals in the seam is not at equilibrium at 1 at. Coals do not re-arrange to their equilibrium form without some treatment because they are glassy. If made rubbery, then re-arrangement will occur.

ACKNOWLEDGEMENT

I thank the Department of Energy and Exxon Research and Engineering Co. for finanacial support of this work. This paper is a summary of experimental work carried out by a variety of students and collaborators. Their names are listed in the references and I am most grateful to them for the opportunity to have worked with them and for their help and encouragement. The insights and ideas of Dr. Masaharu Nishioka have been especially important and are gratefully acknowledged.

REFERENCES

1. Larsen, J. W.; Green, T.K.; Kovac. J. J. Org. Chem. **1985**, 50, 4729-4735.

2. Larsen, J. W.; Baskar, A. J. Energy Fuels **1987**, 1, 230-222.

3. Stock, L. M.; Mallaya, N. Fuel, **1986**, 65, 736-738.

4. Quinga, E. M. Y.; Larsen, J. W. Energy Fuels **1987**, 1, 300-304.

5. Kaufmann, W. "Quantum Chemistry," Academic Press; New York; 1957.

6. Miller, J. H.; Mallard, W. G.; Smyth, K. C. J. Phys. Chem. **1984**, 88, 4963-4970 and references therein.

7. Cody, G., Jr.; Larsen, J. W.; Siskin, M. Energy Fuels, **1988**, 2, in press and references therein.

8. Hirsch, P. B. Proc. R. Soc. London, **1954**, A226, 143.

9. Szwilski, A. B. Int. J. Rock Mech. Min. Sci. Geomech. Abstr. **1984**, 21, 3-12. Klepaczko, J. R.; Hsu, T. R.; Bassim, M. N. Can. Geotech. J. **1984**, 21, 203-212. Szwilski, A. B. Min. Sci. Technol. **1985**, 2, 181-189.

10. Thiessen, W. E.; Larsen, J. W.; Narten, A. H. Energy Fuels **1988**, 2, submitted.

11. Peppas, N. A.; Larsen, J. M.; Lucht, L. M.; Sinclair, G. W. Proc.-Int. Conf. Coal Sci. **1983**, 1983, 280.

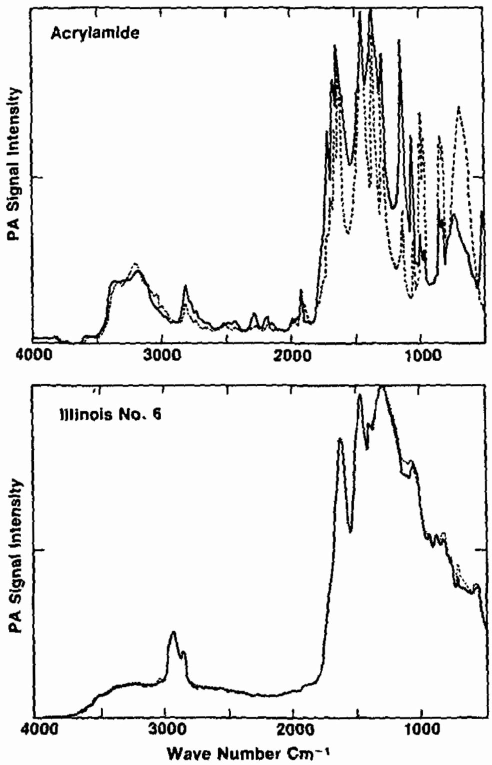

Figure 1. Photoacoustic FTIR Spectra Obtained with Polarized Light
a) Single Crystal Acrylamide; ——— Light Polarized Parallel to C Axis, ----- Polarized Parallel to B Axis
b) Ill. No. 6 Coal; ——— Light Polarized Parallel to Bedding Plane, ----- Polarized Perpendicular to Bedding Plane

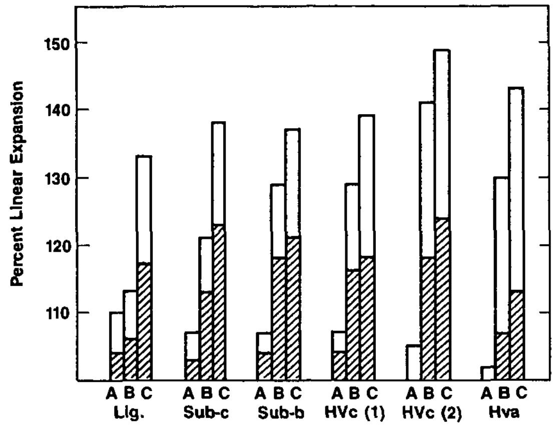

Figure 2. Linear Expansion of Coals in Chlorobenzene (A), THF (B), and Pyridine (C) Measured Parallel (crosshatched) to and Perpendicular to the Bedding Plane. Lig. = Big Brown (Texas); Sub-c = Smith Seam; Sub-b = Wandoan; HVc(1) = Correjón (Columbia); HVc(2) = Ill. No. 6; HVa = Pittsburgh No. 8.

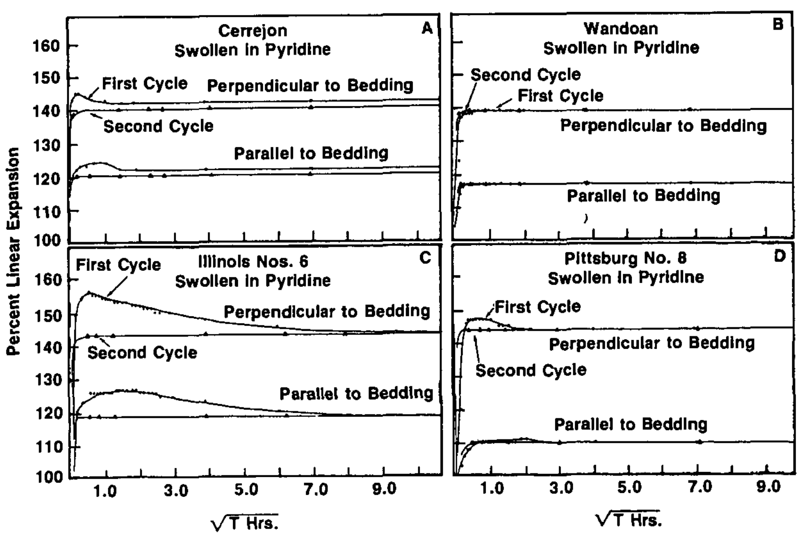

Figure 3. Time Dependence of Linear Expansion of Coals Swollen in Pyridine Parallel to and Perpendicular to the Bedding Plane

AROMATIC STRUCTURES IN WHOLE COALS AND COAL MACERALS

Randall E. Winans, Ryoichi Hayatsu, Robert L. McBeth,
Robert G. Scott and Robert E. Botto
Chemistry Division, Argonne National Laboratory,
9700 South Cass Avenue, Argonne, IL 60439 USA

ABSTRACT

New information on the chemical and physical structure of coals and separated coal macerals strongly suggests that polycyclic aromatics do not dominate the aromatic structure except in the very high-rank coals and in inertinites. Two very different approaches have led to these conclusions. First, a very mild, selective oxidation method has been used to break down the coal macromolecular structure into molecules which can be readily characterized. The products are dominated by single ring aromatics. Second, small-angle neutron scattering has been used to study solvent swollen coals. There is no evidence from the scattering data for the existence of a layered structure, instead long tubular pores are being formed apparently as a result of changes in the hydrogen-bonding in the matrix.

INTRODUCTION

In the past, coal scientists have thought that coal consists mainly of polycyclic aromatic structures. Figure 1 depicts an extreme example. Even recently, three ring aromatics have been proposed as an average aromatic structural unit on the basis of NMR spectroscopic evidence. Our recent findings strongly suggest that polycyclic aromatics are not the most abundant structures in the lower rank bituminous coals as has been previously thought. Our results have significant implications for the development of mild coal-solubilization processes.

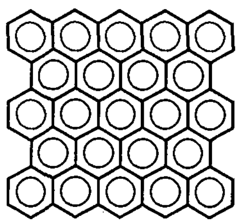

Figure 1. Early thoughts on the aromatic structure of coals.

A major problem in coal characterization and in coal utilization is the intractability of the coal macromolecular network. High temperature treatments yield smaller, volatile and soluble molecules, which can be greatly altered from their original structures, along with a significant amount of a non-volatile char. Mild oxidation should provide a soluble mixture of compounds in higher yields and with structural characteristics more like the original coal. The approach described here oxidatively cleaves activated benzylic sites which are activated by the formation of pyridinium salts at that carbon from the reaction with pyridine and iodine. This reaction sequence has been described in an initial communication for whole coals (1) and the results of the first reaction step on the macerals have been published (2). This report summarizes the results on the yields of the oxidation step and the characterization of the products (3). Also, a solvent refined coal (SRC) has been reacted to test the selectivity of the method.

A few oxidative degradation studies on separated coal macerals have been published (4-6). In these studies there was extensive oxidation and only small molecules were identified. In this study, both smaller and higher molecular weight fractions, which were separated on the basis of solubility, have been characterized by using gel permeation chromatography (GPC), GCMS, Pyrolysis MS (PyMS) in the precise mass measurement mode, and NMR. Compounds in the higher molecular weight range are not volatile enough for GCMS and are broken down into smaller fragments by PyMS. While rearrangements may occur in PyMS, their likelihood is reduced when pyrolysing the oxidation products in comparison to the whole coals or maceral concentrates. It is interesting to note the remarkable lack of large polycyclic aromatics in the soluble products. The significance of this result will be discussed.

Coal porosity has been studied by SANS in the dry state (7,8,9) and in non-swelling deuterated solvents (7,9). These studies suggested that this technique can be useful for examining pore structure. In the second part of this study, changes in the physical structure of coals upon swelling in an organic solvent have been examined. It is known that bituminous coals will swell in solvents such as pyridine (10). The phenomenon of coal solvent swelling is being used to characterize coal structure, especially in determining molecular sizes between crosslinks. Swelling can affect coal reactivity in thermolysis reactions. Also, it is important to note that swelling increases reagent accessibility in chemical modification of coals (11). SANS is being used in this study to examine the changes in pore structure in a Pittsburgh seam hvA bituminous coal, Argonne Premium Coal Sample #4 (12,13). Two perdeuterated solvents are used, benzene for non-swelling and pyridine for swelling conditions. The deuterated solvent provides a large contrast between the solvent and the solid coal for neutron scattering.

EXPERIMENTAL

A description of the coals and SRC is given in Table 1. The Argonne Premium Coal Samples (APCS) have been recently mined and have been stored under nitrogen in sealed glass ampules (14).

The pyridine salts of the samples were prepared by refluxing 1 g of the coal, maceral or polymer in 60 ml of pyridine with 4 g of iodine for 70 hrs (2). The reaction mixture was poured into 10% aqueous $NaHSO_3$ and the solution filtered. The derivatized coal was washed free of pyridine, dried and analyzed. In a typical oxidation, fresh Ag_2O prepared from 9.5 g of $AgNO_3$ and sodium hydroxide, was refluxed with 1.0 g of the substate in 50 ml of 10% aqueous NaOH

TABLE 1. Characteristics of Coal and Maceral Samples.

Sample	Source	Rank	%C	Empirical Formula	Py^+/100°C	Ag_2O Oxidation Yields* Organic Soluble, %	Ag_2O Oxidation Yields* Humic Acid, %
APCS #1	Upper Freeport	mv Bituminous	85.5	$C_{100}H_{66}N_{1.5}S_{0.3}O_{6.6}$	2.8	27	5
APCS #2	Wyodak-Anderson	Subbituminous	75.0	$C_{100}H_{86}N_{1.3}S_{0.2}O_{18.0}$	4.1	40	26
APCS #3	Illinois Herrin	hvC Bituminous	77.7	$C_{100}H_{77}N_{1.5}S_{1.1}O_{13.0}$	3.7	25	34
APCS #4	Pittsburgh	hvA Bituminous	83.2	$C_{100}H_{77}N_{1.7}S_{0.4}O_{8.0}$	3.3	30	30
APCS #8	Beulah-Zap	Lignite	72.9	$C_{100}H_{80}N_{1.3}S_{0.4}O_{20.9}$	3.6	39	21
SRC	Wilsonville (Pittsburgh coal)		86.9	$C_{100}H_{76}N_{1.8}S_{0.5}O_{3.8}$	2.6	21	9

*Based on carbon composition.

for 20 hrs. The silver and unoxidized samples were removed by filtration and the filtrate acidified with aqueous HCl. Products which were alkaline soluble but insoluble in the slightly acidic solution are termed humic acids. The solubles were extracted with Et_2O-MeOH. Yields were determined by analyzing the products for carbon. The products were methylated with diazomethane for further analysis.

GCMS and PyMS data were obtained on a Kratos MS-25 mass spectrometer. A 60 m x 0.25 mm DB-1701 fused silica column was used in GCMS analysis. The details of the PyMS experiment have been reported (2). The samples were all heated at 50°/min on a platinum screen and the instrument was operated in the precise mass measurement mode.

For the very high resolution experiments, the samples were inserted into an all glass heated inlet system (300°C) and leaked into the source of a Kratos MS 50 ultra high resolution mass spectrometer. A dynamic resolution of 80,000 was obtained for the low voltage (11 eV) electron impact LVHRMS experiment with a scan rate of 1000 seconds/decade. The 70 eV EI spectra were obtained with 50,000 dynamic resolution with a scan rate of 100 seconds/decade. Both spectrometers were operated with a Kratos DS 90 data system. Data were transferred to a Micro VAX II for final analysis.

RESULTS AND DISCUSSIONS

The yields for the oxidation step are very sample dependent, as is shown in Table 1. The yields are calculated on the basis of carbon content of the starting material and of the products, with the values given being an average of at least two experiments.

Proton NMR data lends support to the observation of the lack of polycyclic aromatics in the products. Since even the solvent-soluble fractions contained compounds which were too large and nonvolatile for GCMS, the proton NMR spectra were taken. The methyl ester region is the most informative and is shown for several coal samples and the SRC sample in Figure 2. From the spectra of a number of known methyl esters, three regions can be assigned: 3.6-3.8 aliphatic, 3.8-4.0 single-ring aromatics and heteroaromatics, and 4.0-4.2 polycyclic aromatics and heteroaromatics. Single-ring aromatics and aliphatics are the most abundant species in these samples, except in the SRC. A general trend is observed in which the relative amount of polycyclic aromatics increases with rank. This observation is important in that it shows that the procedure does not destroy many of the polycyclic aromatics.

Compounds that can be separated by GCMS are mostly benzene and hydroxybenzene carboxylic acids. The total ion chromatograms for subbituminous and Pittsburgh Seam coals are shown in Figure 3. Although this is a fairly mild oxidant, tetra-, penta-, and hexa-carboxylic acids are still formed. Also note that even the hydroxybenzene tetra- and penta-carboxylic acids are formed. More model compounds are being examined to understand this result better. In addition to benzene and hydroxybenzene carboxylic acids, significant amounts of furan carboxylic acids are found in the subbituminous coal.

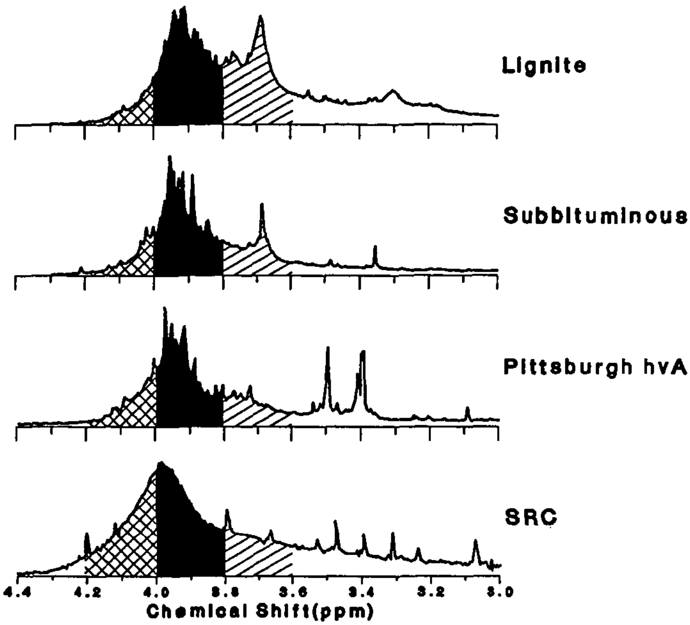

Figure 2. Methyl ester region of the ^{1}H NMR spectra of the methylated solvent-soluble fractions from the Ag_2O oxidation recorded on a Nicolet 200 MHz instrument with $CDCl_3$ as the solvent. (-aliphatic, -single ring aromatic, -polycyclic aromatic.)

Fragments found by PyMS with the premium coal samples and the vitrinites (3) are dominated by aliphatics, single-ring aromatics, and hydroxylated aromatics. PyMS of the humic products results in volatilization at lower temperatures than with the coal. Comparing the pyrolysis products between the two samples, the most striking difference is the reduction in aliphatics in the humic acid fraction. All of these results strongly suggest that, for our vitrinite samples and the coals with a carbon content of less than 83%, the single-ring aromatics dominate. Unlike many other experiments, most of the carbon is characterized with this approach.

From preliminary small-angle neutron scattering results, we conclude that in a good swelling solvent the tertiary structure of this bituminous coal undergoes major rearrangement (12,13). Whereas the original coal contains a broad size range of roughly spherical pores, the swollen coal contains elongated pores with several distinct sizes. The pyridine appears to be determining the new

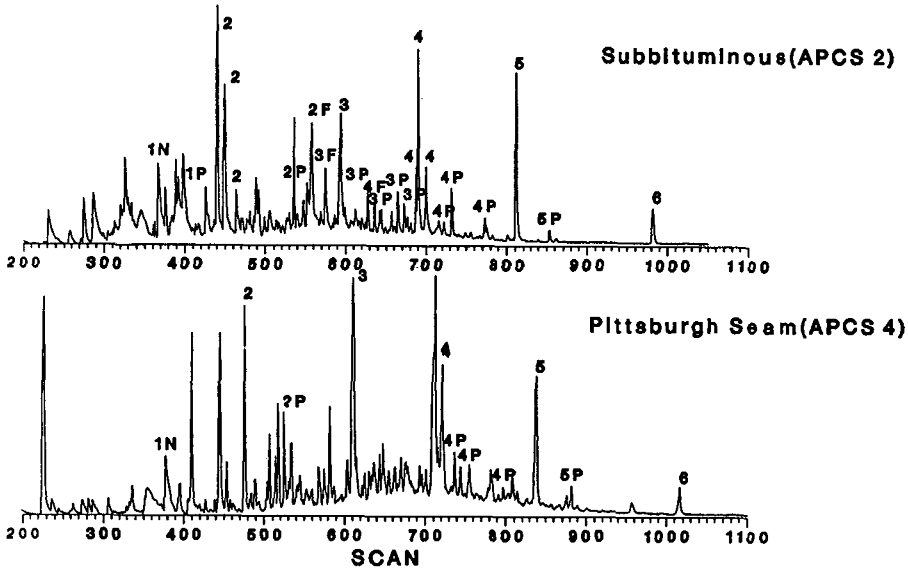

Figure 3. Total ion chromatograms of solvent soluble fractions from the Ag_2O oxidation of two premium coals. Major peaks: 2-6 number of methyl carboxylates on benzene; 1P-5P, on phenol; 1N, on pyridine; 2F-4F, on furan.

pore dimension. Exactly five pyridines can be fitted into a 9 Å radius circle. The size of the pyridine molecule has been estimated from space-filling computer models based on the van der Waals radii of the individual atoms. It is important to note that we are observing relatively narrow elongated pores. These results could be explained by invoking hydrogen bonding between the pyridines and the phenols or other acidic hydroxyls on the surface of the tubular pores. In addition, it is thought from the NMR and ESR experiments that the motion of pyridine in a coal is restricted (15). Our SANS data argues against a layered, polycyclic aromatic structure for this coal.

In summary, the results from both oxidation and SANS strongly suggest that polycyclic aromatics do not dominate the structures of hv bituminous, subbituminous, and lignite coals. These can be contrasted with the calculations made by NMR spectroscopists (16,17) which suggest that the average aromatic ring size is three. This number does not seem to be rank dependent (16) which is a little difficult to rationalize. We know that for vitrinites the starting material is mostly lignin (18) which does not contain polycyclic aromatics. Therefore, one would expect a gradual increase in the amount of polycyclic aromatics in vitrinites with increasing rank. The remnants of lignin are easily identified in low rank coals (19). Our results do not rule out the possibility of microdomains of layered structure, but they do suggest that stacking of planar polycyclics is unlikely. Figure 4 displays two generalized structural arrangements for coals. The lower one appears to be more likely with hydrogen bonding, represented by the filled circles, playing a critical role in determining the overall structure.

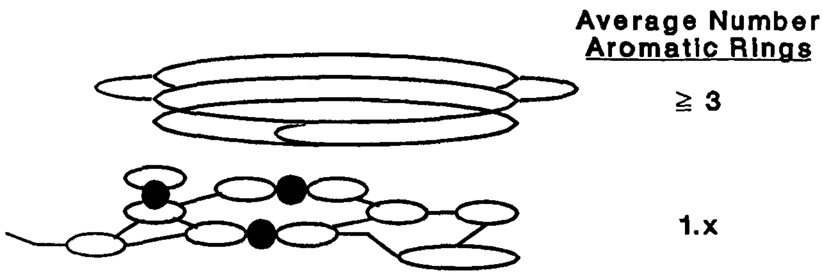

Figure 4. Possible coal structural arrangements. Top-stacked polycyclic aromatics, bottom-single ring aromatics with hydrogen bonding.

ACKNOWLEDGMENTS

This work was performed under the auspices of the Office of Basic Energy Sciences, Division of Chemical Sciences, U.S. Department of Energy, under contract number W-31-109-ENG-38.

REFERENCES

1. R. Hayatsu, R. G. Scott, R. E. Winans, R. L. McBeth, and R. E. Botto, Proceedings International Conference on Coal Science, p. 322 (1983).

2. R. E. Winans, R. Hayatsu, R. G. Scott, and R. L. McBeth, in "Chemistry and Characterization of Coal Macerals", Winans, R. E.; Crelling, J. C., Eds., ACS Symposium Series No. 252, ACS:Washington, p. 137 (1984).

3. R. E. Winans, R. Hayatsu, R. L. McBeth, R. G. Scott, and R. E. Botto, Preprints, Div. Fuel Chem., ACS, 31(4), 94 (1986).

4. R. E. Winans, G. R. Dyrkacz, R. L. McBeth, R. G. Scott, and R. Hayatsu, Proceedings International Conference on Coal Science, p. 22 (1981).

5. J. Allan and S. R. Larter, "Advances in Organic Geochemistry 1981", M. Bjoroby, Ed., Wiley:Chichester, U.K., p. 534 (1983).

6. C.-Y. Choi, S. H. Wang and L. M. Stock, Energy & Fuels, 2, 37 (1988).

7. H. Kaiser and J. S. Gethner, Proceedings International Conference on Coal Science, p. 300 (1981).

8. M. J. Tricker, A. Grint, G. J. Audley, S. M. Church, V. S. Rainey and C. J. Wright, Fuel, 62, 1092 (1983).

9. J. S. Gethner, J. Appl. Phys., 59, 1068 (1986).

10. T. Green, J. Kovac, D. Brenner, and J. W. Larsen, in "Coal Structure", R. A. Meyers, Ed., Academic Press, p. 199 (1982).

11. R. Liotta, Fuel, 58, 724 (1979).

12. R. E. Winans and P. Thiyagarajan, Preprints, Div. Fuel Chem., ACS, 32(4), 227 (1987).

13. R. E. Winans and P. Thiyagarajan, Energy & Fuels (in press).

14. K. S. Vorres and S. K. Janikowski, Preprints, Div. Fuel Chem., ACS, 32(1), 492 (1987).

15. B. G. Silbernagel, L. B. Ebert, R. H. Schlosberg, and R. B. Long, in "Coal Structure", M. L. Gorbaty and K. Ouchi, Eds., ACS Adv. Chem. Series, 182, 23 (1981).

16. B. C. Gerstein, P. D. Murphy, and L. M. Ryan, in "Coal Structure", R. A. Meyers, Ed., Academic Press, p. 87 (1982).

17. M. Solum, R. J. Pugmire, and D. M. Grant, Preprints, Div. Fuel Chem., ACS, 32(4), 273 (1987).

18. R. Hayatsu, R. E. Botto, R. G. Scott, R. L. McBeth, and R. E. Winans, Fuel, 65, 821 (1986).

19. R. Hayatsu, R. E. Winans, R. L. McBeth, R. G. Scott, L. P. Moore, and M. H. Studier, in "Coal Structure", Adv. in Chem. Series, No. 192, M. L. Gorbaty and K. Ouchi, Eds., ACS, p. 133 (1981).